C A N A D A

PROVINCE OF QUEBEC

DISTRICT OF MONTREAL

DOCKET No. R-3770-2011

RÉGIE DE L'ÉNERGIE / ENERGY BOARD

AUTHORIZATION OF AN INVESTMENT BY HYDRO-QUEBEC DISTRIBUTION – ADVANCED METERING PROJECT PHASE 1

HYDRO-QUEBEC
As Electricity Distributor

Petitioner

-and-

STRATEGIES ENERGETIQUES (S.E.) / ENERGY STRATEGIES (E.S.)

ASSOCIATION QUEBECOISE DE LUTTE CONTRE LA POLLUTION ATMOSPHERIQUE (AQLPA) / QUEBEC ASSOCIATION TO FIGHT AGAINST AIR POLLUTION

Interveners

ARTICLES MENTIONED IN SECTION 44 OF DR. CARPENTER'S REPORT

(MECHANISMS OF INTERACTION BETWEEN RF/MW RADIATION AND BIOLOGIC SYSTEMS AT THE CELLULAR LEVEL)

Referred to in **David O. CARPENTER**, *Expert Report*, Revised on May 14, 2012, C-SE-AQLPA-0072, SE-AQLPA-7, Doc. 1.1, parag. 44, 55.

Filed on May 15, 2012

ARTICLES MENTIONED IN SECTION 44 OF DR. CARPENTER'S REPORT

(MECHANISMS OF INTERACTION BETWEEN RF/MW RADIATION AND BIOLOGIC SYSTEMS AT THE CELLULAR LEVEL)

44. The following studies explain the mechanisms of interaction between RF/MW radiation and biologic systems at the cellular level.

a. The cell membrane recognition process -- which includes signal transduction and 'heat-shock protein' release -- was first discerned by Litovitz and his co-workers at Catholic University of America in the mid-1990s.

   Below are a few references that make the point.

   i. Litovitz, T., C. Montrose, et al. (1994). "Superimposing spatially coherent electromagnetic noise inhibits field induced abnormalities in developing chick embryos." Bioelectromagnetics 15(2): 105-113.

   ii. DiCarlo, A., J. Farrell, et al. (1998). "A simple experiment to study electromagnetic field effects: Protection induced by short term exposures to 60 Hz magnetic fields." Bioelectromagnetics 19(8): 498-500.

   iii. Penafiel, L., T. Litovitz, et al. (1997). "Role of modulation on the effect of microwaves on ornithine decarboxylase activity in L929 cells." Bioelectromagnetics 18(2): 132-141.

   iv. Dicarlo, A. L., Michael T. Hargis, L. Miguel Penafiel, Theodore A. Litovitz, A. (1999). "Short-term magnetic field exposures (60Hz) induce protection against ultraviolet radiation damage." International journal of radiation biology 75(12): 1541-1549.

   v. Litovitz, T., C. Montrose, et al. (1990). "Amplitude windows and transiently augmented transcription from exposure to electromagnetic fields." Bioelectromagnetics 11(4): 297-312.

   vi. Litovitz, T., M. Penafiel, et al. (1997). "The role of temporal sensing in bioelectromagnetic effects." Bioelectromagnetics 18(5): 388-395.

vii. Litovitz, T., L. Penafiel, et al. (1997). "Role of modulation in the effect of microwaves on ornithine decarboxylase activity in L929 cells." Biolectomagnetics 18: 132-141.]

viii. Litovitz, T., D. Krause, et al. (1993). "The role of coherence time in the effect of microwaves on ornithine decarboxylase activity." Bioelectromagnetics 14(5): 395-403.

b. Cell membrane reaction is lipid peroxidation.

i. Serban, M. and V. Ni (1994). "Lipid peroxidation and change of plasma lipids in acute ischemic stroke." Romanian journal of internal medicine= Revue roumaine de médecine interne 32(1): 51. [English summary filed only]

ii. Vileno, B., S. Jeney, et al. (2010). "Evidence of lipid peroxidation and protein phosphorylation in cells upon oxidative stress photogenerated by fullerols."Biophysical chemistry.

iii. Maaroufi, K., E. Save, et al. (2011). "Oxidative stress and prevention of the adaptive response to chronic iron overload in the brain of young adult rats exposed to a 150 kilohertz electromagnetic field." Neuroscience.

iv. Nelson, S. K., S. K. Bose, et al. (1994). "The toxicity of high-dose superoxide dismutase suggests that superoxide can both initiate and terminate lipid peroxidation in the reperfused heart." Free Radical Biology and Medicine 16(2): 195-200.

v. Alvarez, J. G. and B. T. Storey (1989). "Role of glutathione peroxidase in protecting mammalian spermatozoa from loss of motility caused by spontaneous lipid peroxidation." Gamete research 23(1): 77-90.

vi. Devasagayam, T., K. Boloor, et al. (2003). "Methods for estimating lipid peroxidation: An analysis of merits and demerits." Indian journal of biochemistry & biophysics 40(5): 300-308. [Not included]

c. Free-Radical Damage :

i. Ozgur, E., G. Güler, et al. (2010). "Mobile phone radiation-induced free radical damage in the liver is inhibited by the antioxidants n-acetyl cysteine and epigallocatechin-gallate." International journal of radiation biology(00): 1-11.

ii. Gutteridge, J. and X. C. Fu (1981). "Enhancement of bleomyciniron free radical damage to DNA by antioxidants and their inhibition of lipid peroxidation." FEBS letters 123(1): 71.

d. mRNA :

i. Yan, J. G., M. Agresti, et al. (2009). "Qualitative Effect on mRNAs of Injury-Associated Proteins by Cell Phone Like Radiation in Rat Facial Nerves. Electromagnetic Biology and Medicine 28(4): 383-390.

ii. Yan, J. G., M. Agresti, et al. (2008). "Upregulation of specific mRNA levels in rat brain after cell phone exposure." Electromagnetic Biology and Medicine 27(2): 147-154.

iii. Simbürger, E., A. Stang, et al. (1997). "Expression of connexin43 mRNA in adult rodent brain."Histochemistry and cell biology 107(2): 127-137.

iv. Chen, J., H. C. He, et al. (2010). "Effects of Pulsed Electromagnetic Fields on the mRNA Expression of RANK and CAII in Ovariectomized Rat Osteoclast-Like Cell." Connective Tissue Research 51(1): 1-7.

e. Epigenetic changes.... environmentally induced genetic change:

i. Migliore, L. and F. Copped (2009). "Genetics, environmental factors and the emerging role of epigenetics in neurodegenerative diseases." Mutation Research/Fundamental and Molecular Mechanisms of Mutagenesis 667(1-2): 82-97.

f. Micronuclei formation :

i. Tice, R. R., G. G. Hook, et al. (2002). "Genotoxicity of radiofrequency signals. I. Investigation of DNA damage and micronuclei induction in cultured human blood cells." Bioelectromagnetics, 23(2): 113-126.

ii. Lerchl, A. (2009). "Comments on "Radiofrequency electromagnetic fields (UMTS, 1,950 MHz) induce genotoxic effects in vitro in human fibroblasts but not in lymphocytes" by Schwarz et al. (Int Arch Occup Environ Health 2008: doi: 10.1007/s00420-008-0305-5)." Int Arch Occup Environ Health 82(2): 275-278.

iii. Vijayalaxmi and T. J. Prihoda (2009). "Genetic damage in mammalian somatic cells exposed to extremely low frequency electro-magnetic fields: a meta-analysis of data from 87 publications (1990-2007)." Int J Radiat Biol 85(3): 196-213.

iv. Sannino, A., M. Sarti, et al. (2009). "Induction of adaptive response in human blood lymphocytes exposed to radiofrequency radiation." Radiat Res 171(6): 735-742.

g. DNA repair disruption :

i. Brusick, D., R. Albertini, et al. (1998). "Genotoxicity of radiofrequency radiation. DNA/Genetox Expert Panel." Environ Mol Mutagen 32(1): 1-16. http://www.ncbi.nlm.nih.gov/pubmed/9707093 and http://onlinelibrary.wiley.com/doi/10.1002/(SICI)1098-2280(1998)32:1%3C1::AID-EM1%3E3.0.CO;2-Q/abstract;jsessionid=426C74204A95D2EAD8182A0C624B7C3F.d03t04

ii. Belyaev, I. Y., E. Markova, et al. (2009). "Microwaves from UMTS/GSM mobile phones induce long-lasting inhibition of 53BP1/gamma-H2AX DNA repair foci in human lymphocytes."Bioelectromagnetics 30(2): 129-141.

iii. Sun, L. X., K. Yao, et al. (2006). "[Effect of acute exposure to microwave from mobile phone on DNA damage and repair of cultured human lens epithelial cells in vitro]." Zhonghua Lao Dong Wei Sheng Zhi Ye Bing Za Zhi 24(8): 465-467. [Not included]

h. Immune response suppression :

i. Lyle, D. B., P. Schechter, et al. (1983). "Suppression of Tlymphocyte cytotoxicity following exposure to sinusoidally amplitude-modulated fields." Bioelectromagnetics 4(3): 281-292.

ii. Elekes, E., G. Thuroczy, et al. (1996). "Effect on the immune system of mice exposed chronically to 50 Hz amplitude-modulated 2.45 GHz microwaves." Bioelectromagnetics 17(3): 246-248.

iii. Dabala, D., D. Surcel, et al. (2008). "Oxidative and Immune Response in Experimental Exposure to Electromagnetic Fields." Electromagnetic field, health and environment: proceedings of EHE'07: 105.

iv. Surcel, D., D. Dabala, et al. (2009). "Free Radicals, Lipid Peroxidation and Immune Response in Experimental Exposure to Electromagnetic Fields." Epidemiology 20(6): S118. [Not included]

Bioelectromagnetics 15:105–113(1994)

Superimposing Spatially Coherent Electromagnetic Noise Inhibits Field-Induced Abnormalities in Developing Chick Embryos

T.A. Litovitz, C.J. Montrose, P. Doinov, K.M. Brown, and M. Barber

Department of Physics, The Catholic University of America, Washington, D.C. (T.A.L., C.J.M., P.D., M.B.) and Biological Sciences Department, George Washington University, Washington, D.C. (K.M.B.)

Living cells exist in an electrically noisy environment. This has led to the so-called "signal-to-noise" problem whereby cells are observed to respond to extremely-low-frequency (ELF) exogenous fields that are several orders of magnitude weaker than local endogenous fields associated with thermal fluctuations. To resolve this dilemma, we propose that living cells are affected only by electromagnetic fields that are spatially coherent over their surface. The basic idea is that a significant number of receptors must be simultaneously and coherently activated (biological cooperativity) to produce effects on the biochemical functioning of the cell. However, like all physical detection systems, cells are subject to the laws of conventional physics and can be confused by noise. This suggests that a spatially coherent but temporally random noise field superimposed on a coherent ELF signal will defeat the mechanism of discrimination against noise, and any observed field-induced bioeffects would be suppressed. An experimental test of this idea was conducted using morphological abnormalities in developing chick embryos caused by electromagnetic field exposure as the endpoint. At an impressed noise amplitude comparable to the ELF field strength (but roughly one-thousandth of the thermal noise field), the increased abnormality rate observed with only the ELF field present was reduced to a level essentially the same as for the control embryos. ©1994 Wiley-Liss, Inc.

Key words: noise, cooperativity, signal-to-noise, embryo development, abnormalities

INTRODUCTION

The association of biological effects at the cellular level with exposure to weak ELF electromagnetic fields (EMFs) has remained a controversial subject despite nearly a decade of such reports. Theoretical arguments based on signal-to-noise considerations are in large measure responsible for the skepticism [Weaver and Astumian, 1990; Adair, 1991]. The dilemma arises because cells, existing in an

Received for review October 12, 1992; revision received July 6, 1993.

Address reprint requests to C.J. Montrose, Department of Physics, Catholic University of America, Washington, DC 20064

electrically noisy environment, respond to external EMFs some 100 to 1000 times weaker than local noise fields resulting from the thermally driven movements of ions in the vicinity of cells. In this context Adair [1991] has concluded that "...it does not appear to be possible for weak external ELF electromagnetic fields to affect biological processes significantly at the cell level." Yet the data unambiguously demonstrate that they do [see Byus et al., 1987; Rubin et al., 1989; and Litovitz et al., 1991, for example]. How can the externally impressed fields possibly influence cell behavior when cells have evolved in such a way as to function normally in the presence of the much larger local noise fields?

To address this question, Weaver and Astumian [1990] have proposed that cells integrate the electromagnetic signals, effectively narrowing their acceptance bandwidth, and thus averaging out the thermal noise. However, their calculations yield averaging times much longer than exposure intervals observed to produce bioeffects. For cells of 20 μm diameter, they estimate that to achieve the required signal-to-noise improvement at 100 Hz requires averaging over 4.3×10^4 s (about 12 h) yet there are many cases of bioeffects being observed with exposure intervals on the order of (or even less than) 1 h. It is clear that a simple time averaging mechanism cannot explain the data.

The essence of this paper is the formulation of a hypothesis that confronts the problem of how cells discriminate against the large endogenous thermal noise fields, enabling them to respond to the weak exogenous fields. We propose that living cells discriminate against thermal noise fields by recognizing them as *spatially incoherent*, i.e., uncorrelated at different locations on the cell membrane. Adey [1975a,b, 1981, 1988] and Blackman [1988, 1989] have conjectured that coherence plays some role in the interaction of electromagnetic fields with cells. The specific character of the hypothesis developed here is shaped by an experimental study designed to elucidate the effect of electromagnetic noise on biological response.

EXPERIMENTAL METHODS AND RESULTS

Fertilized White Leghorn eggs (Truslow Farms, Chestertown, MD) were used within 24 h of their being received. The apparatus and techniques followed the "Project Henhouse" protocols [Berman et al., 1990] with several exceptions. Six VWR water-jacketed incubators were employed in the study. Their temperature control systems were modified to avoid the possible introduction of unwanted stray magnetic fields: the coiled heater elements located below the water jackets at the bottom of the incubators were disconnected; the water was heated externally using RTE Model 110 FRC Bath/Circulators. Incubators were used interchangeably and randomly for the various exposure configurations.

Electromagnetic fields were produced by passing current through Helmholtz coils wound and connected as described by Berman et al. [1990]. Three exposure conditions were examined: 1) control or "sham" exposed, 2) "pulse" exposed, and 3) "pulse-plus-noise" exposed. In the first, no current was allowed to flow in the Helmholtz coils. In the "pulse" exposure, the pulsed EMF signal prescribed by "Henhouse" (100 Hz, 500 μs pulse duration, 2 μs rise and decay times and, 1 μT nominal peak strength) was imposed on the incubating embryos. The signal in the "pulse-plus-noise" condition consisted of the same pulsed EMF as in (2) on which was superimposed a noise EMF—a *confusion field.*

The pulsed signal was produced using a Wavetek Model 801 50 Mhz pulse generator. The noise was generated by a General Radio Model 13090-B random noise generator. The output of the noise generator was filtered with a Krohn-Hite Model 3323 bandpass filter and used to drive a Realistic Model MPA-90 audio amplifier. The filter was set for a nominal 30 to 100 Hz bandpass. The amplitude of the noise was adjusted to produce an rms magnetic field strength of 1 μT. In Figure 1 the Fourier spectra of the pulse and the noise are presented. The spectrum of the pulse contains significant contributions out to nearly 10 kHz, as is to be expected of a nearly "square" pulse; only the first few harmonics are shown here to provide a comparison with the spectrum of the noise. These frequency spectra were measured with an Ono Sokki Model CF-910 dual channel FFT spectrum analyzer.

The eggs were exposed during the first 48 h of incubation, with the control sample being incubated simultaneously. After the 48 h incubation, embryos were removed from their shells and examined by the procedures used in "Henhouse." This evaluation was performed under blind conditions. Eggs were first examined for fertility and the embryos were determined to be live or dead. Live embryos were examined for abnormal gross morphologies. Embryos were considered to be abnormal if they differed markedly from the Hamburger and Hamilton [1951] 48 h developmental stages. Malformations were classified as cephalic nervous system, truncal neural tube, heart, blood vessels, and somites. Of these only the first two occurred with any significant frequency. Indeed, over 90% of those embryos (both control and exposed samples) that were characterized as abnormal exhibited truncal neural tube malformations (as well as possibly other abnormalities).

The experiments were carried out in two groups of replicates (two runs), the second run being done roughly one year after the first. Each replicate consisted of 10, 20, or 30 eggs in each sample group. Summaries of the results are presented in Table 1 and displayed in Figure 2. It seems apparent that there is an increase in the fraction of abnormally developed embryos when the eggs are subjected to a pulsed external EMF. It also seems evident that this increase is greatly reduced when a

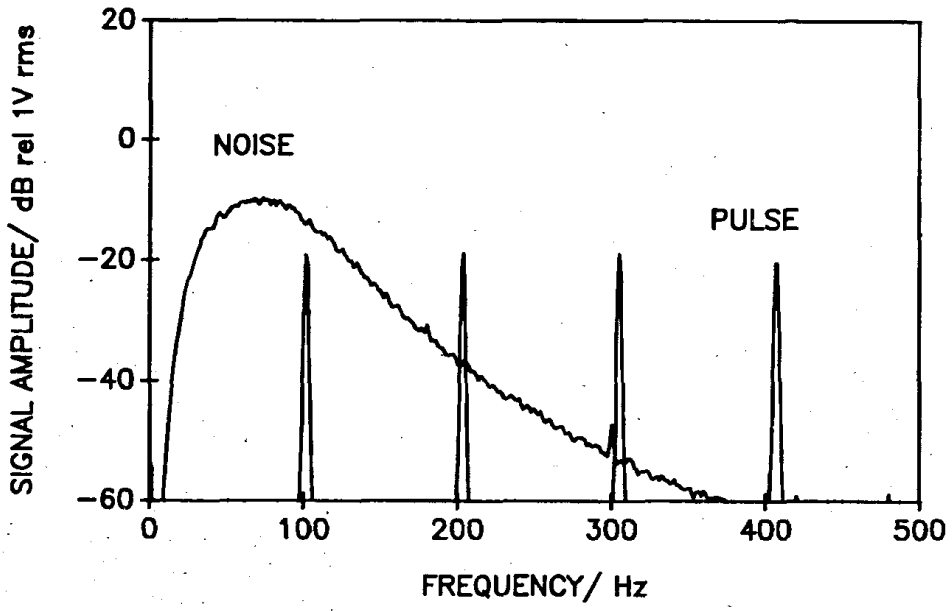

Fig. 1. Frequency spectra of the pulsed signal and of the superimposed noise field.

TABLE 1. Results for Embryos Subjected to Pulse EMFs and Pulse EMFs With Noise EMFs.

Exposure conditions	Live	Abnormal	Percent
Run 1			
Sham exposed (control)	255	16	6.3
Pulse EMF exposed	152	29	19.1
Pulse EMF + noise exposed	110	8	7.3
Run 2			
Sham exposed (control)	206	6	2.9
Pulse EMF exposed	203	22	10.8
Pulse EMF + noise exposed	181	6	3.3

confusion field is present. The data were not pooled because during the nearly 1 year interval between the two runs, the supplier changed the laying flock. From the difference in the abnormal development frequencies in the sham-exposed control samples for the two runs, about a factor of two, it is clear that the two flocks represent different experimental models.

Analysis of the Data

A detailed chronicle of the experiments is given in Table 2. The record is a rather consistent one; no single replicate gave results that stand out as so unusual that they should be regarded as "tainted." Indeed there is quite a remarkable consis-

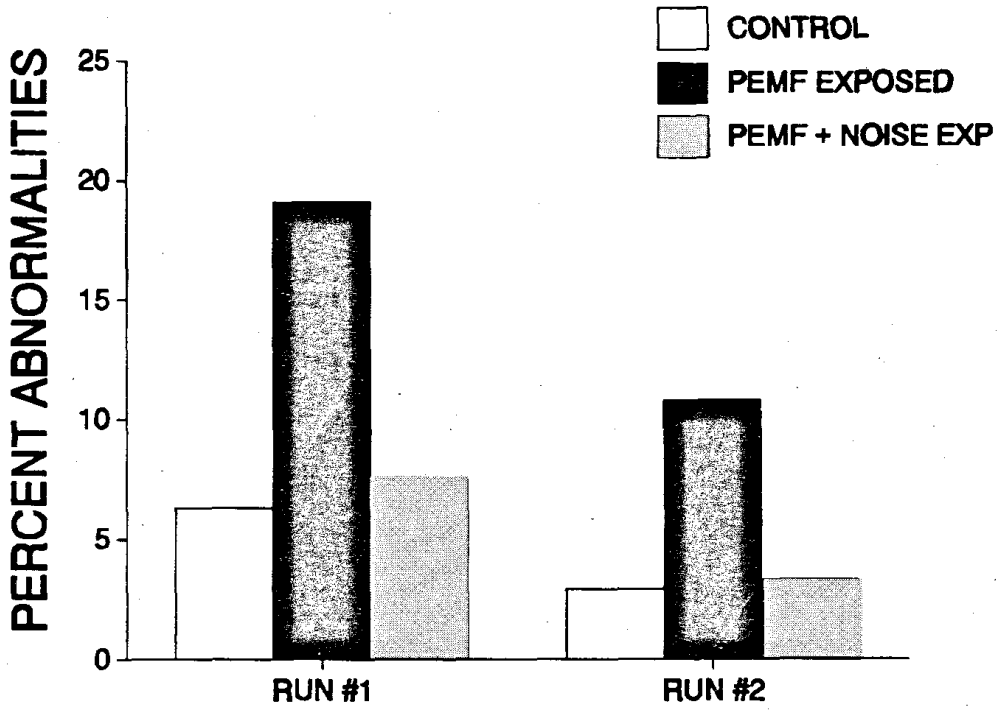

Fig. 2. The abnormal development rate for chick embryos following a 48 h incubation period during which the embryos were exposed to pulsed electromagnetic fields. The abnormality rates for sham-exposed (control) embryos and for embryos exposed to a field in which a noise signal was superimposed on the temporally coherent signal are also given.

TABLE 2. Chronological Summary of the Experimental Replicates

Replicate number and date[a]	Control sample			Pulse exposed			Pulse + noise exposed		
	Live	Abn	Remarks	Live	Abn	Remarks	Live	Abn	Remarks
1 24 Nov 91	19[b]	2		10	2		10	2	
2 27 Nov 91	26	2		9	2	1 De	16	3	2 De, 1 Tw
3 29 Nov 91	27	2	2 De	10	2		19	1	1 De
4 1 Dec 91	29	1		19	2	1 De	10	1	
5 4 Dec 91	29	2	1 De	18	3	1 De	10	0	
6 6 Dec 91	28	3		20	5		8	0	2 De
7 8 Dec 91	28	1	1 De, 1 Tw	18	3	1 De, 1 Tw	10	1	
8 11 Dec 91	30	2		10	2		17	0	2 De
9 13 Dec 91	30	1		29	7	1 De	None[c]		
10 15 Dec 91	9	0		9	1		10	0	
RUN 1 totals	255	16 (6.3%)		152	29 (19.1%)		110	8 (7.3%)	
11 9 Dec 92	19	0		20	2		17	1	1 De, 1 Tw
12 11 Dec 92	18	1	2 De	17	2	3 De	18	0	
13 13 Dec 92	18	0	1 De	19	2		20	1	
14 16 Dec 92	20	1		19	2	1 De	18	0	
15 18 Dec 92	19	0		18	2	1 De	20	1	
16 20 Dec 92	20	1		19	2		19	0	1 De
17 23 Dec 92	20	2		19	0	1 De	16	2	
18 6 Jan 93	15	0	3 De	19	1		19	0	
19 9 Jan 93	20	0		17	3	2 De, 1 Tw	None[d]		
20 12 Jan 93	20	0		19	2	1 De	18	0	1 De
21 18 Jan 93	17	1	3 De	17	4	2 De	16	1	3 De, 1 Tw
RUN 2 totals	206	6 (2.9%)		203	22 (10.8%)		181	6 (3.3%)	

[a]This is the date on which the 48 h incubation interval was completed.
[b]Unless noted (De, dead; Tw, twin embryo), missing embryos were broken during analysis.
[c]The noise field was inadvertently not switched on; thus there is no "pulse + noise exposed" sample for this replicate.
[d]The noise field was switched off after 30 h incubation; there is no "pulse + noise exposed" sample for this replicate.

tency to the results with the pulsed-EMF (PEMF) exposed abnormality rate exceeding the sham-exposed rate in 20 of the 21 replicates and exceeding the pulsed-EMF-plus-noise (PEMF + N) exposed abnormality rate in 17 of 19 replicates (with one being tied). The data lend themselves to various statistical analyses so that the tentative conclusions of the preceding paragraph can be subjected to quantitative scrutiny.

The overall null hypothesis that all three treatments, sham-exposure, PEMF-exposure, and PEMF + N-exposure, yield the same rate of abnormal development was tested using the non-parametric Friedman rank test [Lehmann, 1975]. This procedure ranks the abnormality rate for each of the three treatments (from low to high) within each replicate. For run 1, the hypothesis can be rejected with a P value $< .001$ and for run 2 with $P < .004$. The Friedman test can also be used to study whether or not differential treatment effects exist [Neder et al., 1985]. The results are that for both runs the differences between the PEMF-exposed and the sham-exposed samples are significant at $P < .05$. Similarly, the differences between the PEMF-exposed and the PEMF + N-exposed samples are significant at $P < .05$.

The differences between the sham-exposed and PEMF + N-exposed samples are not statistically significant. Paired t tests were also used to evaluate the differences. For run 1 the abnormal development rates in the PEMF-exposed samples exceeds those for the sham-exposed and PEMF + N-exposed samples at the $P < .001$ level; for run 2 the same comparisons yield $P < .01$. While these tests are not independent, they do serve to bear out the results obtained using the Friedman test, corrected for multiple comparisons.

The data demonstrate that imposing the pulsed EMF on the developing embryos brings about an increase in the frequency of abnormal development (at least at the 48 h point in the incubation process). Moreover, they show that superimposing a temporally incoherent noise field on an electromagnetic field that by itself induces embryo abnormalities, greatly curtails, or essentially eliminates its capacity to induce adverse developmental effects.

The conclusions that can be drawn are the following: 1) Impressing pulsed electromagnetic fields with amplitudes on the order of a microTesla significantly increases the fraction of embryos exhibiting developmental abnormalities after a 48 h incubation period; 2) Superimposing a confusion field (a spatially coherent, temporally incoherent field) of rms amplitude comparable to the pulsed field suppresses the effect of the latter on the abnormal development frequency; 3) For the noise fields considered here, the abnormality rates with no field imposed and with both the temporally coherent and noise fields are nearly the same, that is, the confusion field masks the effect of the imposed EMF even though it contains significant energy only near the fundamental frequency of the pulsed field.

DISCUSSION

The results presented above establish that the presence of noise, comparable in magnitude to the EMF signal, can nullify the bioeffects of that signal. In so doing, they confer on those effects the kind of respectability that derives from their being in harmony with fundamental scientific principles. In addition, they focus attention on the issue of how the externally imposed noise, the confusion field, differs from the thermal noise that is always present and several orders of magnitude larger. An obvious, and we believe the crucial, difference has to do with the spatial variation of thermally generated fields compared with that of external fields. Because the Debye screening length (roughly the range over which a given ion is not shielded from other ions) in the extracellular fluid is about 1 nm, localized charge density fluctuations produce thermal noise fields that are spatially uncorrelated. Conversely, externally impressed fields (including externally imposed noise) are spatially coherent over distances substantially larger than cellular dimensions.

We assume that the vital electromagnetic field-cell interaction occurs in the immediate vicinity of the cell surface; this interaction triggers a transmission to the cell interior where some modification of the biochemical reaction pathway is effected. A plausible supposition is that the field affects the binding of ligands to the roughly 10000 receptor proteins (sensors) that are integral to the cell membrane (we envision the effect as arising from charge redistribution caused by the local induced electric field, although this specific mechanism is not crucial to the picture). Ligand binding causes the production of effector molecules (second messengers) within the cell; the net effect is the transducing of the extracellular signal into an

intracellular one. Cooperativity is required in such processes in that "more than one intracellular effector molecule must bind to some target macromolecule in order to induce a response" [Alberts et al., 1983].

The average spacing between receptors for a particular hormone at the cell membrane is on the order of 100 nm. This is estimated by considering that there are roughly 10000 such receptors per cell [Darnell et al., 1990] and by using 10 μm as the approximate cell diameter. Hence, the idea that a multiplicity of cellular receptors must be simultaneously activated if modified cell functioning is to result requires that an essentially uniform stimulating field be presented to the receptors for some required "coherence interval." Litovitz et al. [1991] have already demonstrated that *temporal* coherence for times on the order of 5–10 s is necessary if EMF-produced bioeffects are to be observed. The operative mechanism in discriminating against fields from thermal fluctuations is analogous to a *coincidence detection* scheme, a significant number of receptors at the cell membrane must be simultaneously and coherently activated to produce an effect on the biochemical functioning of the cell. Externally imposed electromagnetic fields are thus able to affect cell functioning because they are spatially coherent at various receptor sites in the membrane; consequently, they produce the required number of effector molecules to initiate a cytoplasmic response. In contrast, the uncorrelated thermal noise fields can produce no such synchronous effects. This biological coincidence detection scheme allows the cell to be exquisitely sensitive to very weak *spatially correlated* electromagnetic fields while discriminating against the much stronger but spatially random (on the relevant distance scale) thermal noise fields.

This discrimination mechanism cannot operate if the noise signal is itself spatially correlated. The spatially coherent but temporally random confusion fields are thus able to frustrate the cellular detection scheme and eliminate any electromagnetic field-induced bioeffects. The experimental result given above, nullifying the EMF-caused developmental abnormalities in chick embryos by the superposition of a confusion field, is completely consistent with this interpretation. Preliminary work by Farrell et al. [1993] on field-modified ornithine decarboxylase (ODC) activity in developing embryos, and the abolition of this effect with a confusion field further supports the conclusion. Mullins et al., [1993] have reported a similar elimination of sinusoidal EMF-enhanced ODC activity in murine fibroblast cell cultures.

Comparison of the results reported here with those of Mullins et al. [1993] is informative. They find that imposition of a weak sinusoidal 60 Hz EMF induces roughly a two-fold increase in ODC activity in L929 cells. Similar to the result reported here they find that a 30–100 Hz bandwidth confusion field essentially eliminates this enhancement. Note that in their case the Fourier components of the coherent signal (the 60 Hz sinusoid) lie completely within the noise spectrum. In contrast for the pulsed EMF signal, most of the energy lies outside of the spectral range of the noise. A straightforward interpretation of these results is that living cells respond to coherent signals as a broadband detector, not distinguishing between different frequencies over a rather wide range. This is supported by the work of Juutilainen and Saali [1986] and Juutilainen et al. [1987] who have shown that developmental abnormalities in chick embryos result from exposure to sinusoidal fields stronger than about 1 μT at frequencies ranging from 50–100 kHz.

SUMMARY

We have hypothesized that living cells discriminate against random thermally generated electromagnetic fields by a cellular coincidence detection mechanism that responds only to fields that are spatially coherent over the cell membrane. We have rationalized this hypothesis by ascribing it to biological cooperativity in which a significant number of membrane-integral receptor proteins must be simultaneously activated in order to cause signal transduction to the cytoplasm. Because all physical detection systems are ultimately limited by noise constraints, one test of this hypothesis involves the superposition of spatially coherent temporally random noise on a pulsed electromagnetic field that has been demonstrated to cause a bioeffect.

We have carried out such an experiment using developmental abnormalities in incubating chick embryos as the endpoint. Initially, it was established that weak pulsed EMFs (100 Hz rep rate) caused an increase in the embryo abnormality rate following exposure during the first 48 h of incubation. It was found that superimposing externally generated noise fields of roughly the same strength (although several orders of magnitude smaller than the endogenous thermal noise field) on the pulsed fields essentially eliminated the field-induced abnormalities. The results with the exogenous noise fields were statistically indistinguishable from those for the sham-exposed embryos.

This finding supports our proposal that it is their sensitivity only to *spatially coherent* EMFs that enables living cells to respond to weak exogenous fields while remaining unaffected by the relatively large (but spatially incoherent) endogenous noise fields that are always present. The idea that cells distinguish between exogenous and endogenous fields by recognizing the latter's spatial incoherence offers a viable explanation of the signal-to-noise dilemma. Far from being "magically" exempt from signal-to-noise considerations, cellular detection mechanisms are subject to the same laws of nature as all physical systems. The masking that is provided by a spatially coherent confusion field could prove to be a basis for protecting humans against possible adverse health risks associated with environmental electromagnetic fields.

ACKNOWLEDGMENTS

The authors thank Dr. Sam Greenhouse of the George Washington University Biostatistics Center for his help with the statistical analysis of the data. They also acknowledge the Walter Reed Army Institute of Research for support of this work under contract DAMD17-86-C-6260.

REFERENCES

Adair RK (1991): Constraints on biological effects of weak extremely-low-frequency electromagnetic fields. Phys Rev A 43:1039–1048.

Adey WR (1975a): Introduction: Effects of electromagnetic radiation on the nervous system. Ann NY Acad Sci 247:15–20.

Adey WR (1975b): Evidence for cooperative mechanisms in the susceptibility of cerebral tissue to environmental and intrinsic electric fields. In Schmitt FO, Schneider DM, Crothers DM (eds): "Functional Linkage in Biomolecular Systems." New York: Raven Press, pp 325–342.

Adey WR (1981): Tissue interaction with non-ionizing electromagnetic fields. Physiol Rev 61:435–514.

Adey WR (1988): Physiological signalling across cell membranes and cooperative influences of extremely low frequency electromagnetic fields. In Frohlich H (ed): "Biological Coherence and Response to External Stimuli." Heidelberg, Germany: Springer, pp 148–170.

Alberts B, Bray D, Lewis J, Raff M, Roberts K, Watson JD (1983): "Molecular Biology of the Cell." New York: Garland Publishing, Inc., p 752.

Berman E, Chacon L, House D, Koch BA, Koch WE, Leal J, Løvtrup S, Mantiply E, Martin AH, Martucci GI, Mild KH, Monahan JC, Sandström M, Shamsaifar K, Tell R, Trillo MA, Ubeda A, Wagner P (1990): The effects of a pulsed magnetic field on chick embryos. Bioelectromagnetics 11:169–187.

Blackman CF (1988): Influence of electromagnetic fields on the efflux of calcium ions from brain tissue in vitro: Three models consistent with the frequency response up to 510 Hz. Bioelectromagnetics 9:215–227.

Blackman CF (1989): Multiple power-density windows and their possible origin. Bioelectromagnetics 10:115–128.

Byus CV, Pieper SE, Adey WR (1987): The effects of low-energy 60-Hz environmental fields upon the growth-related enzyme ornithine decarboxylase. Carcinogenesis (Lond.) 8:1385–1389.

Darnell J, Lodish H, Baltimore D (1990): "Molecular Cell Biology," 2nd Ed. New York: W.H. Freeman and Co., p 719.

Farrell JM, Barber M, Doinov P, Krause D, Litovitz TA (1993): Effect of 60 Hz sinusoidal magnetic fields on ornithine decarboxylase activity in developing chick embryos. In Blank M (ed): "Electricity and Magnetism in Biology and Medicine." San Francisco, CA: San Francisco Press, Inc.

Hamburger V, Hamilton HL (1951): A series of normal stages in the development of the chick embryo. J Morphol 88:49–92.

Juutilainen J, Läära E, Saali K (1987): Relationship between field strength and abnormal developments in chick embryos exposed to 50 Hz magnetic fields. J Radiat Biol 52:787–793.

Juutilainen J, Saali K (1986): Development of chick embryos in 1 Hz to 1 Khz magnetic fields. Radiat Environ Biophys 25:135–140.

Lehmann E (1975): "Non-Parametric Statistics." San Francisco, CA: Holden-Day Publishers, pp 262–264.

Litovitz TA, Mullins JM, Krause D (1991): Effect of coherence time of the applied magnetic field on ornithine decarboxylase activity. Biochem Biophys Res Comm 178:862–865.

Mullins JM, Krause D, Litovitz TA (1993): Simultaneous application of a spatially coherent noise field blocks the response of cell cultures to a 60 Hz electromagnetic field. In Blank M (ed): "Electricity and Magnetism in Biology and Medicine" San Francisco, CA: San Francisco Press, Inc.

Neder J, Wasserman W, Kutner MH (1985): "Applied Linear Statistical Models," 2nd Ed. Homewood, IL: Irwin, pp 950–952.

Rubin CT, McLeod KJ, Lanyon LE (1989) Prevention of osteoporosis by pulsed electromagnetic fields. J Bone Joint Surg 71A:411–417.

Weaver JC, Astumian RD (1990): The response of living cells to very weak electric fields: The thermal noise limit. Science 247:459–462.

Bioelectromagnetics 19:498–500 (1998)

Brief Communication

A Simple Experiment to Study Electromagnetic Field Effects: Protection Induced by Short-term Exposures to 60 Hz Magnetic Fields

A.L. DiCarlo,[1] J.M. Farrell,[2] and T.A. Litovitz[1]*

[1]Vitreous State Laboratory, Catholic University of America, Washington, DC
[2]Harvard/MIT Division for Health Science and Technology, Cambridge, Massachusetts

Stress proteins are important in protection during cardiac ischemia/reperfusion (cessation and return of blood flow) and are reportedly induced by electromagnetic (EM) fields. This suggests a possible ischemia protection role for EM exposures. To test this, chick embryos (96 h) were exposed to 60 Hz magnetic fields prior to being placed into anoxia. Survival was 39.6% (control), and 68.7% (field-exposed). As a positive control, embryos were heated prior to anoxia (57.6% survival). We conclude that: 1) 60 Hz magnetic field exposures reduce anoxia-induced mortality in chick embryos, comparable to reductions observed following heat stress, and 2) this is a simple and rapid experiment to demonstrate the existence of weak EM field effects. Bioelectromagnetics 19:498–500, 1998. © 1998 Wiley-Liss, Inc.

Key words: chick embryos; anoxia; stress proteins; protective effect; magnetic field

Work in electromagnetics has long been plagued by problems with replication [Berman et al., 1990]. The current report details a replicable experiment which provides an easily observed biomarker for electromagnetic (EM) field effects. We describe a method to utilize EM field exposures to protect against simulated heart attack (i.e., anoxia) in a chick embryo model. Use of the chick embryo is ideal in that it is a readily available, inexpensive animal model requiring minimal care and handling. The experiment itself is straightforward, and the ease with which it can be performed minimizes error. Additionally, results are obvious (e.g., alive or dead) and not subject to investigator bias.

Nearly all organisms possess stress response mechanisms which help to protect them from harmful stimuli. One method is via induction of a family of protective compounds known collectively as stress proteins [Morimoto, 1993]. A common inducer of these proteins is sudden elevated temperatures (heat shock) [Kelley and Schlesinger, 1978; Lindquist, 1986]. In addition to heat shock, cardiac cells also respond to hypoxia and metabolic stress with increased synthesis of stress proteins (especially heat shock protein 70 [hsp70]), indicating a possible protective role for these proteins against ischemia/reperfusion. Recently, cross-protection (use of one nonlethal stress to protect against the lethal effects of another stress) was demonstrated by Mestril et al. [1994], who showed that cardiac cells which were heated to 42 °C for 30 min prior to onset of ischemia exhibited higher survival than non-heat-shocked cells. It has also been reported that stress protein levels following elevated temperatures correlate with myocardial protection [Hutter et al., 1994].

Contract Grant Sponsor: National Institute of Environmental Health Sciences (NIEHS), National Institutes of Health (NIH); Contract grant Number: 5 R01 ES0687-02.

Submitted as partial fulfillment of degree requirements for A.L. DiCarlo for Doctor of Philosophy, Department of Biology, University of Maryland, College Park, MD.

The described project's contents are solely the responsibility of the authors and do not necessarily represent the official views of the NIEHS, NIH.

*Correspondence to: Theodore A. Litovitz, PhD, Director, Vitreous State Laboratory, Catholic University of America, 620 Michigan Avenue, NE, Washington, DC 20064. E-mail: litovitz@cua.edu

Received 19 February 1998; Revision received 28 July 1998

Recent studies indicate that HL60 cells exposed to EM fields show activation of heat shock factor and binding to heat shock element, one of the first steps in activation of the heat shock response pathway [Lin et al., 1997], as well as increased levels of stress protein transcripts [Goodman et al., 1994]. This work suggests that EM field exposures induce responses similar to those caused by heat and other stressors. We hypothesized, therefore, that EM fields could confer protection against ischemia/reperfusion.

Fertilized White Leghorn eggs (Truslow Farms, Chestertown, MD) were incubated at 37.8 (±0.1) °C for 96 h to developmental stage 24 [Hamburger and Hamilton, 1992] in six VWR water-jacketed incubators. Eggs were randomly distributed in cartons among the incubators and periodically moved between incubators to ensure no bias. Control and exposed groups were randomly chosen from all cartons. Incubator temperatures were continuously measured using permanent thermocouples affixed to the center of each incubator, which were then wired into a temperature monitoring computer program. Incubators were modified to minimize stray magnetic field emissions, and measurements indicated that magnetic fields were less than 0.5 μT at all egg positions. Exposures were produced by passing current through Helmholtz coils wound and connected as described previously with slight modifications [Berman et al., 1990]. Two types of 20-min, 37.8 °C exposure conditions were examined: 1) by rewiring the incubator heaters we were able to maintain control or ''sham'' magnetic field strengths at <0.5 μT, and 2) 60 Hz magnetic field exposures at strengths of 4, 6, 8, and 10 μT (all data combined).

As a positive control in 10 of the experiments, additional embryos were subjected to 43 °C for 20 min. Hyperthermia (heat shock) was achieved by placing the intact eggs into a sand bath enclosed in a steel container which was placed into a 43 °C circulating water bath (direct immersion of the eggs in 43 °C water would have inadvertently caused anoxia in the embryos due to the blockage of gas exchange across the shell). A thermocouple was placed into one of the eggs at the site of the embryo and timing of exposure was begun when the temperature reached 43 °C. Measurements of magnetic fields in the water bath apparatus indicated that field strengths were below 0.5 μT. Magnetic field signals were generated using a function/arbitrary waveform generator (Hewlett-Packard; Palo Alto, CA, Model #33120A) and a 35 watt P.A. amplifier (Radio Shack; Fort Worth, TX). Magnetic fields were measured using a 60 Hz calibrated dosimeter (Integrity Design and Research Corp.; Buffalo, NY).

Following heat shock or EM field exposures, embryos were held at 37.8 °C for 1 h, during which time portions of the shells and inner shell membranes were removed to reveal the embryos. Embryos were windowed at room temperature and then immediately returned to the incubator. Approximately 30 s was required to window each embryo. Any unusual eggs (abnormal, bleeding, or at the incorrect developmental stage) were discarded to eliminate the possibility that they might die during anoxia due to causes unrelated to the insult. To achieve blinded conditions, embryos were coded by one individual and the code was entered into a computer program specifically designed to keep the observer blinded during evaluations.

Once coded, eggs containing the embryos (in open cartons) were placed into plastic, air-tight bags such that all treatment conditions (control, heat shocked, and field-exposed) were equally represented in each bag. Experiments consisted of at least 8–12 eggs per experimental condition. Bags contained between 12 and 18 embryos, with each experiment having two or three separate bags. Air was evacuated from the bags using gentle suction and bags were then filled with argon and sealed. A sensor (Model STX70, Industrial Scientific, Oakdale, PA) placed in the bags confirmed that oxygen levels remained below 1% during the experiment. Bags were then returned to the incubators where the temperature was maintained at 37.8 °C.

At 30-min intervals, embryos were evaluated by observing the heart beat. Mortality data (heart beating or stopped) was entered into the computer program, which then, without indicating specifically which eggs were control or exposed, provided the researcher with percent survival for both control and exposed embryos in each bag. When between 15 and 45% of control embryo hearts were still beating, bags were opened to allow for re-oxygenation. This targeted percent survival range in the control embryos was chosen because survival below 15% indicated that the timing of the anoxic insult was too long, and survival above 45% in control embryos suggested that the anoxia was not administered for long enough to observe differential protection between control and exposed embryos. Final observations were taken after 30 min recovery in ambient air (21% O_2) at 37.8 °C. Any bleeding embryos were not considered in final counts, since it would be impossible to determine if death was due to anoxia or bleeding injury.

Field exposure results represent 80 experiments. In 10 of these experiments, heat shock positive controls were also performed. Eight to twelve embryos were used per exposure condition, with a total of 24–36 embryos total per experiment (minus damaged and unusable embryos). A final total of 1,023 embryos were

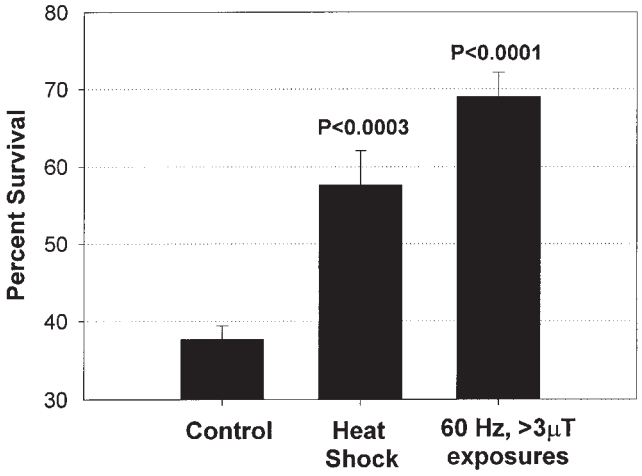

Fig. 1. Heat shock and EM field anoxia protection. Percent survival of chick embryos pre-exposed to the following 20-min treatments: control (sham field exposure), heating at 43 °C, or 60 Hz, 4, 6, 8, and 10 μT rms exposure (data combined), and then placed into anoxia is shown. Means for *n* experiments (n = 10 heat-shocked and 80 field-exposed) are given. The *P*-value indicates the significance level achieved by comparison of individual treatment data with control using the χ^2 test. Error bars represent SEM.

analyzed; 451 control, 66 heat-shocked, and 506 exposed to 60 Hz magnetic fields.

The data in Figure 1 indicate that embryos exposed to 60 Hz EM fields exhibited a higher percent survival (68.7%) than controls (39.6%). Treatment is significant at $P < 0.0001$ (χ^2 test). Heat-shocked embryos also showed improved survival following anoxia compared to controls (57.7%, $P < 0.0003$).

This laboratory has conducted more than 80 EM field exposure assays at 60 Hz (4, 6, 8, and 10 μT magnetic field strengths combined) utilizing more than 2,000 eggs (combined control and exposed) in the past year, and we have consistently observed the described protection. The assay in our hands was found to be simple, consistent, and effective in both procedure and the rapidity with which results could be obtained. In one day, 5–6 experiments (up to 150 embryos) could be evaluated, with 50 embryos per exposure condition. This yields, in one day's results, statistically significant data at $P < 0.05$. Additionally, this biomarker is well suited to studying the many possible permutations of EM field exposure effects, such as frequency dependence, field constancy, and time duration of exposure.

REFERENCES

Berman E, Chacon L, House D, Koch BA, Koch WE, Leal J, Lovtrup S, Mantiply E, Martin AH, Martucci GI, Mild KH, Monahan JC, Sandström M, Shamsaifar K, Tell R, Trillo MA, Ubeda A, Wagner P (1990): Development of chicken embryos in a pulsed magnetic field. Bioelectromagnetics 11:169–187.

Goodman R, Blank M, Lin H, Dai R, Khorkova O, Soo L, Weisbrot D, Henderson A (1994): Increased levels of HSP70 transcripts induced when cells are exposed to low frequency electromagnetic fields. Bioelectrochem Bioenerg 33:115–120.

Hamburger V, Hamilton HL (1992): A series of normal stages in the development of the chick embryo. 1951 (classical article; see comments). Dev Dyn 195:231–272.

Hutter MM, Sievers RE, Barbosa V, Wolfe CL (1994): Heat-shock protein induction in rat hearts. A direct correlation between the amount of heat-shock protein induced and the degree of myocardial protection. Circulation 89:355–360.

Kelley PM, Schlesinger MJ (1978): The effect of amino acid analogues and heat shock on gene expression in chicken embryo fibroblasts. Cell 15:1277–1286.

Lin H, Opler M, Head M, Blank M, Goodman R (1997): Electromagnetic field exposure induces rapid, transitory heat shock factor activation in human cells. J Cell Biochem 66:482–488.

Lindquist S (1986): The heat-shock response. Annu Rev Biochem 55:1151–1191.

Mestril R, Chi SH, Sayen MR, O'Reilly K, Dillmann WH (1994): Expression of inducible stress protein 70 in rat heart myogenic cells confers protection against simulated ischemia-induced injury. J Clin Invest 93:759–767.

Morimoto RI (1993): Cells in stress: Transcriptional activation of heat shock genes. Science 259:1409–1410.

Bioelectromagnetics 18:132–141 (1997)

Role of Modulation on the Effect of Microwaves on Ornithine Decarboxylase Activity in L929 Cells

L. Miguel Penafiel,[2] Theodore Litovitz,[2]* David Krause,[1] Abiy Desta,[1] and J. Michael Mullins[1]

[1]*Department of Biology, The Catholic University of America, Washington, DC*
[2]*Vitreous State Laboratory, The Catholic University of America, Washington, DC*

The effect of 835 MHz microwaves on the activity of ornithine decarboxylase (ODC) in L929 murine cells was investigated at an SAR of ~2.5 W/kg. The results depended upon the type of modulation employed. AM frequencies of 16 Hz and 60 Hz produced a transient increase in ODC activity that reached a peak at 8 h of exposure and returned to control levels after 24 h of exposure. In this case, ODC was increased by a maximum of 90% relative to control levels. A 40% increase in ODC activity was also observed after 8 h of exposure with a typical signal from a TDMA digital cellular telephone operating in the middle of its transmission frequency range (~840 MHz). This signal was burst modulated at 50 Hz, with approximately 30% duty cycle. By contrast, 8 h exposure with 835 MHz microwaves amplitude modulated with speech produced no significant change in ODC activity. Further investigations, with 8 h of exposure to AM microwaves, as a function of modulation frequency, revealed that the response is frequency dependent, decreasing sharply at 6 Hz and 600 Hz. Exposure with 835 MHz microwaves, frequency modulated with a 60 Hz sinusoid, yielded no significant enhancement in ODC activity for exposure times ranging between 2 and 24 h. Similarly, exposure with a typical signal from an AMPS analog cellular telephone, which uses a form of frequency modulation, produced no significant enhancement in ODC activity. Exposure with 835 MHz continuous wave microwaves produced no effects for exposure times between 2 and 24 h, except for a small but statistically significant enhancement in ODC activity after 6 h of exposure. Comparison of these results suggests that effects are much more robust when the modulation causes low-frequency periodic changes in the amplitude of the microwave carrier. *Bioelectromagnetics 18:132–141, 1997.*

Key words: cellular phones; EMFs

INTRODUCTION

Particular attention has been focused recently on the potential health effects of radio frequency (RF) and microwave fields, which are used extensively in telecommunications. The transmission of information via RF or microwave signals is accomplished by applying some form of modulation to a carrier wave, which changes some aspect of this wave as a function of the transmitted information. Basic modulation schemes modify the carrier wave's amplitude, frequency, or phase. However, more complex modulation schemes are often used to minimize transmission errors and increase bandwidth in telecommunications. For instance, in North America, digital cellular telephones transmit information in bursts, thereby introducing an amplitude modulation component onto the carrier. Clearly, a careful assessment of potential biological effects that might result from exposure to such fields must examine the role of modulation.

Because of the prevalence of cellular phone use, part of our investigation focuses on signals of the type used in cellular phone communications. Cellular phones may be broadly classified as analog or digital depending on the modulation scheme employed. Analog cellular phones generally use narrow band FM, which causes phase variations in the carrier with very little amplitude change. The analog standard most com-

Contract Grant sponsor: Department of the Army; Contract Grant number: DAMD 17-86-C-62601.

*Correspondence to: Dr. Theodore Litovitz, Vitreous State Laboratory, The Catholic University of America, Washington, DC 20064.

Received for review 24 November 1995; Final revision received 10 June 1996.

monly used in the United States is the advanced mobile phone system (AMPS). We refer to fields generated using this standard as analog cellular fields. Digital cellular phones operate under various standards. GSM (global system for mobile communications), the pan-European digital system, has gained wide acceptance in Europe. DAMPS (digital AMPS) is still the most commonly used standard in the United States. DAMPS uses a type of modulation referred to as ''time division multiple access'' (TDMA), which quadruples the channel bandwidth by splitting the spectrum of each assigned analog channel [Boucher, 1992]. Under this scheme, cellular phones transmit encoded, digitized information using some form of phase or frequency modulation. Consequently, minimal or no fluctuations in amplitude occur when using this basic modulation scheme. However, transmission is generally implemented in burst mode, which introduces a periodic variation in the amplitude of the carrier. By one commonly used protocol, code bursts, approximately 7 ms in duration, are transmitted at a rate of 50 Hz. We refer to the fields generated by cellular phones operating in this fashion as digital cellular fields.

Previous investigations of biological effects from exposure to RF and microwave fields include a large number of both animal and in vitro studies. Included in the latter category are a number of experiments suggesting that, at SARs <5 W/kg, cellular effects occur primarily from exposure to microwaves that are amplitude modulated or pulse modulated at ELF frequencies. Reported effects include changes in calcium ion efflux [Bawin et al., 1975; Blackman et al., 1979, 1985; Dutta et al., 1984, 1989], changes in enzymatic activity [Byus et al., 1984, 1988; Litovitz et al., 1993], and induction of cellular transformations [Balcer-Kubiczek and Harrison, 1985, 1989, 1991; Czerska et al., 1992]. Some effects in in vitro preparations have also been observed with CW microwaves [Cleary et al., 1990; Krause et al., 1991; Saffer and Profenno, 1992; Garaj-Vrhovac et al., 1992]. However, all the latter studies used SARs greater than or equal to 10 W/kg. The evidence seems to indicate that modulation plays an important role in eliciting a biological response, particularly when exposing with weak (<5 W/kg) microwaves.

In the work reported herein, we investigated the biological response of L929 murine fibroblasts to ELF-modulated and CW 835 MHz microwave fields. The 835 MHz frequency was chosen because it is within the range currently used in many wireless personal communication applications in North America and is therefore of practical relevance. Various modulation methods were examined, including sinusoidal AM and FM, speech AM, analog cellular, and digital cellular. The specific activity of ornithine decarboxylase (ODC), which performs a rate-limiting step in the synthesis of polyamines [Hayashi and Murakami, 1995], was selected as the biological marker for this work. ODC activity has been shown to be a reliable indicator of EMF-induced cellular response [Litovitz et al., 1991]. Additionally, ODC is of interest because recent work has shown that overexpression of the ODC gene in cultured cells facilitates, and in some cases causes, cell transformation [Hibshoosh et al., 1990; Auvinen et al., 1992; Moshier et al., 1993; Ḧoltẗa et al., 1994]. Furthermore, overexpression of ODC in transgenic mice enhances the tumor-promoting effects of PMA [Halmekyẗo et al., 1992]. Given these facts, it is conceivable that the enhancement of ODC activity as the result of EMF exposure is of relevance to questions of potential health risk posed by ambient EM fields.

MATERIALS AND METHODS

Exposure System

All exposures were carried out using a Crawford cell that was housed in a 37 °C, water-jacketed incubator. The Crawford cell, designed for operation between DC and 1,000 MHz (model CC110-SPEC; Instruments for Industry, Farmingdale, NY), was mounted vertically on a rotary table. This arrangement allowed easy access to both sample chambers, located at either side of the center conductor, through doors installed on opposite sides of the Crawford cell. A Hewlett Packard signal generator, model 8657B with RF plug-in 83522A, was used as the microwave signal source.

Amplitude and frequency modulation were accomplished by using the built-in AM and FM inputs of the signal generator. A function generator (TENMA model 72-380; MCM Electronics, Centerville, OH) was used as the signal source for sinusoidal modulation. Modulation with speech was implemented by using the signal available at the speaker output of a radio receiver tuned to a station broadcasting speech. Square wave modulation was implemented with a Hewlett Packard 8403A modulator to control a Hewlett Packard 8730B PIN modulator. Exposure with the cellular telephone signals was accomplished by using a hands-free adapter to couple the output from the telephone antenna to a coaxial line. The telephone was powered by a DC power supply (Hewlett Packard 6267B) to allow long-term operation. The modulated microwave signals (from the signal generator or the cellular telephones) were amplified to the required power level by using a 10 W solid-state microwave amplifier (model 10W1000; Amplifier Research, Souderton, PA). A double stub tuner was used to match the impedance of the loaded Crawford cell.

All amplitude modulation experiments were car-

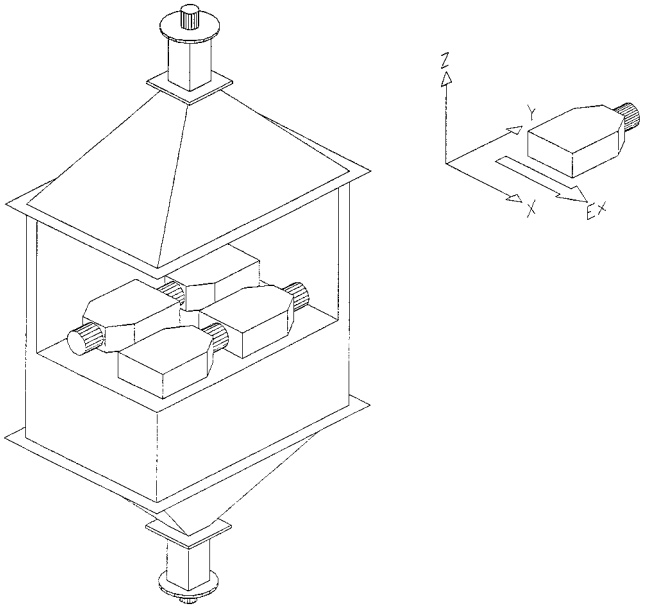

Fig. 1. Detail of the exposure chamber showing placement of the sample flasks. For ease of visualization, a section of the Crawford cell has been cut out and the center conductor is not shown. The samples are placed on nonconducting shelves located at a height of approximately 7 cm from the junction between the center rectangular section of the exposure chamber and the lower tapered end. In this exposure arrangement, the electric field is perpendicular to the direction of wave propagation, which is parallel to the long axis of the exposure chamber. The orientation of the electric field is shown in the inset in relation to the position of a sample flask.

ried out with a modulation index of 0.23, calculated by using the relation $P_t = P_c\ (1 + m^2/2)$, where P_t is the microwave power with modulation, P_c is the microwave power without modulation, and m is the modulation index. When using speech as the modulating signal, P_t was set to the value needed for m = 0.23, on average. All frequency modulation experiments were carried out with the frequency deviation set to approximately ±60 kHz (3 mV signal at the FM input). The square wave modulation experiments were conducted at 50% duty cycle (i.e., the carrier amplitude was zero for 50% of the time during each cycle).

Experiments with cellular telephone signals were conducted using a Motorola Micro TAC Lite analog cellular telephone and a Motorola Digital Cellular Personal Communicator. The test signal was generated by placing the phone in test mode, selecting a transmission channel in the middle of the available range (approximately 840 MHz), selecting the transmission mode (AMPS for analog or TDMA for digital), and enabling continuous transmission of a pseudorandom test sequence. Examination of the output signal from the digital phone with a diode detector and oscilloscope revealed that transmission was executed in bursts lasting approximately 7 ms with a uniform repetition rate of 50 Hz. By contrast, the output signal from the analog phone was found to be constant (i.e., no amplitude modulation).

For each exposure, four 25 cm^2 flasks of L929 cells were used. The flasks, each containing 5 ml of culture medium, were placed as pairs, end to end, on either side of the center conductor (Fig. 1). This configuration ensured overall symmetry, if not complete uniformity, of the electric field distribution within the samples. The SAR distribution for this exposure arrangement has been previously reported [Litovitz et al., 1993]. To determine this distribution, measurements were made on two flasks located at one side of the center conductor. Because of symmetry, the SAR distribution within the other two flasks was assumed to be similar. The experimental SAR is specified as a simple average of the set of measurements within the two flasks, which were taken on a grid of 48 points within each flask. All experiments reported here were conducted with an input power of 0.96 W, which yielded an average SAR of 2.5 W/kg. The SAR distribution corresponding to this average SAR is shown in Figure 2. This SAR produced no measurable temperature increase within the samples.

The average electric field within the sample can be calculated from the average SAR by using the equation $SAR = (\sigma/\rho)|E|^2$ [NCRP report No. 67, 1981],

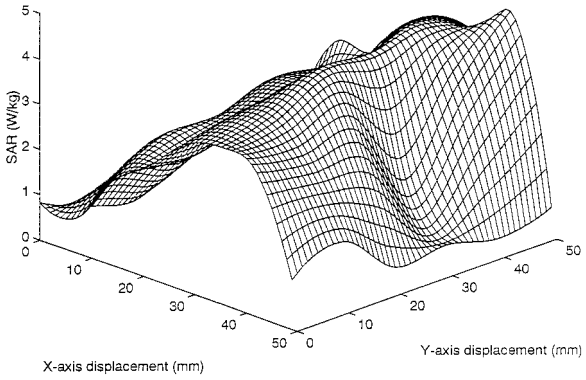

Fig. 2. SAR distribution measured inside the left front flask (see Fig. 1) over the 50 × 50 mm cell growth region located at the bottom of the flask. X and Y axis displacements are measured relative to the left front corner of the square region at the base of the flask. The region of maximal SAR is skewed towards the right back corner of the flask. The SAR decreases by as much as 25% of maximum across the width of the flask and by as much as 75% of maximum across the length of the flask. A somewhat similar distribution was measured inside the left rear flask. In this case, the region of maximal SAR is skewed towards the front right corner of the flask. In the rear flask, the SAR decreases by as much as 25% across both the width and the length of the flask. In both flasks, the regions of maximal SAR are located towards the junction between flasks.

where σ and ρ are, respectively, the conductivity and the density of the aqueous sample. For an SAR of 2.5 W/kg with $\sigma = 1.5$ S/m and $\rho = 1$ g/cm^3, the E-field is on the order of 0.6 V/cm. The field inside the Crawford cell can be calculated by using the relation $E = (PZ_o/d^2)^{1/2}$, where P is the input power, $Z_o = 50\Omega$ is the characteristic impedance of the Crawford cell, and d = 7 cm is the distance between the center conductor and the outer plate. For P = 0.96 W, the electric field within the Crawford cell is on the order of 1 V/cm [correction of our previous calculation of 0.7 V/cm, Litovitz et al., 1993]. The computations of the electric field, both inside the Crawford cell and within the aqueous samples, yield values of the same order of magnitude. This suggests that the SAR measurements are a reasonably good indicator of the electric field in the aqueous interface at the base of the flask, where the tangential components of the electric field must be continuous.

Cell Culture Preparation

Actively growing cultures of the murine L929 fibroblast cell line were maintained in Eagle's minimum essential medium, supplemented as previously reported [Litovitz et al., 1991]. Cell cultures to be used for exposures were initiated approximately 20 h prior to an experiment at a density (3×10^6 cells in 5 ml of culture medium per 25 cm^2 flask) to produce midlogarithmic phase growth by the time of use. Prior to exposure, cells were kept at 37 °C in a 95% air/5% CO_2 atmosphere. Microwave exposures were conducted without CO_2 flow; flasks were sealed for the duration of exposure. Experiments were conducted over approximately a 3 year period. To ensure uniformity of the cell cultures during this time, we maintained multiple ampules of our original L929 cell stocks in liquid nitrogen. New cultures were started from these frozen stocks approximately every 6 months.

Field Exposure Protocol

For each experimental run, four flasks of cells were placed into the Crawford cell for microwave exposure. An incubator shelf, cut to form a platform around the Crawford cell, provided for positioning of four control flasks within the same incubator chamber and at the same height as the flasks within the Crawford cell. Exposure times ranged between 2 and 24 h. Immediately after exposure, the cells in each flask were washed twice with 3 ml of ice-cold phosphate-buffered saline (PBS) and were then collected by gentle scraping in an additional 3 ml of PBS. To provide sufficient protein for the ODC assay, cells were pooled to provide one exposed and one control sample from each experimental run. Cells were pelleted for 5 min at 200*g*, and the resultant cell pellet was resuspended in 1 ml PBS and centrifuged again for 5 min at 200*g*. After removal of the supernatant, the cell pellets were dried by briefly placing the inverted centrifuge tubes onto absorbent paper. These pellets were stored at −75 °C until assay (typically for 3–4 days).

ODC Assay

ODC activity was determined through minor modifications of the method of Seely and Pegg [1983], as previously reported [Litovitz et al., 1991]. Units of ODC activity were expressed as pmol $^{14}CO_2$ generated/30 min/mg protein at 37 °C. Protein analysis was performed with the Bradford method by using a BioRad kit (BioRad Laboratories, Melville, NY). Each cell pellet was lysed in 140 µl of lysis buffer and centrifuged for 5 min at 13,000 rpm. One hundred microliters of the supernatant from each sample was added separately to 150 µl aliquots of the ^{14}C-labeled reaction mixture. $^{14}CO_2$ generated by ODC activity from each sample was absorbed with 100 µl of 1.0 N NaOH. The reaction was allowed to proceed for 1 h with the samples placed in a shaker water bath at 37 °C. At the end of this period, 400 µl of 20% trichloroacetic acid (TCA) was added to each sample to terminate the enzymatic reactions. To measure the ^{14}C activity, each NaOH sample was transferred to a scintillation vial containing 7 µl of acetic acid and 10 ml of fluor. After 2 h, samples were counted in a scintillation counter. Background activity was determined by the use of samples in which ODC activity was eliminated by acid denaturation with TCA.

RESULTS

ODC activity is an effective marker for EM field-induced effects, provided that variations in ODC activity displayed by cell cultures established at different times are accounted for. To allow comparisons of results obtained on different days, we express our data as an ''ODC activity ratio,'' obtained by dividing the mean activity of EMF-exposed samples from a given run by that of matched control samples. The validity of this approach was demonstrated in our previously published work [Litovitz et al., 1993, 1994]. Because some scientists are uncomfortable with the use of such ratios, the results of this work are also expressed in terms of the mean and standard deviation of the measured ODC activity for each exposure condition (see Tables 1–8). The standard deviation of the mean ODC activity data reflects the day-to-day variations in this parameter. Because these variations were often large, the analysis to determine whether the mean difference between exposed and control samples was statistically significant was performed on paired observations by using a standard two-tailed t test. The two-tailed test

was selected because there is no a priori knowledge of the direction of the differences between exposed and control samples.

Because of the large number of experiments performed and exposure conditions examined, the tabulated data summarize separately the results for each exposure condition. Included in the tables are the mean ODC activities of the control and exposed samples, the *P* value of the two-tailed t test, and the mean activity ratio. It should be stressed that the ODC activity ratio is not the ratio of mean E over mean C but rather the ratio of the mean activity of EMF-exposed samples over that of matched control samples.

Exposure With CW Microwaves

We have previously reported that 8 h of exposure with CW microwaves (835 MHz, 8 h, 2.5 W/kg) yielded no measurable changes in ODC activity [Litovitz et al., 1993]. Because AM-induced biological effects were shown to be transient, we decided that a more complete time course of CW exposure should be examined. To this end, experiments were carried out with 835 MHz CW microwaves for exposure times in the range of 2 to 24 h. Table 1 shows the results of these experiments. Exposures of 2, 4, 8, 12, 16, and 24 h yielded no measurable effects and confirmed previous results. However, a statistically significant effect was obtained after 6 h of exposure, which yielded an ODC activity ratio of 1.3.

Exposure With AM Microwave Fields

The ODC response of L929 cells exposed to AM, 835 MHz microwaves was examined as a function of exposure time (2–24 h) at two frequencies, 16 Hz and 60 Hz, and as a function of frequency in the range of 6–600 Hz for the exposure time that produced the most robust response in the time course experiments (8 h). In all cases, the modulation amplitude was adjusted to give a modulation index of 23%.

Dependence on time. Exposure with either 16 Hz or 60 Hz AM microwaves produced a transient enhancement in ODC activity that peaked after 8 h and returned to control levels by 24 h of continuous exposure. Table 2 shows the results of exposure with 16 Hz AM microwaves. Continuous 6 and 8 h exposures of cells produced enhancements in ODC activity that were statistically significant relative to control levels. The other exposure times tested did not induce statistically significant changes in ODC activity. Table 3 shows the results of exposure with 60 Hz AM microwaves. Statistically significant effects were observed after 6, 8, 12, and 16 hours of continuous exposure, but no statistically significant effects were seen after 2, 4, and 24 h of exposure. The peak field-induced ODC activity ratios were 1.5 for 16 Hz AM and 1.9 for 60 Hz AM.

Dependence on frequency. Having determined that an exposure time of 8 h produced a peak in the ODC response at two AM frequencies, we examined the variation of the response for this exposure time as a function of frequency in the range of 6–600 Hz. Table 4 shows the results of these experiments. Statistically significant enhancements of ODC activity were obtained at frequencies in the range between 16 Hz and 65 Hz, whereas no significant effects were obtained at either 6 Hz or 600 Hz. The field-induced response peaked in the 60 Hz range, at which the ODC activity ratio approximately doubled. Because no experimental points were obtained between 65 Hz and 600 Hz, these results provide only a general idea of the variation of the frequency response.

Dependence on coherence. We previously demonstrated that the enhancement of ODC activity by AM microwaves requires a minimum coherence time of the modulating signal [Litovitz et al., 1993]. Optimal enhancement was obtained when the coherence time was 10 s or greater, whereas no enhancement resulted when the coherence time was 1 s or less. A case of some practical interest is that of RF or microwave signals amplitude modulated with speech. Because the coherence time of speech is less than 1 s, we predicted, based on our earlier work, that no effect on ODC activity would be elicited by exposure to such signals. The experimental data confirmed this prediction (see Table 8). Eight hour exposures with microwaves amplitude modulated with speech yielded no statistically significant effects as measured using a paired t test. Whereas the coherence time is an accurate predictor of the biological response in some cases, further research, to be reported elsewhere, has led us to conclude that the ability of an electromagnetic field to induce biological effects is best characterized in terms of a ''constancy'' interval, defined as the time interval over which the field parameters (e.g., amplitude, frequency) remain constant.

Exposure With FM Microwave Fields

The effects of frequency modulation with a 60 Hz sinusoid were examined as a function of exposure time in the range of 2–24 h. The modulation frequency, ω_m, and exposure times were selected to allow direct comparison to similar experiments using amplitude modulation. The maximum deviation, $\Delta\omega$, of the FM signal was set to 60 kHz to correspond approximately to the maximum deviation of commercial FM (75 kHz). The corresponding modulation index, $\beta = \Delta\omega/\omega_m$, was on the order of 1,000, which defines this signal as

wideband FM. Table 5 summarizes the results of exposure with FM microwaves. No statistically significant changes in ODC activity were induced by exposure of cultures to this signal.

Exposure With Cellular Phone-Type Signals

The results of the AM and FM experiments described above suggest that biological effects can be induced when the modulation causes periodic changes in the amplitude of the carrier, as is the case in sinusoidal AM. FM, which causes changes in phase but minimal changes in amplitude, appears to produce no measurable effect. A situation of practical interest is that of cellular phone transmissions. If amplitude modulation of the carrier is a significant factor in determining a biological response, then the extent to which cellular phones can induce a response would depend on whether the modulation schemes used for transmission impart a periodic ELF modulation component onto the carrier. Digital phones, which operate in burst mode, have periodic fluctuations of the carrier amplitude in the ELF range. Analog phones, which do not operate in burst mode, have relatively constant carrier amplitude (assuming no changes in reception between the cellular phone and the nearest cell). A series of exposures was conducted to determine whether either of these cellular phone signals produce enhancement of ODC activity in exposed cells.

Exposures were carried out with both the analog and the digital cellular fields and also with an 835 MHz carrier amplitude modulated with a 50 Hz square wave. This latter condition was intended to simulate the low-frequency burst modulation of the digital cellular field. Exposures with the analog cellular field produced no statistically significant enhancement in ODC activity for exposure times between 4 and 10 h (Table 6). Exposures with the digital cellular field produced statistically significant enhancements in ODC activity for 6, 8, and 10 h of exposure. The other two exposure times tested, 4 and 16 h, produced no statistically significant enhancement in ODC activity (Table 7). The square wave modulated signal was tested only after 8 h of exposure, yielding results similar to those for the corresponding condition with the digital cellular phone signal.

Table 8 and Fig. 3 summarize the results of 8 h exposures with the various signals tested. We note from this table that, in all cases tested with this exposure time, exposures with modulated microwaves produced statistically significant enhancements in ODC activity only when the modulation introduced low-frequency periodic changes in the amplitude of the carrier.

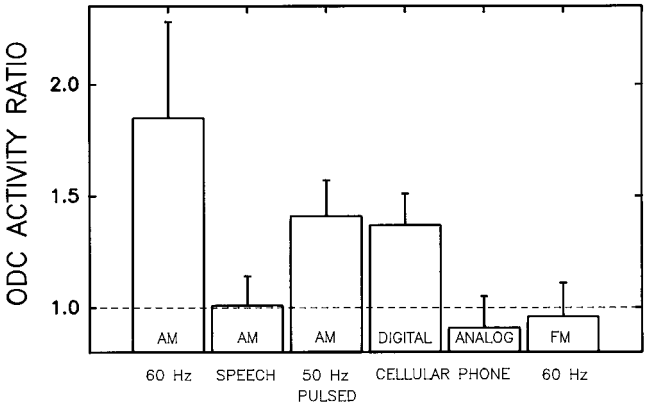

Fig. 3. ODC activity ratios for L929 murine cells exposed for 8 h with 835 MHz microwaves modulated by various methods.

DISCUSSION

The ODC activity of L929 fibroblasts was transiently enhanced by exposure to some, but not all, of the modulated 835 MHz microwave fields we examined. Exposure to an unmodulated, CW field also produced a response. These results are consistent with other reports that demonstrate enhanced ODC activity after EMF exposure. EMF-induced changes in ODC activity have been documented for cultured cells exposed to 60 Hz electric or magnetic fields [Byus et al., 1987; Litovitz et al., 1991, 1994; Mullins et al., 1993], for chicken embryos exposed to 60 Hz magnetic fields [Farrel et al., 1993], and for cultured cells exposed to amplitude-modulated microwave fields [Byus et al., 1988; Litovitz et al., 1993]. Thus, ODC activity appears to provide a consistent and reliable measure of cellular response to both ELF and RF EM fields. As such, it represents one of the few replicated examples of a bioeffect being induced by a weak electromagnetic field.

Microwave-Induced ODC Response: The Role of Modulation

Whether a given microwave field induces an ODC response seems to be dependent upon the modulation scheme employed. Enhancements in ODC activity were observed for L929 cells exposed to 835 MHz fields that were amplitude modulated with sinusoidal 16 and 60 Hz signals or with a 50 Hz square wave signal. Use of digital cellular signals burst modulated at 50 Hz, which produces a pattern of amplitude modulation very similar to that of the 50 Hz square wave, also induced increases in ODC activity.

In contrast to these results, neither the 60 Hz sinusoidal frequency-modulated 835 MHz carrier nor the frequency-modulated microwave field produced by analog cellular telephones induced an ODC response in L929 cells. These frequency-modulation schemes

TABLE 1. Results of Exposures With 835 MHz Continuous Wave Microwaves. The Mean E and Mean C Values Are the Average ODC Activities and Corresponding Standard Deviations, Expressed in Terms of pmol $^{14}CO_2$ Generated/30 Min/mg Protein, of the N Exposed (E) and N Control (C) Samples of Each Exposure Condition. The P Value Is the Probability That the Observed Differences Between Control and Exposed Samples in Each Set of N Paired Observations Is Due to Chance. The ODC Activity Ratio Is the Mean Value of the Ratios of the ODC Activity in Exposed Samples to That of Corresponding Control Samples, Computed from N Paired Observations of Each Exposure Condition. The ODC Activity Ratio is Not the Ratio of Mean E Over Mean C

Exp time (hrs)	N	Mean C	Mean E	*P*	ODC activity ratio
2	5	13.8 ± 6.3	12.9 ± 6.4	>0.52	0.9 ± 0.2
4	6	9.2 ± 6.1	8.7 ± 5.2	>0.69	1.0 ± 0.2
6	11	13.3 ± 12.2	16.5 ± 13.7	<0.004	1.3 ± 0.2
8	16	16.8 ± 13.8	15.9 ± 15.2	>0.41	0.9 ± 0.2
12	8	8.9 ± 1.7	8.3 ± 2.2	>0.34	0.9 ± 0.2
16	10	5.3 ± 4.1	4.8 ± 3.3	>0.32	1.0 ± 0.3
24	9	5.4 ± 2.3	5.0 ± 2.2	>0.32	0.9 ± 0.2

TABLE 2. Results of Exposures With 835 MHz Microwaves Amplitude Modulated (23%) With 16 Hz Sinusoids. Column Headings Are as Defined in Table 1

Exp time (hrs)	N	Mean C	Mean E	*P*	ODC activity ratio
2	7	12.1 ± 4.1	11.5 ± 4.2	>0.77	1.0 ± 0.3
4	7	12.0 ± 7.9	13.2 ± 10.0	>0.38	1.1 ± 0.3
6	13	14.2 ± 18.9	15.8 ± 20.3	<0.045	1.2 ± 0.3
8	11	9.9 ± 8.5	13.6 ± 11.8	<0.012	1.5 ± 0.3
12	6	12.8 ± 7.4	10.5 ± 6.1	>0.17	0.8 ± 0.2
16	7	6.7 ± 3.7	7.2 ± 4.0	>0.49	1.1 ± 0.3
24	9	10.3 ± 11.2	10.3 ± 9.2	>0.97	1.1 ± 0.1

TABLE 3. Results of Exposure With 835 MHz Microwaves Amplitude Modulated (23%) With 60 Hz Sinusoids. Column Headings Are as Defined in Table 1

Exp time (hrs)	N	Mean C	Mean E	*P*	ODC activity ratio
2	8	8.4 ± 3.4	9.8 ± 4.6	>0.15	1.2 ± 0.3
4	9	16.3 ± 12.8	16.1 ± 10.9	>0.91	1.1 ± 0.5
6	13	7.2 ± 4.0	11.6 ± 5.3	<0.0001	1.7 ± 0.4
8	22	24.0 ± 32.7	40.0 ± 47.2	<0.0001	1.9 ± 0.4
12	9	7.4 ± 3.4	11.1 ± 4.9	<0.0017	1.5 ± 0.3
16	9	7.6 ± 2.0	9.5 ± 2.6	<0.0058	1.3 ± 0.2
24	9	7.4 ± 2.4	6.7 ± 2.3	>0.13	0.9 ± 0.2

TABLE 4. Results of Exposure With 835 MHz Microwaves Amplitude Modulated (23%) With 6-600 Hz Sinusoids. Column Headings Are as Defined in Table 1

Freq (Hz)	N	Mean C	Mean E	*P*	ODC activity ratio
6	7	7.1 ± 5.0	6.6 ± 3.1	>0.61	1.1 ± 0.2
16	11	9.9 ± 8.5	13.6 ± 11.8	<0.012	1.5 ± 0.3
55	6	10.4 ± 4.8	18.5 ± 6.7	<0.009	1.9 ± 0.5
60	22	24.0 ± 32.7	40.0 ± 47.2	<0.0001	1.9 ± 0.4
65	6	10.0 ± 1.9	20.5 ± 4.7	<0.0011	2.1 ± 0.4
600	7	7.8 ± 5.3	9.4 ± 8.7	>0.37	1.3 ± 0.5

TABLE 5. Results of Exposure With 835 MHz Microwaves Frequency Modulated (60 kHz Deviation) With 60 Hz Sinusoids. Column Headings Are as Defined in Table 1

Exp time (hrs)	N	Mean C	Mean E	*P*	ODC activity ratio
2	9	35.9 ± 14.2	36.8 ± 14.5	>0.72	1.0 ± 0.1
4	6	17.7 ± 9.8	17.5 ± 7.7	>0.84	1.0 ± 0.1
6	8	22.0 ± 11.5	20.7 ± 11.5	>0.28	0.9 ± 0.1
8	7	18.9 ± 7.2	18.4 ± 7.7	>0.69	1.0 ± 0.2
12	6	13.0 ± 4.3	12.5 ± 2.9	>0.51	1.0 ± 0.1
16	7	12.4 ± 5.8	10.7 ± 5.6	>0.29	0.9 ± 0.2

TABLE 6. Results of Exposures With an AMPS Analog Cellular Phone Signal. Column Headings Are as Defined in Table 1

Exp time (hrs)	N	Mean C	Mean E	*P*	ODC activity ratio
4	6	28.9 ± 8.2	28.6 ± 8.6	>0.86	1.0 ± 0.1
6	6	33.4 ± 7.3	34.2 ± 11.7	>0.74	1.0 ± 0.1
8	6	17.5 ± 6.9	15.8 ± 6.7	>0.06	0.9 ± 0.1
10	6	33.9 ± 23.1	27.7 ± 16.1	>0.11	0.9 ± 0.2

TABLE 7. Results of Exposure With a DAMPS Digital Cellular Phone Signal. Column Headings Are as Defined in Table 1

Exp time (hrs)	N	Mean C	Mean E	*P*	ODC activity ratio
4	11	36.3 ± 20.1	40.0 ± 19.4	>0.07	1.2 ± 0.2
6	12	24.6 ± 12.5	29.1 ± 13.3	<0.0085	1.2 ± 0.2
8	9	26.6 ± 11.3	35.6 ± 13.4	<0.0002	1.4 ± 0.2
10	8	27.0 ± 8.8	31.4 ± 10.1	<0.0008	1.2 ± 0.1
16	3	8.9 ± 7.3	9.0 ± 5.9	>0.97	1.1 ± 0.1

TABLE 8. Results of 8 Hour Exposures to 835 MHz Microwaves Modulated by Various Methods. Column Headings Are as Defined in Table 1

Modulation type	N	Mean C	Mean E	*P*	ODC activity ratio
FM 60 Hz	7	18.9 ± 7.2	18.4 ± 7.7	>0.69	1.0 ± 0.2
AM speech	7	14.6 ± 11.7	14.1 ± 9.3	>0.69	1.0 ± 0.1
AM 60 Hz	22	24.0 ± 32.7	40.0 ± 47.2	<0.0001	1.9 ± 0.4
Sq wave 50 Hz	8	25.9 ± 6.6	36.4 ± 9.5	<0.0004	1.4 ± 0.2
Digital cellular	9	26.6 ± 11.3	35.6 ± 13.4	<0.0002	1.4 ± 0.2
Analog cellular	6	17.5 ± 6.9	15.8 ± 6.7	>0.06	0.9 ± 0.1

produce no measurable changes in carrier amplitude. The results suggest that, to induce a cellular response through microwave exposure, the microwave field must be modulated by a method that produces periodic alterations in the amplitude of the carrier wave. For example, the fact that the square wave and digital phone signals induced similar responses suggests that the cells responded to the 50 Hz pulsing of the carrier amplitude common to both signals. Thus, it appears that the cells did not respond to the very-high-frequency digitized information transmitted within the envelope of each pulse of the cellular signal.

The data obtained by using modulated microwaves are all consistent with the concept that the ELF amplitude modulation is critical in causing a biological effect. However, the results of our CW experiments

present an exception. Exposure of L929 cells to the 835 MHz CW field produced a statistically significant enhancement in ODC activity after 6 h of exposure. However, the time course of this response seemed unusual in that the increase in ODC activity was sharply demarcated in time, with no indication of rising or falling activity at the 4 or 8 h exposure time points. Nonetheless, we believe this effect to be real, having obtained the same result in two separate sets of experiments that were conducted more than 3 years apart, each set having independently yielded a statistically significant enhancement. How this CW effect relates to the ODC enhancements observed in cells exposed to AM fields is not clear. The obvious distinctions are that the enhancements induced by AM fields peaked 2 h later than those caused by the CW field and that the most robust response, that produced by the 60 Hz AM field, was significantly larger than the response produced by the CW field.

In each instance for which a time course was measured, the enhancement in ODC activity induced by AM microwave exposure was transient. ODC activity peaked after 8 h of exposure and then returned to control values despite continued exposure. Byus et al. [1988] also showed the transient enhancement of ODC activity in three different cultured cell lines exposed to AM microwaves. Approximately 15–60% increases in ODC activity were observed after 1 h exposures to 450 MHz microwaves sinusoidally amplitude modulated at 16 Hz. Under the exposure conditions used by Byus et al., 60 Hz amplitude modulation failed to elicit changes in ODC activity. However, direct comparisons to our results are not possible, because their carrier frequency, cell lines, exposure time, and modulation index differed from ours. For example, our data indicate that it is not until at least 6 h after onset of exposure to the 60 Hz AM microwave field that a clearly discernible effect on ODC activity is observed. The longest time that Byus et al. observed ODC activity was only 4 h after onset of exposure. It is possible that, had they waited longer, they would have observed an effect similar to that observed by us when using a 60 Hz AM exposure. Regardless, the observations of Byus et al. underscore the fact that exposure to a sinusoidal, amplitude-modulated microwave field can enhance ODC activity.

Microwave-Induced ODC Responses Resemble Those Induced by ELF Fields

The basic response to 60 Hz AM microwaves (i.e., a transient, approximately twofold increase in ODC activity) is similar to that observed after exposure of cells to a 60 Hz ELF magnetic field. The major distinction is that the timing of the two responses is different. The ELF field-induced ODC response peaks at 4 h of exposure, with a return to control values by 8 h of exposure. The 60 Hz AM microwave response peaked at 8 h and returned to control levels after approximately 24 h. Our results, considered with those of others, suggest that the responses induced by ELF and AM microwave fields are fundamentally similar and that it is the ELF modulation frequency of the microwave field that plays a critical role in determining the characteristics of the response.

For example, the ODC responses to ELF and AM microwave fields display similar requirements for temporal coherence of the stimulating field's ELF frequency. Cells exposed to an ELF magnetic field for which the frequency was switched between 55 and 65 Hz at regular intervals yielded a twofold enhancement in ODC activity only when each frequency was maintained over intervals $\geq$ 10 s throughout exposure [Litovitz et al., 1991]. When the frequency was switched at intervals $\leq$ 1 s, ODC activities remained at control levels. This temporal requirement for frequency coherence was also demonstrated by the fact that L929 cells showed no enhancement of ODC activity after exposure to ELF random noise fields of amplitude comparable to that of the 60 Hz stimulating field [Litovitz et al., 1994]. A similar temporal coherence requirement determines the response of L929 cells exposed to AM microwaves [Litovitz et al. 1993]. If the modulation frequency is switched between 55 and 65 Hz at regular intervals throughout the 8 h exposure period, the ODC response is determined by the duration of the constant frequency interval. As with the ELF studies, switching at an interval $\geq$ 10 s produced an approximate doubling in ODC activity, but intervals $\leq$ 1 s produced no ODC response. This result is reinforced by the data presented herein, which demonstrate that amplitude modulation using speech (which has a coherence time of $<$1 s) produced no enhancements in ODC activity. However, in this case, the decrease in the response may also be attributed in part to the frequency spectral distribution of speech. Our data show that the ODC response to AM microwaves decreases as the modulation frequency increases (Table 3). Speech is generated mostly in the range between 50 Hz and 10 kHz, but the highest concentration of sounds is in the range 100–600 Hz [Denes and Pinson, 1963]. Consequently, regardless of other effects, a decreased response relative to 60 Hz AM would be expected.

SUMMARY AND CONCLUSIONS

Our results indicate that amplitude-modulated microwaves at an SAR of 2.5 W/kg, corresponding to a plane wave equivalent power density of approximately 1 mW/cm^2, are capable of altering biological activity in in vitro cell cultures. Frequency-modulated micro-

waves at this power level appear to have no effect at all. The radiation from TDMA digital cellular phones can cause significant changes in ODC activity, whereas that from analog phones does not (evidently because they are FM). The data suggest that the same coherence requirements necessary for ELF-induced bioeffects apply to the modulation of ELF amplitude-modulated microwaves. It is clear from this study that the use of SAR alone is inadequate for setting safety standards. The type of modulation must also be considered.

ACKNOWLEDGMENTS

This work was partially supported by funds from the Department of the Army (DAMD17-86-C-6260). The authors gratefully acknowledge the support and advice of Col. Edward Elson.

REFERENCES

Auvinen M, Paasinen A, Andersson LC, Ḧoltẗa E (1992): Ornithine decarboxylase activity is critical for cell transformation. Nature 360:355–358.

Balcer-Kubiczek EK, Harrison GH (1985): Evidence for microwave carcinogenesis in vitro. Carcinogenesis 6:859–864.

Balcer-Kubiczek EK, Harrison GH (1989): Induction of neoplastic transformations in $C^3H/T10\frac{1}{2}$ cells by 2.45-GHz microwaves and phorbol ester. Radiat Res 117:531–537.

Balcer-Kubiczek EK, Harrison GH (1991): Neoplastic transformation of $C^3H/T10\frac{1}{2}$ cells following exposure to 120 Hz modulated 2.45-GHz microwaves and phorbol ester tumor promotor. Radiat Res 126:65–72.

Bawin SM, Kaczmarek LK, Adey WR (1975): Effects of modulated VHF fields on the central nervous system. Ann NY Acad Sci 247:74–81.

Blackman CF, Elder JA, Weil CM, Benane SG, Eichinger DC, House DE (1979): Induction of calcium ion efflux from brain tissue by radio-frequency radiation: Effects of modulation frequency and field strength. Radio Sci 14(6S):93–98.

Blackman CF, Benane SG, House DE, Joines WT (1985): Effects of ELF (1–20 Hz) and modulated (50 Hz) RF field on the efflux of calcium ions from brain tissue in vitro. Bioelectromagnetics 6:1–11.

Boucher NJ (1992): ''The Cellular Radio Handbook.'' Mendecino, CA: Quantum Publishing.

Byus CV, Lundak RL, Fletcher RM, Adey WR (1984): Alterations in protein kinase activity following exposure of cultured human lymphocytes to modulated microwave fields. Bioelectromagnetics 5:341–351.

Byus CV, Pieper SE, Adey WR (1987): The effects of low-energy 60-Hz environmental fields upon the growth-related enzyme ornithine decarboxylase. Carcinogenesis 8:1385–1389.

Byus CV, Kartun K, Pieper SE, Adey WR (1988): Increased ornithine decarboxylase activity in cultured cells exposed to low energy modulated microwave fields and phorbol ester tumor promoters. Cancer Res 48:4222–4226.

Cleary SF, Liu LM, Merchant RE (1990): Glioma proliferation modulated in vitro by isothermal radiofrequency radiation exposure. Radiat Res 121:38–45.

Czerska EW, Elson EC, Davis CC, Swicord ML, Czerski P (1992): Effects of continuous and pulsed 2,450-MHz radiation on spontaneous lymphoblastoid transformation of human lymphocytes in vitro. Bioelectromagnetics 13:247–259.

Denes PB, Pinson EN (1963): ''The Speech Chain: The Physics and Biology of Spoken Language.'' Bell Telephone Laboratories, pp 115–116.

Dutta SK, Subramoniam A, Ghosh B, Parshad R (1984): Microwave radiation induced calcium ion efflux from human neuroblastoma cells in culture. Bioelectromagnetics 5:71–78.

Dutta SK, Gosh B, Blackman CF (1989): Radiofrequency radiation-induced calcium ion efflux enhancement from human and other neuroblastoma cells in culture. Bioelectromagnetics 10:7–202.

Farrel JM, Barber M, Doinov P, Krause D, Litovitz TA (1993): Superposition of a temporally incoherent magnetic field suppresses the change in ornithine decarboxylase activity in developing chick embryos induced by a 60 Hz sinusoidal field. In Blank M (ed): ''Electricity and Magnetism in Biology and Medicine.'' San Francisco: San Francisco Press, pp 342–344.

Garaj-Vrhovac V, Fucic A, Horvat D (1992): The correlation between the frequency of micronuclei and specific chromosome aberrations in human lymphocytes exposed to microwave radiation in vitro. Mutat Res 281:182–186.

Halmekyö M, Syrjänen K, Jänne J, Alhonen L (1992): Enhanced papilloma formation in response to skin tumor promotion in transgenic mice overexpressing the human ornithine decarboxylase gene. Biochem Biophys Res Commun 187:493–497.

Hayashi S, Murakami Y (1995): Rapid and regulated degradation of ornithine decarboxylase. Biochem J 306:1–10.

Hibshoosh H, Johnson M, Weinstein IB (1990): Effects of overexpression of ornithine decarboxylase (ODC) on growth control and oncogene-induced cell transformation. Oncogene 6:739–743.

Ḧoltẗa E, Auvinen M, Paasinen A, Kangas A, Andersson LC (1994): Ornithine decarboxylase-induced cellular transformation: The involvement of protein tyrosine kinase(s) and pp130. Biochem Soc Trans 22:853–859.

Krause D, Mullins JM, Penafiel LM, Meister R, Nardone RM (1991): Microwave exposure alters the expression of 2-5A-dependent RNase. Radiat Res 127:164–170.

Litovitz TA, Krause D, Mullins JM (1991): Effect of coherence time of the applied magnetic field on ornithine decarboxylase activity. Biochem Biophys Res Commun 178:862–865.

Litovitz TA, Krause D, Penafiel M, Elson EC, Mullins JM (1993): The role of coherence time in the effect of microwaves on ornithine decarboxylase activity. Bioelectromagnetics 14:395–403.

Litovitz TA, Krause D, Montrose CJ, Mullins JM (1994): Temporally incoherent magnetic fields mitigate the response of biological systems to temporally coherent magnetic fields. Bioelectromagnetics 15:399–409.

Moshier JA, Dosescu J, Skunca M, Luk GD (1993): Transformation of NIH/3T3 cells by ornithine decarboxylase overexpression. Cancer Res 53:2618–2622.

Mullins JM, Krause D, Litovitz TA (1993): Simultaneous application of a spatially coherent noise field blocks the response of cell cultures to a 60 Hz electromagnetic field. In Blank M (ed): ''Electricity and Magnetism in Biology and Medicine.'' San Francisco: San Francisco Press, pp 345–346.

NCRP (1981): ''Radiofrequency Electromagnetic Fields: Properties, Quantities and Units, Biophysical interaction, and Measurements.'' Bethesda, MD: National Council on Radiation Protection and Measurements, Report No. 67.

NCRP (1986): ''Biological Effects and Exposure Criteria for Radio Frequency Electromagnetic Fields.'' Bethesda, MD: National Council on Radiation Protection and Measurements, Report No. 86.

Saffer JD, Profenno LA (1992): Microwave-specific heating affects gene expression. Bioelectromagnetics 13:75–78.

Seely JE, Pegg AE (1983): Ornithine decarboxylase (mouse kidney). Methods Enzymol 94:158–161.

INT. J. RADIAT. BIOL 1999, VOL. 75, NO. 12, 1541–1549

Short-Term Magnetic Field Exposures (60 Hz) Induce Protection Against Ultraviolet Radiation Damage

ANDREA L. DICARLO†, MICHAEL T. HARGIS, L. MIGUEL PENAFIEL and THEODORE A. LITOVITZ*

(Received 19 February 1999; accepted 18 May 1999)

Abstract.
Purpose: To investigate the ability of electromagnetic (EM) field pre-exposures to induce protection in chick embryos against subsequent ultraviolet (UV) light exposure.
Materials and Methods: Chick embryos in the 4th day of gestation were exposed for 20 minutes (short term) or 96 hours (long term) to 60 Hz, 8 μT magnetic or sham fields (controls) followed by 30 minutes rest. They were then exposed to UV radiation of either low ($30\,J/m^2$) or high ($45\,J/m^2$) intensity (long term was exposed only to $30\,J/m^2$) for 75 minutes. Mortality measurements were made every 30 minutes following UV exposure.
Results: At both UV intensities, short-term, EM field-exposed embryos showed significantly *higher* post-UV survival ($p < 0.05$) at each time point as compared to controls. Long-term EM field exposures, however, offered no protection against low intensity UV light, in fact, 96 hour-EM field-exposed embryos were significantly *less* protected than non-EM field-exposed controls ($p < 0.05$).
Conclusions: Results of the present study demonstrate that EM field exposures of appropriate duration induce protection against damage from UV light exposure. Because EM field exposures have been reported to activate stress protein response pathways and protect against anoxia/re-oxygenation damage, stress proteins are thought to play a role in the observed UV protection.

1. Introduction

Organisms protect themselves against harmful stimuli by activation of a number of different cellular protection pathways. Among these is the classical heat shock response, in which heat shock proteins (hsp's) are synthesized (Morimoto and Fodor 1984). The hsp's, which are a class of stress proteins, are a family of molecular chaperones which are induced by a variety of environmental stresses such as heat, chemicals and oxidative injury. These induced chaperone proteins are responsible for the repair of damaged proteins, and their induction contributes to protection from and adaptation to cellular stress. It is now generally accepted that prior exposure of a cell or tissue to a mild stressor can confer protection against a subsequent lethal stressor, and induction of stress proteins are involved (Mestril and Dillmann 1995). This effect is known as pre-conditioning, and can be achieved by pre-exposure to the same type of stimulus (auto-protection), or by exposure to an unrelated stimulus (cross-protection).

Induction of the heat shock stress response, via the cross-protection mechanism, has been shown to be protective against ultraviolet radiation. Protection against ultraviolet B (UVB) radiation has been achieved by brief, hyperthermic pre-exposures in a human keratinocyte cell line (Maytin *et al.* 1993). It has been shown that a major protein in the heat shock protein (hsp) family, hsp72, is the mediator of this observed resistance (Trautinger *et al.* 1995). Over-expression of hsp72 in a transfected murine fibroblast cell line has also been shown to yield increased viability following UVB treatment (Simon *et al.* 1995). Other groups (Maytin 1992; Maytin *et al.* 1993) have replicated these findings in cultured keratinocytes. Finally, it has been demonstrated that heat shock transcription factors (HSF, required for the expression of hsp genes) are activated following UVC radiation treatment in human glioblastoma cell lines (Ohnishi *et al.* 1996). The concept of cross-protection has also been extensively studied in ischemia/reperfusion, another form of cell stress. Pre-exposure to heat or certain chemicals has been shown to minimize ischemic damage to both myocardial cells and tissues (Marber *et al.* 1994; Mestril and Dillmann 1995). These findings, taken with evidence that induction of the heat shock response can protect against UV damage suggest that heat shock protein responses may play a role in protection against various forms of oxidative stress.

That heat shock proteins are protective against oxidative stress is intriguing, given the recent findings of our laboratory, which demonstrated that short (20 minute) pre-exposures to 60 Hz magnetic fields could induce protection against anoxia/re-oxygenation in a chick embryo model (Di Carlo *et al.* 1998; Di Carlo

*Author for correspondence; e-mail: litovitz@cua.edu
Vitreous State Laboratory, Catholic University of America, Washington, DC, USA.
†Submitted as partial fulfillment of degree requirements for Doctorate of Philosophy Department of Biology, University of Maryland, College Park, MD 20742, USA.

International Journal of Radiation Biology ISSN 0955-3002 print/ISSN 1362-3095 online © 1999 Taylor & Francis Ltd
http://www.tandf.co.uk/JNLS/rab.htm
http://www.taylorandfrancis.com/JNLS/rab.htm

et al. 1999). That work was based on earlier studies done by Blank *et al.* (1994) which showed that 60 Hz magnetic field exposures yielded the same patterns of protein synthesis as heat shock. Later studies confirmed this finding by demonstrating that fields activate HSF (Goodman *et al.* 1994) and enhance transcription of hsp70 (Lin *et al.* 1997). The induction of the hsp70 protein by 60 Hz magnetic field exposure was found to be rapid, with maximum accumulation of the protein in as little as 40 minutes after exposure (Han *et al.* 1998). The same group also demonstrated that AP-1, AP-2, and SP-1, other stress-induced transcription factors, were activated in response to EM field exposures (Lin *et al.* 1998). Preliminary evidence from our laboratory shows that activation of HSF in chick embryos occurs within 10 minutes after the start of a 60 Hz, 8 μT magnetic field exposures (data not shown). Thus, we hypothesized that the anoxia protection that was observed in response to the 60 Hz magnetic field exposures might be due, in part, to field-enhanced activation of cellular stress responses similar to those seen during thermal stress. Given the evidence that 60 Hz magnetic field exposures activate cellular stress responses, which are then protective against subsequent lethal stress, an experiment was designed to determine if field exposures could stimulate the stress response system of chick embryos (i.e. pre-condition) in such a way that protection against UV radiation could be induced.

2. Materials and methods

2.1. *Embryos*

Fertilized White Leghorn eggs (Truslow Farms, Chestertown, MD) were held at 10°C and used within 48 hours of receipt. The holding refrigerator was monitored periodically to insure that ambient magnetic field strengths were below 0.5 μT. Embryos were incubated (37.8 ± 0.1°C) for 96 hours (developmental stages ranged from 22 to 25) (Hamburger and Hamilton 1951) in water-jacketed incubators (VWR) maintained at > 55% humidity. Embryos of these stages were readily visible with conspicuous blood vessels surrounding them. The heart consisted of one atrial and one ventricular chamber. The two chambers were well defined, and the flow of blood was clearly visible between them as the heart beat. Separation of the heart into left and right hemispheres (i.e. the formation of two atria and ventricles) by the interventricular groove, had not yet occurred, making analysis of heart function (described below) a more straightforward procedure.

The 4-day-old chick embryos used in this study do not fall under the category of 'vertebrate animal' and thus, were not subject to committee approval. Although the chick embryo model has been criticized because it 'affords no parallel with the anatomical... relationship existing between the pregnant mammal and her conceptus' (Klug *et al.* 1997), others have stated that '...the chicken embryo may be considered an exciting model... lying on the borderline between cell cultures and adult laboratory animals' (Tempel and Schleifer 1995). Additionally, the effects of UV light exposure on the chick embryo had been previously investigated (Lwin, 1971), and provided a basis for the experiments described here.

Incubators were modified to minimize stray magnetic field emissions, and ambient measurements indicated that magnetic fields were below 0.5 μT at all egg placement positions. Typical geomagnetic fields measured in all of our incubators were ~40–50 μT. During all experiments, the embryos were maintained at 37.8°C except for brief intervals (30 to 60 seconds) required to handle the eggs or transfer them to different treatment conditions. During these intervals, embryos experienced ambient, room temperature air (approximately 22°C).

2.2 *Field exposure*

Signals were generated using a 15 MHz function/arbitrary waveform generator (Hewlett-Packard model 33120A, Palo Alto, CA, USA), and 35 watt P.A. amplifier (Radio Shack MPA-46, Fort Worth, TX, USA). Fields were produced by passing current through paired coils arranged in the Helmholtz configuration, wound and connected as described previously (Berman *et al.* 1990). A coil diameter of 15 inches provided a region of nearly uniform magnetic field (± 5%), sufficiently large so that 24 embryos could be exposed at one time. Exposures were randomly done in one of six pairs of exposure coils. Embryos were exposed to EM fields (60 Hz, 8 μT) for either 20 minutes (short-term) or 96 hours (long-term).

Each set of coils was housed within a water-jacketed cell culture incubator (VWR Scientific Inc., West Chester, PA) so that temperature could be maintained at 37.8°C. The relative humidity in the incubation chambers was held at > 55% by placing a pan of saturated aqueous NaCl solution on the bottom of the incubator chamber. Magnetic fields were measured using 60 Hz-calibrated magnetic dosimeters (Model IDR-109; Integrity Design and Research Corp., Essex, VT). Embryos were exposed to either sham (double-wound coil, canceled field) or 60 Hz magnetic fields (8 μT) for either 20 minutes, or 96 hours. Both sham and 60 Hz exposures were carried out at 37.8°C.

2.3. *Sham field coils*

Paired coils were wired such that one of the pair could be configured to produce a canceled field while the other coil produced a 60 Hz, 8 μT magnetic field. Each exposure coil was wound from two, adjacent sets of conducting wires connected so that electric current could flow in either the same, or in opposite directions in the paired conductors. In the first case the induced magnetic fields from each loop reinforced each other, producing the field to which the chick embryos were exposed. In the latter case the fields from each loop canceled each other so that control embryos received no field exposure, but did experience all other environmental conditions (*e.g.* generation of heat or vibration) that might be produced by the activated coil. Such canceled field conditions provide the best sham (negative control) exposure conditions so that effects resulting only from the applied field can be clearly determined.

2.4. *Temperature controls*

To eliminate the possibility that heating by 60 Hz magnetic field exposure was responsible for observed protection, and because chick embryos are sensitive to temperature changes, thermocouples were placed into 8 eggs to record temperature changes during 20 minute, 60 Hz, 8 μT magnetic field exposures. To position the thermocouples, eggs were candled (a light source was placed behind the egg to visualize the location of the embryo) while in the incubator, and a small hole was made in the shell, just large enough to insert the thin wire of the thermocouple (HH82 digital thermometer—Omega, Stamford, CT). The end of the thermocouple was placed immediately adjacent to the embryo. The same procedure was repeated in control embryos to insure there was no heat lost due to the hole in the shell. The thermocouples used had an accuracy of measurement to within $\pm 0.1^{\circ}$C. No measurable temperature changes were noted in either the control or 60 Hz magnetic field-exposed embryos.

2.5. *UV exposure*

Embryos were maintained at 37.8°C, for 30 minutes following the 20 minute, or 96 hour 60 Hz magnetic field exposures, during which time, a portion of the shells were removed, and the inner shell membranes were drawn back to reveal the embryos. The windowing process took approximately 30 seconds per egg. Windowing allowed ready observation of the embryos and facilitated effective exposure of the embryo to ultraviolet light. Special care was taken to insure that similar surface areas of the embryos were exposed. Embryos were coded by an individual who was not the person making the mortality observations. This coding insured that the observer was blinded during the course of the experiment. Embryos were exposed to a germicidal lamp (Ecometrics—Silverdale, PA) with either 30 or 45 J/m^2 (0.7 or 1 μW/cm^2 for 75 minutes) of UVC (254 nm) in two separate sets of experiments. According to the manufacturer, the spectral distribution of the lamp was approximately 75% UVC, 20%, UVB and 5% UVA and visible light. The intensity of the incident radiation at the site of the embryos was determined using a power meter (Model 1815-C, Newport, Irvine, CA, USA). The probe was calibrated by the manufacturer and UV intensity was determined using calibration curves provided by Newport. The meter was equipped with a UV filter and thus, detected any wavelengths within the UV region of the spectrum (200–400 nm), including UVA and UVB light. This experiment was designed using lethal doses of UV so that large amounts of statistically significant data could be obtained in a short time period. Large doses of UV light insure that mortality occurs within several hours.

As an additional control, embryos ($n = 24$) were windowed in exactly the same manner and were placed into an incubator for the duration of the experiment. This was done to insure that the windowing procedure itself was not responsible for any observed embryo death. All of the embryo treated in this way (no sham or 60 Hz magnetic field exposure and no exposure to ultraviolet light) were observed following a 5 hour period, and survival was 100%.

2.6. *Observations*

At the end of UV exposure, and every thirty minutes, UV-exposed embryos were evaluated visually to determine if they were alive (heart beating) or dead (heart stopped). For the 45 J/m^2 UV exposure, mortality observations were made for one hour following the end of UV. Three hours of post UV observations were made for the 30 J/m^2 exposure. Fewer time points were recorded for the 45 J/m^2 UV intensity because the higher intensity exposure led to a more rapid embryo death.

2.7. *Statistical analysis*

The standard error of the mean (shown as error bars on all data points) was determined for each time point on figures 1 and 2. For figure 3, error bars represent the standard error of the mean for the percent survival of field-exposed embryos one hour

following UV exposure. The P values and statistical significance of the data were determined by χ^2 analysis using the Instat (©1993) statistical analysis program version 2.04 (GraphPad software, San Diego, CA).

3. Results

Table 1 gives a brief overview of the exposure conditions and timing for each of the three figures. In figure 1, a time course is shown for survival of short-term, 60 Hz magnetic field-exposed and control embryos after 45 J/m^2 UV irradiation (1 μW/cm^2, higher dose). Timing was begun at the start of UV exposure, and continued until 60 minutes after the end of UV. At time 0, there was 100% survival prior to UV treatment. No observations were made during UV irradiation. As can be seen in the graph, 60 Hz magnetic field-exposed embryos had consistently higher survival ($p < 0.05$) at all time points after UV exposure. Data comprised 100 control and 97 exposed embryos (13 experiments).

Figure 2 shows data for a separate set of embryos (short-term, 60 Hz magnetic field-exposed and control) exposed to a lower dose of UV (30 J/m^2). In these experiments, time of UV exposure was the same (75 minutes) as for figure 1, however the intensity of the incident radiation at the site of the embryos was lower (0.7 μW/cm^2). Time shown on the x-axis is from the start of UV exposure. Data (7 experiments) consisted of 58 control and 59 exposed embryos.

Figure 3 illustrates how the time duration of the applied 60 Hz magnetic field is critical in whether protection or de-protection against UV radiation is achieved in the chick embryo model. Embryos were exposed to electromagnetic fields for either 20 minutes or 96 hours prior to the low intensity of UVC irradiation (30 J/m^2). Survival, shown in the graph, was recorded one hour after UV exposure. Bars shown represent the percent increase or decrease in protection from the 60 Hz magnetic field exposure as compared to controls. Note that the 20-minute exposure yields 60% more protection than was seen in non-field-exposed embryos, however, survival of the 96-hour-exposed embryos was 30% lower than that of the controls. Changes in survival following UV were significantly higher in 60 Hz magnetic field-exposed embryos as compared to controls ($p < 0.05$).

In all of the data presented here, the marker for possible 60 Hz magnetic field protection was mortality, however an examination of the gross morphology of the embryos following the UV exposure revealed extensive vascular deterioration and hemorrhage.

Table 1. Exposure conditions.

Figure	EM Field Exposure Time	Germicidal Bulb Intensity	Time Points Shown
1	20 min	45 J/m^2	up to 1 h post-UV
2	20 min	30 J/m^2	up to 3 h post-UV
3	20 min or 96 h	30 J/m^2	at 1 h post-UV

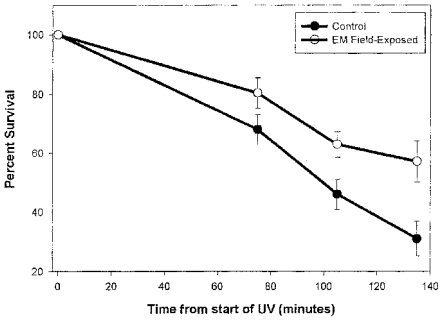

Figure 1. Time course for 60 Hz magnetic field-induced protection against the higher intensity of UV light (45 J/m^2). Embryos were exposed to a 60 Hz, 8 μT magnetic field for 20 min and were then exposed to UV light 30 min after the end of EM field exposure. Data shown consist of a total of 13 separate experiments for which mortality observations were made immediately following UV radiation and every thirty minutes thereafter. Error bars shown represent the standard error of the mean. Survival data for control embryos is given by closed circles (–●–), and exposed embryos are shown with open circles (–○–).

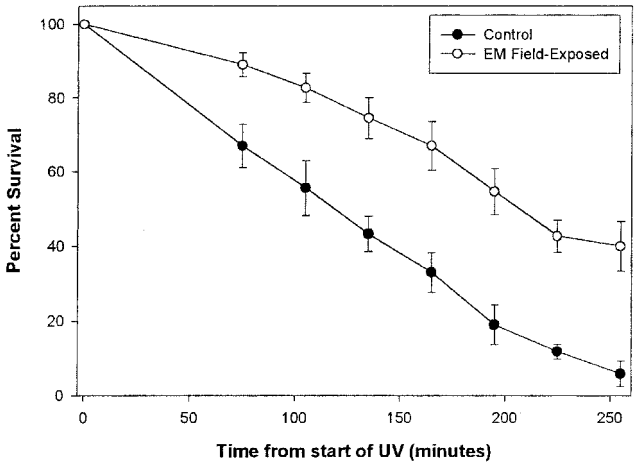

Figure 2. Time course for 60 Hz magnetic field-induced protection against the lower intensity of UV (30 J/m^2). Embryos were exposed to a 60 Hz, 8 μT magnetic field for 20 min and were then exposed to UV light 30 min after the end of EM field exposure. Control and exposed embryos were studied in a total of 7 separate experiments. Error bars shown represent the standard error of the mean. Survival data for control embryos is given by closed circles (–●–), and exposed embryos are shown with open circles (–○–).

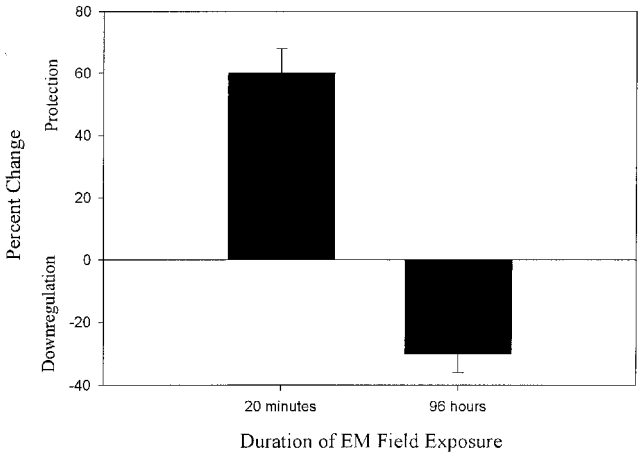

Figure 3. 60 Hz magnetic field exposures of varied time duration can affect EM field-induced UV radiation protection. Chick embryos (96 h) were exposed to 60 Hz, 8 μT magnetic fields for 20 min (50 EM-exposed and 48 control, $n = 5$ replicates) or 96 h (48 EM-exposed and 52 control, $n = 5$ replicates) 30 min prior to UVC irradiation ($30\,J/m^2$). Mortality measurements reported here were recorded at one hour following the end of UV exposure. Data plotted in the figure represent the percent increase in protection from the 60 Hz magnetic field exposure as compared to control values. Error bars represent the standard error of the mean for the per cent survival of field-exposed embryos.

4. Discussion

The aim of this study was to evaluate the use of 60 Hz magnetic field exposures to pre-condition chick embryo tissue against the damaging effects of UV irradiation. We showed that EM field pre-treatment was effective in extending the life span of the embryos following UV irradiation. At the two intensities of UV that were investigated, there was, at all time points, significant induced protection (damage repair) in the 20 minute, EM field-exposed embryos as compared to controls (figures 1,2). All of the embryos ultimately died; however, the finding that EM field exposures are more protective at the $30\,J/m^2$ intensity of UV light than at the $45\,J/m^2$ dose is interesting in that it suggests that 60 Hz magnetic field exposures may be even more effective in protecting against UV light exposures which are not immediately lethal, but instead lead only to cell damage. At the dose levels used here, the UV light insult caused damage which exceeded the repair capacity of the EM field-induced protective mechanism. In cells, there exists a balance between damage caused by a stressor and the corresponding cellular response to minimize that damage. In addition to causing direct damage to proteins and DNA, UV exposures can lead to the formation of reactive oxygen species (ROS) which cause secondary damage to many cellular components. This damage, whether direct or indirect, leads to activation of the cell's innate protection mechanisms. Therefore, it is useful to discuss the damage and repair mechanisms involved in UV light exposures.

4.1. *UV light exposures and cell damage: a role for ROS*

The primary damage from exposure to germicidal wavelengths of UV is to DNA (maximum absorption from 240–290 nm). We therefore asked if damage to DNA was an important mechanism involved in the chick embryo mortality observed. This is improbable, because in contrast to the 3–4 hour post-UV survival of the chick embryos in our study; UVB-induced DNA fragmentation, a known biochemical process of apoptosis, does not peak until 12–24 hours after irradiation of rat skin (Iwasaki *et al.* 1996). Due to the rapid onset of mortality in the chick embryos, it did not seem likely that the DNA damage sustained by the embryos was the main cause of death. The germicidal bulb that was used in these studies, however, also emits UVA and UVB wavelengths which have been shown to lead to the formation of ROS. In addition, singlet oxygen is produced by UVC light exposure (Zhang *et al.* 1997). Thus, it appears that the formation of ROS by the spectra of UV light emitted by the bulb may be the primary mechanism for the damage and ultimately, the mortality observed in these studies.

It is accepted that the ROS induced by UV light can cause widespread cellular damage. For example, in our chick embryo model, we observed extensive vascular deterioration in the UV light-exposed embryos which likely played a significant role in their deaths. This deterioration of the vascular system could be attributed to denaturation of membrane structural proteins and lipid peroxidation of the endothelial cell membranes by ROS. This would render the chick embryo vasculature leaky and prone to hemorrhage, as was seen in the present study. Others have noted similar damage following UV exposure of chick embryos (Lwin 1971). Singlet oxygen (Ryter and Tyrrell 1998), as well as exposures to UVB and UVC light (Costanza *et al.* 1995) have been shown to increase lipid peroxidation. In addition, there is evidence that oxidative destruction of lipids can cause cellular damage similar to that which we observed in the chick embryo vasculature. For example, lipid peroxidation generated by cocaine-induced oxidative stress leads to vascular disruption and hemorrhage in mouse embryos (Zimmerman *et al.* 1994).

4.2. *ROS induce hsp's which confer protection against oxidative stress*

The presence of ROS in the cytoplasm has been linked to activation of the heat shock stress response (Becker *et al.* 1991; Liu and Thiele 1996). Consistent with this fact is the finding that the addition of exogenous ROS to a system can directly activate HSF (Bruce *et al.* 1993). Increased levels of ROS can lead to modifications of intracellular proteins, which is a major source of damage from UV (Davies 1987). The ROS also denature proteins. The accumulation of damaged or denatured proteins within a cell has also been demonstrated to induce the heat shock protein response pathway (Ananthan *et al.* 1986). Over-expression of the hsp70 protein has been shown to be involved in protection against H_2O_2, and HO^-, and hypoxia/re-oxygenation (all of which are forms of oxidative stress) in cardiac myocytes (Chong *et al.* 1998). There is also direct evidence that induction of hsp72 is critical in protection against oxidative stress (Musch *et al.* 1998). When hsp72 induction by glutamine was specifically inhibited with anti-sense constructs in intestinal epithelial cells, viability following oxidant treatment was significantly decreased. Several studies have also implicated hsp's in the attenuation of lipid-peroxidation damage (Jacquier-Sarlin *et al.* 1994; Calabrese *et al.*, 1996; Wong *et al.* 1998). Although the role of the hsp's in our protection model is not completely clear, the EM field exposures are likely inducing protection against some form of oxidant injury, as evidenced by increased longevity of field-exposed embryos following UV irradiation as compared to controls. Thus, we explore possible connections between EM field-induced cellular responses and oxidative stress.

4.3. *EM field exposures and the generation of ROS*

Several studies have shown a connection between EM field exposures and evolution of ROS. Acting synergistically with phorbol myristate acetate (an inducer of oxidative burst in neutrophils), EM fields have been shown to cause an increased generation of free radical species (Roy *et al.* 1995). In a later study, the addition of anti-oxidants (catalase, superoxide dismutase, and vitamin E) to cultures of chick embryo fibroblasts (CEF) cells was found to inhibit EM field-induced increases in cell proliferation (Katsir and Parola 1998). The findings of Katsir *et al.* are consistent with studies which show that increased activity of the growth-related enzyme ornithine decarboxylase (ODC) is induced by ROS (Marsh and Mossman 1991; Hunt and Fragonas 1992; Lovaas 1995). Increased ODC activity is critical for enhanced cell proliferation (Luk *et al.* 1982; Willey *et al.* 1985), and EM fields have been shown to increase the activity of ODC (Byus *et al.* 1987; Farrell *et al.* 1997a). The above studies support the hypothesis that EM field-enhanced proliferation in CEF cells involves ROS. Exposure to EM fields have also been shown to stimulate anti-oxidant systems including glutathione peroxidase and glutathione reductase (Pafkova and Jerabek 1994), further supporting a connection between EM field exposures and the induction of oxidative stress.

4.4. *Possible mechanisms for EM field-induced protection*

Taken together, all of the above findings suggest that the generation of ROS may be involved in a number of EM field-induced biological effects, including those reported here. Brief 60 Hz magnetic field exposures have been shown to induce typical stress response pathways (Goodman *et al.* 1994; Lin *et al.* 1997). This study extends those results to a chick embryo model to show that this induction of protection by EM fields can be used to minimize subsequent damage caused by UV light exposure. In fact, in our chick embryo model, EM fields have been shown to cause activation of HSF (data not shown). There are several explanations for the mechanism by which EM fields might provide protection against UV. These include induction of stress proteins and/or alteration of oxidative repair mechanisms. It is clear that the first mechanism is operative in our model, however, there is less evidence for direct EM field stimulation of anti-oxidant systems. We suggest that EM fields are increasing the levels of ROS within the cell. This increased ROS can then mediate activation of the stress protein pathway, conferring protection against UV light by minimizing damage to proteins and lipids.

4.5. *EM fields: protective or damaging? A question of timing*

This finding that 60 Hz magnetic field exposures can induce a beneficial effect is in contrast to some previous findings (Farrell *et al.* 1997b, Berman *et al.* 1990, Ubeda *et al.* 1994, Youbicier-Simo *et al.* 1997), which demonstrate adverse effects in chick embryo models as a result of EM field exposures. For example, Youbicier-Simo *et al.* found that continuous exposure of embryos to EM fields emitted by video display units led to significantly increased embryonic death. However, the exposures involved in the above studies were long-term (on the order of 48–96 hours). To better understand the ability of an electromagnetic field stimulus to be either beneficial or adverse, we

exposed embryos to 60 Hz magnetic fields for 96 hours to more closely mimic the long-term exposures investigated previously. Following these long-term exposures, the chick embryos appeared to be 'de-protected' against the subsequent UV insult as compared to their non-field-exposed counterparts. We hypothesized that the observed 'de-protection' following long term exposure to 60 Hz magnetic fields was due to a down-regulation of the stress protein response.

This hypothesis of down-regulation of stress proteins as a result of long-term EM field exposures is not unreasonable. Whereas acute exposure to a stimuli elicits one type of cellular response, chronic stimulation tends to give the opposite result (Hellriegel and D'Mello 1997, Marti *et al.* 1994, Giralt *et al.* 1993). There is evidence that it is possible to down-regulate the heat shock stress response. For example, Blake *et al.* (1995) monitored hsp72 expression in response to both acute restraint stress, and chronic plus acute restraint stress. Induction of hsp72 following acute restraint stress was demonstrated, however, when acute immobilization was preceded by chronic restraint, no significant increase in hsp72 could be detected. Thus, biological effects resulting from magnetic field exposures might, as with other stimuli, depend on the dose (e.g. duration of exposure). Short term EM field exposures up-regulate cell repair mechanisms, whereas long term exposures appear to down-regulate protective responses.

4.6. *EM fields: DNA damage and repair*

The concept of up– and down-regulation is not limited to heat shock proteins. Phillips *et al.* (1998) showed that following low intensity field exposures, DNA damage (strand breaks) was decreased in T-lymphoblastoid cells. High intensity field exposures, however, yielded an increase in the number of DNA strand breaks. Since the field strengths employed did not have sufficient energy to directly affect chemical bonds in the DNA, it was hypothesized that the fields might be up and down-regulating innate DNA repair mechanisms. This conclusion was supported by Phillips' earlier work (1995), which showed that the activity of a DNA repair enzyme, poly-ADP-ribose polymerase could be changed by exposure to EM fields. This is consistent with our results. Although Phillips' 1998 study was done with high frequency (835 MHz) fields, studies have shown that 60 Hz and 835 MHz fields can have similar effects. For example, exposure of murine L929 cells to both frequencies causes similar changes in ODC activity (Penafiel *et al.* 1997).

5. Conclusions

We conclude that 60 Hz magnetic field exposures can provide protection against subsequent damaging insults such as UV. It appears that EM fields of a proper magnitude and duration can stimulate cellular repair processes. These might include induction of the heat shock stress protein pathway mediated by EM field-induced ROS, and/or enhancement of anti-oxidant, ROS detoxification systems. In addition, the finding of protection or de-protection, depending on the duration of field exposure provides insight into a possible mechanism for negative health effects linked to long-term EM field exposures.

Acknowledgements

This project described was supported by grant number 5 R01 ES06872-02 from the National Institute of Environmental Health Sciences (NIEHS), NIH. Its contents are solely the responsibility of the authors and do not necessarily represent the official views of the NIEHS, NIH.

References

Ananthan, J., Goldberg, A. L. and Voellmy, R., 1986, Abnormal proteins serve as eukaryotic stress signals and trigger the activation of heat shock genes. *Science*, **232,** 522–524.

Berman, E., Chacon, L., House, D., Koch, B. A., Koch, W. E., Leal, J., Lovtrup, S., Mantiply, E., Martin, A. H., Martucci, G. I., Mild, K. H., Monahan, J. C., Sandstrom, M., Shamsaifar, K., Tell, R., Trillo, M. A., Ubeda, A. and Wagner, P., 1990, Development of chicken embryos in a pulsed magnetic field. *Bioelectromagnetics*, **11,** 169–187.

Blake, M. J., Klevay, L. M., Halas, E. S. and Bode, A. M., 1995, Blood pressure and heat shock protein expression in response to acute and chronic stress. *Hypertension*, **25,** 539–544.

Blank, M., Khorkova, O. and Goodman, R., 1994, Changes in polypeptide distribution stimulated by different levels of electromagnetic and thermal stress. *Bioelectrochemistry and Bioenergetics*, **33,** 109–114.

Bruce J. L., Price, B. D., Coleman, C. N. and Calderwood, S. K., 1993, Oxidative injury rapidly activates the heat shock transcription factor but fails to increase levels of heat shock proteins. *Cancer Research*, **53,** 12–15.

Byus, C. V., Pieper, S. E. and Adey, W. R., 1987, The effects of low-energy 60-Hz environmental electromagnetic fields upon the growth-related enzyme ornithine decarboxylase. *Carcinogenesis*, **10,** 1385–1389.

Calabrese, V., Renis, M., Calderone, A., Russo, A., Barcellona, M. L. and Rizza, V., 1996, Stress proteins and SH-groups in oxidant-induced cell damage after acute ethanol administration in rat. *Free Radicals in Biology and Medicine*, **20,** 391–397.

Chong, K. Y., Lai, C. C., Lille, S., Chang, C. and Su, C. Y., 1998, Stable over-expression of the constitutive form of

heat shock protein 70 confers oxidative protection. *Journal of Molecular and Cellular Cardiology*, **30,** 599–608.

COSTANZA, L. L., DE GUIDI, G., GIUFFRIDA, S., SORTINO, S. and CONDORELLI, G., 1995, Antioxidant effect of inorganic ions on UVC and UVB induced lipid peroxidation. *Journal of Inorganic Biochemistry*, **59,** 1–13.

DAVIES, K. J., 1987, Protein damage and degradation by oxygen radicals. I. General aspects. *Journal of Biological Chemistry*, **262,** 9895–9901.

DI CARLO, A. L., FARRELL, J. M. and LITOVITZ, T. A., 1998, A simple experiment to study electromagnetic field effects: protection induced by short-term exposures to 60 Hz magnetic fields. *Bioelectromagnetics* , **19,** 498–500.

DI CARLO, A. L., FARRELL, J. M. and LITOVITZ, T. A., 1999, Myocardial protection conferred by electromagnetic fields. *Circulation* , **99,** 813–816.

FARRELL, J. M., BARBER, M., KRAUSE, D. and LITOVITZ, T. A., 1997a, Effects of low frequency electromagnetic fields on the activity of ornithine decarboxylase in developing chick embryos. *Bioelectrochemistry and Bioenergetics*, **43,** 91–96.

FARRELL, J. M., LITOVITZ, T. L., PENAFIEL, M., MONTROSE, C. J., DOINOV, P., BARBER, M., BROWN, K. M. and LITOVITZ, T. A., 1997b, The effect of pulsed and sinusoidal magnetic fields on the morphology of developing chick embryos. *Bioelectromagnetics* , **18,** 431–438.

GIRALT, M., ARMARIO, A. and HIDALGO, J., 1993, Chronic stress reduces serum but not liver metallothionein response to acute stress. *Chemico-Biological Interactions*, **88,** 1–5.

GOODMAN, R., BLANK, M., LIN, H., DAI, R., KHORKOVA, O., SOO, L., WEISBROT, D. and HENDERSON, A., 1994, Increased levels of HSP70 transcripts induced when cells are exposed to low frequency electromagnetic fields. *Bioelectrochemistry and Bioenergetics*, **33,** 115–120.

HAMBURGER, V. and HAMILTON, H. L., 1951, A series of normal stages in the development of the chick embryo. 1951. *Journal of Morphology*, **88,** 49–67.

HAN, L., LIN, H., HEAD, M., JIN, M., BLANK, M. and GOODMAN, R., 1998, Application of magnetic field-induced heat shock protein 70 for presurgical cytoprotection. *Journal of Cellular Biochemistry*, **71,** 577–583.

HELLRIEGEL, E. T. and D'MELLO, A. P., 1997, The effect of acute, chronic, and chronic intermittent stress on the central noradrenergic system. *Pharmacology, Biochemistry and Behavior*, **57,** 207–214.

HUNT, N. H. and FRAGONAS, J. C., 1992, Effects of anti-oxidants on ornithine decarboxylase in mitogenically-activated T lymphocytes. *Biochimica et Biophysica Acta*, **1133,** 261–267.

IWASAKI, K., IZAWA, M. and MIHARA, M., 1996, UV-induced apoptosis in rat skin. *Journal of Dermatological Science*, **12,** 31–35.

JACQUIER-SARLIN, M. R., FULLER, K., DINH-XUAN, A. T., RICHARD, M. J. and POLLA, B. S., 1994, Protective effects of hsp70 in inflammation. *Experentia*, **50,** 1031–1038.

KATSIR, G. and PAROLA, A. H., 1998, Enhanced proliferation caused by a low frequency weak magnetic field in chick embryo fibroblasts is suppressed by radical scavengers. *Biochemical and Biophysical Research Communications*, **252,** 753–756.

KLUG, S., HETSCHER, M., GILES, S., KOHLSMANN, S. and KRAMER, K., 1997, The lack of effects of nonthermal RF electromagnetic fields on the development of rat embryos grown in culture. *Life Sciences*, **61,** 1789–1802.

LIN, H., OPLER, M., HEAD, M., BLANK, M. and GOODMAN, R., 1997, Electromagnetic field exposure induces rapid, transitory heat shock factor activation in human cells. *Journal of Cellular Biochemistry*, **66,** 482–488.

LIN, H., BLANK, M., HEAD, M. and GOODMAN, R., 1998, Magnetic field activation of protein-DNA binding. *Journal of Cellular Biochemistry*, **70,** 297–303.

LOVAAS, E., 1995, Hypothesis: spermine may be an important epidermal antioxidant. *Medical Hypotheses*, **45,** 59–67.

LUK, G. D., CIVIN, C. I., WEISSMAN, R. M. and BAYLIN, S. B., 1982, Ornithine decarboxylase: essential in proliferation but not differentiation of human promyelocytic leukemia cells. *Science*, **216,** 75–77.

LWIN, K., 1971, Sensitivity of chick embryos to ultraviolet radiation during early embryogenesis. *Photochemistry and Photobiology* , **13,** 289–291.

MARBER, M. S., WALKER, J. M., LATCHMAN, D. S. and YELLOW, D. M., 1994, Myocardial protection after whole body heat stress in the rabbit is dependent on metabolic substrate and is related to the amount of the inducible 70-kD heat stress protein. *Journal of Clinical Investigation*, **93,** 1087–1094.

MARSH, J. P. and MOSSMAN, B. T., 1991, Role of asbestos and active oxygen species in activation and expression of ornithine decarboxylase in hamster tracheal epithelial cells. *Cancer Research*, **51,** 167–173.

MARTI, O., GAVALDA, A., GOMEZ, F. and ARMARIO, A., 1994, Direct evidence for chronic stress-induced facilitation of the adrenocorticotropin response to a novel acute stressor. *Neuroendocrinology* , **60,** 1–7.

MAYTIN, E. V., 1992, Differential effects of heat shock and UVB light upon stress protein expression in epidermal keratinocytes. *Journal of Biological Chemistry*, **267,** 23 189–23 196.

MAYTIN, E. V., MURPHY, L. A. and MERRILL, M. A., 1993, Hyperthermia induces resistance to ultraviolet light B in primary and immortalized epidermal keratinocytes. *Cancer Research*, **53,** 4952–4959.

MESTRIL, R. and DILLMANN, W. H., 1995, Heat shock proteins and protection against myocardial ischemia. *Journal of Molecular and Cellular Cardiology*, **27,** 45–52.

MORIMOTO, R. and FODOR, E., 1984, Cell-specific expression of heat shock proteins in chicken reticulocytes and lymphocytes. *Journal of Cell Biology*, **99,** 1316–1323.

MUSCH, M. W., HAYDEN, D., SUGI, K., STRAUS, D. and CHANG, E. B., 1998, Cell-specific induction of hsp72-mediated protection by glutamine against oxidant injury in IEC18 cells. *Proceedings of the Association of American Physicians*, **110,** 136–139.

OHNISHI, K., MATSUMOTO, H., TAKAHASHI, A., WANG, X. and OHNISHI, T., 1996, Heat shock transcription factor, HSF, is activated by ultraviolet irradiation. *Photochemistry and Photobiology* , **64,** 949–952.

PAFKOVA, H. and JERABEK, J., 1994, Interaction of MF 50 Hz, 10 mT with high dose x-rays: Evaluation of embryotoxicity in chick embryos. *Reviews on Environmental Health*, **10,** 235–241.

PENAFIEL, L. M., LITOVITZ, T. A., KRAUSE, D., DESTA, A. and MULLINS, J. M., 1997, Role of modulation on the effect of microwaves on ornithine decarboxylase activity in L929 cells. *Bioelectromagnetics* , **18,** 132–141.

PHILLIPS, J. L., CAMPBELL-BEACHLER, M., ISHIDA-JONES, T., HAGGREN, W. and ADEY, W. R., 1995, Exposure of PC12 cells to a 1 G sinusoidal magnetic field at 60 Hz: Effect on the activity of the DNA repair enzyme poly(ADP-ribose) polymerase (Abstr.). *Annual Review of Research on Biological Effects of Electric and Magnetic Fields from the Generation, Delivery and Use of Electricity* (Palm Springs, CA).

PHILLIPS, J. L., IVASCHUK, O., ISHIDA-JONES, T., JONES, R. A., CAMPBELL-BEACHLER, M. and HAGGREN, W., 1998, DNA

damage in Molt-4 T-lymphoblastoid cells exposed to cellular telephone radiofrequency fields *in vitro*. *Bioelectrochemistry and Bioenergetics*, **45,** 103–110.

ROY, S., NODA, Y., ECKERT, V., TRABER, M. G., MORI, A., LIBURDY, R. and PACKER, L., 1995, The phorbol 12-myristate 13-acetate (PMA)-induced oxidative burst in rat peritoneal neutrophils is increased by a 0.1 mT (60 Hz) magnetic field. *FEBS Letters*, **376,** 164–166.

RYTER, S. W. and TYRRELL, R. M., 1998, Singlet molecular oxygen ((1)O2): a possible effector of eukaryotic gene expression. *Free Radical Biology and Medicine*, **24,** 1520–1534.

SIMON, M. M., REIKERSTORFER, A., SCHWARZ, A., KRONE, C., LUGER, T. A., JAATTELA, M. and SCHWARZ, T., 1995, Heat shock protein 70 overexpression affects the response to ultraviolet light in murine fibroblasts. Evidence for increased cell viability and suppression of cytokine release. *Journal of Clinical Investigation*, **95,** 926–933.

TEMPEL, K. and SCHLEIFER, S., 1995, Adaptive response of the chicken embryo to low doses of x-irradiation. *Radiation and Environmental Biophysics*, **34,** 177–183.

TRAUTINGER, F., KINDAS-MUGGE, I., BARLAN, B., NEUNER, P. and KNOBLER, R. M., 1995, 72-kD heat shock protein is a mediator of resistance to ultraviolet B light. *Journal of Investigative Dermatology*, **105,** 160–162.

UBEDA, A., TRILLO, M. A., CHACON, L., BLANCO, M. J. and LEAL, J., 1994, Chick embryo development can be irreversibly altered by early exposure to weak extremely-low-frequency magnetic fields. *Bioelectromagnetics* , **15,** 385–398.

WILLEY, J. C., LAVECK, M. A., MCCLENDON, I. A. and LECHNER, J. F., 1985, Relationship of ornithine decarboxylase activity and cAMP metabolism to proliferation of normal human bronchial epithelial cells. *Journal of Cellular Physiology*, **124,** 207–212.

WONG, H. R., MENENDEZ, I. Y., RYAN, M. A., DENENBERG, A. G. and WISPE, J. R., 1998, Increased expression of heat shock protein-70 protects A549 cells against hyperoxia. *American Journal of Physiology*, **275,** L836–L841.

YOUBICIER-SIMO, B. J., BOUDARD, F., CABANER, C. and BASTIDE, M., 1997, Biological effects of continuous exposure of embryos and young chickens to electromagnetic fields emitted by video display units. *Bioelectromagnetics* , **18,** 514–523.

ZHANG, X., ROSENSTEIN, B. S., WANG, Y., LEBWOHL, M. and WEI, H., 1997, Identification of possible reactive oxygen species involved in ultraviolet radiation-induced oxidative DNA damage. *Free Radical Biology and Medicine*, **23,** 980–985.

ZIMMERMAN, E. F., POTTURI, R. B., RESNICK, E. and FISHER, J. E., 1994, Role of oxygen free radicals in cocaine-induced vascular disruption in mice. *Teratology*, **49,** 192–201.

Bioelectromagnetics 11:297–312 (1990)

Amplitude Windows and Transiently Augmented Transcription From Exposure to Electromagnetic Fields

T.A. Litovitz, C.J. Montrose, Reba Goodman, and Edward C. Elson

Vitreous State Laboratory, Catholic University of America (T.A.L., C.J.M.) and Walter Reed Army Institute of Research (E.C.E), Washington, DC, Department of Pathology, Columbia University Health Sciences, New York (R.G.)

The exposure of cells to relatively low-intensity, pulsed, low-frequency electromagnetic fields can result in a transient augmentation of mRNA synthesis. Under certain conditions of irradiation, the augmentation is a function of the strength of the electromagnetic field. A linear, multi-step, chemical-reaction model accounts for many of the principal features that are observed in both the time- and intensity-dependent variations of transcriptional effects. The crucial assumption in the model is that the direct effect of electromagnetic fields on exposed cells is an increase in the rate constant that characterizes one of the intermediate sequential reactions in the synthesis of mRNA.

Key words: ELF fields, transient response, chemical-reaction model, rate constant, RNA synthesis

INTRODUCTION

Under certain exposure conditions the effect of extremely low-frequency (ELF) exogenously applied electromagnetic fields on certain measured properties of a biological system is transient [Goodman et al., 1983, 1989ab; Goodman and Henderson, 1986]. The system's response, determined by some well-defined endpoint, first rises following the switching on of the field, reaches some maximal value, and then decays, ultimately approaching some steady-state value (which may be the original equilibrium of basal value). It has also been reported that the magnitude of a system's response, both to ELF fields and to microwave fields amplitude-modulated at ELF, depends on the field strength, exhibiting maxima [Goodman et al., 1989a,b; Blackman et al., 1989] when regarded as a function of the exogenous field strength. In this paper we suggest an intimate connection between these two observations, in particular, that the maxima may arise simply from observing the transient response at a fixed exposure time following the switching-on of the exogenous field.

As an example, suppose that we are monitoring the concentration of some

Received for review June 27, 1990; revision received August 23, 1990.

Address reprint requests to T.A. Litovitz, Vitreous State Laboratory, The Catholic University of America, Washington, DC 20064.

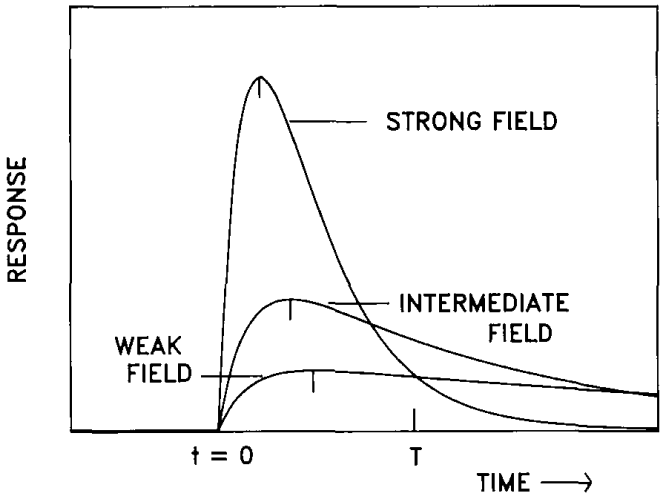

Fig. 1. The schematic representation of a transient response by a system to three different exposure levels of an electromagnetic field switched on at time t = 0.

particular species of messenger RNA as a function of time following the switching on of the field at t = 0. We suppose that, as a function of time, the mRNA concentration initially rises to some maximal value and then decays to a steady-state level (the exogenous field remaining on). Let us further suppose that the system's response depends on the strength or power density of the incident field such that increasing the strength 1) increases the maximal value of the system's response (the peak is higher) and 2) accelerates the system's response (the peak occurs sooner after switching on the field). Under such conditions the responses associated with three different field strengths will look something like the curves shown in Figure 1.

Next, consider that rather than being monitored as a function of time, the mRNA (or any other suitable end point) is measured only for some fixed exposure time T following the initial switching on of the field. Such an experiment might be designed to probe, for instance, the response of the system to the exposure for a time = T as a function of the field strength (irradiating power density). For the curves shown in Figure 1, the time = T exposure data would be represented by the bar graph in Figure 2. There is apparently a region of maximal sensitivity even though our assumptions above would seem to legislate explicitly against such behavior. This peaking of the response as a function of the strength of the applied field is sometimes termed (rather inexactly, to be sure) a "power window." The conclusion to be drawn is clear: Observations of amplitude windows must be viewed cautiously, especially if they involve measurements made not as a function of exposure time, but rather for a single exposure duration.

Observe that this conclusion rests on three, perhaps not-too-unreasonable assumptions: 1) there is a transient response to an impressed field; 2) there is a maximal response that increases with increasing strength of the irradiating field; and 3) there is a peak location that shifts to an earlier time as the field strength is increased. Is there some simple physical model that contains this kind of behavior? In the next section, we suggest that there is, and that this simple model—which is surely much too crude to portray accurately a process as complex as, for instance, RNA or protein synthesis—can nevertheless prove useful as a guide for designing and as a vehicle for interpreting in vitro experiments involving electromagnetic fields.

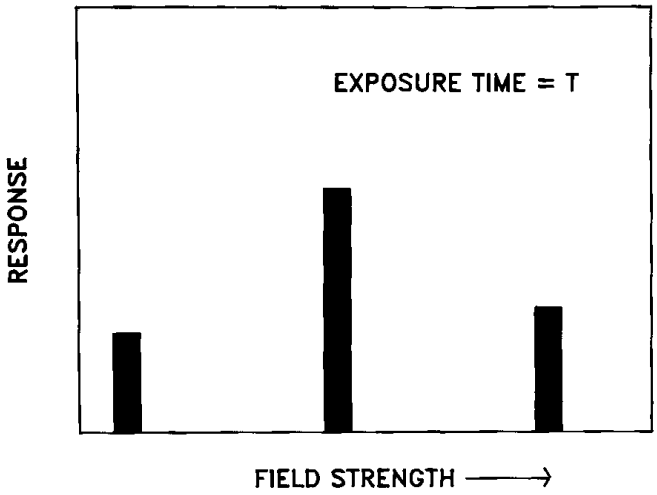

Fig. 2. The schematic representation of an apparent power window resulting from observing the system's response only for a fixed exposure time T in Figure 1.

I. DESCRIPTION OF THE MODEL

For the sake of definiteness we shall present the model as one intended to describe field-enhanced transcription, although it can profitably be used to conceptualize a variety of field-altered processes. We envision a series of events, modeled by a set of sequential, first-order chemical reactions:

$$\begin{bmatrix}\textit{Nucleotide}\\ \textit{reservoir}\end{bmatrix} \rightarrow \begin{bmatrix}\textit{Positioned}\\ G,\ C,\ A,\ U\end{bmatrix} \rightarrow [mRNA] \rightarrow \cdots$$

Diffusion Polymerization Degradation

$$[A] \xrightarrow[k_1]{} [X] \xrightarrow[k_2]{} [Y] \xrightarrow[k_3]{} \cdots$$

The first step (rate constant = k_1) represents the diffusion-controlled migration to, and the "positioning" and orienting of, the various nucleotides from the cellular pool (we designate the nucleotide reservoir concentration by A) in their "correct" sites in the neighborhood of the DNA molecule. The second reaction step (rate constant = k_2) is the polymerization of the positioned and oriented G, C, A, and U nucleotides (the concentration of which we designate by x) to form messenger RNA (concentration denoted by y). The final step (rate constant = k_3) is the degradation of messenger RNA by cytoplasmic nucleases. We assume that the reactions are strongly biased in the forward direction, and that only these rate constants need be considered.

Of course, we recognize that what we have described as a *single* reaction step in actuality consists of a number of complex individual processes. Our assumption is that among these processes there is one that is "rate-determining" so that the simplification shown above is meaningful. No qualitative changes in the model's predictions would result if additional steps were added to the sequence, although the equations would become more complicated and the exact shapes of the response curves would be altered.

TABLE 1. Definition of Symbols

Symbol	Definition
A	Concentration in nucleotide pool; assumed constant
K	Rate constant for protein formation reaction
k_1	Rate constant for $A \rightarrow X$ reaction (diffusion controlled positioning of nucleotides)
k_2	Rate constant for $X \rightarrow Y$ reaction (mRNA polymerization) reaction with no exogenous field
k_2^*	Rate constant for $X \rightarrow Y$ reaction (mRNA polymerization) in presence of exogenous field
k_3	Rate constant for degradation of Y (mRNA) assuming this to be unaffected by an exogenous field
k_3^*	Rate constant for degradation of Y (mRNA) assuming this to be altered by an exogenous field
t	Time after switching on the external field
t_{max}	Time at which y reaches a maximum
x, y, z	Time-dependent concentrations of X, Y, and Z
x_0, y_0	Zero-field equilibrium concentrations of X and Y
y_{max}	Concentration of Y (mRNA) at time t_{max}
α	Rate of degradation of Z (protein)
δy	*Change in* y for $t > 0$, $y(t) - y_0$
Δk	$k_2 - k_2^*$, field-produced change in k_2

Mathematical Formulation

In the development of the mathematical ideas presented below all symbols are defined explicitly when they are first used. For convenience these definitions are also collected in Table 1.

We assume that the nucleotide reservoir is rapidly replenished (that is, that it is not depleted) and, as noted above, that any back-reactions can be neglected. We then describe these reactions by a set of linear first-order differential equations

$$dx/dt = + k_1A - k_2x; \tag{1a}$$

$$dy/dt = + k_2x - k_3y. \tag{1b}$$

The equilibrium values (in the absence of any external electromagnetic fields) are easy to determine from $dx/dt = dy/dt = 0$:

$$x_{eq} = x_0 = k_1A/k_2; \tag{2a}$$

$$y_{eq} = y_0 = k_2x_0/k_2 = k_1A/k_3. \tag{2b}$$

We now make our hypothesis regarding the effect of the exogenous electromagnetic field: Switching on the electromagnetic field at t = 0 produces a "sudden" increase in k_2, that is

$$k_2 \rightarrow k_2^*$$

with this change occurring on a time scale that is short compared with the inverse reaction rates.

With this hypothesis, it is now a straightforward matter to solve the differential equations to determine the concentrations as functions of time:

$$x(t) = \frac{k_1 A}{k_2^*}\left[1 + \frac{\Delta k}{k_2} e^{-k_2^* t}\right]; \tag{3}$$

and

$$y(t) = \frac{k_1 A}{k_3} + \frac{k_1 A}{k_3 - k_2^*}\frac{\Delta k}{k_2}\left[e^{-k_2^* t} - e^{k_3 t}\right], \tag{4}$$

where

$$\Delta k = k_2^* - k_2. \tag{5}$$

The quantities $x(t)$ and $y(t)$ (the mRNA concentration) are plotted in Figures 3 and 4 for three values of the altered rate constant k_2^*.

The parameters for the plots are given in a set of reduced units. From the differential equations (1), it is clear that the rate constants (the k_j) have units of $(\text{time})^{-1}$. It is therefore sensible to choose one of them as defining the basic time unit: we do this by setting $k_1 = 1$. In a similar fashion, we take A as the basic concentration unit, i.e., $A = 1$. Equivalently, we may regard all rate constants and concentrations as being given by ratios with k_1 and A, respectively:

$$k_j \rightarrow k_j/k_1,\ x \rightarrow x/A \text{ and } y \rightarrow y/A.$$

Similarly times can be regarded as products with k_1:

$$t \rightarrow k_1 t$$

For the plots in Figures 3 and 4 we have taken $k_2 = 1$, $k_3 = 10$, and $k_2^* = 3$, 10, and 30.

Observe from Figure 4 that, independent of the value of k_2^*, the long-time, steady-state, field-on concentration is the same as the zero-field concentration—the basal level, i.e., $y(\infty) = y(0)$. The transient character of the response in this model is relatively easy to understand. The initial increase in $y(t)$ arises from the enhanced rate k_2^* (the polymerization rate); the drop off at long times (back to the equilibrium value) comes from the depletion of the precursors x (the "positioned and oriented" nucleotides). Note in particular that 1) the position of the maximum of $y(t)$ marked by "|" on the plots moves toward t = 0 with increasing k_2^* and 2) the peak height increases with increasing k_2^*.

Apparent Amplitude Windows

If we were now to assume that Δk increases with irradiating field strength (or power density), that is, the change in the rate constant governing the $X \rightarrow Y$ reaction (the production of mRNA) increases with the intensity of the electromagnetic field, *then all features of the transient responses would be qualitatively reproduced by this simple model.*

Note in particular that for the parameters chosen for this sample calculation, an exposure time $t_x = 0.25$ (marked on Figure 4 by a vertical line) leads to the appearance of a maximum in the response considered as a function of k_2^*, the field strength or power density. This window is illustrated on the bar graph in Figure 5. Note that

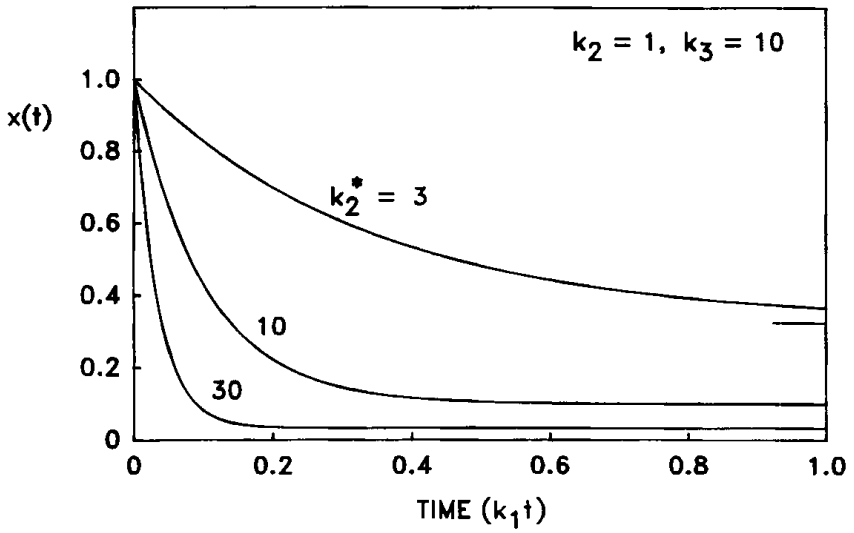

Fig. 3. The prediction of the multi-step model for the temporal evolution of the concentration x(t) following the switching on of the exogenous electromagnetic field at time = 0. The curves are calculated from equation 3 for the three values of k_2* shown.

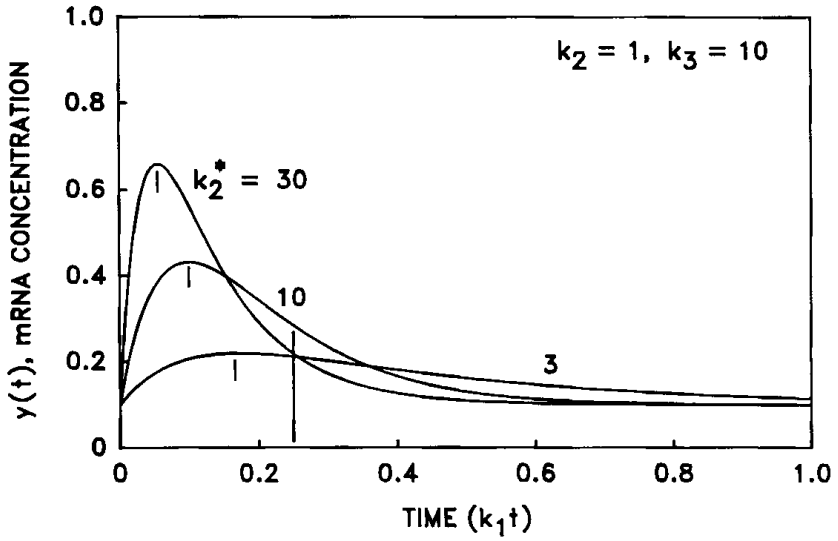

Fig. 4. The prediction of the multi-step model for the temporal evolution of the concentration y(t) following the switching on of the exogenous electromagnetic field at time = 0. The curves are calculated from equation 3 for the three values of k_2* shown.

for shorter exposure times (illustrated in Figure 5 is the case of an exposure time $t_x = 0.12$) the maximum shifts at higher power densities. The point is that, within the context of the linear-reaction model, fixed observation times will *always* lead to the appearance of a maximum in the response regarded as a function of the field strength, with the location of the maximum a function of the exposure times.

The Peak in the Transient Response

The location in time of the peak that is observed in the response of the system can be determined by differentiating equation 4. The result is

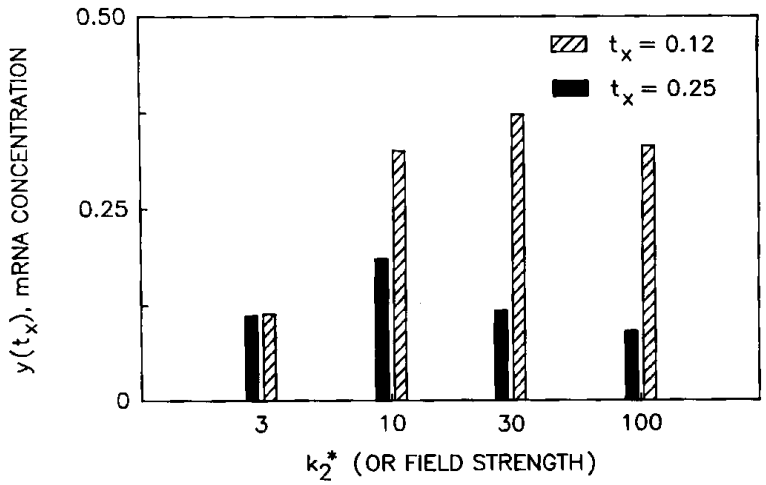

Fig. 5. The amplitude windows that result from observing the response shown in Figure 4 as a function of field strength (k_2^*) for two fixed exposure times: $t_x = 0.12$ and $t_x = 0.25$.

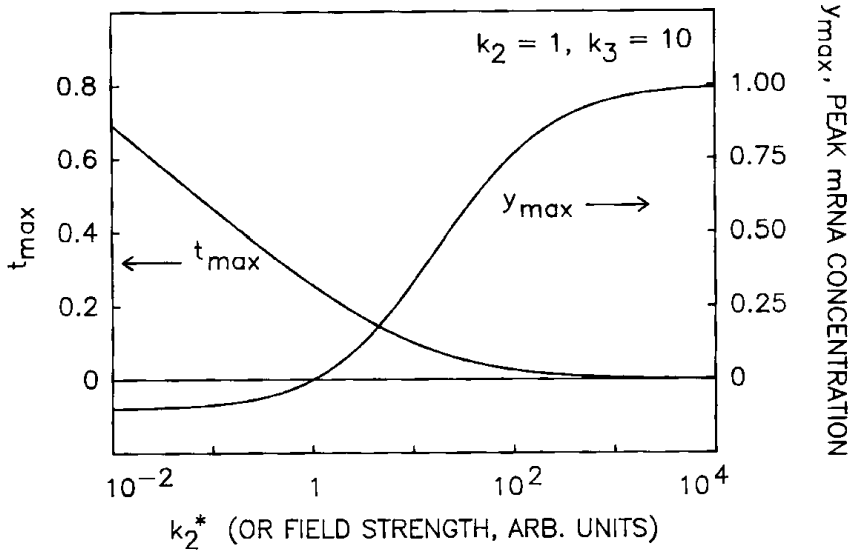

Fig. 6. The dependence on field strength (or k_2^*) of the location in time (left scale) of the peak value of $y(t)$, i.e., t_{max} and the variation of the magnitude of the peak value $y_{max} = y(t_{max})$ (right scale) with field strength.

$$t_{\max} = \frac{1}{k_3 - k_2^*} \ln (k_3/k_2^*) \tag{6}$$

and the magnitude of the maximal response is given by substituting this back in equation 4. Defining $y_{\max} = y(t_{\max})$ leads to

$$y_{\max} = \frac{k_1 A}{k_3} + \frac{k_1 A}{k_3 - k_2^*} \frac{\Delta k}{k_2^*} [(k_2^*/k_3)^{k_2^*/(k_3 - k_2^*)} - (k_2^*/k_3)^{k_3/(k_3 - k_2^*)}]. \tag{7}$$

Both t_{max} and y_{max} are plotted as functions of the changed rate constant k_2^* in Figure 6. Observe that $y_{\max}$ saturates as k_2^* is increased so that the peak height cannot be

used as a measure of the change in k_2. That is, for large values of k_2^* the peak height does not change although the location of the peak does shift to shorter times. This saturation occurs when k_2^* has become so large that it no longer limits the polymerization rate; the production of mRNA is controlled exclusively by the availability of the positioned nucleotide precursors.

Short-time and Long-time Behavior

The change in k_2 produced by switching on the field can be found from the initial rate of change of the response. Expanding equation 4 about t = 0 shows that y increases linearly for short times:

$$y(t) - y_0 \equiv \delta y(t) \approx \frac{k_3}{k_2} \Delta k \; t \qquad (t << t_{max}). \tag{8}$$

From this it follows that the initial slope of the response is directly proportional to the magnitude of the change in k_2, that is to Δk.

Note also the behavior of the response at long times. With the field remaining on, the system marked (mRNA) returns to its equilibrium value at a rate determined by the *smaller* of the reaction rates k_2^* and k_3. Specifically, if one of the rates is much larger than the other, we have

$$\left[\frac{d}{dt} \ln \delta y\right]_{t \to \infty} \approx -k_< \qquad (k_< << k_>), \tag{9}$$

where $k_<$ ($k_>$) is the smaller (larger) of k_2^* and k_3.

The Effect of mRNA Stabilization

In the reaction model just described, the transient increase and subsequent fall of the measured marker (mRNA) was produced by assuming that the effect of the impressed field is to *increase the polymerization rate (the rate of mRNA production).* It is reasonable to inquire if a similar result can be derived if we assume that the effect of the field is to stabilize the mRNA, that is, to decrease its rate of degradation. The answer is that within the context of this elementary linear picture, it is not. If we had assumed, for example, that switching on the field at t = 0 causes k_3 to be suddenly changed to some new value k_3^* ($<k_3$), then we would obtain for the response

$$x = \frac{k_1 A}{k_2} = a \; constant, \; i.e., \; no \; change,$$

and

$$y(t) = \frac{k_1 A}{k_3^*}\left[1 - \left(\frac{k_3 - k_3^*}{k_3}\right) e^{-k_3^* t}\right].$$

The mRNA concentration simply rises montonically from its initial level k_1A/k_3 to an increased level k_1A/k_3^*; there is no later return to the pre-exposure level.

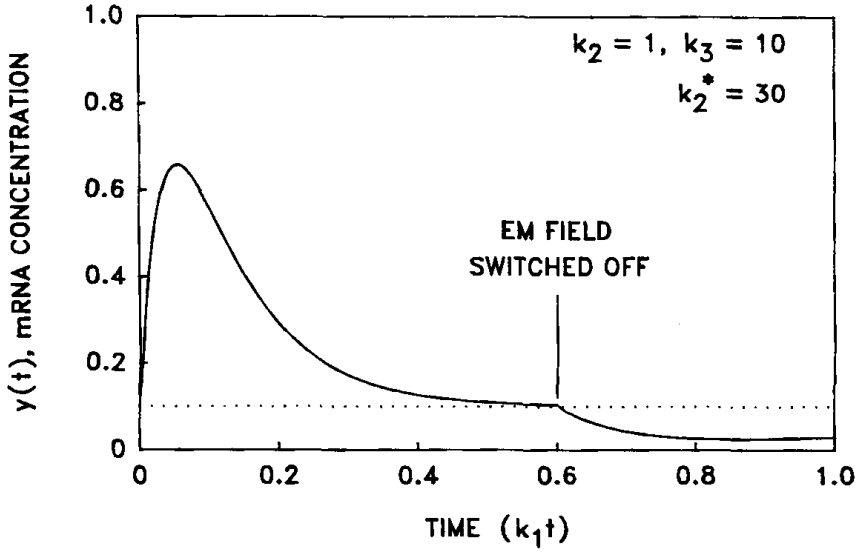

Fig. 7. The time dependence of the concentration $y(t)$ for exposure conditions in which the EM field is switched on at time = 0 and off at time = 0.6 (after y has returned to its basal level). At long times (not shown) the "rebound effect" vanishes as the concentration returns to its pre-exposure, equilibrium value, here 0.1.

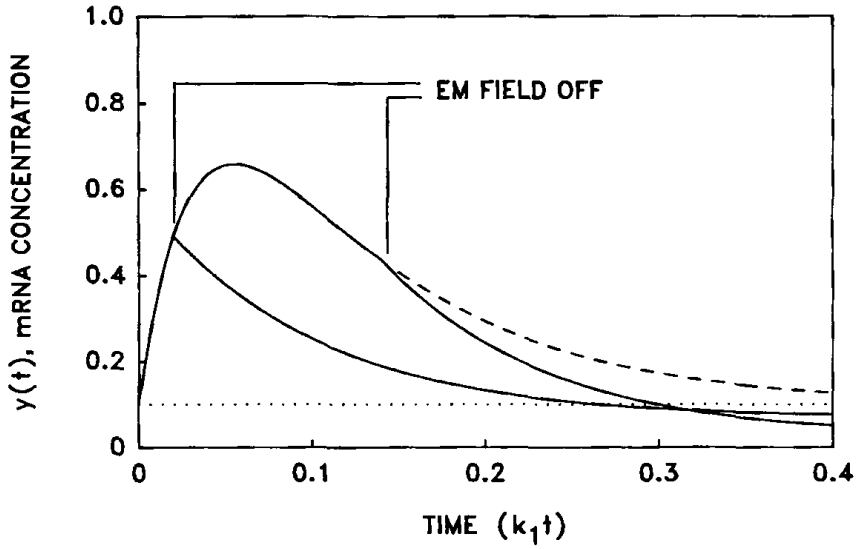

Fig. 8. The time dependence of the concentration of $y(t)$ for exposure conditions under which the EM field is switched on at time = 0 and off at two different times (0.03 and 0.14) during the transient-response period. The broken curve illustrates behavior when the field is allowed to remain on. All curves return to the equilibrium level of 0.1 at long times.

The Rebound Effect

We close this section by noting the effect of switching *off* the impressed field. Assuming that the effect of the electromagnetic field on the rate constant is reversible (which seems reasonable because we are considering relatively weak fields), then the task is to solve again the differential equations for $t \geq t_0$ (the time at which the field is switched off) using k_2 rather than k_2^*. For simplicity we consider first the effect of

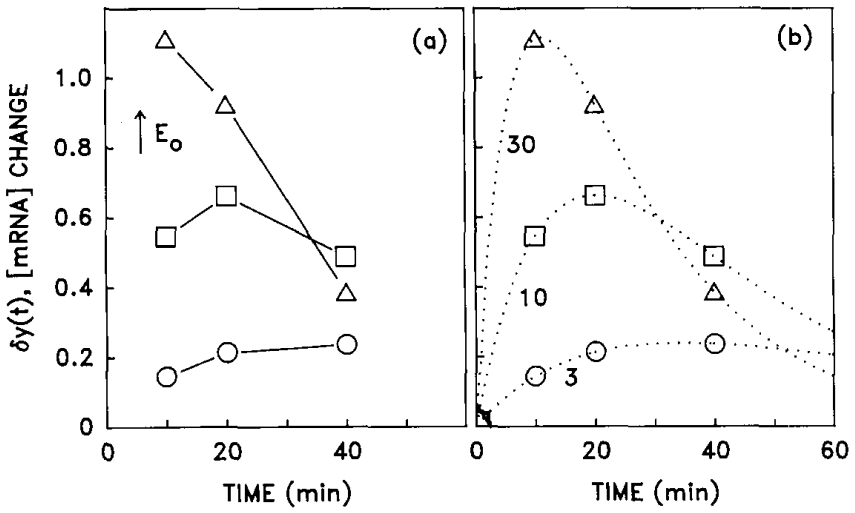

Fig. 9. **(a):** "Data" on the deviation of y from its equilibrium value obtained from evaluating equation 4 at times of 10, 20, and 40 minutes assuming $k_1 = 0.005\ min^{-1}$ and other parameters as shown in Figure 4. The circles, squares, and triangles, respectively, represent values of $k_2^*/k_1 = 3$, 10, and 30. **(b):** The same data with the time = 0 data points and the full curves shown in Figure 4 added.

turning off the field *after the mRNA concentration has returned to its pre-irradiation equilibrium value.* This is shown for $k_2^* = 30$ in Figure 7. Note the drop below the steady-state value immediately following the cessation of irradiation; the concentration reaches a minimum, and then slowly returns to its equilibrium value. The "rebound" is easily understood as resulting from the suddenly decreased rate of mRNA production ($k_2 < k_2^*$) coupled with the depleted population of appropriately positioned nucleotides.

If the exposure field is switched off at a time prior to the system's response returning to its pre-exposure level, then the effect is a sudden decrease in the system's response (the mRNA concentration) leading to an overshoot of the basal value, and, finally, to a slow return to this equilibrium value. This behavior is illustrated for two different "switch-off" times in Figure 8.

II. IMPLICATIONS OF THE MODEL FOR EXPERIMENTATION

For a variety of reasons experiments are seldom carried out as a function of exposure duration. Even in those instances in which time-dependent responses are measured, the data are usually confined to measurements made at rather widely separated times, and perhaps at only a few field strengths so that the actual character of the variation may not be apparent. In the paragraphs below, we consider a few examples of the difficulties that may be encountered.

A. Experimental Difficulties: Detecting Transient Responses

Generally, experimental measurements of, for example, mRNA production are not made continuously as a function of time after switching on the external field, nor are they routinely carried on for very long times. Consequently, it is quite possible for the specific set of experimental parameters chosen for a given investigation that the "true" nature of the system's behavior might be missed. This situation is illustrated

by considering the "data" shown in Figure 9. These data were created by use of the same parameters as those that generated Figures 3 and 4, taking as the defining time unit $k_1 = 0.3\ hr^{-1}$ ($= 0.005\ min^{-1}$, and then assuming that measurements of mRNA concentration were made after exposure intervals of 10, 20, and 40 minutes. These "data" are plotted in Figure 9(a) for three external field strengths $E_0 = E_1, E_2$, and E_3 ($E_1 < E_2 < E_3$) that correspond to the three values of k_2^* used to generate Figure 4. No unifying theme is obvious in these plots: at the highest field strength, the data decrease monotonically; at the lowest field strength they increase; and at the intermediate field strength they exhibit a maximum at t = 20 minutes. When the time = 0 point ($\delta y(0) = 0$) is added, and the set of curves computed from the model is superimposed, as in Figure 9(b), a coherent picture emerges. Of course, when the data are based on "real" laboratory measurements, there are no predetermined curves to superimpose on the results and, consequently, the interpretation of the measurements is not nearly so straightforward. The point is that it is difficult (at best) to infer the correct nature of a transient biological response from a small set of isolated points measured over a limited range of time.

B. Experimental Difficulties: Non-zero Quenching Times

Another factor complicating measurements, especially at higher field strengths (larger k_2^* values), is the rapid fall in the system's response that occurs immediately after the sample is removed from the electromagnetic field (see Fig. 8). To clarify the nature of this problem we consider a specific example.

Consider the "data" shown in Figure 9. If these had been real data, they would have been obtained by exposing a suitably prepared sample of cells to the desired electromagnetic field (produced perhaps by a solenoid or a Helmholtz coil) with adequate provision being made to maintain the experimental system at the desired temperature, usually 37 °C. After exposure for desired time, the sample is removed from the exposure chamber and is quenched—its temperature is quickly reduced to the neighborhood of 0 °C—so that biological processes are thermally arrested. Suitable assays are then carried out to obtain the desired concentration values (or quantities that are proportional to them).

Suppose that samples are removed for assay after 5, 10, 20, and 40 minutes of exposure to the electromagnetic field. Suppose, too, that an interval of 3 minutes is required to quench the samples; that is, for 3 minutes following their removal from the field, the mRNA levels decrease in the manner shown in Figure 8 because of the reduction in the polymerization rate from k_2^* to the original rate k_2. As a result, the measured mRNA concentrations will differ from the "correct" values; this is shown in Table 2. The differences are in a range from about 10–15%, but the qualitative behavior of the data is unchanged. Also shown is a similar comparison obtained by assuming that 1 minute is required to quench the samples. Here the differences are significantly less (only 3–5%), as expected.

If the first point (the 5-minute point) is used to determine the initial slope of the response-versus-time curve, and then this initial slope is combined with equation 8 to obtain Δk, one must be concerned both with the errors that are introduced due to non-zero quenching times and because the curves may not be linear at times as long as 5 minutes. For the examples discussed in this section with $k_2^* = 0.05$ and 0.15 min^{-1} ($k_1 = k_2 = 0.005\ min^{-1}$ and $k_3 = 0.05\ min^{-1}$), the errors in Δk that would result from assuming linearity out to 5 minutes are of the order of 30–40%. As a

TABLE 2. The Effect of "Slow" Quenching

Exposure time (min)	Strong field ($k_2^* = 0.15$)[a] "Measured" [mRNA]	Strong field ($k_2^* = 0.15$)[a] "Actual" [mRNA]	Weak field ($k_2^* = .05$)[a] "Measured" [mRNA]	Weak field ($k_2^* = .05$)[a] "Actual" [mRNA]
Three-Minute Quenching				
5	0.475	0.544	0.248	0.275
10	0.568	0.656	0.330	0.373
20	0.484	0.561	0.377	0.431
40	0.253	0.293	0.299	0.344
One-Minute Quenching				
5	0.520	0.544	0.266	0.275
10	0.635	0.656	0.358	0.373
20	0.534	0.561	0.412	0.431
40	0.279	0.293	0.328	0.344

[a]The value of k_2^* is given here in units of min^{-1}. These are related to the reduced unit values of k_2^* by taking $k_1 = 0.005\ min^{-1} = 0.3\ hr^{-1}$. Given here are results for $k_2^* = 30\ k_1$ and $k_2^* = 10\ k_1$, with $k_2 = k_1$ and $k_3 = 10\ k_1$.

specific case, examine the data set corresponding to $k_2^* = 0.05\ min^{-1}$ ($\Delta k = 0.045\ min^{-1}$). The peak in the response-versus-time curve occurs at about t = 20 minutes. Assuming a linear increase and using equation 8 one would calculate an increased mRNA concentration at 5 minutes of

$$y(t) = 0.100 + (0.045\ min^{-1})(5\ min) = 0.325$$

(all concentrations in reduced units, i.e., relative to $A = 1$); the correct value is $y(t) = 0.275$. Using this value, one would obtain a value for the slope, and thus for Δk, some 22% too low even with instantaneous quenching. For the finite (1- and 3-minute) quenching times illustrated in Table 2, the $y(t)$ values of 0.266 and 0.248 increase these errors, respectively, to 26% and 34%. Even for measurements made 2 minutes after switching on the field the errors would still be 10%, 16%, and 28%, respectively, for 0-, 1-, and 3-minute quenching times.

At lower field strengths, the situation is somewhat better. For $k_2^* = 0.015\ min^{-1}$ ($\Delta k = 0.010\ min^{-1}$, peak at about 35 minutes), the errors resulting from a 5-minute measurement are 15%, 19%, and 28% for 0-, 1-, and 3-minute quenching times. For a 2-minute measurement the comparable errors are 6%, 13%, and 26%. The message is simply that although (we feel) the multi-step reaction model is useful for the conceptualization and understanding of the responses to exogenous fields, as well as for guiding and designing experiments, experimental determinations of the model's parameters are subject to quite large errors (as high as 30–40%), even without accounting for uncertainties in the data. These latter uncertainties may also lead to errors of the same order.

C. Relationship Between k_2^* and the External Field Strength

In the "Introduction" the appearance of a so-called "power" window was shown to follow from some elementary considerations regarding transient phenomena. These were embodied in the multistep reaction model discussed in Section I provided that we assume a monotonically increasing relationship between the change

in k_2 (or k_2^*) and the strength of the impressed field E_0. Examples of possible functional dependencies of Δk on E_0 that one might think about include

$$\Delta k \propto E_0, \ \Delta k \propto E_0^2, \text{ and } \Delta k \propto \exp(\mu E_0/k_B T) - 1,$$

among others (in the last of these μ is a constant parameter, k_B is Boltzmann's constant, and T is the temperature). To determine the relationship between Δk and E_0 it is probably simplest to make use of equation 8, which connects the initial slope of the response-versus-time curve to the change in k_2. We have already noted that neither y_{max} or t_{max} are simply related to k_2^*. Observe from Figure 4 that for large changes in k_2, i.e., high field strengths, these might well be very difficult measurements in that data at rather short times would be required. For instance, if the units of the time axis in Figure 4 were assumed to be hours (the rate constants would then be measured in hours^{-1}), then, for the larger values of k_2^* or field strength, measurements would have to be made on time scales on the order of a few minutes. This is a very challenging experimental task, and it indicates that the dependence of Δk on E_0 can most effectively be determined by measurements made with relatively weak impressed fields. Of course the fields must be large enough that the system's response (the increase in mRNA levels over the unexposed controls) can be accurately determined.

III. A FEW SPECULATIVE IDEAS

A. Protein Synthesis

We can think about the effect of the time-varying mRNA levels on the production of protein in the cytoplasm by recognizing that the rate of synthesis of a protein is proportional to the amount of its corresponding mRNA that is present. The increased amount of mRNA resulting from the EM field ($k_2^* > k_2$) means an enhanced rate of protein production. Designating the excess protein concentration as z, we can then write the governing differential equation as

$$dz/dt = K\delta y - \alpha z, \tag{10}$$

where K is the rate constant describing the protein production and α is the reciprocal lifetime describing the rate at which it is degraded. The solution to equation 10 is straightforward:

$$z = K \frac{k_1 A}{k_3 - k_2^*} \frac{\Delta k}{k_2} \left[\frac{e^{-k_2^* t} - e^{-\alpha t}}{\alpha - k_2} - \frac{e^{-k_3 t} - e^{-\alpha t}}{\alpha - k_3} \right]. \tag{11}$$

This result is plotted—along with $x(t)$ and $y(t)$ from equations 3 and 4—in Figure 10 for the intermediate field value (i.e., $k_2^* = 10$) considered in Figures 3–5. Observe that the peak in excess protein concentration is delayed relative to the mRNA peak. This delay is significant in terms of the field's effect on the organism, as it is certainly the altered protein production that would be most significant. Note also that the peak in the protein response is generally broader than that for mRNA.

B. Regulatory Feedback Effects

A central feature in the mathematical model presented in this paper as well as in the discussion is that of *linearity*. Once the rate constant k_2 is altered by the field,

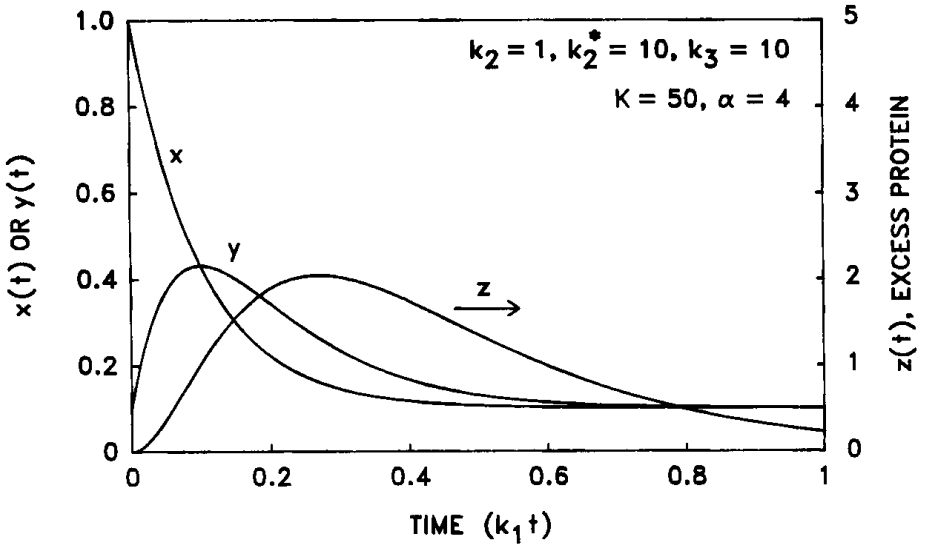

Fig. 10. The time variation of the excess protein, z(t) (right side scale), calculated from equation 11, for an EM-field exposure switched on at time = 0 (note that reduced units are used). The time evolution of x(t) and y(t) (left side scale) for the same conditions are shown for comparison.

the subsequent behavior is prescriptively and predictively determined by a set of rate equations *in which the governing rate parameters* (k_1, k_2, k_3, K, α) *are independent of the local concentrations* (x, y, z) *of the various species*. This is, of course, not the situation at long times. Cells do indeed regulate the production of proteins by a rather complex set of biochemical *sense-and-feedback* mechanisms. Depending on what precisely is sensed, the regulatory processes will operate in different ways to restore basal levels.

Consider the situation depicted in Figure 10 at time = 0.8. At this point the mRNA concentration has returned to its basal level. However the nucleotide concentration, x, is not at its pre-exposure equilibrium level, being reduced by the ratio k_2^*/k_2. Suppose that the cell senses this low value and attempts to correct the deficiency by, for example, increasing the rate k_1 at which nucleotides are brought to the immediate vicinity of DNA. The effect would be to cause a second rise in the production of mRNA and also of its corresponding protein. This second rise might also trigger additional regulatory responses.

Alternatively, suppose that it is the presence of excess protein that is sensed by the cell. Possible responses designed to eliminate the excess could include destabilizing the protein (increasing α) to hasten the degradation of the excess, or decreasing the protein production rate K. Alternatively, it is not inconceivable that the cellular response would be to effect an increase in k_3, the rate of mRNA degradation. This would have the desired effect of reducing the excess protein, but would also cause the mRNA to drop below its basal level to which it has returned by $t \approx 0.6$.

In the preceding few paragraphs, we have anticipated the likelihood that the simple linear model presented in this paper is incomplete. We would like to emphasize that a valuable feature of such a linear model is that it can provide a "baseline" against which to compare the results of experiments. From these paragraphs we see that by probing the directions and magnitude of the deviations from the predictions of

the linear model one can hope to acquire insight into the cell's regulatory responses. For instance, we have suggested that one possibility is the cell's sensing a low value of x and reacting by increasing k_1, leading to a *rise* in mRNA levels. In comparing this rise with the possibility of the second rise in mRNA discussed in the preceding paragraph (in which an excess of protein causes an increase in k_3 and subsequently a *fall* in the mRNA level), we suggest a class of experiments that might prove useful in probing the nature of cellular regulatory mechanisms.

Additional information might be available in this regard by exploiting the "rebound effect" that results when the field is switched off to examine the response to sub-equilibrium values of mRNA. Indeed, one might find that, although the field has been switched off (at say time ≈ 0.6 in Fig. 10), the delayed cellular regulatory processes might lead to "unexpected" time dependences in the mRNA or protein concentrations that act to enhance or to offset the predicted variations.

SUMMARY

The main results of this work include the following:

1. The demonstration that a transient response to EM fields can lead to apparent amplitude windows;
2. The description of a multi-step-reaction model that predicts transient behavior and amplitude windows if one assumes that
   a. Switching on the field causes a sudden increase in an intermediate reaction rate, and
   b. The change in the reaction rate increases with the strength of the EM field;
3. The prediction that switching off the field leads to a "rebound effect" in which the mRNA levels drop below the basal levels;
4. The recognition that these predictions imply certain precautions that must be taken to avoid significant errors in experimentally determining the model's parameters; and
5. The suggestion that deviations from the model's predictions provide a useful probe for attempting to gain insight into the nature of cellular regulatory mechanisms.

ACKNOWLEDGMENTS

This work was supported in part by Contract Number DAMD17-86-6260 with the Walter Reed Army Institute of Research, United States Army Medical Command. That support is gratefully acknowledged by the authors.

REFERENCES

Blackman CF, Kinney LS, House DE, Joines WT (1989): Multiple power-density windows and their possible origin. Bioelectromagnetics 10:115–128. See also the references cited in this paper's "Introduction."

Goodman R, Bassett CAL, Henderson AS (1983): Pulsing electromagnetic fields induce cellular transcription. Science 22:1283–1285.

Goodman R, Henderson AS (1986): Sine waves enhance cellular transcription. Bioelectromagnetics 7:23–29.

Goodman R, Wei L-X, Xu J-C, Henderson AS (1989a): Relationship of Transcript Quantity to Signal

Amplitudes. Presented at the Eleventh Annual Meeting of the Bioelectromagnetics Society, Tucson, AZ, June 18–22, 1989.

Goodman R, Wei L-X, Xu J-C, Henderson AS (1989b): Exposure of Human Cells to Low-Frequency Electromagnetic Fields Results in Quantitative Changes in Transcrips. *Biochimica et Biophysica Acta* 1009:216–220.

Bioelectromagnetics 18:388–395 (1997)

The Role of Temporal Sensing in Bioelectromagnetic Effects

T.A. Litovitz,[1] M. Penafiel,[1] D. Krause,[2] D. Zhang,[2] and J.M. Mullins[2]*

[1]*Department of Physics, The Catholic University of America, Washington, DC*
[2]*Department of Biology, The Catholic University of America, Washington, DC*

Experiments were conducted to see whether the cellular response to electromagnetic (EM) fields occurs through a detection process involving temporal sensing. L929 cells were exposed to 60 Hz magnetic fields and the enhancement of ornithine decarboxylase (ODC) activity was measured to determine cellular response to the field. In one set of experiments, the field was turned alternately off and on at intervals of 0.1 to 50 s. For these experiments, field coherence was maintained by eliminating the insertion of random time intervals upon switching. Intervals $\leq$ 1 s produced no enhancement of ODC activity, but fields switched at intervals $\geq$ 10 s showed ODC activities that were enhanced by a factor of approximately 1.7. These data indicate that it is the interval over which field parameters (e.g., amplitude or frequency) remain constant, rather than the interval over which the field is coherent, that is critical to cellular response to an EMF. In a second set of experiments, designed to determine how long it would take for cells to detect a change in field parameters, the field was interrupted for brief intervals (25–200 ms) once each second throughout exposure. In this situation, the extent of EMF-induced ODC activity depended upon the duration of the interruption. Interruptions $\geq$ 100 ms were detected by the cell as shown by elimination of field-induced enhancement of ODC. That two time constants (0.1 and 10 s) are involved in cellular EMF detection is consistent with the temporal sensing process associated with bacterial chemotaxis. By analogy with bacterial temporal sensing, cells would continuously sample and average an EM field over intervals of about 0.1 s (the ''averaging'' time), storing the averaged value in memory. The cell would compare the stored value with the current average, and respond to the EM field only when field parameters remain constant over intervals of approximately 10 s (the ''memory'' time). *Bioelectromagnetics 18:388–395, 1997.*

Key words: ornithine decarboxylase; cell culture; 60 Hz fields; ''averaging'' time; ''memory'' time

INTRODUCTION

Specific effects induced by exposure of cells to weak, extremely low frequency (ELF), electromagnetic fields (EMFs) continue to be reported but the mechanisms that underlie cellular detection of EM fields are still not understood. It is clearly important to determine the specific molecular interactions involved in EMF detection. Until such information is known, however, aspects of the detection mechanism may be revealed by characterizing the parameters of EM fields that are critical for initiation of a cellular response.

To this end, we previously examined the question of whether cellular response to an EM field requires that the field be coherent, i.e., that field parameters be predictable over time [Litovitz et al., 1991]. Magnetic fields with frequencies of 55, 60, or 65 Hz induce a doubling of ornithine decarboxylase (ODC) activity in L929 cells. To assess the role of field coherence, we exposed these cells to a magnetic field whose frequency was incoherently switched between 55 and 65 Hz at set intervals (coherence times). The resulting enhancement of ODC activity depended upon the time duration of the switching interval. It was necessary to maintain each frequency for approximately 10 s or longer to obtain the same enhancement of ODC activity that was induced by exposure to a field of constant frequency.

The possibility that this 10-s time constant re-

Contract Grant sponsor: National Institute of Environmental Health Sciences (NIEHS), National Institutes of Health (NIH); Contract Grant number: 5 R01 ES0687-02.

*Correspondence to: J. Michael Mullins, Department of Biology, The Catholic University of America, Cardinal Station, Washington, DC 20064.

Received for review 6 May 1996; final revision received 21 January 1997

flected a fundamental property of the cell's ability to detect, and respond to, EMFs was intriguing. Nonetheless, some basic questions were unanswered. (1) Was this fundamental 10-s time constant related only to shifts in field frequency or, as seemed likely to us, would changes in other field parameters (e.g., amplitude, wave form) produce similar results? (2) In the original work, the time duration of each frequency interval was slightly randomized by adding to the basic interval a random period ranging from 0 to 50 ms. This randomization produced phase incoherence, and was the rationale for our use of the term ''coherence time'' to describe the switching intervals. The question remained, however, whether the significant factor was truly the coherence.

Could it be that simply the constancy of field parameters (e.g., frequency or amplitude) determines whether there is a field-induced bioresponse? The work reported here addresses this question. The *amplitude* of the applied magnetic field was varied at regular intervals throughout EMF exposure, and the resultant enhancement of ODC activity was assessed. For these experiments, field coherence was maintained by eliminating the insertion of random time intervals upon switching. Results of this work allow us to determine whether it is the coherence or the simple constancy of the applied field parameters that determines a cellular response.

In considering possible mechanisms for EM field detection that underlie these data, we drew ideas from the well-characterized body of information on bacterial chemotaxis [Koshland, 1981; Segall, et al., 1982; Morimoto and Koshland, 1991]. Motile bacteria use a rudimentary system of memory to sense average values for concentrations of extracellular attractants and repellents, to compare a ''remembered'' average value with a current one, and to direct their swimming based upon measured variation in the average concentration over time. Functioning of this memory depends upon specific interactions between two biochemical events, one that occurs over a few tenths of a second (the averaging time) and one that occurs over intervals of a few seconds (the memory time). Given that our earlier work [Litovitz et al., 1991] demonstrated a time constant on the order of 10 s for the cellular-ODC response to an EM field, we wondered whether a memory function might also be involved in EM field detection and response. To explore this possibility, a series of experiments was initiated to look for a second, shorter time constant comparable to that of the averaging time of the bacterial system. The results of these experiments are discussed in the context of a mechanism that would govern cellular response to EMFs based on the constancy, over time, of EM field parameters.

MATERIALS AND METHODS

Cell Culture, ODC Assay, and Statistical Analysis

Methods for the maintenance of L929 cell cultures, and for the assay of ODC specific activity were done following the procedures described by Litovitz et al. [1994]. To provide blinded experimental conditions, samples were coded by one individual so that neither the exposure condition to which each corresponded, nor the exposure system used to produce it, were known to the person doing the ODC assays. After ODC activities were calculated and recorded, this code was ''broken,'' and the results of the experiment were analyzed. As in our previous work, the results of each exposure were expressed as an ODC activity ratio, obtained by dividing the activity of an EMF-exposed sample by that of its matched, sham-exposed control. Because the ODC activities of control L929 cultures display day-to-day variation, use of the ODC activity ratio allows normalization of experimental results from one day to the next.

We previously demonstrated [Litovitz et al., 1993, 1994] the consistency and effectiveness of the ODC activity ratio for determining the cellular response to applied EM fields. However, some scientists have expressed reservations about the use of ratios to determine whether EMF-induced responses exist. Accordingly, we have also included in this report the results of a statistical analysis done using a paired, two-tailed *t* test to determine the statistical significance of each experimental condition. Tables provided for each experimental condition list the mean ODC activities, $\pm$ standard deviation, for both sham and exposed samples. The paired *P* value for each condition was determined with INSTAT, a statistics program distributed by GraphPad Software, Inc. (San Diego, CA).

Exposure System

All exposures were carried out using a Helmholtz-coil type, ELF exposure system. Sham exposures were concurrently carried out in such a system with the field turned off. The Helmholtz coils, which are E-field shielded and have an average radius of 4.125 inches, were enclosed in a $10 \times 10 \times 10$ inch mu-metal box constructed of mil-annealed Amumetal (Amuneal Manufacturing Corp., Philadelphia, PA). Measurements showed that the magnetic field shielding efficiency of this mu-metal box is approximately a factor of 5 in the ELF range of interest. Each Helmholtz coil unit was housed within a water jacketed, cell culture incubator maintained at 37 °C.

Each exposure condition was carried out using three, stacked, 75 cm^2 tissue culture flasks that were centered between the paired coils and were positioned

so that the magnetic field was parallel to their growth surfaces. The magnetic field distribution within the region occupied by the cells varied by less than ± 15% from the nominal value at the center of the Helmholtz coil.

The Helmholtz coils were operated with a pulse modulated 60 Hz sinusoidal current. The exposure signal was produced using a function generator (TENMA model 72-380, MCM Electronics, Centerville, OH), either of two custom made pulse modulators, and a 35 watt audio amplifier (Realistic model MPA-45, Tandy Corporation, Fort Worth, TX). The Helmholtz coils and a 3Ω series resistor were connected to the 8Ω speaker output of the amplifier. The pulse modulators were used to introduce periodic changes in the signal amplitude. One pulse modulator allowed switching of the signal amplitude between zero and a fixed level, on successive equal time intervals of 0.1, 1, 5, 10, 20, and 50 s. The other modulator allowed momentary interruption of the signal on successive 1-s intervals. The interruption interval was selectable in the range 0 to 500 ms. Additionally, these devices were used to expose cells to fields for which the amplitude was regularly switched between 5 and 15 μT, providing a mean amplitude of 10 μT during the course of exposure.

The on-off transitions used in our experiments resulted in the production of switching transients by the inductive elements, chiefly the Helmholtz coils and power amplifier, in the exposure system. Because the input signal to the amplifier was not synchronized for zero cross-switching, the transients were of variable peak amplitude (less than 25% of the peak-to-peak signal amplitude). Their duration was less than 10 ms. For some exposures input signals were switched at zero crossing points using an Arbitrary Waveform Generator (Hewlett Packard model 33120A). In this case the switching transients were of constant peak amplitude, approximately equal to 25% of the peak-to-peak signal amplitude. The time duration of these transients was also of the order of 10 ms.

To study the bioeffects of transient-free variations in signal amplitude, ODC activity was examined for cells exposed to a 60 Hz signal whose amplitude was varied periodically by amplitude modulating the 60 Hz sinusoid with a 1 Hz sinusoid. The modulation depth was adjusted so that amplitude of the 60 Hz signal varied sinusoidally at 1 Hz between 0 and 10 μT.

RESULTS

Amplitude Switching and the Role of Incoherence

To determine whether variations in field parameters other than frequency would affect the cellular response to EMFs, we conducted a series of exposures in which the amplitude of the applied 60 Hz field was switched between 0 and 10 μT. This was done at intervals, t_c, of 0.1, 1, 5, 10, 20 or 50 s throughout the 4-h exposure period. The field thus alternated between being completely off and then on at an amplitude known to induce enhanced ODC activity. In contrast to our previous experiments with frequency switching, there was no randomization of the intervals by inclusion of additional, random time periods.

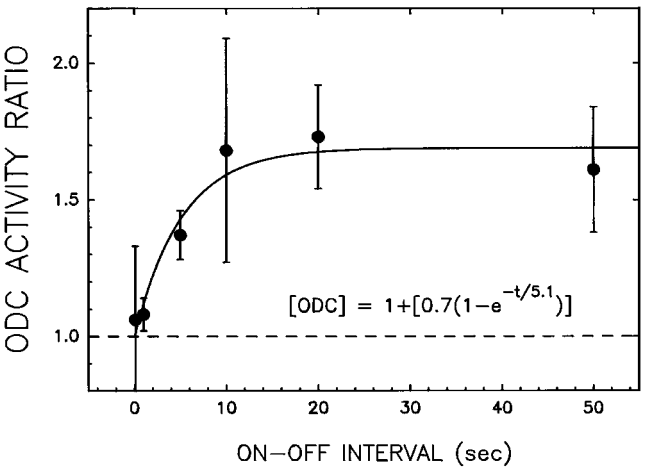

Fig. 1. Response of L929 cultures to 60 Hz fields, which were turned off and on at an interval of 0.1, 1, 5, 10, 20, or 50 s throughout exposure. Results are expressed as the mean ornithine decarboxylase (ODC) activity ratios ± standard deviation. Numbers of separate experiments performed for each data point are given in Table 1.

The results of these experiments are shown in Figure 1. Cells exposed to fields that were turned off and on at t_c intervals ranging from 5 to 50 s displayed statistically significant enhancements in ODC activity. Intervals of 10, 20, or 50 s produced comparable enhancements, with ODC activity ratios of about 1.7. ODC activities of cultures exposed to fields switched at a 5-s t_c interval were also elevated, but to a lesser extent (ODC ratio = 1.4) than those obtained with the longer t_c intervals. In contrast, a t_c interval of 0.1 or 1 s produced no statistically significant enhancement of ODC activity. A statistical analysis of the ODC activity (see ''Materials and Methods'') obtained from these exposures is presented in Table 1. It can be seen from the table that only when t_c was 1 s or less were ODC activities statistically equivalent to those obtained with sham exposure conditions. For longer t_c's, p values were less than .05 indicating that the enhancement of ODC activity shown in Table 1 is statistically significant.

These results are essentially the same as those

TABLE 1. Two-Tailed, Paired *t* Test Analysis of the Effect of Turning the 10 μT, 60 Hz Field Off and On at Regular Intervals Throughout Exposure*

On-off interval (s)	*n*	Mean ODC activity: sham	Mean ODC activity: exposed	*P* value	ODC activity ratio
0.1	6	11.7 ± 4.3	12.9 ± 7.2	0.47	1.1 ± 0.3
1.0	5	54.8 ± 14.9	59.3 ± 16.9	0.06	1.1 ± 0.1
5.0	3	13.0 ± 2.6	17.7 ± 2.7	0.01	1.4 ± 0.1
10.0	11	20.9 ± 8.7	35.9 ± 18.2	0.001	1.7 ± 0.4
20.0	6	13.0 ± 3.2	22.5 ± 5.6	0.001	1.7 ± 0.2
50.0	4	26.0 ± 12.3	38.6 ± 16.5	0.02	1.6 ± 0.2

*Actual units of ODC activity for cultures exposed to the on-off fields were compared with those for the matched, sham-exposed cultures. The ODC activities and activity ratios in this and subsequent tables are expressed as the mean ± standard deviation.

obtained in our previously reported coherence studies in which frequency switching was employed. The obvious difference between the data from these two studies is that the maximum enhancement in ODC activity produced with the on-off fields (ODC ratio ≈ 1.7) was less than that obtained with either frequency-switched or continuous 60 Hz fields (ODC ratio ≈ 2.0). This slight reduction in response may be due to the fact that cells were actually exposed to the applied field for only half of the exposure period during the on-off experiments. Plotted in Figure 2 is a comparison of the results from the two different studies. The data are plotted as percentage of maximum response. In this way, the differences in the maximum response between the two studies do not obscure the similarities. It is clear that the time duration of constancy of the field amplitude determines the magnitude of the cellular response in the same manner as does the time duration of constancy of the frequency of the EMF.

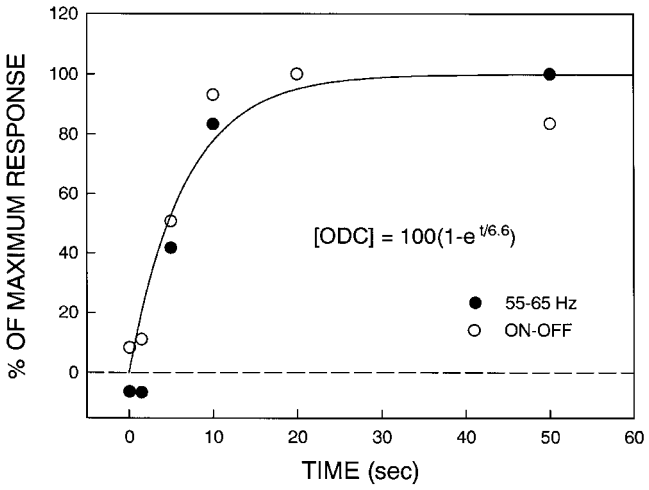

Fig. 2. Comparison of the field-induced ornithine decarboxylase (ODC) responses of L929 cells to on-off fields, as shown in Figure 1, and to fields for which the frequency was shifted between 55 and 65 Hz at the same intervals. Results are normalized as percent of maximum response to allow direct comparisons of the two sets of data. Note that the 0.1- and 1-s time points for the 55–65 Hz data fall below the line that denotes a 0% increase. Mean ODC activities for cells exposed to these conditions were slightly lower than those of their matched control samples, but were not statistically distinguishable from them.

Amplitude switching, as described above, involved turning the field off and on at regular intervals. To be certain that the effects observed were due to time-dependent variations in amplitude level, and not simply to the field being turned off and on, an additional series of exposures was conducted in which the field was constantly applied, but with regular variations in field amplitude. In these experiments the amplitude of the 60 Hz field was switched between 5 and 15 μT every 1 or 10 s throughout the 4-h exposure period. Amplitude thus varied ± 50% around a mean of 10 μT, which value induces a doubling of ODC activity in constant-amplitude exposures. The results of these experiments are shown in Table 2. The ± 50% amplitude fields displayed the same basic time dependency observed with fields for which amplitude was varied between 0 and 10 μT. Amplitude switching at 1.0-s intervals produced no enhancement in ODC activity, but switching at 10-s intervals produced an ODC response that was comparable to that obtained with a 60 Hz field of constant, 10 μT amplitude.

All the results of the amplitude switching experiments were obtained using coherent fields. Thus, the magnitude of the EMF-induced ODC enhancement appears to be determined by the time over which field parameters remain constant, rather than by the time duration of field coherence.

Amplitude Variation Without Transient Fields

In the experiments described above, the variation in amplitude of current delivered to the Helmholtz coils resulted in transient applied fields, which persisted for intervals up to 10 ms during the ''off period'' of field

TABLE 2. Two-Tailed, Paired *t* Test Analysis of the Effect of Switching the Amplitude of the 60 Hz Field Between 5 and 15 μT at Regular Intervals

Exposure condition	*n*	Mean ODC activity: sham	Mean ODC activity: exposed	*P* value	ODC activity ratio
5 to 15 μT, each 1 s	14	15.8 ± 8.3	15.5 ± 9.7	0.69	0.9 ± 0.2
5 to 15 μT, each 10 s	6	16.0 ± 8.7	29.0 ± 14.3	0.006	1.5 ± 0.5

*Actual units of ODC activity for cultures exposed to the amplitude-switched fields were compared with those for the matched, sham-exposed cultures.

exposure. These transient fields are described in detail under ''Materials and Methods.'' To determine whether the transient fields might be a significant factor in the results obtained, an additional set of exposures was conducted in which field amplitude was varied between 0 and 10 μT, but under conditions that produced no transient fields. This was done by using an applied field in which amplitude was varied by slowly modulating the 60 Hz field with a 1 Hz sinusoid. The relationship describing the input voltage to the Helmholtz coil needed to produce this field is given by,

$$V = V_0\,(1 + \cos(\omega_m t))\cos(\omega_c t) \qquad (1)$$

where V_o is the peak amplitude of the 60 Hz input voltage, ω_m is the angular frequency of the modulating signal, ω_c is the angular frequency of the 60 Hz signal, and t is time. The waveform of a field modulated in this manner is represented in Figure 3.

By amplitude modulating the applied field with a 1 Hz sinusoid the introduction of transient fields was avoided, while still varying the amplitude of the field between 0 and 10 μT at a 1 Hz rate. This modulated 60 Hz field yielded an ODC activity ratio of 1.1 ± 0.1 (n = 4). The *t* test analysis of the ODC activities for these exposures is presented in Table 3. Since this result is indistinguishable from those obtained with on-off switching at either 0.1- or 1.0-s constancy times, these results demonstrate that transient fields were not a significant factor in determining the cellular response.

Intermittent Amplitude Variations—Search for the Averaging Time

The results described above indicate that the cell ''knows'' whether or not the field has been on for at least 10 s. For this to be so, detection of the presence of the field would have to occur on a time scale significantly less than 10 s. By analogy with the bacterial chemotaxis system, we reasoned that cells might continuously sample the EM field, ''averaging'' some aspect of the field parameters over a limited time interval (the averaging time) lasting a fraction of a second. Successive, averaged field values would then be compared. If such comparison were to indicate that field parameters had remained constant over an interval of about 10 s, then the cell would initiate, or continue, its response to the applied field. However, if successive comparisons were to indicate a substantial inconstancy of field parameters, no EMF-induced cellular response would occur.

On the basis of this hypothesis, an experiment was devised to search for the putative averaging time. L929 cells were exposed to magnetic field conditions (60 Hz, 10 μT field, 4 h) that normally induce a doubling of ODC activity, but the field was modified by being turned off for a brief interval, Δt, once each second throughout the exposure period. The values of Δt used ranged from 25 to 200 ms. This introduction of periodic ''gaps'' in the field is illustrated by the waveform shown in Figure 4. The idea was that if a memory system were operative for detection of EM

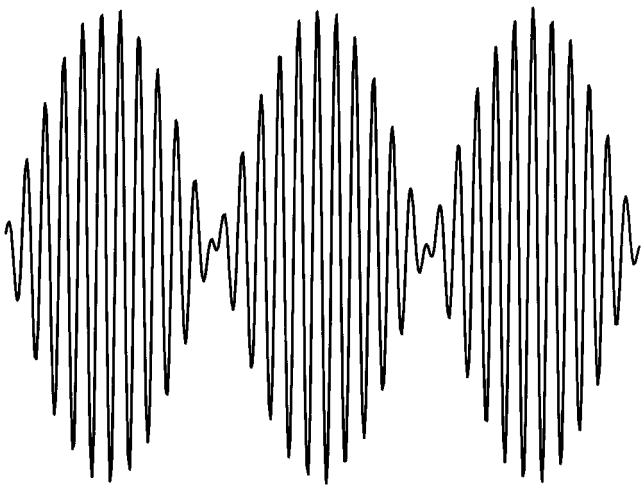

Fig. 3. Diagrammatic representation of the waveform produced by amplitude modulation of a sinusoidal, ELF signal.

TABLE 3. Two-Tailed, Paired *t* Test Analysis of the Effect of Amplitude Modulation of the 60 Hz Field Between 0 and 10 μT at a Frequency of 1 Hz

Exposure condition	*n*	Mean ODC activity: sham	Mean ODC activity: exposed	*P* value[a]	ODC activity ratio
1 Hz AM of 60 Hz Field	4	39.9 ± 10.4	41.5 ± 13.0	0.46	1.1 ± 0.1

[a] The *P* values compare units of ODC activity for cultures exposed to the 1 Hz AM field with those for the matched, sham-exposed cultures.

fields, then a gap in the field, over an interval equal to or longer than the averaging time, would be sensed by the cell as a change in field constancy. Repeating these periodic interruptions throughout the exposure period would, thus, prevent an EMF-induced enhancement in ODC activity. Interruptions lasting only a small fraction of the averaging time, however, would not alter the value of the averaged measurements enough to indicate a change in field parameters. Under these conditions no inhibition of ODC enhancement would occur.

Experiments were performed using both the custom-made modulator, which produced transients with variable peak amplitude at the on to off transitions, and the HP33120A Random Wave Function Generator, which was programmed to generate signals switched at the zero cross points and therefore produced transients with fixed peak amplitude. The response of cells exposed to both types of interrupted fields is displayed in Figure 5. As the figure shows, the ODC response is equivalent in both cases, offering further evidence that the transients do not play a role in the response process.

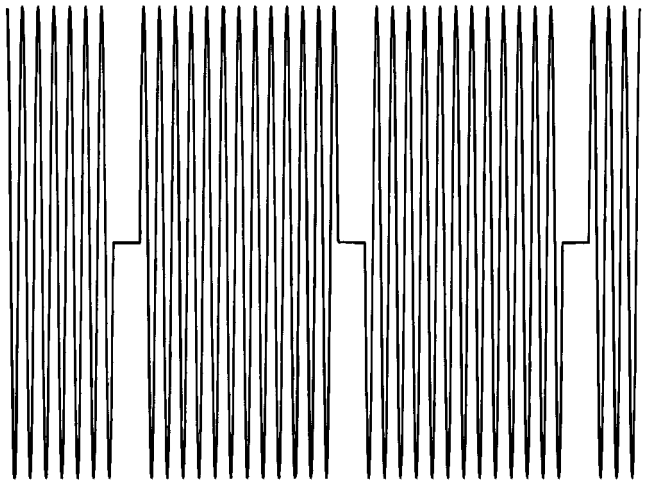

Fig. 4. Diagrammatic representation of the waveform produced by introducing brief, periodic intervals of zero amplitude (''gaps'') into a sinusoidal, ELF signal.

The magnitude of field-induced enhancement of ODC activity decreased with increasing Δt. The shortest Δt examined, 25 ms, resulted in an ODC enhancement which was approximately 60% of that induced by exposure to an uninterrupted field . As Δt was increased to 50 and 75 ms, there were corresponding decreases in ODC activity ratios. At Δt's of 100 or 200 ms, ODC activities of exposed cells were statistically indistinguishable from those of matched, sham-exposed cultures. Field-induced ODC enhancement was, thus, completely eliminated when $\Delta t \geq 100$ ms. Table 4 presents the results of paired, *t* test analysis of the ODC activity for these exposures. The resultant *P* values show that there was a statistically significant difference

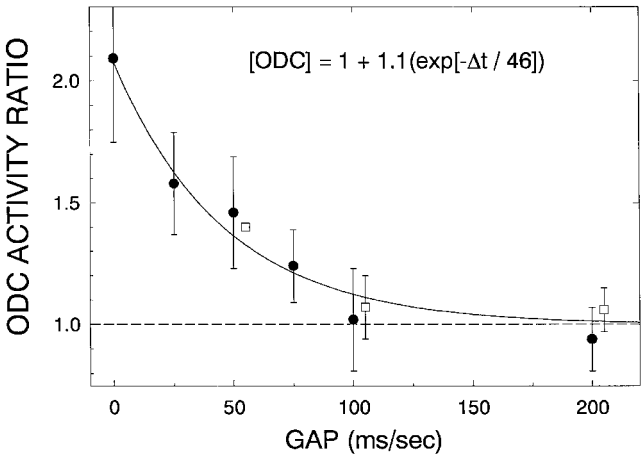

Fig. 5. The effect of the introduction of brief intervals of zero amplitude (''gaps'') into the 10 μT, 60 Hz field once each second throughout exposure. Gap durations (Δt) ranged from 25 to 200 ms. Results are expressed as the mean ornithine decarboxylase (ODC) activity ratios ± standard deviation. Data obtained with our custom-made, amplitude switching device are displayed as filled circles. Data obtained using the Hewlett Packard (33120A) Arbitrary Waveform Generator are plotted as hollow squares. To avoid overlap of data points, the HP-generated data were displaced horizontally by adding 5 ms to their actual Δt's. The numbers of separate experiments performed for each data point using the custom switching device are given in Table 3. Numbers of experiments performed for the HP-generated data are: 50 ms, n = 3; 100 ms, n = 9, 200 ms, n = 5.

TABLE 4. Two-Tailed, Paired *t* Test Analysis of the Effect of Introducing Brief, Zero Amplitude Gaps, Once Each Second, Into the 10 μT, 60 Hz Field*

GAP interval (ms)	*n*	Mean ODC activity: sham	Mean ODC activity: exposed	*P* value	ODC activity ratio
25	7	10.1 ± 2.2	15.9 ± 3.7	0.001	1.6 ± 0.2
50	11	12.6 ± 3.9	18.4 ± 6.3	0.0001	1.5 ± 0.2
75	6	13.4 ± 5.0	16.4 ± 6.7	0.03	1.2 ± 0.2
100	7	15.4 ± 5.2	15.5 ± 5.8	0.92	1.0 ± 0.2
200	6	12.0 ± 3.4	11.6 ± 4.0	0.31	0.9 ± 0.1

*Actual units of ODC activity for cultures exposed to the ''gapped'' fields were compared with those for the matched, sham-exposed cultures.

in activities between sham-exposed cultures and cultures exposed to fields with Δt's of 25 and 50 ms, but not for cultures exposed to fields with Δt's of 75, 100, and 200 ms.

The data in Figure 5 were fit by nonlinear regression techniques to the following expression, in which Δt is the time duration (in ms) of the interruption:

$$[O\,D\,C] = 1 + 1.1*\exp(-\Delta t/46) \qquad (2)$$

DISCUSSION

Cellular Response to Electromagnetic Fields: Temporal Sensing

We have attempted to synthesize a picture of the biological EMF detection process that takes into account the approximately 0.1- and 10-sec time constants characterized in this, and in earlier work [Litovitz et al., 1991]. Our thinking has been influenced by the apparent similarities between cellular EMF detection, and the well-understood sensing mechanism of bacterial chemotaxis.

Chemotactic activity of motile bacteria directs their movements toward higher concentrations of attractants, and away from higher concentrations of repellents. Detection of the concentration of a chemotactant molecule depends on a mechanism by which an actively swimming bacterium utilizes memory to compare the concentrations of the molecule that are sampled at different times. As with other memory systems the bacterial memory functions through two processes that occur over different time scales [Koshland, 1981; Segall, et al., 1982; Morimoto and Koshland, 1991]. The first process, a change in signal transduction in response to the binding of chemotactant molecules to cell surface receptors, is rapid, occurring on a time scale $\sim$ 0.04 s. The second process, a reversible, covalent modification of receptors that is promoted if the bacterium encounters uniform concentrations of a chemotactant, occurs more slowly, taking place over a period $\sim$ 5 s. Interplay of these two processes provides the rudimentary, memory that allows the bacterium's swimming pattern to be appropriately modified. Essentially, averaged measurements of concentration are continuously made by the bacterium, which compares successive measurements, and responds to the *difference* between them. This process has been termed *temporal sensing*.

Based on the work reported here, we suggest that cellular detection of EM fields also employs a system of memory, and that this memory functions to determine the extent of the cellular response to the EM field. Details of this proposed mechanism are described in the following sections.

The Memory Time

Results shown here and in previous work [Litovitz, et al., 1991] indicate that unless field amplitude or frequency is fixed over intervals (constancy times) of about 10 s or longer, there is a reduced enhancement of ODC activity compared with that induced by a field whose parameters remain constant in time. When either the amplitude or frequency was varied at intervals (constancy times) of 1 s or less, no EMF-induced enhancement of ODC activity was observed. For intermediate constancy times ($1\text{ s} \leq t_c \leq 10\text{ s}$), the measured ODC enhancement increased between the $t_c \leq 1$ s value (no enhancement) and the $t_c \geq 10$ s value (full enhancement).

The work reported here extends and clarifies our earlier results in two ways:

(1) The elimination of time randomization at each switching point gave the same response as those obtained with insertion of random time intervals. Thus, in our earlier experiments the critical factor was the interval over which frequency was constant, not the interval over which the field was coherent. Accordingly, we have adopted the term ''constancy time,'' rather than ''coherence time,'' to describe the fundamental time constant of this EMF detection process. We now use the symbol τ_c (previously used to denote coherence time) to denote constancy time.

(2) Since essentially identical results were obtained when either frequency or amplitude was varied, the constancy time phenomenon is not limited to field frequency variations. It is reasonable to expect that variations in waveform (which implicitly involve variations in frequency content) would similarly affect ODC response.

Because the cells responded differently to a field whose amplitude, for example, was changed at 5-s intervals versus one whose amplitude was changed at 10-s intervals, it can be inferred that each cell was able to *remember* the field characteristics for a time that was longer than 5 s, so that it could make this comparison. That the results were approximately the same for intervals longer than 10 seconds implies that the memory duration was not necessarily longer than about 10 s. These facts suggest that there is a biological memory mechanism, characterized by a time scale in the 5- to 10-s range, over which some aspect of the imposed EM field is ''sensed,'' enabling this to be remembered and examined for constancy. When there is a substantial change in one of the field parameters (e.g., 100% variation in amplitude at t_c = 1.0 s), the memory is apparently ''reset'' in a much shorter time, and the accumulation of sensed field information begins again.

The Averaging Time

In the discussion below we use the term ''averaging time.'' It should be noted that the average of a sine wave is always zero. Thus the ''averaging'' to which we refer must be either the average of the square of the field, of a rectified signal, or of some similar, nonlinear aspect of the EM field.

Changes in field characteristics at intervals less than about 10 s led to an inhibition of EMF-induced ODC enhancement. However, because sinusoidal fields are continuously changing (a 60 Hz field, for example, exhibits significant changes in the instantaneous values of the field over times as short as 0.001 s — about 5% of a period), it is clear that the biological system must examine for constancy some field characteristic that has been averaged over a time significantly longer than a period of a 60 Hz signal (that is, longer than about 0.01 s). Conversely, because the L929 cells studied here were unresponsive to fields whose constant-amplitude intervals were shorter than 1 s, the EMF detection process must be able to recognize amplitude changes that occur on a time scale less than about 1 s.

Combining the facts and ideas above, we postulated the existence of a time over which the cell averages the EM field to determine its characteristics. To reveal this *averaging time* we conducted the series of gap exposures in which the field was switched off for a brief interval, Δt, each second throughout EMF exposure. The results of the exposure gap experiments are compatible with the existence of an averaging time for EMF detection. Field-induced enhancement of ODC activity was completely suppressed for $\Delta t \approx 0.1$ s or longer, but was greatly reduced when Δt was 0.025 s. Equation 2 suggests that the averaging process utilizes a ''moving average'' by which all the previous values of the field parameters are included in the average. The cell puts emphasis on the more recently obtained values by ''forgetting'' past values exponentially in time. The important time constant here is approximately 50 ms. Thus measurements over the most recent period of about 100 ms play the dominant role in determining the average at any given time.

We recognize that the results presented here are only consistent with, but do not prove, the functioning of a memory system in the ODC response of cells exposed to weak, 60 Hz fields. Clarification of the memory role in EMF detection will require a detailed knowledge of the signal transduction mechanism involved, as has been done for bacterial chemotaxis. Furthermore, it should be recognized that the averaging and memory times determined here are biological constants for the L929/ODC system. Nonetheless, we are impressed that our two time constants are remarkably similar to those observed in bacterial chemotaxis. Whether other EMF-induced bioresponses will display similar time constants, of course, remains to be determined.

ACKNOWLEDGMENTS

The described project's contents are solely the responsibility of the authors and do not necessarily represent the official views of the NIEHS, NIH.

REFERENCES

Litovitz TA, et al. (1991): Effect of coherence time of the applied magnetic field on the enhancement of ornithine decarboxylase activity. Biochem Biophys Res Commun 178:862–865.

Litovitz TA, et al. (1993): The role of coherence time in the effect of microwaves on ornithine decarboxylase activity. Bioelectromagnetics 14:395–403.

Litovitz TA, et al. (1994): Temporally incoherent magnetic fields mitigate the response of biological systems to temporally coherent magnetic fields. Bioelectromagnetics 15:399–409.

Koshland DE Jr. (1981): Biochemistry of sensing and adaptation in a simple bacterial system. Annu Rev Biochem 50:765–782.

Morimoto BH, Koshland DE Jr. (1991): Short-term and long-term memory in single cells. FASEB J 5:2061–2067.

Segall JE, Manson MD, Berg HC (1982): Signal processing times in bacterial chemotaxis. Nature 296:855–857.

Bioelectromagnetics 18:132–141 (1997)

Role of Modulation on the Effect of Microwaves on Ornithine Decarboxylase Activity in L929 Cells

L. Miguel Penafiel,[2] Theodore Litovitz,[2]* David Krause,[1] Abiy Desta,[1] and J. Michael Mullins[1]

[1]*Department of Biology, The Catholic University of America, Washington, DC*
[2]*Vitreous State Laboratory, The Catholic University of America, Washington, DC*

The effect of 835 MHz microwaves on the activity of ornithine decarboxylase (ODC) in L929 murine cells was investigated at an SAR of ~2.5 W/kg. The results depended upon the type of modulation employed. AM frequencies of 16 Hz and 60 Hz produced a transient increase in ODC activity that reached a peak at 8 h of exposure and returned to control levels after 24 h of exposure. In this case, ODC was increased by a maximum of 90% relative to control levels. A 40% increase in ODC activity was also observed after 8 h of exposure with a typical signal from a TDMA digital cellular telephone operating in the middle of its transmission frequency range (~840 MHz). This signal was burst modulated at 50 Hz, with approximately 30% duty cycle. By contrast, 8 h exposure with 835 MHz microwaves amplitude modulated with speech produced no significant change in ODC activity. Further investigations, with 8 h of exposure to AM microwaves, as a function of modulation frequency, revealed that the response is frequency dependent, decreasing sharply at 6 Hz and 600 Hz. Exposure with 835 MHz microwaves, frequency modulated with a 60 Hz sinusoid, yielded no significant enhancement in ODC activity for exposure times ranging between 2 and 24 h. Similarly, exposure with a typical signal from an AMPS analog cellular telephone, which uses a form of frequency modulation, produced no significant enhancement in ODC activity. Exposure with 835 MHz continuous wave microwaves produced no effects for exposure times between 2 and 24 h, except for a small but statistically significant enhancement in ODC activity after 6 h of exposure. Comparison of these results suggests that effects are much more robust when the modulation causes low-frequency periodic changes in the amplitude of the microwave carrier. *Bioelectromagnetics 18:132–141, 1997.*

Key words: cellular phones; EMFs

INTRODUCTION

Particular attention has been focused recently on the potential health effects of radio frequency (RF) and microwave fields, which are used extensively in telecommunications. The transmission of information via RF or microwave signals is accomplished by applying some form of modulation to a carrier wave, which changes some aspect of this wave as a function of the transmitted information. Basic modulation schemes modify the carrier wave's amplitude, frequency, or phase. However, more complex modulation schemes are often used to minimize transmission errors and increase bandwidth in telecommunications. For instance, in North America, digital cellular telephones transmit information in bursts, thereby introducing an amplitude modulation component onto the carrier. Clearly, a careful assessment of potential biological effects that might result from exposure to such fields must examine the role of modulation.

Because of the prevalence of cellular phone use, part of our investigation focuses on signals of the type used in cellular phone communications. Cellular phones may be broadly classified as analog or digital depending on the modulation scheme employed. Analog cellular phones generally use narrow band FM, which causes phase variations in the carrier with very little amplitude change. The analog standard most com-

Contract Grant sponsor: Department of the Army; Contract Grant number: DAMD 17-86-C-62601.

*Correspondence to: Dr. Theodore Litovitz, Vitreous State Laboratory, The Catholic University of America, Washington, DC 20064.

Received for review 24 November 1995; Final revision received 10 June 1996.

monly used in the United States is the advanced mobile phone system (AMPS). We refer to fields generated using this standard as analog cellular fields. Digital cellular phones operate under various standards. GSM (global system for mobile communications), the pan-European digital system, has gained wide acceptance in Europe. DAMPS (digital AMPS) is still the most commonly used standard in the United States. DAMPS uses a type of modulation referred to as ''time division multiple access'' (TDMA), which quadruples the channel bandwidth by splitting the spectrum of each assigned analog channel [Boucher, 1992]. Under this scheme, cellular phones transmit encoded, digitized information using some form of phase or frequency modulation. Consequently, minimal or no fluctuations in amplitude occur when using this basic modulation scheme. However, transmission is generally implemented in burst mode, which introduces a periodic variation in the amplitude of the carrier. By one commonly used protocol, code bursts, approximately 7 ms in duration, are transmitted at a rate of 50 Hz. We refer to the fields generated by cellular phones operating in this fashion as digital cellular fields.

Previous investigations of biological effects from exposure to RF and microwave fields include a large number of both animal and in vitro studies. Included in the latter category are a number of experiments suggesting that, at SARs <5 W/kg, cellular effects occur primarily from exposure to microwaves that are amplitude modulated or pulse modulated at ELF frequencies. Reported effects include changes in calcium ion efflux [Bawin et al., 1975; Blackman et al., 1979, 1985; Dutta et al., 1984, 1989], changes in enzymatic activity [Byus et al., 1984, 1988; Litovitz et al., 1993], and induction of cellular transformations [Balcer-Kubiczek and Harrison, 1985, 1989, 1991; Czerska et al., 1992]. Some effects in in vitro preparations have also been observed with CW microwaves [Cleary et al., 1990; Krause et al., 1991; Saffer and Profenno, 1992; Garaj-Vrhovac et al., 1992]. However, all the latter studies used SARs greater than or equal to 10 W/kg. The evidence seems to indicate that modulation plays an important role in eliciting a biological response, particularly when exposing with weak (<5 W/kg) microwaves.

In the work reported herein, we investigated the biological response of L929 murine fibroblasts to ELF-modulated and CW 835 MHz microwave fields. The 835 MHz frequency was chosen because it is within the range currently used in many wireless personal communication applications in North America and is therefore of practical relevance. Various modulation methods were examined, including sinusoidal AM and FM, speech AM, analog cellular, and digital cellular. The specific activity of ornithine decarboxylase (ODC), which performs a rate-limiting step in the synthesis of polyamines [Hayashi and Murakami, 1995], was selected as the biological marker for this work. ODC activity has been shown to be a reliable indicator of EMF-induced cellular response [Litovitz et al., 1991]. Additionally, ODC is of interest because recent work has shown that overexpression of the ODC gene in cultured cells facilitates, and in some cases causes, cell transformation [Hibshoosh et al., 1990; Auvinen et al., 1992; Moshier et al., 1993; Ḧoltẗa et al., 1994]. Furthermore, overexpression of ODC in transgenic mice enhances the tumor-promoting effects of PMA [Halmekyẗo et al., 1992]. Given these facts, it is conceivable that the enhancement of ODC activity as the result of EMF exposure is of relevance to questions of potential health risk posed by ambient EM fields.

MATERIALS AND METHODS

Exposure System

All exposures were carried out using a Crawford cell that was housed in a 37 °C, water-jacketed incubator. The Crawford cell, designed for operation between DC and 1,000 MHz (model CC110-SPEC; Instruments for Industry, Farmingdale, NY), was mounted vertically on a rotary table. This arrangement allowed easy access to both sample chambers, located at either side of the center conductor, through doors installed on opposite sides of the Crawford cell. A Hewlett Packard signal generator, model 8657B with RF plug-in 83522A, was used as the microwave signal source.

Amplitude and frequency modulation were accomplished by using the built-in AM and FM inputs of the signal generator. A function generator (TENMA model 72-380; MCM Electronics, Centerville, OH) was used as the signal source for sinusoidal modulation. Modulation with speech was implemented by using the signal available at the speaker output of a radio receiver tuned to a station broadcasting speech. Square wave modulation was implemented with a Hewlett Packard 8403A modulator to control a Hewlett Packard 8730B PIN modulator. Exposure with the cellular telephone signals was accomplished by using a hands-free adapter to couple the output from the telephone antenna to a coaxial line. The telephone was powered by a DC power supply (Hewlett Packard 6267B) to allow long-term operation. The modulated microwave signals (from the signal generator or the cellular telephones) were amplified to the required power level by using a 10 W solid-state microwave amplifier (model 10W1000; Amplifier Research, Souderton, PA). A double stub tuner was used to match the impedance of the loaded Crawford cell.

All amplitude modulation experiments were car-

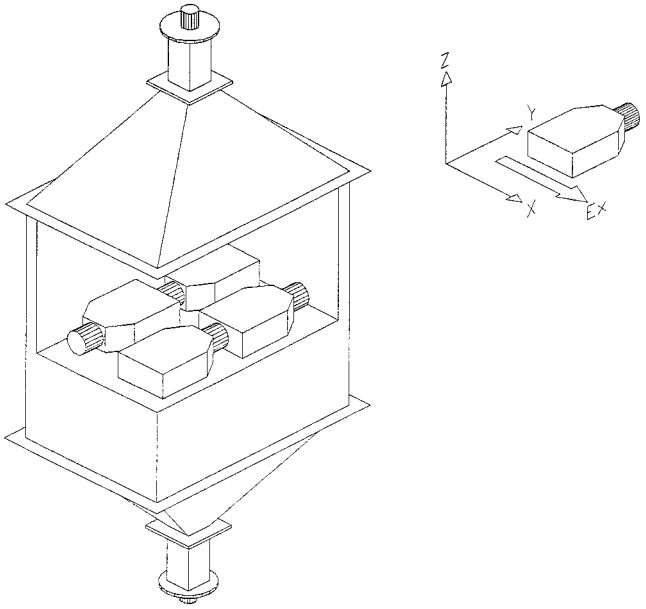

Fig. 1. Detail of the exposure chamber showing placement of the sample flasks. For ease of visualization, a section of the Crawford cell has been cut out and the center conductor is not shown. The samples are placed on nonconducting shelves located at a height of approximately 7 cm from the junction between the center rectangular section of the exposure chamber and the lower tapered end. In this exposure arrangement, the electric field is perpendicular to the direction of wave propagation, which is parallel to the long axis of the exposure chamber. The orientation of the electric field is shown in the inset in relation to the position of a sample flask.

ried out with a modulation index of 0.23, calculated by using the relation $P_t = P_c\ (1 + m^2/2)$, where P_t is the microwave power with modulation, P_c is the microwave power without modulation, and m is the modulation index. When using speech as the modulating signal, P_t was set to the value needed for m = 0.23, on average. All frequency modulation experiments were carried out with the frequency deviation set to approximately ±60 kHz (3 mV signal at the FM input). The square wave modulation experiments were conducted at 50% duty cycle (i.e., the carrier amplitude was zero for 50% of the time during each cycle).

Experiments with cellular telephone signals were conducted using a Motorola Micro TAC Lite analog cellular telephone and a Motorola Digital Cellular Personal Communicator. The test signal was generated by placing the phone in test mode, selecting a transmission channel in the middle of the available range (approximately 840 MHz), selecting the transmission mode (AMPS for analog or TDMA for digital), and enabling continuous transmission of a pseudorandom test sequence. Examination of the output signal from the digital phone with a diode detector and oscilloscope revealed that transmission was executed in bursts lasting approximately 7 ms with a uniform repetition rate of 50 Hz. By contrast, the output signal from the analog phone was found to be constant (i.e., no amplitude modulation).

For each exposure, four 25 cm^2 flasks of L929 cells were used. The flasks, each containing 5 ml of culture medium, were placed as pairs, end to end, on either side of the center conductor (Fig. 1). This configuration ensured overall symmetry, if not complete uniformity, of the electric field distribution within the samples. The SAR distribution for this exposure arrangement has been previously reported [Litovitz et al., 1993]. To determine this distribution, measurements were made on two flasks located at one side of the center conductor. Because of symmetry, the SAR distribution within the other two flasks was assumed to be similar. The experimental SAR is specified as a simple average of the set of measurements within the two flasks, which were taken on a grid of 48 points within each flask. All experiments reported here were conducted with an input power of 0.96 W, which yielded an average SAR of 2.5 W/kg. The SAR distribution corresponding to this average SAR is shown in Figure 2. This SAR produced no measurable temperature increase within the samples.

The average electric field within the sample can be calculated from the average SAR by using the equation $SAR = (\sigma/\rho)|E|^2$ [NCRP report No. 67, 1981],

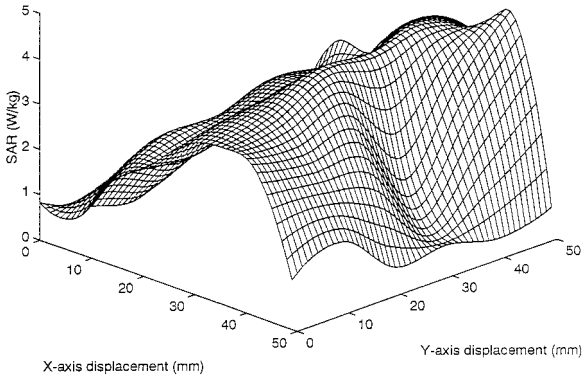

Fig. 2. SAR distribution measured inside the left front flask (see Fig. 1) over the 50 × 50 mm cell growth region located at the bottom of the flask. X and Y axis displacements are measured relative to the left front corner of the square region at the base of the flask. The region of maximal SAR is skewed towards the right back corner of the flask. The SAR decreases by as much as 25% of maximum across the width of the flask and by as much as 75% of maximum across the length of the flask. A somewhat similar distribution was measured inside the left rear flask. In this case, the region of maximal SAR is skewed towards the front right corner of the flask. In the rear flask, the SAR decreases by as much as 25% across both the width and the length of the flask. In both flasks, the regions of maximal SAR are located towards the junction between flasks.

where σ and ρ are, respectively, the conductivity and the density of the aqueous sample. For an SAR of 2.5 W/kg with $\sigma = 1.5$ S/m and $\rho = 1$ g/cm^3, the E-field is on the order of 0.6 V/cm. The field inside the Crawford cell can be calculated by using the relation $E = (PZ_o/d^2)^{1/2}$, where P is the input power, $Z_o = 50\Omega$ is the characteristic impedance of the Crawford cell, and d = 7 cm is the distance between the center conductor and the outer plate. For P = 0.96 W, the electric field within the Crawford cell is on the order of 1 V/cm [correction of our previous calculation of 0.7 V/cm, Litovitz et al., 1993]. The computations of the electric field, both inside the Crawford cell and within the aqueous samples, yield values of the same order of magnitude. This suggests that the SAR measurements are a reasonably good indicator of the electric field in the aqueous interface at the base of the flask, where the tangential components of the electric field must be continuous.

Cell Culture Preparation

Actively growing cultures of the murine L929 fibroblast cell line were maintained in Eagle's minimum essential medium, supplemented as previously reported [Litovitz et al., 1991]. Cell cultures to be used for exposures were initiated approximately 20 h prior to an experiment at a density (3×10^6 cells in 5 ml of culture medium per 25 cm^2 flask) to produce midlogarithmic phase growth by the time of use. Prior to exposure, cells were kept at 37 °C in a 95% air/5% CO_2 atmosphere. Microwave exposures were conducted without CO_2 flow; flasks were sealed for the duration of exposure. Experiments were conducted over approximately a 3 year period. To ensure uniformity of the cell cultures during this time, we maintained multiple ampules of our original L929 cell stocks in liquid nitrogen. New cultures were started from these frozen stocks approximately every 6 months.

Field Exposure Protocol

For each experimental run, four flasks of cells were placed into the Crawford cell for microwave exposure. An incubator shelf, cut to form a platform around the Crawford cell, provided for positioning of four control flasks within the same incubator chamber and at the same height as the flasks within the Crawford cell. Exposure times ranged between 2 and 24 h. Immediately after exposure, the cells in each flask were washed twice with 3 ml of ice-cold phosphate-buffered saline (PBS) and were then collected by gentle scraping in an additional 3 ml of PBS. To provide sufficient protein for the ODC assay, cells were pooled to provide one exposed and one control sample from each experimental run. Cells were pelleted for 5 min at 200*g*, and the resultant cell pellet was resuspended in 1 ml PBS and centrifuged again for 5 min at 200*g*. After removal of the supernatant, the cell pellets were dried by briefly placing the inverted centrifuge tubes onto absorbent paper. These pellets were stored at −75 °C until assay (typically for 3–4 days).

ODC Assay

ODC activity was determined through minor modifications of the method of Seely and Pegg [1983], as previously reported [Litovitz et al., 1991]. Units of ODC activity were expressed as pmol $^{14}CO_2$ generated/30 min/mg protein at 37 °C. Protein analysis was performed with the Bradford method by using a BioRad kit (BioRad Laboratories, Melville, NY). Each cell pellet was lysed in 140 µl of lysis buffer and centrifuged for 5 min at 13,000 rpm. One hundred microliters of the supernatant from each sample was added separately to 150 µl aliquots of the ^{14}C-labeled reaction mixture. $^{14}CO_2$ generated by ODC activity from each sample was absorbed with 100 µl of 1.0 N NaOH. The reaction was allowed to proceed for 1 h with the samples placed in a shaker water bath at 37 °C. At the end of this period, 400 µl of 20% trichloroacetic acid (TCA) was added to each sample to terminate the enzymatic reactions. To measure the ^{14}C activity, each NaOH sample was transferred to a scintillation vial containing 7 µl of acetic acid and 10 ml of fluor. After 2 h, samples were counted in a scintillation counter. Background activity was determined by the use of samples in which ODC activity was eliminated by acid denaturation with TCA.

RESULTS

ODC activity is an effective marker for EM field-induced effects, provided that variations in ODC activity displayed by cell cultures established at different times are accounted for. To allow comparisons of results obtained on different days, we express our data as an ''ODC activity ratio,'' obtained by dividing the mean activity of EMF-exposed samples from a given run by that of matched control samples. The validity of this approach was demonstrated in our previously published work [Litovitz et al., 1993, 1994]. Because some scientists are uncomfortable with the use of such ratios, the results of this work are also expressed in terms of the mean and standard deviation of the measured ODC activity for each exposure condition (see Tables 1–8). The standard deviation of the mean ODC activity data reflects the day-to-day variations in this parameter. Because these variations were often large, the analysis to determine whether the mean difference between exposed and control samples was statistically significant was performed on paired observations by using a standard two-tailed t test. The two-tailed test

was selected because there is no a priori knowledge of the direction of the differences between exposed and control samples.

Because of the large number of experiments performed and exposure conditions examined, the tabulated data summarize separately the results for each exposure condition. Included in the tables are the mean ODC activities of the control and exposed samples, the *P* value of the two-tailed t test, and the mean activity ratio. It should be stressed that the ODC activity ratio is not the ratio of mean E over mean C but rather the ratio of the mean activity of EMF-exposed samples over that of matched control samples.

Exposure With CW Microwaves

We have previously reported that 8 h of exposure with CW microwaves (835 MHz, 8 h, 2.5 W/kg) yielded no measurable changes in ODC activity [Litovitz et al., 1993]. Because AM-induced biological effects were shown to be transient, we decided that a more complete time course of CW exposure should be examined. To this end, experiments were carried out with 835 MHz CW microwaves for exposure times in the range of 2 to 24 h. Table 1 shows the results of these experiments. Exposures of 2, 4, 8, 12, 16, and 24 h yielded no measurable effects and confirmed previous results. However, a statistically significant effect was obtained after 6 h of exposure, which yielded an ODC activity ratio of 1.3.

Exposure With AM Microwave Fields

The ODC response of L929 cells exposed to AM, 835 MHz microwaves was examined as a function of exposure time (2–24 h) at two frequencies, 16 Hz and 60 Hz, and as a function of frequency in the range of 6–600 Hz for the exposure time that produced the most robust response in the time course experiments (8 h). In all cases, the modulation amplitude was adjusted to give a modulation index of 23%.

Dependence on time. Exposure with either 16 Hz or 60 Hz AM microwaves produced a transient enhancement in ODC activity that peaked after 8 h and returned to control levels by 24 h of continuous exposure. Table 2 shows the results of exposure with 16 Hz AM microwaves. Continuous 6 and 8 h exposures of cells produced enhancements in ODC activity that were statistically significant relative to control levels. The other exposure times tested did not induce statistically significant changes in ODC activity. Table 3 shows the results of exposure with 60 Hz AM microwaves. Statistically significant effects were observed after 6, 8, 12, and 16 hours of continuous exposure, but no statistically significant effects were seen after 2, 4, and 24 h of exposure. The peak field-induced ODC activity ratios were 1.5 for 16 Hz AM and 1.9 for 60 Hz AM.

Dependence on frequency. Having determined that an exposure time of 8 h produced a peak in the ODC response at two AM frequencies, we examined the variation of the response for this exposure time as a function of frequency in the range of 6–600 Hz. Table 4 shows the results of these experiments. Statistically significant enhancements of ODC activity were obtained at frequencies in the range between 16 Hz and 65 Hz, whereas no significant effects were obtained at either 6 Hz or 600 Hz. The field-induced response peaked in the 60 Hz range, at which the ODC activity ratio approximately doubled. Because no experimental points were obtained between 65 Hz and 600 Hz, these results provide only a general idea of the variation of the frequency response.

Dependence on coherence. We previously demonstrated that the enhancement of ODC activity by AM microwaves requires a minimum coherence time of the modulating signal [Litovitz et al., 1993]. Optimal enhancement was obtained when the coherence time was 10 s or greater, whereas no enhancement resulted when the coherence time was 1 s or less. A case of some practical interest is that of RF or microwave signals amplitude modulated with speech. Because the coherence time of speech is less than 1 s, we predicted, based on our earlier work, that no effect on ODC activity would be elicited by exposure to such signals. The experimental data confirmed this prediction (see Table 8). Eight hour exposures with microwaves amplitude modulated with speech yielded no statistically significant effects as measured using a paired t test. Whereas the coherence time is an accurate predictor of the biological response in some cases, further research, to be reported elsewhere, has led us to conclude that the ability of an electromagnetic field to induce biological effects is best characterized in terms of a ''constancy'' interval, defined as the time interval over which the field parameters (e.g., amplitude, frequency) remain constant.

Exposure With FM Microwave Fields

The effects of frequency modulation with a 60 Hz sinusoid were examined as a function of exposure time in the range of 2–24 h. The modulation frequency, ω_m, and exposure times were selected to allow direct comparison to similar experiments using amplitude modulation. The maximum deviation, $\Delta\omega$, of the FM signal was set to 60 kHz to correspond approximately to the maximum deviation of commercial FM (75 kHz). The corresponding modulation index, $\beta = \Delta\omega/\omega_m$, was on the order of 1,000, which defines this signal as

wideband FM. Table 5 summarizes the results of exposure with FM microwaves. No statistically significant changes in ODC activity were induced by exposure of cultures to this signal.

Exposure With Cellular Phone-Type Signals

The results of the AM and FM experiments described above suggest that biological effects can be induced when the modulation causes periodic changes in the amplitude of the carrier, as is the case in sinusoidal AM. FM, which causes changes in phase but minimal changes in amplitude, appears to produce no measurable effect. A situation of practical interest is that of cellular phone transmissions. If amplitude modulation of the carrier is a significant factor in determining a biological response, then the extent to which cellular phones can induce a response would depend on whether the modulation schemes used for transmission impart a periodic ELF modulation component onto the carrier. Digital phones, which operate in burst mode, have periodic fluctuations of the carrier amplitude in the ELF range. Analog phones, which do not operate in burst mode, have relatively constant carrier amplitude (assuming no changes in reception between the cellular phone and the nearest cell). A series of exposures was conducted to determine whether either of these cellular phone signals produce enhancement of ODC activity in exposed cells.

Exposures were carried out with both the analog and the digital cellular fields and also with an 835 MHz carrier amplitude modulated with a 50 Hz square wave. This latter condition was intended to simulate the low-frequency burst modulation of the digital cellular field. Exposures with the analog cellular field produced no statistically significant enhancement in ODC activity for exposure times between 4 and 10 h (Table 6). Exposures with the digital cellular field produced statistically significant enhancements in ODC activity for 6, 8, and 10 h of exposure. The other two exposure times tested, 4 and 16 h, produced no statistically significant enhancement in ODC activity (Table 7). The square wave modulated signal was tested only after 8 h of exposure, yielding results similar to those for the corresponding condition with the digital cellular phone signal.

Table 8 and Fig. 3 summarize the results of 8 h exposures with the various signals tested. We note from this table that, in all cases tested with this exposure time, exposures with modulated microwaves produced statistically significant enhancements in ODC activity only when the modulation introduced low-frequency periodic changes in the amplitude of the carrier.

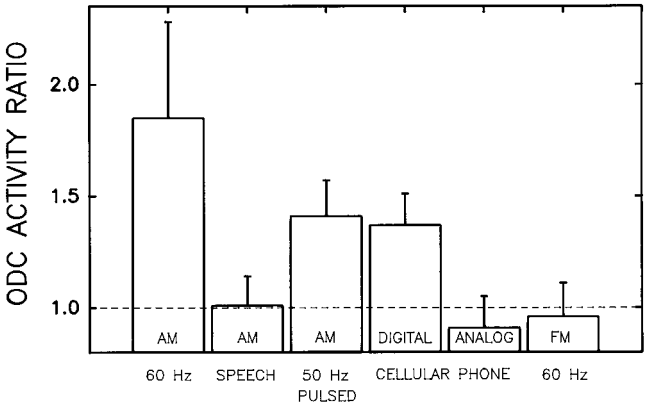

Fig. 3. ODC activity ratios for L929 murine cells exposed for 8 h with 835 MHz microwaves modulated by various methods.

DISCUSSION

The ODC activity of L929 fibroblasts was transiently enhanced by exposure to some, but not all, of the modulated 835 MHz microwave fields we examined. Exposure to an unmodulated, CW field also produced a response. These results are consistent with other reports that demonstrate enhanced ODC activity after EMF exposure. EMF-induced changes in ODC activity have been documented for cultured cells exposed to 60 Hz electric or magnetic fields [Byus et al., 1987; Litovitz et al., 1991, 1994; Mullins et al., 1993], for chicken embryos exposed to 60 Hz magnetic fields [Farrel et al., 1993], and for cultured cells exposed to amplitude-modulated microwave fields [Byus et al., 1988; Litovitz et al., 1993]. Thus, ODC activity appears to provide a consistent and reliable measure of cellular response to both ELF and RF EM fields. As such, it represents one of the few replicated examples of a bioeffect being induced by a weak electromagnetic field.

Microwave-Induced ODC Response: The Role of Modulation

Whether a given microwave field induces an ODC response seems to be dependent upon the modulation scheme employed. Enhancements in ODC activity were observed for L929 cells exposed to 835 MHz fields that were amplitude modulated with sinusoidal 16 and 60 Hz signals or with a 50 Hz square wave signal. Use of digital cellular signals burst modulated at 50 Hz, which produces a pattern of amplitude modulation very similar to that of the 50 Hz square wave, also induced increases in ODC activity.

In contrast to these results, neither the 60 Hz sinusoidal frequency-modulated 835 MHz carrier nor the frequency-modulated microwave field produced by analog cellular telephones induced an ODC response in L929 cells. These frequency-modulation schemes

TABLE 1. Results of Exposures With 835 MHz Continuous Wave Microwaves. The Mean E and Mean C Values Are the Average ODC Activities and Corresponding Standard Deviations, Expressed in Terms of pmol $^{14}CO_2$ Generated/30 Min/mg Protein, of the N Exposed (E) and N Control (C) Samples of Each Exposure Condition. The P Value Is the Probability That the Observed Differences Between Control and Exposed Samples in Each Set of N Paired Observations Is Due to Chance. The ODC Activity Ratio Is the Mean Value of the Ratios of the ODC Activity in Exposed Samples to That of Corresponding Control Samples, Computed from N Paired Observations of Each Exposure Condition. The ODC Activity Ratio is Not the Ratio of Mean E Over Mean C

Exp time (hrs)	N	Mean C	Mean E	*P*	ODC activity ratio
2	5	13.8 ± 6.3	12.9 ± 6.4	>0.52	0.9 ± 0.2
4	6	9.2 ± 6.1	8.7 ± 5.2	>0.69	1.0 ± 0.2
6	11	13.3 ± 12.2	16.5 ± 13.7	<0.004	1.3 ± 0.2
8	16	16.8 ± 13.8	15.9 ± 15.2	>0.41	0.9 ± 0.2
12	8	8.9 ± 1.7	8.3 ± 2.2	>0.34	0.9 ± 0.2
16	10	5.3 ± 4.1	4.8 ± 3.3	>0.32	1.0 ± 0.3
24	9	5.4 ± 2.3	5.0 ± 2.2	>0.32	0.9 ± 0.2

TABLE 2. Results of Exposures With 835 MHz Microwaves Amplitude Modulated (23%) With 16 Hz Sinusoids. Column Headings Are as Defined in Table 1

Exp time (hrs)	N	Mean C	Mean E	*P*	ODC activity ratio
2	7	12.1 ± 4.1	11.5 ± 4.2	>0.77	1.0 ± 0.3
4	7	12.0 ± 7.9	13.2 ± 10.0	>0.38	1.1 ± 0.3
6	13	14.2 ± 18.9	15.8 ± 20.3	<0.045	1.2 ± 0.3
8	11	9.9 ± 8.5	13.6 ± 11.8	<0.012	1.5 ± 0.3
12	6	12.8 ± 7.4	10.5 ± 6.1	>0.17	0.8 ± 0.2
16	7	6.7 ± 3.7	7.2 ± 4.0	>0.49	1.1 ± 0.3
24	9	10.3 ± 11.2	10.3 ± 9.2	>0.97	1.1 ± 0.1

TABLE 3. Results of Exposure With 835 MHz Microwaves Amplitude Modulated (23%) With 60 Hz Sinusoids. Column Headings Are as Defined in Table 1

Exp time (hrs)	N	Mean C	Mean E	*P*	ODC activity ratio
2	8	8.4 ± 3.4	9.8 ± 4.6	>0.15	1.2 ± 0.3
4	9	16.3 ± 12.8	16.1 ± 10.9	>0.91	1.1 ± 0.5
6	13	7.2 ± 4.0	11.6 ± 5.3	<0.0001	1.7 ± 0.4
8	22	24.0 ± 32.7	40.0 ± 47.2	<0.0001	1.9 ± 0.4
12	9	7.4 ± 3.4	11.1 ± 4.9	<0.0017	1.5 ± 0.3
16	9	7.6 ± 2.0	9.5 ± 2.6	<0.0058	1.3 ± 0.2
24	9	7.4 ± 2.4	6.7 ± 2.3	>0.13	0.9 ± 0.2

TABLE 4. Results of Exposure With 835 MHz Microwaves Amplitude Modulated (23%) With 6-600 Hz Sinusoids. Column Headings Are as Defined in Table 1

Freq (Hz)	N	Mean C	Mean E	*P*	ODC activity ratio
6	7	7.1 ± 5.0	6.6 ± 3.1	>0.61	1.1 ± 0.2
16	11	9.9 ± 8.5	13.6 ± 11.8	<0.012	1.5 ± 0.3
55	6	10.4 ± 4.8	18.5 ± 6.7	<0.009	1.9 ± 0.5
60	22	24.0 ± 32.7	40.0 ± 47.2	<0.0001	1.9 ± 0.4
65	6	10.0 ± 1.9	20.5 ± 4.7	<0.0011	2.1 ± 0.4
600	7	7.8 ± 5.3	9.4 ± 8.7	>0.37	1.3 ± 0.5

TABLE 5. Results of Exposure With 835 MHz Microwaves Frequency Modulated (60 kHz Deviation) With 60 Hz Sinusoids. Column Headings Are as Defined in Table 1

Exp time (hrs)	N	Mean C	Mean E	*P*	ODC activity ratio
2	9	35.9 ± 14.2	36.8 ± 14.5	>0.72	1.0 ± 0.1
4	6	17.7 ± 9.8	17.5 ± 7.7	>0.84	1.0 ± 0.1
6	8	22.0 ± 11.5	20.7 ± 11.5	>0.28	0.9 ± 0.1
8	7	18.9 ± 7.2	18.4 ± 7.7	>0.69	1.0 ± 0.2
12	6	13.0 ± 4.3	12.5 ± 2.9	>0.51	1.0 ± 0.1
16	7	12.4 ± 5.8	10.7 ± 5.6	>0.29	0.9 ± 0.2

TABLE 6. Results of Exposures With an AMPS Analog Cellular Phone Signal. Column Headings Are as Defined in Table 1

Exp time (hrs)	N	Mean C	Mean E	*P*	ODC activity ratio
4	6	28.9 ± 8.2	28.6 ± 8.6	>0.86	1.0 ± 0.1
6	6	33.4 ± 7.3	34.2 ± 11.7	>0.74	1.0 ± 0.1
8	6	17.5 ± 6.9	15.8 ± 6.7	>0.06	0.9 ± 0.1
10	6	33.9 ± 23.1	27.7 ± 16.1	>0.11	0.9 ± 0.2

TABLE 7. Results of Exposure With a DAMPS Digital Cellular Phone Signal. Column Headings Are as Defined in Table 1

Exp time (hrs)	N	Mean C	Mean E	*P*	ODC activity ratio
4	11	36.3 ± 20.1	40.0 ± 19.4	>0.07	1.2 ± 0.2
6	12	24.6 ± 12.5	29.1 ± 13.3	<0.0085	1.2 ± 0.2
8	9	26.6 ± 11.3	35.6 ± 13.4	<0.0002	1.4 ± 0.2
10	8	27.0 ± 8.8	31.4 ± 10.1	<0.0008	1.2 ± 0.1
16	3	8.9 ± 7.3	9.0 ± 5.9	>0.97	1.1 ± 0.1

TABLE 8. Results of 8 Hour Exposures to 835 MHz Microwaves Modulated by Various Methods. Column Headings Are as Defined in Table 1

Modulation type	N	Mean C	Mean E	*P*	ODC activity ratio
FM 60 Hz	7	18.9 ± 7.2	18.4 ± 7.7	>0.69	1.0 ± 0.2
AM speech	7	14.6 ± 11.7	14.1 ± 9.3	>0.69	1.0 ± 0.1
AM 60 Hz	22	24.0 ± 32.7	40.0 ± 47.2	<0.0001	1.9 ± 0.4
Sq wave 50 Hz	8	25.9 ± 6.6	36.4 ± 9.5	<0.0004	1.4 ± 0.2
Digital cellular	9	26.6 ± 11.3	35.6 ± 13.4	<0.0002	1.4 ± 0.2
Analog cellular	6	17.5 ± 6.9	15.8 ± 6.7	>0.06	0.9 ± 0.1

produce no measurable changes in carrier amplitude. The results suggest that, to induce a cellular response through microwave exposure, the microwave field must be modulated by a method that produces periodic alterations in the amplitude of the carrier wave. For example, the fact that the square wave and digital phone signals induced similar responses suggests that the cells responded to the 50 Hz pulsing of the carrier amplitude common to both signals. Thus, it appears that the cells did not respond to the very-high-frequency digitized information transmitted within the envelope of each pulse of the cellular signal.

The data obtained by using modulated microwaves are all consistent with the concept that the ELF amplitude modulation is critical in causing a biological effect. However, the results of our CW experiments

present an exception. Exposure of L929 cells to the 835 MHz CW field produced a statistically significant enhancement in ODC activity after 6 h of exposure. However, the time course of this response seemed unusual in that the increase in ODC activity was sharply demarcated in time, with no indication of rising or falling activity at the 4 or 8 h exposure time points. Nonetheless, we believe this effect to be real, having obtained the same result in two separate sets of experiments that were conducted more than 3 years apart, each set having independently yielded a statistically significant enhancement. How this CW effect relates to the ODC enhancements observed in cells exposed to AM fields is not clear. The obvious distinctions are that the enhancements induced by AM fields peaked 2 h later than those caused by the CW field and that the most robust response, that produced by the 60 Hz AM field, was significantly larger than the response produced by the CW field.

In each instance for which a time course was measured, the enhancement in ODC activity induced by AM microwave exposure was transient. ODC activity peaked after 8 h of exposure and then returned to control values despite continued exposure. Byus et al. [1988] also showed the transient enhancement of ODC activity in three different cultured cell lines exposed to AM microwaves. Approximately 15–60% increases in ODC activity were observed after 1 h exposures to 450 MHz microwaves sinusoidally amplitude modulated at 16 Hz. Under the exposure conditions used by Byus et al., 60 Hz amplitude modulation failed to elicit changes in ODC activity. However, direct comparisons to our results are not possible, because their carrier frequency, cell lines, exposure time, and modulation index differed from ours. For example, our data indicate that it is not until at least 6 h after onset of exposure to the 60 Hz AM microwave field that a clearly discernible effect on ODC activity is observed. The longest time that Byus et al. observed ODC activity was only 4 h after onset of exposure. It is possible that, had they waited longer, they would have observed an effect similar to that observed by us when using a 60 Hz AM exposure. Regardless, the observations of Byus et al. underscore the fact that exposure to a sinusoidal, amplitude-modulated microwave field can enhance ODC activity.

Microwave-Induced ODC Responses Resemble Those Induced by ELF Fields

The basic response to 60 Hz AM microwaves (i.e., a transient, approximately twofold increase in ODC activity) is similar to that observed after exposure of cells to a 60 Hz ELF magnetic field. The major distinction is that the timing of the two responses is different. The ELF field-induced ODC response peaks at 4 h of exposure, with a return to control values by 8 h of exposure. The 60 Hz AM microwave response peaked at 8 h and returned to control levels after approximately 24 h. Our results, considered with those of others, suggest that the responses induced by ELF and AM microwave fields are fundamentally similar and that it is the ELF modulation frequency of the microwave field that plays a critical role in determining the characteristics of the response.

For example, the ODC responses to ELF and AM microwave fields display similar requirements for temporal coherence of the stimulating field's ELF frequency. Cells exposed to an ELF magnetic field for which the frequency was switched between 55 and 65 Hz at regular intervals yielded a twofold enhancement in ODC activity only when each frequency was maintained over intervals $\geq$ 10 s throughout exposure [Litovitz et al., 1991]. When the frequency was switched at intervals $\leq$ 1 s, ODC activities remained at control levels. This temporal requirement for frequency coherence was also demonstrated by the fact that L929 cells showed no enhancement of ODC activity after exposure to ELF random noise fields of amplitude comparable to that of the 60 Hz stimulating field [Litovitz et al., 1994]. A similar temporal coherence requirement determines the response of L929 cells exposed to AM microwaves [Litovitz et al. 1993]. If the modulation frequency is switched between 55 and 65 Hz at regular intervals throughout the 8 h exposure period, the ODC response is determined by the duration of the constant frequency interval. As with the ELF studies, switching at an interval $\geq$ 10 s produced an approximate doubling in ODC activity, but intervals $\leq$ 1 s produced no ODC response. This result is reinforced by the data presented herein, which demonstrate that amplitude modulation using speech (which has a coherence time of $<$1 s) produced no enhancements in ODC activity. However, in this case, the decrease in the response may also be attributed in part to the frequency spectral distribution of speech. Our data show that the ODC response to AM microwaves decreases as the modulation frequency increases (Table 3). Speech is generated mostly in the range between 50 Hz and 10 kHz, but the highest concentration of sounds is in the range 100–600 Hz [Denes and Pinson, 1963]. Consequently, regardless of other effects, a decreased response relative to 60 Hz AM would be expected.

SUMMARY AND CONCLUSIONS

Our results indicate that amplitude-modulated microwaves at an SAR of 2.5 W/kg, corresponding to a plane wave equivalent power density of approximately 1 mW/cm^2, are capable of altering biological activity in in vitro cell cultures. Frequency-modulated micro-

waves at this power level appear to have no effect at all. The radiation from TDMA digital cellular phones can cause significant changes in ODC activity, whereas that from analog phones does not (evidently because they are FM). The data suggest that the same coherence requirements necessary for ELF-induced bioeffects apply to the modulation of ELF amplitude-modulated microwaves. It is clear from this study that the use of SAR alone is inadequate for setting safety standards. The type of modulation must also be considered.

ACKNOWLEDGMENTS

This work was partially supported by funds from the Department of the Army (DAMD17-86-C-6260). The authors gratefully acknowledge the support and advice of Col. Edward Elson.

REFERENCES

Auvinen M, Paasinen A, Andersson LC, Ḧoltẗa E (1992): Ornithine decarboxylase activity is critical for cell transformation. Nature 360:355–358.

Balcer-Kubiczek EK, Harrison GH (1985): Evidence for microwave carcinogenesis in vitro. Carcinogenesis 6:859–864.

Balcer-Kubiczek EK, Harrison GH (1989): Induction of neoplastic transformations in $C^3H/T10\frac{1}{2}$ cells by 2.45-GHz microwaves and phorbol ester. Radiat Res 117:531–537.

Balcer-Kubiczek EK, Harrison GH (1991): Neoplastic transformation of $C^3H/T10\frac{1}{2}$ cells following exposure to 120 Hz modulated 2.45-GHz microwaves and phorbol ester tumor promotor. Radiat Res 126:65–72.

Bawin SM, Kaczmarek LK, Adey WR (1975): Effects of modulated VHF fields on the central nervous system. Ann NY Acad Sci 247:74–81.

Blackman CF, Elder JA, Weil CM, Benane SG, Eichinger DC, House DE (1979): Induction of calcium ion efflux from brain tissue by radio-frequency radiation: Effects of modulation frequency and field strength. Radio Sci 14(6S):93–98.

Blackman CF, Benane SG, House DE, Joines WT (1985): Effects of ELF (1–20 Hz) and modulated (50 Hz) RF field on the efflux of calcium ions from brain tissue in vitro. Bioelectromagnetics 6:1–11.

Boucher NJ (1992): ''The Cellular Radio Handbook.'' Mendecino, CA: Quantum Publishing.

Byus CV, Lundak RL, Fletcher RM, Adey WR (1984): Alterations in protein kinase activity following exposure of cultured human lymphocytes to modulated microwave fields. Bioelectromagnetics 5:341–351.

Byus CV, Pieper SE, Adey WR (1987): The effects of low-energy 60-Hz environmental fields upon the growth-related enzyme ornithine decarboxylase. Carcinogenesis 8:1385–1389.

Byus CV, Kartun K, Pieper SE, Adey WR (1988): Increased ornithine decarboxylase activity in cultured cells exposed to low energy modulated microwave fields and phorbol ester tumor promoters. Cancer Res 48:4222–4226.

Cleary SF, Liu LM, Merchant RE (1990): Glioma proliferation modulated in vitro by isothermal radiofrequency radiation exposure. Radiat Res 121:38–45.

Czerska EW, Elson EC, Davis CC, Swicord ML, Czerski P (1992): Effects of continuous and pulsed 2,450-MHz radiation on spontaneous lymphoblastoid transformation of human lymphocytes in vitro. Bioelectromagnetics 13:247–259.

Denes PB, Pinson EN (1963): ''The Speech Chain: The Physics and Biology of Spoken Language.'' Bell Telephone Laboratories, pp 115–116.

Dutta SK, Subramoniam A, Ghosh B, Parshad R (1984): Microwave radiation induced calcium ion efflux from human neuroblastoma cells in culture. Bioelectromagnetics 5:71–78.

Dutta SK, Gosh B, Blackman CF (1989): Radiofrequency radiation-induced calcium ion efflux enhancement from human and other neuroblastoma cells in culture. Bioelectromagnetics 10:7–202.

Farrel JM, Barber M, Doinov P, Krause D, Litovitz TA (1993): Superposition of a temporally incoherent magnetic field suppresses the change in ornithine decarboxylase activity in developing chick embryos induced by a 60 Hz sinusoidal field. In Blank M (ed): ''Electricity and Magnetism in Biology and Medicine.'' San Francisco: San Francisco Press, pp 342–344.

Garaj-Vrhovac V, Fucic A, Horvat D (1992): The correlation between the frequency of micronuclei and specific chromosome aberrations in human lymphocytes exposed to microwave radiation in vitro. Mutat Res 281:182–186.

Halmekyö M, Syrjänen K, Jänne J, Alhonen L (1992): Enhanced papilloma formation in response to skin tumor promotion in transgenic mice overexpressing the human ornithine decarboxylase gene. Biochem Biophys Res Commun 187:493–497.

Hayashi S, Murakami Y (1995): Rapid and regulated degradation of ornithine decarboxylase. Biochem J 306:1–10.

Hibshoosh H, Johnson M, Weinstein IB (1990): Effects of overexpression of ornithine decarboxylase (ODC) on growth control and oncogene-induced cell transformation. Oncogene 6:739–743.

Ḧoltẗa E, Auvinen M, Paasinen A, Kangas A, Andersson LC (1994): Ornithine decarboxylase-induced cellular transformation: The involvement of protein tyrosine kinase(s) and pp130. Biochem Soc Trans 22:853–859.

Krause D, Mullins JM, Penafiel LM, Meister R, Nardone RM (1991): Microwave exposure alters the expression of 2-5A-dependent RNase. Radiat Res 127:164–170.

Litovitz TA, Krause D, Mullins JM (1991): Effect of coherence time of the applied magnetic field on ornithine decarboxylase activity. Biochem Biophys Res Commun 178:862–865.

Litovitz TA, Krause D, Penafiel M, Elson EC, Mullins JM (1993): The role of coherence time in the effect of microwaves on ornithine decarboxylase activity. Bioelectromagnetics 14:395–403.

Litovitz TA, Krause D, Montrose CJ, Mullins JM (1994): Temporally incoherent magnetic fields mitigate the response of biological systems to temporally coherent magnetic fields. Bioelectromagnetics 15:399–409.

Moshier JA, Dosescu J, Skunca M, Luk GD (1993): Transformation of NIH/3T3 cells by ornithine decarboxylase overexpression. Cancer Res 53:2618–2622.

Mullins JM, Krause D, Litovitz TA (1993): Simultaneous application of a spatially coherent noise field blocks the response of cell cultures to a 60 Hz electromagnetic field. In Blank M (ed): ''Electricity and Magnetism in Biology and Medicine.'' San Francisco: San Francisco Press, pp 345–346.

NCRP (1981): ''Radiofrequency Electromagnetic Fields: Properties, Quantities and Units, Biophysical interaction, and Measurements.'' Bethesda, MD: National Council on Radiation Protection and Measurements, Report No. 67.

NCRP (1986): ''Biological Effects and Exposure Criteria for Radio Frequency Electromagnetic Fields.'' Bethesda, MD: National Council on Radiation Protection and Measurements, Report No. 86.

Saffer JD, Profenno LA (1992): Microwave-specific heating affects gene expression. Bioelectromagnetics 13:75–78.

Seely JE, Pegg AE (1983): Ornithine decarboxylase (mouse kidney). Methods Enzymol 94:158–161.

Bioelectromagnetics 14:395-403 (1993)

The Role of Coherence Time in the Effect of Microwaves on Ornithine Decarboxylase Activity

T.A. Litovitz, D. Krause, Miguel Penafiel, Edward C. Elson, and J.M. Mullins

Vitreous State Laboratory (T.A.L., M.P.), Department of Biology (D.K., J.M.M.), Catholic University of America, and Walter Reed Army Institute of Research (E.C.E.), Washington, DC

Previously, we demonstrated the requirement for a minimum coherence time of an applied, small amplitude (10 μT) ELF magnetic field if the field were to produce an enhancement of ornithine decarboxylase activity in L929 fibroblasts. Further investigation has revealed a remarkably similar coherence time phenomenon for enhancement of ornithine decarboxylase activity by amplitude-modulated 915 MHz microwaves of large amplitude (SAR 2.5 W/kg). Microwave fields modulated at 55, 60, or 65 Hz approximately doubled ornithine decarboxylase activity after 8 h. Switching modulation frequencies from 55 to 65 Hz at coherence times of 1.0 s or less abolished enhancement, while times of 10 s or longer provided full enhancement. Our results show that the microwave coherence effects are remarkably similar to those observed with ELF fields. ©1993 Wiley-Liss, Inc.

Key words: coherence time, microwave, amplitude modulation, ornithine decarboxylase

INTRODUCTION

A considerable controversy has surrounded the question of biological response to weak electromagnetic fields. The mechanisms by which cells might detect and respond to these fields are unknown. It is argued [Adair, 1991] that a cellular response is impossible since the magnitudes of such fields are lower than those of the electrical noise fields produced by random thermal motion of ions in and about the cell. Nonetheless, a number of reports detailing responses to weak, extremely low frequency (ELF) fields [e.g., Goodman et al., 1989; Wei et al., 1990; Litovitz et al., 1991] and to amplitude-modulated microwave fields [e.g., Byus et al., 1988] are found in the literature.

In order to understand these results, Weaver and Astumian [1990] proposed that signal averaging over time might provide a mechanism for cellular response to weak fields. Unfortunately their calculations showed that the averaging times necessary were much longer than the exposure times found to be effective.

Received for review July 27, 1992; revision received March 22, 1993.

Address reprint requests to Dr. J. Michael Mullins, Department of Biology, The Catholic University of America, Washington, DC 20064.

Recently Litovitz et al. [1991] examined the hypothesis that cells do not respond to the local thermal noise fields because these fields are not temporally coherent, in contrast to the temporal coherence of the exogenous, applied fields used in the above experiments. They investigated the role of the coherence time of an exogenous ELF field in effecting a biological response. Ornithine decarboxylase (ODC) activity was selected as the biological marker for that study. Enhancement of ornithine decarboxylase specific activity following exposure of L929 cells to an ELF magnetic field of 10 μT rms (with an associated electric field of approximately 0.04 μV/cm) was found to depend upon the coherence time of the applied field. During a 4-h exposure the frequency of the field was shifted between 55 and 65 Hz at slightly random intervals termed coherence times (τ_{coh}). The coherence time here is loosely defined as the time interval over which one can reasonably predict the frequency, phase, and amplitude of the field. When (τ_{coh}) was 1 s or less no enhancement of ornithine decarboxylase activity resulted, while (τ_{coh}) of 10 s or greater yielded a significant enhancement of activity. The observed coherence times needed for full cellular response were too short to account for the signal averaging phenomenon hypothesized by Weaver and Astumian [1990]. However, the coherence time was revealed to be an important factor in determining the magnitude of the cellular response.

We report here the ornithine decarboxylase response of L929 cultures to microwave fields. Our results show that the microwave coherence effects are remarkably similar to those observed with ELF fields.

MATERIALS AND METHODS

Microwave Exposure System

Microwave exposure was accomplished using a Crawford cell placed within an incubator chamber maintained at 37 °C. A block diagram of the exposure system is shown in Figure 1. A model CC110 Crawford cell (Instruments for Industry, Farmingdale, NY) was vertically mounted on a rotary table and provided with an additional access door to facilitate sample insertion. The 915 MHz driving signal was produced by a signal generator (Hewlett Packard, 8657B) followed by a travelling wave tube amplifier (Amplifier Research #10W1000, Souderton, PA). A double stub tuner was used to match the impedance of the loaded Crawford cell for optimum power delivery to the sample.

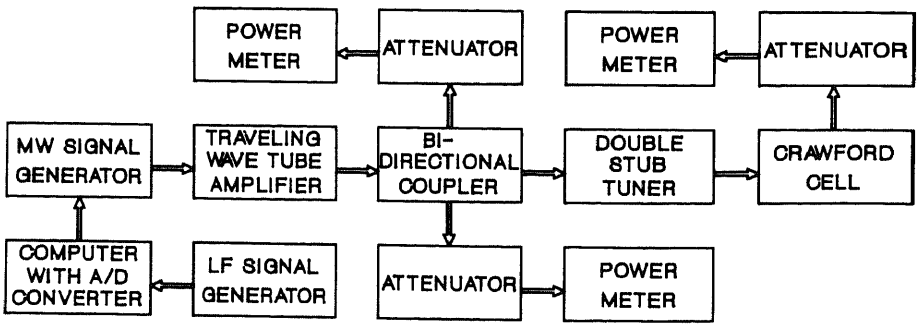

Fig. 1. Block diagram of the modulated microwave exposure system.

To investigate the role of the coherence time of the modulation, the signal was periodically switched between 55 Hz and 65 Hz. The time interval within which the signal was operated at each frequency was selected as a fixed period τ plus a randomly selected period $\Delta\tau$ of duration between 0 and 50 ms. The interval τ was varied between 0.1 and 50 s. The coherence time (τ_{coh}) is $\tau+\Delta\tau$. Since $\tau>>\Delta\tau$, (τ_{coh}) is closely equal to τ. The frequency of the sinusoidal output of the function generator was varied by a computer-generated signal to the voltage controlled oscillator (VCO) of the generator. The system was operated at 915 MHz with amplitude modulation at 55, 60, and 65 Hz. The modulation index was set at 0.23 and was calculated using the relation $P_t = P_c(1 + m^2/2)$, where P_t is the microwave power with modulation, P_c is the microwave power without modulation, and m is the modulation index.

Crawford cells are generally chosen for exposure of biological samples because, under special conditions, they allow uniform electric field exposure. To achieve uniform exposure the sample should be positioned perpendicular to the direction of wave propagation and parallel to the electric field. Additionally it should occupy no more than one-third of the distance between the center conductor and the outer plate. Due to constraints imposed by the availability of commercially fabricated tissue culture flasks, it was not possible to meet the requirements for the ideal exposure configuration. The flasks used in our experiments (25 cm^2, 50 ml) had a width approximately equal to 70% of the distance between the center conductor and the outer plate. Two flasks were placed end to end on both sides of the center conductor. This configuration insured overall symmetry, if not complete uniformity, of the electric field distribution within the samples.

To determine the uniformity of the field, SAR measurements were made within each tissue culture flask with the flasks filled with 5 ml of culture medium and positioned in the arrangement used for exposures. The SAR was determined by measuring the rate of temperature increase after switching on a high power field. The temperature was measured using a fiber optic thermometer (Luxtron model 3000) with two MPM 4 sensor probes. The temperature distribution at the base of the flask, where cells were located, was mapped at 7 mm intervals along the width of the flask and at 10 mm intervals along its length for a total of 48 points. Measurements were made on both flasks positioned on one side of the center conductor. Due to symmetry the SAR distribution on the other side was assumed to be similar. The optical probes were inserted into the flask through small holes made on the top of the flask. Each run of eight simultaneous measurements was carried out with an input power of 69 watts for a period of 20 s. This measuring interval allowed a 0.5–1 °C temperature rise from the starting temperature of 21 °C at the measuring site. To minimize the error due to heat loss the SAR was determined using the temperature vs. time data for the first 10 s after the power was turned on.

The SAR was calculated using the well-known relation $SAR = C_P\Delta T/\Delta t$, where C_P is the specific heat of the exposed sample medium and $\Delta T/\Delta t$ is the rate of temperature increase per unit time. For these calculations, C_P was assumed to be 3.95 J/°C/g. The results indicate that the SAR varied with an asymmetrical overall distribution if both flasks at either side of the center conductor were taken together. The SAR across the width of the flasks varied from low points (approximately 25% of maximum) at the edges to a maximum skewed toward the center conductor. Similarly, the SAR increased from the back end of the rear flask (approximately

25% of the maximum) to a maximum in the proximity of the junction between flasks and decreased again toward the front end of the front flask (approximately 75% of the maximum). An effective SAR of approximately 180 W/kg, corresponding to an input power of 69 watts, was calculated by performing a simple average over all the measured points.

In the cell culture exposures reported here, an input power of 0.96 watts was used. Accordingly, the corresponding average SAR was approximately 2.5 W/kg. With this input power no measurable temperature increase was expected within the samples. Measurements with a fiber optic thermometer demonstrated that within the resolution of the probe (±0.1 °C) no temperature change occurred at any location within the culture medium. The electric field within the Crawford cell, associated with an input power of 0.96 watts, was of the order of 0.7 V/cm. This field was calculated, assuming a uniform field, using the relation $E = (PZ_0/d^2)^{1/2}$, where $P = P_t/2$ is the power distributed to the Crawford cell at each side of the conductor, $Z_0 = 50\ \Omega$ is the characteristic impedance of the Crawford cell, and $d = 7$ cm is the distance between the center conductor and the outer plate (dimension slightly larger than the standard CC110).

Cell Cultures

Actively growing cultures of the murine L929 fibroblast cell line (NCTC clone 929; American Type Culture Collection, Rockville, MD) were maintained in Eagle's minimum essential medium supplemented with 5% calf serum and 10 mM HEPES buffer. Cells were kept at 37 °C in a 95% air, 5% CO_2 atmosphere. Cultures to be used for exposure were initiated approximately 20 h prior to an experiment, at a density (3×10^6 cells in 5 ml of culture medium per 25 cm^2 flask) to produce mid-logarithmic phase growth by the time of use. To avoid large increases in ODC activity due to serum stimulation, the culture medium was not replaced prior to exposure.

Electromagnetic Field Exposure and Harvesting of Cells

From 5–12 separate experiments were conducted for each exposure condition (i.e., for each modulation frequency or coherence time). The order in which exposures were conducted was random with regard to the values of τ_{coh} used, so that different exposure conditions were intermixed in sequence during the approximately 12-month duration of the project.

For microwave exposure four, 25 cm^2 flasks were inserted into the Crawford cell as described above. Four 25 cm^2 flasks of cells, serving as control cultures, were placed in the same incubator chamber at the same height as the exposed cultures within the Crawford cell. In the experiments described below, an average SAR of 2.5 W/kg, modulation index of 0.23, and an 8 h exposure time were consistently employed.

Immediately following exposures the cells in each flask were washed twice with 5 ml ice-cold phosphate buffered saline (PBS) and then gently scraped from their growth surface in a third aliquot of cold PBS. In order to provide sufficient protein for ODC assay the cells from the four exposed or four control flasks were combined for a single determination of ODC activity. Released cells were washed with cold PBS, pelleted at 350*g* for 5 min, and the supernatant aspirated. Cell pellets were frozen and stored at -75 °C until assay.

Determination of ODC Activity

ODC activity was determined by the method of Seely and Pegg [1983] modified by the addition of 50 μM pyridoxal 5′-phosphate, 50 μg/ml leupeptin, and 0.2% Nonidet P-40 to the cell lysis buffer. Absorption of generated $^{14}CO_2$ was accomplished with 150 μl of 1.0 N NaOH, and addition of 400 μl 20% TCA was done to terminate reactions. Background counts were determined by counting preparations in which ODC activity was eliminated by acid denaturing. ODC activity units were expressed as picomoles $^{14}CO_2$ generated/30 min/mg protein. Protein concentrations were determined by the method of Bradford [1976].

Evaluation of Data

ODC activities of control L929 cultures assayed on different days varied over an approximately five fold range, from about 5 to 25 units. Most of this variation appeared to be inherent to the cell cultures. ODC activity is readily altered by changes in cell growth conditions [Heby et al., 1975; reviewed by Jänne et al., 1978], and despite our rigorous attempts to assure constant culture parameters, variations in control activities occurred. To deal with such day-to-day variations in control ODC activity and to allow ready comparisons among experiments, the results of each experiment were expressed as an ODC activity ratio, calculated by dividing the ODC activity of an exposed culture with that of its matched control. An activity ratio of 1.8 would thus indicate an ODC activity in an exposed culture that was 1.8 times that of the control.

Figure 2 provides a demonstration of the validity of the ODC activity ratio for assessing enhancement of ODC activity due to EM field exposure. Results are shown for a total of 59 separate experiments in which L929 cells were exposed to a 60 Hz, sinusoidally varied magnetic field of 10 μT rms amplitude. Time of exposure was 4 h, which was previously found [Litovitz et al., 1991] to induce a maximum ODC response to such a field. Mean activity ratios (and standard deviations) are plotted against 5 groups of control ODC activities spanning the range from 5–30 units. The ODC activity ratio for each group was approximately 2 (range 2.0 ± 0.2 to 2.1 ± 0.3; mean for all 59 exposures = 2.1 ± 0.2). Nearly identical activity ratios were obtained for cultures varying as much as five fold in control ODC specific activities. These values demonstrate the effectiveness of the ODC activity ratio for assessing EMF-induced cellular response.

RESULTS

Initially, a series of exposure times (2–24 h) was conducted using 60 Hz amplitude-modulated, 915 MHz microwaves, with modulation index of 0.23 and an average SAR of approximately 2.5 W/kg. These conditions produced a transient, approximately two-fold increase in ODC activity which peaked after 8 h of exposure. Using SARs as low as 0.5 W/kg or a modulation index of 0.60 also produced an approximate doubling of ODC specific activity after 8 h exposure.

An approximate doubling of ornithine decarboxylase activity (ODC activity ratio = 1.9 ± 0.3 (S.D.), n = 11) was obtained for L929 cultures exposed to the 60 Hz amplitude modulated microwave field for 8 h. However, no ornithine decarboxylase enhancement was observed for cultures exposed for 8 h to the unmodulated 915 MHz

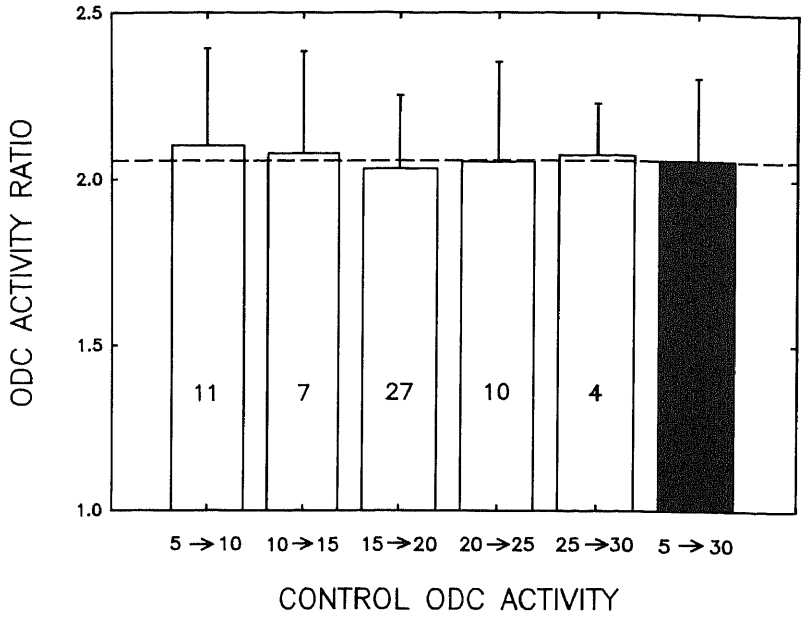

Fig. 2. Plot of ODC activity ratios (ODC activities of exposed cultures/ODC activities of matched controls) against control ODC specific activities for 59 experiments in which cultures were exposed for 4 h to a 60 Hz, 10 μT field. The number of experiments that fell in each specific activity range are indicated in the open bars. Mean ODC activity ratio for all 59 experiments is indicated by the filled bar and the dashed line.

microwave field (ODC activity ratio = 0.9 ± 0.1, n = 10). Thus, the extremely low frequency of the amplitude modulation, was the critical factor in eliciting cellular response. In order to examine the importance of the coherence time (τ_{coh}) for the microwave response, we also assessed the ornithine decarboxylase activities of cultures exposed for 8 h to microwave fields amplitude modulated at 55 or 65 Hz. Results, 1.9 ± 0.5 (n = 6) and 1.9 ± 0.3 (n = 5), respectively, were statistically indistinguishable from those obtained with 60 Hz modulation.

Results of the coherence time studies are plotted in Figure 3. When the modulation frequency was shifted with τ_{coh} of 0.1 or 1.0 s no significant enhancement of ornithine decarboxylase activity over control levels was observed. However, a τ_{coh} of 10 s yielded an enhancement of ornithine decarboxylase activity equivalent to that obtained with constant amplitude modulated frequencies of 55, 60, or 65 Hz. Increasing the τ_{coh} five fold to 50 s produced an enhancement equivalent to that obtained at 10 s. Thus, approximately two-fold increases in activity were obtained with values of τ_{coh} of 10.0 s or greater. A 5 s coherence time produced a level of enhancement that was intermediate between control values and those obtained with τ_{coh} of 10 s or longer. The differences in ODC activity ratios between τ_{coh} of 1 s or less, and τ_{coh} of 10 s or more are very significant. Analysis by independent t-test yielded p values $\leq 1.3 \times 10^{-4}$.

The ODC activity ratio, [ODC], was fit to the function

$$[ODC] = 1 + A\left(1 - e^{-\frac{t_{coh}}{t_{cell}}}\right), \qquad (1)$$

where A is a constant associated with the magnitude of the enhancement and τ_{cell}

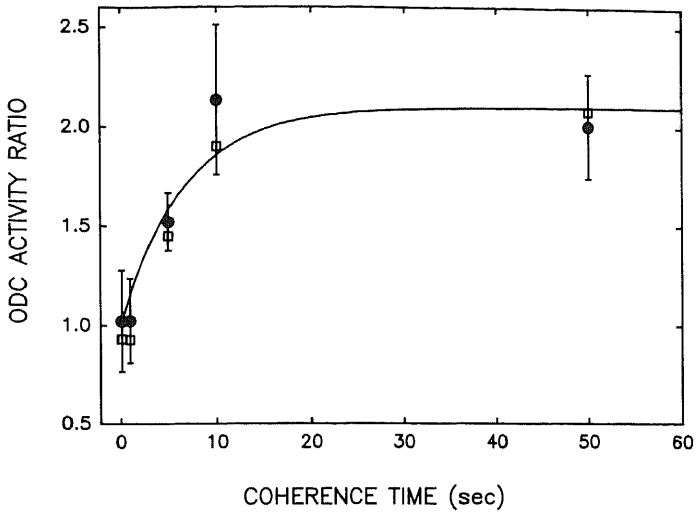

Fig. 3. ODC activity ratio is plotted against coherence time. Numbers of exposures used to determine each time point were as follows: 0.1 s, n = 5; 1.0 s, n = 8; 5.0 s, n = 6; 10.0 s, n = 12; 50.0 s, n = 6. Values from the previously reported ELF coherence time analysis [Litovitz et al., 1991] are plotted (open squares) for purposes of comparison. The solid line represents values calculated for τ_{coh} according to equation 1.

is a time constant apparently associated with the cell detection mechanism. The fit parameters are listed in Table 1.

DISCUSSION

Enhancement of ornithine decarboxylase activity by exposure to microwaves requires that the microwave carrier be amplitude modulated. It is thus the extremely low frequency of the modulating signal which is critical to producing the ornithine decarboxylase response. The mechanism by which the amplitude modulated signal affects the cell is not known. However, it does appear that the cell somehow demodulates the microwave signal and that the demodulated ELF stimulus is what affects cell function.

Previously we used a Helmholtz coil configuration for exposures at ELF frequencies [Litovitz et al., 1991]. The coils were driven by a computer-controlled function generator followed by an audio amplifier. Monolayer cultures of L929 cells,

TABLE 1. Comparison of Fit Parameters in the Microwave and ELF Experiments

Parameter	Microwave exposed	ELF exposed	Combined ELF and microwave data
A	1.08 ± .15	1.11 ± .15[a]	1.1 ± .16
τ_{cell} (s)	5.3 ± 2.2	8.2 ± 2.9	6.6 ± 1.6

[a]The originally published value of A (the constant in equation 1) for ELF-exposed cells (1.26 [Litovitz et al., 1991]) was calculated using a subset of the complete data and was published by mistake. The data given in the text and in Figure 1 of that report are, however, correct. The value of 1.11 for A, as given here, is correct.

oriented parallel to the direction of a 60 Hz, 10 μT rms magnetic field and experiencing an induced electric field of 0.04 μV/cm [Bassen et al., 1992; Wang et al., 1993], displayed a transient doubling of ODC activity that peaked at 4 h of exposure.

We have thus demonstrated that 60 Hz ELF fields [Litovitz et al., 1991] and 60 Hz amplitude modulated 915 MHz microwave fields both produce a transient increase in the ornithine decarboxylase activity of L929 cells. The maximum value of this increase is, in both experiments, a factor of about 2. Data presented here show that the ELF and amplitude-modulated microwave effects share an additional and striking similarity in the requirement for maintenance of coherence over some minimum time interval.

In each case the use of a τ_{coh} of 1.0 s or less resulted in no ornithine decarboxylase enhancement, 5.0 s produced a value intermediate between control and the maximum electromagnetic field-induced values, and 10.0 s or longer yielded full enhancement. In Figure 3 the ODC activity ratios (ODC), for the ELF data are plotted. It can be seen by comparing the microwave and ELF data that the variation of [ODC] with τ_{coh} is quite similar.

In our earlier study on the role of coherence in ELF effects on ornithine decarboxylase activity [Litovitz et al., 1991] we were also able to fit the results to equation 1. The fit parameters are listed in Table 1. It can be seen that there is good agreement between the fit parameters for the two experiments. The values of τ_{cell} for the modulated microwave and ELF are the same to within the uncertainty of the fit. This is further indication that τ_{cell} is truly some fundamental time constant of the mammalian cell.

ACKNOWLEDGMENTS

This work was supported by contract DAMD17-86-C-6260 from the Walter Reed Institute of Research, Department of the Army. The authors wish to express appreciation for the expert technical assistance of Mr. Abiy Desta.

REFERENCES

Adair R (1991): Constraints on biological effects of weak, extremely low frequency electromagnetic fields. Phys Rev A 43:1039–1049.

Bassen H, Litovitz T, Penafiel M, Meister R (1992): ELF in vitro exposure systems for inducing uniform electric and magnetic fields in cell culture media. Bioelectromagnetics 13:183–198.

Bradford, M (1976): A rapid and sensitive method for the quantitation of microgram quantities of protein utilizing the principle of protein-dye binding. Anal Biochem 72:248–254.

Byus CV, Kartun K, Pieper S, Adey RW (1988): Increased ornithine decarboxylase activity in cultured cells exposed to low energy modulated microwave fields and phorbol ester tumor promoters. Cancer Res 48:4222–4226.

Goodman RL, Wei LX, Xu JC, Henderson A (1989): Exposure of human cells to low-frequency electromagnetic fields results in quantitative changes in transcripts. Biochim Biophys Acta 1009:216–220.

Heby O, Marton LJ, Zardi L, Russell DH, Baserga R (1975): Changes in polyamine metabolism in WI38 cells stimulated to proliferate. Exp Cell Res 90:8–14.

Jänne J, Pösö H, Raina A (1978): Polyamines in rapid growth and cancer. Biochem Biophys Acta 473:241–293.

Litovitz T, Krause D, Mullins JM (1991): Effect of coherence time of the applied magnetic field on ornithine decarboxylase activity. Biochem Biophys Res Comun 178:862–865.

Seely JE, Pegg AE (1983): Ornithine decarboxylase (mouse kidney). Methods Enzymol 94:158–161.

Wang W, Litovitz TA, Penafiel LM, Meister R (1993): Determination of the induced ELF electric field distribution in a two layer in vitro system simulating biological cells in nutrient solution. Bioelectromagnetics 14:29–39.

Weaver JC, Astumian, RD (1990): The response of living cells to very weak electric fields—the thermal noise limit. Science 247:459–462.

Wei LX, Goodman R, Henderson A (1990): Changes in levels of c-myc and histone H2B following exposure of cells to low-frequency sinusoidal electromagnetic fields: Evidence for a window effect. Bioelectromagnetics 11:269–272.

Rom J Intern Med. 1994 Jan-Mar;32(1):51-6.

Lipid peroxidation and change of plasma lipids in acute ischemic stroke.

Serban MG, Niţă V.

Source

C. Davilla University of Medicine and Pharmacy, Department of Physiopathology, Bucharest, Romania.

Abstract

An estimation was made of the changes of the plasma lipid components and of the level of lipid peroxidation in acute ischemic stroke either as a transient accident (TLA) or as a cerebral vascular accident (CVA). The level of serum triglycerides was found significantly increased in the patients with CVA, in correlation with a decrease of the total HDL values due to the decrease of the HDL subfraction. As compared with the control group the LDL/HDL ratio presented increased values due to the decrease of the serum HDL concentration (respectively of the HDL2). The lipid peroxidation presented a more marked increase in patients with transient ischemic accident.

PMID:
8081312
[PubMed - indexed for MEDLINE]
http://www.ncbi.nlm.nih.gov/pubmed/8081312

Biophysical Chemistry 152 (2010) 164–169

Contents lists available at ScienceDirect

Biophysical Chemistry

journal homepage: http://www.elsevier.com/locate/biophyschem

Evidence of lipid peroxidation and protein phosphorylation in cells upon oxidative stress photo-generated by fullerols

B. Vileno [a,*], S. Jeney [a], A. Sienkiewicz [a], P.R. Marcoux [b], L.M. Miller [c], L. Forró [a]

[a] NN Group, Institute of Physics of Condensed Matter, School of Basic Sciences (Station 3), Swiss Federal Institute of Technology (EPFL), CH-1015 Lausanne, Switzerland
[b] LETI/DTBS/Equipe commune CEA–bioMérieux, 17 rue des Martyrs 38054 Grenoble cedex 9, France
[c] National Synchrotron Light Source, Brookhaven National Laboratory, Upton, NY 11973, United States

ARTICLE INFO

Article history:
Received 26 July 2010
Received in revised form 18 September 2010
Accepted 18 September 2010
Available online 27 September 2010

Keywords:
IR
Infrared Spectroscopic Microscopy
Synchrotron
Fullerols
Reactive Oxygen Species
Oxidative stress

ABSTRACT

An oxidative stress (OS) state is characterized by the generation of Reactive Oxygen Species (ROS) in a biological system above its capacity to counterbalance them [1]. Exposure to OS induces the accumulation of intracellular ROS, which in turn causes cell damage in the form of protein, lipid, and/or DNA oxidations. Such conditions are believed to be linked to numerous diseases or simply to the ageing of tissues. However, the controlled generation of ROS *via* photosensitizing drugs or photosensitizers (PS) is now widely used to treat various tumors and other infections [2,3]. Here we present a method to track the chemical changes in a cell after exposure to oxidative stress. OS is induced *via* fullerols, a custom made water soluble derivative of fullerene (C_{60}), under visible light illumination. Synchrotron-based Fourier Transform InfraRed Microspectroscopy (S-FTIRM) was used to assess the chemical makeup of single cells after OS exposure. Consequently, a chemical fingerprint of oxidative stress was probed in this study through an increase in the bands linked with lipid peroxidation (carbonyl ester group at 1740 cm^{-1}) and protein phosphorylation (asymmetric phosphate stretching at 1240 cm^{-1}).

1. Introduction

Reactive Oxygen Species (ROS) are important intermediates in photo-oxidative processes. ROS include non-exhaustively, hydroxyl radical (OH•), superoxide anion (O_2•), electronically-excited dioxygen, *i.e.* singlet oxygen ($^1\Delta_g$), peroxynitrite (ONOO•) and hydrogen peroxide (H_2O_2). If ROS play important roles in living systems, both as key intermediates in physiological processes and as strong oxidants, they are also responsible for the oxidative stress (OS) underlying various deleterious processes. In living cells, OS occurs when enhanced ROS generation exceeds the basal level of cellular protective mechanisms. The cells are then damaged by oxidization of their subcellular components, which can lead to cell apoptosis or necrosis. In particular, elevated ROS levels in cells are associated with the aging process [4], as well as with many pathological disease processes [1,5]. Among various ROS involved in bio-oxidative and bio-photo-oxidative processes, $^1\Delta_g$ plays a significant role. In particular, $^1\Delta_g$ is involved in light-induced photo-damage to the eyes and skin [6]. $^1\Delta_g$ is known to be almost as reactive as atomic oxygen and to react directly with proteins and unsaturated lipids located in the cytosol and cell membranes to give the corresponding peroxides. Consequently, cell apoptosis, bacterial and viral inactivation are identified effects of $^1\Delta_g$ action [7,8] with higher yields than hydroxide (OH•) or superoxide (O_2•) radicals [9].

Pristine fullerene (C_{60}), due to its unique electronic π-system, can generate $^1\Delta_g$ and other ROS in organic solvents under UV or visible light illumination [10]. It has also been shown that the polyhydroxylated and highly water-soluble derivatives of C_{60}, also known as fullerols, are potent photosensitizers of ROS. In particular, evidence of generation of superoxide radicals via the so-called Type I mechanism, as well as $^1\Delta_g$ via an effective resonant energy transfer (Type I photosensitization pathway) was demonstrated for fullerol $C_{60}(OH)_{24}$ [11]. In a previous study we have shown that a custom-synthesized fullerol ($C_{60}(OH)_{19}(ONa)_{17}$,18$H_2O$) can efficiently generate $^1\Delta_g$ in aqueous milieus under visible light illumination and also pointed to a strong photo-toxicity of this compound towards cells [12] and cell compounds [13].

In this work, the oxidative stress on living monkey fibroblasts was mediated *via* ROS, which was photo-sensitized in the presence of the above-mentioned fullerol $C_{60}(OH)_{19}(ONa)_{17}$,18$H_2O$ [12]. First, the generation of $^1\Delta_g$ by this water-soluble derivative of C_{60} *via* Type II photodynamic process was confirmed in a cell-free EPR experiment using a $^1\Delta_g$ selective substrate, 2,2,6,6-tetramethyl-4-piperidinol (TMP-OH). Then, the OS-induced biochemical alterations in living fibroblasts were tracked by Fourier Transform InfraRed Microspectroscopy (FTIRM) at the

* Corresponding author. Present address: POMAM Lab. Institut de Chimie de Strasbourg, UMR7177, CNRS-UDS. 1, rue Blaise Pascal, BP296/R8, 67008 Strasbourg France.
E-mail address: vileno@unistra.fr (B. Vileno).

0301-4622/$ – see front matter © 2010 Elsevier B.V. All rights reserved.
doi:10.1016/j.bpc.2010.09.004

single cell level. To achieve the required subcellular spatial resolution, an IR beam size smaller than the cell size itself is needed. However, existing IRMS instruments using a conventional thermal (globar) source, encounter a Signal-to-Noise ratio (S/N) limitation when apertures confine the IR to an area of below 30 μm^2 [14]. Hence, for single cell imaging, the InfraRed (IR) synchrotron source delivers the entire infrared wavelength at much higher brightness than a globar source [15]. For a 10 by 10 μm^2 aperture, the S/N ratio is improved by a few orders of magnitude compared to globar sources [16]. In order to account for heterogeneities in living matter, we also looked for spectral anomalies for a given functional group in a population of at least 75 cells, allowing statistical sampling.

2. Materials and methods

2.1. Fullerol synthesis and ROS generation

The fullerol synthesis was adapted from Chiang et al. [17], based on the oxidation of C_{60} under strongly acidic conditions. The synthesis and characterization is detailed in [12]. The final stoichiometry used here was $C_{60}(OH)_{19}(ONa)_{17}$,18$H_2O$. White light illumination of an aqueous solution of fullerol leads to ROS generation. Depending on experimental conditions, either oxygen based radicals (OH•, O_2•) are generated via charge transfer (Type I pathway) or $^1\Delta_g$ following a resonant energy transfer pathway (Type II) [18]. Throughout all experiments, a 500 μM solution of fullerol in Phosphate Buffered Saline (PBS, pH = 7.4, Sigma), saturated with oxygen gas by bubbling for at least 30 min, was used. All solutions were prepared with ultrapure water (18.2 MΩcm^{-1}; Milli-Q purification system, Millipore).

2.2. ROS detection

To confirm the generation of $^1\Delta_g$, we employed Electron Paramagnetic Resonance (EPR) in conjunction with reactive scavenging of $^1\Delta_g$ with a diamagnetic substrate, 2,2,6,6-tetramethyl-4-piperidinol (TMP-OH, Sigma). This approach, introduced firstly by Lion et al. [19], is now customarily considered as a highly specific technique for the detection of $^1\Delta_g$ in aqueous media [20]. The formation of a stable paramagnetic N-oxyl radical, 4-hydroxy-2,2,6,6,-tetramethyl-piperidineN-oxyl (TEMPOL) is monitored by EPR, resulting from the attack of $^1\Delta_g$ on TMP-OH. The unpaired electron in TEMPOL is primarily located in the π-orbital of the nitrogen ^{14}N atom, which has a nuclear spin $I = 1$. This gives rise to a characteristic EPR spectrum consisting of three equidistant and approximately equi-intense hyperfine features ($A_N = 1.69$ mT, $g = 2.0066$, $\Delta H_{pp} = 0.158$ mT). The EPR reactive scavenging of $^1\Delta_g$ is summarized in Fig. 1A. The aqueous PBS solution (pH ~ 7.4) containing 500 μM of fullerol was supplemented with TMP-OH at 50 mM. Prior to the EPR measurements, the oxygen saturated solutions were directly transferred into thin quartz capillaries (0.6/0.87 mm inner/outer diameter, with a sample height of 25 mm, VitroCom, NJ, USA) and sealed on both ends with Cha-Seal™ tube sealing compound (Medex International, Inc., USA). Solutions were then exposed to illumination with the white light from a spot light source (150 W halogen lamp, Model 6000, Intralux, Switzerland). Immediately after exposure to visible light, the sample-holding capillaries were transferred into the EPR cavity of the EPR spectrometer (Model ESP300E from Bruker BioSpin GmbH). All the EPR experiments were carried out at room temperature. EPR spectra were acquired in a conventional field-swept mode. Routinely, for each experimental point, ten-scan field-swept EPR spectra were recorded. The typical instrumental settings were: microwave frequency 9.38 GHz, microwave power 2.0 mW, sweep width 100 G, modulation frequency 100 kHz, modulation amplitude 1 G, receiver gain 1×10^5, time constant 20.48 ms, conversion time 40.96 ms, and time per single scan 41.9 s.

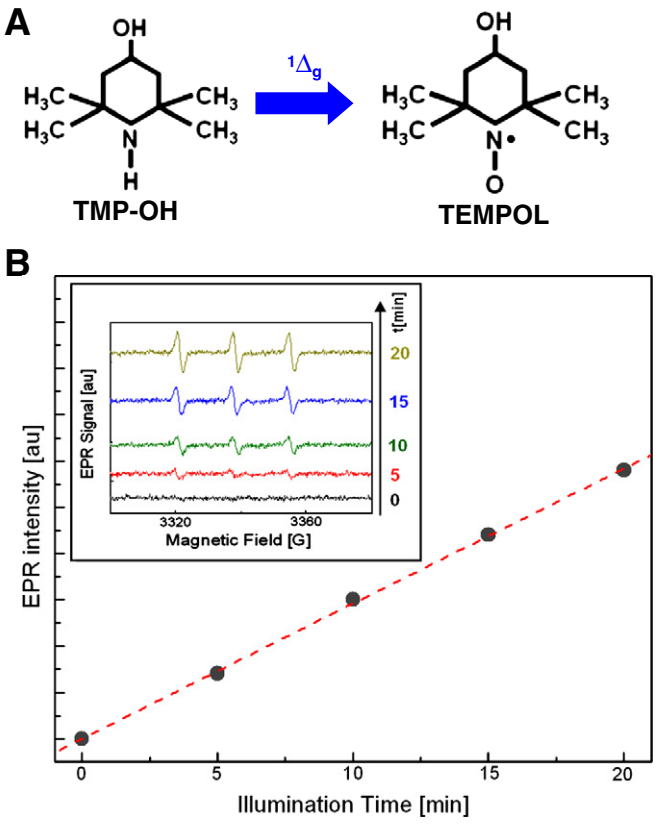

Fig. 1. (A) Reactive mechanism of TEMPOL generation (paramagnetic) resulting from TMP-OH (diamagnetic) scavenging of $^1\Delta_g$. (B) Evolution of the EPR signal of TEMPOL at different illumination times in the process of $^1\Delta_g$-photosensitization in oxygen-saturated 500 μM of $C_{60}(OH)_{19}(ONa)_{17}$ supplemented with 50 mM of TMP-OH.

2.3. Cell culture

The monkey Fibroblast cell line COS-7 was cultured in Dulbecco's Modified Eagle Medium (DMEM, pH 7.4, Sigma) supplemented with 10% Fetal Calf Serum and 2 mM L-Glutamine. Cells were grown at 37 °C, 95% air/5% CO_2, on non-coated calcium fluoride (CaF_2) windows (13 mm diameter, 1 mm thickness, Crystran, UK) using an identical number of passages. CaF_2 is known to be non toxic to cells and fully transparent in the relevant IR range between 1000 and 4000 cm^{-1}. A density of 25,000–30,000 cells per window was deposited, and used for experiment before they reached confluent state (days 2–3), thus single cells were still distinguishable [21].

2.4. Protocol of cell irradiations

The cell—covered CaF_2—windows were removed from the culture medium, rinsed in PBS, placed in the photosensitizing solution (*i.e.* PBS supplemented by 500 μM $C_{60}(OH)_{19}(ONa)_{17}$), and then illuminated for three different exposure times (10, 20 and 30 min). Special care was taken not to heat the sample by the light source (Halogen Philips, 150 W). After exposure, the photosensitizing solution was removed, the cells were rinsed in PBS, incubated for 30 min in DMEM, rinsed again with PBS and left to dry at 4 °C under a soft air flow. Once fully dried, the windows were carefully re-washed with distilled water in order to remove PBS salt crystals on the window surface, fully dried again and kept at 4 °C until S–FTIRM experiments [22–24].

A Trypan Blue (TB, Sigma Aldrich) assay was used to probe the viability of the cells upon OS. TB is negatively charged and typically does not penetrate a cell unless its membrane is damaged. Consequently, all cells including this dye and thus having a blue stained cytoplasm are dead. Inversely all viable cells exclude the dye

and have a clear cytoplasm. Noteworthy, the TB assay cannot differentiate between a necrotic or apoptotic cell.

2.5. Synchrotron infrared microspectroscopy

Synchrotron-based Fourier Transform Infrared Microspectroscopy (S-FTIRM) measurements were performed on dried cells prepared as described previously. The S-FTIRM set-up [14] consists of a Thermo Nicolet Continum IR microscope coupled to a Thermo Nicolet Magna 860 FTIR (Thermo Nicolet Instrument, Madison, WI). An automated X–Y mapping stage allowed sample scanning with a step accuracy of 1 μm. The IR beam, with an aperture of 7×7 to 10×10 μm^2, was positioned on the center of a single flat cell chosen by conventional optical microscopy. Spectra were collected in transmission mode, at a spectral resolution of 4 cm^{-1}, and 128 to 256 scans were co-added to enhance the S/N ratio. Prior to each experiment, a background spectrum was taken at a clean cell-free place on the CaF_2 window and subtracted from the one with the sample. Data were analyzed using Omnic 7.4 (Thermo Fisher Scientific Inc), and Transform (Fortner Software). Few bad pixels were removed and replaced either by the mean value of their neighbor's pixel (e.g. for odd absorbance values) or set to zero (for negative values). It is worth noting that despite the high brightness of the IR source, the total energy delivered to a sample for an aperture of 10 by 10 μm^2 is less than 5 mW [25]. The local rise of temperature under IR synchrotron irradiation has been determined to be lower than 1° [26]. Therefore, we assumed that heating had no effect on our experiment.

3. Results

3.1. Kinetics of ROS-generation by $C_{60}(OH)_{19}(ONa)_{17}$

The EPR measurements confirmed the photosensitization of $^1\Delta_g$ in PBS buffered H_2O solutions in the presence of fullerol $C_{60}(OH)_{19}(ONa)_{17}$,18 H_2O. The typical EPR results on reactive scavenging of $^1\Delta_g$ are shown in Fig. 1B. As shown in the inset, the observed EPR spectra are 1:1:1 triplets, indicative of TEMPOL, the paramagnetic product of the $^1\Delta_g$ attack on TMP-OH. The amplitude of the characteristic EPR signal of TEMPOL increased linearly until 20 min of illumination, pointing to a marked process of $^1\Delta_g$-formation *via* Type II energy transfer from the light-excited triplet states of fullerols to the ground state triplets of dioxygen molecules.

3.2. Cell viability under photo-oxidative stress

As a preliminary study, a cell viability test was performed using a Trypan Blue dye exclusion assay. Cells were incubated after different exposure times to OS in solutions of 0.01% TB in PBS. The buffer was then exchanged with pure PBS and cells were dried as described above. A significant increase of TB stained cells was observed after only 5 minutes of exposure to the combined effects of light and fullerol. The percentage of dead cells increased above 75% after 20 min of OS exposure. Control experiments suggested that neither the lone presence of the photosensitizer in the dark, nor the visible light illumination in the absence of PS, had a detectable effect on cell viability (TB stained cells <4%).

3.3. Spectral IR signature

As individual biochemical components have their specific vibrational fingerprints (see reference [27]), the various organic molecules present in a single cell shape an S–FTIRM spectrum with complex overlapping absorption bands. Hence, one band can be associated with several compounds. A typical S–FTIRM spectrum of a single dried, non-treated fibroblast is shown in Fig. 2 (top spectrum). The main spectral

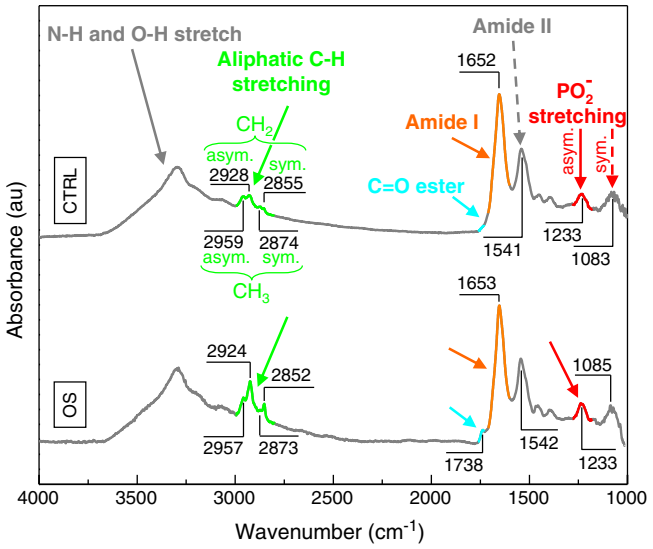

Fig. 2. Infrared spectra of dried single monkey fibroblasts for: (top) a non-treated cell (ctrl) and (bottom) a cell exposed to photo-mediated OS for 30 min in an oxygenated 500 μM fullerol in PBS solution. The aperture was set to 10×10 μm^2, the instrumental resolution to 4 cm^{-1}, and 256 spectra were accumulated. A baseline was subtracted for both spectra.

features observed in the cell with their associated characteristic functional groups were the following:

(i) The wide 3300 cm^{-1} band (gray arrow) originates from both the N–H and O–H bonds present in water traces, polysaccharides, carbohydrates and proteins [28].

(ii) The band in the 2995–2800 cm^{-1} region (green arrow) arises from the symmetric and asymmetric stretching modes of the carbon–hydrogen bond in methylene (CH_2) and methyl (CH_3) group mainly present in lipids and protein [29].

(iii) Between 1740 and 1725 cm^{-1} (blue arrow) the shoulder is attributed to the contributions of the carbonyl ester group (>C=O) in non-hydrogen bonded and hydrogen-bonded states respectively, found in phospholipids [30].

(iv) The two absorption bands centered around 1650 and 1545 cm^{-1} correspond to the intensity of Amide I (orange arrow) and Amide II (dashed gray arrow), respectively. Amide I originate from the C=O hydrogen bonded stretching vibrations. The Amide II peak, is also representative of a protein-based structure, and arises from C–N stretching and C–NH bending vibrations [31,32].

(v) The bands centered around 1235 cm^{-1} and 1085 cm^{-1} originate mainly from asymmetric phosphate ($asPO_2^-$, red arrow) and symmetric phosphate (sPO_2^-, dotted red arrow) stretching vibrations, respectively. They are attributed to the phosphodiester groups of nucleic acids from DNA. These two bands are also attributed to the C–O–P stretching modes present in phosphorylated lipids or proteins [33].

Fig. 2 (bottom spectrum) shows a typical IR spectrum of a single fibroblast after 30 min of exposure to oxidative stress generated by $C_{60}(OH)_{19}(ONa)_{17}$ following the procedure explained above. The spectrum was acquired with the same parameters as for the control experiment. Compared to the non-exposed fibroblast, the most striking change is the appearance of a peak centered at 1740 cm^{-1} (blue arrow). Nevertheless, the absolute increase of this peak could be due to a high number of lipid molecules and/or high lipid density in the cell. This could be especially the case when the aliphatic chains band (region 2995–2800 cm^{-1}, green arrow), which is connected to lipids, also increased. Therefore, we calculated the ratio between the C O representative band and the lipids for N>75 cells at three different time points T = 10, 20 and 30 min. Results are shown in Fig. 3A. All

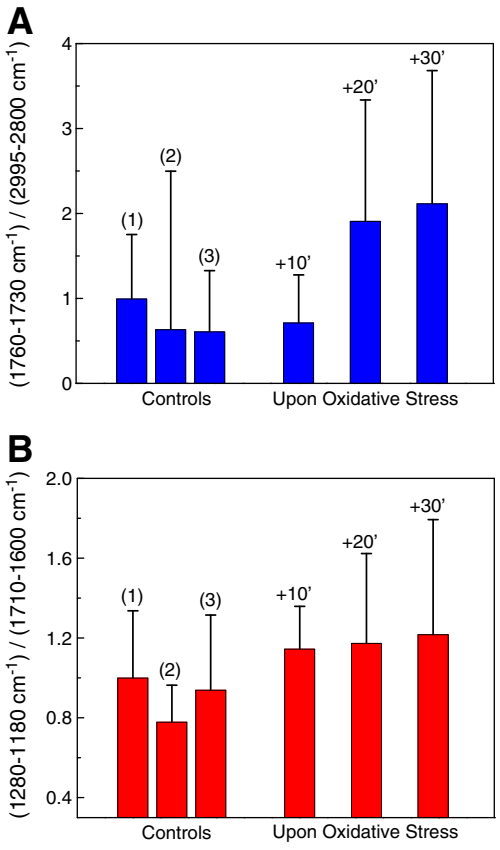

Fig. 3. Histograms of the integrated area ratio between (A) the ester carbonyl stretching mode (1760–1730 cm^{-1} region) and the aliphatic C–H stretch region (2995–2800 cm^{-1} region) and (B) between the phosphorylated protein peak area (asymmetric phosphate stretching band, 1280–1180 cm^{-1}) and the protein peak area (Amide I, 1710–1600 cm^{-1}). Controls were the following: (1) no treatment. (2) 20 min in the presence of fullerols in the dark. (3) 20 min illumination in PBS without PS. OS exposure: cells were illuminated in the presence of 500 μM of $C_{60}(OH)_{19}(ONa)_{17}$ in PBS saturated with oxygen, for different exposure times (10, 20 and 30 min). All the values were normalized by the control (1). Average values were calculated assuming a Gaussian distribution of our experimental values. The error was taken as the full width at half maximum (FWHM) of the Gaussian.

values were normalized to control (1) where the cells were not subjected to any treatment. Controls (2) and (3) were performed respectively in the presence of PS in the dark and after 20 min of illumination but without PS. Even though the distribution of the obtained values is relatively high, due to a strong heterogeneity among cells, the ratio between carbonyl ester groups in non-hydrogen bonded state and lipids, in each experimental group, were consistent and almost doubled after a 20 min OS exposure.

Specific protein-phosphorylation events have been previously demonstrated to occur during apoptosis and play an important role in the regulation of the programmed cell death mechanism [34]. Hence, we also calculated the ratio between the asymmetric phosphate stretching region, 1280–1180 cm^{-1}, and the Amide I peak at 1710–1600 cm^{-1} for $N>75$ cells at three different time points $T=10, 20$ and 30 min (Fig. 3B).

To determine whether the differences in the means of the presented histograms are significant, we performed a two tails t-test comparing the control (1) with the 10, 20 and 30 min oxidative stress statistics. The data were expressed as means and standard errors. The obtained t values for $p=0.1$ or less were considered as significant. All these data fulfilled the imposed t-test conditions.

3.4. Single cell mapping

In order to localize characteristic spectral features at higher resolution we recorded an IR map of a single cell, by scanning the sample. The step size was 8 μm and the aperture was set to 7 μm, the diffraction-limited spatial resolution allowed a detailed mapping of a single cell with a size between ten and a few tens of a micrometer. Flat, well-spread cells were chosen by optical microscopy ensuring that the observed variations in intensity arose mostly from local concentration changes rather than from local thickness changes. Different distributions of the chemical functional groups are presented in Figs. 4 and 5, for a non-treated fibroblast and for a fibroblast cell after a maximal exposure to photo-mediated OS (30 min/500 μM PS in oxygenated PBS solution): (A) optical image of the cell, (B) distribution map of lipids computed from the integration of the aliphatic C–H stretching band area (2995–2800 cm^{-1}), (C) distribution map of proteins represented by the integration of the Amide I band area (1710–1600 cm^{-1}), (D) ester distribution mapped by integration of the carbonyl ester group stretching band (1730–1760 cm^{-1}) and (E) asymmetric phosphate stretching represented by the 1280–1180 cm^{-1} area. The protein distribution (C) for both, treated and non-treated cells exhibited a relatively homogenous distribution and high intensity at the cell center. This corresponded to the thickest part of the cell where the nucleus was also present, and in which a high protein density is found [35]. In contrast, the lipid distribution (B) was more spread, confirming that lipids are well distributed among the intracellular compartments, like the endoplasmic reticulum, the Golgi apparatus, the nuclear and cell membrane. No significant changes in either distribution were visible between the control and the treated cell, except that the treated cell was thicker and gave a stronger signal.

In order to normalize such thickness differences in cells, and detect relative changes in lipid peroxidation and protein phosphorylation from a non-treated to a treated cell (panels D and E in Fig. 4), we also represented the peak ratios: 1730–1760 cm^{-1} (C O) over 2995–2800 cm^{-1} (lipids) and 1280–1180 cm^{-1} (PO_2^-) over 1710–1600 cm^{-1} (Amide I). Both signatures were significantly enhanced upon ROS treatment (see Fig. 5 panels D and E respectively), as it was already observed in single cell spectra (Fig. 2, bottom).

4. Discussion and conclusion

We have shown that $^1\Delta_g$ is generated within the timeframe of fullerol illumination (Fig. 1B). This allowed us to conclude that the detected spectrum anomalies arising in the cells are largely due to the effect of $^1\Delta_g$. The most significant spectrum anomaly observed in cells exposed to OS was an increase of the peak around 1740 cm^{-1}, after 20 min of exposure to OS (Fig. 3A). This was already observed by Holman et al. in dying fibroblasts, and attributed to the non-hydrogen-bonded ester carbonyl stretching mode in phospholipids [36]. Moreover, in previous studies this peak increase was referred to an IR fingerprint of necrotic cells [16,35]. In our case, it can be explained by the generation and accumulation of lipid peroxidation end products, known as Reactive Carbonyl Compound (RCC) such as e.g. malondialdehyde (MDA) [37] or acrolein [38]. Moreover, according to the chemical map of the cell in Figs. 4 and 5 panel D, such increases are predominantly located in the cell periphery, distant from the nucleus (highlighted by a white dashed circle). Hence this pattern can be ascribed to the increase of oxidized lipids present in the membrane of dying cells. This feature, localized around the nucleus, is in excellent agreement with the study performed on necrotic cells by Dumas et al. [16].

On the other hand, the ratio between the peak partially associated with phosphorylated proteins (asymmetric phosphate stretching band, 1280–1180 cm^{-1}) and the protein peak (Amide I, 1710–1600 cm^{-1}) integrated intensities started to increase earlier: after only 10 min of exposure to OS (as shown in Fig. 3B). Specific protein-phosphorylation events are known to occur during apoptosis and also play an important role in the regulation of programmed cell death [39,40]. Cell mapping in Panel E (Figs. 4 and 5) shows an increase in

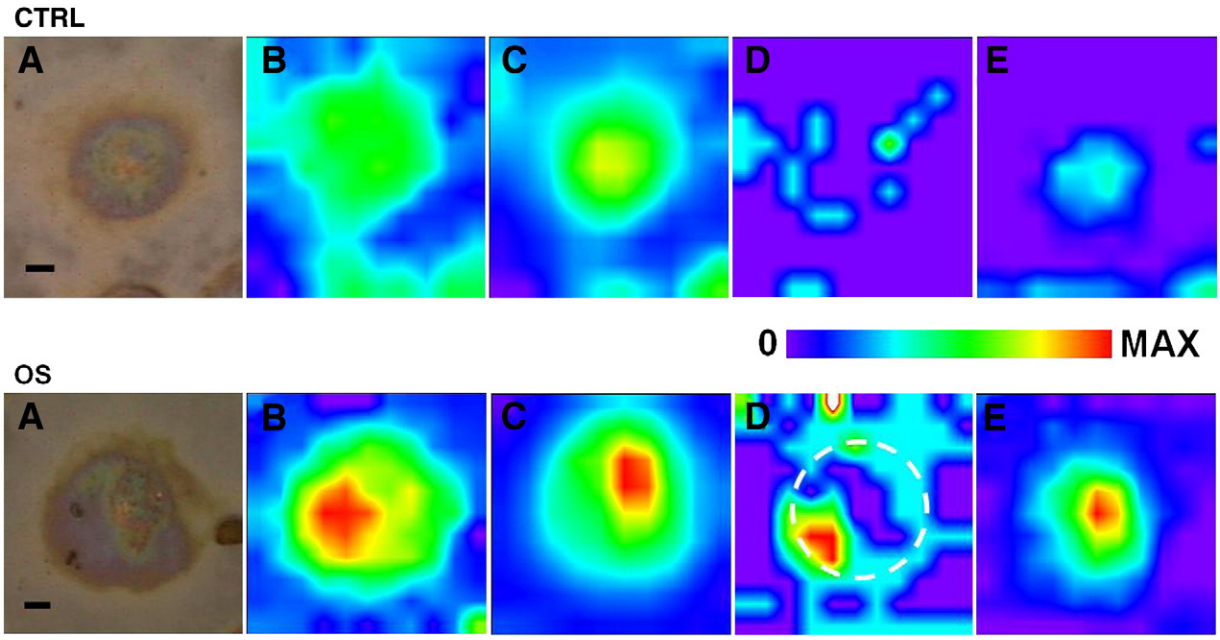

Fig. 4. Single cell mapping of the functional group distribution for a non-treated (CTRL) fibroblast (top row) and exposed for 30 min to OS (bottom row). (A) Optical image of a single cell. (B) Lipid distribution map associated to the aliphatic C–H stretch band (2995–2800 cm^{-1}) (C) Protein distribution map resulting from the Amide I peak integration (1710–1600 cm^{-1}) (D) Asymmetric phosphate stretching distribution (1280–1180 cm^{-1}). (E) Ester distribution map illustrated by carbonyl ester group stretch (1730–1760 cm^{-1}). The spectra were recorded with an aperture of 8×8 μm^2 with a step size of 7 μm, a resolution of 4 cm^{-1}. 256 scans were accumulated. The scale bar on A represents 8 μm. The concentrations of each component scale from blue (0) to red (max).

the phosphate contribution, spread over the whole cell, possibly indicating that cytoskeletal proteins were targeted during this apoptotic process. In summary, exposure to oxidative stress, and in particular $^1\Delta_g$, induces a cascade of lipid peroxidation and phosphorylation reactions within the observed cells. First, protein phosphorylation occurs within the cytoplasm and nucleus and later lipid phosphorylation of membrane structures. However, attributing this OS-induced phosphorylation to an apoptotic or necrotic reaction remains still open. It is very likely that a combination of both pathways exists.

Concerning the distribution in the value obtained in our statistical sampling, it is worth noting that the cells studied after exposure to oxidative stress, might have been those which better resisted the photo-mediated action. Considering the experimental procedure, those cells with more damage had a higher likelihood to detach from the surface and were then washed away during the multiple rinsing steps. Therefore, they were not considered in this study, which compromised the statistics. In conclusion, we successfully used FTIRM to detect small OS-mediated biochemical changes in cells. Especially, lipid peroxidation and protein phosphorylation have been identified as OS fingerprint. These features were characterized by an increase of the ester (1740 cm^{-1}) and phosphate asymmetric stretching (1240 cm^{-1}) related peaks respectively.

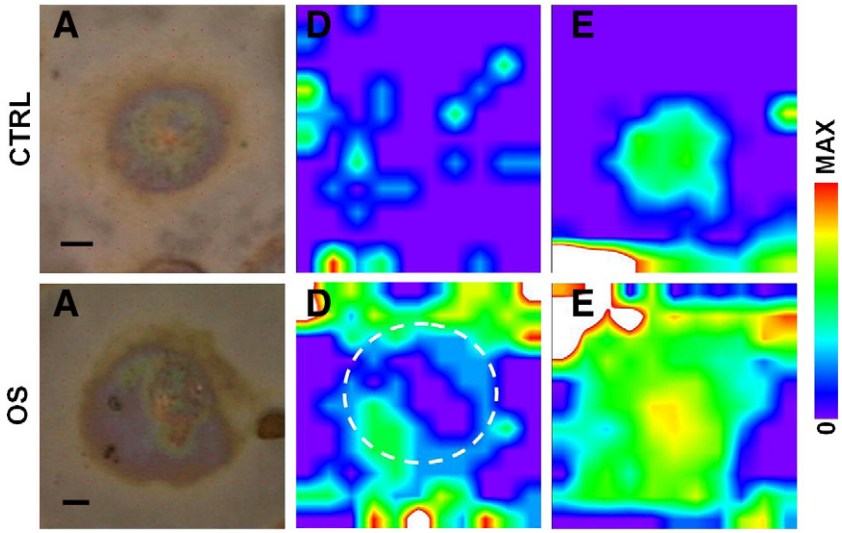

Fig. 5. Single cell mapping of the functional group distribution for a non-treated (CTRL) fibroblast (top row) and exposed for 30 min to OS (bottom row). (A) Optical image of a single cell. (D) Ratio of the bands 1730–1760 cm^{-1} (C=O) and 2995–2800 cm^{-1} (lipids). (E) Ratio of the bands 1280–1180 cm^{-1} (PO_2^-) and 1710–1600 cm^{-1} (Protein). The spectra were recorded with an aperture of 8×8 μm^2 with a step size of 7 μm, a resolution of 4 cm^{-1}. 256 scans were accumulated. The scale bar on A represents 8 μm. The concentrations of each component scale from blue (0) to red (max), white corresponds to values out of range, when the ratio is diverging (obtained for a very low absorbance value *i.e.* when the probed area is empty).

Acknowledgements

The authors are also particularly thankful to Randy Smith for his technical assistance and Dr. Titusz Feher for his constructive discussions. The NSLS is supported by the United States Department of Energy under contract DE-AC02-98CH10886. These studies were also partially supported by the Swiss National Science Foundation, project No. 205320-112164, "Biomolecules under stress: ESR *in vitro* study" (A.S. and L.F.).

References

[1] T. Finkel, N.J. Holbrook, Oxidants, oxidative stress and the biology of ageing, Nature 408 (2000) 239–247.
[2] A.P. Castano, P. Mroz, M.R. Hamblin, Photodynamic therapy and anti-tumour immunity, Nat. Cancer Rev. 6 (2006) 535.
[3] T.J. Dougherty, An update on photodynamic therapy applications, J. Clin. Laser Med. Surg. 20 (2002) 3–7.
[4] K. Scharffetter-Kochanek, P. Brenneisen, J. Wenk, G. Herrmann, W.J. Ma, L. Kuhr, C. Meewes, M. Wlaschek, Photoaging of the skin from phenotype to mechanisms, Exp. Gerontol. 35 (2000) 307–316.
[5] E. Mariani, M.C. Polidori, A. Cherubini, P. Mecocci, Oxidative stress in brain aging, neurodegenerative and vascular diseases: an overview, J. Chromatogr. B 825 (2005) 65–75.
[6] A. Dewilde, C. Pellieux, S. Hajjam, P. Wattre, C. Pierlot, D. Hober, J.-M. Aubry, Virucidal activity of pure singlet oxygen generated by thermolysis of a water-soluble naphthalene endoperoxide, J. Photochem. Photobiol. B 26 (1996) 23–29.
[7] A. Dewilde, C. Pellieux, S. Hajjam, P. Wattre, C. Pierlot, D. Hober, J.-M. Aubry, Virucidal activity of pure singlet oxygen generated by thermolysis of a water-soluble naphthalene endoperoxide, J. Photochem. Photobiol. B 26 (1996) 23–29.
[8] R.W. Redmond, I.E. Kochevar, Spacially resolved cellular responses to singlet oxygen, Photochem. Photobiol. 82 (2006) 1178–1186.
[9] I.E. Kochevar, M.C. Lynch, S. Zhuang, C.R. Lambert, Singlet oxygen, but not oxidizing radicals, induces apoptosis in HL-60 cells, Photochem. Photobiol. 72 (2002) 548–553.
[10] Y. Yamakoshi, N. Umezawa, A. Ryu, K. Arakane, N. Miyata, Y. Goda, T. Masumizu, T. Nagano, Active oxygen species generated from photoexcited fullerene (C_{60}) as potential medicines: O_2^* versus $^1O_2$, J. Am. Chem. Soc. 125 (2003) 12803–12809.
[11] A.R. Badireddy, E.M. Hotze, S. Chellam, P. Alvarez, M.R. Wiesner, Inactivation of bacteriophages via photosensitization of fullerol nanoparticles, Environ. Sci. Technol. 41 (2007) 6627–6632.
[12] B. Vileno, P.R. Marcoux, M. Lekka, A. Sienkiewicz, T. Feher, L. Forró, Spectroscopic and photophysical properties of a highly derivatized C60 fullerol, Adv. Funct. Mater. 16 (2006) 120–128.
[13] A. Sienkiewicz, B. Vileno, K. Pierzchała, M. Czuba, P.R. Marcoux, A. Graczyk, P.G. Fajer, L. Forró, Oxidative stress-mediated protein conformation changes: ESR study of spin-labelled staphylococcal nuclease, J. Phys. Condens. Matter 19 (2007) 285201.
[14] L.M. Miller, R.J. Smith, Synchrotrons versus globars, point-detectors versus focal plane arrays: selecting the best source and detector for specific infrared microspectroscopy and imaging applications, Vib. Spectrosc. 38 (2005) 237–240.
[15] L.M. Miller, P. Dumas, Chemical imaging of biological tissue with synchrotron infrared light, Biochim. Biophys. Acta 1758 (2006) 846–857.
[16] P. Dumas, L.M. Miller, The use of synchrotron infrared microspectroscopy in biological and biomedical investigations, Vib. Spectrosc. 32 (2003) 3–21.
[17] L.Y. Chiang, R.B. Upasani, J.W. Swirczewski, US Patent 5 177 248, 1993.
[18] Z. Markovic, V. Trajkovic, Biomedical potential of the reactive oxygen species generation and quenching by fullerenes (C_{60}), Biomaterials 29 (2008) 3561–3573.
[19] Y. Lion, M. Delmelle, A. van de Vorst, New method of detecting singlet oxygen production, Nature 263 (1976) 442–443.
[20] T. Ando, T. Yoshikawa, T. Tanigawa, M. Kohno, N. Yoshida, M. Kondo, Quantification of singlet oxygen from hematoporphyrin derivative by electron spin resonance, Life Sci. 61 (1997) 1953–1959.
[21] P. Steiner, J.C.F. Sarria, L. Glauser, S. Magnin, S. Catsicas, H. Hirling, Modulation of receptor cycling by neuron-enriched endosomal protein of 21 KD, J. Cell Biol. 157 (2002) 1197–1209.
[22] J. Ramesh, A. Salman, Z. Hammody, B. Cohen, J. Gopas, N. Grossman, S. Mordechai, FTIR microscopic studies on normal and h-ras oncogene transfected cultured mouse fibroblasts, Eur. Biophys. J. 30 (2001) 250–255.
[23] M.A. Cohenford, B. Rigas, Cytologically normal cells from neoplastic cervical samples display extensive structural abnormalities on IR spectroscopy: Implications for tumor biology, Proc. Natl Acad. Sci. 95 (1998) 15327–15332.
[24] K.Z. Liu, H.H. Mantsch, Apoptosis-induced structural changes in leukemia cells identified by IR spectroscopy, J. Mol. Struct. 565 (2001) 299–304.
[25] L.M. Miller, G.D. Smith, G.L. Carr, Synchrotron-based biological microspectroscopy: from the mid-infrared through the far-infrared regimes, J. Biol. Phys. 29 (2003) 219–230.
[26] M.C. Martin, N.M. Tsvetkova, J.H. Crowe, W.R. McKinney, Negligible sample heating from synchrotron infrared beam, Appl. Spectrosc. 55 (2001) 111–113.
[27] B. Stuart, in: D.J. Ando (Ed.), Biological Applications of Infrared Spectroscopy, John Wiley & sons, NY, 1997.
[28] F. Siebert, Infrared-spectroscopy applied to biochemical and biological problems, Meth. Enzymol. 246 (1995) 501–526.
[29] F. Severcan, N. Toyran, N. Kaptan, B. Turan, Fourier transform infrared study of the effect of diabetes on rat liver and heart tissues in the C–H region, Talanta 53 (2000) 55–59.
[30] J. Kneipp, P. Lasch, E. Baldauf, M. Beekes, D. Naumann, Detection of pathological molecular alterations in scrapie-infected hamster brain by Fourier transform infrared (FT-IR) spectroscopy, Biochim. Biophys. Acta 1501 (2000) 189–199.
[31] A. Barth, Infrared spectroscopy of proteins, Biochim. Biophys. Acta 1767 (2007) 1073–1101.
[32] R. Schweitzer-Stenner, Advances in vibrational spectroscopy as a sensitive probe of peptide and protein structure: a critical review, Vib. Spectrosc. 42 (2006) 98–117.
[33] P. Dumas, L.M. Miller, Biological and biomedical applications of synchrotron infrared microspectroscopy, J. Biol. Phys. 29 (2003) 201–218.
[34] B.T. Gjertsen, S.O. Doskeland, Protein-phosphorylation in apoptosis, Biochim. Biophys. Acta Mol. Cell Res. 1269 (1995) 187–199.
[35] N. Jamin, P. Dumas, J. Moncuit, W.H. Fridman, J.L. Teillaud, G.L. Carr, G.P. Williams, Highly resolved chemical imaging of living cells by using synchrotron infrared microspectrometry, Proc. Natl Acad. Sci. 95 (1998) 4837–4840.
[36] H.N. Holman, M.C. Martin, E.A. Blakely, K. Bjornstad, W.R. McKinney, IR spectroscopic characteristics of cell cycle and cell death probed by synchrotron radiation based Fourier transform IR spectromicroscopy, Biopolymers 57 (2000) 329–335.
[37] D. Del Rio, A.J. Stewart, N. Pelligrini, A review of recent studies of malondialdehyde as toxic molecule and biological marker of oxidative stress, Nutr. Metab. Cardiovasc. 15 (2005) 316.
[38] K. Uchida, M. Kanematsu, Y. Morimitsu, T. Osawa, N. Noguchi, E. Niki, Acrolein is a product of lipid peroxidation reaction, J. Biol. Chem. 273 (1998) 16058.
[39] B.T. Gjertsen, S.O. Doskeland, Protein phosphorylation in apoptosis, Biochim. Biophys. Acta 1269 (1995) 187–199.
[40] P.K. Davis, G.V.W. Johnson, Energy metabolism and protein phosphorylation during apoptosis: a phosphorylation study of tau and high-molecular-weight tau in differentiated PC12 cells, Biochem. J. 340 (1999) 51–58.

Neuroscience 186 (2011) 39–47

OXIDATIVE STRESS AND PREVENTION OF THE ADAPTIVE RESPONSE TO CHRONIC IRON OVERLOAD IN THE BRAIN OF YOUNG ADULT RATS EXPOSED TO A 150 KILOHERTZ ELECTROMAGNETIC FIELD

K. MAAROUFI,[a,b] E. SAVE,[a] B. POUCET,[a] M. SAKLY,[b] H. ABDELMELEK[b] AND L. HAD-AISSOUNI[c]*

[a]*Laboratory of Neurobiology and Cognition, Unité Mixte de Recherche 6155 Centre National de la Recherche Scientifique-Université de Provence, 3 place Victor Hugo, 13331 Marseille cedex 3, France*

[b]*Faculty of Sciences of Bizerte, Laboratory of Integrative Physiology, 7021 Jarzouna, Tunisia*

[c]*Developmental Biology Institute of Marseille-Luminy, Unité Mixte de Recherche 6216 Centre National de la Recherche Scientifique-Université de la Méditerranée, Campus de Luminy - Case 907, 13288 Marseille cedex 9, France*

Abstract—Iron surcharge may induce an oxidative stress-based decline in several neurological functions. In addition, electromagnetic fields (EMF) of frequencies up to about 100 kHz, emitted by electric/electronic devices, have been suggested to enhance free radical production through an iron dependent pathway. The purpose of this study was therefore to determine a possible relationship between iron status, exposure to EMF, and brain oxidative stress in young adult rats. Samples were micro-dissected from prefrontal cortex, hippocampus, striatum, and cerebellum after chronic saline or iron overload (IO) as well as after chronic sham exposure or exposure to a 150 kHz EMF or after combining EMF exposure with IO. The brain samples were used to monitor oxidative stress-induced lipid peroxidation and activity of the antioxidant enzymes superoxide dismutase and catalase. While IO did not induce any oxidative stress in young adult rats, it stimulated antioxidant defenses in the cerebellum and prefrontal cortex in particular. On the contrary, EMF exposure stimulated lipid peroxidation mainly in the cerebellum, without affecting antioxidant defenses. When EMF was coapplied with IO, lipid peroxidation was further increased as compared to EMF alone while the increase in antioxidant defenses triggered by the sole IO was abolished. These data suggest that EMF exposure may be harmful in young adults by impairing the antioxidant defenses directed at preventing iron-induced oxidative stress.

Key words: iron overload, electromagnetic exposure, oxidative stress, rat.

Low levels of reactive forms of oxygen, including both radical and nonradical species, are continually produced in cells. They may serve important physiological functions through redox based regulation of signal transduction and gene expression (Sen and Packer, 1996; Lander et al., 1997; Suzuki et al., 1997). However, due to their high reactivity, accumulation of reactive oxygen species (ROS) may induce oxidative damage to critical molecules, such as DNA, proteins, and lipids. If mild oxidative damage to DNA or proteins may be repaired or reversed, oxidative damage to polyunsaturated fatty acids may initiate a chain reaction of peroxidation (Draper and Hadley, 1990) that may affect membrane fluidity and permeability, and subsequently cell structure, function, and viability. Due to the pronounced effect of ROS on lipids, measure of lipid peroxidation is often used as a bio-marker of oxidative tissue damage (Niki et al., 1993; Gutteridge, 1995).

ROS generation is normally controlled by a large number of biological antioxidant defense systems, which act as protective mechanisms and reduce oxidative stress (Halliwell, 1996). The superoxide anion, formed mainly by the electron transport chains in mitochondria through electron leakage, is converted to hydrogen peroxide by the action of superoxide dismutase (SOD; EC 1.15.1.1). Hydrogen peroxide is then degraded by catalase (CAT; EC 1. 11. 1. 6) or other antioxidant enzymes. However, under certain conditions, for example, the presence of elevated concentrations of transition metals such as iron, hydrogen peroxide can also undergo metal ion-catalyzed cleavage by the Fenton reaction to generate the toxic hydroxyl radical that may initiate lipid peroxidation. Lipid hydroperoxide may also interact with iron resulting in new peroxidation chains. These reactions are dependent upon the availability of free iron, which is tightly controlled by metal-binding proteins (Gaasch et al., 2007), and may be enhanced by IO (Zecca et al., 2004a).

Brain tissue is thought to be very sensitive to oxidative stress. Neurons are enriched in mitochondria and possess a very high aerobic metabolism. Indeed, in resting conditions, up to 20% of total oxygen may be used by the brain which accounts for only 2% of total body weight. Knowing that up to 2% of the consumed oxygen may be converted to incompletely reduced ROS during mitochondrial respiration and that this proportion increases with oxygen consumption, ROS production in brain may be higher than in any other organ. Moreover, low levels of some antioxidant enzymes, such as SOD and CAT, high contents of polyunsaturated fatty acids in brain membranes, and high iron content may combine their effects to make the brain a preferential target for oxidative stress-related degeneration

*Corresponding author. Tel: +33-491-269-245; fax: +33-491-269-244.
E-mail address: laurence.had-aissouni@univmed.fr (L. Had-Aissouni).
Abbreviations: CAT, catalase; EMF, electromagnetic fields; IO, iron overload; ROS, reactive oxygen species; SOD, superoxide dismutase; TBARS, thiobarbituric acid-reactive substances.

0306-4522/11 $ - see front matter
doi:10.1016/j.neuroscience.2011.04.003

(Halliwell, 2006). It has been suggested that various neurodegenerative disorders such as Parkinson's disease, Alzheimer's disease, and amyotrophic lateral sclerosis result from the formation of ROS and oxidative stress (Fahn and Cohen, 1992; Benzi and Moretti, 1995; Bergeron, 1995).

Several epidemiological studies suggest a link between electromagnetic field (EMF) exposure resulting from the use of electric/electronic devices, and neurodegenerative disorders (Park et al., 2005; Davanipour et al., 2007; Roosli et al., 2007; Garcia et al., 2008; Huss et al., 2009). In addition, experiments performed to study the cellular effects of extremely low frequency EMF (50–60 Hz), have shown that EMF can disturb the cellular redox balance *in vitro* (Lin et al., 1994; Pessina and Aldinucci, 1997, 1998; Di Loreto et al., 2009) as well as in the rat brain (Amara et al., 2009; Akdag et al., 2010). Magnetic fields of frequencies up to about 10^5 Hz would stabilize free radicals species, increasing their lifetime and thus the probability of oxidative injury (Scaiano et al., 1994; Repacholi and Greenebaum, 1999). In accordance, higher levels of ROS, including superoxide anion, were found in immune cells after EMF exposure (Roy et al., 1995; Rollwitz et al., 2004). EMF exposure was also found to induce DNA damage in lymphocytes and brain cells through a process involving iron and possible formation of hydroxyl radicals (Zmyslony et al., 2000; Lai and Singh, 2004). There is also evidence that exposure to extremely low frequency (0–300 Hz) and radio frequency (10 MHz–300 GHz) EMF alters the blood-brain barrier permeability (Oscar and Hawkins, 1977; Nittby et al., 2008). In this context, it has been suggested that changes in the integrity of the blood-brain barrier may result in excess accumulation of heavy metals and in particular of iron in the brain (Castelnau et al., 1998; Thompson et al., 2001), which could lead to neuronal damage. Moreover, some studies promote the idea that the young brain is particularly sensitive to iron excess, possibly due to an immature iron permeability of the blood-brain barrier. It is therefore possible that neurotoxic effects resulting from EMF-induced iron excess in the brain would be greater in young adult rats.

The vast majority of the studies focusing on the biological and behavioral effects of EMF have used extremely low frequency EMF (0–300 Hz) that are generated by power lines or radiofrequency EMF (10 MHz–300 GHz) that are generated by wireless communications. Intermediate frequencies (300 Hz–10 MHz) have been poorly studied (Litvak et al., 2002) although they result from the operation of increasingly numerous electric/electronic devices (antitheft devices, card readers, metal detectors), household appliances (induction cook tops), and industrial equipments (welding devices, induction heaters). In the case of induction hotplates, users undergo prolonged and repeated exposure to EMF that raises concerns about potential health effects. In a previous study, we have shown in young adult rats that a 21-day iron supplementation treatment induced a deficit in spatial memory processes that could be correlated with modifications of the serotoninergic system. Surprisingly, combining 150 kHz-EMF and iron treatment restored the serotoninergic mechanisms affected by IO while it only attenuated the behavioral effects (Maaroufi et al., 2009b), therefore suggesting that the deficits due to IO and/or 150 kHz-EMF exposure result from the deficiency of multiple biochemical mechanisms. One of these mechanisms may involve oxidative stress. Thus, prolonging Maaroufi et al.'s work, the present study aims to analyze the long-term impact of IO and combination of IO and 150 kHz-EMF in young adult rats on oxidative stress in the brain. We measured (1) lipid peroxidation, using thiobarbituric acid-reactive substances (TBARS) assay, and (2) activity of the antioxidant enzymes SOD and CAT following IO and concurrent IO and EMF exposure in four different brain structures, prefrontal cortex, hippocampus, striatum, and cerebellum.

EXPERIMENTAL PROCEDURES

Subjects

1 month-old male Wistar rats, purchased from a commercial supplier (Janvier, Le Genest-St-Isle, France) and weighting 130–150 g (4 weeks old) served as subjects. Upon arrival, they were housed by groups of two with food and water *ad libitum* and kept in a temperature-controlled room (20±2 °C) with a 12/12 light/dark cycle. Two groups were tested in the IO experiment: IO (n=8), and Saline (n=8) groups; and three in the IO and EMF experiment: EMF-exposed (EMF, n=6), EMF-exposed and IO (EMF-IO, n=6), and Sham exposed without iron treatment (SHAM, n=6) groups. IO and EMF exposure treatment started 1 week after arrival. After the treatment was completed (IO and/or EMF exposure), rats were submitted to several behavioral tests (reported in Maaroufi et al., 2009b). In the present study our aim was to examine the long term effects of such treatments on oxidative stress. For this reason, oxidative stress was measured after completion of the behavioral tests.

Experiments were performed in accordance with the NIH guide for the care and use of laboratory animals (NIH publication no. 86-23, revised 1978), European guidelines (European Community Council Directive, November 2004, 1986, 86/609/EEC) and National guidelines (Council directive n°87848 of the Direction des Services Vétérinaires de la Santé et de la Protection Animale permission n°13.24 from the Ministère de l'Agriculture et de la Pêche to E.S.).

Iron overload

Rats received daily one i.p. injection of ferrous sulfate ($FeSO_4 7H_2O$, Sigma Aldrich, France) dissolved in sodium chloride 0.9% or vehicle (i.p.; 3 mg of $FeSO_4$ per kg of body) during 21 consecutive days. As previously shown, a daily 3 mg/kg dose of iron administrated in adult rats during 5 days results, 16 days after treatment, in significant iron accumulation in the hippocampus, cerebellum, and basal ganglia (Maaroufi et al., 2009a). This accumulation was correlated to behavioral deficits. Based on this result, longer treatment using the same dose is expected to ensure iron accumulation in the brain.

Iron overload and EMF exposure

To generate a 150 kHz magnetic field, we used a custom-made Helmoltz coil built by the "Centre Commun de Ressources en Micro-ondes" (Marseille). The Helmoltz coil was conceived as two parallel 50 cm×35 cm square-based coils, placed symmetrically on each side of the experimental areas along a common axis. The distance between the coils was 24 cm, calculated by approximating a circular coil of same surface (1750 cm^2). Each coil was made

up of six turns (isolated 1.5 mm^2 copper wire) so that a 250 mA electric current was required to generate a 150 kHz, 5 A/m, and 6.25 μT magnetic field. The 5 A/m strength used in the present study corresponds to the reference exposure levels determined by the European Council recommendation (199/519/CE) for a 150 kHz frequency. To generate the magnetic current, we used a low frequency (LW) generator (Thurlby Thandar Instruments, Huntingdon, UK) and an LF amplifier (150 W, 2–4 ohms, Blaupunkt, Hildesheim, Germany) connected to the coils. Control and measure of the magnetic field was made using an F16 current probe (Fischer Custom Communications, Torrance, CA, USA), a single loop antenna SAS 200/560, and an oscilloscope (Agilent, Santa Clara, CA, USA). This allowed us to check the tuning of the generator to produce the appropriate intensity (5 A/m) at 150 kHz and the homogeneity of the field at various points in the experimental area. The field was found to vary between 5 A/m and 5.75 A/m, which is negligible.

The apparatus was placed in a 1.7 m×3.2 m, temperature-controlled (20 °C), ventilated, dimly lit room, on a table. A 40 cm×26 cm×16 cm cage with a plexiglass cover that contained six rats for each assay was placed in the experimental area between the coils. Rats were exposed to 150 kHz EMF, 1 h/day (between 9 and 12 h) during 21 consecutive days. The sham-exposed control rats were placed in the cage using the same procedure as treated rats except that they did not receive irradiation.

Tissue sample preparation

At the end of the behavioral tests (approximately 2 months after the end of treatment), the rats were anesthetized with sodium pentobarbital and then decapitated. The brain was removed, rapidly washed with cold phosphate buffered saline, then immediately frozen on dry ice and finally stored at −80 °C. Thick coronal slices (2–3 mm) of various brain regions (cortex 5.16 mm–2.16 mm; striatum 2.16 mm to −0.48 mm; hippocampus −2.52 mm to −4.56 mm, and cerebellum −9.36 mm to −14.04 mm relative to bregma; (Schwarz et al., 2006)) were made at −20 °C using a cryostat (Leica CM3050). Micropunches were taken from these different sliced brain regions.

Samples were weighed and homogenized (1/10, w/v) in cold 20 mM HEPES buffer, pH 7.2, containing 1 mM EDTA, using a potter-Elvehjem homogenizer fitted with a pestle for microtubes. Homogenates were then centrifuged at 1600 g for 10 min at 4 °C. Part of the resulting supernatant (SN1) was kept at −80 °C until used to determine protein and TBARS contents as well as total SOD activity. The remaining part of SN1 was further centrifuged at 10,000 g for 15 min at 4 °C and supernatant (SN2) was kept at −80 °C until used to determine CAT activity.

Protein content

Protein content was determined in SN1 by the Bradford's method (Bradford, 1976) using the Coomassie Protein Assay Kit (Pierce, Rockford, IL, USA) and bovine serum albumin as standard.

Content in thiobarbituric-acid reactive substances

Lipid peroxidation was measured as TBARS by the method of Richard et al. (1992). Briefly, samples were incubated for 1 h at 95 °C in 0.75 volume of a mixture made of two volumes 55.36 mM thiobarbituric acid and 1 volume 7% perchloric acid. The samples were then chilled on ice to stop the reaction and two volumes of butanol-1 were added to extract the TBARS. After the phases were separated by centrifugation (1500 g, 10 min, 4 °C), the TBARS content was determined in the butanol-1 extract using a fluorescent plate reader (Fluoroskan Ascent FL; λex=530 nm, λem=590 nm). Malondialdehyde standards were included with each assay and TBARS contents were expressed as nmol of malondialdehyde/mg of proteins.

SOD activity

SOD was assayed using the SOD assay kit (Cayman Europe, Tallinn, Estonia) according to manufacturer instructions. This assay uses SOD's ability to inhibit the reduction of a tetrazolium salt by superoxide anions generated by xanthine oxidase. Formation of the formazan product was monitored at 450 nm using a microplate reader. One unit of SOD is defined as the amount of enzyme necessary to have 50% of inhibition. SOD activity was expressed as units/mg of proteins.

CAT activity

CAT was assayed using the CAT assay kit (Cayman Europe, Tallinn, Estonia) according to manufacturer instructions. This assay utilizes the peroxidatic function of CAT for determination of enzyme activity. Formaldehyde production from methanol in presence of optimal concentration of H_2O_2 was monitored at 540 nm on a microplate reader using purpald as chromogen. CAT activity was expressed as nmol/min/mg of proteins.

Data analysis

All results are shown as means±SEM. Student's *t*-test was used to compare the mean of Saline vs. IO groups while data from Sham, EMF, and EMF-IO groups were analyzed using ANOVA followed by Holm-Sidak's test for multiple comparison procedures.

RESULTS

Effects of iron overload

To investigate whether IO would produce oxidative damage in the brain, we measured the concentrations of TBARS as an index of oxidative stress and lipid peroxidation after chronic saline or IO in four different brain structures, prefrontal cortex, hippocampus, striatum, and cerebellum. As shown in Table 1, IO did not increase TBARS levels as compared to saline in any brain region.

We then searched for protective mechanisms that could be triggered following long term chronic IO and prevent oxidative damage. As iron toxicity is dependent partly on hydrogen peroxide, we first looked at the activity of antioxidant enzymes that form hydrogen peroxide. Total SOD activity was significantly increased in the cerebellum after IO ($P<0.01$) (Fig. 1A). This increase

Table 1. TBARS levels in different brain structures following IO as compared to saline

	Cerebellum	Striatum	Hippocampus	Prefrontal cortex
Saline	0.37±0.03	0.81±0.13	1.14±0.28	0.79±0.10
Iron	0.31±0.03	0.89±0.24	1.01±0.23	0.88±0.12

Data are means±SEM of values expressed as nmol/mg proteins and obtained from eight animals for each group.

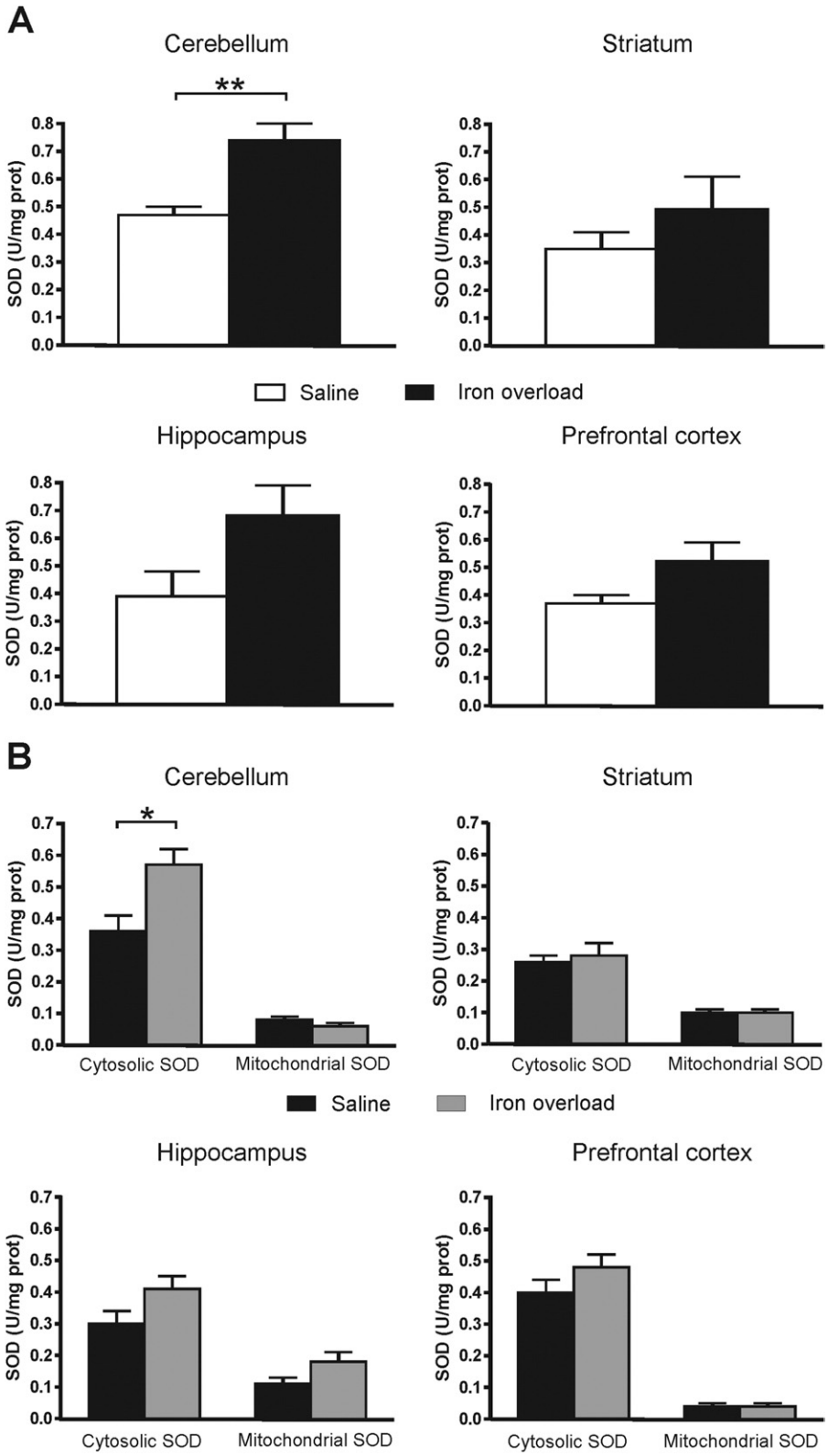

Fig. 1. Effect of IO on total (A) and cytosolic or mitochondrial (B) SOD activity in the cerebellum, striatum, hippocampus, and prefrontal cortex as compared to saline. Data are means±SEM of values obtained from eight animals for each group. * $P<0.05$; ** $P<0.01$.

mainly concerned cytosolic SOD while mitochondrial SOD was not affected (Fig. 1B). In the other brain regions, a slight increase in total SOD activity was also observed but proved to be not significant (Fig. 1A).

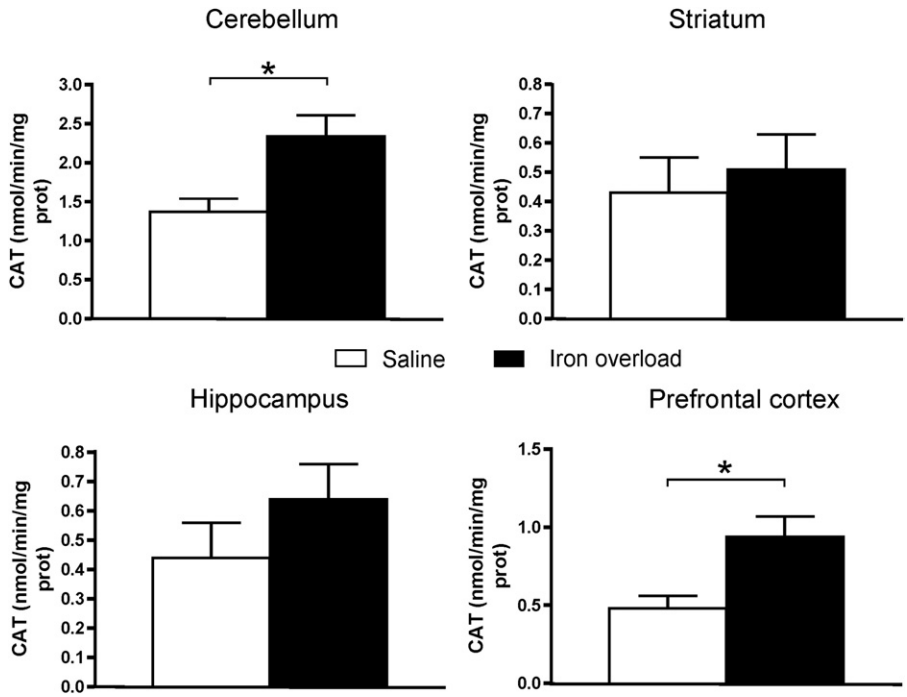

Fig. 2. Effect of IO on CAT activity in the cerebellum, striatum, hippocampus, and prefrontal cortex as compared to saline. Data are means±SEM of values obtained from eight animals for each group. * $P<0.05$.

An increase in SOD activity must be associated with an increased activity of hydrogen peroxide-consuming enzymes such as CAT to prevent iron catalyzed formation of hydroxyl radical and oxidative damage. We therefore monitored CAT activity, which was increased in all brain regions of IO-group; this increase reaching significance in the cerebellum ($P<0.05$) and prefrontal cortex ($P<0.05$) only (Fig. 2).

Effects of combined iron overload and 150 kHz EMF exposure

We evaluated the consequences of EMF exposure in the absence or presence of IO on oxidative stress and lipid peroxidation by measuring the TBARS levels as compared to SHAM exposure. TBARS levels were increased in the cerebellum of the EMF group vs. the SHAM group ($P<0.05$). In addition we noted an increase of TBARS in the cerebellum of EMF-IO group compared to the SHAM group ($P\leq0.001$) and the EMF group ($P<0.05$) (Fig. 3).

As EMF exposure had also been reported to modify antioxidant defenses in rats in an age-dependent way, we therefore evaluated the consequences of EMF exposure in absence or in presence of IO on SOD and CAT activity. EMF exposure alone in young adults did not modify the activity of the antioxidant enzymes tested (Table 2). Moreover, EMF exposure abolished the increase in antioxidant defenses triggered by IO, in particular in the cerebellum (Compare Figs. 1, 2, and Table 2).

DISCUSSION

We investigated whether chronic IO at a dose of 3 mg/kg and/or chronic exposure to intermediate frequency EMF (1 h, 150 kHz) during 21 days could induce oxidative stress in the brain of young adult rats by measuring lipid peroxidation and the activities of major antioxidant enzymes. Among brain structures, we focused our work on the cortex, hippocampus, striatum, and cerebellum. Lipid peroxidation, as an index of ROS production and oxidative damage, was monitored using the TBARS assay. SOD and CAT enzyme activities were measured to evaluate the level of antioxidant defenses. While IO did not induce any oxidative stress in young adult rats, it stimulated antioxidant defenses in the cerebellum and prefrontal cortex. On the contrary, EMF exposure stimulated lipid peroxidation mainly in the cerebellum, without affecting antioxidant defenses. When EMF was co-applied with IO, lipid peroxidation was further increased while EMF exposure prevented the increase in antioxidant defenses triggered by IO alone.

Iron excess is known to be deleterious for both the young and aging brain (Sobotka et al., 1996) where it may irreversibly alter neurological functions (Connor et al., 1992; Gerlach et al., 1994; Thompson et al., 2001). Administration of iron in young rats has been shown to diminish spontaneous locomotor activity, habituation, and reactivity to environmental stimuli as measured by the startle reflex and the prepulse inhibition of startle (Sobotka et al., 1996; Fredriksson et al., 1999, 2000, 2003; Schroder et al., 2001). In addition, iron treated rats and mice were also impaired in the acquisition of a radial maze task (Fredriksson et al., 1999, 2000; Schroder et al., 2001) suggesting a working memory deficit. Note that in most of these studies, deficits were observed when iron was administrated on postnatal days 10–12, suggesting a critical brain sensitivity period to IO (Taylor and Morgan, 1990;

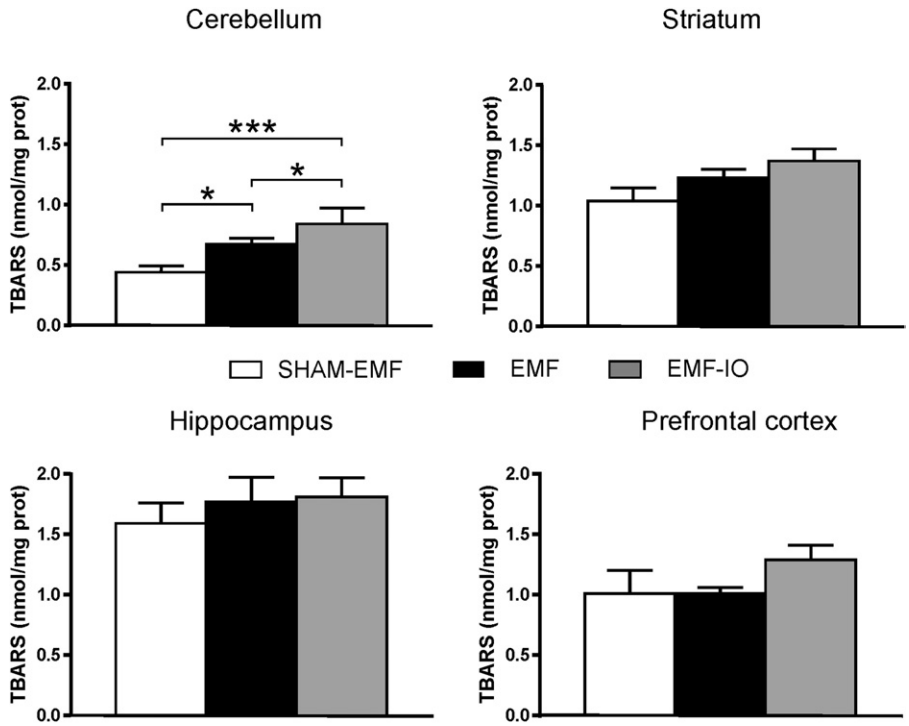

Fig. 3. Effect of EMF exposure alone or in combination with IO on TBARS levels in the cerebellum, striatum, hippocampus, and prefrontal cortex as compared to SHAM exposure. Data are means±SEM of values obtained from six animals for each group. * $P<0.05$; *** $P<0.001$.

Roskams and Connor, 1994; Focht et al., 1997). When administering iron after this critical period, we recently found that excess iron in young adults (4–5 week-old rats) specifically interfered with spatial information processing in a spontaneous object exploration task. These data indicate that the effects of IO may not be limited to those observed following treatment in the postnatal 10–12 day period but may occur when iron is administrated at later periods (Maaroufi et al., 2009b). Iron is also known to accumulate in specific regions of the brain with aging (Connor et al., 1992; Zecca et al., 2004a) and it has been recently shown that iron chelation prevents age-related recognition memory impairment in old rats (de Lima et al., 2008). Specific accumulation of iron has been also demonstrated in various degenerative diseases including Parkinson's, Alzheimer's, and Huntington's diseases (Zecca et al., 2004b) and iron chelators have been proposed as a potential neuroprotective strategy for these diseases (Mandel et al., 2008a,b).

An important issue is whether the behavioral deficits (not presented in this article, see Maaroufi et al., 2009b) are the result of iron-dependent oxidative stress. Memory impairment due to excess iron was shown by de Lima et al. (2005) to be correlated to brain oxidative damage in young rats after short term iron administration. In the present study, we measured the oxidative effects of IO in young adult rats after long-term iron administration (21 days). In contrast with de Lima et al.'s results, we found that the behavioral deficit was not correlated with brain oxidative damage. Indeed, no increase in TBARS levels was measured in any brain region investigated. The absence of oxidative stress is nevertheless surprising since shorter iron treatments are known to increase brain levels of iron in the same structures we investigated (Maaroufi et al., 2009a). A possible explanation is that chronic iron administration has induced adaptive responses involving stimulation of the antioxidant defenses. Indeed, SOD and CAT activities were increased after treatment. These data are

Table 2. SOD and CAT activities in different brain structures after of EMF exposure alone or in combination with IO as compared to sham exposure

		Cerebellum	Striatum	Hippocampus	Prefrontal cortex
S	Sham	0.53±0.04	0.32±0.01	0.42±0.04	0.41±0.07
O	EMF	0.55±0.03	0.35±0.06	0.43±0.04	0.56±0.05
D	EMF+iron	0.56±0.05	0.32±0.03	0.47±0.07	0.48±0.04
C	Sham	1.61±0.17	0.42±0.15	0.46±0.13	0.42±0.05
A	EMF	1.30±0.16	0.32±0.06	0.39±0.06	0.40±0.06
T	EMF+iron	1.42±0.12	0.53±0.16	0.46±0.13	0.52±0.03

Data are means±SEM of values expressed as U/mg proteins (SOD) or nmol/min/mg proteins (CAT) and obtained from six animals for each group.

consistent with those obtained in the rat following different chronic stressors (Pajovic et al., 2006). Short term iron treatment was also shown by de Lima et al. (2005) to produce an increase in SOD and CAT activity when administrated at early stages of life, an effect that seemed to decrease with aging. Nevertheless, our results show that iron administration at older stages of life (4–5 week-old rats) may also produce an increase of SOD and CAT activity. Interestingly, this increase was observed mainly in the cerebellum, a brain structure whose development occurs mostly after birth. Thus, it could be that the capacity to respond to IO by increasing SOD and CAT activities is more important in immature structures. Concerning SOD activity, the increase was found to involve cytosolic SOD only. This enzyme may be protective against iron toxicity by buffering superoxide anions in the cytoplasm, a mechanism that may prevent iron release from ferritin (Harris et al., 1994). The protective effect of CAT may be through degradation of hydrogen peroxide, preventing its interaction with iron and therefore formation of the highly toxic hydroxyl radical.

That iron accumulation in the brain induces neurodegenerative disorders via oxidative stress mechanisms have been abundantly discussed in the literature (e.g. Thompson et al., 2001; Zecca et al., 2004b). In contrast, there are very few studies that address the issue of the links between EMF exposure and oxidative stress. Using mostly cell culture models, it has been shown that EMF exposure enhances endogenous free radical production/stability, disturbing the cellular redox balance and increasing the probability of oxidative injury (Roy et al., 1995; Zmyslony et al., 2000; Lai and Singh, 2004; Rollwitz et al., 2004). After exposure to extremely low EMF (50–60 Hz), there was evidence of oxidative stress in the plasma of American Kestrels (intensity 30 μT; Fernie and Bird, 2001), and increased lipid peroxidation in snails (20 day exposure, 0.15 μT; Regoli et al., 2005). Concerning the brain, 50 Hz EMF exposure had no effects on guinea pigs while oxidative damage to lipids was reported in adult rats (Jelenkovic et al., 2006; Turkozer et al., 2008; Amara et al., 2009; Akdag et al., 2010). In accordance, we found increased levels of TBARS following chronic 150 kHz–6.25 μT EMF exposure in brain of young adult rats. This increase reached significance only in the cerebellum while basal forebrain and frontal cortex were found to be affected in adults (Jelenkovic et al., 2006). The reason for this discrepancy is not clear but may be linked to differences in time and mode of exposure. Interestingly, EMF effects were slightly more severe when co-applied with IO. This is in accordance with previous studies suggesting that EMF effects may be triggered through a process involving iron and possible formation of hydroxyl radicals in brain cells (Lai and Singh, 2004). It is therefore possible that the effect of EMF in the cerebellum is due to EMF-induced iron excess through altered blood-brain barrier permeability. Another way by which EMF exposure may potentiate iron effects is by modifying antioxidant defenses. While it has been reported that EMF exposure may modify cortical antioxidant defenses in an age dependent way (Falone et al., 2008), we found that in young adults it did not affect antioxidant defense per se but abolished the increase normally triggered by IO in the cerebellum.

CONCLUSION

In conclusion, our results show that 150 kHz EMF exposure may be harmful to young adults by increasing ROS levels and by impairing the antioxidant defenses directed at preventing iron-induced oxidative stress. It is likely however that the effects of EMF may depend on a number of parameters including the frequency, intensity, and duration of exposure. Thus, the relationship between oxidative stress and impaired cognitive processes remains to be clarified. However, knowing that IO has been associated with several neurodegenerative insults, that the iron status of the brain is determined during infancy and that this iron status may determine antioxidant defense levels, the interference of EMF exposure with iron effects on young adults may have long term delayed impacts on neurological functions that would result in neurodegenerative disorders as reported by several epidemiological studies.

Acknowledgments—The study was supported by the CNRS, Aix-Marseille University, and the Faculty of Sciences of Bizerte. The authors thank Philippe Pignet of the Centre Commun de Ressources en Microondes, Laboratoire d'Electromagnétisme, Compatibilité électromagnétique et Hyperfréquences in Marseille (CCM) for kindly providing the irradiation apparatus.

REFERENCES

Akdag MZ, Dasdag S, Ulukaya E, Uzunlar AK, Kurt MA, Taşkin A (2010) Effects of extremely low-frequency magnetic field on caspase activities and oxidative stress values in rat brain. Biol Trace Elem Res 138:238–249.

Amara S, Douki T, Garel C, Favier A, Sakly M, Rhouma KB, Abdelmelek H (2009) Effects of static magnetic field exposure on antioxidative enzymes activity and DNA in rat brain. Gen Physiol Biophys 28:260–265.

Benzi G, Moretti A (1995) Are reactive oxygen species involved in Alzheimer's disease? Neurobiol Aging 16:661–674.

Bergeron C (1995) Oxidative stress: its role in the pathogenesis of amyotrophic lateral sclerosis. J Neurol Sci 129(Suppl):81–84.

Bradford MM (1976) A rapid and sensitive method for the quantitation of microgram quantities of protein utilizing the principle of protein-dye binding. Anal Biochem 72:248–254.

Castelnau PA, Garrett RS, Palinski W, Witztum JL, Campbell IL, Powell HC (1998) Abnormal iron deposition associated with lipid peroxidation in transgenic mice expressing interleukin-6 in the brain. J Neuropathol Exp Neurol 57:268–282.

Connor JR, Snyder BS, Beard JL, Fine RE, Mufson EJ (1992) Regional distribution of iron and iron-regulatory proteins in the brain in aging and Alzheimer's disease. J Neurosci Res 31:327–335.

Davanipour Z, Tseng CC, Lee PJ, Sobel E (2007) A case-control study of occupational magnetic field exposure and Alzheimer's disease: results from the California Alzheimer's Disease Diagnosis and Treatment Centers. BMC Neurol 7:13.

de Lima MN, Polydoro M, Laranja DC, Bonatto F, Bromberg E, Moreira JC, Dal-Pizzol F, Schroder N (2005) Recognition memory impairment and brain oxidative stress induced by postnatal iron administration. Eur J Neurosci 21:2521–2528.

de Lima MN, Dias CP, Torres JP, Dornelles A, Garcia VA, Scalco FS, Guimarães MR, Petry RC, Bromberg E, Constantino L, Budni P, Dal-Pizzol F, Schröder N (2008) Reversion of age-related recog-

nition memory impairment by iron chelation in rats. Neurobiol Aging 29:1052–1059.

Di Loreto S, Falone S, Caracciolo V, Sebastiani P, D'Alessandro A, Mirabilio A, Zimmitti V, Amicarelli F (2009) Fifty hertz extremely low-frequency magnetic field exposure elicits redox and trophic response in rat-cortical neurons. J Cell Physiol 219:334–343.

Draper HH, Hadley M (1990) Malondialdehyde determination as index of lipid peroxidation. Methods Enzymol 186:421–431.

Fahn S, Cohen G (1992) The oxidant stress hypothesis in Parkinson's disease: evidence supporting it. Ann Neurol 32:804–812.

Falone S, Mirabilio A, Carbone MC, Zimmitti V, Di Loreto S, Mariggio MA, Mancinelli R, Di Ilio C, Amicarelli F (2008) Chronic exposure to 50Hz magnetic fields causes a significant weakening of antioxidant defence systems in aged rat brain. Int J Biochem Cell Biol 40:2762–2770.

Fernie KJ, Bird DM (2001) Evidence of oxidative stress in American kestrels exposed to electromagnetic fields. Environ Res 86:198–207.

Focht SJ, Snyder BS, Beard JL, Van Gelder W, Williams LR, Connor JR (1997) Regional distribution of iron, transferrin, ferritin, and oxidatively-modified proteins in young and aged Fischer 344 rat brains. Neuroscience 79:255–261.

Fredriksson A, Schroder N, Archer T (2003) Neurobehavioural deficits following postnatal iron overload: I spontaneous motor activity. Neurotox Res 5:53–76.

Fredriksson A, Schroder N, Eriksson P, Izquierdo I, Archer T (1999) Neonatal iron exposure induces neurobehavioural dysfunctions in adult mice. Toxicol Appl Pharmacol 159:25–30.

Fredriksson A, Schroder N, Eriksson P, Izquierdo I, Archer T (2000) Maze learning and motor activity deficits in adult mice induced by iron exposure during a critical postnatal period. Brain Res Dev Brain Res 119:65–74.

Gaasch JA, Lockman PR, Geldenhuys WJ, Allen DD, Van der Schyf CJ (2007) Brain iron toxicity: differential responses of astrocytes, neurons, and endothelial cells. Neurochem Res 32:1196–1208.

Garcia AM, Sisternas A, Hoyos SP (2008) Occupational exposure to extremely low frequency electric and magnetic fields and Alzheimer disease: a meta-analysis. Int J Epidemiol 37:329–340.

Gerlach M, Ben-Shachar D, Riederer P, Youdim MB (1994) Altered brain metabolism of iron as a cause of neurodegenerative diseases? J Neurochem 63:793–807.

Gutteridge JM (1995) Lipid peroxidation and antioxidants as biomarkers of tissue damage. Clin Chem 41:1819–1828.

Halliwell B (1996) Antioxidants in human health and disease. Annu Rev Nutr 16:33–50.

Halliwell B (2006) Oxidative stress and neurodegeneration: where are we now? J Neurochem 97:1634–1658.

Harris LR, Cake MH, Macey DJ (1994) Iron release from ferritin and its sensitivity to superoxide ions differs among vertebrates. Biochem J 301:385–389.

Huss A, Spoerri A, Egger M, Roosli M (2009) Residence near power lines and mortality from neurodegenerative diseases: longitudinal study of the Swiss population. Am J Epidemiol 169:167–175.

Jelenkovic A, Janac B, Pesic V, Jovanovic DM, Vasiljevic I, Prolic Z (2006) Effects of extremely low-frequency magnetic field in the brain of rats. Brain Res Bull 68:355–360.

Lai H, Singh NP (2004) Magnetic-field-induced DNA strand breaks in brain cells of the rat. Environ Health Perspect 112:687–694.

Lander HM, Tauras JM, Ogiste JS, Hori O, Moss RA, Schmidt AM (1997) Activation of the receptor for advanced glycation end products triggers a p21(ras)-dependent mitogen-activated protein kinase pathway regulated by oxidant stress. J Biol Chem 272:17810–17814.

Lin H, Goodman R, Shirley-Henderson A (1994) Specific region of the c-myc promoter is responsive to electric and magnetic fields. J Cell Biochem 54:281–288.

Litvak E, Foster KR, Repacholi MH (2002) Health and safety implications of exposure to electromagnetic fields in the frequency range 300 Hz to 10 MHz. Bioelectromagnetics 23:68–82.

Maaroufi K, Ammari M, Jeljeli M, Roy V, Sakly M, Abdelmelek H (2009a) Impairment of emotional behavior and spatial learning in adult Wistar rats by ferrous sulfate. Physiol Behav 96:343–349.

Maaroufi K, Had-Aissouni L, Melon C, Sakly M, Abdelmelek H, Poucet B, Save E (2009b) Effects of prolonged iron overload and low frequency electromagnetic exposure on spatial learning and memory in the young rat. Neurobiol Learn Mem 92:345–355.

Mandel SA, Amit T, Kalfon L, Reznichenko L, Weinreb O, Youdim MB (2008a) Cell signaling pathways and iron chelation in the neurorestorative activity of green tea polyphenols: special reference to epigallocatechin gallate (EGCG). J Alzheimers Dis 15:211–222.

Mandel SA, Amit T, Weinreb O, Reznichenko L, Youdim MB (2008b) Simultaneous manipulation of multiple brain targets by green tea catechins: a potential neuroprotective strategy for Alzheimer and Parkinson diseases. CNS Neurosci Ther 14:352–365.

Niki E, Noguchi N, Gotoh N (1993) Dynamics of lipid peroxidation and its inhibition by antioxidants. Biochem Soc Trans 21:313–317.

Nittby H, Grafstrom G, Eberhardt JL, Malmgren L, Brun A, Persson BR, Salford LG (2008) Radiofrequency and extremely low-frequency electromagnetic field effects on the blood-brain barrier. Electromagn Biol Med 27:103–126.

Oscar KJ, Hawkins TD (1977) Microwave alteration of the blood-brain barrier system of rats. Brain Res 126:281–293.

Pajovic SB, Pejic S, Stojiljkovic V, Gavrilovic L, Dronjak S, Kanazir DT (2006) Alterations in hippocampal antioxidant enzyme activities and sympatho-adrenomedullary system of rats in response to different stress models. Physiol Res 55:453–460.

Park RM, Schulte PA, Bowman JD, Walker JT, Bondy SC, Yost MG, Touchstone JA, Dosemeci M (2005) Potential occupational risks for neurodegenerative diseases. Am J Ind Med 48:63–77.

Pessina GP, Aldinucci C (1997) Short cycles of both static and pulsed electromagnetic fields have no effect on the induction of cytokines by peripheral blood mononuclear cells. Bioelectromagnetics 18:548–554.

Pessina GP, Aldinucci C (1998) Pulsed electromagnetic fields enhance the induction of cytokines by peripheral blood mononuclear cells challenged with phytohemagglutinin. Bioelectromagnetics 19:445–451.

Regoli F, Gorbi S, Machella N, Tedesco S, Benedetti M, Bocchetti R, Notti A, Fattorini D, Piva F, Principato G (2005) Pro-oxidant effects of extremely low frequency electromagnetic fields in the land snail Helix aspersa. Free Radic Biol Med 39:1620–1628.

Repacholi MH, Greenebaum B (1999) Interaction of static and extremely low frequency electric and magnetic fields with living systems: health effects and research needs. Bioelectromagnetics 20:133–160.

Richard MJ, Portal B, Meo J, Coudray C, Hadjian A, Favier A (1992) Malondialdehyde kit evaluated for determining plasma and lipoprotein fractions that react with thiobarbituric acid. Clin Chem 38:704–709.

Rollwitz J, Lupke M, Simko M (2004) Fifty-hertz magnetic fields induce free radical formation in mouse bone marrow-derived promonocytes and macrophages. Biochim Biophys Acta 1674:231–238.

Roosli M, Lortscher M, Egger M, Pfluger D, Schreier N, Lortscher E, Locher P, Spoerri A, Minder C (2007) Mortality from neurodegenerative disease and exposure to extremely low-frequency magnetic fields: 31 years of observations on Swiss railway employees. Neuroepidemiology 28:197–206.

Roskams AJ, Connor JR (1994) Iron, transferrin, and ferritin in the rat brain during development and aging. J Neurochem 63:709–716.

Roy S, Noda Y, Eckert V, Traber MG, Mori A, Liburdy R, Packer L (1995) The phorbol 12-myristate 13-acetate (PMA)-induced oxidative burst in rat peritoneal neutrophils is increased by a 0.1 mT (60 Hz), magnetic field. FEBS Lett 376:164–166.

Scaiano JC, Cozens FL, McLean J (1994) Model for the rationalization of magnetic field effects *in vivo*. Application of the radical-pair mechanism to biological systems. Photochem Photobiol 59:585–589.

Schroder N, Fredriksson A, Vianna MR, Roesler R, Izquierdo I, Archer T (2001) Memory deficits in adult rats following postnatal iron administration. Behav Brain Res 124:77–85.

Schwarz AJ, Danckaert A, Reese T, Gozzi A, Paxinos G, Watson C, Merlo-Pich EV, Bifone A (2006) A stereotaxic MRI template set for the rat brain with tissue class distribution maps and co-registered anatomical atlas: application to pharmacological MRI. Neuroimage 32:538–550.

Sen CK, Packer L (1996) Antioxidant and redox regulation of gene transcription. FASEB J 10:709–720.

Sobotka TJ, Whittaker P, Sobotka JM, Brodie RE, Quander DY, Robl M, Bryant M, Barton CN (1996) Neurobehavioral dysfunctions associated with dietary iron overload. Physiol Behav 59:213–219.

Suzuki YJ, Forman HJ, Sevanian A (1997) Oxidants as stimulators of signal transduction. Free Radic Biol Med 22:269–285.

Taylor EM, Morgan EH (1990) Developmental changes in transferrin and iron uptake by the brain in the rat. Brain Res Dev Brain Res 55:35–42.

Thompson KJ, Shoham S, Connor JR (2001) Iron and neurodegenerative disorders. Brain Res Bull 55:155–164.

Turkozer Z, Guler G, Seyhan N (2008) Effects of exposure to 50 Hz electric field at different strengths on oxidative stress and antioxidant enzyme activities in the brain tissue of guinea pigs. Int J Radiat Biol 84:581–590.

Zecca L, Stroppolo A, Gatti A, Tampellini D, Toscani M, Gallorini M, Giaveri G, Arosio P, Santambrogio P, Fariello RG, Karatekin E, Kleinman MH, Turro N, Hornykiewicz O, Zucca FA (2004a) The role of iron and copper molecules in the neuronal vulnerability of locus coeruleus and substantia nigra during aging. Proc Natl Acad Sci U S A 101:9843–9848.

Zecca L, Youdim MB, Riederer P, Connor JR, Crichton RR (2004b) Iron, brain ageing and neurodegenerative disorders. Nat Rev Neurosci 5:863–873.

Zmyslony M, Palus J, Jajte J, Dziubaltowska E, Rajkowska E (2000) DNA damage in rat lymphocytes treated *in vitro* with iron cations and exposed to 7 mT magnetic fields (static or 50 Hz). Mutat Res 453:89–96.

(Accepted 2 April 2011)
(Available online 12 April 2011)

Pergamon

Free Radical Biology & Medicine, Vol. 16, No. 2, pp. 195–200, 1994

0891-5849/94 $6.00 + .00

0891-5849(93)E0038-7

Original Contribution

THE TOXICITY OF HIGH-DOSE SUPEROXIDE DISMUTASE SUGGESTS THAT SUPEROXIDE CAN BOTH INITIATE AND TERMINATE LIPID PEROXIDATION IN THE REPERFUSED HEART

SALLY K. NELSON, SWAPAN K. BOSE, and JOE M. MCCORD

Webb-Waring Institute for Biomedical Research, University of Colorado Health Sciences Center, Denver, CO 80262, USA

(*Received* 13 *May* 1993; *Revised* 11 *June* 1993, *Accepted* 16 *June* 1993)

Abstract—Recently, we described an anomalous bell-shaped dose-response curve for the protection of the reoxygenated isolated myocardium by superoxide dismutase (SOD).[19] SOD is dramatically protective up to a point (5 μg/ml in the perfusate) beyond which it loses its ability to protect and, at very high doses (50 μg/ml), exacerbates the injury. We proposed that $O_2^{\cdot -}$ may serve as both initiator and terminator of lipid peroxidation, such that over scavenging the radical may increase net lipid peroxidation via increased chain length. We examined the ability of U74389F, a lipid peroxidation inhibitor, to ameliorate the toxicity of *high-dose* SOD in the isolated perfused rabbit heart preparation. The results show a significant improvement in the percent recovery of developed tension of hearts treated with U74389F and overdosed with MnSOD, as well as a decrease in thiobarbituric acid reactive substances.

Keywords—Superoxide dismutase, Lipid peroxidation, U74389F, Superoxide, Chain termination, Dose–response, Free radicals

INTRODUCTION

The involvement of oxygen-derived free radicals in myocardial reperfusion injury is well documented.[1–5] The production of superoxide radical ($O_2^{\cdot -}$) results in the liberation and reduction of iron from tissue ferritin,[6,7] as well as the secondary formation of H_2O_2 and hydroxyl radical ($HO^{\cdot}$).[8] Tissue iron, therefore, may seriously exacerbate any oxidative injury by the catalysis of the Haber–Weiss chemistry.[9] Because iron and hydroxyl radical are both initiators of lipid peroxidation,[10,11] one might expect lipid peroxidation to be a prominent component of reperfusion injury. Many reports confirm this to be the case.[12–14] Inhibitors of lipid peroxidation accordingly protect the myocardium following ischemia and reperfusion.[15,16] Certain 21-aminosteroids, including U74389F, are useful as potent inhibitors of lipid peroxidation in vitro.[17]

Recently, Bernier et al.[18] described an anomalous bell-shaped dose–response curve for the prevention of reperfusion-induced arrhythmias in the isolated rat heart. Protection increased with dose of cuprozinc superoxide dismutase (SOD), but declined dramatically when the concentration of SOD in the perfusate reached 120,000 U/l (or about 40 mg/l). We reported similar bell-shaped dose–response curves for the protection of reoxygenated rat and rabbit hearts by both cuprozinc- and manganese-SODs, using a variety of different end points including recovery of developed tension, release of marker enzymes, and infarct size.[19,20] SOD was protective in a dose-dependent fashion in every case up to a point (5–20 mg/l in the perfusate). At 50 mg/l, however, it lost its ability to protect and in some cases significantly *exacerbated* the injury. We proposed that $O_2^{\cdot -}$, in addition to initiating lipid peroxidation as discussed above, may also serve as a terminator of lipid peroxidation, such that over scavenging the radical may paradoxically increase net lipid peroxidation. In the present study we document that high-dose SOD does indeed increase net lipid peroxidation and examine the ability of U74389F, a lipid peroxidation inhibitor, to eliminate the toxicity of high-dose SOD in the reperfusion injury model.

This work was supported in part by the Upjohn Co., Kalamazoo, MI. S. K. N. was supported in part by the Institutional Training Grant for Nutrition (T32 DK 07658) from the National Institutes of Health.

Address correspondence to: Sally K. Nelson, Box C-321, University of Colorado Health Sciences Center, Denver, CO 80262, USA.

METHODS

Ischemia/reperfusion experiments

New Zealand white rabbits (2–3 kg) were sacrificed with 60 mg/kg sodium pentobarbital. The hearts and lungs were quickly excised and mounted via the ascending aorta on a nonrecirculating perfusion apparatus, and retrograde aortic perfusion under gravity at 80 mmHg with modified, oxygenated, glucose-containing Krebs–Henseleit buffer was initiated. The buffer also contained 0, 0.5, 5, or 40 mg/l human recombinant MnSOD (4000 U/mg, BioTechnology General, NY), as indicated. Also where indicated the perfusate contained 1 μM U74389F (Upjohn Co., Kalamazoo, MI) via a 1 μM albumin vehicle in the absence of and the presence of 40 mg/l SOD. A saline-filled latex balloon connected through a pressure transducer to a polygraph recorder (Grass Instruments Co., MA) was inserted into the left ventricle through a left atriotomy and secured by a suture to the mitral annulus. The suture was loose enough to allow fluid drainage from the ventricle. After a 15 min equilibration period, the developed pressure was measured, the balloon was deflated, and the hearts were subjected to 90 min global ischemia. This was followed by 30 min of reperfusion, at the end of which the developed pressure was measured again. The results are expressed as percent recovery of preischemic developed pressure. The hearts were not paced. At the end of the experiment the hearts were stored at −70°C until further analysis.

The Krebs–Henseleit buffer employed was composed of (in mM): NaCl, 118; $NaHCO_3$, 24.8; KCl, 4.7; KH_2PO_4, 1.2; $CaCl_2$, 2.5; $MgSO_4$, 1.2; and glucose, 10. Buffers were bubbled continuously with a mixture of 95% O_2 and 5% CO_2. The CO_2 helped maintain the buffers at a physiological pH of 7.4. The apparatus had extensive water jacketing connected to a water heater that maintained the buffers and the hearts at 37°C. All buffers were filtered through a Gelman GA-4, 0.8 micron Metrical membrane before use.

Estimation of carbonyl protein content

The hearts were homogenized in a buffer (1g/4ml) containing (in mM) *N*-(2-hydroxyethyl)piperazine-*N'*-2-ethanesulfonic acid (HEPES), 10; NaCl, 137; KCl, 4.6; KH_2PO_4, 1.1; $MgSO_4$, 0.6; ethylenediaminetetraacetic acid (EDTA), 1.1; Tween-20 (5 mg/l); butylated hydroxytoluene (1 μM); and protease inhibitors (in μg/ml) leupeptin, 0.5; pepstatin, 0.7; phenyl methyl sulfonyl fluoride, 40; and aprotinin, 0.5 to prevent proteolysis of oxidized proteins during preparation. The homogenates were centrifuged at 20,000 *g* for 20 min. Supernates were used for carbonyl protein determinations and for analysis of thiobarbituric acid reactive substance.

Protein carbonyl groups were determined by the method of Oliver et al.[21] Two equal aliquots containing approximately 0.7–1.0 mg of protein each were taken from the supernate. Both aliquots were precipitated with 10% trichloroacetic acid (TCA) (w/v, final concentration). Samples were then centrifuged at 2000 *g* for 10 min. One pellet was treated with 2 N HCl and the other treated with an equal volume of 0.2% (w/v) dinitrophenyl hydrazine (DNPH) in 2 N HCl, at room temperature for 1 h. Samples were then reprecipitated with 10% TCA (final concentration) and subsequently extracted with ethanol:ethyl acetate (1:1, v/v) and then reprecipitated with 10% TCA. This washing step, repeated three times, rendered the ethanol/ethyl acetate extract virtually colorless, indicating complete removal of unreacted and lipid-bound DNPH. Difference in absorbance between DNPH-treated vs. the HCl control was determined at 370 nm. Data were expressed as nmol carbonyl groups/ mg protein using the molar extinction coefficient of 21,000 for DNPH derivatives.

Thiobarbituric acid reactive substances

Thiobarbituric acid reactive substances, or TBARS, were determined by the method of Ohkawa et al.[22] The reaction mixture (total volume of 4 ml) contained 200 μl of 8.1% sodium dodecyl sulfate, 1.5 ml of 20% acetic acid, and 1.5 ml 0.8% thiobarbituric acid, and 800 μl of heart homogenate supernate. The mixture was heated in boiling water for 1 h, cooled with tap water and extracted with *n*-butanol/pyridine (15:1 v/v) by vortexing for 1–2 min. The mixture was then centrifuged at 500–1000 *g* for 10 min or until a good aqueous-organic phase separation occurred. The organic phase was removed and its absorbance at 532 nm was measured against a reaction mixture blank. A standard curve was prepared with 1,1,3,3-tetramethoxypropane, and TBARS are reported as molar equivalents.

Statistics

Data are presented as the mean ± standard error in the figures. Tests for significance were made using a one-way analysis of variance and the differences between specific groups were determined by the Newman–Keuls test.

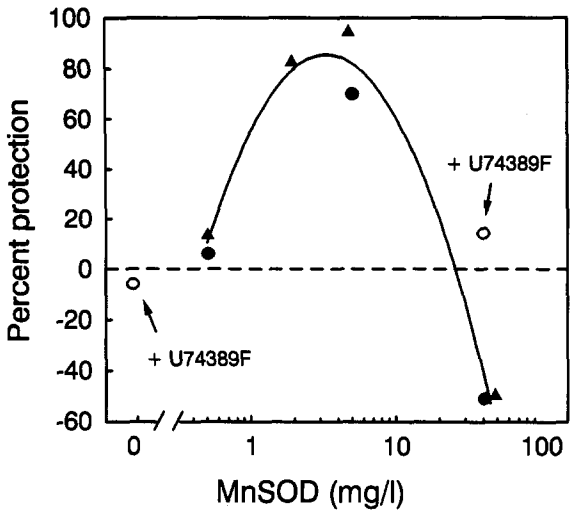

Fig. 1. The dose–response data are plotted as percent protection vs. the logarithm of the SOD concentration. In the present study (indicated by the closed circles) human recombinant Mn-SOD was perfused at 0 mg/l (controls, $n = 6$), 0.5 mg/l ($n = 3$), 5 mg/l ($n = 3$), and 40 mg/l ($n = 3$). These results reproduce those from a previous study[20] (indicated by the triangles). In both cases, while SOD improved the recovery of developed tension at lower doses, it exacerbated the injury at higher doses ($p < 0.0003$). 1 μM U74389F (open circles) failed to protect by itself, but eliminated the toxicity of high dose SOD ($p < 0.0003$).

RESULTS

Functional recovery

The percent recovery of developed tension (relative to preischemic) at the end of 30 min of reperfusion post 90 min ischemia was determined. Control hearts ($n = 6$) showed 33.65 ± 5.5% (mean ± SEM) recovery of developed tension. Hearts perfused with 0.5 mg/l SOD ($n = 3$) recovered by 37.86 ± 6.3% (nonsignificant). Hearts perfused with 5 mg/l ($n = 3$) SOD recovered by 80.3 ± 5.9% ($p < 0.0003$). However, hearts receiving 40 mg/l SOD ($n = 3$) showed 0% recovery and were significantly different from all other groups ($p < 0.0003$). Figure 1 shows the percent protection normalized to the control hearts. Hearts perfused with 1 μM U74389F ($n = 4$) recovered by 27.3 ± 3.3% and were not significantly different from the control, whereas, hearts perfused with 40 mg/l SOD and 1 μM U74389F ($n = 5$) recovered 41.4 ± 9.5% and were significantly different ($p < 0.0003$) from the hearts receiving only the 40 mg/l SOD (Fig. 2).

Carbonyl protein formation

There was a decrease of approximately 20%, although not significantly different, in carbonyl protein formation in the hearts treated with U74389F in the absence of added SOD. In the presence of 40 mg/l SOD, however, carbonyl protein content rose to 1.8 ± 0.4 nmol/mg protein ($n = 3$), and the addition of U74389F reduced this by 67% to 0.6 ± 0.2 nmol/mg protein ($n = 4$, $p < 0.04$).

Thiobarbituric acid reactive substances

Hearts treated with neither SOD nor U74389F contained 1.16 ± 0.1 nmol TBARS/mg protein. TBARS contents in the hearts perfused with 0.5, 5, and 40 mg/l SOD were 0.74 ± 0.13, 0.31 ± 0.098, and 2.28 ± 0.26 nmol/mg protein, respectively. The TBARS content of the heart treated with 5 mg/l SOD was significantly lower than the untreated control ($p < 0.0001$), whereas the TBARS content of the heart treated with 40 mg/l SOD was significantly higher than the untreated control ($p < 0.0001$) (Fig. 3). Treatment with U74389F caused significant decreases in TBARS, whether in the absence or presence of 40 mg/l SOD (0.47 ± 0.1 and 0.98 ± 0.21 nmol/mg protein, respectively, $p < 0.0001$) (Fig. 3).

DISCUSSION

The postischemic isolated rabbit heart was considerably protected by human recombinant MnSOD up to a dose of 5 mg/l of perfusate. With an increase in SOD concentration to 40 mg/l, however, there was complete failure of contractility, illustrating a dramatic toxic effect from too much SOD. The bell-shaped dose–response curve seen in previous studies[18–20] is confirmed in this study.

Iron plays a crucial role in the initiation of lipid-rad-

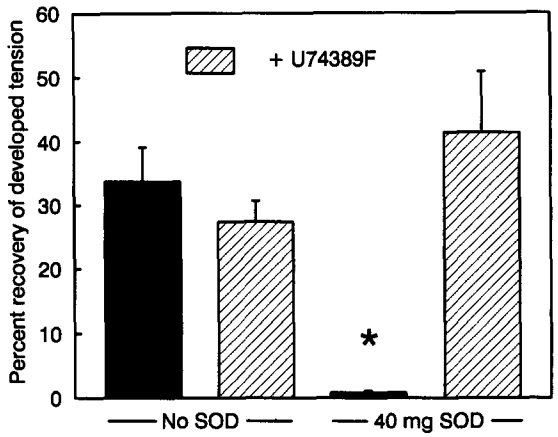

Fig. 2. Dose-dependent effect of human recombinant Mn-SOD on the percent recovery of developed tension in isolated rabbit hearts subjected to 90 min of global ischemia followed by 30 min of reperfusion. Means and standard errors are shown. 1 μM U74389F eliminated the toxicity of high dose SOD ($p < 0.0003$).

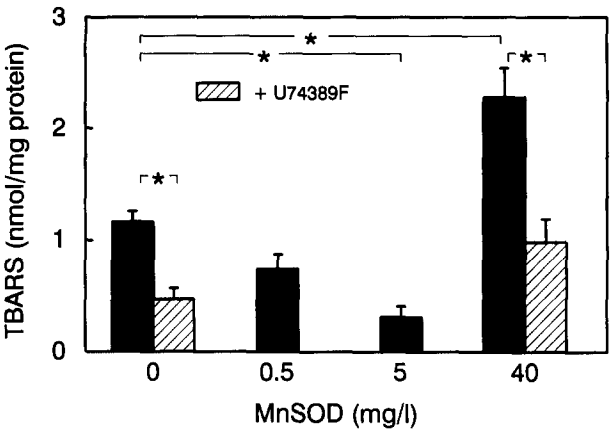

Fig. 3. Dose-dependent effect of human recombinant Mn-SOD on TBARS revealed an inverted bell shaped curve showing a decrease at 5 mg/l SOD ($p < 0.0001$) and an increase at 40 mg/l SOD ($p < 0.0001$). 1 μM U74389F decreased TBARS formation in hearts perfused with 0 or 40 mg/l SOD by about 60% in both cases ($p < 0.0001$).

ical chain reactions.[10,11] Ferrous iron can cause the reductive lysis of the oxygen–oxygen bond in a preexisting lipid hydroperoxide molecule (LOOH) giving rise to the alkoxyl (LO$^{\cdot}$) radical that may then serve as an initiating radical in lipid peroxidation:[23]

$$\text{LOOH} + \text{Fe}^{2+} \rightarrow \text{LO}^{\cdot} + \text{Fe}^{3+} + \text{OH}^{-} \text{ (Initiation)}$$
$$\text{LO}^{\cdot} + \text{LH} \rightarrow \text{LOH} + \text{L}^{\cdot}$$
$$\text{L}^{\cdot} + \text{O}_2 \rightarrow \text{LOO}^{\cdot} \text{ (Propagation)}$$
$$\text{LOO}^{\cdot} + \text{LH} \rightarrow \text{LOOH} + \text{L}^{\cdot}$$

If these alkoxyl or dioxyl radicals were scavenged by $O_2^{\cdot -}$, then entire chains of reactions would be prevented or terminated:

$$\text{LO}^{\cdot} + \text{O}_2^{\cdot -} + \text{H}^{+} \rightarrow \text{LOH} + \text{O}_2 \text{ (termination)}$$
$$\text{LOO}^{\cdot} + \text{O}_2^{\cdot -} + \text{H}^{+} \rightarrow \text{LOOH} + \text{O}_2$$

Therefore, it was hypothesized that $O_2^{\cdot -}$, in addition to being able to liberate iron and initiate lipid peroxidation, may also serve as a *terminator* of lipid peroxidation, such that over scavenging the radical may increase net lipid peroxidation.[19] If this hypothesis is correct, then indices of lipid peroxidation should increase at high doses of SOD, and a potent inhibitor of lipid peroxidation such as U74389F[17] might eliminate the downside of the SOD dose–response curve. We found both of these conditions to be true.

U74389F belongs to a class of 21-aminosteroids that have been shown to be potent inhibitors of iron-catalyzed lipid peroxidation in vitro.[24,25] In addition, these compounds have demonstrated protection in vivo in models of ischemia,[15,16,26,27] neurological recovery,[28,29] and central nervous system trauma.[30,31] These compounds were specifically designed to localize at or near sites within cell membranes where oxidative damage is believed to be initiated. The 21-aminosteroids are membrane soluble.[32] U74006F, which is very similar in structure to U74389F, appears to inhibit lipid peroxidation by a mechanism similar to that of vitamin E by scavenging lipid dioxyl radicals. During the inhibition of lipid peroxidation there is a competition between the 21-aminosteroids and vitamin E, thereby slowing the degradation of the vitamin.[33] In this study, 1 μM U74389F was perfused through the hearts for 15 min prior to ischemia. During this time, the lipophilic compound may have accumulated preferentially in the membranes of the heart. This treatment alone did not show a protective effect on recovery of developed tension by reperfused hearts, although it did suppress lipid peroxidation by about 60%. The reason for this lack of protection of functional recovery in the absence of SOD is not clear, but may relate to the multifactorial nature of the injury. When $O_2^{\cdot -}$ is high, several enzymes vital to cardiac function are vulnerable to inactivation by the radical. These include creatine kinase,[34] myofibrillar ATPase,[35] and aconitase.[36] When no SOD is present in the perfusate, the modest amount of lipid peroxidation taking place may not be contributing greatly to the loss of function. Because lipid peroxidation, once initiated, may continue for long periods of time, it is also possible that the action of U74389F might become more important after a longer period of reperfusion than that observed in the present study (30 min). In combination with 40 mg/l SOD, U74389F likewise suppressed lipid peroxidation by about 60%, and it also clearly ameliorated the toxicity of the high dose SOD with regard to recovery of developed tension (Fig. 2).

Determination of TBARS (Fig. 3) provides yet another end point demonstrating a bell-shaped dose–response curve with SOD. This suggests that lipid peroxidation is high in the presence of *either* low SOD (0.5 mg/l) or high SOD (40 mg/l), but is minimized at the intermediate SOD concentration (5 mg/l). If one considers that free radical chain reactions are both initiated and terminated by free radicals, and that, in theory, the *same* radical may do both operations, the bell-shaped curves are not difficult to rationalize. Figure 4 presents the expected mathematical relationships between SOD concentration (which is inversely related to superoxide concentration) and initiation, termination, and net lipid peroxidation. Panel A shows that as SOD concentration increases (and $O_2^{\cdot -}$

decreases) initiation (at least via superoxide-dependent iron-catalyzed reduction of hydroperoxides) would decrease according to an inverse rectangular hyperbola, asymptotically approaching zero initiating events at infinite SOD. Panel B shows the expected effect on chain length. At the highest concentration of $O_2^{\cdot -}$ (no SOD) the chain length would approach unity. At the lowest concentration of the radical (high SOD) the chain length would be maximal (limited only by other terminators such as vitamin E, or by the mutual annihilation of propagating radicals). This produces another inverse rectangular hyperbolic function in the opposite direction. Net lipid peroxidation, shown in Panel C, is represented by the *product* of initiation events times chain length. Panel C shows the curves from Panels A and B replotted on a semilog coordinate, along with the curve produced by multiplying initiation by chain length. Note that the net amount of lipid peroxidation displays a minimum at a specific, optimal concentration of SOD. It is an inverted bell-shaped curve. Figure 5 shows the remarkable similarity in shape of this theoretically predicted curve (using arbitrarily selected constants) and that obtained experimentally (data from Fig. 3). The closeness of fit of this mathematical model convinces us that the superoxide radical can act both as initiator of lipid peroxidation (indirectly, by the liberation and/or reduction of iron) and terminator of lipid peroxidation. This realization provides a rational basis for the bell-shaped dose–response curves observed for SOD, and argues that, for any specific set of conditions, there is an optimally protective concentration of SOD. It underscores the importance of balance between oxidants and antioxidants.

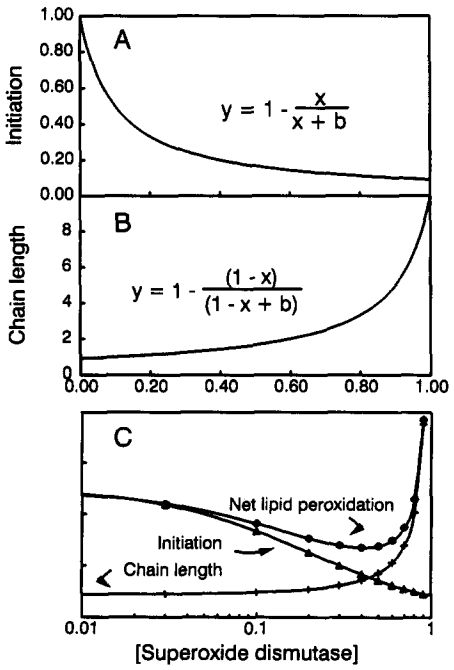

Fig. 4. The expected mathematical relationships between SOD concentration (which is inversely related to superoxide concentration) and initiation (A), termination (B), and net lipid peroxidation (C).

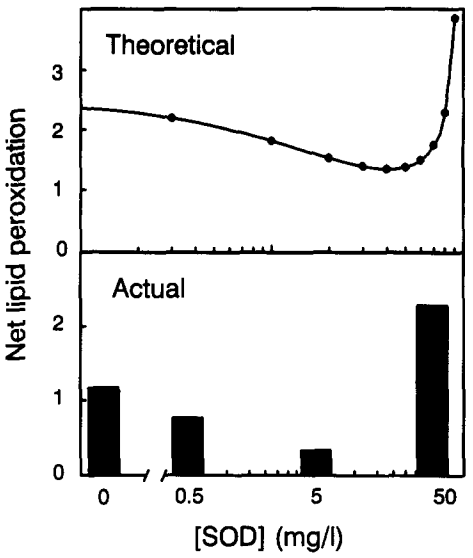

Fig. 5. A comparison of the theoretical and experimental dose–response curves of net lipid peroxidation vs. SOD concentration, showing a remarkable similarity.

Other studies have also observed the detrimental effects of too much SOD. Elroy-Stein et al.[37] have shown increased lipid peroxidation in transfected cells overproducing Cu,Zn-SOD. Ceballos et al.[38] found an increase in the glutathione peroxidase activity in mouse L cells and NS20Y neuroblastoma cells transfected with human Cu,Zn-SOD. Kedziora and Bartosz[39] suggested that the abnormalities observed in Down's syndrome are partially due to an imbalance in the reactive oxygen species caused by excess Cu,Zn-SOD. While other explanations have been offered for the observed toxicity of high dose SOD, we believe the arguments presented above may explain most, if not all, of the published observations.

REFERENCES

1. McCord, J. M. Oxygen-derived free radicals in postischemic tissue injury. *N. Engl. J. Med.* **312**:159–163; 1985.
2. Grill, H. P.; Zweier, J. L.; Kuppusamy, P.; Weisfeldt, M. L.; Flaherty, J. T. Direct measurement of myocardial free radical generation in an invivo model—Effects of postischemic reperfusion and treatment with human recombinant superoxide dismutase. *J. Am. Coll. Cardiol.* **20**:1604–1611; 1992.
3. Arroyo, C. M.; Kramer, J. H.; Dickens, B. F.; Weglicki, W. B. Identification of free radicals in myocardial ischemia/reperfusion by spin trapping with nitrone DMPO. *FEBS Lett.* **221**:101–104; 1987.

4. Garlick, P. B.; Davies, M. J.; Hearse, D. J.; Slater, T. F. Direct detection of free radicals in the reperfused rat heart using electron spin resonance spectroscopy. *Circ. Res.* **61**:757–760; 1987.
5. Bolli, R.; Patel, B. S.; Jeroudi, M. O.; Lai, E. K.; McCay, P. B. Demonstration of free radical generation in "stunned" myocardium of intact dogs with the use of the spin trap α-phenyl *N*-*tert*-butyl nitrone. *J. Clin. Invest.* **82**:476–485; 1988.
6. Biemond, P.; van Eijk, H. G.; Swaak, A. J. G.; Koster, J. F. Iron mobilization from ferritin by superoxide derived from stimulated polymorphonuclear leukocytes. Possible mechanism in inflammation diseases. *J. Clin. Invest.* **73**:1576–1579; 1984.
7. Biemond, P.; Swaak, A. J.; Beindorff, C. M.; Koster, J. F. Superoxide-dependent and -independent mechanisms of iron mobilization from ferritin by xanthine oxidase. Implications for oxygen-free-radical-induced tissue destruction during ischaemia and inflammation. *Biochem. J.* **239**:169–173; 1986.
8. Rubanyi, G. M.; Vanhoutte, P. M. Oxygen-derived free radicals, endothelium, and responsiveness of vascular smooth muscle. *Am. J. Physiol.* **250**:H815-H821; 1986.
9. McCord, J. M.; Day, E. D., Jr. Superoxide-dependent production of hydroxyl radical catalyzed by iron-EDTA complex. *FEBS Lett.* **86**:139–142; 1978.
10. Halliwell, B.; Gutteridge, J. M. The importance of free radicals and catalytic metal ions in human diseases. *Mol. Aspects. Med.* **8**:89–193; 1985.
11. Aust, S. D.; Morehouse, L. A.; Thomas, C. E. Role of metals in oxygen radical reactions. *J. Free Radicals Biol. Med.* **1**:3–25; 1985.
12. Meerson, F. Z.; Kagan, V. E.; Kozlov, Y. P.; Belkina, L. M.; Arkhipenko, Y. V. The role of lipid peroxidation in pathogenesis of ischemic damage and the antioxidant protection of the heart. *Basic Res. Cardiol.* **77**:465–485; 1982.
13. Tavazzi, B.; Lazzarino, G.; Dipierro, D.; Giardina, B. Malondialdehyde production and ascorbate decrease are associated to the reperfusion of the isolated postischemic rat heart. *Free Radic. Biol. Med.* **13**:75–78; 1992.
14. Yamashita, C.; Oobo, H.; Tsuji, F.; Tobe, S.; Yamamoto, H.; Nakamura, H.; Okada, M.; Nakamura, K. Effect of prostaglandin-I2 and superoxide dismutase on reperfusion injury of warm ischemic lung. *Ann. Thorac. Surg.* **54**:921–924; 1992.
15. Carrea, F. P.; Lesnefsky, E. J.; Kaiser, D. G.; Horwitz, L. D. The lazaroid U74006F, a 21-aminosteroid inhibitor of lipid peroxidation, attenuates myocardial injury from ischemia and reperfusion. *J. Cardiovasc. Pharmacol.* **20**:230–235; 1992.
16. Holzgrefe, H. H.; Buchanan, L. V.; Gibson, J. K. Effects of U74006F, a novel inhibitor of lipid peroxidation, in stunned reperfused canine myocardium. *J. Cardiovasc. Pharmacol.* **15**:239–248; 1990.
17. Braughler, J. M.; Pregenzer, J. F.; Chase, R. L.; Duncan, L. A.; Jacobsen, E. J.; McCall, J. M. Novel 21-amino steroids as potent inhibitors of iron-dependent lipid peroxidation. *J. Biol. Chem.* **262**:10438–10440; 1987.
18. Bernier, M.; Manning, A. S.; Hearse, D. J. Reperfusion arrhythmias: Dose-related protection by anti-free radical interventions. *Am. J. Physiol.* **256**:H1344-H1352; 1989.
19. Omar, B. A.; Gad, N. M.; Jordan, M. C.; Striplin, S. P.; Russell, W. J.; Downey, J. M.; McCord, J. M. Cardioprotection by Cu,Zn-superoxide dismutase is lost at high doses in the reoxygenated heart. *Free Radic. Biol. Med.* **9**:465–471; 1990.
20. Omar, B. A.; McCord, J. M. The cardioprotective effect of Mn-superoxide dismutase is lost at high doses in the postischemic isolated rabbit heart. *Free Radic. Biol. Med.* **9**:473–478; 1990.
21. Oliver, C. N.; Ahn, B. W.; Moerman, E. J.; Goldstein, S.; Stadtman, E. R. Age-related changes in oxidized proteins. *J. Biol. Chem.* **262**:5488–5491; 1987.
22. Ohkawa, H.; Ohishi, N.; Yagi, K. Assay for lipid peroxides in animal tissues by thiobarbituric acid reaction. *Anal. Biochem.* **95**:351–358; 1979.
23. Fujii, T.; Hiramoto, Y.; Terao, J.; Fukuzawa, K. Site-specific mechanisms of initiation by chelated iron and inhibition by α-tocopherol of lipid peroxide-dependent lipid peroxidation in charged micelles. *Arch. Biochem. Biophys.* **284**:120–126; 1991.
24. Braughler, J. M.; Pregenzer, J. F. The 21-aminosteroid inhibitors of lipid peroxidation: Reactions with lipid peroxyl and phenoxy radicals. *Free Radic. Biol. Med.* **7**:125–130; 1989.
25. Wolfgang, G. H. I.; Jolly, R. A.; Donarski, W. J.; Petry, T. W. Inhibition of diquat-induced lipid peroxidation and toxicity in precision-cut rat liver slices by novel antioxidants. *Toxicol. Appl. Pharmacol.* **108**:321–329; 1991.
26. Fowl, R. J.; Patterson, R. B.; Gewirtz, R. J.; Anderson, D. K. Protection against postischemic spinal cord injury using a new 21-aminosteroid. *J. Surg. Res.* **48**:597–600; 1990.
27. Natale, J. E.; Schott, R. J.; Hall, E. D.; Braughler, J. M.; D'Alecy, L. G. Effect of the aminosteroid U74006F after cardiopulmonary arrest in dogs. *Stroke* **19**:1371–1378; 1988.
28. Hall, E. D.; Yonkers, P. A.; McCall, J. M.; Braughler, J. M. Effects of the 21-aminosteroid U74006F on experimental head injury in mice. *J. Neurosurg.* **68**:456–461; 1988.
29. Anderson, D. K.; Braughler, J. M.; Hall, E. D.; Waters, T. R.; McCall, J. M.; Means, E. D. Effects of treatment with U-74006F on neurological outcome following experimental spinal cord injury. *J. Neurosurg.* **69**:562–567; 1988.
30. Jacobsen, E. J.; McCall, J. M.; Ayer, D. E.; VanDoornik, F. J.; Palmer, J. R.; Belonga, K. L.; Braughler, J. M.; Hall, E. D.; Houser, D. J.; Krook, M. A.; Runge, T. A. Novel 21-aminosteroids that inhibit iron-dependent lipid peroxidation and protect against central nervous system trauma. *J. Med. Chem.* **33**:1145–1151; 1990.
31. Natale, J. E.; Schott, R. J.; Hall, E. D.; Braughler, J. M.; D'Alecy, L. G. The 21-aminosteroid U74006F reduces systemic lipid peroxidation, improves neurologic function, and reduces mortality after cardiopulmonary arrest in dogs. *Prog. Clin. Biol. Res.* **308**:891–896; 1989.
32. Audus, K. L.; Guillot, F. L.; Braughler, J. M. Evidence for 21-aminosteroid association with the hydrophobic domains of brain microvessel endothelial cells. *Free Radic. Biol. Med.* **11**:361–371; 1991.
33. Braughler, J. M.; Burton, P. S.; Chase, R. L.; Pregenzer, J. F.; Jacobsen, E. J.; VanDoornik, F. J.; Tustin, J. M.; Ayer, D. E.; Bundy, G. L. Novel membrane localized iron chelators as inhibitors of iron-dependent lipid peroxidation. *Biochem. Pharmacol.* **37**:3853–3860; 1988.
34. McCord, J. M.; Russell, W. J. Inactivation of creatine phosphokinase by superoxide during reperfusion injury. *Basic Life Sci.* **49**:869–873; 1988.
35. Ventura, C.; Guarnieri, C.; Caldarera, C. M. Inhibitory effect of superoxide radicals on cardiac myofibrillar ATPase activity. *Ital. J. Biochem.* **34**:267–274; 1985.
36. Gardner, P. R.; Fridovich, I. Superoxide sensitivity of the *Escherichia coli* aconitase. *J. Biol. Chem.* **266**:19328–19333; 1991.
37. Elroy-Stein, O.; Bernstein, Y.; Groner, Y. Overproduction of human Cu/Zn-superoxide dismutase in transfected cells: Extenuation of paraquat-mediated cytotoxicity and enhancement of lipid peroxidation. *EMBO J.* **5**:615–622; 1986.
38. Ceballos, I.; Delabar, J. M.; Nicole, A.; Lynch, R. E.; Hallewell, R. A.; Kamoun, P.; Sinet, P. M. Expression of transfected human CuZn superoxide dismutase gene in mouse L cells and NS20Y neuroblastoma cells induces enhancement of glutathione peroxidase activity. *Biochim. Biophys. Acta* **949**:58–64; 1988.
39. Kedziora, J.; Bartosz, G. Down's syndrome: A pathology involving the lack of balance of reactive oxygen species. *Free Radic. Biol. Med.* **4**:317–330; 1988.

Gamete Research 23:77–90 (1989)

Role of Glutathione Peroxidase in Protecting Mammalian Spermatozoa From Loss of Motility Caused by Spontaneous Lipid Peroxidation

Juan G. Alvarez and Bayard T. Storey

Departments of Obstetrics and Gynecology and Physiology, University of Pennsylvania School of Medicine, Philadelphia, Pennsylvania

Mouse and human spermatozoa, but not rabbit spermatozoa, have long been known to be sensitive to loss of motility induced by exogenous H_2O_2. Recent work has shown that loss of sperm motility in these species correlates with the extent of spontaneous lipid peroxidation. In this study, the effect of H_2O_2 on this reaction in sperm of the three species was investigated. The rate of spontaneous lipid peroxidation in mouse and human sperm is markedly enhanced in the presence of 1–5 mM H_2O_2, while the rate in rabbit sperm is unaffected by H_2O_2. The enhancement of lipid peroxidation, the rate of reaction of H_2O_2 with the cells, the activity of sperm glutathione peroxidase, and the endogenous glutathione content are highest in mouse sperm, intermediate in human sperm, and very low in rabbit sperm. Inactivation of glutathione peroxidase occurs in the presence of H_2O_2 due to complete conversion of endogenous glutathione to GSSG: No GSH is available as electron donor substrate to the peroxidase. Inactivation of glutathione peroxidase by the inhibitor mercaptosuccinate has the same effect on rate of lipid peroxidation and loss of motility in mouse and human sperm as does H_2O_2. This implies that H_2O_2 by itself at 1–5 mM is not intrinsically toxic to the cells. With merceptosuccinate, the endogenous glutathione is present as GSH in mouse and human sperm, indicating that the redox state of intracellular glutathione by itself plays little role in protecting the cell against spontaneous lipid peroxidation. Mouse and human sperm also have high rates of superoxide production. We conclude that the key intermediate in spontaneous lipid peroxidation is lipid hydroperoxide generated by a chain reaction initiated by and utilizing superoxide. Removal of this hydroperoxide by glutathione peroxidase protects these sperm against peroxidation; inactivation of the peroxidase allows lipid hydroperoxide to increase and so increases the peroxidation rate. Rabbit sperm have low rates of superoxide reaction due to high activity of their superoxide dismutase; lack of endogenous glutathione and low peroxidase activity does not affect their rate of lipid peroxidation. As a result, these sperm are not affected by either H_2O_2 or mercaptosuccinate. These results lead us to postulate a mechanism for spontaneous lipid peroxidation in mammalian sperm which involves reaction of lipid hydroperoxide and O_2 as the rate-determining step.

Key words: lipid peroxidation, sperm H_2O_2 toxicity, sperm glutathione peroxidase, sperm glutathione, sperm

Received August 30, 1988; accepted December 1, 1988.

Address reprint requests to Dr. Bayard T. Storey, Department of Obstetrics and Gynecology, John Morgan Building, Room 339, University of Pennsylvania, Philadelphia, PA 19104-6080.

INTRODUCTION

Although deleterious effects of H_2O_2 on mammalian spermatozoa were documented some years ago for a number of species including human [McLeod, 1943; Tosic, 1947; Tosic and Walton, 1950; Wales et al., 1959], the mechanism by which H_2O_2 exerts its effect on sperm motility loss has never been elucidated. The sensitivity of mammalian spermatozoa to damage by exogenous H_2O_2 differs between species for almost all the species tested [Wales et al., 1959]. Mammalian spermatozoa are known to lack catalase activity [Mann, 1964] but to possess the two alternate enzymatic defense systems against the dioxygen species $O_2^{\cdot-}$ and H_2O_2, superoxide dismutase (SOD), and the glutathione peroxidase/reductase pair [Li, 1975; Abu-Erreizh et al., 1978; Menella and Jones, 1980; Holland and Storey, 1981; Alvarez and Storey, 1984; Alvarez et al., 1987]. The relative contribution of these two enzymatic systems to the overall protection against O_2 toxicity mediated by $O_2^{\cdot-}$ and H_2O_2 for the different mammalian species tested is far from clear. Rabbit spermatozoa have glutathione peroxidase (GPX) and glutathione reductase (GRD) activities, but have very low levels of endogenous glutathione (GSH plus GSSG), leaving SOD as the only enzymatic protectant system [Li, 1975; Holland and Storey, 1981; Alvarez and Storey, 1983]. Ejaculated rabbit spermatozoa were reported to be resistant to damage from H_2O_2, although some of the protection appeared to be derived from the seminal plasma [Wales et al., 1959]; epididymal rabbit spermatozoa were not examined. Washed, ejaculated ram spermatozoa were shown to contain both SOD and the components of the glutathione system, but the activity of GPX was an order of magnitude lower than that of GRD, implying that this system is secondary to SOD [Abu-Erreizh et al., 1978]. Washed, ejaculated ram spermatozoa proved to be more sensitive to H_2O_2 toxicity than washed ram epididymal spermatozoa [Wales et al., 1959]. Human spermatozoa from a group of healthy donors showed remarkably uniform activities of GPX and GRD and content of total glutathione, about half of which was in the reduced form [Alvarez et al., 1987]. This uniformity was in marked contrast to the variability in SOD activity determined in the same samples from these donors. The SOD activity of a given fresh sample proved to be an accurate predictor of time to complete loss of motility due to spontaneous lipid peroxidation during aerobic incubation at 37°C, over a time range of 1 to 10 hours. It was concluded that SOD was the prime enzymatic defense in human spermatozoa against damage from spontaneous lipid peroxidation, despite a glutathione content and GPX/GRD activities that should be more than sufficient to provide this defense. Wales et al. also [1959] reported that human spermatozoa were somewhat less resistant to H_2O_2 than ejaculated rabbit spermatozoa and unwashed mouse epididymal spermatozoa were quite resistant to H_2O_2. The glutathione content and the GPX/GRD activities of washed mouse cauda epididymal spermatozoa have been shown to be high, implicating this enzymatic defense system as the principal one operating in these cells [Alvarez and Storey, 1984].

Attempts to correlate sensitivity to H_2O_2 toxicity and the activities of the systems of enzymatic defense towards oxidative damage in the spermatozoa from the different species described above proved difficult because of the variable of washed versus unwashed and ejaculated versus epididymal sperm. In this study, washed cauda epididymal spermatozoa from mouse and rabbit were examined, since these cells should represent the extremes of the glutathione protective system in mammalian male gametes. Washed, ejaculated human spermatozoa were also examined, since these

have an intermediate level of glutathione and GPX/GRD activities and could also provide an insight into the possible clinical utility of assaying for these enzymatic defense mechanisms. Since the cells from all three species were washed, perturbations from antioxidants in the epididymal lumen or in the seminal plasma have been minimized. The results imply that sensitivity to H_2O_2 toxicity is a measure of the importance played by the glutathione system in protecting the spermatozoa from oxidative damage.

MATERIALS AND METHODS

Reagents

Cytochrome *c* (Type VI) from horse heart, mercaptosuccinate, glutathione reductase (type IV) from yeast, oxidized and reduced glutathione, bovine serum albumin Fraction V (BSA), thiobarbituric acid, adenine nucleotides, and N,N-ethylenediaminotetracetic acid, disodium salt (EDTA) were from Sigma Chemical Company (St. Louis, MO). Glutathione peroxidase was from Boehringer Manneheim (Indianapolis, IN). Yeast cytochrome *c* peroxidase was the gift of Professor C.P. Lee, Wayne State University. Malonaldehyde-bis (dimethyl acetal) was from Aldrich Chemical Company (Milwaukee, WI). Hydrogen peroxide, trichloroacetic acid, and inorganic salts were from J.T. Baker (Phillipsburg, NJ). Penicillin-streptomycin was from Gibco Labs (Grand Island, NY). Filipin was obtained from Polysciences, Inc. (Warrington, PA).

Media

Three media were used for sperm incubations. For rabbit sperm, the medium was NTP [Alvarez and Storey, 1982] with the following composition: 113 mM NaCl; 10 mM KCl, 12.5 mM NaH_2PO_4, 2.5 mM Na_2HPO_4, 20 mM Tris, 1.5 mM D-glucose, 0.4 mM EDTA, 0.6% penicillin-streptomycin, adjusted to PH 7.4 ± 0.05 with HCl. For mouse sperm the medium was NTPC [Alvarez and Storey, 1984] with the following composition: 113 mM NaCl, 12.5 mM NaH_2PO_4, 2.5 mM Na_2HPO_4, 1.7 mM $CaCl_2$, 20 mM Tris, 1.5 mM D-glucose, 0.4 mM EDTA, 0.6% penicillin-streptomycin, adjusted to pH 7.4 ± 0.05 with HCl. For human spermatozoa the medium used was a modification of NTPC [Alvarez et al., 1987] with the following composition: 103 mM NaCl, 10 mM KCl, 12.5 mM NaH_2PO_4, 2.5 mM Na_2HPO_4, 1.7 mM $CaCl_2$, 20 mM Tris, 1.5 mM D-glucose, 0.4 mM EDTA, 0.6% penicillin-streptomycin, adjusted to pH 7.4 ± 0.05 with HCl.

Preparation of Spermatozoa

Rabbit spermatozoa were removed from the caudae of excised epididymides of mature male New Zealand white rabbits by retrograde flushing with medium NTP and recovered by centrifugation at 750*g* for 10 min. as described previously [Alvarez and Storey, 1982]. Stock suspensions contained 0.4–2 × 10^9 cells/ml. Hyposmotically treated rabbit epididymal spermatozoa were obtained by treatment of the washed spermatozoa with 10 ml of 10 mM potassium phosphate [Keyhani and Storey, 1973], followed by centrifugation at 750*g* for 10 minutes and resuspension in NTP. Epididymal mouse sperm suspensions were prepared by mincing 16–20 excised caudae epididymides from mature Swiss Webster mice into 2 ml NTPC and allowing the sperm

to disperse for 15 minutes, as described previously [Alvarez and Storey, 1984]. Stock suspensions contained 0.3–3.5 $\times$ 10^8 cells/ml. Mouse sperm with permeabilized plasma membranes were obtained by treatment with filipin [Carey et al., 1981] as described previously [Alvarez and Storey, 1984]. Human ejaculated spermatozoa were obtained from ten healthy donors by masturbation. Each donor provided three samples within a span of 2 weeks. Successive sperm samples were collected with at least 48 hours of abstinence between samples. The spermatozoa were incubated at 37°C for 15 minutes until complete liquifaction was achieved. Processing of sperm was then carried out as described previously [Alvarez et al., 1987]. Only those samples with a motility score above 65% and superoxide dismutase activities above 7 units/10^8 cells were considered suitable for this study. The final concentration in the stock suspension was 0.3–6.4 $\times$ 10^8 cells/ml. Hyposmotically treated human ejaculated spermatozoa were obtained by treatment of the washed spermatozoa with 10 ml of 10 mM potassium phosphate as described previously [Alvarez et al., 1987].

Aerobic Incubation of Spermatozoa

The stock suspension of rabbit epididymal spermatozoa was diluted ten-fold to give a sperm suspension containing 0.4 to 2 $\times$ 10^8 cells/ml. Mouse and human spermatozoa stock suspensions were diluted three-fold to give sperm suspensions containing 0.1–1.2 $\times$ 10^8 cells/ml and 0.1–2.2 $\times$ 10^8 cells/ml, respectively. When indicated, 10 μl aliquots of H_2O_2 and mercaptosuccinate solutions in the corresponding media were added to 1 ml of sperm suspension for rabbit spermatozoa, and to 0.3 ml for mouse and human spermatozoa, to obtain final concentrations of 1 and 5 mM H_2O_2 and 100 and 200 μm mercaptosuccinate as required. The sperm suspensions were placed in wide-mouthed specimen bottles (55 $\times$ 28 mm) held in a shaking water bath at 24°C $\pm$ 1°C. These bottles provide excellent aeration of the samples. The caps of the bottles had liners made of Teflon that prevented contamination of the samples and provided a seal tight enough to prevent loss of malonaldehyde by volatilization from the suspension.

Determination of Lipid Peroxidation by Malonaldehyde Production

The determination of malonaldehyde production by rabbit and mouse spermatozoa was carried out using the spectrophotometric determination of the thiobarbituric acid (TBA) adduct, as described previously [Alvarez and Storey, 1982, 1984]. For human spermatozoa, malonaldehyde production was determined using the modification of this assay described by Alvarez et al. [1987].

Motility Assay

Sperm motility was estimated by the method used in previous studies [Alvarez and Storey, 1982, 1983], in which the percent motility in duplicate aliquots of the sperm suspension was estimated by microscopic examination and then averaged.

Determination of Rate of H_2O_2 Reaction With Sperm

The rate of reaction of H_2O_2 with the sperm cells was obtained by incubating sperm suspensions of different cell concentration ranging from 0.2 to 2 $\times$ 10^7 cells/ml at 24°C $\pm$ 1°C in the presence of 7.9 μM H_2O_2 for 30 minutes. This concentration of H_2O_2 was found to be optimal considering the cell concentration ranges used in these

experiments. Incubation was terminated by rapid ice cooling at the chosen time intervals. The sperm suspensions were centrifuged at 750*g* for 10 minutes, and the supernatant assayed for H_2O_2 content. This was carried out by monitoring the oxidation of acetylated ferrocytochrome *c* catalyzed by cytochrome *c* peroxidase at 24°C, with a dual wavelength spectrophotometer using the wavelength pair 550/540 nm exactly as described by Holland and Storey [1981].

Glutathione Peroxidase and Reductase Activities and Glutathione Content

The enzymatic activities of GPX and GRD and the glutathione content of sperm, untreated and treated either with H_2O_2 or mercaptosuccinate, were determined in hyposmotically treated human and rabbit spermatozoa and in filipin-treated mouse spermatozoa by a slight modification of the methods described previously [Holland and Storey, 1981; Alvarez and Storey, 1984; Alvarez et al., 1987]. After incubation was terminated, the sperm suspensions were centrifuged at 750*g* for 10 minutes to remove either excess H_2O_2 or mercaptosuccinate, followed by membrane permeabilization as described above. Controls were subjected to the same procedure in the absence of H_2O_2 or mercaptosuccinate. GPX was assayed by the coupled enzyme method utilizing excess GRD, which couples oxidation of NADPH to the reduction of GSSG formed by the action of GPX [Smith et al., 1979]. The reaction mixture was composed of 60 μg/ml GRD, 1 mM GSH, and 1 mM cumene hydroperoxide in NTPC. The oxidation of NADPH was monitored by the absorbance decrease at 365/395 nm using a dual-wavelength spectrophotomer [Alvarez et al., 1987]. GRD activity was assayed in the same system using 5 mM GSSG as substrate in the presence of GPX inhibitor. Since 200 μM mercaptosuccinate has been reported to inhibit completely the GPX activity from hamster liver [Chaudiere et al., 1984], this concentration of mercaptosuccinate was used to block both the activity of GPX from sperm and that of the exogenously added GPX used to determine the glutathione content in the sperm cells. The values obtained by inhibiting the enzyme with mercaptosuccinate were comparable to those obtained when the enzyme was inhibited with 0.05 mM $ZnCl_2$ [Splittberger and Tappel, 1979]. Total endogenous glutathione was measured by conversion of endogenous GSH to GSSG with 1 mM cumene hydroperoxide and GPX added at 2.5 μg/ml for 5 min. The GPX was inhibited with 200 μM mercaptosuccinate, and the total GSSG determined as for GRD activity as described above. Endogenous GSSG was determined in the absence of GPX pretreatment and GSH was calculated by difference between endogenous GSSG and total glutathione.

RESULTS

The effects of H_2O_2 at 1 mM and 5 mM on the loss of motility of rabbit, human, and mouse spermatozoa are shown in Figures 1 and 2, respectively. Washed epididymal rabbit sperm were essentially unaffected by either concentration of H_2O_2, while washed epididymal mouse and washed ejaculated human spermatozoa were adversely affected in a dose-dependent manner. In previous studies, it was shown that loss of sperm motility in response to O_2 was due to spontaneous lipid peroxidation (as opposed to induced or promoted lipid peroxidation) and that a linear correlation existed between the two parameters [Alvarez and Storey, 1982, 1984; Alvarez et al., 1987]. The rate of spontaneous lipid peroxidation in the presence of H_2O_2 was therefore

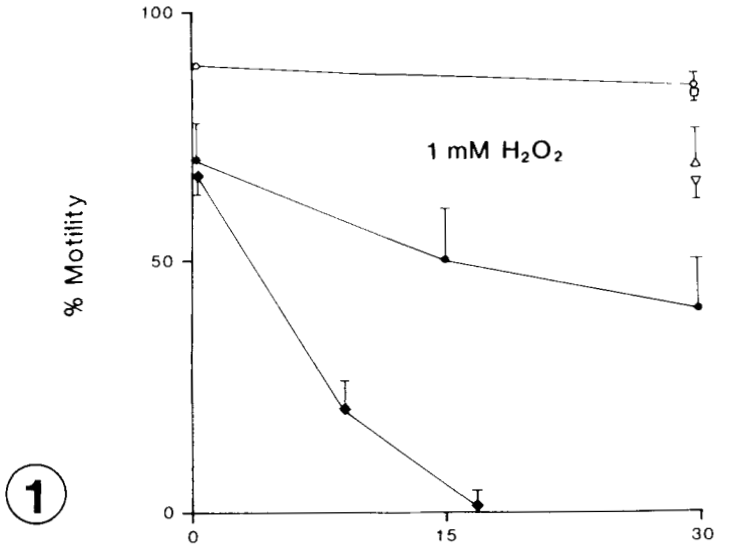

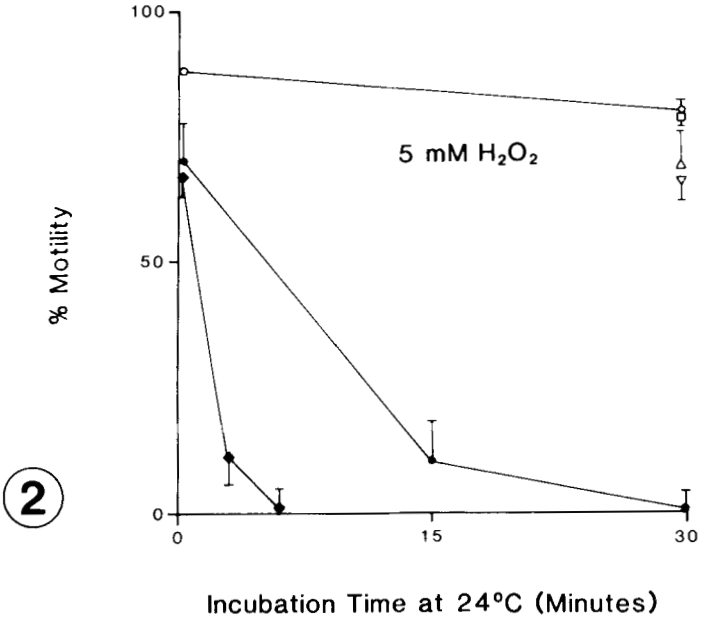

Fig. 1. Effect of 1 mM H_2O_2 on loss of percent motility in mouse, human, and rabbit sperm during aerobic incubation at 24°C. Sperm cell concentrations ranged from 0.5 to 1.0 × 10^6 cell/ml. Each point is the mean of 10 experiments; error bars are standard deviations. Experimental points for rabbit sperm are open circles (○); for human sperm, solid circles (●); and for mouse sperm, solid diamonds (♦). Control point at 30 min for rabbit sperm is open square (□); for human sperm, open triangles (△); and for mouse sperm, inverted open triangles (▽).

Fig. 2. Effect of 5 mM H_2O_2 on loss of percent motility in mouse, human, and rabbit sperm during aerobic incubation at 24°C. Symbols for experimental and control points are the same as in Figure 1.

TABLE 1. Effect of H_2O_2 on the Rate of Lipid Peroxidation in Mouse, Human, and Rabbit Spermatozoa, Expressed as Malonaldehyde (MA) Production*

Species	Rate as MA produced nmol/hr-10^8 cells		
	Control	1 mM H_2O_2	5 mM H_2O_2
Mouse	0.061 ± 0.004	1.7 ± 0.1	2.2 ± 0.2
Human	0.012 ± 0.001	0.10 ± 0.07	0.24 ± 0.02
Rabbit	0.0057 ± 0.0005	0.0057 ± 0.0006	0.0060 ± 0.0006

*Values of rates represent the mean ± S.D., n = 10. Human samples were obtained from 10 separate donors, each providing 3 separate samples. Aerobic incubations were carried out at 24°C.

examined. The rate in rabbit spermatozoa remained unchanged, but there was a marked increase of the lipid peroxidation rate in mouse and human spermatozoa in the presence of H_2O_2 (Table 1).

The question of whether the rate of reaction between the cells and exogenous H_2O_2 would reflect their sensitivity to this oxidant, as reflected by increased rate of lipid peroxidation, was addressed by the experimental protocol shown for mouse spermatozoa in Figure 3. The cells were incubated in the presence of 7.9 μM H_2O_2 for set times at the different cell concentrations indicated. The remaining H_2O_2 was then determined by the cytochrome *c* peroxidase catalyzed oxidation of acetylated ferrocy-

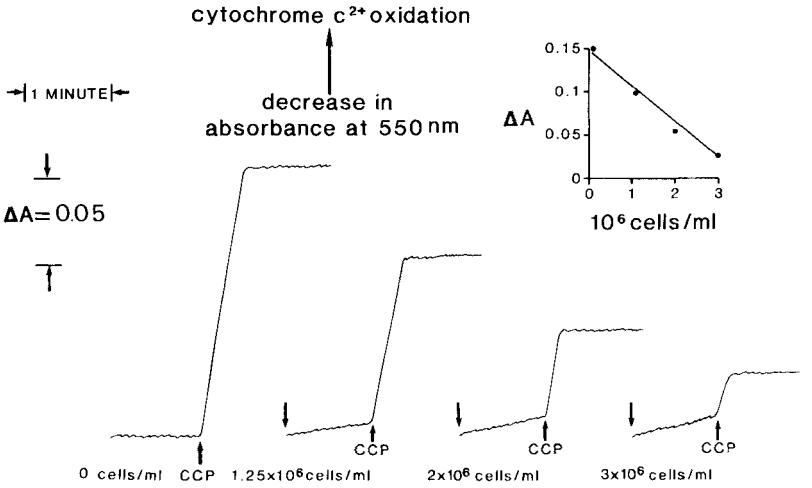

Fig. 3. Reaction of exogenous H_2O_2 with mouse spermatozoa as determined with cytochrome *c* cytochrome *c* peroxidase by dual wavelength spectrophotometry. Shown are direct tracings from the recorder. The reaction mixture contained in a final volume of 1 ml, 113 mM NaCl, 1.7 mM Ca Cl_2, 15 mM sodium phosphate, 1.5 mM D-glucose. 0.4 mM EDTA, 20 mM Tris/HCl, ph 7.4, 86 μM acetylated ferrocytochrome *c*. At the point indicated by the arrows, the supernatant from a suspension of mouse epididymal sperm incubated at 24°C in the presence of 7.9 mM H_2O_2 was added to the reaction, followed 2 minutes later by 0.2 μM cytochrome *c* peroxidase (CCP) at the point marked with the arrow and CCP. The absorbance decrease corresponding to oxidation of acetylated ferrocytochrome at the wavelength pair 550/540 nm appears as an upward deflection of the trace. The insert shows a linear decrease in absorbance with cell concentration for the fixed time interval of 2 minutes up to about 3 × 10^6 cells/ml. At higher cell concentrations, the curve plateaus due to interference from H_2O_2 produced by the cells.

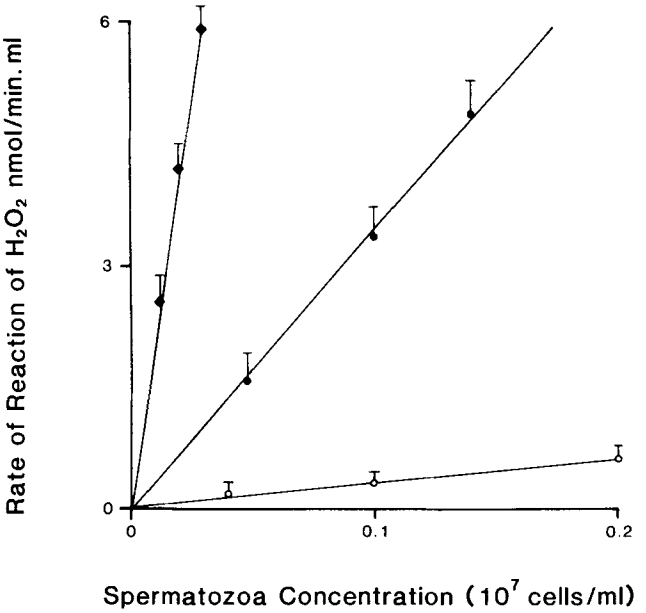

Fig. 4. Rate of reaction of H_2O_2 with spermatozoa from mouse, human, and rabbit sperm as a function of cell concentration defined by the linear region of dependence shown in the inset to Figure 3. Experimental conditions were as described in Figure 3. Regression equation calculated through the origin for mouse spermatozoa (♦) was y = 153 x (r = 0.99) for the concentration range (0.01–0.2) × 10^7 cells/ml. For human spermatozoa (●) the equation was y = 36.4 x (r = 0.999) for the concentration range (0.05–0.2) × 10^7 cells/ml. For rabbit spermatozoa (○) the equation was y = 3 x (r = 0.99) for the concentration range (0.04–0.2) × 10^7 cells/ml. At low rabbit sperm concentration, the rate of reaction of H_2O_2 with the cells nears the limit of sensitivity of the assay. Each point represents the mean of 10 experiments. Error bars are the standard deviations. Note that the symbols for each species correspond to those in Figures 1 and 2.

tochrome *c*. Increasing the cell concentration for a constant incubation time decreases the H_2O_2 content of the medium in linear manner up to 2 × 10^6 cells/ml (Fig. 3, inset). At higher cell concentrations, the production of H_2O_2 by the cells becomes significant enough to cause the curve to level off. Within the range of linearity with cell concentration, the rates of reaction of H_2O_2 with rabbit, human, and mouse spermatozoa (Fig. 4) are markedly different and in the direction expected for the results in Figures 1 and 2. The slopes of the lines in Figure 3 define a second-order rate constant k_p with the units $(10^8 \text{ cells/ml})^{-1}$ min^{-1} for the reaction of exogenous H_2O_2 with the cells, analogous to the constant found for reaction with exogenous O_2 [Alvarez and Storey, 1985]. The rate constants are listed in Table 2, along with the activity of GPX and glutathione content of the sperm cells of each of the three species. GPX is the major enzyme reactive with H_2O_2 in these cells [Holland and Storey, 1981; Alvarez and Storey, 1984; Alvarez et al., 1987]. Rabbit spermatozoa, which have negligible glutathione content, low peroxidase activity, and the lowest value of k_p, are the cells most resistant to H_2O_2, whereas mouse spermatozoa, with the highest glutathione content, highest peroxidase activity, and largest value of k_p, are the most sensitive to immobilization by H_2O_2.

TABLE 2. Rate Constants k_p for Reaction With H_2O_2, Activities of Glutathione Peroxidase (GPX), and Glutathione Content Compared in Mouse, Human, and Rabbit Sperm*

Species	k_p [$(10^8$ cells/ml$)^{-1}$ min^{-1}][a]	GPX activity (nmol/min − 10^8 cells)	Glutathione (nmol/10^8 cells)		
			Total	GSSG	GSH
Mouse	194	194 ± 15	90 ± 6	33 ± 5	57
Human	46	21.0 ± 0.1	6.7 ± 0.4	2.8 ± 0.2	3.9
Rabbit	4	4.0 ± 0.2	<0.1[b]	—	—

*Glutathione content expressed as GSH equivalents. Total (GSSG + GSH) and GSSG were measured as described in Materials and Methods; values represent the mean ± S.D., n = 10. GSH was calculaed as the difference between the total and GSSG. GPX activities represent the mean ± S.D., n = 10, determined at 24°C.

[a]Obtained from the slopes of the lines in Figure 4, divided by 7.9 μM H_2O_2 used as reactant, as described in Materials and Methods. Determinations carried out at 24°C.

[b]Value from Holland and Storey [1981], confirmed in this study.

This finding indicated that impairment of the GPX system could have serious consequences with regard to lipid peroxidation in both mouse and human sperm. Exogenous H_2O_2 could functionally inactivate the system by converting all the intracellular GSH to GSSG, thereby depriving the peroxidase of the reductant substrate needed to reduce lipid hydroperoxides to the far less harmful alcohols. This was shown to occur. At 5 mM H_2O_2, the GSH content of mouse and human sperm was negligible; all the glutathione originally in the cells could be accounted for as GSSG. There was no loss of GSSG from the cells.

The effects of rendering the peroxidase nonfunctional in the absence of H_2O_2 could be assessed by inhibition of the enzyme. A suitable inhibitor for mammalian sperm GPX was found to be mercaptosuccinate (thiomalate) [Chaudiere et al., 1984], as shown in Table 3. With spermatozoa from all three species, 200 μM mercaptosuccinate inhibited the peroxidase by over 90% but had no effect on the reductase. The

TABLE 3. Effect of Mercaptosuccinate (MCS) on the Enzymatic Activities of Glutathione Reductase (GDG), Glutathione Peroxidase (GPX), and on the Rate of Lipid Peroxidation, Expressed as Malonaldehyde (MA) Production, in Mouse, Human, and Rabbit Spermatozoa*

Species	MCS (μM)	Enzyme activity (nmol/min − 10^8 cells)		Rate of lipid peroxidation (MA, nmol/hr − 10^8 cells)
		GDR	GPX	
Mouse	0	117 ± 9	194 ± 15	0.061 ± 0.004
	100	120 ± 10	80 ± 6	0.75 ± 0.04
	200	118 ± 11	2.1 ± 0.1	1.5 ± 0.1
Human	0	45.0 ± 0.4	21.0 ± 0.1	0.012 ± 0.001
	100	42.0 ± 0.3	10.0 ± 0.7	0.16 ± 0.10
	200	43.0 ± 0.3	1.2 ± 0.1	0.20 ± 0.06
Rabbit	0	1.0 ± 0.1	4.0 ± 0.2	0.0057 ± 0.0005
	100	1.1 ± 0.1	1.6 ± 0.1	0.0060 ± 0.0006
	200	0.9 ± 0.04	0.04 ± 0.01	0.0060 ± 0.0010

*Values represent mean ± S.D., n = 10. Enzyme activities and lipid peroxidation rates determined at 24°C.

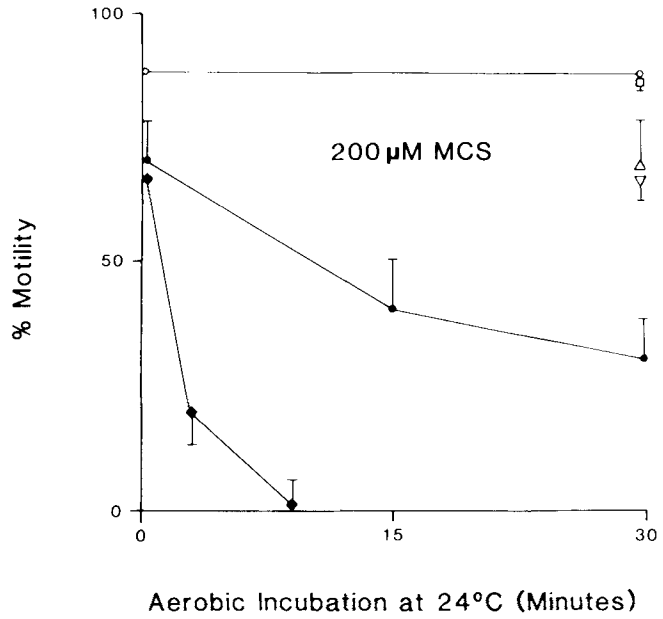

Fig. 5. Effect of 200 μM mercaptosuccinate (MCS) on loss of percent motility in mouse, rabbit, and human sperm during aerobic incubation at 24°C. Symbols for experimental and control points are the same as in Figure 1.

effect of 200 μM mercaptosuccinate on loss of motility in spermatozoa from the three species is shown in Figure 5. The effects observed at 100 μM are very similar (data omitted for clarity). The loss of motility parallels that observed with exogenous H_2O_2 (Figs. 1, 2). A parallel increase in the rate of lipid peroxidation over controls is also observed in the presence of mercaptosuccinate (Table 3). Rabbit spermatozoa showed no increase in the rate of peroxidation with the peroxidase inhibitor, consistent with the result obtained with exogenous H_2O_2. Comparison of the data for peroxidase inhibition by mercaptosuccinate in Table 3 and for rate of peroxidation in Figure 4 indicates that 50%–60% inhibition of the peroxidase activity is sufficient to produce a tenfold increase in the rate of lipid peroxidation. Endogenous GSH is powerless to inhibit the increased rate of peroxidation in the presence of mercaptosuccinate. With the peroxidase inhibited, nearly 90% of the glutathone was determined to be GSH. This is just the opposite of what is observed in the presence of H_2O_2. The redox state of the endogenous glutathione in mouse and human sperm under control conditions and in the presence of 5 mM H_2O_2 or 200 μM mercaptosuccinate is shown in Table 4 for convenient comparison.

DISCUSSION

In spermatozoa from the three mammalian species examined in this study, sensitivity to loss of motility from exogenous H_2O_2 parallels the activity of the glutathione/GPX enzyme defense system in the cells. In mouse and human sperm, the calculated second-order rate constant k_p for the reaction of H_2O_2 with the cells seems to be a

TABLE 4. Comparison of Total Glutathione, GSSG, and GSH Content of Mouse and Human Sperm in the Presence of 5 mM H_2O_2 and 200 μM Mercaptosuccinate (MCS)*

Species	Addition	Total	GSSG	GSH
Mouse	0	90 ± 6	33 ± 5	57
	5 mM H_2O_2	90 ± 5	90 ± 5	0
	200 μM MCS	90 ± 6	2.8 ± 0.2	87
Human	0	6.7 ± 0.4	2.8 ± 0.2	3.9
	5 mM H_2O_2	6.7 ± 0.3	6.7 ± 0.5	0
	200 μM MCS	6.8 ± 0.3	0.40 ± 0.03	6.4

*Values represent mean ± S.D., n = 10. GSH obtained by difference from determinations of total (GSSG + GSH) and GSSG. Content expressed as GSH equivalents.

reliable indicator of GPX activity (Table 2). The effect of H_2O_2 is due to loss of GPX function by complete conversion of its substrate GSH to the disulfide GSSG. Direct inactivation of the peroxidase by the inhibitor mercaptosuccinate causes the same rapid decrease in motility and increase in lipid peroxidation as does H_2O_2, even though the GSH content of the cells actually increases. Comparison of the effects of 5 mM H_2O_2 (Fig. 2) and 200 μM mercaptosuccinate (Fig. 4) suggest that GSH, if present in the absence of functional peroxidase, has only a minor protective effect. These findings indicate that both H_2O_2 and mercaptosuccinate provide a convenient means of estimating both the activity of GPX and its contribution to enzymatic defense against O_2 toxicity in mammalian spermatozoa. It was an unexpected, but useful result in this regard that mercaptosuccinate is a permeant anion, which can readily enter intact, motile spermatozoa.

The rapid loss of motility in human spermatozoa, brought about by inactivation of GPX, requires revision of the conclusion from a previous study [Alvarez et al., 1987] that SOD activity plays a major role in protecting these cells against peroxidative damage. The conclusion was based on the observation that SOD activity in human sperm samples was highly variable, and that this activity correlated well ($r = 0.97$) with the time to complete loss of motility due to lipid peroxidation in a given sample. The times to motility loss varied from 1 to 10 hours for these samples. In contrast, the activities of GRFD and GPX, the glutathione content, and the GSH/GSSG ratio were remarkably constant in the same samples examined for dismutase activity. These samples were all from normal healthy donors, which may explain this constancy. From the present study, it is apparent that the glutathione system provides a basal defense, without which the superoxide dismutase system would be overwhelmed. The glutathione system may be less active in those men with abnormal sperm samples, and so measurement of its activity in samples from patients of suspected infertility may prove clinically useful.

Two questions are posed by the insensitivity of rabbit spermatozoa to H_2O_2, which in turn reflects the minimal activity of the glutathione system. The first is, to what extent is H_2O_2 itself toxic to mammalian spermatozoa? The answer would seem to be that it is virtually nontoxic. Spermatozoa from the three species lack catalase [Mann, 1964] and produce H_2O_2 at a rate entirely accounted for by the activity of their endogenous SOD [Alvarez and Storey, 1982, 1984; Alvarez et al., 1987] with no apparent ill effects from this agent. The second related question is, why should the

formation and breakdown of endogenous hydroperoxides be sufficiently rapid in mouse and human spermatozoa that these cells require the GPX protective system, while rabbit spermatozoa do not? The answer would seem to lie in the intrinsic rates of superoxide production by the sperm cells of the three species. The average intrinsic rate of $O_2^{\cdot-}$ production, v_{int}, in rabbit sperm was found to be 0.17 nmol/min-10^8 cells, compared to 2.0 nmol/min-10^8 cells in mouse and 2.1 nmol/min-10^8 cells in human sperm (the range in human sperm for the samples studied was 0.9–7.0 in these units). These values were obtained in fresh cells with fully functional SOD. In rabbit spermatozoa, the maximum value of v_{int} is 1.61 nmol/min-10^8 cells, obtained in the presence of 10 mM KCN to block SOD activity. The rabbit sperm SOD activity is thus capable of removing nearly 90% of the $O_2^{\cdot-}$ produced by the cells. In contrast, the average removal in human sperm cells is 75% and in mouse sperm cells only 50%. The intracellular steady state concentration of $O_2^{\cdot-}$ would be expected to be far higher in mouse and human spermatozoa, which in turn would mean higher concentrations of its conjugate acid, the very active perhydroxyl radical, $HO_2\cdot$ [Gebicki and Bielski, 1981; Bielski et al., 1983]. The high reactivity of $HO_2\cdot$ in spontaneous lipid peroxidation in rabbit spermatozoa has been demonstrated previously [Alvarez et al., 1984].

From the findings in this and previous studies on the spontaneous lipid peroxidation in mammalian sperm, a more complete set of the reactions involved in this process can be compiled. Spontaneous lipid peroxidation in mammalian sperm, as measured by production of malonaldehyde, is a far slower process than peroxidation induced by the normally used ascorbate/Fe^{2+} system [Jones and Mann, 1973, 1976]. Further, the rate of spontaneous lipid peroxidation in unperturbed sperm from all three species, as measured by malonaldehyde formation, is of the order of 0.006 to 0.06 nmol/hr-10^8 cells (Table 1), corresponding to 0.0001 to 0.001 nmol/min-10^8 cells and is three to four orders of magnitude lower than v_{int}, the intrinsic rate of $O_2^{\cdot-}$ production. Even allowing for yields of 10% to 1% of malonaldehyde from peroxidation breakdown products [Pryor and Stanley, 1975], it is evident that, if the superoxide species $O_2^{\cdot-}$ and $HO_2\cdot$ are to contribute to lipid peroxidation, it must be through a process not directly related to their rate of production. The simplest explanation for the contribution of the superoxide species is relatively rapid formation of lipid hydroperoxide R_2 CHOOH by reaction of HO_2 with the allylic CH_2 group of an unsaturated acyl or alkenyl moiety:

$$R_2CH_2 + HO_2\cdot \rightarrow R_2CH\cdot + H_2O_2 \quad (1)$$

$$R_2CH\cdot + O_2^{\cdot-} + H^+ \rightarrow R_2CHOOH \quad (2)$$

The initiation reaction (1) has been demonstrated by Bielski et al. [1983]. The termination reaction (2) is that expected in the presence of excess $O_2^{\cdot-}$ over the carbon radical; other propagation reactions leading to short chain reactions may also play a role [Pryor and Stanley, 1975; Gebicki and Bielski, 1981; Chan, 1987]. The rate-determining step for malonaldehyde production would be direct reaction of O_2 with the hydroperoxide by abstraction of a H atom. This reaction is spin forbidden, and so would be expected to be slow and have high activation energy [Hamilton, 1974]. Spontaneous lipid peroxidation in these cells has the very high activation energy of 77 to 79 kcal/mol, in accord with this expectation [Alvarez and Storey, 1985]. The steps leading from the reaction product of lipid hydroperoxide and O_2 to various products

are complex but would inevitably yield malonaldehyde in some constant yield under the given set of experimental conditions [Pryor and Stanley, 1975; Chan, 1987]. Removal of R_2CHOOH by the GPX system would keep the steady-state concentration sufficiently low to maintain a low rate of peroxidation by this route. Inactivation of the GPX system in human and mouse sperm evidently allows the peroxidation rate to increase by tenfold and thirtyfold, respectively, presumed to be due to an equivalent rise in the R_2CHOOH. In rabbit sperm, the steady-state production of R_2CHOOH is determined by the low concentrations of superoxide species and so remains low. GPX has little effect on the rate of spontaneous lipid peroxidation in these cells, presumably because it lacks both substrates, R_2CHOOH and GSH.

ACKNOWLEDGMENTS

This work was supported by NIH grants HD 15842 and HL 19737. We thank Mrs. Dorothy Rivers for technical assistance and Ms. Debbie Coffin for expert secretarial input.

REFERENCES

Abu-Erreizh G, Manges L, Li TK (1978): Isolation and properties of superoxide dismutase from ram spermatozoa and erythrocytes. Biol Reprod 18:554–560.

Alvarez JG, Storey BT (1982): Spontaneous lipid peroxidation in rabbit epididymal spermatozoa. Biol Reprod 27:1102–1108.

Alvarez JG, Storey BT (1983): Role of superoxide dismutase in protecting rabbit spermatozoa from O_2 toxicity due to lipid peroxidation. Biol Reprod 28:1129–1136.

Alvarez JG, Storey BT (1984): Lipid peroxidation and the reactions of superoxide and hydrogen peroxide in mouse spermatozoa. Biol Reprod 30:833–841.

Alvarez JG, Storey BT (1985): Spontaneous lipid peroxidation in rabbit and mouse epididymal spermatozoa: Dependence of rate on temperature and oxygen concentration. Biol Reprod 32:342–351.

Alvarez JG, Holland MK, Storey BT (1984): Spontaneous lipid peroxidation in rabbit spermatozoa: a useful model for the reaction of O_2 metabolites with single cells. In DW Lubbers, H Acker, E Leniger-Follert, TK Goldstick (eds): "Oxygen Transport to Tissue," Vol. 5. New York: Plenum, pp 433–443.

Alvarez JG, Touchstone JC, Blasco L, Storey BT (1987): Spontaneous lipid peroxidation and production of hydrogen peroxide and superoxide in human spermatozoa. Superoxide dismutase as major enzyme protectant against oxygen toxicity. J Androl 8:338–348.

Bielski BHJ, Arudi RL, Sutherland MW (1983): A study of the reactivity of HO_2/O_2^- with unsaturated fatty acids. J Biol Chem 258:4759–4761.

Carey JE, Olds-Clarke P, Storey BT (1981): Oxidative metabolism of spermatozoa from inbred and random bred mice. J Exp Zool 216:285–292.

Chan HW-S (1987): The mechanism of autoxidation. In HW-S Chan (ed): "Autoxidation of Unsaturated Lipids." London: Academic Press, pp 1–16.

Chaudiere J, Wilhelmsen EC, Tappel AL (1984): Mechanism of selenium-glutathione peroxidase and its inhibition by mercaptocarboxylic acids and other mercaptans. J Biol Chem 259:1043–1050.

Gebicki JM, Bielski BHJ (1981): Comparison of the capacities of the perhydroxyl and the superoxide radicals to initiate chain oxidation of linoleic acid. J Am Chem Soc 103:7020–7022.

Hamilton GA (1974): Chemical models and mechanisms for oxygenases. In O Hayaishi (ed): "Molecular Mechanisms of Oxygen Activation." New York: Academic Press, pp 405–451.

Holland MK, Storey BT (1981): Oxygen metabolism of mammalian spermatozoa. Generation of hydrogen peroxide by rabbit epididymal spermatozoa. Biochem J 198:273–280.

Jones R, Mann T (1973): Lipid peroxidation in spermatozoa. Proc R Soc Lond [Biol] 184:103–107.

Jones R, Mann T (1976): Lipid peroxides in spermatozoa: Formation, role of plasmalogen, and physiological significance. Proc R Soc Lond [Biol] 193:317–333.

Keyhani E, Storey BT (1973): Energy conservation capacity and morphological integrity of mitochondria in hypotonically treated rabbit epididymal spermatozoa. Biochim Biophys Acta 305:557–569.

Li TK (1975): The glutathione and thiol content of mammalian spermatozoa and seminal plasma. Biol Reprod 12:641–646.

Mann T (1964) "The Biochemistry of Semen and the Male Reproductive Tract." London: Methuen, pp 130–131.

McLeod J (1943): The role of oxygen in the metabolism and motility of human spermatozoa. Am J Physiol 138:512–518.

Menella MRF, Jones R (1980): Properties of spermatozoal superoxide dismutase and lack of involvement of superoxides in metals ion-catalyzed lipid peroxidation reactions in semen. Biochem J 191:289–297.

Pryor WA, Stanley JP (1975): A suggested mechanism for the production of malonaldehyde during the autooxidation of polyunsaturated fatty acids. Nonenzymatic production of prostaglandin endoperoxides during autooxidation. J Org Chem 40:3615–3617.

Smith DG, Senger PL, McCutchan JF, Landa CA (1979): Selenium and glutathione peroxide distributin in bovine semen and selenium-75 retention by the tissue of the reproductive tract of the bull. Biol Reprod 20:377–383.

Splittberger AG, Tappel AL (1979): Inhibition of glutathione peroxidase by cadmium and other metal ions. Arch Biochem Biophys 197:534–542.

Tosic J (1947): Mechanism of hydrogen peroxide formation by spermatozoa and the role of amino-acids in sperm motility. Nature 159:544.

Tosic J, Walton A (1950): Metabolism of spermatozoa. Formation of hydrogen peroxide by spermatozoa and its effects on motility and survival. Biochem J 47:199–212.

Wales RG, White IG, Lamond DR (1959): The spermicidal activity of hydrogen peroxide in vitro and in vivo. J Endocrinol 18:236–244.

Int. J. Radiat. Biol., Vol. 86, No. 11, November 2010, pp. 935–945

informa
healthcare

Mobile phone radiation-induced free radical damage in the liver is inhibited by the antioxidants n-acetyl cysteine and epigallocatechin-gallate

ELCIN OZGUR, GÖKNUR GÜLER, & NESRIN SEYHAN

Department of Biophysics and Gazi Non-Ionizing Radiation Protection Center, Gazi University Medical Faculty, Ankara, Turkey

(Received 29 January 2010; Revised 10 May 2010; Accepted 11 May 2010)

Abstract

Purpose: To investigate oxidative damage and antioxidant enzyme status in the liver of guinea pigs exposed to mobile phone-like radiofrequency radiation (RFR) and the potential protective effects of N-acetyl cysteine (NAC) and epigallocatechin-gallate (EGCG) on the oxidative damage.

Materials and methods: Nine groups of guinea pigs were used to study the effects of exposure to an 1800-MHz Global System for Mobile Communications (GSM)-modulated signal (average whole body Specific Absorption Rate (SAR) of 0.38 W/kg, 10 or 20 min per day for seven days) and treatment with antioxidants.

Results: Significant increases in malondialdehyde (MDA) and total nitric oxide (NO_x) levels and decreases in activities of superoxide dismutase (SOD), myeloperoxidase (MPO) and glutathione peroxidase (GSH-Px) were observed in the liver of guinea pigs after RFR exposure. Only NAC treatment induces increase in hepatic GSH-Px activities, whereas EGCG treatment alone attenuated MDA level. Extent of oxidative damage was found to be proportional to the duration of exposure ($P < 0.05$).

Conclusion: Mobile phone-like radiation induces oxidative damage and changes the activities of antioxidant enzymes in the liver. The adverse effect of RFR may be related to the duration of mobile phone use. NAC and EGCG protect the liver tissue against the RFR-induced oxidative damage and enhance antioxidant enzyme activities.

Keywords: *Mobile phone radiation, oxidative stress, liver, antioxidants, (-)-epigallocatechin-gallate, N-acetyl cysteine*

Introduction

Nowadays, people are voluntarily exposed to radio-frequency radiation (RFR) by using devices such as mobile phones and microwave ovens, and also passively subjected to the radiation due to living or working in areas near television and radio transmitters and mobile phone base stations. The possible health effects of RFR have been a concern in the past decades.

Even though there is no consensus about the non-thermal effects of RFR exposure below present guidelines, there is an agreement on the need for further research particularly on the investigation of interaction mechanisms. One of the proposed mechanisms for interaction between RFR and biological tissues is the formation of free radicals-molecules with an unpaired electron that may act as direct targets for the electromagnetic fields, as they are charged particles (Challis 2005). Free radicals are normally highly reactive and hence short lived, and their roles in diseases such as cancer are well established. Many studies have been carried out to investigate free radical formation in cells and animals under the influence of mobile phone radiation (Irmak et al. 2002, Ayata et al. 2004, Ilhan et al. 2004, Oktem et al. 2005, Ozguner et al. 2005a, 2005b, 2005c, 2006, Köylü et al. 2006, Balci et al. 2007, Guney et al. 2007, Meral et al. 2007, Oral et al. 2006, Sokolovic et al. 2008).

Free radicals and potent *radical* derivatives, such as reactive oxygen species (ROS) and reactive nitrogen species (RNS) are present in low concentration at normal states of metabolism in cells and tissues, and they play a vital role in many biochemical processes (Dröge 2002, Pacher et al. 2007, Valko et al. 2007).

Correspondence: Prof. Nesrin Seyhan, Gazi Üniversitesi Tıp Fakültesi Biyofizik Abd., Dekanlık Binası 5. Kat 06500 Beşevler, Ankara, Turkey. Tel: +90 312 202 46 02. Fax: +90 312 212 90 23. E-mail: nesrin@gazi.edu.tr

ISSN 0955-3002 print/ISSN 1362-3095 online © 2010 Informa UK, Ltd.
DOI: 10.3109/09553002.2010.496029

Over-production of free radicals may result in oxidative and nitrosative damages, known as oxidative stress and nitrosative stress (Halliwell and Gutteridge 1999). Lipid peroxidation is one of the major consequences of oxidative stress. Malondialdehyde (MDA) is the end-product of lipid peroxidation by reactive oxygen species. It is therefore generally used as a biomarker for the oxidative stress of an organism (Nair et al. 1986). In nitrosative stress, nitric oxides (NO_x) are produced excessively. Under such circumstances, NO_x produces highly reactive nitrogen species. Nitric oxide derivatives (nitrate [NO_3], nitrite [NO_2] and total level of NO_x) are used as biomarkers of nitrosative stress (Hausladen and Stamler 1999). The level of free radical damage is determined by the balance between the rate of damage induced and the rate of damage repaired and removed. The rate at which the damage is induced is determined by how fast the free radical species are generated and then inactivated by antioxidants and endogenous defense agents (Mathews et al. 1997). When a free radical gains electron from an antioxidant, the chain reaction of oxidation is broken. At this stage, the antioxidants are not harmful as they have the ability to accommodate the change in electrons without becoming reactive. Those that are manufactured within the body of living organisms are called enzymatic antioxidants. In addition, excessive free radicals in cells are removed by enzymatic activities. Superoxide dismutase (SOD) is a class of closely related enzymes that catalyse the breakdown of the super-oxide anion into oxygen and hydrogen peroxide. Myeloperoxidase (MPO) and glutathione peroxidase (GSH-Px) are in the family of enzymes with peroxidase activity, the main biological role of these enzymes is to protect an organism from oxidative damage (Eberhardt 2000).

Taking antioxidants or eating antioxidant-rich foods are highly recommended by the physicians as a health promoter against aging and many diseases such as cancer (Valko et al. 2007, Lambert et al. 2008). There are also many studies on the protective effect of different antioxidants against mobile phone radiation (Ayata et al. 2004, Ilhan et al. 2004, Oktem et al. 2005, Ozguner et al. 2005a, 2005b, 2005c, 2006, Köylü et al. 2006, Oral et al. 2006, Balci et al. 2007, Guney et al. 2007).

It is well-known that N-acetyl cysteine (NAC) is a powerful antioxidant that is essential in liver detoxification; besides, it is a precursor of glutathione. Epigallocatechin-Gallate (EGCG), the main active component of green tea leaves, may provide beneficial health effects, including prevention of cancer, by protecting cells from oxidative damage from free radicals (McKenna et al. 2002). Thus, we chose these antioxidants in the present study to investigate their protective effects on mobile phone radiation-induced oxidative stress.

The aim of this research is to study, in the liver of guinea pigs: (i) Whether exposure to a 1800-MHz GSM (Global System for Mobile Communications) mobile phone radiation induces oxidative and nitrosative stress by determining MDA and NO_x, and activities of the antioxidant enzymes SOD, GSH-Px and MPO, and (ii) whether treatments with NAC and EGCG can attenuate mobile-phone radiation-induced oxidative damage.

To our knowledge, no research on 1800-MHz GSM mobile phone radiation on oxidative damage and antioxidant enzyme activities in liver tissue has been carried out. In addition, this is a unique study in which NAC and EGCG were used as antioxidants for reducing the effects of mobile phone radiation.

Materials and methods

Animals

The experimental protocol was reviewed and approved by the Laboratory Animal Care Committee of the Gazi University, Ankara, Turkey. All the animal procedures were performed in accordance with the approved protocol. Adult male guinea pigs (approximately 14-week-old, weighing 250–300 g) were obtained from the Public Health Institute, Ankara, Turkey. Before the experiment, animals were adapted to the laboratory conditions for two weeks. Since placing more than one animal in a cage could create a stress factor, only one animal was placed in a cage during mobile phone radiation and sham exposure. All the animals were kept at an ambient temperature of 23°C and a relative humidity of 50%. A 12-h light/night cycle (light on 07:00–19:00 h) was set up and the animals were fed a standard laboratory chow and carrot, and provided with water *ad libitum*.

Exposure conditions

Exposure level and quality control

GSM-like signals at 1800 MHz were produced by using a signal generator (Agilent Technologies 8648C, 9 kHz–3.2 GHz, Santa Clara, USA) with an integrated pulse modulation unit and a horn antenna (Schwarzbeck, Doppelsteg Breitband Horn antenna BBHA 9120 L3F, 0.5–2.8 GHz, Schönau, Germany) in a shielded room. The generated power was controlled by a spectrum analyser (Agilent Technologies N9320A, 9 kHz–3 GHz, Santa Clara, USA) integrated to the signal generator. The signals were amplitude-modulated by rectangular pulses with a repetition frequency of 217 Hz and a duty

cycle of 1:8 (pulse width 0.576 ms), corresponding to the dominant modulation component of the GSM.

The signals were controlled by means of a spectrum analyser connected to the signal generator, and a electromagnetic radiation meter (EMR 300 meter with type 26.1 probe, NARDA Safety Test Solutions, Pfullingen, Germany) were used for measurement of the output radiation. Measurements were taken during the entire experiment and the data were saved in a computer which was connected to the device via a fiber optic cable. The average whole body specific absorption rate (SAR) was estimated to be 0.38 W/kg using the Finite Domain of Time Difference (FDTD) method (Taflove and Hagness 2005).

Ten identical cages were used in order to provide the same exposure conditions for every animal. Cages were made of Plexiglas ($8 \times 10 \times 18$ cm) with ventilation holes. Animals were placed in individual cages just at the beginning of exposure in order to reduce stress.

Grouping of animals

Ninety-six male guinea pigs were randomly divided into nine groups. Twelve animals were included in each of the three sham-exposed groups (Groups I–III described below). In each of these groups, six animals were subjected to 10-min sham exposure and the other six for 20-min sham exposure. Ten animals were used in each of the other six treatment groups that included animals that received daily RFR exposure of 10 or 20 min, and treatments with the antioxidants NAC or EGCG. All animals were injected intraperitoneally either with 1 ml saline or 1 ml antioxidant solution, NAC or EGCG, then they were returned to their home cages for 30 min before starting the exposure procedures. Our previous experience shows that this allows time for the antioxidants to become effective and the animals to recover from the stress of injection (Güler et al. 2008, 2009). NAC solutions were purchased and prepared in an ampule containing 300 mg of NAC dissolved in 3 ml of sterile water with 3 mg of sodium ethylenediaminetetraacetic acid (EDTA) and 73 mg of sodium hydroxide (NaOH) (73 mg), (Hüsnü Arsan Medicine, İstanbul, Turkey). The amount of NAC administrated to animals was proportional to their individual weights (300 mg/kg). 300 mg/3 ml solution was diluted according to the animals' weight and applied to them. EGCG was dissolved in distilled water at 5 mg/ml (Sigma-Aldrich Corp, St Louis, MO, USA). The amount of EGCG in 1 ml solution was proportional to the animals' weight (12.5 mg/kg).

Group I: Sham/saline. Daily for seven days, 1 ml of isotonic saline solution was injected intraperitoneally into each animal. They were then kept individually in a cage for either 10 ($n = 6$) or 20 ($n = 6$) minutes without exposure to RFR. These animals served as sham-exposed injection-controls.

Group II: Sham/NAC. 1 ml NAC solution (300 mg/kg) was injected intraperitoneally into each animal daily for seven days. Guinea pigs were then kept in individual cages for either 10 or 20 min without RFR exposure.

Group III: Sham/EGCG. 1 ml EGCG solution (12.5 mg/kg) was injected intraperitoneally into each animal daily for seven days. Animals were then kept in individual cages for either 10 or 20 min without RFR exposure

Group IV: 10-min RFR-exposure/saline. Daily for seven days, 1 ml of isotonic saline solution was injected intraperitoneally into each animal at 30 min before a daily 10-min RFR exposure.

Group V: 20-min RFR-exposure/saline. Daily for seven days, 1 ml of isotonic saline solution was injected intraperitoneally into each animal at 30 min before a daily 20-min RFR exposure.

Group VI: 10-min RFR-exposure/NAC. Daily for seven days, 1 ml NAC solution (300 mg/kg) was injected intraperitoneally into each animal at 30 min before a daily 10-min exposure to RFR.

Group VII: 20-min RFR-exposure/NAC. Daily for seven days, 1 ml NAC solution (300 mg/kg) was injected intraperitoneally into each animal at 30 min before a daily 20-min exposure to RFR.

Group VIII: 10-min RFR-exposure/EGCG. Daily for seven days, 1 ml EGCG solution (12.5 mg/kg) was injected intraperitoneally into each animal at 30 min before a daily 10-min RFR exposure.

Group IX: 20-min RFR-exposure/EGCG. Daily for seven days, 1 ml EGCG solution (12.5 mg/kg) was injected intraperitoneally into each animal at 30 min before a daily 20-min RFR exposure.

After the last exposure on Day 7, guinea pigs were anaesthetised by ketamine (40 mg/kg, Intramuscular [IM]) and xylazine (10 mg/kg, IM). They were then killed by decapitation. Following this, liver tissues were obtained immediately for biochemical analyses. The specimens were rinsed with ice-cold buffered saline to remove blood and then stored at -85°C for assay later.

Determination of MDA levels

MDA level in liver tissue was determined according to the spectrophotometric method of Cassini et al.

(1986). Lipid peroxidation was quantified by measuring the formation of thiobarbituric acid reactive substances (TBARS). Liver samples weighing 100 mg were homogenised (Disperser T10 basic D-79219, IKA-WERKE, Staufen, Germany) in nine volumes of cold 10% Trichloroacetic acid (TCA) solution and the homogenate was centrifuged (Mikro 22/22R, Hettich-Zentrifugen GmbH & Co, Tuttlingen, Germany) for 15 min at 3,000 *g* at 4°C. The supernatants were then transferred to glass test tubes containing 0.375% (w/v) thiobarbituric acid and 0.02% (w/v) butylated hydroxytoluene to prevent further peroxidation of lipids during the subsequent steps. The samples were then heated for 15 min at 100°C in a boiling water bath (Stuart Orbital Shaker, Bibby Scientific Ltd, Staffordshire, UK), cooled and centrifuged to remove the precipitant. The relative absorbance values of each sample were determined at 532 nm (Ultraviolet [UV]- 1601 Shimadzu spectrophotometer, Chiyoda-ku, Japan).

Determination of NO_x levels

NO_x levels, stable end-products of nitric oxide, in liver tissues were determined by the Griess reaction (Green et al. 1982). Tissue samples (150–200 mg) were homogenised in five volumes of phosphate buffer (pH 7.5) and centrifuged at 2,000 *g* for 5 min at 4°C. To the supernatant (0.5 ml), 0.25 ml of 0.3 M NaOH was added. After incubation for 5 min at room temperature, 0.25 ml of 10% (w/v) zinc sulfate ($ZnSO_4$) was added for deproteinisation. This mixture was then centrifuged at 14,000 *g* for 5 min and supernatants were used for the Griess assay. Nitrate levels in tissue homogenates were determined at 540 nm spectrophotometrically based on the reduction of NO_3 to NO_2 by vanadium (III) chloride (Miranda et al. 2001). Sodium nitrite and nitrate solutions (1, 10, 50, 100 μM) were used as standards.

Determination of SOD activity

Total (Cu-Zn and Mn) SOD activity was determined according to the method of Sun et al. (1988) with a slight modification by Durak et al. (1993). The principle of this method is based on the inhibition of nitrobluetetrazolium (NBT) reduction by the xanthine/xanthine oxidase system as a superoxide generator. Activity was assessed in the ethanol phase of the supernatant, after 1.0 ml ethanol/chloroform mixture (5/3 v/v) was added to the same volume of sample and centrifuged at 18,000 *g* for 60 min at 4°C. The conversion of NBT to formazan was determined at 560 nm spectrophotometrically. One unit of SOD was defined as the enzyme amount causing 50% inhibition in the NBT reduction rate. Medium blue colour was an index of both the presence of SOD and the rate of O_2 consumption. Activity was expressed as units per gram protein (Ug^{-1}). Protein concentration was assayed by the method of Lowry et al. (1951).

Determination of GSH-Px activity

Tissue GSH-Px activity was measured by the method of Paglia and Valentine (1967). Liver tissues were homogenised in phosphate-buffer saline (pH 7.0) at 4°C. Homogenates were centrifuged at 10,000 *g* for 10 min and supernatants were used to measure the GSH-Px activity. Each sample (5 μl) was incubated for 10 min at 37°C in a 495 μl incubation mixture containing (50 μl of 100 mM potassium phosphate buffer (PPB) (pH 7.0), 5 μl of 100 mM reduced glutathione (GSH), 10 μl of 200 mM EDTA, 5 μl of 400 mM sodium azide (NaN3), 50 μl of 2 mM nicotinamide adenine dinucleotide phosphate (NADPH), 325 μl of distilled water and 50 μl glutathione reductase (GR) (10 U/mg). After the 10-min incubation period, the reaction was initiated by addition of 5 μl of a 10 mM hydrogen peroxide (H_2O_2) solution. The rate of change of absorbance during the conversion of NADPH to NADP+ was recorded spectrophotometrially at 340 nm. GSH-Px activity was expressed as μmol of NADPH oxidised to NADP+ per min per mg tissue protein. Protein concentration was determined by the method of Lowry et al. (1951).

Determination of MPO activity

Tissues weighing 300 mg were homogenised in 700 μl of 20 mM PPB (pH 7.4) for 60 sec and the homogenates were centrifuged for 15 min at 20,000 *g* at 4°C. The supernatant was discarded, and the pellet was re-suspended in 500 μl of 50 mM PPB (pH 6.0) containing 0.5% hexadecyltrimethylammonium bromide (HETAB) and 0.146% EDTA. The re-suspended homogenates were then frozen (−20°C), and melted in room temperature, then sonicated for 30 sec, incubated for 2 h in a water bath (60°C), and then centrifuged at 12,500 *g* at 4°C for 30 min. The supernatants were used for MPO assay.

MPO activity was assessed by measuring the H_2O_2-dependent oxidation of o-dianisidin. One unit (U) of enzyme activity was defined as the amount of MPO present that caused a change in absorbance of 1.0/min at 410 nm and 37°C (Hillegass et al. 1990).

Statistical analysis

Statistical analysis was carried out by using the SPSS software (SPSS 11.5 for windows, SPSS Inc.,

Chicago, USA). All results were expressed as mean and standard error of the mean (SEM). The non-parametric Kruskal-Wallis test was applied to evaluate differences among all groups, whereas difference between two groups was evaluated by the Mann-Whitney U-test. A difference at $P < 0.05$ was considered statistically significant.

Results

The results and the assessment of significance are presented in Tables I and II, and Figures 1–5. In the sham-exposed groups (Groups I, II, and III), there was no significant difference between 10- and 20-min sham exposures, therefore, their data were combined and used for data analysis.

Data on free radical levels

Concentrations of MDA and total NO increased significantly in all RFR-exposed groups (Group IV: 10-min RFR-exposure/saline; Group V: 20-min RFR-exposure/saline; Group VI: 10-min RFR-exposure/NAC; Group VII: 20-min RFR-exposure/NAC; Group VIII: 10-min RFR-exposure/EGCG; Group IX: 20-min RFR-exposure/EGCG) compared to control (Group I: Sham/saline) ($P < 0.05$).

In addition, MDA levels of 20-min exposure group (Group V: 20-min RFR-exposure/saline) were significantly higher when compared with those of the 10-min exposure group (Group IV: 10-min RFR-exposure/saline) ($P < 0.05$). EGCG treatment attenuated the effect on MDA levels in the 10-min exposure group (Group VIII: 10-min RFR-exposure/EGCG compared to Group IV: 10-min RFR-exposure/saline, $P < 0.05$). Furthermore, NAC (Group VII: 20-min RFR-exposure/NAC) and EGCG (Group IX: 20-min RFR-exposure/EGCG) treatments significantly attenuated the effects of RFR on MDA in the 20-min exposure group (Group V: 20-min RFR-exposure/saline) ($P < 0.05$).

A significantly larger increase in total NO_x level was observed in the 20-min RFR-exposure group (Group V: 20-min RFR-exposure/saline) than in the 10-min exposure group (Group IV: 10-min RFR-exposure/saline). EGCG-treatment (Group IX:

Table I. Effect of 1800-MHz mobile phone-like radiation exposure and treatments with the antioxidants N-acetyl cysteine (NAC) and epigallocatechin-gallate (EGCG) on guinea pig hepatic levels of malondialdehyde (MDA), nitrite (NO_2), nitrate (NO_3), and total level of nitric oxide (NO_x).

Group	MDA (nmol/g)	NO_2 (μmol/g)	NO_3 (μmol/g)	NO_x (μmol/g)
I. Sham/saline	19.5 ± 1.9	59.3 ± 4.0	293.4 ± 9.8	352.7 ± 12.3
II. Sham/NAC	19.5 ± 0.6	71.1 ± 7.8	275.7 ± 13.9	346.9 ± 10.1
III. Sham/EGCG	15.5 ± 0.4^{a}	55.9 ± 3.8	284.8 ± 10.2	340.7 ± 9.4
IV. 10-min RFR-exposure/saline	51.8 ± 2.1^{a}	64.5 ± 4.9	354.7 ± 14.5^{a}	419.1 ± 16.4^{a}
V. 20-min RFR-exposure/saline	$59.4 \pm 2.5^{a\ b}$	87.0 ± 13.3	440.5 ± 8.6^{ab}	527.4 ± 13.4^{ab}
VI. 10-min RFR-exposure/NAC	45.7 ± 0.5^{a}	61.6 ± 5.4	366.0 ± 27.7^{a}	434.3 ± 30.0^{a}
VII. 20-min RFR-exposure/NAC	$45.8 \pm 3.6^{a\ c}$	79.8 ± 3.4^{a}	456.6 ± 10.5^{a}	536.4 ± 11.1^{a}
VIII. 10-min RFR-exposure/EGCG	$39.2 \pm 2.0^{a\ b}$	85.4 ± 11.3^{a}	374.8 ± 18.0^{a}	460.2 ± 20.0^{a}
IX. 20-min RFR-exposure/EGCG	50.6 ± 1.6^{ac}	68.0 ± 7.2	$354.9 \pm 9.0^{a\ c}$	422.8 ± 14.3^{ac}

Data are mean $\pm$ SEM ($n = 12$ in Group I, II and III; $n = 10$ for the other groups). $^{a}P < 0.05$, when each group was compared with controls (Group I). $^{b}P < 0.05$, when Group IV was compared with Group V, Group VI and Group VIII. $^{c}P < 0.05$, when Group V was compared with Group VII and Group IX.

Table II. Effect of 1800-MHz mobile phone-like radiation exposure and treatments with the antioxidants N-acetyl cysteine (NAC) and epigallocatechin-gallate (EGCG) on superoxide dismutase (SOD), glutathione peroxidase (GSH-Px) and myeloperoxidase (MPO) activities in guinea pig liver tissue.

Group	SOD (U/g protein)	GSH-Px (U/g protein)	MPO (U/g protein)
I. Sham/saline	38.7 ± 0.8	31.1 ± 0.6	29.4 ± 1.0
II. Sham/NAC	38.8 ± 1.6	34.5 ± 1.0^{a}	28.8 ± 1.5
III. Sham/EGCG	30.2 ± 1.8^{a}	29.6 ± 1.6	27.1 ± 0.4
IV. 10-min RFR-exposure/saline	26.4 ± 1.1^{a}	26.8 ± 1.3^{a}	24.9 ± 1.2^{a}
V. 20-min RFR-exposure/saline	29.7 ± 0.7^{a}	27.7 ± 0.7^{a}	24.8 ± 0.7^{a}
VI. 10-min RFR-exposure/NAC	25.6 ± 2.8^{a}	24.8 ± 1.4^{a}	23.6 ± 1.9^{a}
VII. 20-min RFR-exposure/NAC	$16.5 \pm 0.9^{a\ c}$	26.5 ± 0.6^{a}	23.1 ± 0.8^{a}
VIII. 10-min RFR-exposure/EGCG	22.2 ± 1.2^{a}	25.8 ± 1.3^{a}	25.1 ± 1.1^{a}
IX. 20-min RFR-exposure/EGCG	$20.3 \pm 1.1^{a\ c}$	26.7 ± 1.2^{a}	24.4 ± 1.3^{a}

Data presented are mean $\pm$ SEM ($n = 12$ in Group I, II and III; $n = 10$ for the other groups). $^{a}P < 0.05$, when each group was compared with controls (Group I). $^{b}P < 0.05$, when Group IV was compared with Group V, Group VI and Group VIII. $^{c}P < 0.05$, when Group V was compared with Group VII and Group IX.

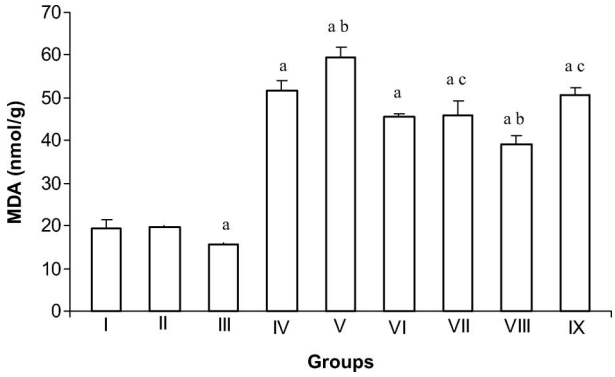

Figure 1. Effect of 1800-MHz mobile phone-like radiation exposure and treatments with the antioxidants N-acetyl cysteine (NAC) and epigallocatechin-gallate (EGCG) on guinea pig hepatic malondialdehyde (MDA) levels (nmol/g). Group I: Sham/saline; Group II: Sham/NAC; Group III: Sham/EGCG; Group IV: 10-min RFR-exposure/saline; Group V: 20-min RFR-exposure/saline; Group VI: 10-min RFR-exposure/NAC; Group VII: 20-min RFR-exposure/NAC; Group VIII: 10-min RFR-exposure/EGCG; Group IX: 20-min RFR-exposure/EGCG. Data presented are mean ± SEM ($n = 12$ in Group I, II and III; $n = 10$ for the other groups). $^{a}P < 0.05$, when each group was compared with controls (Group I). $^{b}P < 0.05$, when Group IV was compared with Group V, Group VI and Group VIII. $^{c}P < 0.05$, when Group V was compared with Group VII and Group IX.

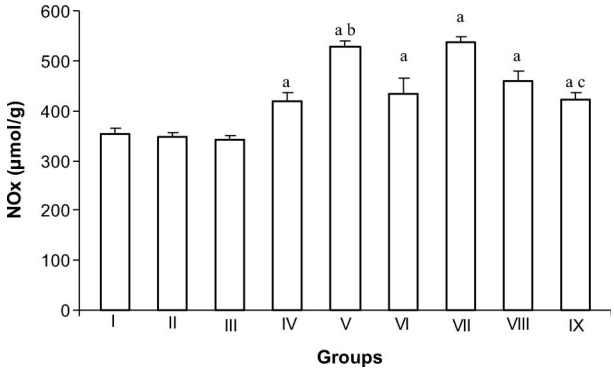

Figure 2. Effect of 1800-MHz mobile phone-like radiation exposure and treatments with the antioxidants N-acetyl cysteine (NAC) and epigallocatechin-gallate (EGCG) on guinea pig hepatic total level of nitric oxide (NO_x) (summation of nitrite (NO_2) and nitrate (NO_3)) levels (μmol/g). Group I: Sham/saline; Group II: Sham/NAC; Group III: Sham/EGCG; Group IV: 10-min RFR-exposure/saline; Group V: 20-min RFR-exposure/saline; Group VI: 10-min RFR-exposure/NAC; Group VII: 20-min RFR-exposure/NAC; Group VIII: 10-min RFR-exposure/EGCG; Group IX: 20-min RFR-exposure/EGCG. Data presented are mean ± SEM ($n = 12$ in Group I, II and III; $n = 10$ for the other groups). $^{a}P < 0.05$, when each group was compared with controls (Group I). $^{b}P < 0.05$, when Group IV was compared with Group V, Group VI and Group VIII. $^{c}P < 0.05$, when Group V was compared with Group VII and Group IX.

20-min RFR-exposure/EGCG) significantly attenuated the effect on NO_x level in the 20-min RFR-exposure group (Group V: 20-min RFR-exposure/saline) ($P < 0.05$).

MDA level of sham-EGCG administrated group (Group III: Sham/EGCG) decreased ($P < 0.05$) when compared to Sham/saline group (Group I: Sham/saline), while it was increased in all other groups.

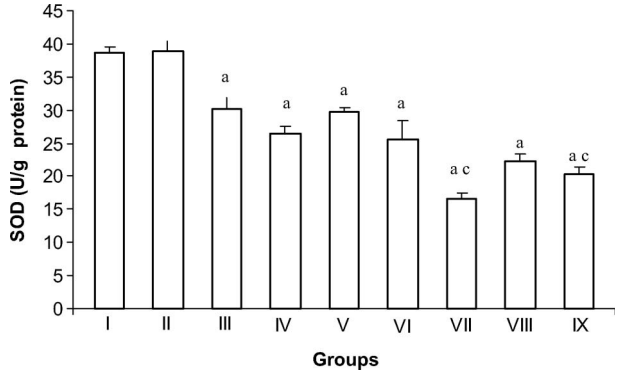

Figure 3. Effect of 1800-MHz mobile phone-like radiation exposure and treatments with the antioxidants N-acetyl cysteine (NAC) and epigallocatechin-gallate (EGCG) on superoxide dismutase (SOD) activities (U/g protein) in guinea pig liver tissue. Group I: Sham/saline; Group II: Sham/NAC; Group III: Sham/EGCG; Group IV: 10-min RFR-exposure/saline; Group V: 20-min RFR-exposure/saline; Group VI: 10-min RFR-exposure/NAC; Group VII: 20-min RFR-exposure/NAC; Group VIII: 10-min RFR-exposure/EGCG; Group IX: 20-min RFR-exposure/EGCG. Data presented are mean ± SEM ($n = 12$ in Group I, II and III; $n = 10$ for the other groups). $^{a}P < 0.05$, when each group was compared with controls (Group I). $^{c}P < 0.05$, when Group V was compared with Group VII and Group IX.

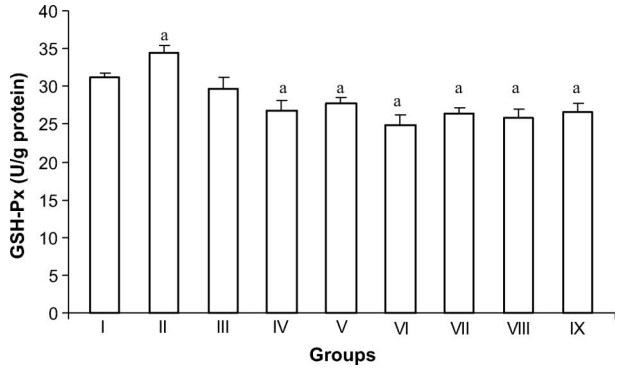

Figure 4. Effect of 1800-MHz mobile phone-like radiation exposure and treatments with the antioxidants N-acetyl cysteine (NAC) and epigallocatechin-gallate (EGCG) on glutathione peroxidase (GSH-Px) activities (U/g protein) in guinea pig liver tissue. Group I: Sham/saline; Group II: Sham/NAC; Group III: Sham/EGCG; Group IV: 10-min RFR-exposure/saline; Group V: 20-min RFR-exposure/saline; Group VI: 10-min RFR-exposure/NAC; Group VII: 20-min RFR-exposure/NAC; Group VIII: 10-min RFR-exposure/EGCG; Group IX: 20-min RFR-exposure/EGCG. Data presented are mean ± SEM ($n = 12$ in Group I, II and III; $n = 10$ for the other groups). $^{a}P < 0.05$, when each group was compared with controls (Group I).

Data on antioxidant enzyme levels

SOD, MPO and GSH-Px activities for all exposure groups were also decreased significantly when

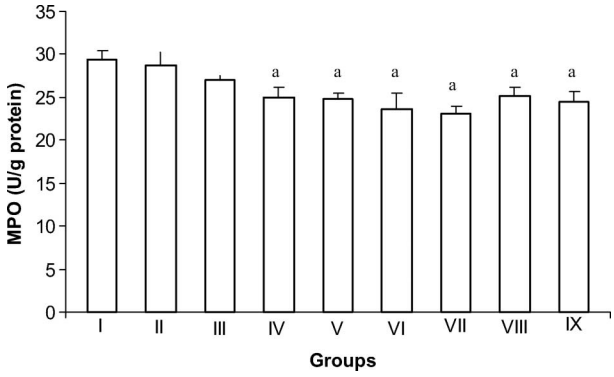

Figure 5. Effect of 1800-MHz mobile phone-like radiation exposure and treatments with the antioxidants N-acetyl cysteine (NAC) and epigallocatechin-gallate (EGCG) on myeloperoxidase (MPO) activities (U/g protein) in guinea pig liver tissue. Group I: Sham/saline; Group II: Sham/NAC; Group III: Sham/EGCG; Group IV: 10-min RFR-exposure/saline; Group V: 20-min RFR-exposure/saline; Group VI: 10-min RFR-exposure/NAC; Group VII: 20-min RFR-exposure/NAC; Group VIII: 10-min RFR-exposure/EGCG; Group IX: 20-min RFR-exposure/EGCG. Data presented are mean $\pm$ SEM ($n = 12$ in Group I, II and III; $n = 10$ for the other groups). $^{a}P < 0.05$, when each group was compared with controls (Group I).

compared to Group I: (Sham/saline) ($P < 0.05$). SOD activities in Group VII: (20-min RFR-exposure/NAC) and Group IX: (20-min RFR-exposure/EGCG) were significantly less with respect to Group V: (20-min exposure with saline injection). However, NAC and EGCG treatments did not significantly reversed the effect of RFR exposure on GSH-Px and MPO activities. GSH-Px activities were significantly increased only in Group II: (Sham/NAC) when compared to Group I: (Sham/saline).

Discussion and conclusion

Due to the widespread use of wireless devices with technological developments, people are exposed to RFR at different frequencies and strengths for long duration, which may lead to adverse health effects. An important tool for wireless telecommunication is the mobile phone which has become an important part of daily life. In addition to genetic (Lai and Singh 1996, Verschaeve 2009), immunologic (Gatta et al. 2003, Nasta et al. 2006), reproduction and developmental effects (Fejes et al. 2005, Agarwal et al. 2008, Desai et al. 2009, Güler et al. 2010, Tomruk et al. 2010), one of the intriguing subjects for research on adverse health effects of mobile phone radiation is oxidative damages to nucleic acids, lipids, and proteins, which is implicated in the genesis of diseases including cancer.

GSM, the most popular standard for mobile phones in the world, operates in a number of different frequency ranges. Although the third-generation GSM networks are starting to operate with simultaneous use of speech and data services at higher data rates, most countries are still using GSM networks operating in the 900-MHz and 1800-MHz bands. There are many studies on the effects of 900-MHz RFR on free radicals and antioxidant enzyme activities (Irmak et al. 2002, Ayata et al. 2004, Ilhan et al. 2004, Oktem et al. 2005, Ozguner et al. 2005a, 2005b, 2005c, 2006, Köylü et al. 2006, Oral et al. 2006, Balci et al. 2007, Guney et al. 2007, Meral et al. 2007, Sokolovic et al. 2008). However, the effects of 1800-MHz RFR on free radical and antioxidant enzyme levels have not been published yet.

This study was planned to investigate the influence of exposure to mobile phone like radiation in the 1800-MHz band for 10 min and 20 min a day for seven days on free radical and antioxidant enzyme levels in the liver tissue. MDA, marker of lipid peroxidation and NO and its derivatives were studied to analyse hepatic oxidative and nitrosative damages. SOD, GSH-Px and MPO, enzymatic antioxidants that play protective roles in healthy individuals by preventing oxidant-mediated damage, were also studied. In addition, the protective effects of the antioxidants NAC or EGCG were investigated.

The reason for investigating the effects of mobile phone radiation on hepatic free radical activity was that the liver, which has a number of functions in the body, including glycogen storage, decomposition of red blood cells and plasma protein synthesis, plays a vital role in metabolism. In addition to this metabolic role, detoxification processes take place in the liver, during which metabolic toxic substances are removed from the body.

RFR absorption in tissues is directly related to the dielectric properties and the conductivity of tissues. Besides the brain, tissues like those of the liver, lung and kidney, that contain large amounts of water, have greater conductivity than the ones that contain less water, such as the bone and adipose tissue. For instance, liver conductivity (0.98 S/m) is nearly twenty times higher than the conductivity of bone (0.05 S/m) in 1 GHz frequency (Foster and Schwan 1996). During whole-body exposure, tissues having higher conductivity absorb RFR more than the others. In vivo studies have reported that 900-MHz RFR affected free radical formation and antioxidant status in the brain (Ilhan et al. 2004, Köylü et al. 2006, Meral et al. 2007, Sokolovic et al. 2008), skin (Ayata et al. 2004), kidney (Oktem et al. 2005, Ozguner et al. 2005a, 2005b), endothelium (Oral et al. 2006, Guney et al. 2007), eye (Ozguner et al. 2006, Balci et al. 2007), heart (Ozguner et al. 2005c), and serum (Irmak et al. 2002). Thus, there is ample evidence that 900-MHz RFR can cause biological changes associated in tissues that have high electrical conductivity.

In this study, we have found that lipid peroxidation and nitrosative stress increased in the liver tissue of guinea pigs exposed to 1800-MHz mobile phone radiation with a decrease in the activity of the antioxidant enzymes SOD, GSH-Px and MPO. We also found that 20-min daily exposure is more effective than 10-min exposure.

There is still no consensus among the scientists about the validity of the hypotheses for the interaction mechanism of RFR with living tissues (Michaelson and Elson 1996). There are reviews on the biophysical mechanisms of RFR which may take place through either thermal or non-thermal mechanism (Schwan and Foster 1980, Adair 2003, Belyaev 2005, Challis 2005). Thermal mechanisms are those resulting from the temperature change of the tissue caused by the RFR. Non-thermal mechanisms are those that are not directly associated with this temperature change but rather to some other change produced in the tissue by RFR (Challis 2005). Adair (2003) examined important special cases of electromagnetic interactions: 'Direct' interactions where biology is modified simply by the motion of charged elements generated by the electric field; resonance interactions; the effects of electrostrictive forces and induced dipole moments; and modifications of radical pair recombination probabilities. He claims that it is unlikely that low intensity fields below the thermal levels generate significant physiological consequences. On the other hand, Belyaev suggests that the physical mechanisms of the non-thermal microwave effects must be based on quantum-mechanical approach and physics of non-equilibrium and non-linear systems. He also discusses that one of the interaction mechanisms of RFR with biological matter is the biochemical mechanism that is based on the responses caused by activating secondary chemical messengers such as ions, radicals or molecules (Belyaev 2005). Some other researchers have also hypothesised a possible role of free radicals in this process, and proposed mathematical models explaining how the weak electromagnetic fields could impair radical re-combination, thus increasing the generation of the free radicals (Grissom 1995, Timmel et al. 2001, Ferreira et al. 2006). Friedman et al. (2007) also recently reported a free radical related mechanism through which mobile phones affect the expression of proteins. Moreover, the radical pair mechanism explained by Woodward et al. (2001) was developed theoretically for radiofrequency magnetic field exposure.

In support of the free radical hypothesis, many researchers have reported that treatment with antioxidants could attenuate the effects of RFR. Antioxidants studied included vitamin C (Oral et al. 2006, Balci et al. 2007, Guney et al. 2007), vitamin E (Oral et al. 2006, Guney et al. 2007), caffeic acid phenethyl ester (Ozguner et al. 2005a, 2005b, 2005c, 2006), melatonin (Lai and Singh 1997, Ayata et al. 2004, Oktem et al. 2005, Ozguner et al. 2005a, 2006, Köylü et al. 2006) Ginkgo Biloba (Ilhan et al. 2004), and N-tert-butyl-α-phenylnitrone (Lai and Singh 1997).

Numerous studies have demonstrated that NAC and EGCG can also inhibit oxidative stress induced by different stimuli. Mansour et al. (2008) showed that pretreatment with NAC prevented the damage induced by ionising radiation and significantly decreased the levels of MDA, NO_x, and increased the levels of antioxidant enzymes and GSH level. Yildirim et al. (2005) reported that NAC significantly prevented increases in nitric oxide and malondialdehyde levels and increased the glutathione peroxidase activity produced by bleomycin toxicity in the lung tissue. Majano et al. (2004) documented that NAC treatment in human hepatocytes modulated NO synthase expression and Nuclear factor-kappaB activity, the key responses of hepatocytes to inflammatory mediators. Furthermore, Alvarez et al. (2002) reported that EGCG is capable of modulating free radical production during the respiratory burst of the rat peritoneal macrophages by acting as a superoxide anion scavenger. Chan et al. (1997) reported that EGCG reduces NO production by reduction of inductible nitric oxide synthase (iNOS) gene expression and inhibition of iNOS enzyme activity in cell culture. However, our present study is the first study in which NAC and EGCG are found to be antioxidants working against mobile phone-like radiation.

We determined in a previous study that both NAC and EGCG treatments were effective in suppressing the oxidative stress caused by Extremely Low Frequency (ELF) electric fields (Güler et al. 2008). The results of that study indicated a significant increase in the levels of oxidant products (MDA, NO_3, NO_2, NO_x), and a significant decrease in antioxidant enzyme (SOD, GSH-Px and MPO) activities. It was also found that the individual or combined application of NAC and EGCG resulted in the reduction of oxidative stress prior to ELF electric field application (Güler et al. 2008). Consistent results were found in the present study that demonstrated a significant decrease in hepatic SOD, GSH-Px and MPO activities in the groups that were only exposed to mobile phone radiation compared with the sham/saline group ($P < 0.05$). Both SOD and GSH-Px enzymes are mainly responsible for preventing cellular damage by oxidants and oxidative stress (Valko et al. 2007). Significant reduction in the activities of antioxidant enzymes (GSH-Px and SOD) in RFR-exposure groups as compared with the Sham/saline group was found in accordance with

the increased MDA and NO levels in these groups. We propose that the significant decrease in SOD and GSH-Px activities ($P < 0.05$) could be due to their utilisation by the enhanced production of ROS and oxidative inactivation of enzyme protein by ROS generation. It has been shown that moderate levels of ROS can induce an increase in antioxidant enzyme activities, whereas very high levels of these reactants were shown to decrease the activities of antioxidant enzymes (Warner et al. 2004). Furthermore, the decrease in GSH-Px activity in RFR exposure may be due to a depletion of its co-substrate, i.e., GSH and NADPH. Additionally, the depletion of the enzyme substrates and/or the downregulation of transcription and translation processes would lead to the changes in SOD and GSH-Px activities (Misra and Fridovich 1972, Meister 1994). We believe that the utilisation of SOD increases if the MDA level increases. This conjecture is supported by our observations that MDA level of 20-min RFR exposure/NAC group (Group VII) and 20-min RFR exposure/EGCG group (Group IX) were significantly lower than the level of 20 min RFR exposure group (Group V) ($P < 0.05$), and the SOD levels were lower in the antioxidant treated groups (Group VII and IX) than the 20-min RFR exposure group (Group V) ($P < 0.05$).

This study also demonstrated that treatment with EGCG or NAC markedly decreased lipid peroxidation and nitrite oxide levels and affected the antioxidant status in animals exposed to mobile phone radiation. Results also revealed that antioxidant administration have different impacts on different parameters. For instance, EGCG is more effective than NAC on the MDA level, but GSH-Px activity responded to NAC administration.

To conclude, the outcome of the present study indicates that exposure to a mobile phone-like radiation was associated with increases in free radical production and lipid peroxidation in guinea pig liver. In addition, it decreased activities of antioxidant enzymes in liver tissue with larger effect observed at longer duration of exposure. Furthermore, treatment with EGCG or NAC may provide protection against oxidative and nitrosative stress-induced liver injury caused by RFR. We aim to design a future study to research the oxidative effects of both RFR and ELF field on other tissues beside the liver.

Acknowledgements

This work was supported by the Gazi University Research funds. The authors wish to thank the Hacettepe University Faculty of Engineering for kindly providing their laboratory equipments for the experiment.

Declaration of interest: The authors report no conflicts of interest. The authors alone are responsible for the content and writing of the paper.

References

Adair RK. 2003. Biophysical limits on athermal effects of RF and microwave radiation. Bioelectromagnetics 24:39–48.

Agarwal A, Deepinder F, Sharma RK, Ranga G, Li J. 2008. Effect of cell phone usage on semen analysis in men attending infertility clinic: An observational study. Fertility and Sterility 89:124–128.

Alvarez E, Leiro J, Orallo F. 2002. Effect of (-)-epigallocatechin-3-gallate on respiratory burst of rat macrophages. International Immunopharmacology 2:849–855.

Ayata A, Mollaoglu H, Yilmaz HR, Akturk O, Ozguner F, Altuntas I. 2004. Oxidative stress-mediated skin damage in an experimental mobile phone model can be prevented by melatonin. The Journal of Dermatology 31:878–883.

Balci M, Devrim E, Durak I. 2007. Effects of mobile phones on oxidant/antioxidant balance in cornea and lens of rats. Current Eye Research 32:21–25.

Belyaev I. 2005. Non-thermal biological effects of microwaves. Microwave Review 11:13–29.

Cassini A, Pompelam A, Maellaro A, Comborti M. 1986. Lipid peroxidation and cellular damage in extrahepatic tissues of bromobenzene intoxicated mice. American Journal of Pathology 123:520–531.

Challis LJ. 2005. Mechanisms for interaction between RF fields and biological tissue. Bioelectromagnetics 7:98–106.

Chan MMY, Fong D, Ho CT, Huang HI. 1997. Inhibition of inducible nitric oxide synthase gene expression and enzyme activity by epigallocatechin gallate, a natural product from green tea. Biochemical Pharmacology 54:1281–1286.

Desai NR, Kesari KK, Agarwal A. 2009. Pathophysiology of cell phone radiation: Oxidative stress and carcinogenesis with focus on male reproductive system. Reproductive Biology and Endocrinology 22;7:114. Review.

Dröge W. 2002. Aging-related changes in the thiol/disulfide redox state: Implications for the use of thiol antioxidants. Experimental Gerontology 37:1333–1345.

Durak I, Yurtarslani Z, Canbolat O, Akyol O. 1993. A methodological approach to superoxide dismutase (SOD) activity assay based on inhibition of nitroblue tetrazolium (NBT) reduction. Clinica Chimica Acta 214:103–104.

Eberhardt MK. 2000. Reactive oxygen metabolites: Chemistry and medical consequences. 1st ed. New York: CRC Press: 117–149.

Fejes I, Zavaczki Z, Szollosi J, Koloszar S, Daru J, Kovacs L, Pal A. 2005. Is there a relationship between cell phone use and semen quality? Archives of Andrology 51:385–393.

Ferreira AR, Knakievicz T, Pasquali MA, Gelain DP, Dal-Pizzol F, Fernández CE, de Salles AA, Ferreira HB, Moreira JC. 2006. Ultra high frequency-electromagnetic field irradiation during pregnancy leads to an increase in erythrocytes micronuclei incidence in rat offspring. Life Science 80:43–50.

Foster KR, Schwan HP. 1996. Dielectric properties of tissues. In: Polk C, Postow E, editors. CRC handbook of biological effects of electromagnetic fields. Boca Raton, FL: Chemical Rubber Co. pp 25–102.

Friedman J, Kraus S, Hauptman Y, Schiff Y, Seger R. 2007. Mechanism of short-term ERK activation by electromagnetic fields at mobile phone frequencies. Biochemical Journal 405:559–568.

Gatta L, Pinto R, Ubaldi V, Pace L, Galloni P, Lovisolo GA, Marino C, Pioli C. 2003. Effects of in vivo exposure to GSM-modulated 900 MHz radiation on mouse peripheral lymphocytes. Radiation Research 160:600–605.

Green LC, Wagner DA, Glogowski J, Skipper PL, Wishnok JS, Tannenbaum SR. 1982. Analyses of nitrate, nitrite and [15N] nitrate in biological fluids. Analytical Biochemistry 126:131–138.

Grissom CB. 1995. Magnetic field effects in biology: A survey of possible mechanisms with emphasis on radical-pair recombination. Chemical Review 95:3–24.

Güler G, Tomruk A, Ozgur E, Seyhan N. 2010. The effect of radiofrequency radiation on DNA and lipid damage in non-pregnant and pregnant rabbits and their newborns. General Physiology Biophysics 29:59–66.

Güler G, Türközer Z, Tomruk A, Seyhan N. 2008. The protective effects of N-acetyl L-cysteine and epigallocatechin 3-gallate on electric field-induced hepatic oxidative stress. International Journal of Radiation Biology 84:669–680.

Güler G, Türközer Z, Ozgur E, Seyhan N. 2009. Antioxidants alleviate electric field-induced effects on lung tissue based on assays of heme oxygenase-1, protein carbonyl content, malondialdehyde, nitric oxide, and hydroxyproline. Science of the Total Environment 407:1326–1332.

Guney M, Ozguner F, Oral B, Karahan N, Mungan T. 2007. 900 MHz radiofrequency-induced histopathologic changes and oxidative stress in rat endometrium: Protection by vitamins E and C. Toxicology and Industrial Health 23:411–420.

Halliwell B, Gutteridge JMC. 1999. Free radicals in biology and medicine. 3rd ed, New York: Oxford University Press.

Hausladen A, Stamler JS. 1999. Nitrosative stress. Methods in Enzymology 300:389–395.

Hillegass LM, Griswold DE, Brickson B, Albrightson-Winslow C. 1990. Assessment of myeloperoxidase activity in whole rat kidney. Journal of Pharmacological Methods 24:285–295.

Ilhan A, Gurel A, Armutcu F, Kamilsi S, Iraz M, Akyol O, Ozen S. 2004. Ginkgo biloba prevents mobile phone-induced oxidative stress in rat brain. Clinica Chimica Acta 340:153–162.

Irmak MK, Fadıllıoğlu E, Gülec M, Erdogan H, Yagmurca M, Akyol O. 2002. Effects of electromagnetic radiation from a cellular telephone on the oxidant and antioxidant levels in rabbits. Cell Biochemistry and Function 20:279–283.

Köylü H, Mollaoglu H, Ozguner F, Nazyroglu M, Delibab N. 2006. Melatonin modulates 900 Mhz microwave-induced lipid peroxidation changes in rat brain. Toxicology and Industrial Health 22:211–216.

Lai H, Singh NP. 1996. Single- and double-strand DNA breaks in rat brain cells after acute exposure to radiofrequency electromagnetic radiation. International Journal Radiation Biology 69:513–521.

Lai H, Singh NP. 1997. Melatonin and a spin-trap compound block radiofrequency electromagnetic radiation-induced DNA strand breaks in rat brain cells. Bioelectromagnetics 18:446–454.

Lambert JD, Sang S, Yang CS. 2008. N-Acetylcysteine enhances the lung cancer inhibitory effect of epigallocatechin-3-gallate and forms a new adduct. Free Radical Biology and Medicine 44:1069–1074.

Lowry OH, Roseberg NJ, Farr AL, Randell RJ. 1951. Protein measurement with Folin phenol reagent. Journal of Biological Chemistry 193:265–275.

Majano PL, Medina J, Zubı I, Sunyer L, Lara-Pezzi E, Maldonado-Rodriguez A, Lopez-Cabrera M, Moreno-Otero R. 2004. N-Acetyl-cysteine modulates inducible nitric oxide synthase gene expression in human hepatocytes. Journal of Hepatology 40:632–637.

Mansour HH, Hafez HF, Fahmy NM, Hanafi N. 2008. Protective effect of N-acetylcysteine against radiation-induced DNA damage and hepatic toxicity in rats. Biochemical Pharmacology 75:773–780.

Mathews CK, Van Holde KE, Ahern KG. 1997. Biochemistry. 3rd ed. San Francisco: Addison-Wesley Publishing Company.

McKenna DJ, Jones K, Hughes K. 2002. Botanical medicines: The desk reference for major herbal supplements. 2nd ed. New York: The Haworth Herbal Press.

Meister A. 1994. Glutathione-ascorbic acid antioxidant system in animals. Journal of Biological Chemistry 269(13):9397–9400.

Meral I, Mert H, Mert N, Deger Y, Yoruk I, Yetkin A, Keskin S. 2007. Effects of 900-MHz electromagnetic field emitted from cellular phone on brain oxidative stress and some vitamin levels of guinea pigs. Brain Research 1169:120–124.

Michaelson SM, Elson EC. 1996. Dielectric properties of tissues. In: Polk C, Postow E, editors. CRC handbook of biological effects of electromagnetic fields. Boca Raton, FL: Chemical Rubber Co. pp 435–534.

Miranda KM, Espey MG, Wink DA. 2001. A rapid simple spectrophotometric method for simultaneous detection of nitrate and nitrite. Nitric Oxide 5:67–71.

Misra HP, Fridovich I. 1972. The role of superoxide anion in the autoxidation of epinephrine and a simple assay for superoxide dismutase. Journal of Biological Chemistry 247:3170–3175.

Nair V, Cooper CS, Vietti DE, Turner GA. 1986. The chemistry of lipid peroxidation metabolites: Crosslinking reactions of malondialdehyde. Lipids 21:6–9.

Nasta F, Prisco MG, Pinto R, Lovisolo GA, Marino C, Pioli C. 2006. Effects of GSM-modulated radiofrequency electromagnetic fields on B-cell peripheral differentiation and antibody production. Radiation Research 165:664–670.

Oktem F, Ozguner F, Mollaoglu H, Koyu A, Uz E. 2005. Oxidative damage in the kidney induced by 900-MHz-emitted mobile phone: Protection by melatonin. Archives of Medical Research 36:350–355.

Oral B, Guney M, Ozguner F, Karahan N, Mungan T, Comlekci S, Cesur G. 2006. Endometrial apoptosis induced by a 900-MHz mobile phone: Preventive effects of vitamins E and C. Advances in Therapy 23:957–973.

Ozguner F, Altinbas A, Ozaydin M, Dogan A, Vural H, Kisioglu AN, Cesur G, Yildirim NG. 2005c. Mobile phone-induced myocardial oxidative stress: Protection by a novel antioxidant agent caffeic acid phenethyl ester. Toxicology and Industrial Health 21:223–230.

Ozguner F, Bardak Y, Comlekci S. 2006. Protective effects of melatonin and caffeic acid phenethyl ester against retinal oxidative stress in long-term use of mobile phone: A comparative study. Molecular and Cellular Biochemistry 282:83–88.

Ozguner F, Oktem F, Armagan A, Yilmaz R, Koyu A, Demirel R, Vural H, Uz E. 2005a. Comparative analysis of the protective effects of melatonin and caffeic acid phenethyl ester (CAPE) on mobile phone-induced renal impairment in rat. Molecular and Cellular Biochemistry 276:31–37.

Ozguner F, Oktem F, Ayata A, Koyu A, Yilmaz HR. 2005b. A novel antioxidant agent caffeic acid phenethyl ester prevents long-term mobile phone exposure-induced renal impairment in rat. Molecular and Cellular Biochemistry 277:73–80.

Pacher P, Beckman JS, Liaudet L. 2007. Nitric oxide and peroxynitrite in health and disease. Physiological Reviews 87:315–424.

Paglia DE, Valentine WN. 1967. Studies on the quantitative and qualitative characterization of erythrocyte glutathione peroxidase. Journal of Laboratory and Clinical Medicine 70:158–170.

Schwan HP, Foster KR. 1980. RF-field interactions with biological systems: Electrical properties and biophysical mechanisms. Proceeding of the IEEE 68:104–113.

Sokolovic D, Djindjic B, Nikolic J, Bjelakovic G, Pavlovic D, Kocic G, Krstic D, Cvetkovic T, Pavlovic V. 2008. Melatonin reduces oxidative stress induced by chronic exposure of microwave radiation from mobile phones in rat brain. Journal of Radiation Research (Tokyo) 49:579–586.

Sun Y, Oberley LW, Li Y. 1988. A simple method for clinical assay of superoxide dismutase. Clinical Chemistry 34:497–500.

Taflove A, Hagness SC. 2005. Computational electrodynamics: The finite-difference time-domain method. 3rd ed. Norwood, MA: Artech House.

Timmel CR, Cintolesi F, Brocklehurst B, Hore PJ. 2001. Model calculations of magnetic fields effects on the recombination reactions of radicals with anisotropic hyperfine interactions. Chemical Physics Letters 334:387–395.

Tomruk A, Güler G, Dincel AS. 2010. The influence of 1800 MHz GSM-like signals on hepatic oxidative DNA and lipid damage in non-pregnant, pregnant, and newly born rabbits. Cell Biochemistry Biophysics 56:39–47.

Valko M, Leibfritz D, Moncol J, Cronin MT, Mazur M, Telser J. 2007. Free radicals and antioxidants in normal physiological functions and human disease. International Journal of Biochemistry and Cell Biology 39:44–84.

Verschaeve L. 2009. Genetic damage in subjects exposed to radio frequency radiation. Mutation Research 681:259–270.

Warner DS, Sheng H, Batinic-Haberle I. 2004. Oxidants, antioxidants and the ischemic brain. The Journal of Experimental Biology 207:3221–3231.

Woodward JR, Timmel CR, McLauchlan KA, Hore PJ. 2001. Radio frequency magnetic field effects on electron-hole recombination. Physical Review Letters 87:077602.

Yildirim Z, Kotuk M, Iraz M, Kuku I, Ulu R., Armutcu F, Ozen S. 2005. Attenuation of bleomycin-induced lung fibrosis by oral sulfhydryl containing antioxidants in rats: Erdosteine and N-acetylcysteine. Pulmonary Pharmacology Therapeutics 18:367–373.

ENHANCEMENT OF BLEOMYCIN–IRON FREE RADICAL DAMAGE TO DNA BY ANTIOXIDANTS AND THEIR INHIBITION OF LIPID PEROXIDATION

John M. C. GUTTERIDGE and FU Xiao-Chang*

Division of Antibiotics, National Institute for Biological Standards and Control, Holly Hill, London NW3 6RB, England and **Division of Antibiotics, Institute of Drug Control of Chengdu, Sichuan, China*

Received 17 November 1980

1. Introduction

The antitumour antibiotic bleomycin binds to and degrades DNA both in vivo and in vitro. This damaging activity has been shown to be dependent on the chelation of ferrous ions, which under aerobic conditions leads to the formation of the hydroxyl radical [1,2]. This damage can be measured by the release of malondialdehyde (MDA) which reacts with thiobarbituric acid (TBA) to give the chromogenic MDA–TBA adduct [3]. Iron-catalysed autoxidation of polyunsaturated fatty acids results in the formation of numerous lipid peroxides and long-chain aldehydes. When subjected to acid conditions and heating during the TBA test these decompose to give malondialdehyde and the same MDA–TBA adduct. Metal-ion catalysed peroxidation of phospholipid like that of bleomycin–iron damage to DNA has been shown to involve reduction intermediates of dioxygen [4]. Unlike bleomycin–iron-mediated damage to DNA, which takes only minutes, lipid peroxidation is a slower autocatalytic reaction characterised by a long induction period during which changes do not appear to take place.

Previous studies have shown that the antioxidant propyl gallate greatly enhances bleomycin–iron-dependent damage to DNA resulting in the increased formation of the MDA–TBA adduct [5]. This work has now been extended to examine the effect of a variety of water-soluble mono-, di- and trihydroxyphenols on the iron-catalysed free radical damage to lipids and DNA resulting in the formation of the MDA–TBA adduct. Phenols with reducing properties inhibited lipid peroxidation but greatly enhanced bleomycin–iron-dependent damage to DNA. One possible implication of this finding is that the clinical administration of phenolic compounds with reducing properties could potentiate the tumour damaging properties of the drug bleomycin while at the same time protecting normal lipid membranes from deleterious free radical damage.

2. Materials and methods

2.1. *Reagents*

Bathophenanthroline sulphonate, nitro blue tetrazolium (NBT) D,L-dihydroxyphenyl alanine (DOPA), L-adrenaline, catechol, phloroglucinol, L-tyrosine and DNA calf thymus type 1 were obtained from Sigma Chemical Co. Bleomycin sulphate complex was from Lundbeck Ltd. All other chemicals were of the highest grades available and obtained from BDH Ltd.

2.2. *Peroxidation of phospholipid*

The phospholipid and liposomes were prepared as in [6], the latter were used as a substrate for the lipid peroxidation studies. Phospholipid (5 mg/ml) was vortex-mixed with 0.15 M NaCl, buffered to pH 7.4 with sodium hydrogen carbonate, for 2 min and the preparation allowed to swell for 1 h at 4°C under nitrogen. Incubation mixtures consisted of 0.5 ml phospholipid liposomes, 0.1 ml phenolic compound, 0.3 ml phosphate saline buffer (pH 7.4) (0.024 M phosphate, 0.15 M NaCl) and 0.1 ml ferrous ions 0.5 mM freshly prepared. Samples were incubated for 2 h at 37°C followed by the addition of 1 ml 25% (v/v) HCl and 1 ml 1% TBA reagent then heated at 100°C for 15 min to develop the MDA–TBA chromogen which was read at 532 nm.

2.3. *Bleomycin–iron-mediated degradation of DNA*

DNA (0.5 ml) (1 mg/ml in 0.15 M NaCl, buffered

to pH 7.4 with sodium hydrogen carbonate) together with 0.1 ml 1 mg bleomycin/ml, 0.2 ml phosphate–saline buffer (pH 7.4) and 0.1 ml phenolic compound were mixed together and the reaction started by the addition of 0.1 ml 0.5 mM ferrous ions. The tubes were incubated at 37°C for 20 min followed by the addition of 1 ml 25% (v/v) HCl and 1 ml of 1% TBA reagent. The tubes were heated at 100°C for 15 min to develop the MDA–TBA chromogen which was read at 532 nm.

2.4. *Iron-reducing properties of phenols*

The method used for measuring the ferric ion reducing properties of the phenols was based on a vitamin E assay procedure [7]. Bathophenanthroline sulphonate (0.1 ml, 1 mg/ml), 0.1 ml ferric ions 0.5 mM and 0.1 ml phenolic compound were reacted together at room temperature for a few minutes in 0.6 ml phosphate–saline buffer (pH 7.4) before the addition of 0.1 ml 6% (v/v) orthophosphoric acid. Distilled water (2.0 ml) was added to each tube and the absorbance at 532 nm measured in a spectrophotometer.

2.5. *Reduction of NBT*

Phosphate–saline buffer (0.6 ml, pH 7.4), 0.1 ml EDTA 0.1 mM, 0.1 ml Triton X-100 16% (v/v) and 0.1 ml NBT 1 mM were mixed together before the addition of 0.1 ml test phenolic compound. The tubes were incubated at 37°C for 15 min followed by the addition of 2.0 ml phosphate–saline buffer (pH 7.4) and the absorbance read at 540 nm.

3. Results

Bovine brain phospholipids containing high levels of unsaturated fatty acids were used as a substrate in the form of multi-lamella liposomal membranes. Following iron-catalysed peroxidation, an MDA–TBA adduct was formed and measured as in [6]. Addition of a variety of mono-, di- and trihydroxyphenols either inhibited or had no effect on the iron-catalysed lipid peroxidation (table 1). Iron chelated by bleomycin enhanced lipid peroxidation by nearly 40% when the iron/bleomycin molar ratio approached 1. Similar enhancement of lipid peroxidation by chelated iron has been described for EDTA and diethylenetriaminepentaacetic acid (DETAPAC) and bathophenanthroline sulphonate [8]. Addition of phenols to bleomycin–iron-catalysed lipid peroxidation gave essentailly the same pattern of inhibition seen with iron alone, but with different degrees of inhibition (table 1).

Table 1
Inhibition of MDA formation during the iron-catalysed peroxidation of phospholipid by mono-, di- and trihydroxyphenols

Phenolic compound	Ferrous ions		Bleomycin–ferrous ions	
	A_{532}	% Inhibition	A_{532}	% Inhibition
Control	0.35		0.50	
Phenol	No change		No change	
Tyrosine	No change		No change	
Catechol	0.16	56%	0.13	74%
Adrenaline	0.27	25%	0.22	56%
Dihydroxyphenyl alanine (DOPA)	0.19	46%	0.35	30%
Resorcinol	No change		No change	
Quinol	0.22	38%	0.32	37%
Pyrogallol	0.22	38%	0.42	15%
Phloroglucinol	No change		No change	
Propyl gallate	0.17	54%	0.18	63%

Peroxidation of phospholipid catalysed by ferrous ions 0.05 mM and by 0.1 mg bleomycin/ml together with ferrous ions 0.05 mM. Inhibition by phenols 0.1 mM is expressed as a percentage of the control value, to which phenols were not added, based on the mean of 4 seperate assays

The TBA–MDA adduct formed from DNA after bleomycin–iron damage was measured by the same method used for the lipid MDA–TBA adduct. Those phenolic compounds which reacted as the most effective antioxidants against iron-catalysed lipid peroxidation were the most reactive pro-oxidants in the bleomycin–iron-catalysed damage to DNA (table 2). In the absence of added phenols but presence of bleomycin only ferrous ions were capable of mediating this DNA damage. Activity with ferric and enhancement with ferrous ions could be related to the reducing properties of the phenols (table 3). Measurement of the reduction of ferric ions as well as that of NBT indicated that the reducing properties of the phenols were essential to both its lipid antioxidant properties as well as to the enhancement of DNA damage by bleomycin–iron.

4. Discussion

Malondialdehyde can be formed by iron-catalysed damage to polyunsaturated fatty acids as well as to

Table 2
Enhancement of MDA formation during bleomycin-iron catalysed damage to DNA by mono-, di- and trihydroxyphenols

Phenolic compound	Bleomycin–ferrous ions A_{532}	% Enhancement	Bleomycin–ferric ions Increase in A_{532}
Control	0.42		0
Phenol	No change		No change
Tyrosine	No change		No change
Catechol	0.63	49%	0.063
Adrenaline	0.60	44%	0.355
Dihydroxyphenyl alanine (DOPA)	1.82	333%	0.480
Resorcinol	No change		No change
Quinol	1.78	326%	0.250
Pyrogallol	1.85	342%	1.600
Phloroglucinol	No change		No change
Propyl gallate	1.14	171%	0.393

Damage to DNA catalysed by 0.1 mg bleomycin/ml together with ferrous 0.05 mM or ferric ions 0.05 mM. Bleomycin–ferrous ion enhancement expressed as a percentage of the control value based on the mean of 4 separate assays. Bleomycin–ferric ion damage expressed as the change in absorbance at 532 nm

Table 3
Reducing properties of phenols

Phenolic compound	Reduction of ferric ions (measured as the BPS–ferrous complex) A_{532}	Reduction of NBT A_{540}
Phenol	No change	No change
Tyrosine	No change	No change
Catechol	0.190	0.022
Adrenaline	0.170	0.126
Dihydroxyphenyl alanine (DOPA)	0.180	0.148
Resorcinol	No change	No change
Quinol	0.200	0.115
Pyrogallol	0.215	0.640
Phloroglucinol	No change	No change
Propyl gallate	0.200	0.100

Reduction of 0.05 mM ferric ions and 0.1 mM NBT by 0.1 mM phenols

DNA. In both instances, evidence points to a dioxygen-dependent free radical mechanism. The peroxidation of unsaturated fatty acids has been studied in great detail during the last 40 years particularly with reference to the edible oils and fats of our foodstuff. Hydrogen abstraction by a free radical thereby leads to an autocatalytic sequence which eventually destroys the lipid molecule:

$$LH\,(\text{lipid}) + R^{\cdot}\,(\text{free radical}) \rightarrow L^{\cdot}\,(\text{lipid radical}) + RH$$

$$L^{\cdot} + O_2 \rightarrow LOO^{\cdot}\,(\text{lipid peroxy radical})$$

$$LOO^{\cdot} + LH \rightarrow LOOH\,(\text{lipid hydroperoxide}) + L^{\cdot}$$

Transition metal ions, particularly iron and copper, can initiate radical formation as well as catalyse the branching sequence by decomposing lipid peroxides to further free radical intermediates. Most of the scavenging lipid antioxidants, such as the phenols, are reducing substances which act by hydrogen donation. Early studies [9], still valid today, suggest that the reducing antioxidants (AH) react primarily with the lipid peroxy radicals ($LOO^{\cdot}$) terminating the radical sequence by forming stable complexes (2A) or new radicals ($A^{\cdot}$) which do not continue the chain reaction:

$$AH + LOO^{\cdot} \rightarrow LOOH + A$$

$$A^{\cdot} + A^{\cdot} \rightarrow 2A$$

Application of the TBA test to peroxidised lipid results in the formation of an MDA–TBA adduct; most of the MDA being derived by the acid or thermal decomposition of peroxides during the test tube reaction. When the same test is applied to DNA damaged by bleomycin–iron it is possible that the MDA forming the TBA adduct is 'free MDA' derived from the deoxyribose sugar moiety of DNA. This iron–dioxygen-dependent damage to DNA is thought to occur by an iron-catalysed Haber-Weiss reaction which results in the formation of a hydroxyl radical opposite the deoxyribose sugar [10,11]. Attempts to inhibit this reaction, on linear duplex DNA, with specific and non-specific radical scavengers have been unsuccessful [5], with only metal chelators preventing such damage. This can be partly explained by the catalytic nature of the bleomycin–iron damage to DNA [12]. Bleomycin has been shown to act as a 'ferroxidase' catalysing the rapid oxidation of ferrous ions to the ferric state [13]. This 'enzymic' free radical producing reaction has here been shown to be enhanced by reducing phenols which re-cycle iron to the ferrous state

via a radical intermediate or the superoxide radical.

The ability of bleomycin to enhance iron-catalysed damage to lipid membranes could account for some of the deleterious effects of bleomycin observed during treatment with the drug. Activity of bleomycin towards the cancer cell is probably dependent on its free radical-mediated damage to DNA. Any enhancement of this activity by phenolic compounds, which at the same time protect normal lipid membranes from unwanted free radical damage, may suggest a rational basis for exploring their use as adjuvants to bleomycin therapy during cancer treatment.

Acknowledgement

Dr Fu Xiao-Chang is a WHO Research Fellow.

References

[1] Sugiura, Y. and Kikuchi, T. (1978) J. Antibiot. 31, 1310–1312.
[2] Oberley, L. W. and Buettner, G. R. (1979) FEBS Lett. 97, 47–49.
[3] Gutteridge, J. M. C. (1979) FEBS Lett. 105, 278–282.
[4] Gutteridge, J. M. C. (1977) Biochem. Biophys. Res. Commun. 77, 379–386.
[5] Gutteridge, J. M. C. and Shute, D. J. (1981) submitted.
[6] Gutteridge, J. M. C. (1977) Anal. Biochem. 82, 76–82.
[7] Hashim, S. A. and Schuttringer, G. R. (1966) Am. J. Clin. Nutr. 19, 137–145.
[8] Gutteridge, J. M. C., Richmond, R. and Halliwell, B. (1979) Biochem. J. 184, 469–472.
[9] Bolland, J. L. and Ten Havre, P. (1947) Trans. Faraday Soc. 43, 201–210.
[10] Lown, J. W. (1979) in: Bleomycin. Chemical, biochemical and biological aspects (Hecht, M. ed) pp. 184–194, Springer-Verlag, Berlin, New York.
[11] Sausville, E. A., Peisach, J. and Horwitz, S. B. (1978) Biochemistry 17, 2740–2746.
[12] Povirk, L. F. (1979) Biochemistry 18, 3989–3995.
[13] Caspary, W. J., Niziak, C., Lanzo, D. A., Friedman, R. and Bachur, N. R. (1979) Mol. Pharmacol. 16, 256–260.

Electromagnetic Biology and Medicine, 28: 383–390, 2009

ISSN 1536-8378 print/1536-8386 online
DOI: 10.3109/15368370903287614

informa
healthcare

Qualitative Effect on mRNAs of Injury-Associated Proteins by Cell Phone Like Radiation in Rat Facial Nerves

JI-GENG YAN, MICHAEL AGRESTI, LIN-LING ZHANG, YUHUI YAN, AND HANI S. MATLOUB

Department of Plastic and Reconstructive Surgery, Medical College of Wisconsin, Milwaukee, Wisconsin, USA

Rats were exposed to cell phone radiation for 6 hours per day for 18 weeks. The buccal and mandibular branches of the facial nerve were evaluated for this study. The mRNA levels of four proteins that are usually up regulated when an injury has occurred were investigated; included were Calcium ATP-ase, Endothelin, Neural Cell Adhesion Molecule, and Neural Growth Factor. These isolated mRNAs were subjected to RT-PCR and all four were up regulated. The mandibular nerve showed a higher and broader level of up regulation than the buccal nerve. All four mRNA up regulations for the mandibular nerve and two for the buccal nerve were also statistically significant. These specific injury-related findings were mild. As the use of these cell phones continues, there most likely will be permanent damage to these tissues over the years and the likelihood of tumors, cancers, and system failures will potentially increase.

Keywords Injury; Cell phone; Rat facial nerves.

Introduction

Every year, the use of cell phones increases. Many people spend several hours using these phones every day. The debate regarding cell phone safety needs to be addressed further. The vast amount of data on cell phone effects has been gathered via whole body exposure of small lab animals. These data can be analyzed and major assumption can be made with regard to the total biology of the animal. The major drawback is that small lab animals do not react as humans do. However, since a small animal's life span is shorter, its metabolism is faster than a human's, and a shorter exposure time (several months) can mimic the effects of long-term human usage (several years).

Due to the close proximity of the head to the microwave emitting cell phone antenna, it has been investigated more thoroughly than any other part of the lab animal. Most investigations have focused on the brain with conflicting results. There is no acute change in c-Fos levels in the brains of rats after 1 h of exposure (Finnie, 2005). The rat pineal gland did not change its secretions of melatonin or serotonin

Address correspondence to Ji-Geng Yan, 8700 Watertown Plank Road, Milwaukee, WI, 53226, USA; E-mail: jyan@mcw.edu

when acutely exposed (Hata et al., 2005). Hamsters exposed 24 h/day for 60 days similarly showed no effects of RF-EMF on melatonin levels in vivo or in vitro (Lerchl et al., 2008). An exposure of 20 min per day for 1 month to the radiation emitted from 900 MHz cellular phones did not alter anti-apoptotic bcl-2 protein in the brain of rats (Yilmaz et al., 2008). When mice were acutely exposed to global system for mobile communication (GSM) 1800 MHz signals for 1 h at a whole body SAR of 1.1 W/kg, no consistent indication of gene expression modulation in whole mouse brain was found (Paparini et al., 2008). Some similar results have been published using cultured cells. The morphology of cultured astroglial cells and microglia was studied and appeared to be unaffected by microwave irradiation (Thorlin et al., 2006). A 900 MHz radio frequency exposure of 24–72 h does not induce significant alterations on proliferation, differentiation, and apoptosis processes in a neuroblastoma cell line (Merola et al., 2006).

Highlighting the division with regard to the actual effects brought on by cell phone exposure, our lab has shown that a chronic exposure of 6 h/day, everyday, for 18 weeks causes mRNA up regulation of injury-associated proteins in the rat brain (Yan et al., 2008). There are other labs that report significant damage done to the rat brain after just 2 h (Salford et al., 2003) as well as changes in brain function (Marino et al., 2003). Rats were exposed for 2 h each week for 55 weeks and showed no difference in open field exploratory behavior but had impaired memory for objects and their temporal order of presentation suggesting significantly reduced memory functions (Nittby et al., 2008). After a single 2 h exposure, no PFGE-detectable induced DNA double-stranded breaks or changes in chromatin conformation were found, but 11 cerebellar genes were up regulated and 1 gene was down regulated (Belyaev et al., 2006). In work measuring GFAP expression in rat glial cells several days after a single GSM exposure, a temporary effect, probably due to a hypertrophy of glial cells, with a temporal and a spatial modulation was seen (Brillaud et al., 2007). After a 24 h intermittent exposure, 24 up regulated genes and 10 down regulated genes were identified from a total of 1,200. These results indicated that the gene expression of rat cerebral cortical and hippocampal neurons could be altered by exposure to RF EMF (Zhao et al., 2007). Studies on the ear, which for the most part is in direct contact with the cell phone, have shown little effect on the inner ear of rats (Kizilay et al., 2003). Other long-term exposures also failed to link cell phones to severe problems (Shirai et al., 2005; Elder, 2003). An interesting finding is that there appeared to be no effect on rat testis after 1 month (Dasdag et al., 2003), but our lab has results to contradict this (Yan et al., 2007). Also contradicting the above data, several reports have shown severe effects on exposed lab animals. Increased NO levels in rat sinus and nasal mucosa (Yariktas et al., 2005), a decrease in rat serum TSH, T3, and T4 levels after 1 month (Koyu et al., 2005) and after 10 days many rat epidermal changes were reported (Ozguner et al., 2004). Several groups from Isparta, Turkey have also reported problems in rats. In the kidney, they have shown that a lipid peroxidation marker MDA as well as the renal tube damage marker NAG were up regulated and the oxidative mechanism induction molecules SOD, CAT, and GSH were down regulated (Oktem et al., 2005; Ilhan et al., 2004). Similar down regulations were reported in rat epidermis after exposure times of between 7–10 days (Ayata et al., 2004).

This all shows that there are still many different conclusions with regard to the actual effects of cell phone like radiation (CPLR) exposure. As seen from the published data, there seems to be less conclusive results when it comes to cancers,

tumors, and other system-wide diseases. However, when the aim was to show smaller problems like changes in NO levels, thyroid hormone levels, and kidney damage marker levels, the results showed there was an effect from the exposure. We feel this is the more correct approach to whether cell phones actually do cause detrimental effects to the user.

Our lab exposed rats to cell phones for 6 h per day every day for 18 weeks. These data will show that this exposure does indeed cause injuries to the mandibular and buccal branches of the facial nerve which are close to the microwave source. To our knowledge, there are no published reports focusing on peripheral nerve exposure to CPLR. We have looked at several proteins that are usually up regulated when an injury has occurred to a specific tissue. Those included in this study were Calcium ATP-ase, Endothelin, Neural Cell Adhesion Molecule (NCAM), and Neural Growth Factor (NGF). These specific injuries might not have caused any acute permanent damage; however, when these injuries continue to occur over years and years of exposure, there will be permanent damage to these tissues and the likelihood of tumors, cancers and system failures will increase.

Materials and Methods

For the care and use of laboratory animals, this study utilized the guidelines of the Biomedical Resource Center (BRC) of the Medical College of Wisconsin. The proposal was carefully designed and approved by BRC of the Medical College of Wisconsin. Twelve 3-month-old male Sprague-Dawley rats weighing 250–300 g were the subjects of this research. The rats were divided into two groups of six. One group acted as a sham control and the other group was exposed to cell phone radiation. The cell phones used in the study were Nokia 3588i (Keilalahdentie, Finland) and within the personal communications service code division multiple access (PCS CDMA) frequency band of 1.9 GHz, 800 MHz digital, and 800 MHz analog. The Nokia cell phone used in the study had three different modes: AMPS, CELL mode, and PCS mode. In AMPS mode, the specific absorbance rate (SAR) at 2.2 cm was 1.80 watts/kg and the power ranged from 0.0063–0.607 watts. The SAR at 2.2 cm in CELL mode was 0.9 watts/kg and the power ranged from 0.00001–0.487 watts. The range of power in PCS mode ranged from 0.00001–0.335 watts and the SAR at 2.2 cm was 1.18 watts/kg. The different modes on the cellular phone are used depending on antenna use, signal reception, and other factors associated with picking up different types of radio frequency signals. The frequencies and specific modes mentioned above fall within the cell phone radiation parameters set by the Federal Communications Commission in a June 30, 2005 report.

For this study, customized holding units and cell phone platforms were made (Yan et al., 2007, 2008). A $2'' \times 6''$ PVC tube fitted with a 20-oz clear plastic bottle top on one end and a common $3''$ bolt with nut at the other end were made to accommodate the rats. Air holes were placed throughout the tube in order for fresh air to circulate. As the rats grew larger during this study, new tubes were fashioned using cut 1-liter bottles, a $4''$ bolt with nut, PVC pipe formed to $3.5''$ in diameter, and air holes for circulation. Rats, by nature, enjoy small, restricted spaces and, in other studies by our lab, fall asleep in the aforementioned tubes while experiments were performed. During the exposure time, the rats were never anesthetized.

The experimental rat group was exposed to 3 h of cell phone radiation, then allowed to rest outside of the tubes for 30 min and re-exposed for 3 more hours per day. During the 30-min rest period, the rats were taken out of the tubes and free to

move, play, eat, and drink. The six rats in the sham control group were placed in identical tubes for the same amount of time as the experimental rats, but without the cell phones and, thus, no radiation. Three cell phones of the same type were used in this study. One cell phone was put between two rats in holding chambers. The phones were placed at equal distances between each rat and kept 1 cm from the head of the rat. Each phone was on with an active line for the entire exposure time. The cell phone exposures were done for 6 h a day, 7 days per week, for 18 weeks.

After week 18, the rats were sacrificed and the madibular and buccal branches of the facial nerve were harvested and frozen at −80°C. Total RNA was extracted using a SV Total RNA Isolation Kit (Promega, Wisconsin). The RNA was quantified by 260/280 ratio using a Beckman Spectrophotometer (Beckman, California). RT-PCR was performed using a SuperScript III One Step RT-PCR Kit (Invitrogen, California). Each reaction had 50 ng RNA with 0.5 ul of each specific forward and reverse primer (10 uM). The primers used were as follows: Beta Actin forward 3′-AGC-CATGTACGTAGCCATCC-5′ and reverse 3′-CTCTCAGCTGTGGTGGTGAA-5′, CATPase forward 3′-CTGTCCATGTCCCTCCACTT-5′ and reverse 3′-GGGTGG-TTATCCCTCCAGAT-5′, NGF-B forward 3′-CTGTGTGCAGGAGAGATGGA-5′ and reverse 3′-ATTGAGACCAGGGGACTGTG-5′, NCAM forward 3′-AAAGG ATGGGGAACCCATAG-5′ and reverse 3′-TAGGTGATTTTGGGCTTTGC-5′, Endothelin forward 3′-ACCACAGACCAAGGGAACAG-5′ and reverse 3′-GGTC-TTGATGCTGTTGCTGA-5′.

The reactions ran at 55° for 30 min, 94° for 2 min, then 94°C for 15 s, 55°C for 30 s and 72°C for 1 min for 40 cycles. The DNA was run on a 1% Agarose gel containing ethidium bromide in TAE buffer. A photo of the gel was taken on a Fotodyne 21 UV box (Fotodyne, Wisconsin) with an Electrophoresis Photo Documentation Camera and Hood (Fisher Scientific, Pennsylvania). The photo was then quantitated in a MultiImage Light Cabinet with AlphImager 2000 software (Alpha Innotech Corporation, California). All numbers generated by this software are in Relative Fluorescent Units (RFU).

Results

We tested the mRNA level of four proteins that are up regulated after cellular injury: Calcium ATPase, Neural Cell Adhesion Molecule (NCAM), Neural Growth Factor (NGF), and Endothelin. Beta actin mRNA levels were used as the internal controls since it is a house-keeping protein and its level of expression is not affected by cellular injury. The mean beta actin mRNA level of all the rats was 57802 RFU. This value was used with the actual beta actin mRNA level of each rat to calculate the normalization coefficient (data not shown). Normalization was necessary to standardize the variation in the amount of mRNA extracted and amplified in each rat, so meaningful comparison between the mRNA levels of each protein could be made (Yan et al., 2007, 2008). The means, standard deviations, and *T*-test *p* values (experimental vs. control) of the proteins are as follows.

- Mandibular branch: Calcium ATPase is 58933 ± 1366 vs. 48032 ± 4551 with $p < 0.005$; Endothelin is 46004 ± 8740 vs. 32867 ± 8332 with $p < 0.05$; NCAM is 51009 ± 3734 vs. 39147 ± 7106 with $p < 0.01$; and NGF is 56713 ± 3494 vs. 45652 ± 8872 with $p < 0.05$ (Table 1, Figure 1).
- Buccal branch: Calcium ATPase is 53019 ± 5686 vs. 40382 ± 6574 with $p < 0.01$; Endothelin is 33810 ± 11415 vs. 22719 ± 5816 with $p>0.05$; NCAM is 31468 ± 9345

Table 1
Normalized mandibular nerve RT-PCR data. The RT-PCR agarose gel band intensity measured in RFU of each of the four proteins was normalized by multiplying the original measured levels with the normalization coefficients as calculated by each specific Beta Actin RFU as controls of mRNA integrity (Yan, 2007, 2008). Included are the averages (Ave) and standard deviations (SD)

E-Rat#	CATP	ENDO	NCAM	NGF	C-Rat#	CATP	ENDO	NCAM	NGF
1	56784	34952	48156	51308	7	53769	28136	39447	53322
2	60240	34748	55845	61801	8	43714	25090	33575	56106
3	60173	52787	54328	57664	9	53046	32923	28891	32181
4	58868	50484	46989	54751	10	46782	25133	45999	39244
5	59607	53257	48109	57030	11	43004	43508	47462	47362
6	57928	49789	52631	57718	12	47878	42420	39511	45700
Ave	58933	46004	51010	56713	Ave	48032	32868	39148	45652
SD	1366	8740	3735	3494	SD	4551	8333	7107	8872

E-Rat = Experimental rats, C-Rat = Control rats, CATP = Calcium ATPase, ENDO = Endothelin, NCAM = Neural Cell Adhesion Molecule and NGF = Neural Growth Factor.

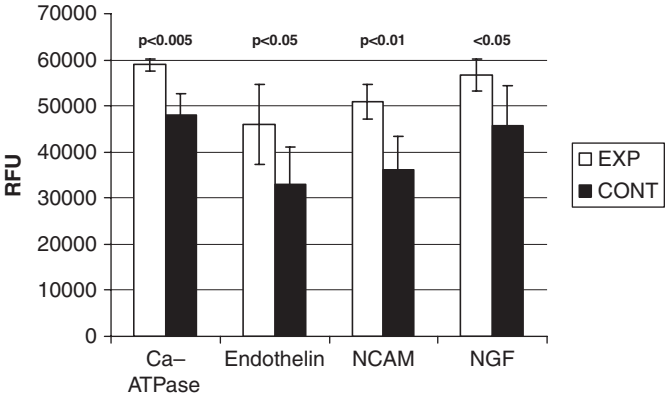

Figure 1. Mandibular branch. This Mandibular Nerve bar graph shows the RFU (y-axis) differences between the control and the experimental rats with regard to the levels of the four mRNAs tested. The standard deviations and *T* test p values are noted on the tops of the bars. These data are from Table 1.

vs. 24371 ± 8728 with p>0.05; NGF is 37511 ± 12016 vs. 23451 ± 7650 with $p < 0.05$ (Table 2, Figure 2).

Discussion

This article is part of our larger series of experiments exposing rats to long-term/high-dose CPLR. Due to the large number of animals, cytokines tested, and tissue samples involved in this study, Real-Time qPCR would have been cost prohibitive at the time we started this project, therefore, we used RT-PCR and agarose gel electrophoresis. We are well aware of the limitations of traditional RT-PCR when compared to qPCR

Table 2
Normalized buccal nerve RT-PCR data. The RT-PCR agarose gel band intensity measured in RFU of each of the four proteins was normalized by multiplying the original measured levels with the normalization coefficients as calculated by each specific Beta Actin RFU as controls of mRNA integrity (Yan, 2007, 2008). Included are the averages (Ave) and standard deviations (SD)

E-Rat#	CATP	ENDO	NCAM	NGF	C-Rat#	CATP	ENDO	NCAM	NGF
1	42241	19031	19513	18624	7	29465	17037	16759	21879
2	56161	26315	45417	29501	8	40966	27904	26545	12976
3	57834	38285	34305	50770	9	36881	16307	18396	21937
4	54365	41097	36664	47748	10	48585	19524	16864	24393
5	55942	50216	23818	41930	11	43975	25830	28980	22779
6	51574	27917	29093	36495	12	42420	29718	38687	36748
Ave	53019	33810	31468	37511	Ave	40382	22720	24372	23452
SD	5686	11416	9346	12017	SD	6575	5817	8728	4650

E-Rat = Experimental rats, C-Rat = Control rats, CATP = Calcium ATPase, ENDO = Endothelin, NCAM = Neural Cell Adhesion Molecule and NGF = Neural Growth Factor.

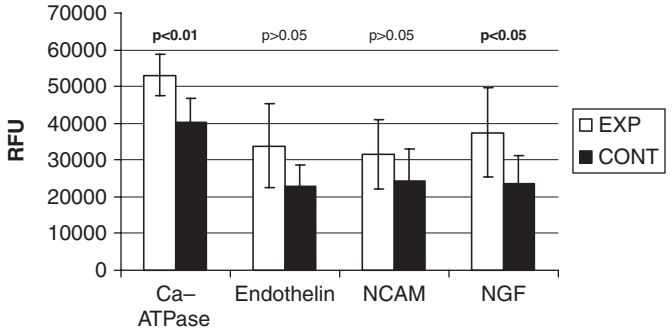

Figure 2. Buccal branch. This Buccal Nerve bar graph shows the RFU (y-axis) differences between the control and the experimental rats with regard to the levels of the four mRNAs tested. The standard deviations and *T* test p values are noted on the tops of the bars. These data are from Table 2.

and will not make any statements regarding the quantitative effects on mRNA up regulation from cell phone exposure.

The exposures of lab animals need to be of a sufficient length to generate measurable responses. It will take years for an accurate answer to be achieved in humans through medical examinations and tests. Some of the endpoints (cancer or tumors) need to be rethought because of the length of incubation time needed for these to be observed. When the endpoints are modified as in studying protein levels, changes in cellular permeability and regulation of mRNA's, there is still evidence on both sides but a greater amount of data show that there is an effect from even a relatively short exposure. We feel this is the correct approach.

There has been much work done on the various types of biological signaling factors that arise or disappear after an injury or trauma has occurred. We have looked at several proteins that are known to be up regulated after injury. Those included in this

study were, Calcium ATP-ase, Neural Cell Adhesion Molecule, Neural Growth Factor, and Endothelin. Ca-ATPase is an energy-dependant transport protein in the plasma membrane that removes calcium ions from all eukaryotic cells. The up regulation of Ca-ATPase indicates an increase in calcium ion accumulation inside the nerve tissue which will cause micro vascular spasms, nerve ischemia, and directly damages nerve fibers. It is these nerve cell membranes which have been compromised after cell phone exposure resulting in the influx of calcium. Widely distributed in the body, receptors for Endothelin are present in blood vessels, cells of the brain, and peripheral nerves. Endothelin is part of a group of proteins that constricts blood vessels and raises blood pressure. It also causes thromboses, vascular spasms, and is neuroactive, causing an increase in tissue metabolism. These effects seem to be mediated by the activity of calcium channels which might have been affected by the cell phone radiation which explains the up-regulation. The neuroactive and vascular properties might also be in response to the injuries sustained during the exposure. Neural cell adhesion molecule (NCAM) is a homophilic binding glycoprotein expressed on the surface of neurons, glia and skeletal muscle cells. Major roles of NCAM include cell to cell adhesion and neurite outgrowth via the fibroblast growth factor receptors. After injuries to nerve tissues, NCAM mRNA should be up regulated, aiding in healing and recovery. Neural Growth Factor (NGF) is a small secreted protein which induces the differentiation of particular target nerve cells. It is critical for the survival and maintenance of sympathetic and sensory neurons. NGF is released from the target cells, binds to and activates its high affinity receptor, and is internalized into the responsive neuron. This binding and activation is required for NGF-mediated neuronal survival and differentiation. These functions are required for the neurons to grow after injuries have occurred and recovery begins. All four of these proteins showed up regulation of their mRNAs in the exposed group compared to the control group in both nerve samples. Using *T*-test analysis, these differences were statistically significant for all four proteins in the mandibular branch and two for the buccal branch. The other two proteins for the buccal branch (Endothelin and NCAM) were up regulated but not enough to be statistically significant.

Due to this exposure, we believe that these up regulations have occurred in the cell phone exposed group because there have been injuries to the surrounding nerve tissue. These tissues are now going through the process of repair. Prolonged exposure to these phones over several years will keep causing these types of injuries and recovery will be incomplete. At some point these might overwhelm the body and secondary problems will arise. These problems, most likely, will be far worse and could include tumors, cancers, or system failures. This is only a hypothesis, but the facts and results from this study, as well as our other results, show the potential for serious consequences from the prolonged use of cell phones.

References

Ayata, A., Mollaoglu, H., Yalmaz, H. R., et al. (2004). Oxidative stress-mediated skin damage in an experimental mobile phone model can be prevented by melatonin. *J. Dermatol.* 31:878–883.

Belyaev, I. Y., Koch, C. B., Terenius, O., et al. (2006). Exposure of rat brain to 915 MHz GSM microwaves induces changes in gene expression but not double stranded DNA breaks or effects on chromatin conformation. *Bioelectromagnetics* 27:295–306.

Brillaud, E., Piotrowski, A., de Seze, R. (2007). Effect of an acute 900 MHz GSM exposure on glia in the rat brain: A time-dependent study. *Toxicology* 238:23–33.

Dasdag, S., Zulkuf Akdag, M., Aksen, F., et al. (2003). Whole body exposure of rats to microwaves emitted from a cell phone does not affect the testes. *Bioelectromagnetics* 24:182–188.

Elder, J. A. (2003). Survival and cancer in laboratory mammals exposed to radiofrequency energy. *Bioelectromagnetics Suppl*. 6:S101–106.

Finnie, J. W. (2005). Expression of the immediate early gene, c-fos, in mouse brain after acute global system for mobile communication microwave exposure. *Pathology* 37:231–233.

Hata, K., Yamaguchi, H., Tsurita, G., et al. (2005). Short term exposure to 1439 MHz pulsed TDMA field does not alter melatonin synthesis in rats. *Bioelectromagnetics* 26:49–53.

Ilhan, A., Gurel, A., Armutcu, F., et al. (2004). Ginkgo biloba prevents mobile phone-induced oxidative stress in rat brain. *Clin. Chim. Acta*. 340:153–162.

Kizilay, A., Ozturan, O., Erdem, T., et al. (2003). Effects of chronic exposure of electromagnetic fields from mobile phones on hearing in rats. *Auris Nasus Larynx* 30:239–245.

Koyu, A., Cesur, G., Ozguner, F., et al. (2005). Effects of 900 MHz electromagnetic field on TSH and thyroid hormones in rats. *Toxicol. Lett*. 157:257–262.

Lerchl, A., Krüger, H., Niehaus, M., et al. (2008). Effects of mobile phone electromagnetic fields at nonthermal SAR values on melatonin and body weight of Djungarian hamsters (Phodopus sungorus). *J. Pineal. Res*. 44:267–272.

Marino, A. A., Nilsen, E., Frilot, C. (2003). Nonlinear changes in brain electrical activity due to cell phone radiation. *Bioelectromagnetics* 24:339–346.

Merola, P., Marino, C., Lovisolo, G. A., et al. (2006). Proliferation and apoptosis in a neuroblastoma cell line exposed to 900 MHz modulated radiofrequency field. *Bioelectromagnetics* 27:164–171.

Nittby, H., Grafström, G., Tian, D. P., et al. (2008). Cognitive impairment in rats after long-term exposure to GSM-900 mobile phone radiation. *Bioelectromagnetics* 29:219–232.

Oktem, F., Ozguner, F., Mollaoglu, H., et al. (2005). Oxidative damage in the kidney induced by 900-MHz-emitted mobile phone: protection by melatonin. *Arch. Med. Res*. 36:350–355.

Ozguner, F., Aydin, G., Mollaoglu, H., et al. (2004). Prevention of mobile phone induced skin tissue changes by melatonin in rat: an experimental study. *Toxicol. Ind. Health* 20:133–139.

Paparini, A., Rossi, P., Gianfranceschi, G., et al. (2008). No evidence of major transcriptional changes in the brain of mice exposed to 1800 MHz GSM signal. *Bioelectromagnetics* 29:312–323.

Salford, L. G., Brun, A. E., Eberhardt, J. L., et al. (2003). Nerve cell damage in mammalian brain after exposure to microwaves from GSM mobile phones. *Environ. Health Perspect*. 111:881–883: discussion A408.

Shirai, T., Kawabe, M., Ichihara, T., et al. (2005). Chronic exposure to a 1.439 GHz electromagnetic field used for cellular phones does not promote N-ethylnitrosourea induced central nervous system tumors in F344 rats. *Bioelectromagnetics* 26:59–68.

Thorlin, T., Rouquette, J. M., Hamnerius, Y., et al. (2006). Exposure of cultured astroglial and microglial brain cells to 900 MHz microwave radiation. *Radiat. Res*. 166:409–421.

Yan, J. G., Agresti, M., Bruce, T., et al. (2007). Effects of cellular phone emissions on sperm motility in rats. *Fertil. Steril*. 88:957–964.

Yan, J. G., Agresti, M., Zhang, L. L., et al. (2008). Upregulation of specific mRNA levels in rat brain after cell phone exposure. *Electromagn. Biol. Med*. 27:147–154.

Yariktas, M., Doner, F., Ozguner, F., et al. (2005). Nitric oxide level in the nasal and sinus mucosa after exposure to electromagnetic field. *Otolaryngol. Head Neck Surg*. 132:713–716.

Yilmaz, F., Dasdag, S., Akdag, M. Z., et al. (2008). Whole-body exposure of radiation emitted from 900 MHz mobile phones does not seem to affect the levels of anti-apoptotic bcl-2 protein. *Electromagn. Biol. Med*. 27:65–72.

Zhao, R., Zhang, S., Xu, Z., et al. (2007). Studying gene expression profile of rat neuron exposed to 1800 MHz radiofrequency electromagnetic fields with cDNA microassay. *Toxicology* 235:167–175.

The Federal Communications Commission and the Food and Drug Administration. (2005, June 30). Cell Phone Facts: Consumer information on Wireless Phones. [Online] Available: http://www.fda.gov/cellphones/wireless.html

Electromagnetic Biology and Medicine, 27: 147–154, 2008

ISSN 1536-8378 print/1536-8386 online
DOI: 10.1080/15368370802072208

informa
healthcare

Upregulation of Specific mRNA Levels in Rat Brain After Cell Phone Exposure

JI-GENG YAN, MICHAEL AGRESTI, LIN-LING ZHANG, YUHUI YAN, AND HANI S. MATLOUB

Department of Plastic and Reconstructive Surgery, Medical College of Wisconsin, Milwaukee, Wisconsin, USA

Adult Sprague-Dawley rats were exposed to regular cell phones for 6 h per day for 126 days (18 weeks). RT-PCR was used to investigate the changes in levels of mRNA synthesis of several injury-associated proteins. Calcium ATPase, Neural Cell Adhesion Molecule, Neural Growth Factor, and Vascular Endothelial Growth Factor were evaluated. The results showed statistically significant mRNA up-regulation of these proteins in the brains of rats exposed to cell phone radiation. These results indicate that relative chronic exposure to cell phone microwave radiation may result in cumulative injuries that could eventually lead to clinically significant neurological damage.

Keywords Cell phones; mRNA; Rat brain.

Introduction

Cell phones are major emitters of microwave radiation. Effects of this radiation on humans have been studied but the results are contradictory. Finnie et al. (2002) and Kuribayashi et al. (2005) found no change in the permeability of the blood-brain barrier (BBB) using a rat model. In contrast, Salford et al. (2003) found, after a 2 h exposure, significant leakage across the rat BBB. Finnie (2005) reported there was no change in the proto-oncogene c-fos protein level in the mouse brain after a short-term exposure. Hata et al. (2005), studying the secretion of melatonin and serotonin from the rat pineal gland, found no changes either. One long-term study exposed rats for 90 min per day, 5 days per week for 104 weeks; this chronic exposure did not induce tumor growth in the rat central nervous system (Shirai et al., 2005). This study, although long term, did not evaluate early or subtle effects of exposure including changes in gene expression. Very little data has been published on this topic. The change in mRNA levels of apoptotic, heat shock, and general cellular proteins after exposure has been evaluated. Human HeLa-60 and Mono-Mac-6 cells exposed to intermittent non-thermalizing levels of 1.9 GHz

Address correspondence to Ji-Geng Yan, Department of Plastic and Reconstructive Surgery, Medical College of Wisconsin, 8700 Watertown Plank Road, Milwaukee, WI 53226, USA; E-mail: jyan@mcw.edu

pulse-modulated RF fields did not cause any detectable change in stress-related gene expression (Chauhan et al., 2006). No statistically significant effects on murine fibroblasts gene expression after 24 h exposure at 5 W/kg were found either (Whitehead et al., 2006). Up-regulation of the heat shock protein Hsp70 in human lens epithelial cells was found after RF exposure but this might be involved in protecting these cells from DNA damage and maintaining the cellular capacity for proliferation (Lixia et al., 2006). A short-term exposure of 2 h showed up-regulation of apoptotic proteins caspase-2, caspase-6 in murine neurons and astrocytes (Zhao et al., 2007). There has not been enough data generated on changing mRNA levels after long-term cell phone exposure using a whole animal model. Using these criteria, subtle neural or vascular injuries over prolonged exposure times could be found by measuring the mRNA level changes of injury associated proteins that are necessary for cellular repair and known to respond to cellular injury. These proteins include: Calcium ATP-ase ($Ca2^{+}$-ATPase) (Chen et al., 2002; Kurnellas et al., 2005), Neural Cell Adhesion Molecule 1 (NCAM-1) (Skaper, 2005; Skibo et al., 2005; Thornton et al., 2005), Neural Growth Factor B (NGF-B) (Blesch et al., 2005; Moore et al., 2006), and Vascular Endothelial Growth Factor A (VEGF-A) (Greenberg and Jin, 2005; Zachary, 2005). We hypothesize that cellular damage to the rat brain; leading to increased mRNA transcription of these injury-associated proteins will be caused by chronic exposure to cell phone radiation leading to gradual degenerative and functional loss.

Materials and Methods

Fourteen 3-month-old male Sprague-Dawley rats, weighing 250–300 g, were the subjects of this research. (Note: For the care and use of laboratory animals, this study used the guidelines of the Biomedical Resource Center of the Medical College of Wisconsin. The Institutional Animal Care and Use Committee of the Medical College of Wisconsin approved the protocol.) The rats were divided into two groups of eight rats each. One group received cell phone radiation exposure, and the other group acted as a control group.

The four cell phones used in the study were Nokia 3588i (Keilalahdentie, Finland), which have a personal communications service code division multiple access (PCS CDMA) frequency band of 1.9 GHz (800 MHz digital and 800 MHz analog). These cell phones have three different modes: AMPS mode, CELL mode, and PCS mode. The various modes can be used based on signal reception, antenna use, and other factors associated with reception of different types of radiofrequency signals. In AMPS mode, the specific absorbance rate (SAR) at a distance of 2.2 cm was measured to be 1.80 W/kg, and the power range was 0.0063–0.607 W. The SAR at a distance of 2.2 cm in CELL mode was 0.9 W/kg, and the power range was 0.00001–0.487 W. The SAR at 2.2 cm away in PCS mode was 1.18 W/kg, and the power range was 0.00001–0.335 W. The frequencies and specific modes of this phone fall within the cell phone radiation parameters set by the U.S. Federal Communications Commission (FCC) (19). Each cell phone was positioned 1 cm from the head of the rats, at equal distances between two rats in holding chambers.

Customized holding units (Fig. 1) and cell phone platforms were constructed for this study. The holding units for the rats consisted of 5.1 cm × 15.2 cm PVC tubes with holes for circulation, fitted with 0.59-liter clear plastic bottle tops on one end and common 7.6-cm bolts with nuts at the other end. As the rats grew larger during this study, new tubes were fashioned using 8.9 cm-diameter PVC pipes with holes for air circulation, 1-liter bottles, and 10.2 cm bolts with nuts. The holding units were plastic, because metal can absorb radiation energy.

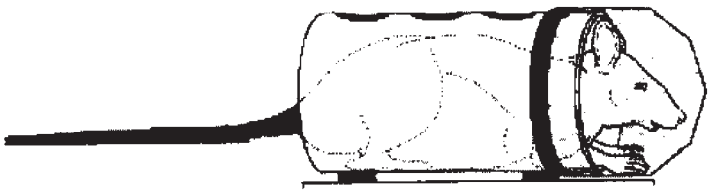

Figure 1. Rat in plastic PVC holding tube. The tube has a clear plastic bottle top and numerous air holes for adequate ventilation.

The rats were acclimated to these holding units for 1 week before the beginning of testing by placing the units in the rat cages to allow the rats to become familiar with their smell and feel. After less than one day, the rats voluntarily entered the units to rest and sleep in them. By the end of the week, the rats would enter the holding units as soon as they saw them. Owing to this acclimation process, anesthesia was not required during the exposure time. Therefore, the rats did not have any ill effects or altered physiology from anesthesia, rendering the comparison to humans more relevant.

The experimental rat group was exposed to 3 h of cell phone radiation, followed by a 30 min rest period outside of the tubes and a second exposure for 3 more hours per day. During the 30 min rest period, the rats were removed from the tubes and were free to walk around, eat, and drink. The rats received this daily cell phone exposure for 18 weeks. The 8 rats in the control group were placed in identical tubes for the same amount of time as the experimental rats but without cell phone exposure.

To address the concern that the harmful effects of cell phones are due to heat given off by the phone rather than the radiation emitted, we took temperatures from both groups during a standard day of exposure. Temperatures of the rats were taken at the side of the face surface nearest the phone, using a Mini-Alarm thermometer with a probe (Fisher Scientific, Hampton, NH). These readings were taken approximately every 12 min during both of the 3-h exposures. Final rectal temperatures were taken at the end of each of the two exposure times with a Big-Digit thermometer (Fisher Scientific). Because the rectal measurements irritated the animals, repeated measurements were not practical.

After week 18, the rats were sacrificed. Brain tissue was harvested and flash frozen in liquid nitrogen and stored at -80°C. Total RNA was extracted using a SV Total RNA Isolation Kit (Promega, USA). The RNA was quantified by 260/280 ratio using a Beckman Spectrophotometer (Beckman, USA). RT-PCR was performed using a SuperScript III One Step RT-PCR Kit (Invitrogen, USA). Each reaction had 50 ng RNA with 0.5 µl of each specific forward and reverse primer (10 µM). The primers (PE Applied Biosystems, USA) used were as follows:

Beta Actin (BA) forward 3′-AGCCATGTACGTAGCCATCC-5′, reverse 3′-CTCTCAGCTGTGGTGGTGAA-5′, $Ca2^{+}$ATPase forward 3′-CTGTCCA TGTCCCTCCACTT-5′, reverse 3′-GGGTGGTTATCCCTCCAGAT-5′, NGF-B forward 3′ CTGTGTGCAGGAGAGATGGA-5′, reverse 3′-ATTGAGACCAGGGGACTGTG-5′, NCAM-1 forward 3′-AAAGGATGG GGAACCCATAG-5′, reverse 3′-TAGGTGATTTTGGGCTTTGC-5′ and VEGF-A forward 3′-CAATGATGAAGCCCTGGAGT-5′ and reverse 3′-TTTCTTGCGCTTTCGTTTTT-5′.

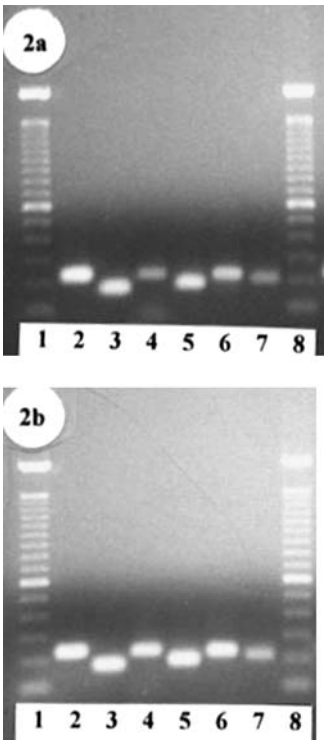

Figure 2. (a, b) Examples of fluorescent pictures of the agarose gels used in the quantitation of the RT-PCR band intensity. (a) Control and (b) Experimental. Lanes are as follows: 1-MWM (100Bp), 2-BA, 3-CaATPase, 5-NCAM-1, 6-NGF-B, 7-VEGF-A, and 8-MWM (100Bp).

The reactions ran at 55°C for 30 min, 94°C for 2 min and 15 sec, 55°C for 30 sec, and 72°C for 1 min for 40 cycles. The DNA was run on a 1% Agarose gel containing ethidium bromide in TAE buffer. A photo of the gel was taken on a Fotodyne 21 UV box (Fotodyne, USA) with an Electrophoresis Photo Documentation Camera and Hood (Fisher Scientific, USA) (Fig. 2). The photo was then quantitated in a MultiImage Light Cabinet with AlphaImager 2000 software (Alpha Innotech Corporation, USA).

Results

The intensity of the bands of interest was read by the AlphaImager 2000 software and was assigned a unitless number. The greater the amount of specific cDNA amplified the more intense the agarose gel band was and a higher number was generated by the software. These numbers will now be identified in relative intensity units (RIU).

The mRNA levels of the four injury-associated proteins ($Ca2^+$ ATPase, NCAM-1, NGF-B, and VEG-F) were examined. The Beta Actin mRNA level was used as the internal control since it is a housekeeping protein and its level of expression does not change. The mean Beta Actin intensity of the 14 rats in this study was 60916 (data not shown). This value was used along with the individual Beta Actin intensities to obtain a normalization coefficient for each value (data not shown). The final values in Table 1 were obtained by multiplying the specific protein RIU with the corresponding normalization coefficient. Normalization of the data is a routine and accepted practice necessary to standardize the experimental variations inherent in any type of PCR.

Table 1
Normalized RT-PCR Data. The RT-PCR agarose gel band intensity measured in RIU of each protein was normalized by multiplying the measured levels with the normalization coefficients calculated using each specific Beta Actin RIU as controls of RNA integrity. Included are the averages (AVE) and standard deviations (SD). These data are in Fig. 3

Rat	Ca-ATPase	NCAM	NGF	VEGF
Experimental				
1	56706	64634	66846	55515
2	57430	55601	32073	53240
3	62401	59774	36596	41464
4	58590	59039	55911	46599
5	60948	55179	54698	49964
6	56973	57389	59043	53192
7	60462	58463	44401	47375
Ave	59073	58583	49938	49621
SD	2216	3167	12616	4855
Control				
8	56074	59378	32245	40788
9	55485	45441	36068	35378
10	44934	44519	43644	41152
11	54502	54560	53210	51302
12	44383	38860	16697	23838
13	51001	51291	48746	51811
14	51497	50128	36621	41979
Ave	51125	49168	38176	40893
SD	4810	6838	12049	9575

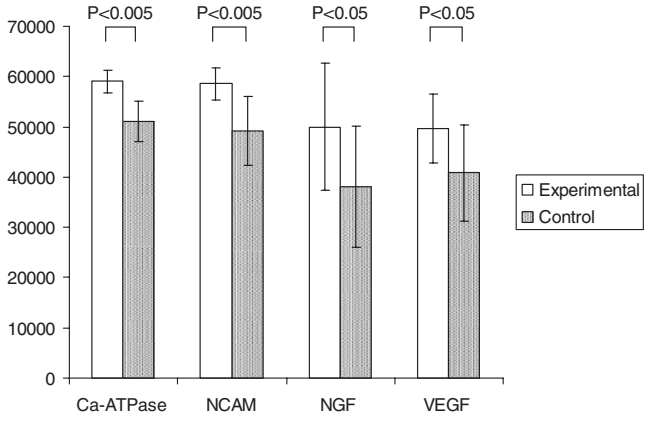

Figure 3. This bar graph shows the RIU (y axis) differences between the control and experimental rats with regard to the levels of the four mRNAs tested. The standard deviations are noted on the tops of the bars as well as the *T* test *p* values. These data are from Table 1.

Meaningful and accurate comparisons between mRNA levels of each protein could now be made.

As seen in Table 1, the normalized RIU of the four specific proteins were as follows.

- The control group mean values were: 51125 ± 4801 for $Ca2^+$ATPase; 49168 ± 6838 for NCAM-1; 38176 ± 12049 for NGF-B; and 40893 ± 9575 for VEGF-A.
- The experimental group mean values were: 59073 ± 2216 for $Ca2^+$ATPase; 58583 ± 3167 for NCAM-1; 49938 ± 12616 for NGF-B; and 49621 ± 4855 for VEGF-A.

The RIU difference of each protein between two groups was all statistically significant. (Using a standard independent *T*-test. See Table 1: $P < 0.005$ for $Ca2^+$-ATPase; $P < 0.005$ for NCAM-1; $P < 0.05$ for NGF-B; and $P < 0.05$ for VEGF-A).

Data were gathered to show whether the heat given off by phone exposure might increase facial surface or internal temperatures of the rats. In our previous study (Yan et al., 2007), the mean surface temperature of the head after 3 h of radiation exposure was $33.3 \pm 0.5^\circ$C for the experimental group and $33.5^\circ\text{C} \pm 1.1^\circ$C for the control group. Similarly, after the full 6 h of exposure, the mean surface temperature was $33 \pm 0.6^\circ$C for the experimental group and $32 \pm 0.8^\circ$C for the control group. The mean rectal temperature after 3 h of exposure was $35.6 \pm 0.3^\circ$C in the experimental group and $36.4 \pm 0.5^\circ$C in the control group. The mean rectal temperature after 6 h of exposure was $35.9 \pm 0.6^\circ$C in the experimental group and $35.9 \pm 0.5^\circ$C in the control group. The differences in temperatures measured by a standard independent *T*-test were not statistically significant ($p > 0.5$).

Discussion

Long-term, high-dose, whole-body exposures are needed to accurately assess the effects of cell phone microwave radiation. Short to moderate exposure times using animal models, cell cultures, or questionnaires filled out by human subjects have been the methodologies of choice. These methods have not yielded satisfactory results to settle the controversy involving cell phones. To generate accurate data, whole-body exposure time of a sufficient length is needed to correspond to that of the average person's use of a cell phone. An intensive long term exposure with a total time of 756 h was therefore performed. Given the expected lifespan of rats are 1–2 years (8,760–17,520 h), this total exposure time translates into 4–9% of their lifespan. This is comparable to human subjects who use cell phones for between 0.96–2.16 h per day for over 30 years. Irreparable cellular injury can occur and subsequently lead to tissue and system damage without reaching the stage of causing cancerous growth. Various proteins that are up or down regulated after injuries have been investigated. For this reason, four injury-associated proteins, which serve as indicators of acute cellular injuries, were chosen. $Ca2^+$-ATPase is the major enzyme responsible for the concentration gradient in healthy nerves. If an injury occurs, calcium influx causes edema and cell death. This protein is needed in increased amounts to restore the gradient prior to nerve healing. NCAM-1 contributes to nerve regeneration by increasing the ability of Schwann cells to adhere to the axon. An increase in syaptogenesis, fasciculation, and general nerve growth are also functions of this protein.

NGF-B stimulates nerve sprouting and neurite growth. The increased production of this protein under conditions of tissue injury or inflammation also aids in angiogenesis using a VEGF mediated pathway. VEGF-A in concert with NGF-B aids in nerve regeneration and wound healing. Injuries stimulate the neurotropic and neuroprotective properties of this protein. These proteins showed mRNA up-regulation in the exposed group compared to the controls. These increases were all statistically significant. These up-regulations, we believe, were stimulated by cellular damage caused by cell phone radiation. Although these proteins aid in cellular repair after acute injury, if some injuries are only partially repaired, repetitive insults over a long period of time may result in cumulative cellular injuries, leading to cellular dysfunction. Even though the inherent plasticity of the brain may compensate partially or completely for the cellular dysfunction, the plasticity and the self-repair ability of the brain decrease over time. At some point, when the compensatory mechanisms of the brain are overwhelmed, the effects of cellular dysfunction will then manifest as clinically significant functional disabilities. The exact mechanism of cell phone exposure induced injury is still unknown; perhaps the electromagnetic effect does play an important role. It would seem prudent for people to keep their cell phone exposure to a minimum in case there are small but irreversible injuries taking place.

References

Blesch, A., Conner, J., et al. (2005). Regulated lentiviral NGF gene transfer controls rescue of medial septal cholinergic neurons. *Mol. Ther*. 11:916–925.

Chauhan, V., Mariampillai, A., et al. (2006). Analysis of proto-oncogene and heat-shock protein gene expression in human derived cell-lines exposed in vitro to an intermittent 1.9 GHz pulse-modulated radiofrequency field. *Int. J. Radiat. Biol*. 82(5):347–354.

Chen, L., Yang, Y., et al. (2002). Changes of neuronal calcium channel following brain damage induced by injection of pertussis bacilli in rats. *Chin. J. Traumatol*. 5:224–227.

The Federal Communications Commission and the Food and Drug Administration. (2005). *Cell Phone Facts: Consumer information on Wireless Phones*. [Online] Available: http://www.fda.gov/cellphones/wireless.html

Finnie, J. W. (2005). Expression of the immediate early gene, c-fos, in mouse brain after acute global system for mobile communication microwave exposure. *Pathology* 37:231–233.

Finnie, J. W., Blumbergs, P. C., et al. (2002). Effect of long-term mobile communication microwave exposure on vascular permeability in mouse brain. *Pathology* 34:344–347.

Greenberg, D. A., Jin, K. (2005). From angiogenesis to neuropathology. *Nature* 438:954–959.

Hata, K., Yamaguchi, H., et al. (2005). Short term exposure to 1439 MHz pulsed TDMA field does not alter melatonin synthesis in rats. *Bioelectromagnetics* 26:49–53.

Kuribayashi, M., Wang, J., et al. (2005). Lack of effects of 1439 MHz electromagnetic near field exposure on the blood-brain barrier in immature and young rats. *Bioelectromagnetics* 26:578–588.

Kurnellas, M. P., Nicot, A., et al. (2005). Plasma membrane calcium ATPase deficiency causes neuronal pathology in the spinal cord: a potential mechanism for neurodegeneration in multiple sclerosis and spinal cord injury. *FASEB J*. 19:298–300.

Lixia, S., Yao, K., et al. (2006). Effects of 1.8 GHz radiofrequency field on DNA damage and expression of heat shock protein 70 in human lens epithelial cells. *Mutat. Res*. 602(1–2):135–142.

Moore, K., Macsween, M., Shoichet, M. (2006). Immobilized concentration gradients of neurotrophic factors guide neurite outgrowth of primary neurons in macroporous scaffolds. *Tissue Eng*. 12:267–278.

Munshi, A., Jalali, R. (2002). Cellular phones and their hazards: the current evidence. *Nat. Med. J. India* 15:275–277.

Salford, L. G., Brun, A. E., et al. (2003). Nerve cell damage in mammalian brain after exposure to microwaves from GSM mobile phones. *Environ. Health Perspect.* 111:881–883.

Shirai, T., Kawabe, M., et al. (2005). Chronic exposure to a 1.439 GHz electromagnetic field used for cellular phones does not promote N-ethylnitrosourea induced central nervous system tumors in F344 rats. *Bioelectromagnetics* 26:59–68.

Skaper, S. D. (2005). Neuronal growth-promoting and inhibitory cues in neuroprotection and neuroregeneration. *Ann. N Y Acad. Sci.* 1053:376–385.

Skibo, G. G., Lushnikova, I. V., et al. (2005). A synthetic NCAM-derived peptide, FGL, protects hippocampal neurons from ischemic insult both in vitro and in vivo. *Eur. J. Neurosci.* 22:1589–1596.

Thornton, M. R., Mantovani, C., et al. (2005). Quantification of N-CAM and N-cadherin expression in axotomized and crushed rat sciatic nerve. *J. Anat.* 206:69–78.

Whitehead, T. D., Moros, E. G., et al. (2006). Gene expression does not change significantly in C3H 10T(1/2) cells after exposure to 847.74 CDMA or 835.62 FDMA radiofrequency radiation. *Radiat. Res.* 165(6):626–635.

Yan, J. G., Agresti, M., et al. (2007). Effects of cellular phone emissions on sperm motility in rats. *Fertil. Steril.* 88(4):957–964.

Zachary, I. (2005). Neuroprotective role of vascular endothelial growth factor: signalling mechanisms, biological function, and therapeutic potential. *Neurosignals* 14:207–221.

Zhao, T. Y., Zou, S. P., et al. (2007). Exposure to cell phone radiation up-regulates apoptosis genes in primary cultures of neurons and astrocytes. *Neurosci. Lett.* 412(1):34–38.

Histochem Cell Biol (1997) 107:127–137

ORIGINAL PAPER

Eva Simbürger · Alexander Stang · Marian Kremer
Rolf Dermietzel

Expression of connexin43 mRNA in adult rodent brain

Accepted: 1 October 1996

Abstract The expression of connexin43 mRNA was detected in adult rat brains by in situ hybridization methods. Specific digoxigenin riboprobes were generated by *in vitro* transcription of two PCR-amplified fragments of connexin43 cDNA which lack homology with any other published connexin. Following immunohistochemical detection, the digoxigenin cRNA was found to occur in various neuronal populations including Purkinje cells of the cerebellum, pyramidal cells of the neocortex and the hippocampal formation, as well as granule cells of the dentate gyrus and various neurons of diverse hindbrain nuclei. This ubiquituous expression of connexin43 mRNA in adult neurons, in particular in neocortical pyramidal cells, is surprising insofar as gap junction communication in adult bains has been considered to be confined to specific subpopulations of neurons revealing a high incidence of synchronized electrical activities in contrast to the postnatal brain where interneuronal coupling via gap junctions precedes the formation of chemical transmission. In addition, connexin43 is regarded as being preferentially expressed in astrocytes, although its presence in adult neurons has not definitely been excluded. We propose that adult neurons preserve their capability of expressing functional gap junctions more frequently than presently considered and that connexin43 is a most likely neuronal gap junction protein candidate.

Introduction

Gap junctions constitute intercellular channels that allow neighboring cells to directly exchange electrical and metabolic signals (Loewenstein 1981). The channel-forming elements are transmembrane proteins, collectively called connexins, which oligomerize in the trans Golgi network to hemichannels (connexons; Musil and Goodenough 1992). Adjacent cells contact each other by coupling via hemichannels which then form functionally competent cell-to-cell channels for direct signal exchange between adjoining cells (for recent reviews see Dermietzel et al. 1990; Bennett et al. 1991; Beyer 1993). In the mammalian central nervous system (CNS), morphological and electrophysiological studies describe gap junctions in distinct neuronal cell populations and predominantly in glial cells (for reviews see Sotelo and Korn 1978; Dermietzel and Spray 1993; Spray and Dermietzel 1995). The identification and characterization of a variety of connexins accordingly implied the existence of different types of gap junctions. Different brain tissues express distinct sets of connexins (for review see Dermietzel and Spray 1993). By means of antibodies raised against three different connexins (connexin 26, connexin32 and connexin43) the distribution of gap junction immunoreactivity in developing and mature brain tissue (Dermietzel et al. 1989) has been studied. According to this investigation, some neurons, as well as oligodendrocytes, were found to express connexin32, whereas connexin26 and connexin43 were coexpressed in leptomeningeal and ependymal cells. Connexin43 immunoreactivity was most abundant in astrocytes, as was evident from ultrathin brain sections and postnatal cultured astrocytes (Dermietzel et al. 1989; Shiosaka et al. 1989; Yamamoto et al. 1990; Dermietzel et al. 1991; Giaume et al. 1991). The expression of connexins in the CNS was further examined by northern blot hybridization with specific probes for connexin43 and connexin32 cRNA to total RNA preparations of different regions of the brain (Naus et al. 1990). According to this study, connexin43 mRNA is homogeneously distributed in different regions of adult rat brain, whereas connexin32 shows a heterogeneous distribution throughout the brain. In situ hybridization was performed to further evaluate the cellular distribution of connexin mRNAs in adult (Micevych and Abelson 1991) and developing (Belliveau and Naus 1995) rat brains. These studies using cRNA probes for connexin32 and connexin43 were based on *in situ* autoradiography. After hybridization, signals for connexin43 mRNA seemed to be predominantly associated with astrocytes, but expression of con-

E. Simbürger · A. Stang · M. Kremer · R. Dermietzel (✉)
Institute of Anatomy, Universität Regensburg,
Universitätsstraße 31, D-91049 Regensburg, Germany;
Tel. +49941 943 2520; fax +49941 943 2568

nexin43 mRNA in neurons could not be excluded. Connexin32 mRNA matched with subpopulations of neurons and with oligodendrocytes, especially in the hippocampal cortex, the neocortex, and the cerebellum of the adult rat brain (Micevych and Abelson 1991). Because of the abundance of connexin43 protein in astrocytes and the close relationship of these cells to neurons, the problem of a correct assignment of this connexin to a particular cell class arises. Single cell resolution is therefore an essential requirement to unequivocally attribute connexin43 mRNA expression to one of these cell types.

Here we report on in situ hybridization of brain slices using the digoxigenin technique which allows the identification of individually stained cells. Our data provide evidence that the mRNA of connexin43 is ubiquitiously expressed in a variety of neurons including pyramidal cells of the hippocampus, cortical neurons, and Purkinje cells of the cerebellar cortex. It also occurs in various concentrations in multiple nuclei of the hindbrain. The functional implications of this observation is discussed in the context of the concept of gap junction-mediated cell-to-cell communication in brain tissue.

Materials and methods

Tissue preparation

Tissues were collected from adult (2–3 months) Wistar rats of both sex (Charles River, Sulzfeld, Germany). Animals were deeply anesthetized in ether and subsequently decapitated. The brain was dissected immediately by separating the cortex, cerebellum, and brainstem. The specimens were embedded in Tissue Tek (Miles, USA) and directly frozen in liquid nitrogen.

cRNA probes

Two specific regions of rat connexin43 cDNA (Beyer et al. 1987) were amplified by polymerase chain reaction (P1: positions 940–1347, the C terminus; P2: positions 517–630, the cytoplasmatic loop; see Fig. 1 for positions). Screening of the EMBL gene bank indicated that both probes do not show any major homology with other published sequences. P1 was subcloned into vector pGEM-3Z (Promega, Heidelberg, Germany) and P2 into vector (pCR II (Invitrogen, San Diego, USA). Both cRNA probes were synthesized and digoxigenin-labelled by means of an *in vitro* transcription kit according to the manufacturer's recommendation (Boehringer, Mannheim, Germany). To produce antisense cRNA strands of the C-terminal region (P1), the plasmid was linearized with *Eco*RI followed by *in vitro* transcription with SP6 RNA polymerase. In the same way, but using *Bam*HI and T7 RNA polymerase, the sense cRNA strands of the same region were synthesized. Transcripts of the cytoplasmatic loop region (P2) were produced using the enzymes *Bam*HI and T7 RNA polymerase for the antisense cRNA strands, *Xho*I and SP6 RNA polymerase for the sense cRNA strands. All *in vitro* transcriptions were performed with digoxigenin-labelled UTP.

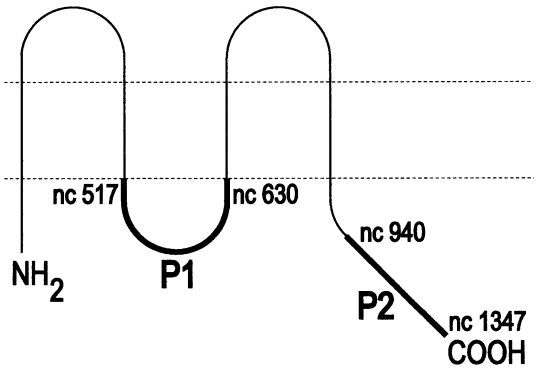

Fig. 1 Positions of the two connexin43 cRNA probes (P1, P2). The nucleotide positions are projected on the assumbed protein structure of connexin43. The *numbers* indicate the nucleotide positions (*nc*) within connexin43 cDNA (Beyer et al. 1987). This scheme is used throughout the figures to indicate the probes used for hybridization

Northern blots

Total RNA from rat heart was isolated according to Chomczynski and Sacchi (1987). Aliquots of 20 µg were separated in agarose gels and blotted onto nitrocellulose membranes. Blotted membranes were prehybridized at 55° C in 50% formamide, 0.02% SDS, 0.1% Sarkosyl, 2×Denhardt's reagent, and 5×SSC (1×SSC is 150 mM NaCl, 15 mM sodium citrate, pH 7.2) for 3 h. Hybridization was performed applying a total of 500 ng of RNA in the prehybridization mixture to each membrane strip for 16 h at 55° C. After hybridization, the membranes were washed and the hybridized probes were further processed with an anti-digoxigenin antibody (see below). Controls included blotting with labelled sense strand cRNA as well as hybridizing the probes to total RNA from rat liver, which, under non-regenerating conditions, expresses only low levels of connexin43.

In situ hybridization histochemistry

For in situ hybridization histochemistry, 8- to 15-µm-thick sections were cut in a cryostat, placed on silanated cover slips, and freeze dried at –20° C for several hours before application of the fixative (4% formaldehyde in phosphate-buffered saline, PBS). Sections were rinsed in PBS, 0.1 M glycine thereafter and incubated in 0.1 M TRIS, pH 8, containing 50 mM EDTA and 3 µg/ml proteinase K for 20 min at 37° C. Proteinase activity was stopped by applying the fixative for 10 min. After rinsing in PBS containing 0.1 M glycine, the sections were acetylated using 0.25% acetic anhydride in 0.1 M triethanolamine at pH 8, followed by dehydration in an ascending series of ethanol, and subsequent air drying. Prehybridization was achieved by incubating the sections at 45° C in 50% formamide, 0.3 M NaCl, 20 mM TRIS, pH 8, 1 mM EDTA, 10% dextran sulfate, 1×Denhardt's solution, and 500 µg/ml yeast tRNA (Song et al. 1994).

For hybridization with P1, sections were incubated for 16 h at 50° C in 15 µl prehybridization mixture containing 50 ng digoxigenin-labelled RNA probe. After hybridization, the sections were washed 3 times in 2×SSC at 55° C. Subsequently, the non-hybridized probe was removed by incubating the sections in 10 mM TRIS, 1 mM EDTA, 0.5 M NaCl containing 6 µg/ml ribonuclease A at 37° C for 10 min. The sections were then washed 3 times in 0.1×SSC at 55° C and once in 0.1×SSC at 55° C and once in 0.1×SSC at room temperature. Controls were performed by hybridization with labelled sense strand RNA (Uhl et al. 1985).

Slight modifications were performed when sections were hybridized with the P2 probe. Before treatment with fixative, a heat fixation step (5 min, 50° C) was inserted. Sections were rinsed in PBS without glycine. Before incubation for 1 h at 50° C in prehybridization mixture, sections were rinsed twice in 2×SSC for 5 min. Proteinase K treatment and subsequent steps were not performed. Hybridization was done for 16 h at 50° C in prehybridization mixture containing 12 ng digoxigenin-labelled cRNA probe. The sections were then washed once in 2×SSC, 3 times in 2×SSc containing 60% formamide at 37° C, and twice in 2×SSC at room temperature. Controls for P2 were also performed with appropriate labelled sense strand cRNA.

In both cases (P1, P2) the hybridization products were visualized by immunolabelling of the digoxigenin-labelled hybrid with a specific polyclonal anti-digoxigenin antibody coupled to alkaline

phosphate (Boehringer) and subsequent staining of the alkaline phosphatase with 5-bromo-4-chloro-3-indolyl phosphate (BCIP)/ nitro blue tetrazolium (NBT). Briefly, sections were rinsed twice in 0.1 M TRIS-buffered saline (TBS) and blocked with 1% blocking reagent (Boehringer) in TBS for at least 30 min. The antibody was diluted in TBS containing 0.2% blocking reagent and 0.1% Triton X-100. The sections were incubated overnight at 4° C, rinsed twice in TBS, and once in 100 mM TRIS/100 mM NaCl/50 mM $MgCl_2$. The staining was performed in the latter buffer containing 4.5 µl NBT/ml and 3.5 µl BCIP/ml for 7–16 h. The reaction was stopped by washing the sections several times in double-distilled water. Slices hybridized with cRNA probes containing the cytoplasmatic loop region (P2) were counterstained with methyl green for 7 min. All sections were embedded in aqueous mounting medium (Shandon Southern Products, Astmoor, USA).

Additionally, simultaneous fluorescence in situ hybridization (FISH) of connexin43 and immunocytochemistry of a glial marker (glial fibrillar acidic protein, GFAP) was performed in order to assess the contribution of astrocytes to the expression of connexin43 mRNA in brain slices. In these experiments the hybridized sections were incubated in a mixture of anti-digoxigenin Fab2 fragments raised in sheep (diluted 1:50, Boehringer) and a monoclonal anti-GFAP antibody (diluted 1:400, Dianova, Hamburg, Germany). Incubation was performed overnight at 4° C, followed by labelling with secondary antibodies. The anti-digoxigenin Fab2 fragments were detected by anti-sheep IgG coupled to fluorescein isothiocyanate (FITC; diluted 1:100, Boehringer) and the anti-GFAP IgG with goat anti-rabbit IgG conjugated to Texas Red (diluted 1:500, Dianova). After three washes in 0.1% BSA/PBS, sections were embedded in FITC-Guard (Testoc, Chicago, USA) and examined with a confocal laser microscope (BioRad 500) equipped with a multi-laser irradiation device.

Results

Determination of the specificity of the cRNA probes

In order to evaluate the specificity of the anti-sense cRNA probes (P1, P2), the digoxigenin-labelled transcripts were hybridized to total RNA of rat heart. Heart tissue was chosen since connexin43 is the major gap junction protein in cardiac cells. Northern blots showed distinct bands at 3.0 kb (Fig. 2a, c) which correspond with the expected length of connexin43 mRNA (Beyer et al. 1987). No additional bands were detected, indicating specific binding of the probes to connexin43 mRNA. Controls were performed using the digoxigenin-labelled sense probes (Fig. 2b, d) as well as hybridizing sense and anti-sense probes to total RNA from rat liver, which expresses connexin43 only in fibroblasts of the Glisson capsule and in endothelial cells, but is enriched in connexin32 and connexin26. Incubation of liver RNA yielded no signals with the connexin43 cRNA probes at exposure times which gave a discrete signal in heart samples (data not shown).

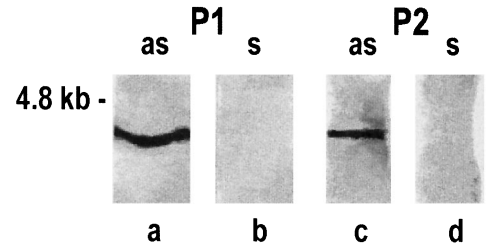

Fig. 2 Northern blot of total RNA from rat heart hybridized with P1 (**a, b**) digoxigenin-labelled antisense (*as*) and sense (*s*) probes. Position of 28S RNA is indicated on the left side in kilobases. P2 (**c, d**) indicates corresponding Northern blots with the cytoplasmic loop probe

Distribution pattern of connexin43 mRNA in the cerebellum

In situ hybridization performed on coronal sections of the cerebellum (Fig. 3A) showed consistent staining of Purkinje cells (Fig. 3B, C). The reaction product was localized preferentially in the cytoplasm of individual perikarya. In the stratum granulosum, hybridized probe was detected in randomly distributed cells which exhibited large pericarya. By their localization, size, and abundance they can be considered to represent Golgi cells (Fig. 3B). Staining was confined to the somata of these cells. The stratum moleculare revealed various numbers of preferentially staining, relatively small cells, in close proximity to Purkinje cells (Fig. 3C). A definitive identification of these cells according to their localization could not be assessed by the alkaline phosphatase staining. Controls using sense probes exhibited no labelling of the sections (Fig. 3D).

Neocortical localization of connexin43 mRNA

The mRNA hybridization of P1 could be detected in cells distributed throughout all layers of the fronto-parietal cortex. The most intense staining was observed in the pericarya of pyramidal cells in layer V and in cell bodies located at the innermost cortical layer (lamina VIb; Fig. 4A, B). Layers II, III, and IV as well as layer VIa showed homogeneously distributed cells with variable staining intensities. In the molecular layer as well as in the white matter few connexin43 mRNA-positive cells were detected, which, according to their localization, can be considered to represent astrocytic pericarya. The staining intensitiy of these cells was lower than in most of the pyramidal cells. Apart from the pyramidal cells which could be identified by their characteristic morphology (Fig. 4C), the attribution of the other label to a specific cell class was less accurate. They may either represent astrocytes or interneurons such as spindle cells, basked or stellate cells. When comparing hybridized sections with subsequent sections counterstained with toluidine blue (Fig. 4A, B), the larger and more prominently stained cells can be considered to represent neurons because of their phenotypical appearance and laminated localization, whereas the population of randomly dispersed cells revealing mostly a weaker reaction are likely to represent astrocytes (Fig. 4C). Hybridization of coronal sections with P2 revealed an identical labelling pattern (Fig. 4E). In general, labelling intensity with P2 was less prominent than with P1. This difference is probably due to the length of the probe which is about 290 nucleotides shorter than P1 and therefore allows less dUTP label per cRNA molecule. Again, sense controls were devoid of any reaction product (Fig. 4D, F).

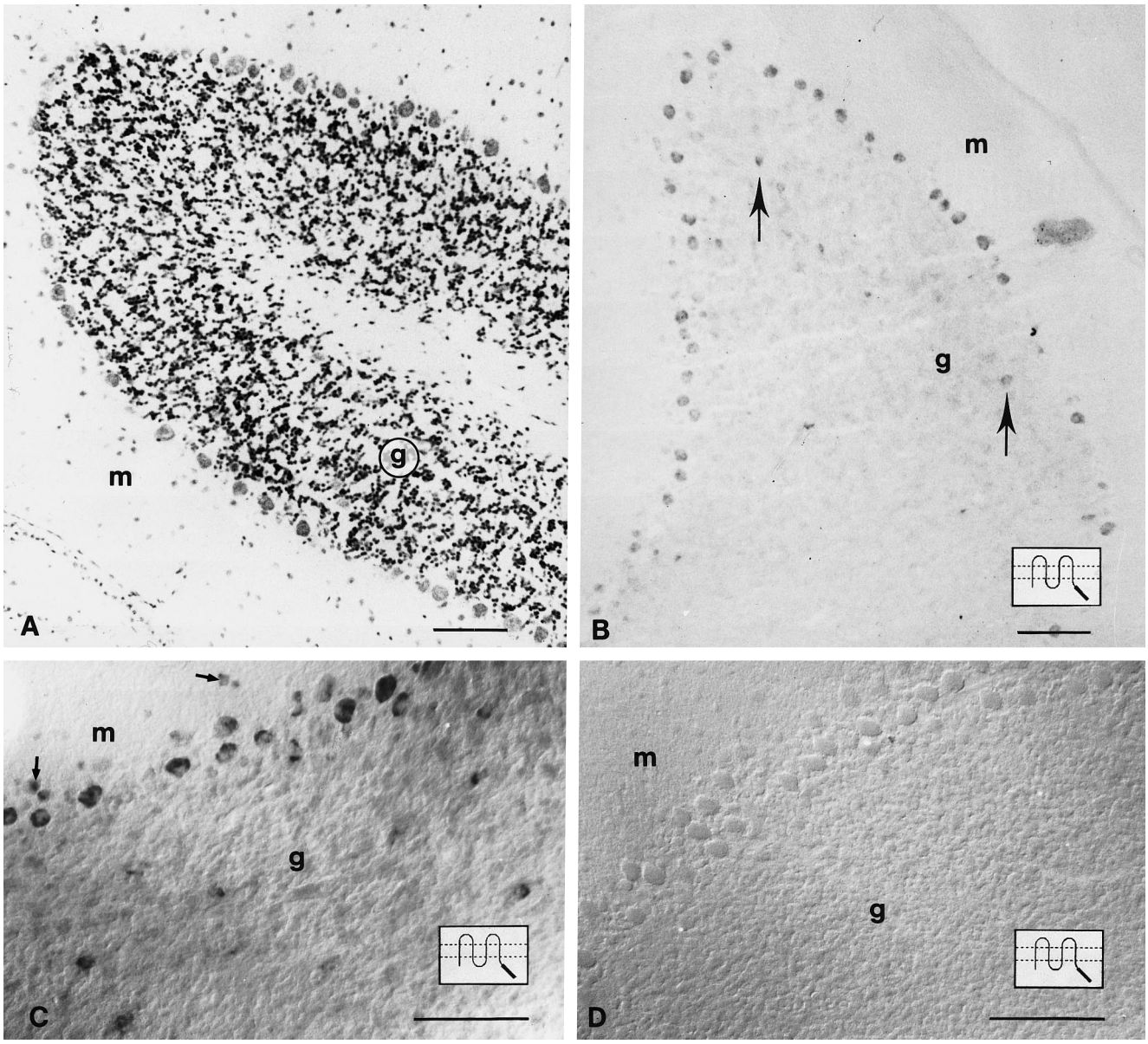

Fig. 3 Sagittal section of the cerebellum stained with toluidine blue (**A**). Localization of connexin43 mRNA in the cerebellum by in situ hybridization with digoxigenin-labelled antisense (**B, C**) and sense (**D**) P1 probes. Hybridized probes were visualized with an enyzme-linked antibody/alkaline phosphatase-conjugated anti-digoxigenin antibody with nitro blue tetrazolium/5-bromo-4-chloro-3-indolyl phosphate (NBT/BCIP) as substrate. **B** A low magnifiation of the cerebellar cortex with regularly stained Purkinje cells and some Golgi cells in the granular layer (*arrows*). **C** Higher magnification showing the presence of connexin43 mRNA in perikarya of smaller cells (*arrows*) located in the Purkinje cell layer. (*m* Molecular layer, *g*, granule cell layer) Normaski contrast (**C, D**). *Bars* 100 μm

The hippocampal cortex shows a distinct pattern of connexin43 mRNA expression

In situ hybridization of coronal sections of hippocampal slices with the labelled cRNA probe containing the antisense sequence of the C-terminus of connexin43 (P1) showed a specific labelling pattern of connexin43 mRNA-positive cells. The cell bodies of pyramidal cells at the hilus as well as in the CA3 and CA2 regions were intensively stained (Fig. 5A). A decrease in staining intensity was found in pyramidal cells of the CA1 region (Fig. 5B). The granule cells of the dentate gyrus were also positive for connexin43 but the signal was much fainter than that of the pyramidal cell layer (Fig. 5A, C). However, in most of the granule cells, prominent spots of

Fig. 4 Coronal section of the fronto-parietal cortex stained with toluidine blue (**A**). Localization of connexin43 mRNA in the fronto-parietal cortex by in situ hybridization with digoxigenin-labelled antisense (**B, C, E**) and sense (**D, F**) riboprobes. Staining is most intense in the pyramidal cells of layers V and VIb (**B**). **C** A high magnification micrograph of layer V indicating a considerable degree of variability of mRNA concentrations between the different cell types. **E** A section through cortical layers IV and V, labelled with P2. Nuclei are counterstained with methyl green (**E, F**). (*cc* Corpus callosum, *I-VI* indication of cortical layers) Normaski contrast (**C–F**). *Bars* **A, B, E, F** 100 μm, **C, D** 50 μm

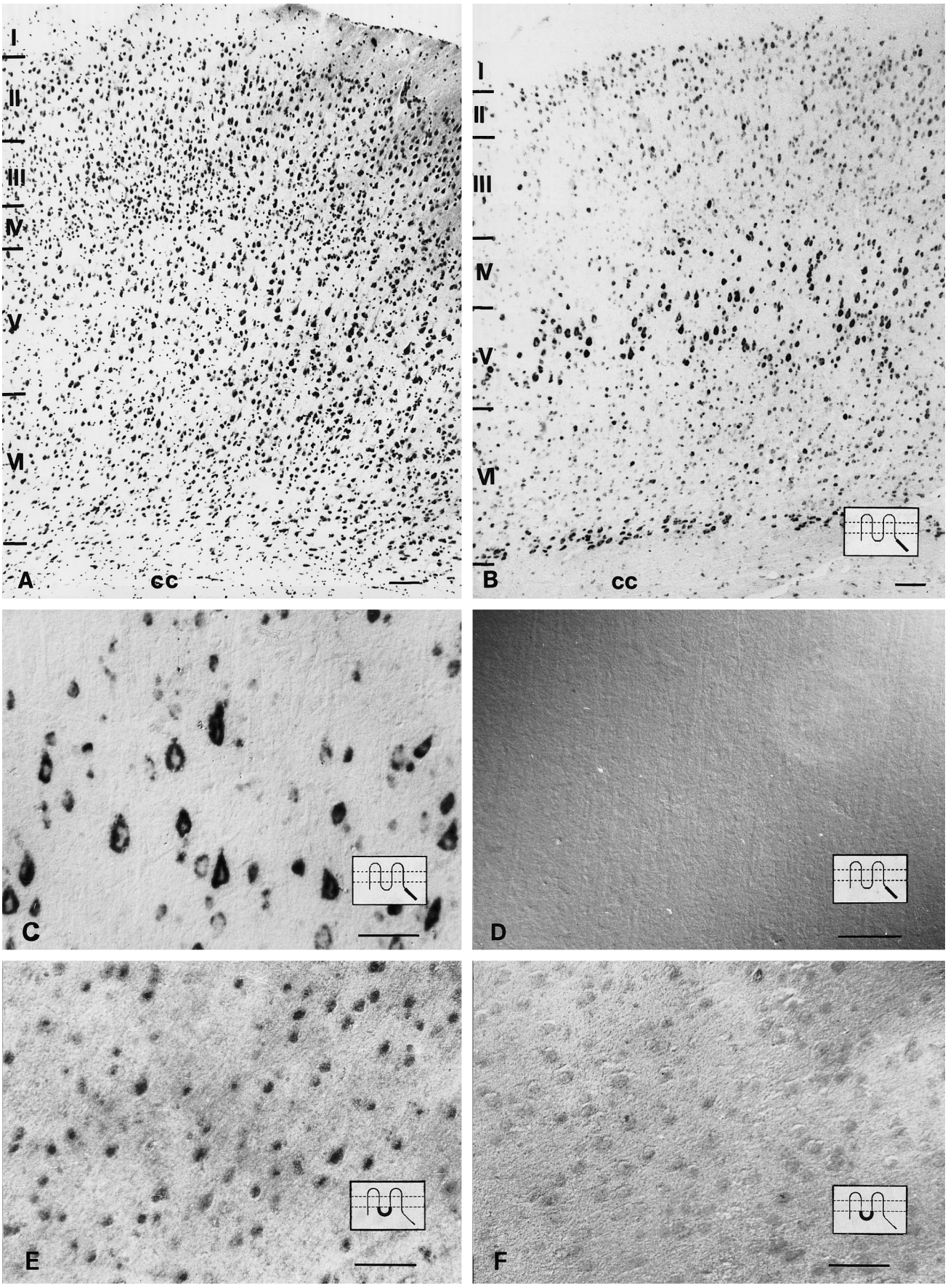
I
II
III
IV
V
VI
A
cc
I
II
III
IV
V
VI
B
cc
C
D
E
F

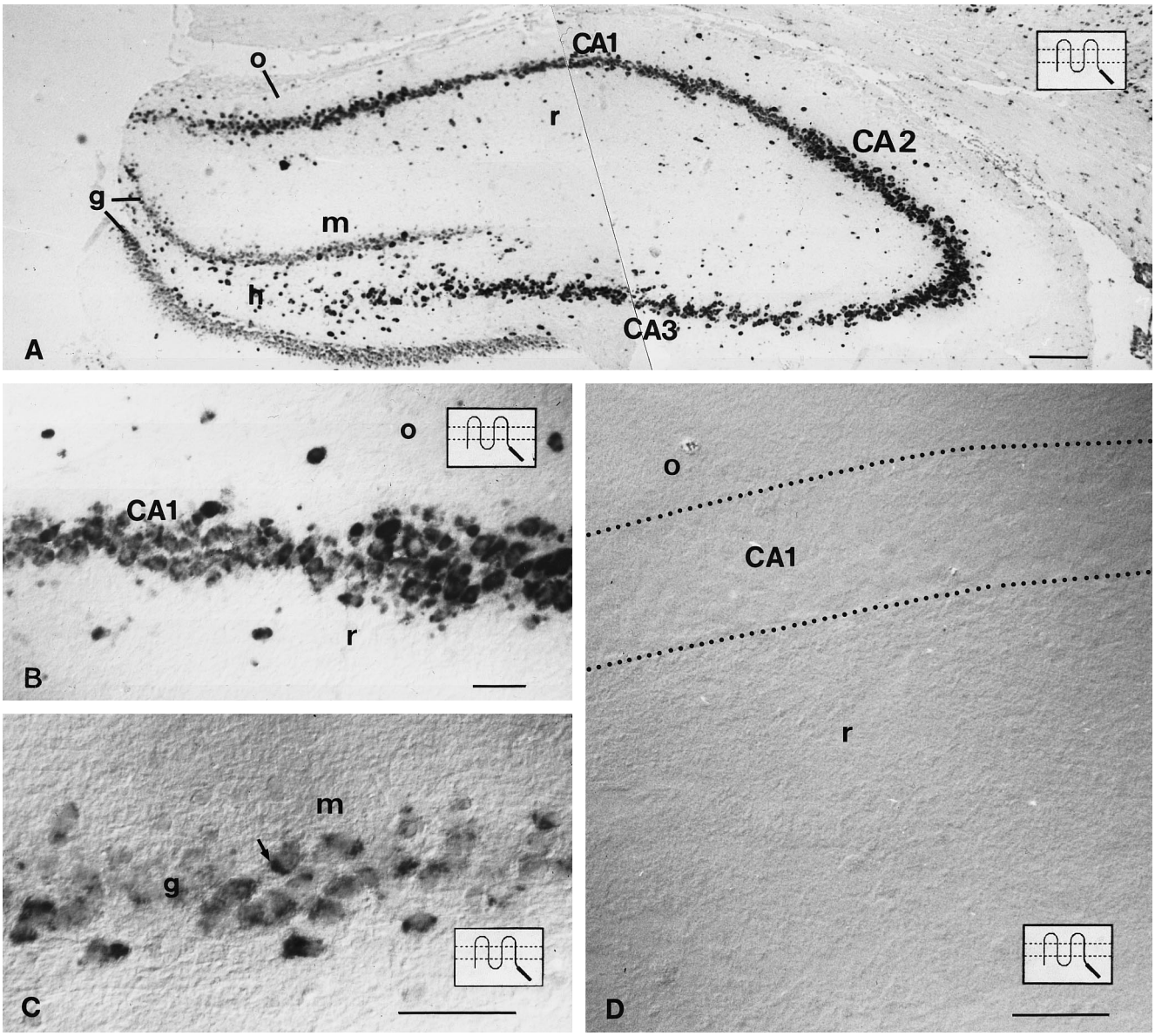

Fig. 5 Localization of connexin43 mRNA in a coronal section of the hippocampal formation with digoxigenin-labelled antisense (**A–C**) and sense (**D**) P1 riboprobes. Low magnification (**A**) indicates the differences in staining intensities between the dentate gyrus (*g*) and the pyramidal cells of the hippocampus (**CA3, CA2, CA1**). **B** The transition zone between the CA2 and CA1 regions which reveals a gradient in staining intensity indicative of lower amounts of connexin43 mRNA in CA1 pyramidal cells. **C** Granule cells of the dentate gyrus with clusters of mRNA (*arrows*). (*o* Stratum oriens, *r* stratum radiatum, *m* stratum moleculare, *h* hilus, *g* granular cells of the dentate gyrus) Normaski contrast (**B–D**). *Bars* **A** 200 μm, **B–D** 50 μm

the hybridization product were found, which are likely to represent clusters of mRNA (Fig. 5C). The molecular layer of the dentate gyrus revealed only very few connexin43 mRNA-positive cells. Additionally, connexin43 mRNA was abundant in cells probably representing interneurons located mainly in the stratum oriens along the CA2 region and the subsequent part of the CA1 region. In the stratum radiatum, immunopositive cells were more homogeneously distributed. The stratum lacunosum moleculare was devoid of connexin43 mRNA-positive cells. No reactivity was found with P1 sense controls (Fig. 5D). Hybridization of hippocampal sections with P2 yielded identical patterns of labelling (Fig. 7D). As indicated above, labelling intensity with P2 was less prominent than with P1 but reached significant levels, especially when compared with the sense controls (Fig. 7E).

Fig. 6A–C Localization of connexin43 mRNA in coronal sections of the hindbrain using digoxigenin-labelled antisense P1 riboprobes. **A** Low magnification of a section taken from the level of the hypoglossal nucleus (*h*). **B, C** Higher magnifications showing individual stained neurons of the inferior olivary complex (**B**) and the gigantocellular nucleus (**C**). (*o* Inferior olivary complex, *g* gigantocellular nucleus, *p* pyramidal tract, *h* hypoglossal nucleus, *s* solitary nucleus, *r* reticular nuclei, *t* spinal trigeminal nucleus, *c*, nucleus cuneatus, *v* dorsal vagal nucleus, *l* lateral reticular nucleus) Normaski contrast (**B, C**). *Bars* **A** 200 μm, **B, C** 100 μm ▶

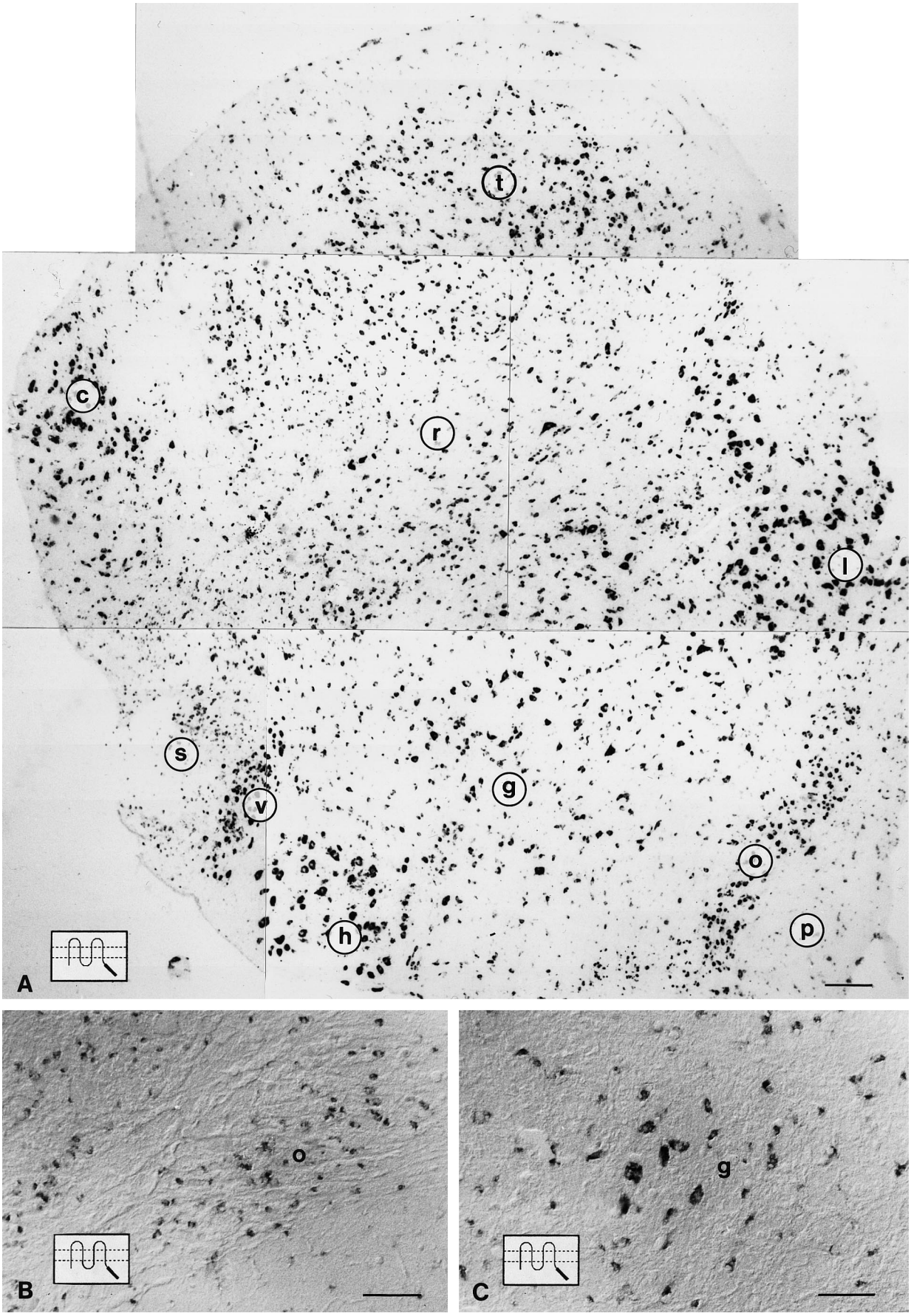
t
c
r
l
s
v
g
o
h
p
A
o
B
g
C

Table 1 Expression of connexin43 mRNA in different nuclei of the hindbrain. Expression is indicated in relative terms: + positive reaction, +/– low reaction, – no reaction

Hindbrain nuclei	Connexin43 mRNA-positive neurons
Inferior olive	+
Lateral reticular nucleus	+
Subtrigeminal lateral reticular nucleus	+
Parvocellular lateral reticular nucleus	+/–
Intermediate reticular nucleus	+
Paramedian reticular nucleus	–
Nucleus gigantocellularis	+
Spinal trigeminal nucleus	+
Nucleus cuneatus	+
Nucleus solitary tract	+/–
Dorsal motor nucleus vagus	+
Nucleus hypoglossus	+

Distribution of connexin43 mRNA in the hindbrain

For analysis of connexin43 mRNA distribution in the hindbrain, frontal sections of the brainstem at the level of the inferior olivary complex were used for in situ hybridization with the P1 probe. Connexin43 mRNA-positive cells could be detected in various nuclei of the hindbrain. According to their cell shape, the large cells were identified as neurons while the small cells, which were found to be randomly distributed, are considered to represent astrocytes (Fig. 6A). The intensity of connexin43 mRNA in the nuclei of the hindbrain showed a high degree of variability. Very prominent staining was observed in pericarya of neurons of the hypoglossal nucleus as well as in the complex of the lateral reticular nucleus including the subtrigeminal part (Fig. 6A). Similarly, intense staining was detected in the external nucleus cuneatus and the inferior olivary complex (Fig. 6B). Neurons revealing equal amounts of the hybridization products were also found in the paragigantocellular nucleus and the spinal trigeminal nucleus. For a summary of connexin43 mRNA distribution in the hindbrain see Table 1 (nomenclature according to Paxinos and Watson 1986).

Comparison of connexin43 mRNA levels in astrocytes and neurons

In order to assess the contribution of astrocytic connexin43 mRNA expression in the diverse brain regions, we performed simultaneous fluorescence in situ hybridization and indirect immunofluorescence cytochemistry of GFAP as an astrocytic marker protein. Although an exact correllation of GFAP localization and connexin43 mRNA could not consistently be achieved because of the more peripheral concentration of GFAP in astrocytic processes in contrast to the pericaryonal localization of mRNA, the double labelling approach confirmed our single enzymatic staining experiments insofar as the most prominent connexin43 labelling occurred in neurons. This became particularly evident in the cerebellar cortex (Fig. 7A) where high concentrations of GFAP in the granular layer did not correspond to equivalent amounts of connexin43 mRNA. In contrast, Purkinje cells and some perikarya of the molecular layer stained positively for connexin43 mRNA (Fig. 7A). In cases of colocalization of the GFAP signals (Texas Red) and signals for connexin43 mRNA (FITC) the latter was less pronounced than the signals derived from the neuronal connexin43 mRNA in the same section. This phenomenon proved valid for all brain regions examined by means of the double labelling technique including the hindbrain (Fig. 7B) and the hippocampus (Fig. 7C). Apparently, the bulk concentration of connexin43 mRNA is higher in neurons than in astrocytes.

Discussion

Methodological considerations

In situ hybridization histochemistry using radioactively labelled probes is a sensitive method to detect mRNA molecules in tissues or cultured cells. The number of RNA molecules that can be visualized ranges between 20 and 75 per cell (Cox et al. 1984). However, a major problem of this method concerns the cellular resolution of the signals. In sections of rather heterogeneous tissue it is difficult to assign the signals to individual cells. With respect to the *in situ* labelling of brain slices this problem becomes particularly serious. Glial cells and neurons are often located in close proximity. The observation that the signal of an *in situ*-hybridized radioactively labelled cRNA probe specific for RNA of connexin43 matches predominantly with astrocytes (Miceviych and Abelson 1991; Belliveaun and Naus 1995) does not exclude the possibility of connexin43 mRNA being expressed in neuronal cells as well. In situ hybridization histochemistry using non-radioactively labelled cRNA probes followed by immunocytochemical detection provides a better resolution and subsets of individually stained cells can be differentiated by their typical morphology. The general sensitivity of this method has been shown to be comparable to that achieved by radioactive in situ hybridization (Peterson and McCrone 1994). However, a critical parameter seems to be the concentration of mRNA molecules in a single cell (Gee et al. 1983). High levels of transcripts can reproducibly be detected with both methods, whereas at low levels of mRNA, differences in the sensitivity of both techniques are likely to occur. In particular, the digoxigenin method seems less sensitive than the autoradiographic approach in cases of critical mRNA levels. This may explain the inconsistency of staining in astrocytes which, according to their weaker reactivity, seem to contain less connexin43 mRNA, thereby escaping detectability by the digoxigenin technique.

Cross-hybridization is another serious problem which frequently produces false-positive results. To exclude the possibility that our unexpectedly high labelling frequency of neurons is attributable to artificial cross-hybridization with non-connexin mRNAs, we used a second probe, P2, with no overlap in sequence with the C-termi-

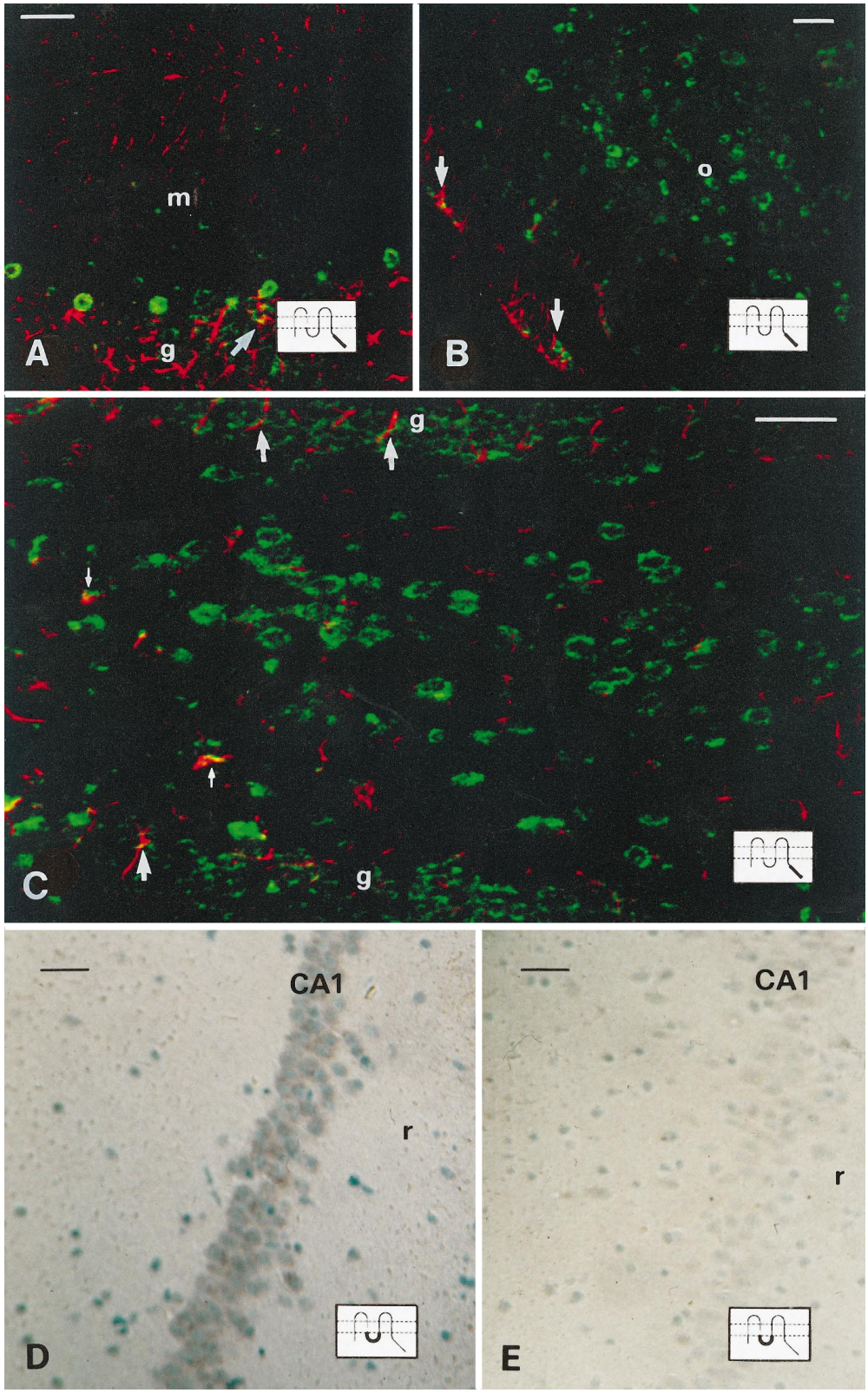

Fig. 7 Simultaneous fluorescence in situ hybridization and indirect immunofluorescence cytochemistry of connexin43 mRNA (fluorescein isothiocyanate, FITC; green) and glial fibrillar acidic protein, GFAP (Texas Red; red) as an astrocytic marker (**A–C**) and localization of connexin43 mRNA in a coronal section of the hippocampal formation with digoxigenin-labelled antisense (**D**) and sense (**E**) P1 riboprobes. **A** The Purkinje cell layer of the cerebellar cortex with part of the molecular layer (*m*) and granular layer (*g*). Note the low concentration of connexin43 mRNA in the granular layer as compared with the intensive staining in Purkinje cells. In some places, colocalization of the mRNA signal (green) and the GFAP signal (red) is achieved, yielding a yellow color (*arrow*). **B** Coronal section of the hindbrain at the level of the inferior olivary nuclei (*o*). Colocalization is only prevelant in the marginal glia (*arrows*). **C** Section through the hippocampal formation. Granular cell layer of the dentate gyrus is shown at the top and bottom (*g*). Pyramidal cells of the CA3/CA4 region are indicated in the center of the micrograph. Colocalization of GFAP immunoreactivity and connexin43 mRNA occurs in several radial astrocytic fibers of the granular layer (*large arrows*) and in some astrocytic processes of the pyramidal layer (*small arrows*). **D** A high magnification of the CA1 region of the hippocampus with staining of pyramidal cells after hybridization with P2. **E** Control with P2 sense probe. Nuclei are counterstained with methyl green (**D, E**). (*r* Stratum radiatum) *Bars* **A–E** 50 µm

nal probe, P1. Both probes were selected from two cDNA portions of Cx43 (Beyer et al. 1987) which show no homology with any other published connexin sequence. Cross-checking of the gene data bank of EMBL also indicated only neglible homologies with some arbitrarily selected viral genes. Since both probes gave consistently identical patterns of labelling in the hippocampus and brain cortex, we consider the data to be most reliable. However, we cannot definitely exclude the possibility of a cross-hybridization of our connexin43 probes with unknown connexins of higher homology than the isoforms published to date.

Neuronal connexin43 expression and functional implications

Using the digoxigenin approach for in situ hybridization with two different cRNA probes specific for connexin43, we detected mRNA of this gap junction protein in a high number of neurons in adult brains such as Purkinje cells and Golgi cells of the cerebellum, pyramidal cells of the neocortex and the hippocampal formation, and in granule cells of the dentate gyrus. Furthermore, neurons expressing connexin43 mRNA were found in distinct nuclei of the hindbrain. These findings are surprising insofar as gap junction-mediated electrical coupling has been considered to be confined to specific populations of neurons in the adult brain which exhibit a high incidence of synchronized electrical activities (Sotelo and Llinás 1972; Llinás et al. 1974; Sotelo and Korn 1978; Llinás 1985; Llinás and Sasaki 1989; Sasaki et al. 1989). In contrast, postnatal brains show extensive coupling of cortical neurons, phenomenon which is regarded to be involved in the postnatal development of the modular architecture of the neocortex (Yuste et al. 1992; Peinado et al. 1993). In the progress of brain maturation, electrical coupling is thought to be downregulated in favor of stabilizing chemical transmission (Kandler and Katz 1995).

Additionally, immunocytochemical studies on slices from adult brains have failed to confirm the expression of connexin43 in neurons. Several reasons may account for the apparent lack of knowledge concerning the neuronal connexin type(s). Firstly, in *situ* labelling of connexin43 by immunocytochemistry does not allow the signals to be attributed to neurons because of the abundance of the protein in astrocytes. Even at the electron microscopical level, a definite attribution of immunogold label to neuronal profiles proved difficult, since minute astrocytic processes with gap junctional contacts can be frequently observed in close proximity to neuronal perikarya (Miragall et al. 1992). Secondly, electrophysiological *in vitro* approaches have failed to characterize unitary conductances of gap junction channels in differentiated neurons due to the low incidence of coupling under *in vitro* conditions (Kessler et al. 1985). Thirdly, the expression of neuronal connexins may be regulated by strict translational control which affects translational efficacy. The latter argument implies that the presence of connexin mRNAs is not indicative of constitutive expression of the protein. Discrepancies between connexin mRNA concentrations and protein levels have been described, for instance, in lung, where connexin37 and connexin40 are enriched at the mRNA level without any detectable protein concentrations (Willecke et al. 1991; Hennemann et al. 1992). Translational efficacy may, thus, be an important regulatory principle in connexin expression (Saez et al. 1989; Kren et al. 1993). From the standpoint of metabolic effectiveness, it seems most likely that the expression of high levels of mRNA is also followed by at least transient translation of the finite gene product, i.e., the protein. We therefore consider the idea reasonable that neurons exhibit a constitutive pool of connexin43 mRNA which may be transiently expressed, for example in an activity-dependent manner. Arguments for a rapid recruitment of gap junctional coupling come from two different sources. We have recently shown that ligation of the facial nerve induces a fast upregulation of connexin43 expression in its central motor nuclei. The increase of detectable connexin43 occurs within less than an hour and is the earliest response described thus far in this experimental paradigm (Rohlmann et al. 1994). In this case, the upregulation is considered to occur in astrocytes. On the other hand, evidence for rapid recruitment of electrical coupling between neurons is provided by electrophysiological and dye injection studies of hippocampal slices (MacVicar and Dudek 1981). The hippocampal paradigm has been frequently used to evaluate the generation of synchronized populations of spikes and its relevance for seizure discharge. Since synchronized action potentials can occur after chemical transmission has been blocked (in calcium-free solutions), electrical transmission is most likely to play a role in spike synchronization (Perez-Velazquez et al. 1994). The strengthening o electrical coupling between hyperexcitable neurons can either be explained by gating mechanisms at the channel level or *de novo* assembly of functional channels from a pool of preexisting connexons. Such a pool can be considered to be transiently fuelled by translation of the appropriate mRNA. The double labelling experiments indicate that the concentation of connexin43 mRNA is higher in neurons than in astrocytes. It remains to be clarified whether this discrepancy in connexin43 mRNA concentrations reflects differences in the regulatory principles governing the expression of connexin43 in both cell classes.

The recent discovery that astroglial-neuronal coupling occurs, at least under *in vitro* conditions (Nedergaard 1994), is indicative of the latent capability of neurons to establish functional gap junctions. Our detection of connexin43 in a variety of neurons does not exclude the possibility of co-expression of another connexin in the same neuronal type, i.e., connexin32, which has been described as a connexin in some subpopulations of neurons (Dermietzel et al. 1989; Micevych and Abelson 1991). Alternatively, a diversified expression of connexins in neurons of different types seems feasible. Double in situ hybridization is necessary to finally answer this issue. Since the different connexin isoforms exhibit considerable differences in their regulatory properties when assembled in gap junction channels, such a diversified expression of neuronal connexins would provide a new aspect to the issue of direct interneuronal communication.

The question then arises, how can the formation of functional connexin43 channels be controlled to avoid promiscuous junctional interaction between neurons and glial cells? The powerful trait of neurons and/or glial cells to establish functionally correct gap junctions could occur via the interaction of homophilic cell adhesion molecules. One would except that strict control mechanisms regulate the successful achievement of interneuronal and/or glial-neuronal gap junction formation in vivo. Further studies using some of the established experimental models, in particular preparations of brain slices,

should allow a better definition of the functional significance of neuronal connexin43 expression.

Acknowledgements We gratefully acknowledge the assistence of Uwe DeVries in preparing the confocal laser images and Irmgard Herting for her help with the immunodetection work. This study was supported by a grant from the Deutsche Forschungsgemeinschaft to R.D. (De 292/6-1).

References

Belliveau DJ, Naus CG (1995) Cellular localization of gap junction mRNAs in developing rat brain. Dev Neurosci 17:81–96

Bennett MVL, Barrio TA, Bargiello DC, Spray DC, Hertzberg E, Saez J (1991) Gap junctions: new tools, new answers, new questions. Neuron 6:305–320

Beyer EC (1993) Gap junctions. Int Rev Cytol 137C:1–36

Beyer EC, Paul DL, Goodenough DA (1987) Connexin43: a protein from rat heart homologous to a gap junction protein from liver. J Cell Biol 105:2621–2629

Chomczynski P, Sacchi N (1987) Single-step method of RNA isolation by acid guanidinium thiocyanate-phenol-chloroform extraction. Anal Biochem 162:156–159

Cox KH, DeLeon DV, Angerer LM, Angerer RC (1984) Detection of mRNAs in sea urchin embryos by in situ hybridization using asymmetric RNA probes. Dev Biol 101:485–502

Dermietzel R, Spray DC (1993) Gap junctions in the brain: where, what type, how many and why? Trends Neurosci 16:186–192

Dermietzel R, Traub O, Hwang TK, Beyer E, Bennett MVL, Spray DC, Willecke K (1989) Differential expression of three gap junction proteins in developing and mature brain tissue. Proc Natl Acad Sci USA 86:10148–10152

Dermietzel R, Hertzberg EL, Kessler JA, Spray DC (1991) Gap junctions in cultured astrocytes: immunocytochemical, molecular, and electrophysiological analysis. J Neurosci 11:1421–1432

Gee CE, Chen CL, Roberts JL, Thompson R, Watson SJ (1983) Identification of proopiomelanocortin neurons in rat hypothalamus by in situ cDNA-mRNA hybridization. Nature 306:374–376

Giaume C, Fromaget C, Aoumari AE, Cordier J, Glowinski J, Gros D (1991) Gap junctions in cultured astrocytes. Single channel currents and characterization of the channel-forming protein. Neuron 6:133–143

Hennemann H, Suchyna T, Lichtenberg-Frate H, Jungbluth S, Dahl E, Schwarz J, Nicholson BJ, Willecke K (1992) Molecular cloning and functional expression of mouse connexin40 a second gap junction protein gene preferentially expressed in lung. J Cell Biol 117:1299–1310

Kandler K, Katz LC (1995) Neuronal coupling and uncoupling in the developing nervous system. Curr Opin Neurobiol 5:95–105

Kessler JA, Spray DC, Sáez JC, Bennett MVL (1995) Development and regulation of electrotonic coupling between cultured sympathetic neurons. In: Bennett MVL, Spray DC (eds) Gap junctions. Cold Spring Harbor Laboratory Press, Cold Spring Harbor, NY, pp 231–240

Kren BT, Kumar NM, Wang SQ, Gilula NB, Steer CJ (1993) J Cell Biol 123:707–718

Llinás RR, Baker R, Sotelo C (1974) Electrotonic coupling between neurons in the cat inferior olive. J Neurophysiol 37: 560–571

Llinás RR (1985) Electrotonic transmission in the mammalian central nervous system. In: Bennett MVL, Spray DC (eds) Gap junctions. Cold Spring Harbor Laboratory Press, Cold Spring Harbor, NY, pp 337–353

Llinás RR, Sasaki K (1989) The functional organization of the olivo-cerebellar system as examined by multiple Purkinje cell recordings. Eur J Neurosci 1:587–602

Loewenstein WR (1981) Junctional intercelular communication: the cell-to-cell membrane channel. Physiol Rev 61:829–913

MacVicar BA, Dudek FE (1981) Electrotonic coupling between pyramidal cells: a direct demonstration in rat hippocampal slices. Science 213:782–785

Miragall F, Hwang TK, Traub O, Hertzberg EL, Dermietzel R (1992) Expression of connexins in the developing olfactory system of the mouse. J Comp Neurol 325:359–378

Miceviych PE, Abelson L (1991) Distribution of mRNA coding for liver and heart gap junction proteins in the rat central nervous system. J Comp Neurol 305:96–118

Musil LS, Gooudenough DA (1993) Multisubunit assembly of an integral plasma membrane channel protein, gap junction connexin43, occurs after exit from the ER. Cell 74:1065–1077

Naus CG, Belliveau DJ, Bechberger JF (1990) Regional differences in connexin32 and connexin43 messenger RNAs in rat brain. Neurosci Lett 111:297–302

Nedergaard M (1994) Direct signaling from astrocytes to neurons in cultures of mammalian brain cells. Science 263:1768–1771

Paxinos G, Watson C (1986) The rat brain in sterotaxic coordinates, 2nd edn. Academic Press, San Diego

Peinado A, Yuste R, Katz LC (1993) Extensive dye coupling between rat neocortical neurons during the period of circuit formation. Neuron 10:103–114

Perez-Velazquez JL, Valiante TA, Carlen PL (1994) Modulation of gap junctional mechanisms during calcium-free induced field burst activity: a possible role for electrotonic coupling in epileptogenesis. J Neurosci 14:4308–4317

Peterson SL, McCrone S (1994) Characterization of the receptor complement of individual neurons using dual-label in situ hybridization histochemistry. In: Eberwine JH, Valentino KL, Barchas JD (eds) In situ hybridization in neurobiology. Oxford University Press, New York, pp 78–95

Rohlmann A, Laskawi R, Hofer A, Dermietzel R, Wolff J (1994) Astrocytes as rapid sensors of peripheral axotomy in the facial nucleus of rats. Neuroreport 5:409–412

Sáez JC, Gregory WA, Watanabe T, Dermietzel R, Hertzberg EL, Reid L, Bennett MVL, Spray DC (1989) cAMP delays disappearance of gap junctions between pairs of rat hepatocytes in primary culture. Am J Physiol 257:C1–11

Sasaki JC, Boweer JM, Llinás R (1989) Multiple Purkinje cell recording in rodent cerebellar cortex. Eur J Neurosci 1:572–586

Shiosaka S, Yamamoto T, Hertzberg EL, Nagy Jl (1989) Gap junction protein in rat hippocampus: correlative light and electron microscope immunhistochemical localization. J Comp Neurol 281:282–297

Song L, Ye M, Troyanovskaya M, Wilk E, Wilk S, Healy DP (1994) Rat kidney glutamyl aminopeptidase (aminopeptidase A): molecular identity and cellular localization. Am J Physiol 267:546–557

Sotelo C, Llinás RR (1972) Specialized membrane junctions between neurons in the vertebrate cerebellar cortex. J Cell Biol 53:271–289

Sotelo C, Korn H (1978) Morphological correlates of electrical and other interactions through low-resistance pathways between neurons of the vertebrate central nervous system. Int Rev Cytol 55:67–107

Spray DC, Dermietzel R (1995) X-linked dominant Charcot-Marie-Tooth disease and other potential gap junction diseases of the nervous system. Trends Neurosci 18:256–262

Uhl GR, Zingg HH, Habener JF (1985) Vasopressin mRNA in situ hybridization: localization and regulation studied with oligonucleotide cDNA probes in normal and Braffleboro rat hypothalamus. Proc Natl Acad Sci USA 82:5555–5559

Willecke K, Heynckes R, Dahl E, Stutenkemper R, Hennemann H, Jungbluth S, Suchyna T, Nicholson BJ (1991) Connexin37: cloning and functional expression of a gap junction gene highly expressed in lung. J Cell Biol 114:1049–1057

Yamamoto T, Ochalski A, Hertzberg EL, Nagy JI (1990) On the organization of astrocytic gap junctions in rat brain as suggested by LM and EM immunohistochemistry of connexin43 expression. J Comp Neurol 302:853–883

Yuste R, Peinado A, Katz LC (1992) Neuronal domains in developing neocortex. Science 257:665–669

Connective Tissue Research, 51:1–7, 2010

ISSN: 0300-8207 print / 1607-8438 online
DOI: 10.3109/03008200902855917

informa
healthcare

Effects of Pulsed Electromagnetic Fields on the mRNA Expression of RANK and CAII in Ovariectomized Rat Osteoclast-Like Cell

Jian Chen, Hong-Cheng He, Qing-Jie Xia, Li-Qun Huang, Yu-Jun Hu, and Cheng-qi He

Department of Rehabilitation, West China Hospital, Sichuan University, Chengdu, China; Province Key Laboratory of Rehabilitation Sichuan, Chengdu, China

This study was designed to determine the effects of pulsed electromagnetic fields (PEMF) on the mRNA expression of the receptor activator of NF-κ-B (RANK) and carbonic anhydrase II (CA II) in ovariectomized rat osteoclast-like cells. Marrow cells were harvested from femora and tibiae of rats, from which the ovaries had been totally excised, and cultured in 6-well chamber slides. After 1 day of incubation, the marrow cells were exposed to PEMF for 3 days with 3.8 mT, 8 Hz, and 40 min per day. Osteoclast-like cells were confirmed by both tartrate resistant acid phosphatase (TRAP) stain and bone resorption assay. The expression of RANK and CA II mRNA was determined with real-time fluorescent-nested quantitative polymerase chain reaction. Compared with the sham group, the level of serum estradiol in the ovariectomized group was significantly decreased ($p < 0.05$). The numbers of multinucleated, TRAP-positive osteoclast-like cells and resorption pits formed were observed. In invitro study, the expression of RANK and CA II were measured in sham, ovariectomized without PEMF, and ovariectomized with PEMF treatment. Compared with the ovariectomized (PEMF) experimental group and sham group, CA II mRNA expression was significantly increased in the ovariectomized control group ($p < 0.05$, 0.01, respectively). Compared with the sham group, RANK mRNA expression was significantly increased in the ovariectomized control group ($p < 0.05$). These data suggest that PEMF could regulate the expression of RANK and CA II mRNA in the marrow culture system.

Keywords PEMF; E_2; Osteoclast-Like Cell; RANKmRNA; CAIImRNA

INTRODUCTION

Osteoporosis is a condition of low bone mass and disrupted microarchitecture that results in fractures with minimal trauma. Bone is a complex tissue that remodels continually throughout life via resorption of old bone by osteoclasts and the subsequent formation of new bone by osteoblasts [1]. Osteoclast-mediated bone resorption and osteoblast-induced bone formation are critical factors that determine bone mass. An imbalance between osteoclasts and osteoblasts may leads to various bone-related disorders such as osteoporosis, osteomalacia, and osteopetrosis [2, 3]. Osteoclasts derive from hematopoietic cells of the monocyte/macrophage lineage through differentiation. During this process, the receptor activator of nuclear factor kappa B ligand (RANKL) and macrophage colony-stimulating factor (M-CSF) play crucial roles and have been identified as essential for differentiation and maintenance of osteoclasts.

So far, two types of receptors for RANKL are known: RANK and osteoprotegerin (OPG). RANK expressed on osteoclast precursors and mature osteoclasts transduces RANKL signaling. The RANKL signal in osteoclast precursor cells stimulates the activation of the three major mitogen-activated protein kinases (MAPKs), including extracellular signal-regulated kinase (ERK), c-Jun-N-terminal kinase (JNK), and p38-MAPKs [4]. The phosphoinositide kinase-3/Akt, nuclear factor of activated T-cells c1 (NFATc1), activator protein 1 (AP-1), and nuclear factor kappa B (NF-κ-B) pathways are also affected by RANKL [4–7]. These signaling pathways ultimately lead to induction and activation of the transcription factors involved in the expression of genes that characterize osteoclasts. Carbonic anhydrase isoenzyme II (CA II) also affects osteoclast function and gives rise to metabolic bone disease. CA II deficiency (formerly called osteopetrosis with renal tubular acidosis and cerebral calcification syndrome) is an autosomal recessive inborn error of metabolism that provides significant insight into osteoclast function and osteoclast-mediated bone resorption. CA II and vacuolar H^+-ATPases are involved in the extracellular acidification caused by osteoclasts. The process of acid demineralization in osteoclasts is accomplished through H^+-ATPase, which pumps hydrogen ions formed and released by specific CA II into the extracellular compartment [8, 9]. CA II catalyzes the

Received 31 October 2008; Revised 13 February 2009; Accepted 26 February 2009.

Address correspondence to Cheng-qi He, 37 Guo Xue Xiang, Chengdu 610041, P.R. China. E-mail: hechqi@yahoo.com.cn

reaction between CO_2 and H_2O to synthesize H_2CO_3, which then dissociates into H^+ and HCO_3^- [10]. Therefore, CA II plays an important role in osteoclastic bone resorption [11, 12].

Pulsed electromagnetic fields (PEMFs) are effective therapy for patients with delayed fracture healing and nonunions [13–15] and affect bone metabolism both in vivo and in vitro [16–21]. Cellular studies have demonstrated that PEMF treatment (15 Hz) results in a more differentiated and mature osteoblast [22]. Studies of the effects of PEMFs (7.5 Hz) on osteoclasts have shown that PEMF promotes the apoptosis rate of osteoclasts derived from primary osteoblasts and bone marrow cells cocultures [17] and can regulate osteoclastogenesis, bone resorption, OPG, RANKL, and M-CSF concentrations in marrow culture system [23]. However, although the biological effects of PEMF on osteoblasts and osteoclasts have been studied for many decades, the manner in which electromagnetic fields interact with cells and influence their behavior is still poorly understood.

The purpose of this study was to investigate the effects of PEMF on the expression of RANK and CA II mRNA in osteoclast-like cell cultures derived from the bone marrow of ovariectomized rat.

MATERIALS AND METHODS

Animals

Female rats (SD) at 3 months of age with body weights of 201 ± 18 g were purchased from West China Clinical Medicine College of Sichuan University Laboratory Animal Center, Chengdu, China (certificate no. 0003236). The rats were maintained at 22 ± 2°C with good ventilation, an alternate 12-hr natural light-dark cycle, and unlimited access to standard rat food and tap water. This study was approved by the medical ethics committee of the West China Hospital of Sichuan University and conforms to National Institutes of Health guidelines regarding animal experimentation.

Reagents and Electromagnetic Stimulation System

MEM-alpha and Tris used in this study were obtained from Invitrogen Co (USA). The fetal bovine serum was obtained from GIBCO (USA). Trizol was obtained from MRC Co (USA). DNA markers were obtained from Tiangen Co, (Beijing, China). Taq DNA polymerase and dNTP were obtained from Takara Bio Group (Dalian, China). RevertAid™ first strand cDNA synthesis kits were obtained from MBI Co, (Lithuania). Primer probes were obtained from Shanghai Biological Engineering (Shanghai, China).

A stimulating unit composed of the waveform generator, amplifier, and coils, which can provide a uniform PEMF for treating culture cells, was applied. The waveform generator was an extremely low frequency function generator that can generate potential signals with sinusoidal, triangular, and rectangular waveforms. Triangular wave was applied in this study. After being amplified, the signals were output to the coils. The coils formed a cylindrical solenoid, which consisted of 1000 turns of copper wire (diameter 1 mm) surrounding a plastic tube. The PEMF in the solenoid was approximately uniform. The cells were contained in a chamber that could be placed in the middle of the apparatus on a plastic shelf, and the magnetic flux was vertical to the chamber. In the study, the frequency, intensity, and time of PEMF were 8 Hz, 3.8 mT, and 40 min per day, respectively. The apparatus (Union-2000A osteoporosis treatment system) used in the present study was obtained from the Biomedical Engineering Research Institute, Chinese Academy of Medical Sciences, Tianjin. China.

Ovariectomy

In the first set of the experiments, a 36 healthy female SD rats were randomly assigned to two groups. Sham group included 12 rats in which retroperitoneal fat with the same mass as bilateral ovaries was removed under general anesthesia with 5% chloral hydrate (0.6 ml/100 g). In the ovariectomized (OVX) group 24 rats had ovariectomies performed under similar conditions of anesthesia. After 12 weeks, blood samples were collected and the rats were sacrificed. Serum was separated and stored at −20°C for later measurement of serum estradiol (E_2).

Hormone Measurements

Levels of serum E_2 were determined by chemiluminescence analysis using a Centaur automatic immunoassay apparatus (Bay Co. Germany) and counting with a XH-6010 gamma counter in parallel double-tube tests. The intrabatch and interbatch coefficient of variation (CVs) of E_2 were 2.37% and 3.04%, respectively.

Osteoclast-Like Cell Formation in Rat Marrow Cultures

Rat bone marrow cells were harvested 12 weeks after ovariectomized by the method of Chamber and Magnus [24] with minor modifications. For superficial antisepsis, the sacrificed rats were soaked two times for 5 min each in 1% iodophors liquid. Deiodination was completed with 75% alcohol. After rapid removal of soft tissues under aseptic conditions, the femora and tibiae were cleaned twice with phosphate buffered saline (PBS, pH7.4). They were then rinsed two times with a-MEM culture medium. Bone marrow cells were obtained from both femora and tibiae of the SD rats by flushing the marrow space with α-MEM (α-MEM contained 15% fetal bovine serum [FBS], Invitrogen Co.) and seeded into 6-well chamber slides (Nunc, Naperville, IL, USA) at 2 mL cell suspension/well in α-MEM containing FBS. Bone slices and glass slides were added. After 5 hr, nonadherent cells were removed with α-MEM. Half the medium was replaced every day with fresh medium, and culture was continued for 10 days.

Mature Osteoclast-Like Cell Activity Assay

After 72 hr of culture, cell creeping slices were removed and dried at room temperature. The cells were fixed in 2.5% (v/v)

glutaraldehyde at 4°C for 10 min. TRAP staining fluid was added, and the plates were incubated at 37°C for an additional 50 min. After removal of the TRAP solution, the plates were washed three times with distilled water and air-dried. The slices were sealed with glycerogelatin. Osteoclast morphology, including cellular configuration, size, and nuclei, was observed under a microscope. TRAP staining was also performed 10 days after cell isolation.

After 10 days of culture with osteoclast-like cells as described above, the bone slices were removed and cleaned ultrasonically three times for 10 min each in a 0.25M NH_4OH solution to remove adherent cells. They were then rinsed with PBS, fixed in 2.5% (v/v) glutaraldehyde, postfixed in 1% osmiumtetroxide, dehydrated with an alcohol series, and replaced in alcohol with isopentyl acetate. Finally, the bone slice samples were subjected to CO_2 critical-point drying and gold staining, and the resorptive lacunae were observed by scanning electronic microscopy (SEM, Jeol model 100S, Japan) operated at 20 kV.

TABLE 1
Primer sequences and PCR product lengths

Primer	Sequence 5–3 direction	PCR product length (bp)
RANKF-O	ATGCGAACCAGGAAAG	143
RANKR-O	CCTTGCCTGCATCACA	
RANKF	ACCTGTCTTCTAAATGCACTC	125
RANKR	CTTGCCTGCATCACAGACTT	
RANKTM	TCTGCCCTGTGGCCCAGAT	
CAIIFO:	GAGTTTGATGACTCCCAG	203
CAIIR:	TGCTGCACAGCTTTTCCAAA	
CAIIF:	GATCCAGTTTCACTTTCACTG	138
CAIIR:	TGCTGCACAGCTTTTCCAAA	
CAIITM:	CTTCACTTGGTTCACTGGAACACC	
β-actinF:	GCCAACACAGTGCTGTCT	114
β-actinR:	AGGAGCAATGATCTTGATCTT	
β-actinTM:	ATCTCCTTCTGCATCCTGTC	

Experimental Protocols

Cells derived from the OVX group were randomly and equally divided into the OVX control group and OVX experimental group. After 24 hr of incubation, culture plates (6 well) derived from the OVX experimental group were placed in the center of plastic shelves (mimicking the dimensions of the field) within an incubator, and the cultures were exposed to stimulation by PEMF. The PEMF was generated by a commercial, clinically approved proprietary device. The frequency, intensity, and time of PEMF used in the present study were 8 Hz, 3.8 mT, and 40 min per day, respectively, for 3 days. RANK and CA II mRNA assays were subsequently performed at the end of time points. The OVX control group and the sham group of cells that grew in another identical incubator without PEMF stimulation also were cultured to the same time points, and their RANK and CA II mRNA levels were assayed.

Real-Time Polymerase Chain Reaction Analysis

Total RNA was isolated using the TRIzol reagent (Invitrogen, USA). Reverse transcription and polymerase chain reactions were carried out as nested PCR. The nested RT-PCR conditions were established and optimized for each primer pair. To determine the sensitivity of the nested RT-PCR, definitive amounts of transcripts synthesized from a cloned cDNA of the corresponding gene (RANK or CA II) were used. The synthesis of the cDNA was primed separately for detection of RANK mRNA and CA II mRNA. The threshold cycle (Ct) value was calculated from amplification plots [25]. The ΔCt value for each sample was obtained by subtracting the Ct values of a housekeeping gene (β-actin). Three samples from the control, experimental, and sham groups were included in each experiment, and each experiment was carried out at least 3 times. The sequences of reaction products were confirmed by agarose gel electrophoreses, and the control reactions run in the absence of reverse transcription did not generate any product. The expression levels of RANK and CA II mRNA were determined relative to the expression level of β-actin mRNA.

The specific sequences of the PCR primers for RANK, CA II, and β-actin and the expected PCR product lengths are listed in Table 1.

Statistical Analysis

All values were expressed as mean $\pm$ SD. One-way ANOVA followed by the LSD multiple comparison procedure was performed using SigmaStat (SPSS Science). $p < 0.05$ was considered significant.

RESULTS

Serum Sex Hormones

Levels of serum E_2 in the sham group were significantly higher than those in the OVX group (54.93 $\pm$ 23.52 pg/ml vs. 31.99 $\pm$ 23.45 pg/ml) ($p < 0.05$).

Identification of Osteoclast-Like Cells

There were no osteoclast-like cells found in the bone marrow cells immediately after plating out. Osteoclast-like cells first appeared in the culture at day 3 and increased in number until the end of the culture period. Cell suspensions producing osteoclast-like cells contained osteoclast-like cells, red cells, mononuclear phagocytic systems, and fibroblast-like cells. After nonadherent cells were washed out, the cytoplasms of the osteoclast-like cells with three or more nuclei appeared to have pseudofoot-like activity (Figure 1). The number of multinucleated, TRAP-positive osteoclast-like cells was observed. They were larger than monocytes and often irregular or elliptical in configuration (Figure 2). After 10 days, the osteoclast-like cells were still

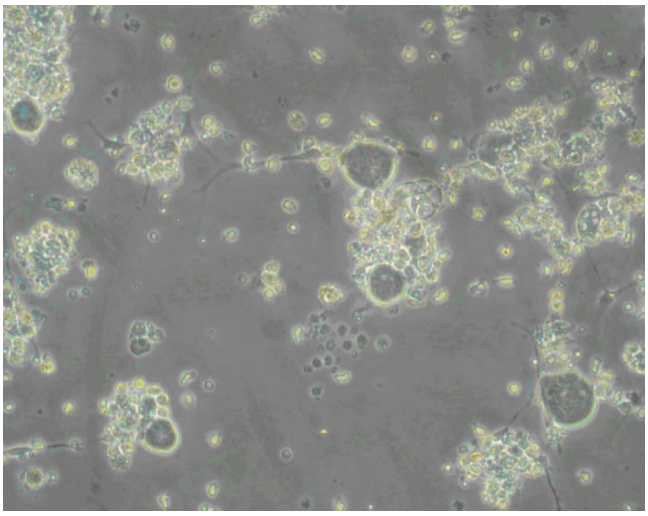

FIG. 1. Inverted phase contrast microscopic appearance of some typical rat osteoclast-like cells with 3 or more nuclei (×100).

observed, but the TRAP staining appeared faintly red. In bone resorption studies, the bone slices cultured with bone marrow cells showed an excavated pit on the surface formed by osteoclast-like cells in vitro at day 10. These lacunae were round, elliptical, or irregular (Figure 3).

Regulation of RANK and CA II mRNA Expression

Real-time fluorescent-nested quantitative PCR was carried out after the high purity of the total RNA was confirmed and the primer design and probe synthesis were validated. The Ct values of the samples were determined by comparison with a standard curve. Expression of RANK mRNA in the OVX control group was significantly higher than that in sham group ($p < 0.05$).

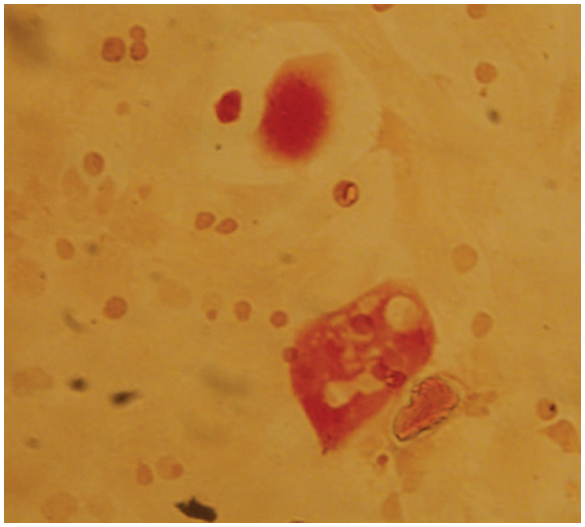

FIG. 2. Inverted phase contrast microscopic appearance of some typical rat osteoclast-like cells stained for tartrate-resistant acid phosphatase (TRAP) activity on chamber slides (×100).

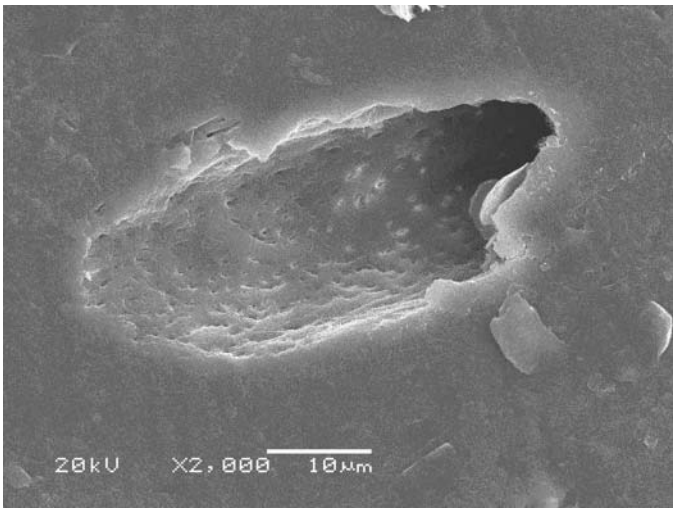

FIG. 3. Scanning electron microscopic photograph of bone slice surface cultured with marrow cells for 10 days. Irregular shape of pit was clearly observed (×2000).

Although RANK mRNA expression increased in PEMF group, no statistically significant difference was found between PEMF group and OVX control group. The expression of CA II mRNA in the OVX control group was significantly higher than that in the sham and OVX experimental groups ($p < 0.01$, $p < 0.05$, respectively) (Figures 4 and 5).

DISCUSSION

Pulsed electromagnetic fields generated by electromagnets are widely used to enhance osteogenesis and have been

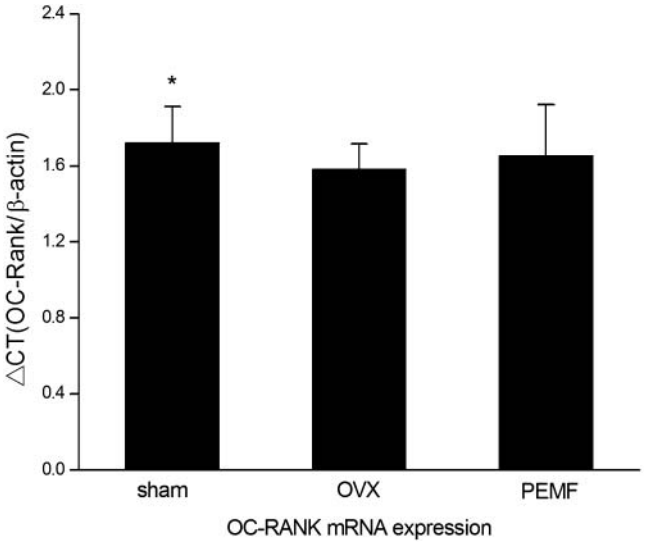

FIG. 4. Effect of PEMF on expression of RANK genes in rat osteoclast-like cell. The expression levels of RANKmRNA was determined with real-time PCR. RANKmRNA expression was increased in OVX control group. The asterisk represents significant decrease ($p < 0.05$) compared with OVX control group. ($n = 12$ in sham group and n = 24 in other two groups).

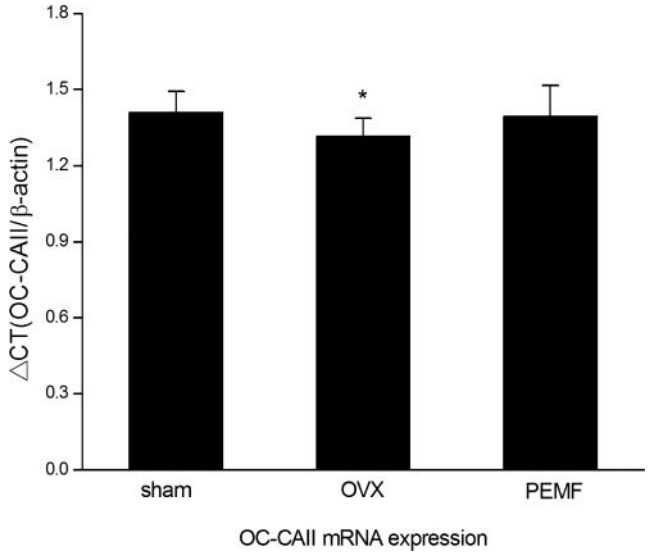

FIG. 5. Effect of PEMF on expression of carbonic anhydrase II genes in rat osteoclast-like cell.The expression levels of CAII gene was determined with real-time PCR. CAII mRNA expression was increased in OVX control group. The asterisk represents significant increase ($p < 0.05, 0.01$, respectively) compared with OVX experimental group and sham group ($n = 12$ in sham group and $n = 24$ in other two groups).

used extensively in patients with fracture nonunions or as an adjunct to assist postsurgical healing for spinal fusions. Clinical evidence shows that regardless of fracture location, therapeutic effects can be achieved for union-delayed and nonunion bone fractures using PEMF treatment [26–29]. PEMF simulation provides marked improvement at the hydroxyapatite/bone interface [30]. PEMF can directly affect not only osteoblasts, but also osteoclasts [31–33]. It is possible that effects of PEMF stimulation on osteoclastogenesis might be responsible for modulation of bone resorption. PEMF stimulation can increase or decrease osteoclastogenesis in bone marrow cells according to different PEMF signal characteristics [33].

The biphasic changes in osteoclast numbers for PEMF intensities, frequency, and time are under dispute. It has been suggested that there was cell specificity toward the electrical stimulation in terms of cyclic AMP and DNA synthesis [34]. That study showed that fibroblast-like cells responded to electric stimulation at low electric field intensity, whereas osteoblast-like cells responded only to electric stimulation at high electric field intensity. In the previous study, we found that osteoclast-like cell and bone resorption can be regulated by PEMF and that the intensity, frequency, and treatment time of PEMF might play an important role [35, 36]. PEMF with 8 Hz, 3.8 mT has maximal effect on the osteoclast and bone resorption in those studies.

RANKL is produced by osteoblasts and exerts its effects through binding to its receptor (RANK) on osteoclast precursor cells. This results in activation of osteoclast-like cells and easily brings about osteoporosis. It is known that NF-κB transcription factors carry out important roles during osteoclast differentiation and activation. Strong evidence for the importance of NF-κB in osteoclastogenesis comes from the osteopetrotic phenotype displayed in NF-κB1 (p50) and NF-κB2 (p52) double knockout mice [37]. RANK stimulation has an influence on gene expression of nuclear factor of activated T cells, calcineurin-dependent 1 (NFATc1) via AP-1. CA II existing in the osteoclastic cytoplasm accompanies variations of osteoclast activity; it appears that high gene expression during the bone absorbing period affects proliferation and activity of osteoclasts. In the process of bone resorption, the inorganic mineral is dissolved by intense acidification of the resorption site between the ruffled border and the bone surface.

CA II is an important factor for producing protons intracellularly, which are transported via vacuolar H^+-ATPases (V-ATPase) through the ruffled border cell membrane into resorption lacuna. Fluid shear stress has an effect on carbonic anhydrase II in polarized rat osteoclasts [38]. It has also been reported that the expression of CA II, cathepsin K, and MMP-9 in RAW264.7 cells was not induced by M-CSF, but by RANKL in the presence of interleuken-1α [39].

In the present study, the level of serum E_2 was significantly decreased in the OVX group compared to that in the sham group. This indicated that the ovaries were totally excised. The protective effect of estrogens on bone tissue is believed to result primarily from their antiresorptive action. Use of the OVX-induced rat osteoporotic model is recommended by the American Food and Drug Administration because it is surmised to better simulate the pathophysiological changes of osteoporosis in postmenopausal women, although the OVX-induced osteoporotic rat shows some side effects including increased weight, hair loss, and decreased activity.

The mechanical anatomical technique that was used to obtain osteoclasts from the long bones of SD rats may be regarded as classic because of several advantages. First, the osteoclasts are derived from resorbing bone tissue. These cells from animal bone marrow are most likely to resemble the characteristics of osteocytes in the physiological condition. Second, this method produces sufficient osteoclasts for the experiments. In this study, the osteoclast-like cells displayed various morphological appearances: most had irregular or elliptical configurations. TRAP staining of the osteoclast-like cells revealed uneven red deposits in the cytoplasm of these large cells. In addition, we found that the resorptive pits excavated by the osteoclast-like cells were round, elliptical, or irregular, which demonstrated the activity of these cells in the resorption experiment. It is believed that osteoclasts are terminally differentiated cells with a short survival time in vitro. At first, the survival time of osteoclasts in vitro was only about 24 hr [40]. As osteoclast culture techniques improved, the survival time of osteoclasts could be extended to as long as 144 hr [41]. In our study, the osteoclast-like cells were still observed after 10 days of culture, but TRAP staining appeared faintly red showing that the activity of the osteoclast-like cells had gradually decreased.

Studies have also demonstrated that PEMF can inhibit bone loss [42–44] and can be applied in clinical treatment. We performed in vitro screening of PEMFs for potential application to prevention and therapy for diseases involving bone loss. Primary bone marrow cells from the OVX experimental group were exposed to PEMFs with 3.8 mT and 8 Hz for 40 min per day. After 3 days, RANK and CA II gene expression was analyzed by real-time fluorescent-nested quantitative PCR. The current results indicated that PEMFs had inhibitory effects on osteoclast-like cells via the pathways of RANK and CA II mRNA expression. We presume that these changes in gene expression might be associated with signaling pathways caused by PEMF.

The activation of a series of biological effects and the release of signaling molecules may modulate various cellular functions [45, 46], including changes in the mRNA expression of multiple genes [47], and some of these regulators can be modulated by PEMF [48–50]. Although the potential for exogenous EMF to inhibit bone loss is not well understood, the expression of RANK and CA II in osteoclasts might be one of the targets of electromagnetic fields. This result suggests that the downregulation of CA II mRNA by PEMFs may be induced by both the RANKL [39] and RANK pathways.

CONCLUSION

Our data demonstrated that PEMFs applied at 3.8 mT, 8 Hz, and 40 min per day for 3 days could regulate the osteoclast-like cellic gene expression of RANK and CA II. On the basis of the current understanding of preosteoblastic/stromal cell regulation of osteoclastogenesis [51] and our own findings, we infer that PEMF might modulate the process of osteoclastogenesis and subsequent bone resorption, at least partially, through RANK and CA II.

ACKNOWLEDGMENT

This work was supported by the National Natural Science Foundation of China, Grant No. 30672215, China.

Declaration of Interest

The authors report no conflicts of interest. The authors alone are responsible for the content and writing of this article.

REFERENCES

1. Boyce, B.F., Hughes, D.E., Wright, K.R., Xing, L., and Dai, A. (1999). Recent advances in bone biology provide insight into the pathogenesis of bone diseases. *Lab Invest.*, 79, 83–94.
2. Alliston, T., and Derynck, R. (2002). Medicine: interfering with bone remodelling. *Nature*, 416, 686–687.
3. Karsenty, G., and Wagner, E.F. (2002). Reaching a genetic and molecular understanding of skeletal development. *Dev. Cell*, 2, 389–406.
4. Lee, Z.H., and Kim, H.H. (2003). Signal transduction by receptor activator of nuclear factor kappa B in osteoclasts. *Biochem. Biophys. Res. Commun.*, 305, 211–214.
5. Anderson, D.M., Maraskovsky, E., Billingsley, W.L., Dougall, W.C., Tometsko, M.E., Roux, E.R., Teepe, M.C., DuBose, R.F., Cosman, D., and Galibert, L. (1997). A homologue of the TNF receptor and its ligand enhance T-cell growth and dendritic-cell function. *Nature*, 390, 175–179.
6. Takayanagi, H., Kim, S., Koga, T., Nishina, H., Isshiki, M., Yoshida, H., Saiura, A., Isobe, M., Yokochi, T., Inoue, J., Wagner, E.F., Mak, T.W., Kodama, T., and Taniguchi, T. (2002). Induction and activation of the transcription factor NFATc1 (NFAT2) integrate RANKL signaling in terminal differentiation of osteoclasts. *Dev. Cell*, 3, 889–901.
7. Wong, B.R., Besser, D., Kim, N., Arron, J.R., Vologodskaia, M., Hanafusa, H, and Choi, Y. (1999). TRANCE, a TNF family member, activates Akt/PKB through a signaling complex involving TRAF6 and c-Src. *Mol. Cell*, 4, 1041–1049.
8. Mattsson, J.P., Skyman, C., Palokangas, H., Vaananen, K.H., and Keeling, D.J. (1997). Characterization and cellular distribution of the osteoclast ruffled membrane vacuolar H+-ATPase B-subunit using isoform-specific antibodies. *J. Bone Miner. Res.*, 12, 753–760.
9. Huang, W.H., Lau, A.T., Daniels, L.L., Fujii, H., Seydel, U., Wood, D.J., Papadimitriou, J.M., and Zheng, M.H. (1998). Detection of estrogen receptor alpha, carbonic anhydrase II and tartrate-resistant acid phosphatase mRNAs in putative mononuclear osteoclast precursor cells of neonatal rats by fluorescence in situ hybridization. *J. Mol. Endocrinol.*, 20, 211–219.
10. Salo, J., Lehenkari, P., Mulari, M., Metsikko, K., and Vaananen, H.K. (1997). Removal of osteoclast bone resorption products by transcytosis. *Science*, 276, 270–273.
11. Zelzer, E., and Olsen, B.R. (2003). The genetic basis for skeletal diseases. *Nature*, 423, 343–348.
12. Mostov, K., and Werb, Z. (1997). Journey across the osteoclast. *Science*, 276, 219–220.
13. Inoue, N., Ohnishi, I., Chen, D., Deitz, L.W., Schwardt, J.D., and Chao, E.Y. (2002). Effect of pulsed electromagnetic fields (PEMF) on late-phase osteotomy gap healing in a canine tibial model. *J. Orthop. Res.*, 20, 1106–1114.
14. Funk, R.H., and Monsees, T.K. (2006). Effects of electromagnetic fields on cells: physiological and therapeutical approaches and molecular mechanisms of interaction. A review. *Cells Tissues Organs.*, 182, 59–78.
15. Repacholi, M.H., and Greenebaum, B. (1999). Interaction of static and extremely low frequency electric and magnetic fields with living systems: health effects and research needs. *Bioelectromagnetics*, 20, 133–160.
16. Panagopoulos, D.J., Karabarbounis, A., and Margaritis, L.H. (2002). Mechanism for action of electromagnetic fields on cells. *Biochem. Biophys. Res. Commun.*, 298, 95–102.
17. Chang, K., Chang, W.H., Tsai, M.T., and Shih, C. (2006). Pulsed electromagnetic fields accelerate apoptotic rate in osteoclasts. *Connect. Tiss. Res.*, 47, 222–228.
18. Zhuang, H., Wang, W., Seldes, R.M., Tahernia, A.D., Fan, H., and Brighton, C.T. (1997). Electrical stimulation induces the level of TGF-beta1 mRNA in osteoblastic cells by a mechanism involving calcium/calmodulin pathway. *Biochem. Biophys. Res. Commun.*, 237, 225–229.
19. Blank, M., and Goodman, R. (2004). Initial interactions in electromagnetic field-induced biosynthesis. *J. Cell Physiol.*, 199, 359–363.
20. Brighton, C.T., Wang, W., Seldes, R., Zhang, G., and Pollack, S.R. (2001). Signal transduction in electrically stimulated bone cells. *J. Bone Joint. Surg. Am.*, 83-A, 1514–1523.
21. Khatib, L., Golan, D.E., and Cho, M. (2004). Physiologic electrical stimulation provokes intracellular calcium increase mediated by phospholipase C activation in human osteoblasts. *FASEB J.*, 18, 1903–1905.
22. Lohmann, C.H., Schwartz, Z., Liu, Y., Guerkov, H., Dean, D.D., Simon, B., and Boyan, B.D. (2000). Pulsed electromagnetic field stimulation of MG63 osteoblast-like cells affects differentiation and local factor production. *J. Orthop. Res.*, 18, 637–646.
23. Chang, K., Chang, W.H., Huang, S., Huang, S., and Shih, C. (2005). Pulsed electromagnetic fields stimulation affects osteoclast formation by

modulation of osteoprotegerin, RANK ligand and macrophage colony-stimulating factor. *J. Orthop. Res.*, 23, 1308–1314.
24. Chambers, T.J., and Magnus, C.J. (1982). Calcitonin alters behaviour of isolated osteoclasts. *J. Pathol.*, 136, 27–39.
25. Aung, H.T., Schroder, K., Himes, S.R., Brion, K., van Zuylen, W., Trieu, A., Suzuki, H., Hayashizaki, Y., Hume, D.A., Sweet, M.J., and Ravasi, T. (2006). LPS regulates proinflammatory gene expression in macrophages by altering histone deacetylase expression. *FASEB J.*, 20, 1315–1327.
26. Bassett, C.A., Mitchell, S.N., and Gaston, S.R. (1981). Treatment of ununited tibial diaphyseal fractures with pulsing electromagnetic fields. *J. Bone Joint. Surg. Am.*, 63, 511–523.
27. Garland, D.E., Moses, B., and Salyer, W. (1991). Long-term follow-up of fracture nonunions treated with PEMFs. *Contemp. Orthop.*, 22, 295–302.
28. Gossling, H.R., Bernstein, R.A., and Abbott, J. (1992). Treatment of ununited tibial fractures: a comparison of surgery and pulsed electromagnetic fields (PEMF). *Orthopedics.*, 15, 711–719.
29. Sharrard, W.J., Sutcliffe, M.L., Robson, M.J., and Maceachern, A.G. (1982). The treatment of fibrous non-union of fractures by pulsing electromagnetic stimulation. *J. Bone Joint Surg. Br.*, 64, 189–193.
30. Fini, M., Giavaresi, G., Giardino, R., Cavani, F., and Cadossi, R. (2006). Histomorphometric and mechanical analysis of the hydroxyapatite-bone interface after electromagnetic stimulation: an experimental study in rabbits. *J. Bone Joint Surg. Br.*, 88, 123–128.
31. Luben, R.A., Cain, C.D., Chen, M.C., Rosen, D.M., and Adey, W.R. (1982). Effects of electromagnetic stimuli on bone and bone cells in vitro: inhibition of responses to parathyroid hormone by low-energy low-frequency fields. *Proc. Natl. Acad. Sci. USA*, 79, 4180–4184.
32. McLeod, K.J., Donahue, H.J., Levin, P.E., Fontaine, M.A., and Rubin, C.T. (1993). Electric fields modulate bone cell function in a density-dependent manner. *J. Bone Miner. Res.*, 8, 977–984.
33. Chang, K., Hong-Shong Chang, W., Yu, Y.H., and Shih, C. (2004). Pulsed electromagnetic field stimulation of bone marrow cells derived from ovariectomized rats affects osteoclast formation and local factor production. *Bioelectromagnetics*, 25, 134–141.
34. Binderman, I., Somjen, D., Shimshoni, Z., Levy, J., Fischler, H., and Korenstein, R. (1985). Stimulation of skeletal-derived cell cultures by different electric field intensities is cell-specific. *Biochim. Biophys. Acta*, 844, 273–279.
35. Huang, L., Wang, W., Xiao, D., Yang, L., Lei, Z., and He, C. (2008). [Effect of pulsed electromagnetic fields of different treatment time on bone mineral density of femur in ovariectomized rats]. *Zhongguo Xiu Fu Chong Jian Wai Ke Za Zhi*, 22, 548–550.
36. Yang, Y.H., He, C.Q., Yang, L., Wang, W., and Lei, Z.J. (2008). [Effects of different intensity pulsed electromagnetic fields on serum estradiol of ovariectomized rats]. *Sichuan Da Xue Xue Bao Yi Xue Ban*, 39, 256–258.
37. Iotsova, V., Caamano, J., Loy, J., Yang, Y., Lewin, A., and Bravo, R. (1997). Osteopetrosis in mice lacking NF-kappaB1 and NF-kappaB2. *Nat. Med.*, 3, 1285–1289.
38. Zhang, Q., Liang, X., Zhu, B., Dong, Q., Xu, L., Xia, L., Hu, J., Fu, J., and Liu, M. (2006). Effects of fluid shear stress on mRNA expression of carbonic anhydrase II in polarized rat osteoclasts. *Cell. Biol. Int.*, 30, 714–720.
39. Fujisaki, K., Tanabe, N., Suzuki, N., Kawato, T., Takeichi, O., Tsuzukibashi, O., Makimura, M., Ito, K., and Maeno, M. (2007). Receptor activator of NF-kappaB ligand induces the expression of carbonic anhydrase II, cathepsin K, and matrix metalloproteinase-9 in osteoclast precursor RAW264.7 cells. *Life Sci.*, 80, 1311–1318.
40. Chambers, T.J., Revell, P.A., Fuller, K., and Athanasou, N.A. (1984). Resorption of bone by isolated rabbit osteoclasts. *J. Cell Sci.*, 66, 383–399.
41. Fenton, A.J., Martin, T.J., and Nicholson, G.C. (1993). Long-term culture of disaggregated rat osteoclasts: inhibition of bone resorption and reduction of osteoclast-like cell number by calcitonin and PTHrP[107–139]. *J. Cell Physiol.*, 155, 1–7.
42. Rubin, C.T., McLeod, K.J, and Lanyon, L.E. (1989). Prevention of osteoporosis by pulsed electromagnetic fields. *J. Bone Joint Surg. Am.*, 71, 411–417.
43. Tabrah, F., Hoffmeier, M., Gilbert, F., Jr., Batkin, S., and Bassett, C.A. (1990). Bone density changes in osteoporosis-prone women exposed to pulsed electromagnetic fields (PEMFs). *J Bone Miner. Res.*, 5, 437–442.
44. Zati, A., Gnudi, S., Mongiorgi, R., Giardino, R., Fini, M., Valdre, G., Galliani, I., and Montagnani, A.M. (1993). Effects of pulsed magnetic fields in the therapy of osteoporosis induced by ovariectomy in the rat. *Boll. Soc. Ital. Biol. Sper.*, 69, 469–475.
45. Falany, M.L., Thames, A.M., 3rd., McDonald, J.M., Blair, H.C., McKenna, M.A., Moore, R.E., Young, M.K., and Williams, J.P. (2001). Osteoclasts secrete the chemotactic cytokine mim-1. *Biochem. Biophys. Res. Commun.*, 281, 180–185.
46. Ye, H., Arron, J.R., Lamothe, B., Cirilli, M., Kobayashi, T., Shevde, N.K., Segal, D., Dzivenu, O.K., Vologodskaia, M., Yim, M., Du, K., Singh, S., Pike, J.W., Darnay, B.G., Choi, Y., and Wu, H. (2002). Distinct molecular mechanism for initiating TRAF6 signalling. *Nature*, 418, 443–447.
47. Rubin, J., Rubin, C., and Jacobs, C.R. (2006). Molecular pathways mediating mechanical signaling in bone. *Gene*, 367, 1–16.
48. Cossarizza, A., Angioni, S., Petraglia, F., Genazzani, A.R., Monti, D., Capri, M., Bersani, F., Cadossi, R., and Franceschi, C. (1993). Exposure to low frequency pulsed electromagnetic fields increases interleukin-1 and interleukin-6 production by human peripheral blood mononuclear cells. *Exp. Cell Res.*, 204, 385–387.
49. Jonai, H., Villanueva, M.B., and Yasuda, A. (1996). Cytokine profile of human peripheral blood mononuclear cells exposed to 50 Hz EMF. *Ind. Health*, 34, 359–368.
50. Pessina, G.P., and Aldinucci, C. (1998). Pulsed electromagnetic fields enhance the induction of cytokines by peripheral blood mononuclear cells challenged with phytohemagglutinin. *Bioelectromagnetics*, 19, 445–451.
51. Khosla, S. (2001). Minireview: the OPG/RANKL/RANK system. *Endocrinology*, 142, 5050–5055.

Mutation Research 667 (2009) 82–97

Contents lists available at ScienceDirect

Mutation Research/Fundamental and Molecular Mechanisms of Mutagenesis

journal homepage: www.elsevier.com/locate/molmut
Community address: www.elsevier.com/locate/mutres

Review

Genetics, environmental factors and the emerging role of epigenetics in neurodegenerative diseases

Lucia Migliore [a,*], Fabio Coppedè [b]

[a] Department of Human and Environmental Sciences, University of Pisa, Via S. Giuseppe 22, 56126 Pisa, Italy
[b] Department of Neuroscience, University of Pisa, Italy

ARTICLE INFO

Article history:
Received 3 April 2008
Received in revised form 29 August 2008
Accepted 24 October 2008
Available online 31 October 2008

Keywords:
Alzheimer's disease (AD)
Parkinson disease (PD)
Amyotrophic lateral sclerosis (ALS)
Genetics
Environmental factors
Epigenetics

ABSTRACT

In the present review we summarize recent advances in the understanding of the interaction between genetics and environmental factors involved in complex multi-factorial neurodegenerative disorders such as Alzheimer's disease (AD), Parkinson's disease (PD) and Amyotrophic Lateral Sclerosis (ALS). The discovery of several genes responsible for the familial forms has led to a better comprehension of the molecular pathways involved in the selective neuronal degeneration which is specific for each of these disorders. However, the vast majority of the cases occurs as sporadic forms, likely resulting from complex gene–gene and gene–environment interplay. Several environmental factors, including, pesticides, metals, head injuries, lifestyles and dietary habits have been associated with increased disease risk or even with protection. Hundreds of genetic variants have been investigated as possible risk factors for the sporadic forms, but results are often conflicting, not repeated or inconclusive. New approaches to environmental health research are revealing us that at the basis there could be chemically induced changes in gene regulation and emphasise the importance of understanding the susceptibility of the human epigenome to dietary and other environmental effects.

Contents

* Corresponding author. Tel.: +39 0502211029; fax: +39 0502211034.
E-mail address: l.migliore@geog.unipi.it (L. Migliore).

0027-5107/$ – see front matter © 2008 Elsevier B.V. All rights reserved.
doi:10.1016/j.mrfmmm.2008.10.011

1. Introduction

Genetic predisposition for a disease is best predicted in the context of environmental exposures, mainly for those so-called human complex diseases, including neurodegenerative disorders such as Alzheimer's diseases (AD), Parkinson's disease (PD) and amyotrophic lateral sclerosis (ALS), which are the 3 major neurodegenerative diseases, affecting several million people worldwide. They are defined as complex multifactorial disorders since both familial and sporadic forms are known. Familial forms represent only a minority of the cases (ranging from 5 to 10% of the total), whereas the vast majority of AD, PD and ALS occurs as sporadic forms, likely resulting from the contribution of complex interactions between genetic and environmental factors superimposed on slow, sustained neuronal dysfunction due to aging. Several causative genes for the familial forms have been discovered in recent years, they are inherited as Mendelian traits and their discovery has led to a better comprehension of the molecular pathways responsible for the selective neuronal degeneration which is specific for each disorder. In parallel, genetic association studies based on the "candidate gene approach" and genome-wide association studies have revealed several genetic variants that might act as susceptibility factors for the sporadic forms, likely in combination with environmental exposure to neurotoxicants. New approaches aimed at a better understanding of the contribution of environmental and dietary factors suggest that some of them could be involved in the development of neurodegeneration by causing epigenetic modifications. Environmental agents and dietary factors can interfere with gene regulation in a long-term fashion, beginning at early developmental stages; however, these perturbations do not have pathological results until significantly later in life. For example available data emphasize that deficiency of folate and vitamin B12 can lead to elevated concentrations of total homocysteine and disturbe methylation pathways in the brain. The emerging connections between reactive oxygen species (ROS) and epigenetic mechanisms offer new insight into those neurodegenerative disorders where oxidative stress has been implicated, among which AD, PD, and ALS.

2. Alzheimer's disease (AD)

Alzheimer's disease represents the most common form of dementia in the elderly, characterized by progressive loss of memory and cognitive capacity severe enough to interfere with daily functioning and the quality of life. AD affects several million people worldwide and both the incidence and the prevalence of the disease increase with advancing age. The estimated number of individuals afflicted with this disease is now approaching 5 million in the United States alone, and around 24 million people have dementia in the world. The demographics of the aging of the general population lead to projections that the incidence of AD will continue to escalate over the next several decades in both industrialised and developing countries, thus becoming a major health concern. Both the prevalence and the incidence of the disease are higher in women compared to men, particularly in individuals aged over 80 years.

Table 1
Causative genes for familial forms of neurodegenerative diseases.

Designation	Locus	Gene	Inheritance	Function or probable function
AD1	21q21.2	*Amyloid precursor protein*	AD	Precursor protein of Aβ peptides
AD3	14q24.3	*Presenilin 1*	AD	Component of the γ-secretase complex
AD4	1q31-q42	*Presenilin 2*	AD	Component of the γ-secretase complex
PARK1 and PARK4	4q21	*α-Synuclein*	AD	Presynaptic protein, component of Lewy Bodies
PARK2	6q25.2-q27	*Parkin*	AR	Ubiquitin E3 ligase
PARK3	2p13	Unknown	AD	Unknown
PARK5	4p14	*UCH-L1*	AD	Ubiquitin C-terminal hydrolase
PARK6	1p35-36	*PINK1*	AR	Mitochondrial kinase
PARK7	1p36	*DJ-1*	AR	Mitochondrial protein, Antioxidant defence
PARK8	12p11.2	*LRRK2*	AD	Protein kinase
PARK9	1p36	*ATP13A2*	AR	Lysosomal 5 P-type ATPase
PARK10	1p32	Unknown	AD	Unknown
PARK11	2q36-37	Unknown	AD	Unknown
PARK12	Xq21-q25	Unknown	Unknown	Unknown
PARK13	2p12	*OMI/HTRA2*	Unknown	Mitochondrial serine protease
ALS1	21q21	*SOD1*	AD	Superoxide dismutase, Antioxidant defence
ALS2	2q33	*Alsin*	AR	Guanine nucleotide exchange factor for RAB5A
ALS3	18q21	Unknown	AD	Unknown
ALS4	9q34	*Senataxin*	AD	DNA/RNA helicase, DNA repair
ALS5	15q15.1-q21.1	Unknown	AR	Unknown
ALS6	16q12.1-q12.2	Unknown	AD	Unknown
ALS7	20pter	Unknown	AD	Unknown
ALS8	20q13.3	*VAPB*	AD	Vesicle associated membrane protein
ALS and FTDP	17q21	*MAPT*	AD	Assembly of microtubules
MND, dynactin type	2p13	*Dynactin 1*	AD	Promotion of synapse stability

Biological explanations for gender-specific differences in the phenotype of AD include different brain morphology and function with higher susceptibility for pathological lesions in women and greater cognitive reserve in men. Sex differences were also reported for the expression of antioxidant enzymes related to post-menopausal hormonal changes. Specifically, the increase in gonadotropin concentrations, and the decrease in estrogens production following menopause/andropause, might work in conjunction for the development of the disease. No striking racial differences appear in the prevalence or incidence of AD and no geographic isolates of the disease are known [1–7].

The occurrence of extracellular amyloid deposits or plaques and the presence of neurofibrillary tangles composed of intraneuronal aggregates of hyperphosphorylated tau protein are the two cardinal histopathologic hallmarks of the disease. One of the most important early discoveries in understanding the etiology of AD was that the primary component of the extracellular amyloid deposits in AD brains was an approximately 40-residue long peptide, known as amyloid β (Aβ) peptide. It was subsequently established that Aβ is the product of the proteolytic processing of its precursor, the amyloid precursor protein (APP). APP can be processed by γ-secretases (presenilins) and α-secretases (ADAM10 and TACE) producing non-amyloidogenic peptides, or by γ- and β-secretases (BACE) producing Aβ peptides. Therefore the balance between different secretase activities is very important in the maintenance of the physiological levels of non-amyloidogenic and amyloidogenic fragments. The two major forms of Aβ that are produced by APP processing under normal conditions are 40 and 42 residues in length (Aβ40 and Aβ42, respectively). In a normal individual, the majority of Aβ produced is of the shorter variety, Aβ40; whereas AD causative mutations lead to altered APP production and/or processing [8,9].

2.1. Genetics of AD

Similarly to many other neurodegenerative diseases, AD is a genetically complex and heterogeneous disorder. Rare, fully penetrant mutations in 3 genes (*APP*, *PSEN 1* and *PSEN 2*) are responsible for familial early-onset (<65 years) autosomal dominant forms (EOAD). Mutations in the *APP* gene either increase total Aβ levels or just Aβ42 alone [8], whereas mutations in *PSEN 1* and *PSEN 2* act differently with regard to Aβ generation, resulting in reduced Aβ40 production or increased Aβ42 levels [9]. AD causative genes are listed in Table 1.

However, the majority of AD cases (90–95%) are non-familial late onset sporadic forms (LOAD >65 years), and there is now strong consensus that risk and/or onset age variation for LOAD is probably conferred by common polymorphisms with relatively low penetrance (Table 2). Over the last two decades more than 300 genes have been investigated as possible genetic determinants of AD by means of association studies; however, with the exception of the *APOE* gene, no consensus has definitively agreed on even one of them, given the absence of consistency of the associations observed within independent populations [10]. The conflicting results in genetic association studies reflect the different genetic constitution in different ethnic backgrounds and are also indicative of a role played by gene–gene and gene–environment interactions in AD pathogenesis. Moreover, factors such as the sample size of the case–control populations have often led to false positive or false negative results. Several associations observed in studies with small populations of fewer than 100 cases and controls have not been repeated in subsequent studies empowered by the sample size. Moreover, negative results obtained in small populations have discouraged further investigations of potential relevant genes [10]. These general observations remain valid also when considering the amount of conflicting results observed in PD or ALS association studies.

In addition to association studies, genetic linkage studies performed on populations with LOAD have defined several chromosomal regions of interest that often extend several centimorgans, making it difficult to find the disease-causing variations. A consensus has emerged for regions on chromosomes 9, 10 and 12, likely containing major AD genetic determinants [11].

Table 2
Some of the proposed susceptibility genes for neurodegenerative diseases.

Genetic variant(s)	Associated with
Alzheimer's disease	
APOE-ε4	Increased risk
SORL1 variants	Increased risk
ACE intron 16 (ins/del)	Increased risk
ACE rs1800764, rs4291, rs4343	Decreased risk
CHRNB2 rs4845378	Decreased risk
CST3 5′UTR-157, 5′UTR-72	Increased risk
CST3 A25T	Increased risk
ESR1 PvuII, XbaI	Increased risk
GAPDHS rs12984928, rs4806173	Decreased risk
IDE rs2251101	Decreased risk
MTHFR A1298C	Decreased risk
NCSTR 119 intron 16	Increased risk
PRPN M129V	Decreased risk
PSEN1 rs165932	Decreased risk
TF P570S	Increased risk
TFAM rs2306604	Decreased risk
TNF rs4647198 (-1031)	Increased risk
GOLPH2 rs10868366[a], rs7019241[a]	Decreased risk
Rs 9886784 (Chromosome 9)[a]	Increased risk
Rs 10519262 (between *ATP8B4* and *SLC27A2*)[a]	Increased risk
Parkinson's disease	
SNCA Rep1	Increased risk
LRRK2 G2385R	Increased risk[b]
MAPT H1 haplotype	Increased risk
UCHL1 S18Y	Decreased risk[c]
GSTM1 null genotype	Increased risk[d 1]
GSTP1 variants	Increased risk[d 2]
CYP2D6 variants	Increased risk[d 3]
FAM 79B Rs 1000291[a]	Increased risk
UNC5C Rs 2241743[a]	Increased risk
Rs 3018626 (Chromosome 11)[a]	Increased risk
Amyotrophic lateral sclerosis	
APE1 D148E	Conflicting results
ANG G110G	Conflicting results
hOGG1 Ser326Cys	Increased risk in males
VEGF variants	Inconclusive results
HFE H63D	Increased risk
SMN1 variable copy number	Increased risk
DPP6 variant[a]	Increased risk

[a] From genome-wide association studies.
[b] Only in Asiatic populations.
[c] Conflicting results.
[d] In combination with environmental factors (1, solvents; 2, pesticides and herbicides; 3, pesticides, tobacco smoking).

2.2. Causative genes for familial AD

2.2.1. Amyloid precursor protein gene: APP

A link between AD and a missense mutation of the *amyloid precursor protein* gene (*APP*), on chromosome 21q21.2, was identified in 1991 [12]. Several *APP* mutations have been subsequently found to be causal of EOAD in different families: all of them are situated at or near secretase cleavage sites and alter APP proteolysis, and therefore Aβ peptides production (for an overview of all APP mutations see the "AD mutation database" at http://molgen.www.uia.ac.be/ADMutations/). In addition to point mutations, there is evidence of APP locus duplication in 5 families with autosomal dominant EOAD and cerebral amyloid angiopathy [13], and in a Finnish family with dementia and intracerebral haemorrhage [14]. These recent findings suggest that the overexpression of the *APP* gene alone is sufficient to cause AD. In addition, there is evidence that *APP* promoter mutations that significantly increase APP expression levels are associated with the risk of AD [15].

A previous suggestion that *APP* over-expression could be responsible of AD came from observations on Down Syndrome (DS) individuals. By the age of 40 years, virtually all adults with DS have sufficient neuropathology for a diagnosis of AD. The overexpression of the *APP* gene, due to the presence of 3 copies of chromosome 21, was the major candidate for the onset of AD in DS subjects [16]. Even if recent findings do not support *APP* overexpression in DS brains, however numerous other genes functionally linked to APP processing were observed to be dysregulated in adult DS brains analysed by microarray or quantitative PCR analysis [17,18].

2.2.2. Presenilin genes: PSEN1 and PSEN2

The *presenilin 1* gene (*PSEN1*) on chromosome 14q24.3, and the *presenilin 2* gene (*PSEN2*) on chromosome 1q31–q42 have been associated with EOAD [19–21]. Since then, more than 160 mutations in *presenilins* have been described: over 150 in *PSEN1* and a few in *PSEN2* (http://molgen.www.uia.ac.be/ADMutations/). The γ-secretase complex is comprised of the integral membrane proteins presenilin, nicastrin, Aph-1, and Pen-2. Presenilins facilitate the cleavage of APP, γ-secretase cleavage, which generates Aβ peptides, and presenilin 1 directly participate in the catalytic core of the γ-secretase complex. Both *PSEN1* and *PSEN2* AD causative mutations cause a subtle shift in the cleavage of the transmembrane domain of APP, resulting in an increased Aβ42/Aβ40 ratio [22].

In addition to AD causative missense mutations, several polymorphisms in non-coding regions of the *PSEN1* gene have been evaluated in association studies as possible AD risk factors; there are some reports of associations between polymorphisms in the *PSEN1* regulatory and intronic regions and AD risk [23,24]. Also polymorphisms in non-coding regions of *PSEN2* are currently under study, as sporadic AD contributors [25,26].

2.3. AD susceptibility genes

2.3.1. Apolipoprotein E gene: APOE

The *apolipoprotein E* gene (*APOE*) on chromosome 19q13 is the most highly replicated genetic risk factor for LOAD. The first description of an association between the *APOE-ε4* allele and LOAD dates back to 1993 [27]. The *APOE-ε4* allele imposes a 2.3–3-fold increased risk of AD for chromosome copy carried by an individual, compared to the common *APOE-ε3* one, while the *APOE-ε2* allele decreases the risk [28]. Also the age at onset of AD is a function of the number of *APOE-ε4* alleles; AD begins early in *APOE-ε4* homozygous individuals, respect to *APOE-ε4* non-carriers; while heterozygous individuals have an intermediate age at onset [10]. Age is the most important factor modulating the impact of the *APOE-ε4* allele. The effect of the *APOE-ε4* allele on the risk of AD decreases with increasing human age; however, it varies also as a function of both sex and ethnic group [28]. The *APOE-ε4* variant is associated with higher plasma cholesterol levels, and is supposed to enhance Aβ deposition and the formation of neuritic plaques, however the presence of the *APOE-ε4* variant is neither necessary nor sufficient to develop the disease [28]. More than 50% of the genetic variance of AD is not due to mutations in *APP*, *PSEN1*, *PSEN2* and *APOE-ε4*, suggesting the existence of additional susceptibility loci. It is considered that there might be as many as 4 additional genes with similar effect size to *APOE* yet to be discovered [29]. However, despite several genes have been associated with the risk of AD, none of them has been repeated and confirmed as an AD susceptibility factor with the same consistency as *APOE-ε4*.

2.3.2. Genes involved in Aβ biosynthesis: BACE1 and BACE2, NCSTN and PEN-2

The production of Aβ42 peptides requires both β-secretase and γ-secretase cleavage. BACE1, located on chromosome 11q23 is the

major β-secretase activity in humans with abundant expression in the central nervous system, while its homologue BACE2 resides in the DS critical region on chromosome 21q22. Polymorphisms in *BACE1* and *BACE2* have been studied for their role in sporadic AD risk, and several papers report association between polymorphisms of *BACE1* and disease risk, mainly in *APOE-ε4* carriers [30,31].

Beside presenilins, 3 other proteins (Aph1, PEN2 and nicastrin) are associated with γ-secretase activity. The *nicastrin* gene (*NCSTN*) has been screened for mutations and polymorphisms in both familial and sporadic AD cases. A sequence variant (N417Y) predicted to change the amino acid sequence of the gene was present in AD cases as well as in controls and did not change Aβ42 production, suggesting no pathological role [32,33]. A polymorphism in intron 16 of the *NCSTN* gene seems to be associated with increased LOAD risk [24]. The analysis of 4 *PEN2* polymorphisms in a large AD family sample comprising over 700 subjects, suggested that *PEN2* is not a major AD risk factor [34]. However, recent findings support a role for *PEN2* variants in Sardinian EOAD patients [35] and in a Chinese LOAD population [36].

2.3.3. The neuronal sortilin-related receptor: SORL1

The *SORL1* gene (also known as *LR11* or *SORLA*) regulates APP processing directing trafficking of APP into recycling pathways; when *SORL1* is under-expressed, APP is sorted into Aβ-generating compartments [37]. There is a broad consensus suggesting that polymorphisms changing *SORL1* expression or function are associated with AD [37,38].

2.3.4. Other genes

Several hundreds of association papers have been published in recent years reporting a total of over 1000 different polymorphisms on more than 300 genes which have been studied as possible AD susceptibility factors (an updated overview can be found at the AlzGene database: http://www.alzgene.org). In most cases a defined polymorphism has been studied only in one or two different labs, often with conflicting results, making it difficult to come to a conclusion. Recently, Bertram et al. [24] published the largest meta-analysis of AD association studies. Their results were based on 789 publications reporting 802 different polymorphisms in 277 genes. Among these papers authors selected those polymorphisms which had been studied in at least 3 independent research articles, for a total of 127 variants in 69 genes which had sufficient genotype data available for meta-analysis. A total of 24 polymorphisms (4 in *APOE*-loci and the remaining in 13 non-*APOE*-loci) yielded significant summary Odds Ratios (ORs), suggesting that in addition to *APOE* there might be other 13 potential AD susceptibility genes. The authors suggested that the 4 associations in *APOE*-loci could be potentially due to linkage disequilibrium with the *APOE-ε4* allele. On the contrary, variants in other 13 genes (*ACE*, *CHRNB2*, *CST3*, *ESR1*, *GAPDHS*, *IDE*, *MTHFR*, *NCSTR*, *PRPN*, *PSEN1*, *TF*, *TFAM*, and *TNF*) resulted in potential LOAD risk or protective alleles (details are shown in Table 2).

More recently, Li et al. [39] published results from a genome-wide association analysis in a case–control study of 753 AD patients and 736 matched controls, providing additional evidence for association between AD and two polymorphisms in the *GOLPH2* gene, another (rs9886784) on chromosome 9, and an intragenic polymorphism (rs10519262) between *ATP8B4* and *SLC27A2*. They are all additional candidate genetic risk factors for AD to be validated in further studies [39].

As a consequence of the increasing emerging role of DNA repair mechanisms in neurodegeneration several polymorphisms in DNA repair genes (including *hOGG1* and *XRCC* genes) have been recently studied as possible LOAD risk factors. However, none of them gave a statistically significant result in association analyses [40,41].

Table 3
Some of the proposed environmental factors for neurodegenerative diseases.

Environmental factor(s)	Associated with
Alzheimer's disease	
Metals (iron, copper, zinc, mercury, aluminium)	Increased risk, inconclusive results
Pesticides	Increased risk
Solvents	Increased risk, inconclusive results
Electromagnetic fields	Increased risk, inconclusive results
Caloric restriction	Protection
Antioxidants	Protection
Mediterranean diet, fruit and vegetables	Protection
Fish and omega-3 fatty acids	Protection
Traumatic brain injuries	Increased risk
Infections and inflammation	Increased risk
Parkinson's disease	
Metals (iron, copper, manganese, lead)	Increased risk, conflicting results
Rural environment (pesticides, herbicides)	Increased risk
Tobacco smoking	Protection
Caffeine (coffee and tea drinking)	Protection
Fruit and vegetables, legumes, nuts	Protection
Fish	Protection
Head injuries with loss of consciousness	Increased risk
Amyotrophic lateral sclerosis	
Metals (lead)	Increased risk
Pesticides and insecticides	Increased risk
Electromagnetic fields	Increased risk
Some sports (soccer, football)	Increased risk
Head injuries	Increased risk
Tobacco smoking	Increased risk, in women

2.4. Environmental factors in AD pathogenesis

Several environmental factors have been studied, in recent years, as possible AD risk factors; among them metals, pesticides, solvents, electromagnetic fields, brain injuries, inflammation, educational levels, lifestyles and dietary factors (Table 3).

2.4.1. Metals, solvents, pesticides and electromagnetic fields

Metals have been extensively studied as potential AD risk factors and even if a direct causal role for aluminium or other transition metals such as zinc, copper, iron and mercury in AD has not yet been definitively demonstrated, epidemiological evidence suggests that elevated levels of these metals in the brain may be linked to the development or the progression of the disease. Ingestion of aluminium in drinking water was associated with an increased risk of AD; however other studies failed to find such association [42,43]. The homeostasis of zinc, copper and iron are altered in the brain of AD individuals, and under mildly acidic conditions, such as those believed to occur in AD brain, iron and zinc ions have been observed to induce Aβ aggregation [44]. Another risk factor for AD is inorganic mercury, often present in dental amalgam applications, and a role for *APOE* as a mediator of the toxic effect of mercury has been largely suggested [45]. A recent analysis of 24 published studies assessing the role of occupational AD risk factors revealed a statistically consistent association only for pesticides, whereas the evidence of association was less consistent for solvents and electromagnetic fields, and absent for aluminium and lead [46].

2.4.2. Diet, lifestyle and exercise

Dementia risk is the result of exposure to both harmful and protective factors along the life course, and among them dietary and lifestyle habits seem to play a very important role. Several reports suggest that serum cholesterol levels and dietary fat intake, as well as increased homocysteinemia and oxidative stress have a role in dementia risk [47,48]. In 1997, with a meta-analysis of community based studies on diet, Grant [49] observed a positive relationship between caloric, as well as fat, intake and the prevalence of AD, providing a strong link between diet and the disease. Moreover, the author observed that both the incidence of the disease and the penetrance of the *APOE-ε4* variant change for ethnic groups when living in different countries with different fat intake [49]. Subsequently, Smith et al. observed a decreased consumption of fruit, vegetables and antioxidant nutrients, as well as an increased caloric intake, in AD subjects compared with healthy controls [50]. Since then, accumulating evidence suggests that dietary restriction, antioxidants, and Mediterranean diet are good nutritional interventions in the prevention and treatment of AD [51,52]. Moreover, there is also evidence that frequent consumption of fruit and vegetables, fish, and omega-3 rich oils may decrease the risk of dementia and AD, especially among *APOE-ε4* non-carriers [46]. Therefore, in older subjects, healthy diets, antioxidant supplements and the prevention of nutritional deficiencies, combined with a moderate physical activity and intellectual stimulation, could be considered the first line of defence against the development and progression of predementia and dementia syndromes [48].

2.4.3. Head injuries and inflammation

Among other factors accumulating evidence implicates traumatic brain injury as a possible predisposing factor in AD development [53]. Moreover, there is also evidence for a role of systemic infections and inflammation in AD pathogenesis [54].

3. Parkinson's disease (PD)

Parkinson's disease is the second most common neurodegenerative disorder affecting 1–2% of the population over the age of 50 years, with a current estimation of 1.5 million cases in the US alone. Clinically, the disease is characterized by resting tremor, rigidity, bradykinesia, and postural instability with some improvement with dopaminergic therapy. Pathologically, PD is characterized by progressive and profound loss of neuromelanin containing dopaminergic neurons in the substantia nigra with the presence of eosinophilic, intracytoplasmic inclusions termed as Lewy bodies (LB) containing aggregates of α-synuclein as well as other substances, and Lewy neurites in surviving neurons [55].

Relatively little is known regarding the mechanisms of PD pathogenesis. It has been suggested that the selective loss of dopaminergic neurons and the accumulation of α-synuclein are influenced by impairments of the ubiquitin–proteasomal system, mitochondrial dysfunction, and decreased protection against oxidative stress and apoptosis. These defects resulting from a genetic causation, an environmental risk factor or a combination of the two superimposed on slow, sustained neuronal dysfunction due to aging [56]. The incidence of PD is greater in men than in women and gender differences have been shown in response to disease treatment, for example in how levodopa is metabolized, with women having greater levodopa bioavailability respect to men. Estrogens are supposed to influence dopamine synthesis, metabolism, and transport; moreover basic research in experimental animals indicates that estrogens protect neurons from various form of injury. However, the effect of post-menopausal estrogen replacement therapy is still debated, given inconsistencies across different studies [57,58].

3.1. Genetics of PD

The majority of PD cases are sporadic; however, in a minority of cases PD is inherited as a Mendelian trait. Studies in PD families have identified 8 causative genes (*a-synuclein*, *parkin*, *UCH-L1*, *PINK1*, *DJ-1*, *LRRK2*, *ATP13A2* and *OMI/HTRA2*) and 4 additional loci of linkage across the genome (PARK3, PARK10, PARK11 and PARK12) pending characterization and/or replication (Table 1).

Most patients with PD, however, have sporadic forms of the disease whose etiology is likely the result of 3 interactive events: an individual's inherited genetic susceptibility, subsequent exposure to environmental risk factors, and aging. As for AD, a great number of PD association studies have been performed in recent years by both candidate gene approaches, based on their roles in the proposed pathways of PD pathogenesis, and genome-wide screenings to detect genetic linkages (Table 2).

3.2. Causative genes for familial PD

3.2.1. α-Synuclein gene (SNCA): PARK1 and PARK 4

A mutation in the *a-synuclein* gene (*SNCA*) on 4q21 (PARK1), causing an Ala53Thr substitution, was found to segregate with the disease in an Italian–American kindred and 3 Greek kindreds [59]. Another mutation in the *SNCA* gene, leading to an Ala30Pro substitution, was subsequently described in a small German family with PD [60], and a third mutation resulting in an Glu46Lys substitution, in a Spanish family [61]. A recent study in a large family identified a triplication of the *a-synuclein* gene (PARK4) as causative of PD [62]. PARK4 individuals have 4 fully functional copies of the *a-synuclein* gene. Three PD families have been subsequently described with *a-synuclein* gene duplication and a disease course less severe of that observed in PARK4 carriers, suggesting the existence of a gene dosage effect [63].

α-Synuclein plays a role in vesicular function with suggested chaperone activity [64]. Mutated α-synuclein has an increased tendency to form aggregates critical to Lewy body formation. Genetic polymorphisms in the *α-synuclein* gene have been associated with PD risk, particularly a recent meta-analysis confirmed the association between a dinucleotide repeat sequence (Rep1) within the promoter and PD risk [65].

3.2.2. Parkin gene: PARK2

Autosomal-recessive juvenile Parkinsonism (AR-JP) is characterized by early-onset and a marked response to levodopa treatment. AR-JP differs from idiopathic PD in that there is no LB formation, although the distribution of neuronal cell loss is similar to that of conventional PD. The genetic locus for AR-JP was identified in Japanese families, which led to identification of homozygous deletions in the *parkin* gene on chromosome 6q25.2–q27 (PARK2) [66]. Subsequently, over 100 mutations in *parkin*, including missense mutations and exonic deletions and insertions, have been observed in PD families [67]. Parkin is an ubiquitin E3 ligase preparing target proteins for their degradation mediated by the ubiquitin–proteosomal system [68].

3.2.3. Ubiquitin carboxy-terminal hydrolase L1 gene (UCH-L1): PARK5

The detection of an Ile93Met mutation in the *ubiquitin carboxy-terminal hydrolase L1* gene (*UCH-L1*) on 4p14 (PARK5) in a German family with autosomal dominant PD [69] suggested a role for an impaired ubiquitin–proteasomal activity in PD pathogenesis.

UCHL1 is a component of LB and possesses both a hydrolase activity to generate the ubiquitin monomer and a ligase activity to link ubiquitin molecules to tag proteins for disposal [70]. A Ser18Tyr polymorphism, affecting mainly the ligase activity, has a protective effect in PD [71].

3.2.4. PTEN-induced putative kinase 1 gene (PINK-1): PARK6

Several mutations in the *PTEN-induced putative kinase 1* gene (*PINK-1*) on chromosome 1p35-36 (PARK6), encoding a protein which is mitochondrially located and whose loss of function is supposed to render neurons more vulnerable to cellular stress, have been linked to autosomal recessive early-onset PD [72,73]. *PINK1* mutations cause mitochondrial deficits contributing to PD pathogenesis; several different mutations have been identified in PD families worldwide [73].

3.2.5. DJ-1 gene: PARK7

Mutations in the *DJ-1* gene on 1p36 (PARK7), including exonic deletions and point mutations, have been associated with a monogenic early-onset autosomal recessive form of parkinsonism characterized by slow progression and response to levodopa [74,75]. DJ1 is a mitochondrial protein involved in the protection against oxidative stress [74].

3.2.6. Leucine-rich repeat kinase 2 gene (LRRK2): PARK 8

Point mutations in the *LRRK2* gene on 12q12 (PARK8) have been identified in different families with autosomal dominant PD; *LRRK2* encodes the protein dardarin which contains several domains including the catalytic domain of a tyrosine kinase, and whose name is derived from *dardara*, the Basque word for tremor. The precise physiological role of dardarin is unknown, but the presence of several domains suggests involvement in a wide variety of functions [76]. All of the identified pathogenic mutations occur in predicted functional domains [77]. A Gly2385Arg mutation, originally identified as a putative pathogenic mutation in a Taiwanese PD family, was subsequently reported to be a common polymorphism and, probably, one of the most frequent genetic risk factors for PD in Asian populations [78].

3.2.7. ATP13A2 gene: PARK9

Clinical features similar to those of idiopatic PD and pallydopyramidal syndrome were observed in a Jordanian family; these included parkinsonism, pyramidal tract dysfunction, supranuclear gaze paresis and dementia. The pattern of transmission was autosomal recessive, and a region of linkage was identified on chromosome 1p36 (PARK9) [79]. The causative gene underlying PARK9 was recently identified as the *ATP13A2* gene encoding a lysosomal 5 P-type ATPase [80].

3.2.8. OMI/HTRA2 gene: PARK 13

A heterozygous Gly399Ser mutation in the *OMI/HTRA2* gene on chromosome 2p12 (PARK 13) was identified in 4 PD patients, but in none of the healthy controls. Moreover, an Ala141Ser polymorphism was associated with increased PD risk in the same population [81]. OMI/HTRA2 is a nuclear-encoded serine protease protein, localised in the inter-membrane space of the mitochondria and involved in mediating caspase-dependent and caspase-independent cellular death. The Gly399Ser mutation compromises mitochondrial function resulting in increased vulnerability to stress-induced cell death [81].

3.3. PD susceptibility genes

As for AD, several hundreds of association studies have been published in recent years claiming or refusing association between variants in candidate genes and the risk of PD. Results published so far are often conflicting and inconclusive, reflecting genetic heterogeneity of the studied populations, inadequate sample size and the possible contribution of environmental factors. The major pathways which have been analysed in PD association studies are those related to dopamine transport metabolism, detoxification of xenobiotics and oxidative stress. Moreover, common variants of PD causative genes have been largely studied for their role as possible PD susceptibility factors. Recent meta-analyses from multiple independent studies have enhanced the assessment of accuracy of the impact of risk allele effects (Table 2).

3.3.1. Common variants of PD causative genes

In the previous paragraph we have discussed that, together with PD causative mutations, several common polymorphisms in PD causative genes have been suggested as possible PD risk factors. Among them, a common S18Y polymorphism of *UCHL1* has been demonstrated to be protective of PD in some association studies, and a recent meta-analysis of published studies, for a total of 1970 PD patients and 2224 controls, confirmed a protective role for the variant allele [71]. However, a subsequent large case–control study involving 3044 PD cases and 3252 controls, failed to replicate the association [82]. Therefore, the role of the S18Y variant needs to be further clarified.

Another common polymorphism (allele-length variability in the dinucleotide repeat sequence, Rep1) in the promoter region of the *SNCA* gene has been largely analysed in genetic association studies. A recent pooled-analysis of published data supports association between the *SNCA* Rep1 polymorphism and increased PD risk [64].

A common G2385R variant of the *LRRK2* gene has been associated with increased PD risk in Chinese and Japanese populations, and a pooled-analysis of published data (2205 PD cases and 1817 controls) supports such association [83].

Mutations in the gene encoding the microtubular associated protein tau (*MAPT*) have been observed in ALS individuals with frontotemporal dementia and Parkinsonism (see Section 4.2.5). A meta analysis of 7 studies (1305 PD patients and 1194 controls) suggests that individuals homozygous for the *MAPT* H1 haplotype are at increased PD risk respect to H2 carriers [84]. A recent study conducted on 932 PD patients and 664 controls confirms association between PD risk and both the *MAPT* H1 haplotype and the *SNCA* Rep1 polymorphism [85]. There is also evidence suggesting that the role of H1 haplotypes in the etiology of PD might be ethnically dependent [86].

3.3.2. Genes involved in dopamine metabolism and in metabolism of xenobiotics

Several variants of genes coding for proteins involved in dopamine transport and metabolism (e.g., DAT, DRD2, COMT, MAO-B), in metabolism of xenobiotics (e.g., CYP2D6, GSTs, NAT2) and in oxidative stress response (e.g., NOS, SOD2), have been largely studied in recent years as possible PD susceptibility factors. However, for the vast majority of them, results are conflicting or still inconclusive. Several authors agree that the inconsistencies observed in the PD risk-factors literature might partly be explained by the fact that, even if several small studies have reported genetic associations between genetic polymorphisms and PD, only a few of them have examined gene–environment interactions [87,88].

A recently published large case–control study [88], based on 959 individuals with parkinsonism (767 with PD) and 1989 controls across 5 European centres (The Geoparkinson study), was designed to analyse gene–environment interplay in PD risk. Exposure to solvents, pesticides and metals (iron, copper and manganese) was evaluated and related to polymorphisms of several PD putative risk genes (*CYP2D6*, *PON1*, *GSTM1*, *GSTT1*, *GSTM3*, *GSTP1*, *NQO1*, *CYP1B1*,

MAO-A, *MAO-B*, *SOD2*, *EPHX*, *DAT1*, *DRD2* and *NAT2*). A modest association was observed between MAO-A polymorphism and PD risk in males. The majority of gene–environment analyses did not show significant interaction effects. However, *GSTM1* null subjects heavily exposed to solvents appeared to be at increased risk of PD.

GSTP1 polymorphisms have been associated with PD in a pesticide exposed population [89], and recent evidence suggests that the relation between *GSTP1* polymorphisms and PD age at onset is modified by herbicide exposure [90].

A recent meta-analysis of published papers, for a total of 1206 PD patients and 1619 controls, did not provide conclusive evidence for an overall association of *NAT2* slow acetylator genotypes to PD [91].

Variants of the *CYP2D6* gene have been extensively studied as genetic risk factors for PD, with inconsistent results [87]. However, there are data suggesting that risk of PD might be modulated by interactions between the *CYP2D6* genotype and environmental factors such as pesticide exposure and cigarette smoking [87,92].

A recent meta-analysis of genome-wide association studies revealed 3 polymorphisms (rs1000291 on chromosome 3, rs2241743 on chromosome 4 and rs3018626 on chromosome 11) that deserve further consideration [93] (Table 2).

3.4. Environmental factors in PD pathogenesis

In 1999 Tanner et al. designed a large-scale study of monozygotic and dizygotic pairs of twins, aimed to assess genetic versus environmental factors in the etiology of PD and suggested a contribution of environmental factors to both early and late onset forms [94]. Several environmental factors, including pesticides and herbicides, metals, tobacco and caffeine, head injuries and others, have been largely studied in recent years as possible PD risk factors (Table 3).

3.4.1. Rural activities, pesticides, metals.

Since the first description of Parkinson-like symptoms among individuals who had taken drugs contaminated with 1-methyl-4-phenyl-1,2,3,6-tetrahydropyridine (MPTP) [95], and the subsequent evidence that paraquat, an herbicide structurally similar to MPTP, induces selective loss of dopaminergic neurons [96], human exposure to chemical compounds of synthetic origin, including herbicide, insecticides and pesticides, has been the focus of active research in PD pathogenesis. The available evidence indicates that rural environment and pesticide exposures are associated with PD, however no one agent has been consistently identified, likely because associations with specific agents may be confounded by exposure to other pesticides, making it difficult to identify the causative agent [97,98]. Human exposure to metals has been the focus of several epidemiological studies aimed at evaluating their possible contribution as PD risk factors. The Geoparkinson study failed to find association between iron, copper and manganese exposure and PD risk [99]. However a recent report based on 110,000 individuals in two Canadian cities suggests that environmental manganese air pollution might contribute to neuronal loss in PD [100]. There is also evidence that occupational lead exposure is a risk factor for PD [101].

3.4.2. Tobacco use, caffeine intake, dietary factors, habits and exercise

There is substantial evidence supporting a protective role for both tobacco smoking and caffeine use and the risk of PD. A recent pooled analysis of tobacco use and risk of PD supports a dose-dependent reduction of PD risk associated with cigarette smoking [102]. A recently published follow-up study based on 29,335 Finnish subjects suggests that coffee drinking is associated with a lower PD risk. Similar results have been observed in individuals drinking 3 or more cups of tea daily [103]. A prospective study of dietary pattern and risk of PD based on 49,626 men and 81,676 women suggests that dietary patterns with high intakes of fruit, vegetables, legumes, whole grains, nuts, fish and poultry, a moderate intake of alcohol and a low intake of saturated fats might protect against PD [104]. There is evidence that excessive daytime sleepiness might be associated with increased PD risk [105], on the contrary physical activity seems not to contribute to PD risk [106].

3.4.3. Head injuries

The Geoparkinson study suggests that repeated traumatic loss of consciousness is associated with increased PD risk [99]. Similar results have been obtained in a case–control study of 93 twins pairs discordant for PD, in which a prior head injury with amnesia or loss of consciousness was associated with an increased risk for PD [107].

4. Amyotrophic lateral sclerosis (ALS)

Amyotrophic lateral sclerosis, also known as motor neuron disease (MND), is one of the major neurodegenerative diseases alongside AD and PD. It is a progressive disorder characterized by the degeneration of motor neurons of the motor cortex, brainstem and spinal cord. The incidence of the disease is similar worldwide and ranges from 1 to 3 cases per 100,000 individuals per year, with the exception of some high-risk areas around the Pacific Rim such as the island of Guam or parts of Western New Guinea. The course of ALS is inexorably progressive, with 50% of the patients dying within 3 years of onset. Overall, the incidence of the disease rises until it peaks around 75 years of age and the disease is more frequent in males than in females; the male to female ratio is reported to be 3:2, and male predominance is particularly marked in some lower motor neuron variants, where the disease is nearly 10 times more common in men than in women. After the menopause the male to female ratio approaches 1:1, suggesting a neuro-protective effect exerted by estrogens. Studies in families with ALS reveal that the compromising of pathways involved in defence against oxidative damage or vesicle trafficking is critical in ALS pathogenesis [108,109].

4.1. Genetics of ALS

ALS is predominantly a sporadic disorder (SALS), and only 5–10% of the cases have a familial origin. Studies in families have led to the identification of different genes responsible for familial or atypical forms (*SOD1*, *alsin*, *SETX*, *VAPB*, *DCTN1* and *MAPT*) and potential ALS loci (ALS3, ALS5, ALS6 and ALS7) still pending characterization (Table 1). However, in spite of the concerted effort in the field, only few sALS risk factors have been identified so far, including increasing age, gender and family history [109,110].

4.2. Causative genes for familial ALS

4.2.1. Copper–zinc superoxide dismutase gene (SOD1): ALS1

The cytosolic *copper–zinc superoxide dismutase* gene (*SOD1*), on chromosome 21q21 (ALS1), was the first ALS identified gene, accounting for autosomal dominant forms [111]. Superoxide dismutases are scavenger enzymes against free radicals mainly produced by mitochondrial respiration, and to date more than 100 *SOD1* mutations have been described occurring at almost any position in the gene, and accounting approximately for 2% of all ALS and 20% of familial cases (http://www.alsod.org.). Studies on ALS animal models indicate that the over-expression of mutant *SOD1* in mice leads to symptoms similar to those observed in humans [112]. A recent study on fALS animal models showed that the mutant G39A-SOD1

is not able to enter the nucleus and protect the DNA against oxidative damage [113], supporting a role for oxidative DNA damage in ALS pathogenesis.

4.2.2. Alsin gene: ALS2

Autosomal recessive familial amyotrophic lateral sclerosis (RFALS) is rare and has been reported in settings of high consanguinity such as Tunisia. A locus for a rare RFALS form with onset before age 25 was mapped to chromosome 2q33 (ALS2) [114], and contains a recently identified gene named *alsin* [115,116], which encodes a guanine nucleotide exchange factor for RAB5A, a key regulator of endocytosis [117].

4.2.3. Senataxin gene SETX: ALS4

Autosomal dominant juvenile FALS was linked to 9q34 (ALS4), and associated with mutations in the *senataxin* gene (*SETX*) [118], which encodes a DNA and RNA helicase protein that participate in DNA repair mechanisms, and is involved in the defence against oxidative DNA damage [119].

4.2.4. The vesicle-associated membrane protein/synaptobrevin-associated membrane protein B gene (VAPB): ALS8

A P56S mutation in the *vesicle-associated membrane protein/synaptobrevin-associated membrane protein B* gene (*VAPB*) on 20q13.3 (ALS8) was observed in 7 Brazilian families: 3 with late-onset atypical ALS, 3 with late-onset spinal muscular atrophy (SMA), and 1 family with both ALS and SMA members [120]. Recent findings support a model in which reduced levels of VAP family proteins result in decreased endoplasmic reticulum anchoring of lipid-binding proteins and cause motor neuron degeneration [121].

4.2.5. ALS and frontotemporal dementia with Parkinsonism: the MAPT gene

Atypical forms of ALS including frontotemporal dementia (FTD) often accompanied by Parkinsonism symptoms are known; the coexistence of ALS with FTD (ALS and FTD) was first described more than 30 years ago [122], and subsequently linked to chromosome9q21–q22 [123]. Recently, a new locus for ALS and FTD has been mapped to 9p21.3–p13.3 in a Swedish family [124]. Mutations in the gene encoding the microtubular associated protein tau (*MAPT*) on chromosome 17q21 have been observed in ALS individuals with FTD and Parkinsonism (ALS and FTDP) [125]. Tau is a microtubule associated protein involved in the assembly of microtubules [126].

4.2.6. Lower motor neuron disease, dynactin type: the DCTN1 gene

Further, mutations in the *dynactin* gene (*DCTN1*) on chromosome 2p13 have been observed in a family with a slowly progressive motor neuron disease, with onset in early adulthood and characterized by breathing difficulties, vocal fold paralysis and distal lower limb muscle weakness and atrophy [127]. Some of the clinical features overlap with ALS, and studies on animal models indicate that dynactin promotes the stability of synapses at the neuromuscular junctions [128].

4.3. ALS susceptibility

Almost 95% of ALS occurs as sporadic forms (sALS); however, although several genes have been studied in recent years as possible sALS susceptibility factors, no single gene has been definitively shown to be consistently associated with disease risk. Recent genome-wide association studies have provided additional candidates requiring further investigation (Table 2).

4.3.1. DNA repair genes: APEX1 and hOGG1

The DNA repair genes *APEX1* and *hOGG1* have been selected as candidate genes for sporadic ALS based on their protective roles against oxidative stress. A study on 117 sALS Scottish patients and 58 controls reported association between the *APEX1* D148E polymorphism and sALS risk [129], but further studies gave conflicting results [130,131]. We have recently performed the largest case–control study aimed at evaluating the role of the *APEX1* D148E polymorphism on sALS and clinical presentation on an Italian cohort of 134 sALS patients and 129 matched controls. No association was found between the polymorphism and disease risk or presentation, including age and site at onset and disease progression [131]. We have also investigated the role of the *hOGG1* Ser326Cys polymorphism on sALS risk and presentation on 136 Italian sALS patients and 129 matched controls, observing association with disease risk in males [132]. Recent findings on mutant *SOD1* and *senataxin* (see Sections 4.2.1 and 4.2.3) support a role for oxidative DNA damage and DNA repair mechanisms in ALS pathogenesis. Therefore, further studies are required to better understand the contribution of DNA repair gene variants in sALS.

4.3.2. Angiogenesis factors: ANG and VEGF

ANG and VEGF, two angiogenesis factors, have been largely studied in recent years as possible sALS risk factors. A synonymous *ANG* G110G polymorphism has been associated with sALS risk in Irish and Scottish populations [130]. However, further studies in other populations have failed to confirm the association [133]. Concerning the *VEGF* gene, a recent pooled analysis of several association studies gave negative or inconclusive results [110].

4.3.3. Others: neurofilaments, paraoxonases, survival motor neuron and haemocromatosis

Among other candidate sALS genes there are those coding for neurofilaments (*NEFL*, *NEFM* and *NEFH*), paraoxonases (*PON1*, *PON2* and *PON3*), survival motor neuron (*SMN1* and *SMN2*) and the *haemocromatosis* gene (*HFE*). Recent pooled analyses suggest a role for the *HFE* H63D variant and for increased copy numbers of the *SMN* genes and ALS risk [110].

Recently, a genome-wide association study identified a polymorphism in the *dipeptidyl-peptidase 6* gene (DPP6) associated with susceptibility to ALS [134].

4.4. Environmental factors in ALS pathogenesis

The environmental factors contributing to neuronal degeneration in ALS have been studied less extensively compared to other neurodegenerative disorders, such as AD and PD, and were largely unknown until recent years; however, as for AD and PD, the etiology of the majority of sALS cases is presumably due to several interactions between genetic and environmental factors. The first evidence of an environmental contribution in ALS came from the observed endemic occurrence of ALS with Parkinsonism and progressive dementia in regions of Western Pacific that could not be fully explained by genetic factors, and was related to the consumption of food made with seeds of the cycad plants [135]. Several other environmental factors have been extensively studied in recent years (Table 3).

4.4.1. Occupational exposure to metals, pesticides, insecticides, neurotoxins and electromagnetic fields

Several studies report an increased ALS risk among individuals occupationally exposed to lead [136,137]. There is also evidence

suggesting that human exposures to agricultural chemicals, such as pesticides and insecticides, are at increased ALS risk [137,138]. To support this hypothesis there is a recent report of a motor neuron disorder simulating ALS induced by chronic inhalation of pyrethroid insecticides [139]. Moreover, increased post-war risk of ALS has been observed in military personnel who were deployed to the Gulf Region during the first Gulf War period, suggesting exposure to neurotoxins as an environmental risk factor [140]. Several Gulf War veterans who developed neurologic symptoms had decreased levels of the enzyme paraoxonase 1 (PON1) which participates in the detoxification of organophosphate pesticides [141]. There is also evidence for an increased ALS risk among welders and other workers exposed to electromagnetic fields [142,143].

4.4.2. Physical activity and related traumas

A few years ago Chiò et al. [144] observed an increased ALS risk in Italian professional soccer players. Subsequently, similar results were observed for National Football League players in the United States [145]. In the same period it was published the case of 3 amateur league soccer players who were friends from the same part of southern England and developed ALS simultaneously, suggesting that also amateur players are at increased ALS risk [146]. The question of whether or not professional or amateur excessive physical activity per se represents an ALS risk factor is largely debated. Several hypotheses have been formulated trying to explain the causative agent of ALS among soccer players, including as possible candidates excessive physical activity, drugs and doping, dietary supplements, pesticides used on the playgrounds, and traumas to the head and to other body parts [147]. Recent evidence suggests that repeated head injuries might increase ALS risk [148].

4.4.3. Others: smoking and education

Among other factors associated with increased ALS risk smoking, particularly in women, has been associated with increased disease risk [149,150]. Increased risk was also observed among individuals with low education levels (elementary school) [150].

5. Epigenetics and neurodegenerative diseases

Epigenetics is the study of heritable changes in gene function that occur independently of alterations to primary DNA sequence. The best-studied epigenetic modifications are DNA methylation, and changes in chromatin structure by histone modifications and RNA-mediated pathways from non-coding RNAs, notably silencing RNA (siRNA) and microRNA (miRNA). Epigenetic modifications have a critical role in important developmental events, including X-inactivation, genomic imprinting, and neuronal development. Moreover, an increasing number of human pathologies have been found to be associated with aberrant epigenetic regulation, including cancer and a great number of human life-threatening diseases, such as neurodegenerative diseases [151,152].

Epigenetic modifications have been compared, in terms of phenotypic consequences, to genetic polymorphisms resulting in variations in gene function [153]. Until now only few environmental agents have been identified to strongly affect the epigenome, including dietary factors, alcohol, and environmental hazard such as cigarette smoking and arsenic [153]. Moreover, a lot remains to do to adequately characterize the critical windows of vulnerability to environmentally induced epigenetic alterations [154,155].

5.1. Dietary factors and epigenetic changes relevant for AD pathogenesis

It is now clear that dietary components can modulate both genome and epigenome, this last by altering genetic expression and potentially modifying the risk and/or severity of a variety of disease conditions including neurodegenerative ones [156]. In an epigenetic context it is likely that the level of expression of several genes could be altered due to the methylation status of their promoters. In Alzheimer's disease, for instance, critical targets for epigenetic insults are likely genes involved in the maintenance of the physiological levels of non-amyloidogenic and amyloidogenic fragments.

Folate and vitamin B12 are essential cofactors for the methionine/homocysteine cycle in the brain. These vitamins mediate the remethylation of homocysteine (Hcy), which affects the production of the universal methyl donor, S-adenosylmethionine (SAM), in the brain among other organs. AD is characterized by hight Hcy and low folate blood levels, meaning that the conversion of Hcy to methionine is altered in AD, as it is the production of SAM [157]. Fuso et al. analysed the levels of methylation of CpG islands in the promoters of the *APP* and the *PSEN1* gene on human neuroblastoma SK-N-SH or SK-N-BE cell lines, observing that in conditions of folates and vitamin B12 deprivation from the media, the status of methylation of the promoter of the *PSEN1* gene underwent a variation, with a subsequent deregulation of the production of presenilin 1, BACE and APP proteins [157]. This study confirmed that some of the genes responsible for the production of Aβ fragments in AD can be regulated through an epigenetic mechanism depending on the cellular availability of folates and B12 vitamins, and involving the production of SAM and the status of methylation of CpG islands in the DNA.

The same authors recently observed, on the same experimental model, that Hcy accumulation induced through vitamin B deprivation could impair the "methylation potential" with subsequent presenilin 1, BACE and amyloid-beta upregulation [158].

5.2. Oxidative stress and epigenetic modifications

The accumulation of oxidative stress-induced damage in brain tissues plays an important role in the pathogenesis of normal aging and neurodegenerative diseases, including AD. Because of its high metabolic rate the brain is believed to be particularly susceptible to ROS, and the effects of oxidative stress on neurons might be cumulative. At the time oxidative damage was observed in AD, it was supposed that amyloid aggregates were the main source of oxidative stress; however, recent evidence suggests that oxidative stress is one of the earliest events in AD [159–161], and drives Aβ production [162], likely through activation of BACE1 [163–165]. Moreover, it seems that Aβ peptides might be produced to function as scavengers of reactive oxidative species [166]. Only with the persistence of oxidative stress, the production of Aβ peptides overcomes their cellular turnover, so that they start to aggregate and their anti-oxidant function evolve into pro-oxidant, ultimately leading to neuronal death [167].

Epigenetic mechanisms leading to transcriptional silencing of genes important in ROS scavenging, such as *MnSOD*, have been observed [168]. Increases in ROS can also effect glutathione (GSH) levels which in turn can change SAM synthesis and hence DNA methylation patterns. GSH is an important endogenous antioxidant, found in millimolar concentrations in the brain; GSH levels have been shown to decrease with aging, and plasma GSH was decreased in AD patients. Increased GSH production influences epigenetic processes including DNA and histone methylation by limiting the availability of SAM, which is the cofactor utilized during

epigenetic control of gene expression by DNA and histone methyltransferases [169]. There are additional ROS related mechanisms involving hydrogen peroxide that can lead to further changes of the chromatin structure [169].

The role of oxidative stress as a molecular link between the β- and the γ-secretase activities has been recently reviewed [170] and a mechanistic explanation of the pathogenesis of sporadic LOAD has been provided: the overproduction of Aβ, dependent on the upregulation of BACE1 induced by oxidative stress, would contribute to the pathogenesis of the common, sporadic, late-onset form of AD, a major risk factor for which is aging. It has been suggested that an increase in the γ-secretase cleavage of APP mediated by oxidative stress (in sporadic AD), or by *PSEN1* mutations (in familial AD forms), leads to an increase in BACE1 expression and activity [170].

Oxidative stress regulates the expression of many genes that might contribute to AD pathophysiology. Recent genome scan studies found that genes involved in several pathways including antioxidant defence, detoxification and inflammation, are induced in response to oxidative stress and in AD. However, genes that are associated with energy metabolism, which is necessary for normal brain function, are mostly down-regulated. DNA methylation signatures distinguish brain regions and may help account for region-specific functional specialization [171].

5.3. Environmental exposure early in life induces epigenetic changes relevant for AD pathogenesis

It has become increasingly evident in recent years that development is under epigenetic control. Prenatal or early life exposures to dietary and environmental factors can have a profound impact on our epigenome, resulting in birth defects and diseases developed later in life. Indeed, examples are accumulating in which environmental exposures can be attributed to epigenetic causes, an encouraging edge towards greater understanding of the contribution of epigenetic influences of environmental exposures [172]. To explain the etiology of LOAD forms and other neuropsychiatric and developmental disorders, it has been hypothesized that environmental factors, including metals and dietary factors, perturb gene regulation in a long-term fashion, beginning at early developmental stages; however, these perturbations do not have pathological results until significantly later in life. These factors can perturb the interaction of methylated CpG clusters with binding proteins, such as MeCP2 and SP1. Promoters can have both positive and negative regulatory elements, and their activity can be altered both by changes in the primary DNA sequence and by epigenetic changes through mechanisms such as DNA methylation at CpG dinucleotides or oxidation of guanosine residues. For example, such actions would perturb *APP* gene regulation at very early stage via its transcriptional machinery, leading to delayed over-expression of *APP* and subsequently of Aβ deposition [173]. Recent studies in rodents have shown that exposure to lead (Pb) during brain development predetermined the expression and regulation of the amyloid precursor protein and its amyloidogenic Aβ product in old age. The expression of AD-related genes (*APP*, *BACE1*) as well as their transcriptional regulator (*SP1*) were elevated in aged (23-year old) monkeys exposed to Pb as infants. Furthermore, developmental exposure to Pb altered the levels, characteristics, and intracellular distribution of Aβ staining and amyloid plaques in the frontal association cortex. These latent effects were accompanied by a decrease in DNA methyltransferase activity and higher levels of oxidative damage to DNA, indicating that epigenetic imprinting in early life influenced the expression of AD-related genes and promoted DNA damage and disease pathogenesis. These data suggest that AD pathogenesis is influenced by early life exposures and argue for both an environmental trigger and a developmental origin of AD [174]. Wu et al. [175] proposed that environmental influences occurring during brain development alter the methylation pattern of the *APP* promoter which results in a latent increase in APP and Aβ levels. Increased Aβ levels promote the production of ROS which damage DNA. Epigenetic changes in DNA methylation impact both gene transcription and the ability to repair damaged DNA and thus imprint susceptibility to DNA damage. This susceptibility plus the programmed increase in Aβ levels via a transcriptional pathway programmed by environmental exposures in early life exacerbates the normal process of amyloidogenesis in the aging brain, thus accelerating the onset of AD [175].

5.4. Possible role of epigenetics in other neurodegenerative diseases, than AD

About possible role of epigenetics in other neurodegenerative diseases, studies are still at the beginning. Few data exists on the occurrence of epigenetic silencing of genes that have a fundamental role in other neurodegenerative diseases than AD, such as ALS and PD. To explain the variable phenotypic expressivity (the age of onset, the severity and or penetrance of the pathological phenotype) disturbances in methylation levels have been involved. In fact DNA methylation is dynamically regulated in the human cerebral cortex throughout the lifespan, involves differentiated neurons, and affects a substantial portion of genes predominantly by an age-related increase [176]. There is also evidence that oxidative stress and defects in mitochondrial function, particularly in complex I, may contribute to PD. Exposure of humans or mice to the environmental toxins MPTP, paraquat, or rotenone results in acute and irreversible parkinsonism. These toxins impair mitochondrial function and consequently increase free radical production and oxidative stress [96]. Sporadic ALS (SALS) results from the death of motor neurons in the brain and spinal cord. It has been proposed that epigenetic silencing of genes vital for motor neuron function could underlie SALS. However, the promoter of genes thought to be implicated in SALS: *SOD1* and *VEGF*, or that of *MT-Ia* and *MT-II* (the most common human isoforms of the metallothionein (MT) family of proteins), has not been found with inappropriate methylation levels [177,178].

6. Conclusions

Active research performed in recent years in the field of neurodegenerative diseases has led to the identification of several causative genes responsible for the familial forms, with a subsequent better comprehension of the molecular mechanisms at the basis of the selective neuronal death. As a consequence, the compromising of several intracellular pathways has been postulated to increase the risk for the development of the sporadic forms. However, despite hundreds of association studies based on the "candidate gene" approach, results are still largely inconclusive, and researchers have tried to obtain more informative results by means of pooled analyses of published data [24]. The hottest new tool in genetics are genome-wide association studies; geneticists scan patient's DNA for half a million or more single nucleotide polymorphisms (SNPs), and then compare the results to those from a healthy control group. Unfortunately, almost none of them has highlighted genes already under suspicion by the "candidate-gene" approach, moreover results from genome-wide association studies are often conflicting and not replicating, thus adding nothing but confusion to the gene hunt [93,179]. Several authors agree that at the basis of the discordant results obtained in association studies, in most of the cases, there might be the lack of the power to

clearly evaluate exposures to environmental agents that, interacting with the genetic background, could really explain the individual susceptibility [87,88].

Many of the processes with a key role in neurodegeneration, such as the formation of senile plaques, the accumulation of ROS, the cleavage of APP by neuroscretases, can be now analysed in light of the new epigenetic knowledge, to facilitate the implementation of future disease prevention strategies [157,175]. The study of specific aberrant patterns of epigenetic marks might be developed as novel predictors to facilitate the implementation of future disease prevention strategies, to lend new insights into the aetiology of a disease, to allow more exact diagnosis and to develop better-targeted therapeutic regimens. Since epigenetic alterations are reversible, modifying epigenetic marks contributing to disease development may provide an approach to designing new therapies such as the use of inhibitors of enzymes controlling epigenetic modifications [180].

Over the last two decades, preclinical and clinical research has implicated epigenetic alterations in the pathogenesis and progression of cancer. Many of the processes can be reversed offering a hope for epigenetic therapies such as inhibitors of enzymes controlling epigenetic modifications, specifically DNA methyltransferases, histone deacetylases, and RNAi therapeutics. Drugs have been developed with functional effects, including DNA hypomethylation and histone acetylation, that serve to restore the normal transcription of cell regulatory genes (e.g, tumor suppressor genes). DNA hypomethylating agents, such as azacitidine, and histone deacetylase inhibitors such as vorinostat have been approved in the US for the treatment of cancer, reinforcing the importance of these pathways in the biology of this disease [180]. If epigenetic alterations will be confirmed to have a pivotal role also in many neurodegenerative diseases, new targets for therapy will be likely identified soon.

References

[1] P.D. Sloane, S. Zimmerman, C. Suchindran, P. Reed, L. Wang, M. Boustani, S. Sudha, The public health impact of Alzheimer's disease, 2000–2050: potential implication of treatment advances, Annu. Rev. Public Health 23 (2002) 213–231.

[2] L.E. Hebert, P.A. Scherr, J.L. Bienias, D.A. Bennett, D.A. Evans, Alzheimer disease in the US population: prevalence estimates using the 2000 census, Arch. Neurol. 60 (2003) 1119–1122.

[3] N.A. Azad, M. Al Bugami, I. Loy-English, Gender differences in dementia risk factors, Gend. Med. 4 (2007) 120–129.

[4] J. Viña, A. Lloret, S.L. Vallés, C. Borrás, M.C. Badía, F.V. Pallardó, J. Sastre, M.D. Alonso, Mitochondrial oxidant signalling in Alzheimer's disease, J. Alzheimer's Dis. 11 (2007) 175–181.

[5] R. Schmidt, E. Kienbacher, T. Benke, P. Dal-Bianco, M. Delazer, G. Ladurner, K. Jellinger, J. Marksteiner, G. Ransmayr, H. Schmidt, E. Stögmann, J. Friedrich, C. Wehringer, Sex differences in Alzheimer's disease, Neuropsychiatrie 22 (2008) 1–15.

[6] G. Casadesus, R.K. Rolston, K.M. Webber, C.S. Atwood, R.L. Bowen, G. Perry, M.A. Smith, Menopause, estrogen, and gonadotropins in Alzheimer's disease, Adv. Clin. Chem. 45 (2008) 139–153.

[7] C. Qiu, D. De Ronchi, L. Fratiglioni, The epidemiology of the dementias: an update, Curr. Opin. Psychiatry 20 (2007) 380–385.

[8] M.A. Findeis, The role of amyloid beta peptide 42 in Alzheimer's disease, Pharmacol. Ther. 116 (2007) 266–286.

[9] M. Bentahir, O. Nyabi, J. Verhamme, A. Tolia, K. Horré, J. Wiltfang, H. Esselmann, B. De Strooper, Presenilin clinical mutations can affect gamma-secretase activity by different mechanisms, J. Neurochem. 96 (2006) 732–742.

[10] J.C. Lambert, P. Amouyel, Genetic heterogeneity of Alzheimer's disease: complexity and advances, Psychoneuroendocrinology 32 (2007) S62–S70.

[11] M.I. Kamboh, Molecular genetics of late-onset Alzheimer's disease, Ann. Hum. Genet. 68 (2004) 381–404.

[12] A. Goate, M.C. Chartier-Harlin, M. Mullan, J. Brown, F. Crawford, L. Fidani, L. Giuffra, A. Haynes, N. Irving, L. James, R. Mant, P. Newton, K. Rooke, P. Roques, C. Talbot, M. Pericak-Vance, A. Roses, R. Williamson, M. Rossor, M. Owen, J. Hardy, Segregation of a missense mutation in the amyloid precursor protein gene with familial Alzheimer's disease, Nature 349 (1991) 704–706.

[13] A. Rovelet-Lecrux, D. Hannequin, G. Raux, N. Le Meur, A. Laquerrière, A. Vital, C. Dumanchin, S. Feuillette, A. Brice, M. Vercelletto, F. Dubas, T. Frebourg, D. Campion, APP locus duplication causes autosomal dominant early-onset Alzheimer disease with cerebral amyloid angiopathy, Nat. Genet. 38 (2006) 24–26.

[14] A. Rovelet-Lecrux, T. Frebourg, H. Tuominen, K. Majamaa, D. Campion, A.M. Remes, APP locus duplication in a Finnish family with dementia and intracerebral haemorrhage, J. Neurol. Neurosurg. Psychiatry 78 (2007) 1158–1159.

[15] J. Theuns, N. Brouwers, S. Engelborghs, K. Sleegers, V. Bogaerts, E. Corsmit, T. De Pooter, C.M. van Duijn, P.P. De Deyn, C. Van Broeckhoven, Promoter mutations that increase amyloid precursor-protein expression are associated with Alzheimer disease, Am. J. Hum. Genet. 78 (2006) 936–946.

[16] V.P. Prasher, M.J. Farrer, A.M. Kessling, E.M. Fisher, R.J. West, P.C. Barber, A.C. Butler, Molecular mapping of Alzheimer-type dementia in Down's syndrome, Ann. Neurol. 43 (1998) 380–383.

[17] F. Argellati, S. Massone, C. d'Abramo, U.M. Marinari, M.A. Pronzato, C. Domenicotti, R. Ricciarelli, Evidence against the overexpression of APP in Down syndrome, IUBMB Life 58 (2006) 103–106.

[18] H.E. Lockstone, L.W. Harris, J.E. Swatton, M.T. Wayland, A.J. Holland, S. Bahn, Gene expression profiling in the adult Down syndrome brain, Genomics 90 (2007) 647–660.

[19] R. Sherrington, E.I. Rogaev, Y. Liang, L.E. Rogaeva, G. Levesque, M. Ikeda, H. Chi, C. Lin, G. Li, K. Holman, T. Tsuda, L. Mar, J.F. Foncin, A.C. Bruni, M.P. Montesi, S. Sorbi, I. Rainero, L. Pinessi, L. Nee, I. Chumakov, D. Pollen, A. Brookes, P. Sanseau, R.J. Polinsky, W. Wasco, H.A.R. Da Silva, J.L. Haines, M.A. Pericak-Vance, R.E. Tanzi, A.D. Roses, P.E. Fraser, J.M. Rommens, P.H. St George-Hyslop, Cloning of a gene bearing missense mutations in early-onset familial Alzheimer's disease, Nature 375 (1995) 754–760.

[20] E.I. Rogaev, R. Sherrington, E.A. Rogaeva, G. Levesque, M. Ikeda, Y. Liang, H. Chi, C. Lin, K. Holman, T. Tsuda, L. Mar, S. Sorbi, B. Nacmias, S. Piacentini, L. Amaducci, I. Chumakov, D. Cohen, L. Lannfelt, P.E. Fraser, J.M. Rommens, P.H. St George-Hyslop, Familial Alzheimer's disease in kindreds with missense mutations in a gene on chromosome 1 related to the Alzheimer's disease type 3 gene, Nature 376 (1995) 775–778.

[21] E. Levy-Lahad, W. Wasco, P. Poorkaj, D.M. Romano, J. Oshima, W.H. Pettingell, C.E. Yu, P.D. Jondro, S.D. Schmidt, K. Wang, A.C. Crowley, Y.H. Fu, S.Y. Guenette, D. Galas, E. Nemens, E.M. Wijsman, T.D. Bird, G.D. Schellenberg, R.E. Tanzi RE, Candidate gene for the chromosome 1 familial Alzheimer's disease locus, Science 269 (1995) 973–977.

[22] D.J. Selkoe, M.S. Wolfe, Presenilin: running with scissors in the membrane, Cell 131 (2007) 215–221.

[23] C.M. van Duijn, M. Cruts, J. Theuns, G. Van Gassen, H. Backhovens, M. van den Broeck, A. Wehnert, S. Serneels, A. Hofman, C. Van Broeckhoven, Genetic association of the presenilin-1 regulatory region with early-onset Alzheimer's disease in a population-based sample, Eur. J. Hum. Genet. 7 (1999) 801–806.

[24] L. Bertram, M.B. McQueen, K. Mullin, D. Blacker, R.E. Tanzi, Systematic meta-analyses of Alzheimer disease genetic association studies: the AlzGene database, Nat. Genet. 39 (2007) 17–23.

[25] Z. Liu, J. Jia, The association of the regulatory region of the presenilin-2 gene with Alzheimer's disease in the Northern Han Chinese population, J. Neurol. Sci. 264 (2008) 38–42.

[26] M. Gacia, K. Safranow, T. Gabryelewicz, M. Styczyńska, B. Pepłońska, V. Dziedziejko, K. Jakubowska, D. Chlubek, C. Zekanowski, M. Barcikowska, Two polymorphisms of presenilin-2 gene (PSEN2) 5′ regulatory region are not associated with Alzheimer's disease (AD) in the Polish population, J. Neural Transm. 115 (2008) 85–90.

[27] W.J. Strittmatter, A.M. Saunders, D. Schmechel, M. Pericak-Vance, J. Enghild, G.S. Salvesen, A.D. Roses, Apolipoprotein E: high-avidity binding to beta-amyloid and increased frequency of type 4 allele in late-onset familial Alzheimer disease, Proc. Natl. Acad. Sci. U.S.A. 90 (1993) 1977–1981.

[28] L.A. Farrer, L.A. Cupples, J.L. Haines, B. Hyman, W.A. Kukull, R. Mayeux, R.H. Myers, M.A. Pericak-Vance, N. Risch, C.M. van Duijn, Effects of age, sex, and ethnicity on the association between apolipoprotein E genotype and Alzheimer disease. A meta-analysis APOE and Alzheimer Disease Meta Analysis Consortium, JAMA 278 (1997) 1349–1356.

[29] E. Warwick Daw, H. Payami, E.J. Nemens, D. Nochlin, T.D. Bird, G.D. Schellenberg, E.M. Wijsman, The number of trait loci in late-onset Alzheimer disease, Am. J. Hum. Genet. 66 (2000) 196–204.

[30] G. Gold, J.L. Blouin, F.R. Herrmann, A. Michon, R. Mulligan, G. Duriaux Saïl, C. Bouras, P. Giannakopoulos, S.E. Antonarakis, Specific BACE1 genotypes provide additional risk for late-onset Alzheimer disease in APOE epsilon 4 carriers, Am. J. Med. Genet. B: Neuropsychiatr. Genet. 119 (2003) 44–47.

[31] R. Kan, B. Wang, C. Zhang, F. Jin, Z. Yang, S. Ji, Z. Lu, C. Zheng, L. Wang, Genetic association of BACE1 gene polymorphism C786G with late-onset Alzheimer's disease in Chinese, J. Mol. Neurosci. 25 (2005) 127–131.

[32] B. Dermaut, J. Theuns, K. Sleegers, H. Hasegawa, M. Van den Broeck, K. Vennekens, E. Corsmit, P. St George-Hyslop, M. Cruts, C.M. van Duijn, C. Van Broeckhoven, The gene encoding nicastrin, a major gamma-secretase component, modifies risk for familial early-onset Alzheimer disease in a Dutch population-based sample, Am. J. Hum. Genet. 70 (2002) 1568–1574.

[33] A. Confaloni, L. Terreni, P. Piscopo, A. Crestini, L.M. Campeggi, C.S. Frigerio, I. Blotta, M. Perri, M. Di Natale, R. Maletta, G. Marcon, M. Franceschi, A.C. Bruni,

G. Forloni, A. Cantafora, Nicastrin gene in familial and sporadic Alzheimer's disease, Neurosci. Lett. 15 (2003) 61–65.
[34] L. Bertram, R. Menon, K. Mullin, M. Parkinson, M.L. Bradley, D. Blacker, R.E. Tanzi, PEN2 is not a genetic risk factor for Alzheimer's disease in a large family sample, Neurology 62 (2004) 304–306.
[35] P. Piscopo, A. Manfredi, L. Malvezzi-Campeggi, A. Crestini, O. Spadoni, R. Cherchi, E. Deiana, M.R. Piras, A. Confaloni, Genetic study of Sardinian patients with Alzheimer's disease, Neurosci. Lett. 398 (2006) 124–128.
[36] L. Jia, J. Ye, W. Wang, C. Zhou, X. Zhang, J. Xu, L. Wang, J. Jia, Genetic association between polymorphisms of Pen2 gene and late onset Alzheimer's disease in the North Chinese population, Brain Res. 1141 (2007) 10–14.
[37] E. Rogaeva, Y. Meng, J.H. Lee, Y. Gu, T. Kawarai, F. Zou, T. Katayama, C.T. Baldwin, R. Cheng, H. Hasegawa, F. Chen, N. Shibata, K.L. Lunetta, R. Pardossi-Piquard, C. Bohm, Y. Wakutani, L.A. Cupples, K.T. Cuenco, R.C. Green, L. Pinessi, I. Rainero, S. Sorbi, A. Bruni, R. Duara, R.P. Friedland, R. Inzelberg, W. Hampe, H. Bujo, Y.Q. Song, O.M. Andersen, T.E. Willnow, N. Graff-Radford, R.C. Petersen, D. Dickson, S.D. Der, P.E. Fraser, G. Schmitt-Ulms, S. Younkin, R. Mayeux, L.A. Farrer, P. St George-Hyslop, The neuronal sortilin-related receptor SORL1 is genetically associated with Alzheimer disease, Nat. Genet. 39 (2007) 168–177.
[38] Y. Meng, J.H. Lee, R. Cheng, P. St George-Hyslop, R. Mayeux, L.A. Farrer, Association between SORL1 and Alzheimer's disease in a genome-wide study, Neuroreport 18 (2007) 1761–1764.
[39] H. Li, S. Wetten, L. Li, P.L. St Jean, R. Upmanyu, L. Surh, D. Hosford, M.R. Barnes, J.D. Briley, M. Borrie, N. Coletta, R. Delisle, D. Dhalla, M.G. Ehm, H.H. Feldman, L. Fornazzari, S. Gauthier, N. Goodgame, D. Guzman, S. Hammond, P. Hollingworth, G.Y. Hsiung, J. Johnson, D.D. Kelly, R. Keren, A. Kertesz, K.S. King, S. Lovestone, I. Loy-English, P.M. Matthews, M.J. Owen, M. Plumpton, W. Pryse-Phillips, R.K. Prinjha, J.C. Richardson, A. Saunders, A.J. Slater, P.H. St George-Hyslop, S.W. Stinnett, J.E. Swartz, R.L. Taylor, J. Wherrett, J. Williams, D.P. Yarnall, R.A. Gibson, M.C. Irizarry, L.T. Middleton, A.D. Roses, Candidate single-nucleotide polymorphisms from a genomewide association study of Alzheimer disease, Arch. Neurol. 65 (2008) 45–53.
[40] F. Coppedè, M. Mancuso, A. Lo Gerfo, M.L. Manca, L. Petrozzi, L. Migliore, G. Siciliano, L. Murri, A Ser326Cys polymorphism in the DNA repair gene hOGG1 is not associated with sporadic Alzheimer's disease, Neurosci. Lett. 414 (2007) 282–285.
[41] S. Doğru-Abbasoğlu, G. Aykaç-Toker, H.A. Hanagasi, H. Gürvit, M. Emre, M. Uysal, The Arg194Trp polymorphism in DNA repair gene XRCC1 and the risk for sporadic late-onset Alzheimer's disease, Neurol. Sci. 28 (2007) 31–34.
[42] D.R. McLachlan, C. Bergeron, J.E. Smith, D. Boomer, S.L. Rifat, Risk for neuropathologically confirmed Alzheimer's disease and residual aluminum in municipal drinking water employing weighted residential histories, Neurology 46 (1996) 401–405.
[43] C.N. Martyn, D.N. Coggon, H. Inskip, R.F. Lacey, W.F. Young, Aluminum concentrations in drinking water and risk of Alzheimer's disease, Epidemiology 8 (1997) 281–286.
[44] R.A. Cherny, J.T. Legg, C.A. McLean, D.P. Fairlie, X. Huang, C.S. Atwood, K. Beyreuther, R.E. Tanzi, C.L. Masters, A.I. Bush, Aqueous dissolution of Alzheimer's disease Abeta amyloid deposits by biometal depletion, J. Biol. Chem. 274 (1999) 23223–23228.
[45] J. Mutter, J. Naumann, C. Sadaghiani, R. Schneider, H. Walach, Alzheimer disease: mercury as pathogenetic factor and apolipoprotein E as a moderator, Neuro Endocrinol. Lett. 25 (2004) 331–339.
[46] M. Santibáñez, F. Bolumar, A.M. García, Occupational risk factors in Alzheimer's disease: a review assessing the quality of published epidemiological studies, Occup. Environ. Med. 64 (2007) 723–732.
[47] M. Kivipelto, A. Solomon, Cholesterol as a risk factor for Alzheimer's disease – epidemiological evidence, Acta Neurol. Scand. Suppl. 185 (2006) 50–57.
[48] V. Solfrizzi, C. Capurso, A. D'Introno, A.M. Colacicco, A. Santamato, M. Ranieri, P. Fiore, A. Capurso, F. Panza, Lifestyle-related factors in predementia and dementia syndromes, Expert Rev. Neurother. 8 (2008) 133–158.
[49] W.B. Grant, Dietary links to Alzheimer's disease, Alzheimer's Dis. Rev. 2 (1997) 42–55.
[50] M.A. Smith, G.J. Petot, G. Perry, Diet and oxidative stress: a novel synthesis of epidemiological data on Alzheimer's disease, J. Alzheimer's Dis. 1 (1999) 203–206.
[51] S.C. Burgener, L. Buettner, Coen K. Buckwalter, E. Beattie, A.L. Bossen, D.M. Fick, S. Fitzsimmons, A. Kolanowski, N.E. Richeson, K. Rose, A. Schreiner, J.K. Pringle Specht, I. Testad, F. Yu, S. McKenzie, Evidence supporting nutritional interventions for persons in early stage Alzheimer's disease (AD), J. Nutr. Health Aging 12 (2008) 18–21.
[52] P. Barberger-Gateau, C. Raffaitin, L. Letenneur, C. Berr, C. Tzourio, J.F. Dartigues, A. Alpérovitch, Dietary patterns and risk of dementia: the Three-City cohort study, Neurology 69 (2007) 1921–1930.
[53] C. Van Den Heuvel, E. Thornton, R. Vink, Traumatic brain injury and Alzheimer's disease: a review, Prog. Brain Res. 161 (2007) 303–316.
[54] V.H. Perry, C. Cunningham, C. Holmes, Systemic infections and inflammation affect chronic neurodegeneration, Nat. Rev. Immunol. 7 (2007) 161–167.
[55] B. Thomas, M.F. Beal, Parkinson's disease, Hum. Mol. Genet. 16 (2007) R183–R194.
[56] S. Rosner, N. Giladi, A. Orr-Urtreger, Advances in the genetics of Parkinson's disease, Acta Pharmacol. Sin. 29 (2008) 21–34.
[57] L.M. Shulman, Gender differences in Parkinson's disease, Gend. Med. 4 (2007) 8–18.
[58] P. Ragonese, M. D'Amelio, G. Savettieri, Implications for estrogens in Parkinson's disease: an epidemiological approach, Ann. NY Acad. Sci. 1089 (2006) 373–382.
[59] M.H. Polymeropoulos, C. Lavedan, E. Leroy, S.E. Ide, A. Dehejia, A. Dutra, B. Pike, H. Root, J. Rubenstein, R. Boyer, E.D. Stenroos, S. Chandrasekharappa, A. Athanassiadou, T. Papapetropoulos, W.G. Johnson, A.M. Lazzarini, R.C. Duvoisin, G.D. Iorio, L.I. Golbe, R.L. Nussbaum, Mutation in the alphasynuclein gene identified in families with Parkinson's disease, Science 276 (1997) 2045–2047.
[60] R. Kruger, W. Kuhn, T. Muller, D. Woitalla, M. Graeber, S. Kosel, H. Przuntek, J.T. Epplen, L. Schols, O. Riess, Ala30 fi Pro mutation in the gene encoding alpha–synuclein in Parkinson's disease, Nat. Genet. 18 (1998) 106–108.
[61] J.J. Zarranz, J. Alegre, J.C. Gómez-Esteban, E. Lezcano, R. Ros, I. Ampuero, L. Vidal, J. Hoenicka, O. Rodriguez, B. Atarés, V. Llorens, E. Gomez Tortosa, D.G. del Ser, T. Muñoz, J.G. de Yebenes, The new mutation, E46K, of alpha-synuclein causes Parkinson and Lewy body dementia, Ann. Neurol. 55 (2004) 164–173.
[62] A.B. Singleton, M. Farrer, J. Johnson, A. Singleton, S. Hague, J. Kachergus, M. Hulihan, T. Peuralinna, A. Dutra, R. Nussbaum, S. Lincoln, A. Crawley, M. Hanson, D. Maraganore, C. Adler, M.R. Cookson, M. Muenter, M. Baptista, D. Miller, J. Blancato, J. Hardy, K. Gwinn-Hardy, alpha-Synuclein locus triplication causes Parkinson's disease, Science 302 (2003) 841.
[63] M.C. Chartier-Harlin, J. Kachergus, C. Roumier, V. Mouroux, X. Douay, S. Lincoln, C. Levecque, L. Larvor, J. Andrieux, M. Hulihan, N. Waucquier, L. Defebvre, P. Amouyel, M. Farrer, A. Destée, Alpha-synuclein locus duplication as a cause of familial Parkinson's disease, Lancet 364 (2004) 1167–1169.
[64] M.T. Lorincz, Clinical implications of Parkinson's disease genetics, Semin. Neurol. 26 (2006) 492–498.
[65] D.M. Maraganore, M. de Andrade, A. Elbaz, M.J. Farrer, J.P. Ioannidis, R. Krüger, W.A. Rocca, N.K. Schneider, T.G. Lesnick, S.J. Lincoln, M.M. Hulihan, J.O. Aasly, T. Ashizawa, M.C. Chartier-Harlin, H. Checkoway, C. Ferrarese, G. Hadjigeorgiou, N. Hattori, H. Kawakami, J.C. Lambert, T. Lynch, G.D. Mellick, S. Papapetropoulos, A. Parsian, A. Quattrone, O. Riess, E.K. Tan, C. Van Broeckhoven, Genetic Epidemiology of Parkinson's Disease (GEO-PD) Consortium. Collaborative analysis of alpha-synuclein gene promoter variability and Parkinson disease, JAMA 296 (2006) 661–670.
[66] T. Kitada, S. Asakawa, N. Hattori, H. Matsumine, Y. Yamamura, S. Minoshima, M. Yokochi, Y. Mizuno, N. Shimizu, Mutations in the Parkin gene cause autosomal recessive juvenile Parkinsonism, Nature 392 (1998) 605–608.
[67] I.F. Mata, P.J. Lockhart, M.J. Farrer, Parkin genetics: one model for Parkinson's disease, Hum. Mol. Genet. 1 (2004) R127–R133.
[68] H. Shimura, N. Hattori, S. Kubo, Y. Mizuno, S. Asakawa, S. Minoshima, N. Shimizu, K. Iwai, T. Chiba, K. Tanaka, T. Suzuki, Familial Parkinson disease gene product, parkin, is a ubiquitin-protein ligase, Nat. Genet. 25 (2000) 302–305.
[69] E. Leroy, R. Boyer, G. Auburger, B. Leube, G. Ulm, E. Mezey, G. Harta, M.J. Brownstein, S. Jonnalagada, T. Chernova, A. Dehejia, C. Lavedan, T. Gasser, P.J. Steinbach, K.D. Wilkinson, M.H. Polymeropoulous, The ubiquitin pathway in Parkinson's disease, Nature 395 (1998) 451–452.
[70] Y. Liu, L. Fallon, H.A. Lashuel, Z. Liu, P.T. Lansbury Jr., The UCH-L1 gene encodes two opposing enzymatic activities that affect alpha-synuclein degradation and Parkinson's disease susceptibility, Cell 111 (2002) 209–218.
[71] D.M. Maraganore, T.G. Lesnick, A. Elbaz, M.C. Chartier-Harlin, T. Gasser, R. Krüger, N. Hattori, G.D. Mellick, A. Quattrone, J. Satoh, T. Toda, J. Wang, J.P. Ioannidis, M. de Andrade, W.A. Rocca, UCHL1 Global Genetics Consortium.UCHL1 is a Parkinson's disease susceptibility gene, Ann. Neurol. 55 (2004) 512–521.
[72] E.M. Valente, P.M. Abou-Sleiman, V. Caputo, M.M. Muqit, K. Harvey, S. Gispert, Z. Ali, D. Del Turco, A.R. Bentivoglio, D.G. Healy, A. Albanese, R. Nussbaum, R. Gonzalez-Maldonado, T. Deller, S. Salvi, P. Cortelli, W.P. Gilks, D.S. Latchman, R.J. Harvey, B. Dallapiccola, G. Auburger, N.W. Wood, Hereditary early-onset Parkinson's disease caused by mutations in PINK1, Science 304 (2004) 1158–1160.
[73] V. Bonifati, C.F. Rohé, G.J. Breedveld, E. Fabrizio, M. De Mari, C. Tassorelli, A. Tavella, R. Marconi, D.J. Nicholl, H.F. Chien, E. Fincati, G. Abbruzzese, P. Marini, A. De Gaetano, M.W. Horstink, J.A. Maat-Kievit, C. Sampaio, A. Antonini, F. Stocchi, P. Montagna, V. Toni, M. Guidi, A. Dalla Libera, M. Tinazzi, F. De Pandis, G. Fabbrini, S. Goldwurm, A. de Klein, E. Barbosa, L. Lopiano, E. Martignoni, P. Lamberti, N. Vanacore, G. Meco, B.A. Oostra, Italian Parkinson Genetics Network. Early-onset parkinsonism associated with PINK1 mutations: frequency, genotypes, and phenotypes, Neurology 65 (2005) 87–95.
[74] C.M. van Duijn, M.C. Dekker, V. Bonifati, R.J. Galjaard, J.J. Houwing-Duistermaat, P.J. Snijders, L. Testers, G.J. Breedveld, M. Horstink, L.A. Sandkuijl, J.C. van Swieten, B.A. Oostra, P. Heutink, Park7, a novel locus for autosomal recessive early-onset parkinsonism, on chromosome 1p36, Am. J. Hum. Genet. 69 (2001) 629–634.
[75] P.J. Lockhart, S. Lincoln, M. Hulihan, J. Kachergus, K. Wilkes, G. Bisceglio, D.C. Mash, M.J. Farrer, DJ-1 mutations are a rare cause of recessively inherited early onset parkinsonism mediated by loss of protein function, J. Med. Genet. 41 (2004) e22.
[76] C. Paisan-Ruiz, S. Jain, E.W. Evans, W.P. Gilks, J. Simon, M. van der Brug, A. Lopez de Munain, S. Aparicio, A.M. Gil, N. Khan, J. Johnson, J.R. Martinez, D. Nicholl, I.M. Carrera, A.S. Pena, R. de Silva, A. Lees, J.F. Marti-Masso, J. Perez-Tur, N.W. Wood, A.B. Singleton, Cloning of the gene containing mutations that cause PARK8-linked Parkinson's disease, Neuron 44 (2004) 595–600.
[77] A.B. West, D.J. Moore, S. Biskup, A. Bugayenko, W.W. Smith, C.A. Ross, V.L. Dawson, T.M. Dawson, Parkinson's disease-associated mutations in leucine-

rich repeat kinase 2 augment kinase activity, Proc. Natl. Acad. Sci. U.S.A. 102 (2005) 16842–16847.
[78] M.J. Farrer, J.T. Stone, C.H. Lin, J.C. Dächsel, M.M. Hulihan, K. Haugarvoll, O.A. Ross, R.M. Wu, Lrrk2 G2385R is an ancestral risk factor for Parkinson's disease in Asia, Parkinsonism Relat. Disord. 13 (2007) 89–92.
[79] D.J. Hampshire, E. Roberts, Y. Crow, J. Bond, A. Mubaidin, A.L. Wriekat, A. Al-Din, C.G. Woods, Kufor-Rakeb syndrome, pallido-pyramidal degeneration with supranuclear upgaze paresis and dementia, maps to 1p36, J. Med. Genet. 38 (2001) 680–682.
[80] A. Ramirez, A. Heimbach, J. Gründemann, B. Stiller, D. Hampshire, L.P. Cid, I. Goebel, A.F. Mubaidin, A.L. Wriekat, J. Roeper, A. Al-Din, A.M. Hillmer, M. Karsak, B. Liss, C.G. Woods, M.I. Behrens, C. Kubisch, Hereditary parkinsonism with dementia is caused by mutations in ATP13A2, encoding a lysosomal type 5 P-type ATPase, Nat. Genet. 38 (2006) 1184–1191.
[81] K.M. Strauss, L.M. Martins, H. Plun-Favreau, F.P. Marx, S. Kautzmann, D. Berg, T. Gasser, Z. Wszolek, T. Müller, A. Bornemann, H. Wolburg, J. Downward, O. Riess, J.B. Schulz, R. Krüger, Loss of function mutations in the gene encoding Omi/HtrA2 in Parkinson's disease, Hum. Mol. Genet. 14 (2005) 2099–2111.
[82] D.G. Healy, P.M. Abou-Sleiman, J.P. Casas, K.R. Ahmadi, T. Lynch, S. Gandhi, M.M. Muqit, T. Foltynie, R. Barker, K.P. Bhatia, N.P. Quinn, A.J. Lees, J.M. Gibson, J.L. Holton, T. Revesz, D.B. Goldstein, N.W. WoodG, UCHL-1 is not a Parkinson's disease susceptibility gene, Ann. Neurol. 59 (2006) 627–633.
[83] E.K. Tan, The role of common genetic risk variants in Parkinson disease, Clin. Genet. 72 (2007) 387–393.
[84] D.G. Healy, P.M. Abou-Sleiman, A.J. Lees, J.P. Casas, N. Quinn, K. Bhatia, A.D. Hingorani, N.W. Wood, Tau gene and Parkinson's disease: a case-control study and meta-analysis, J. Neurol. Neurosurg. Psychiatry 75 (2004) 962–965.
[85] C.C. McCulloch, D.M. Kay, S.A. Factor, A. Samii, J.G. Nutt, D.S. Higgins, A. Griffith, J.W. Roberts, B.C. Leis, J.S. Montimurro, C.P. Zabetian, H. Payami, Exploring gene-environment interactions in Parkinson's disease, Hum. Genet. 123 (2008) 257–265.
[86] S. Winkler, I.R. König, K. Lohmann-Hedrich, P. Vieregge, V. Kostic, C. Klein, Role of ethnicity on the association of MAPT H1 haplotypes and subhaplotypes in Parkinson's disease, Eur. J. Hum. Genet. 15 (2007) 1163–1168.
[87] G.D. Mellick, CYP450, genetics and Parkinson's disease: gene × environment interactions hold the key, J. Neural Transm. Suppl. 70 (2006) 159–165.
[88] F.D. Dick, G. De Palma, A. Ahmadi, A. Osborne, N.W. Scott, G.J. Prescott, J. Bennett, S. Semple, S. Dick, P. Mozzoni, N. Haites, S.B. Wettinger, A. Mutti, M. Otelea, A. Seaton, P. Soderkvist, A. Felice, Geoparkinson Study Group, Gene–environment interactions in parkinsonism and Parkinson's disease: the Geoparkinson study, Occup. Environ. Med. 64 (2007) 673–680.
[89] A. Menegon, P.G. Board, A.C. Blackburn, G.D. Mellick, D.G. Le Couteur, Parkinson's disease, pesticides, and glutathione transferase polymorphisms, Lancet 352 (1998) 1344–1346.
[90] J.B. Wilk, J.E. Tobin, O. Suchowersky, H.A. Shill, C. Klein, G.F. Wooten, M.F. Lew, M.H. Mark, M. Guttman, R.L. Watts, C. Singer, J.H. Growdon, J.C. Latourelle, M.H. Saint-Hilaire, A.L. DeStefano, R. Prakash, S. Williamson, C.J. Berg, M. Sun, S. Goldwurm, G. Pezzoli, B.A. Racette, J.S. Perlmutter, A. Parsian, K.B. Baker, M.L. Giroux, I. Litvan, P.P. Pramstaller, G. Nicholson, D.J. Burn, P.F. Chinnery, P. Vieregge, J.T. Slevin, F. Cambi, M.E. MacDonald, J.F. Gusella, R.H. Myers, L.I. Golbe, Herbicide exposure modifies GSTP1 haplotype association to Parkinson onset age: the GenePD Study, Neurology 67 (2006) 2206–2210.
[91] J. Borlak, S.M. Reamon-Buettner, N-acetyltransferase 2 (NAT2) gene polymorphisms in Parkinson's disease, BMC Med. Genet. 7 (2006) 30.
[92] A. Elbaz, C. Levecque, J. Clavel, J.S. Vidal, F. Richard, P. Amouyel, A. Alpérovitch, M.C. Chartier-Harlin, C. Tzourio, CYP2D6 polymorphism, pesticide exposure, and Parkinson's disease, Ann. Neurol. 55 (2004) 430–434.
[93] E. Evangelou, D.M. Maraganore, J.P. Ioannidis, Meta-analysis in genome-wide association datasets: strategies and application in Parkinson disease, PLoS ONE 2 (2007) e196.
[94] C.M. Tanner, R. Ottman, S.M. Goldman, J. Ellenberg, P. Chan, R. Mayeux, J.W. Langston, Parkinson disease in twins: an etiologic study, JAMA 281 (1999) 341–346.
[95] J.W. Langston, L.S. Forno, J. Tetrud, A.G. Reeves, J.A. Kaplan, D. Karluk, Evidence of active nerve cell degeneration in the substantia nigra of humans years after 1-methyl-4-phenyl-1,2,3,6-tetrahydropyridine exposure, Ann. Neurol. 46 (1999) 598–605.
[96] B. Liu, H.M. Gao, J.S. Hong, Parkinson's disease and exposure to infectious agents and pesticides and the occurrence of brain injuries: role of neuroinflammation, Environ. Health Perspect. 111 (2003) 1065–1073.
[97] F.D. Dick, Parkinson's disease and pesticide exposures, Br. Med. Bull. 79–80 (2006) 219–231.
[98] A. Elbaz, Parkinson's disease and rural environment, Rev. Prat. 57 (2007) 37–39.
[99] F.D. Dick, G. De Palma, A. Ahmadi, N.W. Scott, G.J. Prescott, J. Bennett, S. Semple, S. Dick, C. Counsell, P. Mozzoni, N. Haites, S.B. Wettinger, A. Mutti, M. Otelea, A. Seaton, P. Söderkvist, A. Felice, Geoparkinson study group, Environmental risk factors for Parkinson's disease and parkinsonism: the Geoparkinson study, Occup. Environ. Med. 64 (2007) 666–672.
[100] M.M. Finkelstein, M. Jerrett, A study of the relationships between Parkinson's disease and markers of traffic-derived and environmental manganese air pollution in two Canadian cities, Environ. Res. 104 (2007) 420–432.
[101] S. Coon, A. Stark, E. Peterson, A. Gloi, G. Kortsha, J. Pounds, D. Chettle, J. Gorell, Whole-body lifetime occupational lead exposure and risk of Parkinson's disease, Environ. Health Perspect. 114 (2006) 1872–1876.
[102] B. Ritz, A. Ascherio, H. Checkoway, K.S. Marder, L.M. Nelson, W.A. Rocca, G.W. Ross, D. Strickland, S.K. Van Den Eeden, J. Gorell, Pooled analysis of tobacco use and risk of Parkinson disease, Arch. Neurol. 64 (2007) 990–997.
[103] G. Hu, S. Bidel, P. Jousilahti, R. Antikainen, J. Tuomilehto, Coffee and tea consumption and the risk of Parkinson's disease, Mov. Disord. 22 (2007) 2242–2248.
[104] X. Gao, H. Chen, T.T. Fung, G. Logroscino, M.A. Schwarzschild, F.B. Hu, A. Ascherio, Prospective study of dietary pattern and risk of Parkinson disease, Am. J. Clin. Nutr. 86 (2007) 1486–1494.
[105] R.D. Abbott, G.W. Ross, L.R. White, C.M. Tanner, K.H. Masaki, J.S. Nelson, J.D. Curb, H. Petrovitch, Excessive daytime sleepiness and subsequent development of Parkinson disease, Neurology 65 (2005) 1442–1446.
[106] G. Logroscino, H.D. Sesso, R.S. Paffenbarger Jr., I.M. Lee, Physical activity and risk of Parkinson's disease: a prospective cohort study, J. Neurol. Neurosurg. Psychiatry 77 (2006) 1318–1322.
[107] S.M. Goldman, C.M. Tanner, D. Oakes, G.S. Bhudhikanok, A. Gupta, J.W. Langston, Head injury and Parkinson's disease risk in twins, Ann. Neurol. 60 (2006) 65–72.
[108] P.M. Worms, The epidemiology of motor neuron diseases: a review of recent studies, J. Neurol. Sci. 191 (2001) 3–9.
[109] J.D. Mitchell, G.D. Borasio, Amyotrophic lateral sclerosis, Lancet 369 (2007) 2031–2041.
[110] J.C. Schymick, K. Talbot, B.J. Traynor, Genetics of sporadic amyotrophic lateral sclerosis, Hum. Mol. Genet. 16 (2007) R233–R242.
[111] D.R. Rosen, T. Siddique, D. Patterson, D.A. Figlewicz, P. Sapp, A. Hentati, D. Donaldson, J. Goto, J.P. O'Regan, H.X. Deng, Z. Rahmani, A. Krizus, D. McKenna-Yasek, A. Cayabyab, S.M. Gaston, R. Berger, R.E. Tanzi, J.J. Halperin, B. Herzfeldt, R. Van den Bergh, W. Hung, T. Bird, G. Deng, D.W. Mulder, C. Smyth, N.G. Laing, E. Soriano, M.A. Pericak-Vance, J. Haines, G.A. Rouleau, J.S. Gusella, H.R. Horvitz, R.H. Brown Jr., Nature 362 (1993) 59–62.
[112] M. Nagai, M. Aoki, I. Miyoshi, M. Kato, P. Pasinelli, N. Kasai, R.H. Brown Jr., Y. Itoyama, Rats expressing human cytosolic copper–zinc superoxide dismutase transgenes with amyotrophic lateral sclerosis: associated mutations develop motor neuron disease, J. Neurosci. 21 (2001) 9246–9254.
[113] D. Sau, S. De Biasi, L. Vitellaro-Zuccarello, P. Riso, S. Guarnieri, M. Porrini, S. Simeoni, V. Crippa, E. Onesto, I. Palazzolo, P. Rusmini, E. Bolzoni, C. Bendotti, A. Poletti, Mutation of SOD1 in ALS: a gain of a loss of function, Hum. Mol. Genet. 16 (2007) 1604–1618.
[114] A. Hentati, K. Bejaoui, M.A. Pericak-Vance, F. Hentati, M.C. Speer, W.Y. Hung, D.A. Figlewicz, J. Haines, J. Rimmler, C. Ben Hamida, R.H. Brown Jr., T. Siddique, Linkage of recessive familial amyotrophic lateral sclerosis to chromosome 2q33–q35, Nat. Genet. 7 (1994) 425–428.
[115] S. Hadano, C.K. Hand, H. Osuga, Y. Yanagisawa, A. Otomo, R.S. Devon, N. Miyamoto, J. Showguchi-Miyata, Y. Okada, R. Singaraja, D.A. Figlewicz, T. Kwiatkowski, B.A. Hosler, T. Sagie, J. Skaug, J. Nasir, R.H. Brown Jr., S.W. Scherer, G.A. Rouleau, M.R. Hayden, J.E. Ikeda, A gene encoding a putative GTPase regulator is mutated in familial amyotrophic lateral sclerosis 2, Nat. Genet. 29 (2001) 166–173.
[116] Y. Yang, A. Hentati, H.X. Deng, O. Dabbagh, T. Sasaki, M. Hirano, W.Y. Hung, K. Ouahchi, J. Yan, A.C. Azim, N. Cole, G. Gascon, A. Yagmour, M. Ben-Hamida, M. Pericak-Vance, F. Hentati, T. Siddique, The gene encoding alsin, a protein with three guanine-nucleotide exchange factor domains, is mutated in a form of recessive amyotrophic lateral sclerosis, Nat. Genet. 29 (2001) 160–165.
[117] J. Chandran, J. Ding, H. Cai, Alsin and the molecular pathways of amyotrophic lateral sclerosis, Mol. Neurobiol. 36 (2007) 224–231.
[118] Y.Z. Chen, C.L. Bennett, H.M. Huynh, I.P. Blair, I. Puls, J. Irobi, I. Dierick, A. Abel, M.L. Kennerson, B.A. Rabin, DNA/RNA helicase gene mutations in a form of juvenile amyotrophic lateral sclerosis (ALS4), Am. J. Hum. Genet. 74 (2004) 1128–1135.
[119] A. Suraweera, O.J. Becherel, P. Chen, N. Rundle, R. Woods, J. Nakamura, M. Gatei, C. Criscuolo, A. Filla, L. Chessa, M. Fusser, B. Epe, N. Gueven, M.F. Lavin, Senataxin, defective in ataxia oculomotor apraxia type 2, is involved in the defense against oxidative DNA damage, J. Cell. Biol. 117 (2007) 969–979.
[120] A.L. Nishimura, M. Mitne-Neto, H.C. Silva, A. Richieri-Costa, S. Middleton, D. Cascio, F. Kok, J.R. Oliveira, T. Gillingwater, J. Webb, P. Skehel, M. Zatz, A mutation in the vesicle-trafficking protein VAPB causes late-onset spinal muscular atrophy and amyotrophic lateral sclerosis, Am. J. Hum. Genet. 75 (2004) 822–831.
[121] E. Teuling, S. Ahmed, E. Haasdijk, J. Demmers, M.O. Steinmetz, A. Akhmanova, D. Jaarsma, C.C. Hoogenraad, Motor neuron disease-associated mutant vesicle-associated membrane protein-associated protein (VAP) B recruits wild-type VAPs into endoplasmic reticulum-derived tubular aggregates, J. Neurosci. 27 (2007) 9801–9815.
[122] M.H. Finlayson, J.B. Martin, Cerebral lesions in familial amyotrophic lateral sclerosis and dementia, Acta Neuropathol. 26 (1973) 237–246.
[123] B.A. Hosler, T. Siddique, P.C. Sapp, W. Sailor, M.C. Huang, A. Hossain, J.R. Daube, M. Nance, C. Fan, J. Kaplan, W.Y. Hung, D. McKenna-Yasek, J.L. Haines, M.A. Pericak-Vance, H.R. Horvitz, R.H. Brown Jr., Linkage of familial amyotrophic lateral sclerosis with frontotemporal dementia to chromosome 9q21–q22, JAMA 284 (2000) 1664–1669.
[124] M. Morita, A. Al-Chalabi, P.M. Andersen, B. Hosler, P. Sapp, E. Englund, J.E. Mitchell, J.J. Habgood, J. de Belleroche, J. Xi, W. Jongjaroenprasert, H.R. Horvitz, L.G. Gunnarsson, R.H. Brown Jr., A locus on chromosome 9p confers susceptibility to ALS and frontotemporal dementia, Neurology 66 (2006) 839–844.

[125] M. Hutton, C.L. Lendon, P. Rizzu, M. Baker, S. Froelich, H. Houlden, S. Pickering-Brown, S. Chakraverty, A. Isaacs, A. Grover, J. Hackett, J. Adamson, S. Lincoln, D. Dickson, P. Davies, R.C. Petersen, M. Stevens, E. de Graaff, E. Wauters, J. van Baren, M. Hillebrand, M. Joosse, J.M. Kwon, P. Nowotny, L.K. Che, J. Norton, J.C. Morris, L.A. Reed, J. Trojanowski, H. Basun, L. Lannfelt, M. Neystat, S. Fahn, F. Dark, T. Tannenberg, P.R. Dodd, N. Hayward, J.B. Kwok, P.R. Schofield, A. Andreadis, J. Snowden, D. Craufurd, D. Neary, F. Owen, B.A. Oostra, J. Hardy, A. Goate, J. van Swieten, D. Mann, T. Lynch, P. Heutink, Association of missense and 5′-splice-site mutations in tau with the inherited dementia FTDP-17, Nature 393 (1998) 702–705.
[126] R. Sato-Harada, S. Okabe, T. Umeyama, N. Y- Kanai, Hirokawa, Microtubule-associated proteins regulate microtubule function as the track for intracellular membrane organelle transports, Cell Struct. Funct. 21 (1996) 283–295.
[127] I. Puls, C. Jonnakuty, B.H. LaMonte, E.L. Holzbaur, M. Tokito, E. Mann, M.K. Floeter, K. Bidus, D. Drayna, S.J. Oh, R.H. Brown Jr., C.L. Ludlow, K.H. Fischbeck, Mutant dynactin in motor neuron disease, Nat. Genet. 33 (2003) 455–456.
[128] B.A. Eaton, R.D. Fetter, G.W. Davis, Dynactin is necessary for synapse stabilization, Neuron 34 (2002) 729–741.
[129] C. Hayward, S. Colville, R.J. Swingler, D.J. Brock, Molecular genetic analysis of the APEX nuclease gene in amyotrophic lateral sclerosis, Neurology 52 (1999) 1899–1901.
[130] M.J. Greenway, M.D. Alexander, S. Ennis, B.J. Traynor, B. Corr, E. Frost, A. Green, O. Hardiman, A novel candidate region for ALS on chromosome 14q11.2, Neurology 63 (2004) 1936–1938.
[131] F. Coppedè, A. Lo Gerfo, C. Carlesi, S. Piazza, M. Mancuso, L. Pasquali, L. Murri, L. Migliore, G. Siciliano, Lack of association between the APEX1 Asp148Glu polymorphism and sporadic amyotrophic lateral sclerosis, Neurobiol. Aging, in press.
[132] F. Coppedè, M. Mancuso, A. Lo Gerfo, C. Carlesi, S. Piazza, A. Rocchi, L. Petrozzi, C. Nesti, D. Micheli, A. Bacci, L. Migliore, L. Murri, G. Siciliano, Association of the hOGG1 Ser326Cys polymorphism with sporadic amyotrophic lateral sclerosis, Neurosci. Lett. 420 (2007) 163–168.
[133] R. Del Bo, M. Scarlato, S. Ghezzi, F. Martinelli-Boneschi, S. Corti, F. Locatelli, D. Santoro, A. Prelle, C. Briani, M. Nardini, G. Siciliano, M. Mancuso, L. Murri, N. Bresolin, G.P. Comi, Absence of angiogenic genes modification in Italian ALS patients, Neurobiol. Aging 29 (2008) 314–316.
[134] M.A. van Es, P.W. van Vught, H.M. Blauw, L. Franke, C.G. Saris, L. Van den Bosch, S.W. de Jong, V. de Jong, F. Baas, R. van't Slot, R. Lemmens, H.J. Schelhaas, A. Birve, K. Sleegers, C. Van Broeckhoven, J.C. Schymick, B.J. Traynor, J.H. Wokke, C. Wijmenga, W. Robberecht, P.M. Andersen, J.H. Veldink, R.A. Ophoff, L.H. van den Berg, Genetic variation in DPP6 is associated with susceptibility to amyotrophic lateral sclerosis, Nat. Genet. 40 (2008) 29–31.
[135] G.E. Kisby, M. Ellison, P.S. Spencer, Content of the neurotoxins cycasin (methylazoxymethanol beta-D-glucoside) and BMAA (beta-N-methylamino-L-alanine) in cycad flour prepared by Guam Chamorros, Neurology 42 (1992) 1336–1340.
[136] F. Kamel, D.M. Umbach, H. Hu, T.L. Munsat, J.M. Shefner, J.A. Taylor, D.P. Sandler, Lead exposure as a risk factor for amyotrophic lateral sclerosis, Neurodegener. Dis. 2 (2005) 195–201.
[137] M.M. Qureshi, D. Hayden, L. Urbinelli, K. Ferrante, K. Newhall, D. Myers, S. Hilgenberg, R. Smart, R.H. Brown, M.E. Cudkowicz, Analysis of factors that modify susceptibility and rate of progression in amyotrophic lateral sclerosis (ALS), Amyotroph. Lateral Scler. 7 (2006) 173–182.
[138] V. Govoni, E. Granieri, E. Fallica, I. Casetta, Amyotrophic lateral sclerosis, rural environment and agricultural work in the Local Health Discrict of Ferrara, Italy, in the years 1964–1998, J. Neurol. 252 (2005) 1322–1327.
[139] H. Doi, H. Kikuchi, H. Murai, Y. Kawano, H. Shigeto, Y. Ohyagi, J. Kira, Motor neuron disorder simulating ALS induced by chronic inhalation of pyrethroid insecticides, Neurology 67 (2006) 1894–1895.
[140] R.D. Horner, K.G. Kamins, J.R. Feussner, S.C. Grambow, J. Hoff-Lindquist, Y. Harati, H. Mitsumoto, R. Pascuzzi, P.S. Spencer, R. Tim, D. Howard, T.C. Smith, M.A.K. Ryan, C.J. Coffman, E.J. Kararskis, Occurrence of amyotrophic lateral sclerosis among Gulf War veterans, Neurology 61 (2003) 742–749.
[141] R.W. Haley, S. Billecke, B.N. La Du, Association of low PON1 type Q (type A) arylesterase activity with neurologic symptom complexes in Gulf War veterans, Toxicol. Appl. Pharmacol. 157 (1999) 227–233.
[142] C.Y. Li, F.C. Sung, Association between occupational exposure to power frequency electromagnetic fields and amyotrophic lateral sclerosis: a review, Am. J. Ind. Med. 43 (2003) 212–220.
[143] N. Håkansson, C. P- Gustavsson, B. Johansen, Floderus, Neurodegenerative diseases in welders and other workers exposed to high levels of magnetic fields, Epidemiology 14 (2003) 420–426.
[144] A. Chiò, G. Benzi, M. Dossena, R. Mutani, G. Mora, Severely increased risk of amyotrophic lateral sclerosis among Italian professional football players, Brain 128 (2005) 472–476.
[145] E.L. Abel, Football increases the risk for Lou Gehrig's disease, amyotrophic lateral sclerosis, Percept. Mot. Skills 104 (2007) 1251–1254.
[146] P. Wicks, J. Ganesalingham, C. Collin, M. Prevett, N.P. Leigh, A. Al-Chalabi, Three soccer playing friends with simultaneous amyotrophic lateral sclerosis, Amyotroph. Lateral Scler. 8 (2007) 177–179.
[147] S. Belli, N. Vanacore, Proportionate mortality in italian soccer players: is amyotrophic lateral sclerosis an occupational disease? Eur. J. Epidemiol. 20 (2005) 237–242.
[148] H. Chen, M. Richard, D.P. Sadler, D.M. Umbach, F. Kamel, Head injury and amyotrophic lateral sclerosis, Am. J. Epidemiol. 166 (2007) 810–816.
[149] M.G. Weisskopf, M.L. McCullough, E.E. Calle, M.J. Thun, M. Cudkowicz, A. Ascherio, Prospective study of cigarette smoking and amyotrophic lateral sclerosis, Am. J. Epidemiol. 160 (2004) 26–33.
[150] N.A. Sutedja, J.H. Veldink, K. Fischer, H. Kromhout, J.H. Wokke, M.H. Huisman, D.J. Heederik, L.H. Van den Berg, Lifetime occupation, education, smoking, and risk of ALS, Neurology 69 (2007) 1508–1514.
[151] R.L. Jirtle, M.K. Skinner, Environmental epigenomics and disease susceptibility, Nat. Rev. Genet. 8 (2007) 253–262.
[152] C.B. Santos-Rebouças, M.M. Pimentel, Implication of abnormal epigenetic patterns for human diseases, Eur. J. Hum. Genet. 15 (2007) 10–17.
[153] M. Szyf, The dynamic epigenome and its implications in toxicology, Toxicol. Sci. 100 (2007) 7–23.
[154] T.M. Edwards, J.P. Myers, Environmental exposures and gene regulation in disease etiology, Environ. Health Perspect. 115 (2007) 1264–1270.
[155] J.R. Weidman, D.C. Dolinoy, S.K. Murphy, R.L. Jirtle, Cancer susceptibility: epigenetic manifestation of environmental exposures, Cancer J. 13 (2007) 9–16.
[156] A.P. Feinberg, Phenotypic plasticity and the epigenetics of human disease, Nature 447 (2007) 433–440.
[157] A. Fuso, L. Seminara, R.A. Cavallaro, F. D'Anselmi, S. Scarpa, S-adenosylmethionine/homocysteine cycle alterations modify DNA methylation status with consequent deregulation of PS1 and BACE and beta-amyloid production, Mol. Cell. Neurosci. 28 (2005) 195–204.
[158] A. Fuso, R.A. Cavallaro, A. Zampelli, F. D'Anselmi, P. Piscopo, A. Confaloni, S. Scarpa, gamma-Secretase is differentially modulated by alterations of homocysteine cycle in neuroblastoma and glioblastoma cells, J. Alzheimer's Dis. 1 (2007) 275–290.
[159] A. Nunomura, G. Perry, G. Aliev, K. Hirai, A. Takeda, E.K. Balraj, P.K. Jones, H. Ghanbari, T. Wataya, S. Shimohama, S. Chiba, C.S. Atwood, R.B. Petersen, M.A. Smith, Oxidative damage is the earliest event in Alzheimer disease, J. Neuropathol. Exp. Neurol. 60 (2001) 759–767.
[160] L. Migliore, I. Fontana, F. Trippi, R. Colognato, F. Coppedè, G. Tognoni, B. Nucciarone, G. Siciliano, Oxidative DNA damage in peripheral leukocytes of mild cognitive impairment and AD patients, Neurobiol. Aging 26 (2005) 567–573.
[161] X. Zhu, B. Su, X. Wang, M.A. Smith, G. Perry, Causes of oxidative stress in Alzheimer disease, Cell. Mol. Life Sci. 64 (2007) 2202–2210.
[162] S.D. Yan, S.F. Yan, X. Chen, J. Fu, M. Chen, P. Kuppusamy, M.A. Smith, G. Perry, G.C. Godman, P. Nawroth, J.L. Zweier, D. Stern, Non-enzymatically glycated tau in Alzheimer's disease induces neuronal oxidant stress resulting in cytokine gene expression and release of amyloid beta-peptide, Nat. Med. 1 (1995) 693–699.
[163] E. Tamagno, P. Bardini, A. Obbili, A. Vitali, R. Borghi, D. Zaccheo, M.A. Pronzato, O. Danni, M.A. Smith, G. Perry, M. Tabaton, Oxidative stress increases expression and activity of BACE in NT2 neurons, Neurobiol. Dis. 10 (2002) 279–288.
[164] E. Tamagno, M. Parola, P. Bardini, A. Piccini, R. Borghi, M. Guglielmotto, G. Santoro, A. Davit, O. Danni, M.A. Smith, G. Perry, M. Tabaton, Beta-site APP cleaving enzyme up-regulation induced by 4-hydroxynonenal is mediated by stress-activated protein kinases pathways, J. Neurochem. 92 (2005) 628–636.
[165] E. Tamagno, M. Guglielmotto, L. Giliberto, A. Vitali, R. Borghi, R. Autelli, O. Danni, M. Tabaton, JNK and ERK1/2 pathways have a dual opposite effect on the expression of BACE1, Neurobiol. Aging, in press.
[166] M.A. Smith, G. Casadesus, J.A. Joseph, G. Perry, Amyloid-beta and tau serve antioxidant functions in the aging and Alzheimer brain, Free Radic. Biol. Med. 33 (2002) 1194–1199.
[167] P.I. Moreira, A. Nunomura, K. Honda, G. Aliev, G. Casadenus, X. Zhu, M.A. Smith, G. Perry, The key role of oxidative stress in Alzheimer's disease, in: G. Ali Qureshi, S. Hassan Parvez (Eds.), Oxidative Stress and Neurodegenerative Disorders, Elsevier, Amsterdam, 2007, pp. 451–466.
[168] M.J. Hitchler, K. Wikainapakul, L. Yu, K. Powers, W. Attatippaholkun, F.E. Domann, Epigenetic regulation of manganese superoxide dismutase expression in human breast cancer cells, Epigenetics 1 (2006) 163–171.
[169] M.J. Hitchlerand, F.E. Domann, An epigenetic perspective on the free radical theory of development, Free Radic. Biol. Med. 43 (2007) 1023–1036.
[170] M. Tabaton, E. Tamagno, The molecular link between beta- and gamma-secretase activity on the amyloid beta precursor protein, Cell. Mol. Life Sci. 64 (2007) 2211–2218.
[171] C. Ladd-Acosta, J. Pevsner, S. Sabunciyan, R.H. Yolken, M.J. Webster, T. Dinkins, P.A. Callinan, J.B. Fan, J.B. Potash, A.P. Feinberg, DNA methylation signatures within the human brain, Am. J. Hum. Genet. 81 (2007) 1304–1315.
[172] S.M. Reamon-Buettner, J. Borlak, A new paradigm in toxicology and teratology: altering gene activity in the absence of DNA sequence variation, Reprod. Toxicol. 24 (2007) 20–30.
[173] D.K. Lahiri, B. Maloney, M.R. Basha, Y.W. Ge, N.H. Zawia, How and when environmental agents and dietary factors affect the course of Alzheimer's disease: the "LEARn" model (latent early-life associated regulation) may explain the triggering of AD, Curr. Alzheimer's Res. 4 (2007) 219–228.
[174] J. Wu, M.R. Basha, B. Brock, D.P. Cox, F. Cardozo-Pelaez, C.A. McPherson, J. Harry, D.C. Rice, B. Maloney, D. Chen, D.K. Lahiri, N.H. Zawia, Alzheimer's disease (AD)-like pathology in aged monkeys after infantile exposure to environmental metal lead (Pb): evidence for a developmental origin and environmental link for AD, J. Neurosci. 28 (2008) 3–9.
[175] J. Wu, M.R. Basha, N.H. Zawia, The environment, epigenetics and amyloidogenesis, J. Mol. Neurosci. 34 (2008) 1–7.

[176] K.D. Siegmund, C.M. Connor, M. Campan, T.I. Long, D.J. Weisenberger, D. Biniszkiewicz, R. Jaenisch, P.W. Laird, S. Akbarian, DNA methylation in the human cerebral cortex is dynamically regulated throughout the life span and involves differentiated neurons, PLoS ONE 2 (2007) e895.
[177] N. Oates, R. Pamphlett, An epigenetic analysis of SOD1 and VEGF in ALS, Amyotroph. Lateral Scler. 8 (2007) 83–86.
[178] J.M. Morahan, B. Yu, R.J. Trent, R. Pamphlett, Are metallothionein genes silenced in ALS? Toxicol. Lett. 168 (2007) 83–87.
[179] K. Garber, The elusive ALS genes, Science 319 (2008) 20.
[180] A. Allen, Epigenetic alterations and cancer: new targets for therapy, IDrugs 10 (2007) 709–712.

Bioelectromagnetics 23:113–126 (2002)
DOI 10.1002/bem.104

Genotoxicity of Radiofrequency Signals. I. Investigation of DNA Damage and Micronuclei Induction in Cultured Human Blood Cells

Raymond R. Tice,[1]* Graham G. Hook,[1] Maria Donner,[1] Donald I. McRee,[2] and Arthur W. Guy[3]

[1]*ILS, Inc., Research Triangle Park, North Carolina*
[2]*Wireless Technology Research, LLC, Raleigh, North Carolina*
[3]*Bioelectromagnetics Consulting, Seattle, Washington*

As part of a comprehensive investigation of the potential genotoxicity of radiofrequency (RF) signals emitted by cellular telephones, in vitro studies evaluated the induction of DNA and chromosomal damage in human blood leukocytes and lymphocytes, respectively. The signals were voice modulated 837 MHz produced by an analog signal generator or by a time division multiple access (TDMA) cellular telephone, 837 MHz generated by a code division multiple access (CDMA) cellular telephone (not voice modulated), and voice modulated 1909.8 MHz generated by a global system of mobile communication (GSM)-type personal communication systems (PCS) cellular telephone. DNA damage (strand breaks/alkali labile sites) was assessed in leukocytes using the alkaline (pH $>$ 13) single cell gel electrophoresis (SCG) assay. Chromosomal damage was evaluated in lymphocytes mitogenically stimulated to divide postexposure using the cytochalasin B-binucleate cell micronucleus assay. Cells were exposed at $37 \pm 1\,^{\circ}C$, for 3 or 24 h at average specific absorption rates (SARs) of 1.0–10.0 W/kg. Exposure for either 3 or 24 h did not induce a significant increase in DNA damage in leukocytes, nor did exposure for 3 h induce a significant increase in micronucleated cells among lymphocytes. However, exposure to each of the four RF signal technologies for 24 h at an average SAR of 5.0 or 10.0 W/kg resulted in a significant and reproducible increase in the frequency of micronucleated lymphocytes. The magnitude of the response (approximately four fold) was independent of the technology, the presence or absence of voice modulation, and the frequency (837 vs. 1909.8 MHz). This research demonstrates that, under extended exposure conditions, RF signals at an average SAR of at least 5.0 W/kg are capable of inducing chromosomal damage in human lymphocytes. Bioelectromagnetics 23:113–126, 2002.

Key words: cellular telephones; genotoxicity; human leukocytes; micronuclei; alkaline single cell gel electrophoresis; Comet assay

INTRODUCTION

Exposure to radiofrequency (RF) signals generated by the use of cellular telephones has increased dramatically during the last two decades. In a comprehensive literature review on the potential genotoxicity of RF signals [Brusick et al., 1998], an expert review panel concluded that there was insufficient evidence to indicate that RF signals were directly mutagenic. In reaching this conclusion, the panel found that the majority of published RF studies reporting a positive genotoxic effect were flawed due to poor biological design, inadequate dosimetry, and/or an inability to eliminate potential thermal effects. Despite this, the panel did find that, in the case of the induction of micronuclei in cultured mammalian cells exposed to RF signals, the frequency of positive findings exceeded that expected based simply on the estimated false positive rate for this assay. Also, results from recent studies using the alkaline (pH $>$ 13) single cell gel electrophoresis (SCG) assay suggested that RF signals at power levels purported to be nonthermal are able to induce DNA damage [Lai and Singh, 1995; 1996; 1997].

Contract grant sponsor: Wireless Technology Research, LIC.

Currect address: Maria Donner, E.I. du Pont de Nemours and Company, Haskell Laboratory for Toxicology and Industrial Medicine, Newark, Delaware

*Correspondence to: Dr. Raymond Tice, ILS, Inc., P.O. Box 13501, Research Triangle Park, North Carolina 27709.
E-mail: rtice@ils-inc.com

Received for review 12 August 2000; Final revision received 8 June 2001

We report here on studies to assess the ability of RF signals emitted by various cellular telephones to induce DNA and chromosomal damage in cultured human blood leukocytes and lymphocytes, respectively. The work was conducted as part of a comprehensive investigation of the potential genotoxicity of RF signals. The types of RF signals tested were chosen to reflect historical and current technology, and included (1) voice modulated 837 MHz RF signals generated by an analog signal generator or by a time division multiple access (TDMA) cellular telephone, (2) 837 MHz (not voice modulated) generated by a code division multiple access (CDMA) cellular telephone, and (3) voice modulated 1909.8 MHz generated by a global systems of mobile communication (GSM)-type personal communication systems (PCS) cellular telephone. To assure uniform exposure and the elimination of thermal effects, an RF exposure system was developed specifically for these in vitro studies [Guy et al., 1999].

The primary focus of these studies was to evaluate the ability of RF signals to induce DNA damage in cultured human blood leukocytes, using the alkaline (pH > 13) SCG (or Comet) assay. This is a sensitive technique for the detection of DNA strand breaks, alkali labile sites, cross-linking, and incomplete excision repair sites in individual eukaryotic cells [Singh et al., 1988; Tice, 1995; Anderson et al., 1998; Rojas et al., 1999]. To aid in the interpretation of the biological significance of potential DNA damage induced by RF signals, the Cytochalasin B-binucleate cell micronucleus assay using lymphocytes mitogenically stimulated to divide postexposure was included as part of the study design. Micronuclei arise from either acentric chromosomal fragments (i.e., structural chromosomal damage) or lagging chromosomes (i.e., numerical chromosomal damage) that fail to be incorporated into daughter nuclei during cytokinesis [Heddle et al., 1993; Tucker and Preston, 1996]. Cytochalasin-B prevents cytokinesis without otherwise interfering with cell division, which allows for the selective scoring for micronuclei in proliferating cells that have divided once postexposure [Fenech and Morley, 1985; Lynch and Parry, 1993; Fenech, 1996; 2000].

Both SCG [Maes et al., 1997; Malyapa et al., 1997a,b; Phillips et al., 1998; Vijayalaxmi et al., 2000] and micronucleus [Garaj-Vrhovac et al., 1991; 1992; Maes et al., 1993, 1995; Balode, 1996; Vijayalaxmi et al., 1997, 2001] assays have been used previously to investigate the genotoxicity of RF signals. In the study reported here, nondividing human blood leukocytes were exposed to analog, CDMA, TDMA, or PCS signals for 3 or 24 h at average specific absorption rates (SARs) ranging from 1.0 to 10.0 W/kg. Following exposure, leukocytes were evaluated immediately for DNA damage using the alkaline (pH > 13) SCG assay or cultured at 37 °C in the presence of phytohemagglutinin (PHA) to stimulate lymphocyte proliferation. The frequency of micronucleated cytochalasin B-induced binucleated lymphocytes was determined in cultures terminated at 72 h after the addition of PHA.

MATERIALS AND METHODS

Chemicals

Dimethyl sulfoxide (DMSO), low melting point (LMP) and regular agarose, Triton X-100, glacial acetic acid, methanol, and 5(6)-carboxyflourescein diacetate (CFDA) were obtained from Fisher Scientific Co. (Fairlawn, NJ, USA). Fetal bovine serum (FBS), Hanks balanced salt solution (HBSS), penicillin/streptomycin, PHA, phosphate buffered saline (PBS), and RPMI-1640 media containing GLUTAMAX were obtained from GIBCO-BRL (Grand Island, NY). Ethylenediaminetetraacetic acid–disodium salt (Na_2EDTA), ethidium bromide, sodium hydroxide (NaOH), sodium chloride (NaCl), Cytochalasin B, sodium sarcosinate, Trizma base, and ethylmethane sulfonate (EMS) were obtained from Sigma Chemical Co. (St. Louis, MO). SYBRGreen was obtained from Molecular Probes (Eugene, OR). Giemsa was obtained from J.T. Baker (Phillipsburg, NJ).

Blood Samples

Human blood leukocytes were used because of the need to use cells that could be cultured in suspension, a constraint of the test tube exposure system, and because of a desire to use normal human cells whenever possible. Peripheral blood was obtained with informed consent from two healthy, nonsmoking adult males without a recent history of viral infections, drug usage, or radiotherapy. Due to resource constraints, a single donor was used for each technology. The same donor was used for all analog, CDMA, and TDMA experiments, and the second donor was used for all PCS experiments.

Blood was collected from a donor on the morning of each exposure day. For each culture, 0.6 ml of blood was mixed with 0.4 ml of RPMI-1640 medium containing 15% heat inactivated fetal bovine serum, 2 mM GLUTAMAX, 100 units penicillin/ml, and 100 μg streptomycin/ml (complete media) in a sterile, round-bottom 14 ml Falcon 2059 centrifuge tube (1.42 cm diameter, 9.5 cm length, 0.7 mm wall thickness). To ensure exposure of the cells to the most uniform SARs distribution possible (see Guy et al.

[1999], the blood was first resuspended in the 1 ml volume just prior to exposure. Next, an additional 9 ml of complete medium was carefully layered with minimal disturbance on top of the cell suspension. During the RF exposure, the blood leukocytes were largely located in the bottom 1/3 ml of the exposure tube (data not presented).

Exposure to RF Signals

An in vitro exposure system that provided the most uniform SAR distribution possible and the ability to maintain a constant temperature was developed for these studies. The system utilized two transverse electromagnetic (TEM) cells operated in series in a vertical position as the exposure chambers. It has been described in detail in Guy et al. [1999]. A plastic rack, capable of holding four (for the 1909.8 MHz exposures) or six (for the 837 MHz exposures) 14 ml test tubes (half of the tubes on each side of the septum), positioned the tubes so that they were exposed from the bottom with the long axis parallel to the direction of wave propagation.

Analog RF signals (frequency modulation (FM) 12.5 kHz) were generated by a HP 8648C signal generator with the frequency set at 837 MHz. For digital technologies, the RF fields were generated by a CDMA, TDMA, or GSM-type PCS (217 Hz modulation) cellular telephone (Motorola) at carrier frequencies of 837 MHz (CDMA and TDMA) or 1909.8 MHz (PCS). For analog, TDMA, and PCS studies, the RF signal was voice modulated using a compact disk (CD) player containing a recording that simulated normal speech. For the CDMA signal, the cellular telephone used to generate the signal was operated in a test mode that did not allow voice modulation. For analog, CDMA, and TDMA experiments, the RF signal was amplified using a 500 W amplifier (Kalmus model LA500G, 500–1000 MHz). For the PCS experiments, the RF signal was amplified using a 200 W amplifier (Amplifier Research model 200T1G2, 1–2 GHz). A terminating load absorbed any power not absorbed by the specimens.

The temperature within each TEM cell was controlled using external fans that circulated air through vents in each TEM cell and a water jacket connected to a RC6 CS Lauda (Brinkman) water bath that circulated water around each TEM cell. The culture temperature in each TEM cell was monitored during the exposure period using fiberoptic thermometers (Luxtron model 790). In each TEM cell, two probes were inserted into a test tube containing blood in complete media. One probe was placed on the bottom of the test tube, approximately in the center, while the other probe was placed in the same tube about halfway up the test tube wall. Temperature measurements were obtained at 1 min intervals during the 3 h exposure experiments and at 10 min intervals during the 24 h exposures. For each measurement, the temperature was averaged over 10 s. The inside environment of each TEM cell was maintained at a constant temperature by adjusting the temperature of the water circulating around the TEM cells.

Dosimetry, Dose Rates, Exposure Duration, and Power/Temperature Settings

The maximum average SAR tested (10.0 W/kg) provided a greater than five fold safety factor above the current recommended upper limit for spatial peak absorption (1.6 W/kg averaged over 1 g of tissue) [NCRP, 1986; ANSI/IEEE, 1992]. Leukocytes were exposed for 3 or 24 h to mimic standard in vitro genotoxicity studies being conducted to evaluate the ability of these RF signals to induce structural chromosomal damage in proliferating human lymphocytes (manuscript in preparation).

The procedures used to calculate and measure SARs under these exposure conditions are provided in Guy et al. [1999]. Using a finite difference time domain (FDTD) analysis, average SARs for the entire 10 ml and the bottom 1 ml for both 837 and 1909.8 MHz were calculated. Calculated average SARs over the entire 10 ml volume were based on time–temperature profiles produced using the fiberoptic probes. Input power levels for the first TEM cell were set based on achieving a given average SAR in the bottom one mL of the sample. A length of coaxial cable was used to attenuate the input power for the second TEM cell. Using this arrangement, two treatment groups could be tested at the same time. The power levels used and corresponding calculated average SARs are provided in Table 1. Power level fluctuation during operation of the system was $<10\%$.

TABLE 1. Input Power and Calculated SARs at 837 and 1909.8 MHz

Frequency			
837 MHz		1909.8 MHz	
Input power (W)	SAR (W/kg)	Input power (W)	SAR (W/kg)
17.6	10.0	1.60	10.0
8.9	5.0	0.80	5.0
4.5	2.5	0.46	2.9
1.8	1.0	0.26	1.6
		0.16	1.0

Abbreviations: SAR, Specific absorption rate; MHz, megahertz; W, Watts; W/kg, Watts per kilogram.

The repeatability of SARs from experiment to experiment was assured by using a test tube holder that was positioned precisely inside the TEM cell. Constant monitoring of temperature within a designated test tube provided information on the repeatability of an SAR for a given input power. Negative (zero SAR) controls consisted of cultures in the second TEM cell when it was disconnected from the input power, with the terminating load transferred to the first TEM cell.

For the analog, TDMA, and CDMA RF signal experiments, the average SARs were 1.0, 2.5, 5.0, and 10.0 during the 3 h exposure experiments, and 1.0, 5.0, and 10.0 W/kg during the 24 h exposure experiments. For the PCS RF signal experiments, SARs were altered due to reduced attenuation on the coaxial cable at 1909.8 MHz. The average SARs were 1.6, 2.9, 5.0, and 10.0 W/kg during the 3 h exposure experiments and 1.0 and 10.0 W/kg during the 24 h exposure experiments. Duplicate cultures were tested at each SAR.

Each RF signal treatment group required a separate TEM cell; therefore, only two treatment groups could be exposed concurrently. All treatment groups in the 3 h exposure experiments were tested during the same day. The order in which the SAR pairings were conducted varied between experiments and technologies. However, in all experiments, the negative and positive control groups were processed last. In experiments utilizing the 24 h exposure period, each test consisted of exposure to a single SAR using the first TEM cell in the series with concurrent negative and positive controls in the second TEM cell.

Positive and Negative Controls

Positive and negative controls were included in each experiment. The negative control consisted of duplicate cultures without an applied RF signal. EMS was tested in duplicate in the same TEM cell to demonstrate the adequacy of the experimental conditions to detect a known genotoxic agent.

Dual Stain Viability Assay

Leukocyte viability was measured at the end of the RF exposure period from a 10 µl aliquot of each culture, using the 5–6 carboxyfluorescein diacetate: ethidium bromide staining technique of Strauss [1991]. For each culture, 100 leukocytes were evaluated for the frequency of live (green cytoplasm), compromised (green cytoplasm/red nucleus), and dead (red nucleus) cells.

SCG Assay

The alkaline (pH $>$ 13) SCG assay was conducted according to the method of Singh et al. [1988] with minor modifications. Briefly, following exposure to the RF signals, the blood cells were resuspended and 500 µl removed. The leukocytes in this sample were pelleted, the supernatant removed, the cells mixed with 375 µl of 0.5% LMP agarose at $37 \pm 1\,^{\circ}$C and layered (75 µl per slide) onto 5 conventional microscope slides precoated with 1% normal melting agarose. After solidification of the cell layer under a coverslip, a third layer of 0.5% LMP agarose was added and allowed to solidify under the same coverslip. Next, the slides were placed for at least 1 h in cold lysing solution consisting of 1% sodium sarcosinate, 2.5 M NaCl, 100 mM Na_2EDTA, 10 mM Trizma (pH 10) with 10% DMSO and 1% Triton X-100, added fresh.

Following lysis for 1 h, one slide per culture was removed for an evaluation of the frequency of cells with low molecular weight (LMW) DNA [Tice et al., 1998]. Each slide was rinsed with Tris buffer (pH 7.5), exposed for 5 min to ice cold 100% methanol, air dried, and boxed until scored. Just prior to scoring, the DNA was stained with SYBRGreen using the manufacturer's recommended procedure. One hundred cells were scored for the extent of diffusion (none, minor, extensive) at $250\times$ magnification using epi-illuminated fluorescence microscopy. Coded slides were scored by a person who had no knowledge of the treatment group. In this variation of the SCG assay, cells with LMW DNA indicative of double strand breaks associated with necrosis or apoptosis exhibit extensive diffusion of DNA into the agarose gel under neutral non-electrophoresis conditions.

After 1 h of lysis, slides to be analyzed for DNA migration were rinsed free of detergents using Tris buffer and then treated with proteinase K (0.5 mg/ml in lysis solution without detergents) overnight at $37 \pm 1^{\circ}$C to remove residual protein. The slides were then immersed in electrophoresis buffer (300 mM NaOH and 1 mM Na_2EDTA; pH $>$ 13) for 60 min to allow for DNA unwinding and expression of alkali labile sites as strand breaks. Using the same buffer, electrophoresis was conducted for 20 min at 25 V (0.9 V/cm) and 300 mAmp. After electrophoresis, the alkali in the gels was neutralized using Tris buffer. The gels were then exposed to ice cold 100% methanol, air dried, and boxed until scored. Just prior to scoring, the DNA was stained with SYBRGreen using the manufacturer's recommended procedure. Using the Komet imaging system (Version 3.1; Kinetic Imaging, Ltd., Liverpool, UK), at least 100 comets were analyzed at $250\times$ magnification using epi-illuminated fluorescence microscopy from each of two replicate cultures. The metrics for DNA migration collected included tail length, the percentage of migrated DNA, and tail moment. Tail length was calculated in microns from the estimated leading edge of the head region to the

leading edge of the tail. The percentage of migrated DNA was calculated as the integrated intensity of DNA in the tail divided by the integrated intensity of DNA for the total image and multiplied by 100. Tail moment was calculated as the fraction of DNA in the tail multiplied by tail length. Coded slides were scored by a person who had no knowledge of the treatment group.

Micronucleated Binucleate (MN-BN) Lymphocyte Assay

After removal of a sample for an assessment of viability and DNA damage, the remaining blood leukocytes were pelleted, resuspended in 10 ml complete media containing PHA (final concentration 1%) (i.e., culture initiation), and then incubated at 37 ± 1 °C and 5% CO_2. Cytochalasin B (6 μg/ml final concentration) was added 44 h after the addition of PHA. At 72 h after the addition of PHA, the cells were pelleted by centrifugation, exposed to warm hypotonic solution (0.075 M KCl), and fixed in methanol:glacial acetic acid (3:1 v/v). Slides were prepared using conventional cytogenetic methodology and stained with Giemsa. For each culture, a minimum of 2000 binucleate lymphocytes was examined at $1000\times$ magnification for the presence of a micronucleus. Each culture was also evaluated for the binucleate cell index (BCI = the percentage of binucleate cells per culture) and the replicative index (RI = the number of cells with one nucleus plus two times the number of cells with two nuclei plus three times the number of cells with three or four nuclei, divided by the number of cells scored), based on scoring 1000 nucleated cells. Coded slides were scored by a person who had no knowledge of the treatment group.

Statistical Analysis

A probability level of 0.05 was used to indicate statistical significance. *SCG assay*: Tail moment was the metric statistically analyzed. In addition, to assess for the presence of subpopulations of cells with increased damage, the within culture distribution of tail moment data was analyzed using the dispersion coefficient H, defined as the variance divided by the mean [Tice et al., 1992]. For both tail moment and tail moment H, individual culture data were analyzed using (i) a one tailed linear trend test to assess for a dose response relationship where data at multiple SARs were obtained and (ii) a one-tailed Student's *t*-test pairwise comparison of each treatment group against the concurrent negative control to identify individual RF signal treatment groups exhibiting a significant increase in response.

MN-BN assay: The metric used was the frequency of MN-BN lymphocytes. Data pooled across cultures within the same exposure group were analyzed using (i) a one tailed Cochran–Armitage trend test to assess for a dose response relationship where data at multiple SARs were obtained and (ii) a one-tailed Fisher's exact test pairwise comparison of each treatment group against the concurrent negative control to identify individual RF signal treatment groups exhibiting a significant response.

The individual culture BCI and RI data were analyzed using the same approach used for tail moment, but with a decrease in lymphocyte proliferation assessed for.

A multiple dose rate experiment was considered positive if both a statistically significant dose rate dependent increase and a statistically significant increase for at least one treatment dose rate were detected. An experiment was considered negative if neither of these was detected. In experiments where a positive response was obtained for one but not both of these criteria, a repeat study was conducted to clarify the nature of the response.

RESULTS

For all RF signal exposures and at all power levels, the recorded equilibrium temperature at the bottom of the tube was 37 ± 1 °C. Once an equilibrium temperature had been reached (within <20 min), the variation in temperature was ± 0.3 °C during the 3 h exposure experiments and ± 0.5 °C during the 24 h exposures. At average SARs of 5.0 W/kg and lower, the temperatures at the bottom and at the middle of the culture tube did not differ. However, at 10.0 W/kg, the temperature at the middle of the tube was, on average, 0.5 °C higher than the temperature at the bottom of the culture tube during the 837 MHz exposures and 0.8 °C higher during the 1909.8 MHz exposures. Representative time-temperature profiles are presented in Figure 1.

SCG Assay

There was no evidence of toxicity, as measured by a significant decrease in the percentage of viable leukocytes or by a significant increase in the percentage of leukocytes with LMW DNA, in any RF experiment (data not shown). The average percentage of viable leukocytes exceeded 97% in all control and exposed cultures, while the average percentage of cells with LMW DNA was 12% or less in all cultures.

The resulting SCG data are provided for each technology in Tables 2–5. Two 3 h and one 24-h exposures were conducted to evaluate the ability of voice modulated 837 MHz analog RF signals to induce

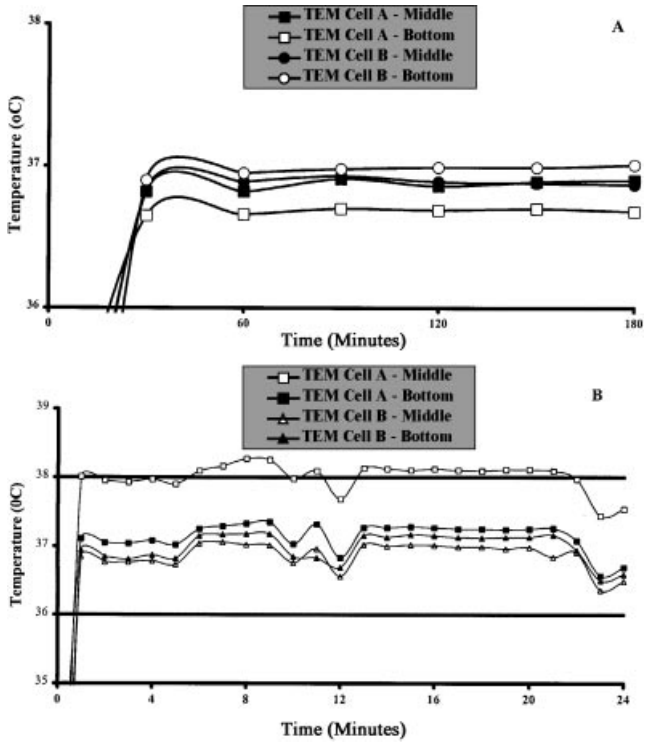

Fig. 1. Representative temperature profiles for 3 h (**A**) and 24 h (**B**) exposures. The 3 h data were collected during the first analog experiment. The SARs for this exposure run were 10 (TEM cell A) and 5 (TEM cell B) W/kg. The 24-h data was collected during the first PCS-GSM experiment. The SARs for this exposure run were 10.0 (TEM cell A) and 0.0 (TEM cell B) W/kg. The profiles presented are based on a representative subset of measurements, with the points connected using a smoothing function.

DNA damage in leukocytes. The replicate 3 h exposure experiment was conducted because of a statistically significant increase in MN-BN lymphocytes at the single average SAR of 5.0 W/kg (see below). In all three experiments, tail moment and tail moment H in the exposed cultures were not significantly increased above that in the concurrent control group. For each of the other cellular telephone technologies, a single experiment of 3 or 24 h exposures was conducted to evaluate the ability of the RF signal to induce DNA damage. For all three technologies and both exposure conditions, tail moment or tail moment H was not significantly increased in exposed leukocytes. EMS, the positive control agent, induced a significant increase in DNA migration in all experiments.

MN-BN Lymphocyte Assay

MN-BN, BCI, and RI data for PHA-stimulated lymphocytes in blood pre-exposed to RF signals using the four different cellular telephone technologies are provided for each technology in Tables 6–9. There was no consistent pattern of toxicity, as measured by a reduction in the BCI or RI, in cultures exposed for 3 h to any signal. However, there was a dose dependent decrease in RI in cultures exposed for 3 h to voice modulated TDMA RF signals, with a significant depression at 10.0 W/kg. In lymphocytes exposed to analog RF signals for 24 h, there was a significant reduction in the BCI at 10.0 W/kg in replicate experiments. There was not a significant reduction in the BCI or RI in cultures exposed for 24 h to CDMA, TDMA, or PCS RF signal technologies.

EMS, the positive control agent, induced a significant increase in the frequency of MN-BN lymphocytes in all 3 h and in most 24 h exposure experiments. In the first analog and the first TDMA RF signal 24 h exposure experiment, cultures treated with EMS could not be scored due to excessive toxicity. The inability to score the positive control cultures in these experiments does not alter the positive experimental findings (see below).

For all cellular telephone technologies tested, with the exception of the first analog RF experiment, a 3 h exposure did not induce a significant increase in the frequency of MN-BN lymphocytes. In the first 3 h analog RF experiment, there was a statistically significant increase in the frequency of MN-BN lymphocytes exposed to an average SAR of 5.0 W/kg. However, in a replicate experiment conducted to evaluate the reproducibility of this response, the frequency of MN-BN lymphocytes was not significantly increased at any SAR. This lack of reproducibility supports a conclusion that analog RF signals also do not induce a significant increase in MN-BN lymphocytes under the exposure conditions tested.

In contrast to the negative micronucleus results obtained using a 3 h exposure protocol, exposure of blood cells to the different cellular telephone RF technologies at 10.0 W/kg for 24 h resulted in a highly significant increase in the frequency of MN-BN lymphocytes. In each case, the positive finding at this SAR was replicated in independent experiments. Based on this positive response at 10.0 W/kg, lower SARs were tested for their ability to induce micronucleated lymphocytes. At an average SAR of 5.0 W/kg, analog and TDMA RF signals also induced a significant increase in the frequency of MN-BN lymphocytes. At an average SAR of 1.0 W/kg, CDMA and PCS RF signals induced a nonsignificant increase in the frequency of MN-BN lymphocytes.

DISCUSSION AND CONCLUSION

The primary focus of these in vitro studies was to evaluate the ability of RF signals generated by various cellular telephone technologies to induce DNA damage, as measured using the alkaline SCG assay, in

TABLE 2. DNA Migration in Human Blood Leukocytes in Cultures Exposed to Voice Modulated 837 MHz Analog RF Signals

Protocol	Dose rate (W/Kg)	Migrated DNA (%) Mean	SEM	Tail Length (microns) Mean	SEM	Tail Moment Mean	SEM	*P*-value+	H	SEM	*P*-value+
3-h	EMS-25[a]	91.8	0.50	118.1	2.26	109.9	1.34	0.004*	10.6	1.41	0.111
Experiment 1	EMS-75[a]	Not scorable due to excessive migration									
	0.0	7.5	0.60	44.6	1.15	4.0	0.40	—	6.5	0.53	—
	1.0	9.1	0.88	54.1	1.91	5.4	0.45	0.070	7.5	0.79	0.189
	2.5	9.8	1.68	53.2	4.45	5.9	1.54	0.218	8.0	0.69	0.110
	5.0	8.4	0.75	57.2	2.43	5.2	0.29	0.067	5.4	0.56	0.854
	10.0	8.3	0.85	56.3	0.11	5.2	0.34	0.071	6.1	0.53	0.673
		Trend test *P*-value				0.314			0.887		
3-h	EMS-1[a]	8.5	0.59	66.7	6.52	6.2	1.21	0.197	6.4	2.23	0.550
Experiment 2	EMS-10[a]	18.0	1.70	75.1	0.34	14.6	1.48	0.012*	10.9	1.01	0.046*
	0.0	6.9	0.03	61.5	1.64	4.9	0.30	—	6.7	0.93	—
	1.0	7.7	0.31	64.7	8.14	5.4	0.72	0.278	6.5	1.58	0.535
	2.5	8.0	0.46	61.4	5.24	5.5	0.68	0.257	8.3	0.62	0.152
	5.0	7.0	0.33	54.6	2.18	4.3	0.39	0.841	6.1	0.43	0.699
	10.0	7.9	0.94	71.0	3.64	6.3	0.91	0.136	7.4	0.29	0.269
		Trend test *P*-value				0.153			0.379		
24-h	EMS-20[a]	90.2	2.66	103.2	2.56	93.1	0.43	<0.001*	2.1	0.14	0.970
Experiment 1	0.0	15.5	0.24	68.6	0.79	11.0	0.39	—	6.6	1.15	—
	10.0	15.2	2.06	66.9	4.78	11.1	2.55	0.484	9.8	4.93	0.295

Abbreviations: Migrated DNA, percentage of total DNA in the tail; Tail Length, length of the comet tail measured from the leading edge of the head to the leading edge of the tail; Tail Moment, fraction of DNA in the tail multiplied by the tail length; SEM, standard error of the mean; H, variance divided by the mean (all SCG data based on 100 comets scored per culture). *P*-value+, pairwise comparison using one-tailed Student's *t*-test; Trend test *P*-value, one-tailed linear trend test for an increase in DNA migration.
[a]Ethylmethane sulfonate (EMS) doses in μg/ml.
*Significantly different at $P < 0.05$.

TABLE 3. DNA Migration in Human Blood Leukocytes in Cultures Exposed to 837 MHz RF Signals Generated by CDMA Technology

Protocol	Dose rate (W/Kg)	Migrated DNA(%) Mean	SEM	Tail Length (microns) Mean	SEM	Tail Moment Mean	SEM	*P*-value+	H	SEM	*P*-value+
3-h	EMS-10[a]	29.6	5.05	127.7	2.28	39.1	7.34	0.026*	11.5	1.82	0.069
Experiment 1	EMS-20	69.7	2.33	122.7	8.25	85.7	8.79	0.006*	5.7	1.41	0.781
	0.0	9.1	0.28	83.2	0.08	8.2	0.15	—	7.1	0.36	—
	1.0	9.2	0.91	99.1	4.49	9.6	1.47	0.226	6.4	2.14	0.617
	2.5	8.5	0.10	89.7	0.44	8.2	0.06	0.596	6.0	0.78	0.830
	5.0	8.3	0.15	90.2	3.13	8.0	0.38	0.712	6.4	0.61	0.792
	10.0	8.8	0.29	95.4	0.92	8.8	0.21	0.086	6.5	0.41	0.810
		Trend test *P*-Value					0.540			0.578	
24-h	EMS-20	92.6	0.90	153.8	1.64	142.6	0.04	<0.001*	4.0	0.44	0.960
Experiment 1	0.0	9.8	1.26	91.1	2.17	9.3	1.40	—	6.7	0.68	—
	10.0	9.5	0.62	100.2	5.25	10.3	1.21	0.331	7.9	1.50	0.263

Abbreviations: Migrated DNA, percentage of total DNA in the tail; Tail Length, length of the comet tail measured from the leading edge of the head to the leading edge of the tail; Tail Moment, fraction of DNA in the tail multiplied by the tail length; SEM, standard error of the mean; H, variance divided by the mean (all SCG data based on 100 comets scored per culture). *P*-value+, pairwise comparison using one-tailed Student's *t*-test; Trend test *P*-value, one-tailed linear trend test for an increase in DNA migration.
[a]Ethylmethane sulfonate (EMS) doses in μg/ml.
*Significantly different at $P < 0.05$.

TABLE 4. DNA Migration in Human Blood Leukocytes in Cultures Exposed to Voice Modulated 837 MHz RF Signals Generated by TDMA Technology

		Migrated DNA (%)		Tail Length (microns)		Tail Moment					
Protocol	Dose rate (W/Kg)	Mean	SEM	Mean	SEM	Mean	SEM	*P*-value+	H	SEM	*P*-value+
3-h	EMS-10[a]	13.6	0.34	52.4	5.41	7.7	0.66	0.025*	5.5	0.58	0.770
Experiment 1	EMS-20	21.4	3.35	53.9	0.69	12.5	1.95	0.027*	7.1	0.60	0.697
	0.0	9.2	0.55	39.0	1.58	4.2	0.45	—	10.4	5.43	—
	1.0	7.7	0.26	33.4	1.39	2.9	0.12	0.945	3.3	0.53	0.840
	2.5	9.1	0.84	40.7	3.79	4.3	0.92	0.454	5.5	1.49	0.766
	5.0	9.7	0.85	45.9	0.38	5.1	0.43	0.149	6.3	1.51	0.730
	10.0	8.7	0.05	36.7	0.02	3.4	0.03	0.895	3.5	0.55	0.834
		Trend test *P*-value				0.550			0.846		
24-h	EMS-20	92.6	0.90	153.8	1.64	142.6	0.04	<0.001*	4.0	0.44	0.960
Experiment 1	0.0	9.8	1.26	91.1	2.17	9.3	1.40	—	6.7	0.68	—
	10.0	9.5	0.62	100.2	5.26	10.3	1.21	0.331	7.9	1.50	0.263

Abbreviations: Migrated DNA, percentage of total DNA in the tail; Tail Length, length of the comet tail measured from the leading edge of the head to the leading edge of the tail; Tail Moment, fraction of DNA in the tail multiplied by the tail length; SEM, standard error of the mean; H, variance divided by the mean (all SCG data based on 100 comets scored per culture). *P*-value+, pairwise comparison using one-tailed Student's *t*-test; Trend test *P*-value, one-tailed linear trend test for an increase in DNA migration
[a]Ethylmethane sulfonate (EMS) doses in μg/ml.
*Significantly different at $P < 0.05$.

human leukocytes. In published in vitro SCG studies, no evidence of an increased level of DNA damage was reported in human lymphocytes exposed to either 935.2 MHz GSM-type RF signals at a maximum SAR of 0.4 W/kg [Maes et al., 1997] or to 2450 MHz pulsed wave RF signals at an average SAR of 2.135 W/kg [Vijayalaxmi et al., 2000]. Similarly, exposure of human glioblastoma U87MG cells and C3H 10 T½ fibroblasts to 2450 MHz continuous wave RF signals at a maximum SAR of 1.9 W/kg [Malyapa et al., 1997a], or to 835.62 MHz frequency-modulated continuous-wave (analog) and 847.74 MHz CDMA RF signals at a SAR 0.6 W/kg did not result in an increased level of DNA damage [Malyapa et al., 1997b]. In contrast, exposure of Molt-4 T-lymphoblastoid cells for 2 or 21 h to pulsed 813.5625 MHz (iDEN) signals at SARs of 2.4 and 24 mW/kg resulted in a significant decrease and increase in DNA migration, respectively, while

TABLE 5. DNA Migration in Human Blood Leukocytes in Cultures Exposed to Voice Modulated 837 MHz RF Signals Generated by PCS Technology

		Migrated DNA (%)		Tail Length (microns)		Tail Moment					
Protocol	Dose rate (W/Kg)	Mean	SEM	Mean	SEM	Mean	SEM	*P*-value+	H	SEM	*P*-value+
3-h	EMS-10[a]	51.7	8.33	109.1	6.98	57.3	12.78	0.032*	7.6	2.28	0.462
Experiment 1	EMS-20	81.3	0.28	115.1	8.12	93.7	6.86	0.003*	2.3	0.35	0.977
	0.0	9.9	0.98	86.5	0.70	8.9	0.78	—	7.3	1.04	—
	1.6	10.6	0.06	97.2	2.81	11.1	0.23	0.059	7.4	0.25	0.459
	2.9	9.6	0.96	86.6	3.42	9.0	1.14	0.489	9.3	1.32	0.175
	5.0	11.0	2.41	90.8	12.49	11.2	3.82	0.307	10.2	1.32	0.111
	10.0	9.4	0.18	86.5	6.30	8.6	0.76	0.597	6.8	0.45	0.647
		Trend test *P*-value				0.611			0.592		
24-h	EMS-20	92.9	0.45	155.1	2.62	144.2	3.15	0.001*	3.0	0.39	0.993
Experiment 1	0.0	11.6	1.06	99.9	0.77	12.3	1.09	—	6.8	0.23	—
	10.0	12.3	0.77	111.6	5.89	14.3	1.87	0.221	7.9	1.78	0.301

Abbreviations: Migrated DNA, percentage of total DNA in the tail; Tail Length, length of the comet tail measured from the leading edge of the head to the leading edge of the tail; Tail Moment, fraction of DNA in the tail multiplied by the tail length; SEM, standard error of the mean; H, variance divided by the mean (all SCG data based on 100 comets scored per culture). *P*-value+, pairwise comparison using one-tailed Student's *t*-test; Trend test *P*-value, one-tailed linear trend test for an increase in DNA migration.
[a]Ethylmethane sulfonate (EMS) doses in μg/ml.
*Significantly different at $P < 0.05$.

TABLE 6. Induction of Micronucleated Binucleate Lymphocytes and Cell Cycle Inhibition in Lymphocyte Cultures Exposed to Voice Modulated 837 MHz Analog RF Signals

Protocol	Dose rate (W/Kg)	MN-BN frequency		Binucleate Cell Index (BCI)			Replicative Index (RI)		
		%	*P*-value+	Mean	SEM	*P*-value+	Mean	SEM	*P*-value+
3-h	EMS-600[a]	0.200	0.808	24.2	3.45	0.475	1.45	0.026	0.738
Experiment 1	0.0	0.325	—	24.5	1.75	—	1.42	0.009	—
	1.0	0.075	0.989	24.7	1.90	0.543	1.44	0.024	0.738
	2.5	0.100	0.976	21.4	2.40	0.206	1.41	0.055	0.472
	5.0	0.600	0.049*	24.1	1.10	0.441	1.48	0.032	0.814
	10.0	0.200	0.808	23.4	1.55	0.342	1.43	0.054	0.528
Trend test *P*-value		0.212		0.376			0.556		
3-h	EMS-800	0.825	<0.001*	37.6	4.75	0.805	1.52	0.056	0.593
Experiment 2	0.0	0.175	—	31.9	2.10	—	1.54	0.008	—
	1.0	0.250	0.315	27.5	1.30	0.108	1.50	0.012	0.065
	2.5	0.100	0.726	28.4	5.50	0.306	1.46	0.073	0.189
	5.0	0.175	0.395	20.9	3.95	0.066	1.31	0.059	0.032*
	10.0	0.175	0.395	26.7	5.50	0.235	1.42	0.128	0.212
Trend test *P*-value		0.584		0.183			0.092		
24-h	EMS-750	Not scorable due to excessive migration							
Experiment 1	0.0	0.450	—	38.9	0.25	—	1.61	0.022	—
	10.0	1.425	<0.001*	36.0	0.25	0.007*	1.51	0.022	0.036*
24-h	EMS-150	0.175	0.274	42.9	1.60	0.036*	1.75	0.029	0.065
Experiment 2	EMS-250	0.750	<0.001*	49.4	4.20	0.567	1.73	0.030	0.046*
	0.0	0.100	—	48.6	0.30	—	1.84	0.021	—
	10.0	0.800	<0.001*	45.8	0.70	0.033*	1.67	0.125	0.161
24-h	EMS-150	0.250	0.151	50.2	0.20	0.979	1.80	0.023	0.820
Experiment 3	EMS-250	0.800	<0.001*	44.7	3.50	0.296	1.72	0.027	0.631
	0.0	0.125	—	47.0	0.65	—	1.68	0.099	—
	5.0	0.325	0.048*	41.0	2.80	0.087	1.75	0.019	0.718

Abbreviations: MN-BN, frequency of micronucleated binucleated cells, based on the analysis of 4000 binucleate cells per treatment group; BCI, Binucleate Cell Index, percantage of binucleate cells per culture, based on scoring 1000 cells per culture; RI, Replicative Index, the number of cells with one nucleus plus two times the number of cells with two nuclei plus three times the number of cells with three or four nuclei divided by the number of cells scored, based on scoring 1000 cells per culture; *P*-value+ = pairwise comparison against concurrent unexposed control; Trend test *P*-Value = one-tailed trend test *P*-value; SEM, standard error of the mean.
[a]Ethylmethane sulfonate (EMS) doses in μg/ml.
*Significantly different at $P < 0.05$.

exposure to 836.55 MHz (TDMA) signals at an SAR of 2.6 and 2.6 mW/kg resulted in a significant decrease in DNA migration [Phillips et al., 1998]. The authors speculated on possible mechanisms of action but reached no firm conclusion, although a decrease in DNA migration is associated with DNA-DNA or DNA-protein cross-linking [Tice, 1995].

Several in vivo SCG studies have also been conducted. Lai and Singh [1995, 1996, 1997] reported that a 2 h whole body exposure of rats to RF signals (2450 MHz continuous wave and pulse modulated; estimated whole body SAR of 0.6 to 1.2 W/kg) resulted in increased levels of DNA damage in brain cells. In contrast, Malyapa et al. [1998] found no increase in DNA migration in the brain cells of rats exposed to a 2450 MHz CW signal (the reported average SAR in the brain was 1.2 W/kg generated using a circular waveguide similar to that used by Lai and Singh).

In the in vitro SCG studies reported here, non dividing blood leukocytes were processed for an analysis of DNA damage immediately after the cessation of a 3 h or 24 h exposure to RF signals. Three measures of DNA migration (the percentage of migrated DNA, the tail length, and tail moment) were obtained for each comet scored by image analysis, with the response averaged across populations of cells within each culture. Tail moment was used as the metric for statistical analysis. In the event of a positive response, data on the percentage of migrated DNA and tail length would have been used to aid in an interpretation of the increase in tail moment. In addition to

TABLE 7. Induction of Micronucleated Binucleate Lymphocytes and Cell Cycle Inhibition in Human Lymphocyte Cultures Exposed to 837 MHz RF Signals Generated by CDMA Technology

Protocol	Dose rate (W/Kg)	MN-BN frequency		Binucleate Cell Index (BCI)			Replicative Index (RI)		
		%	*P*-value+	Mean	SEM	*P*-value+	Mean	SEM	*P*-value+
3-h	EMS-800[a]	2.400	<0.001*	25.4	—	<0.001*	1.54	—	<0.001*
Experiment 1	0.0	0.175	—	39.5	5.60	—	1.61	0.072	—
	1.0	0.150	0.501	42.1	6.10	0.608	1.52	0.024	0.187
	2.5	0.125	0.613	45.6	1.35	0.798	1.60	0.057	0.482
	5.0	0.200	0.498	51.0	1.25	0.908	1.62	0.009	0.569
	10.0	0.200	0.498	51.6	0.30	0.918	1.63	0.037	0.602
Trend test *P*-value		0.271		0.989			0.164		
24-h	EMS-250	0.750	<0.001*	52.1	2.45	0.763	1.63	0.025	0.568
Experiment 1	0.0	0.125	—	49.8	0.95	—	1.62	0.042	—
	10.0	0.750	<0.001*	46.8	5.10	0.314	1.56	0.081	0.298
24-h	EMS-150	1.950	<0.001*	41.8	2.70	0.056	1.71	0.028	0.959
Experiment 2	0.0	0.150	—	49.8	1.05	—	1.61	0.015	—
	10.0	0.775	<0.001*	50.3	0.90	0.635	1.56	0.015	0.079
24-h	EMS-150	1.700	<0.001*	43.4	1.20	0.052	1.66	0.013	0.968
Experiment 3	0.0	0.100	—	46.9	0.15	—	1.53	0.031	—
	1.0	0.175	0.274	46.4	2.75	0.436	1.56	0.003	0.751

Abbreviations: MN-BN, frequency of micronucleated binucleated cells, based on the analysis of 4000 binucleate cells per treatment group; BCI, Binucleate Cell Index, percantage of binucleate cells per culture, based on scoring 1000 cells per culture; RI, Replicative Index, the number of cells with one nucleus plus two times the number of cells with two nuclei plus three times the number of cells with three or four nuclei divided by the number of cells scoring, based on scored 1000 cells per culture; *P*-value+ = pairwise comparison against concurrent unexposed control; Trend test *P*-Value = one-tailed trend test *P*-value; SEM, standard error of the mean.
[a]Ethylmethane sulfonate (EMS) doses in μg/ml.
*Significantly different at $P < 0.05$.

mean tail moment, the tail moment dispersion coefficient H, a measure of the heterogeneity of the individual comet values within a culture, was evaluated to assess for the presence of subpopulations of cells with increased DNA migration. Such heterogeneity in response might occur if more sensitive cells occur within a larger population of nonresponsive cells.

The tail moment results of all RF signal experiments are compared graphically in Figure 2 (3 h exposure experiments) and Figure 3 (24 h exposure experiments). Under both exposure conditions and for all four RF technologies, there was no evidence for an increased level of DNA damage in the SCG experiments at average SARs of up to 10.0 W/kg. These negative in vitro DNA damage results are consistent with published in vitro reports using other types of mammalian cells and other wavelengths and/or RF signal technologies.

The primary focus of these RF signal studies was for an evaluation of DNA damage using the alkaline (pH > 13) SCG assay. As a potential aid in data interpretation, we also evaluated the induction of structural and numerical chromosomal damage using the MN-BN lymphocyte assay [Fenech and Morley, 1985; Fenech, 1996, 2000]. The MN-BN lymphocyte results for all RF signal experiments using a 3 h or a 24 h exposure period are compared graphically in Figures 4 and 5, respectively. In the 3 h exposure experiment, none of the RF signal technologies induced a significant increase in the frequency of MN-BN lymphocytes. In contrast, in the 24 h exposure experiments, the frequency of MN-BN lymphocytes was consistently and reproducibly increased by approximately fourfold for all RF signal technologies at an average SAR of 10.0 W/kg. The significant increase in the frequency of MN-BN lymphocytes was independent of the technology, the presence or absence of voice modulation, and the frequency (837 vs. 1909.8 MHz). Based on the experimental design, donor variability in response cannot be assessed. A significant increase in the frequency of MN-BN lymphocytes was detected also when leukocytes were exposed for 24 h to an average SAR of 5.0 W/kg, using analog and digital (TDMA) technologies (both voice modulated), although the magnitude of the increase varied between the technologies. In contrast, a nonsignificant increase in the frequency of MN-BN lymphocytes was observed

TABLE 8. Induction of Micronucleated Binucleate Lymphocytes and Cell Cycle Inhibition in Human Lymphocyte Cultures Exposed to Voice-Modulated 837 MHz RF Signals Generated by TDMA Technology

		MN-BN frequency		Binucleate Cell Index (BCI)			Replicative Index (RI)		
Protocol	Dose rate (W/Kg)	%	*P*-value+	Mean	SEM	*P*-value+	Mean	SEM	*P*-value+
3-h	EMS-900[a]	3.225	<0.001*	53.4	5.70	0.465	1.91	0.023	0.075
Experiment 1	0.0	0.525	—	54.0	2.00	—	1.97	0.016	—
	1.0	0.350	0.846	57.4	1.30	0.855	1.97	0.031	0.460
	2.5	0.425	0.688	50.4	3.25	0.220	1.93	0.015	0.121
	5.0	0.300	0.919	55.2	3.60	0.601	1.94	0.055	0.332
	10.0	0.300	0.894	50.5	3.75	0.246	1.81	0.022	0.013*
Trend test *P*-value		0.805		0.16			0.001*		
24-h	EMS-750			Not scorable due to excessive migration					
Experiment 1	0.0	0.475	—	53.4	1.15	—	1.74	0.013	—
	10.0	1.600	<0.001*	60.4	0.65	0.983	1.69	0.019	0.079
24-h	EMS-150	0.725	<0.001*	46.9	3.40	0.706	1.77	0.038	0.984
Experiment 2	EMS-250	0.925	<0.001*	49.5	2.45	0.884	1.61	0.002	0.998
	0.0	0.175	—	44.5	1.60	—	1.56	0.003	—
	10.0	0.800	<0.001*	48.5	2.90	0.825	1.66	0.106	0.774
24-h	EMS-150	0.950	<0.001*	44.1	3.85	0.183	1.57	0.004	0.035*
Experiment 3	EMS-250	0.850	<0.001*	48.2	—	—	1.64	—	—
	0.0	0.200	—	49.8	3.05	—	1.72	0.044	—
	5.0	0.800	<0.001*	48.5	3.15	0.397	1.65	0.047	0.190

Abbreviations: MN-BN, frequency of micronucleated binucleated cells, based on the analysis of 4000 binucleate cells per treatment group; BCI, Binucleate Cell Index, percantage of binucleate cells per culture, based on scoring 1000 cells per culture; RI, Replicative Index, the number of cells with one nucleus plus two times the number of cells with two nuclei plus three times the number of cells with three or four nuclei divided by the number of cells scored, based on scoring 1000 cells per culture; *P*-value+ = pairwise comparison against concurrent unexposed control; Trend test *P*-Value = one-tailed trend test *P*-value; SEM, standard error of the mean.
[a]Ethylmethane sulfonate (EMS) doses in μg/ml.
*Significantly different at $P < 0.05$.

when leukocytes were exposed for 24 h to an average SAR of 1.0 W/kg using CDMA (837 MHz without voice modulation) and PCS (1909.8 MHz, voice modulated) technologies.

The biological relevance of the positive MN-BN response detected at SARs of 5 and 10 W/kg is uncertain. Mechanistically, micronuclei result either from acentric fragments (structural chromosomal aberrations) or from lagging chromosomes (numerical chromosomal damage). Differentiation between the two processes can most easily be accomplished using a specialized immunofluorescence staining technique to assess for the presence of a kinetochore, which is indicative of a lagging chromosome rather than an acentric fragment in each micronuclei. Due to the manner in which the cells were fixed, this type of analysis was not possible in the studies reported here. The lack of a significant increase in DNA damage in leukocytes under the same exposure conditions might suggest that numerical chromosomal aberrations are involved in the increased frequency of micronucleated cells. However, such events generally occur when the inducing agent is present during cell division, and these studies involved the exposure of nondividing cells.

One potential mechanism for the induction of micronuclei by microwave radiation is hyperthermia. Although the temperature measured at the location of the cells never exceeded 37.5 °C, the variation in absorption reported by Guy et al. [1999] is such that higher localized temperatures could have been produced. Hyperthermia, defined as 40 °C or higher, is capable of inducing micronuclei in proliferating cultured cells, including human lymphocytes, and in vivo in mouse bone marrow [Asanami and Shimono, 1999; Komae et al., 1999]. Findings from examinations of the chromosome status of hyperthermia-induced micronuclei are consistent with a mechanism involving interference with the segregation of chromosomes during nuclear division (i.e., numerical chromosomal damage) [Komae et al., 1999]. Whether hyperthermia induces numerical chromosomal damage in nondividing cells subsequently stimulated to divide has not been determined.

TABLE 9. Induction of Micronucleated Binucleate Lymphocytes and Cell Cycle Inhibition in Human Lymphocyte Cultures Exposed to Voice Modulated 1909.8 MHz RF Signals Generated by PCS Technology

Protocol	Dose rate[a] (W/Kg)	MN-BN frequency		Binucleate Cell Index (BCI)			Replicative Index (RI)		
		%	*P*-value+	Mean	SEM	*P*-value+	Mean	SEM	*P*-value+
3-h	EMS-600	2.778	<0.001*	24.0	1.15	0.017*	1.24	0.011	<0.001*
Experiment 1	0.0	0.175	—	47.7	4.10	—	1.66	0.003	—
	1.6	0.125	0.613	43.4	3.05	0.242	1.78	0.044	0.949
	2.9	0.150	0.501	43.0	1.75	0.199	1.74	0.124	0.724
	5.0	0.050	0.910	45.3	0.45	0.306	1.81	0.030	0.982
	10.0	0.075	0.829	44.9	2.35	0.304	1.78	0.005	0.999
Trend test *P*-value		0.928		0.398			0.882		
24-h	EMS-250	2.500	<0.001*	35.3	3.25	0.056	1.39	0.031	0.073
Experiment 1	0.0	0.250	—	44.4	0.75	—	1.53	0.056	—
	10.0	1.025	<0.001*	34.2	0.65	0.005*	1.44	0.011	0.116
24-h	EMS-250	1.200	<0.001*	48.0	1.45	0.126	1.63	0.044	0.063
Experiment 2	0.0	0.125	—	52.4	2.35	—	1.75	0.018	—
	10.0	0.650	<0.001*	47.9	1.05	0.111	1.65	0.029	0.055
24-h	EMS-250	1.950	<0.001*	42.4	1.25	0.063	1.71	0.012	0.995
Experiment 3	0.0	0.175	—	48.3	1.95	—	1.57	0.008	—
	1.0	0.200	0.498	51.4	1.85	0.816	1.64	0.076	0.760

Abbreviations: MN-BN, frequency of micronucleated binucleated cells, based on the analysis of 4000 binucleate cells per treatment group; BCI, Binucleate Cell Index, percantage of binucleate cells per culture, based on scoring 1000 cells per culture; RI, Replicative Index, the number of cells with one nucleus plus two times the number of cells with two nuclei plus three times the number of cells with three or four nuclei divided by the number of cells scoring, based on scored 1000 cells per culture; *P*-value+ = pairwise comparison against concurrent unexposed control; Trend test *P*-Value = one-tailed trend test *P*-value; SEM, standard error of the mean.
[a]Ethylmethane sulfonate (EMS) doses in μg/ml.
*Significantly different at $P < 0.05$.

The finding of an increased frequency of micronucleated cells following exposure to RF signals is consistent with published reports on other in vitro studies [Garaj-Vrhovac et al., 1991; 1992; Maes et al., 1993; 1995; Balode, 1996]. However, Vijaylaxmi et al. [1997, 2001] did not find any indication of an induction of micronuclei in mitogen stimulated peripheral blood lymphocytes exposed to 2450 MHz signals at an average SAR of 12.46 W/kg or to 835.62 MHz frequency division multiple access (FDMA) signals at a maximum average SAR of 5.0 W/kg. Considered together, the positive micronuclei data do not provide sufficient information to establish dose rate or frequency guidelines but do support the need for additional research to (1) independently assess the reliability of the results reported here in other

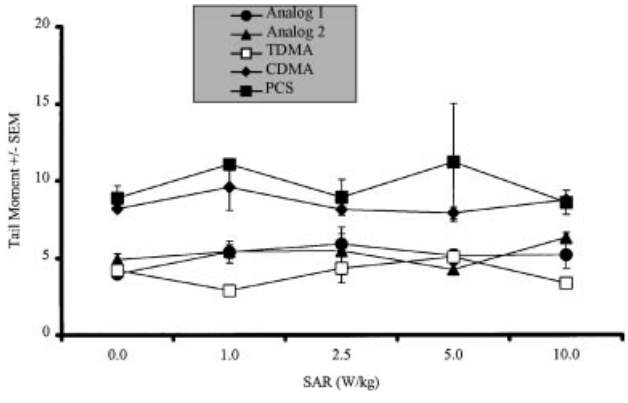

Fig. 2. Effect of exposure to RF signals for 3 h on DNA migration in human blood leukocytes.

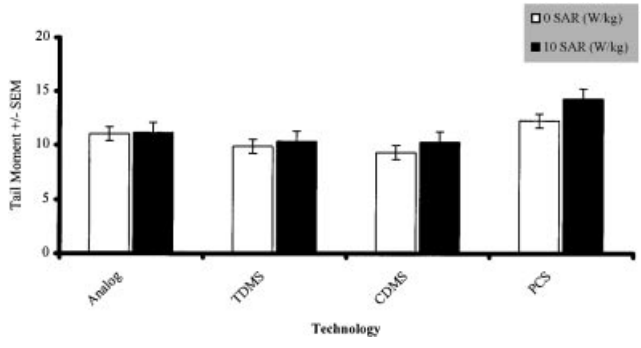

Fig. 3. Effect of exposure to RF signals for 24 h on DNA migration in human blood leukocytes.

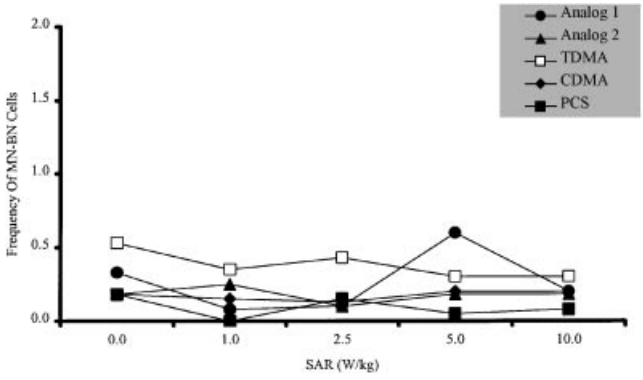

Fig. 4. Effect of exposure to RF signals for 3 h on the frequency of MN-BN human blood lymphocytes.

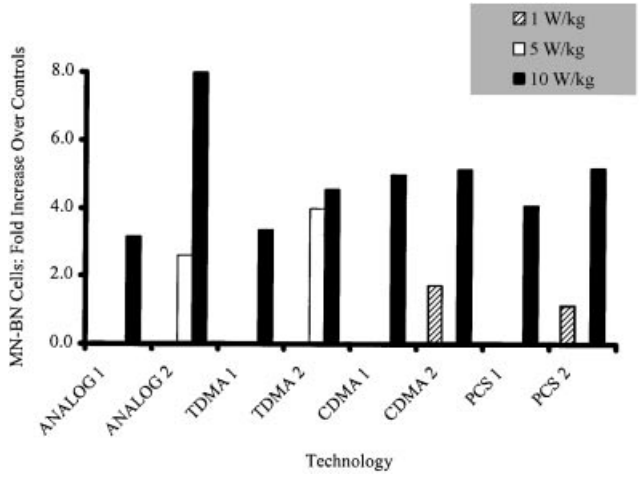

Fig. 5. Fold increase in MN-BN response over concurrent negative controls in human blood lymphocyte exposed to RF signals for 24 h.

laboratories; (2) evaluate the extent of inter-donor variability in micronucleus induction by RF signals; (3) more closely evaluate the shape of the dose–response curve as a function of exposure duration and dose rate; (4) determine the mechanistic basis for the induction of micronuclei, (e.g., evaluate for the presence or absence of a kinetochore); (5) under the experimental conditions used, determine the possible role of hyperthermia in these results potentially by evaluating the relationship between culture temperature and the induction of micronucleated lymphocytes; and (6) evaluate the biological relevance of the finding to human health.

ACKNOWLEDGMENTS

The authors thank Motorola Inc. for donating the cellular telephones adapted for use with our exposure system and the compact disk voice recording used in these studies. We thank Mr. Carroll Sorensen for fabricating the TEM cells and Mr. John McDougall for his assistance in establishing the RF exposure system at ILS, including finding the dielectric constants and associated exposure parameters for 837 MHz and 1909.8 MHz exposures and developing the temperature and power level monitoring systems. We also acknowledge the considerable assistance of Dr. C.K. Chou and thank Ms. M. Vasquez and Ms. D. Blackwell for their technical assistance during this research and Mr. E. Hendricks for assistance with manuscript preparation.

REFERENCES

Anderson D, Yu TW, McGregor DB. 1998. Comet assay responses as indicators of carcinogen exposure. Mutagenesis 13:539–555.

ANSI/IEEE. 1992. IEEE standard for safety levels with respect to human exposure to radio frequency electromagnetic fields, 3 KHz to 300 GHz. ANSI/IEEE C95.1-1992, New York: IEEE.

Asanami S, Shimono K 1997. High body temperature induces micronuclei in mouse bone marrow. Mutation Res 390(1-2):79–83.

Balode Z. 1996. Assessment of radio-frequency electromagnetic radiation by the micronucleus test in bovine peripheral erythrocytes. Science Total Environment 180:81–85.

Brusick D, Albertini R, McRee D, Peterson D, Williams G, Hanawalt P, Preston J. 1998. Genotoxicity of radiofrequency radiation. Environ Molecular Mutagen 32:1–16.

Fenech M, Morely AA. 1985. Measurement of micronuclei in lymphocytes. Mutation Res 1477:29–36.

Fenech MF. 1996. The cytokinesis-block micronucleus technique. In: Pfeifer GP, editor, Technologies for Detection of DNA Damage and Mutations, New York: Plenum Press, p 25–36.

Fenech MF. 2000. The in vitro micronucleus technique. Mutation Res. 455:81–95.

Garaj-Vrhovac V, Horvat D, Koren Z. 1991. The relationship between colony-forming ability, chromosome aberrations and incidence of micronuclei in V79 Chinese hamster cells exposed to microwave radiation. Mutation Res. 263:143–149.

Garaj-Vrhovac V, Fucic A, Horvat D. 1992. The correlation between the frequency of micronuclei and specific chromosome aberrations in human lymphocytes exposed to microwave radiation in vitro. Mutation Res 281:181–186.

Guy AW, Chou CK, McDougall JA. 1999. A quarter century of in vitro research: a new look at exposure methods. Bioelectromagnetics 20(Supplement 4):21–39.

Heddle JA, Hite M, Kirkhart B, Mavrournin K, MacGregor JT, Newell GW, Salamone MF. 1993. The induction of micronuclei as a measure of genotoxicity. A report of the U.S. Environmental Protection Agency Gene-Tox Program. Mutation Res 123:61–118.

Komae N, Hibino Y, Sugano 1999 Analysis of micronuclei induced under hyperthermic conditions in human lymphocyte cultures by fluorescence in situ hybridization (FISH) and spectral karyotyping (SKY) methods. Yakugaku Zasshi, 119(10):763–772.

Lai H, Singh NP. 1995. Acute low-intensity microwave exposure increases DNA single-strand breaks in rat brain cells. Bioelectromagnetics 16:207–210.

Lai H, Singh NP. 1996. Single- and double-strand DNA breaks in rat brain cells after acute exposure to radiofrequency electromagnetic radiation. Int J Radiat Biol 69:513–521.

Lai H, Singh NP. 1997. Melatonin and a spin-trap compound block radiofrequency electromagnetic radiation-induced DNA strand breaks in rat brain cells. Bioelectromagnetics 18:446 – 454.

Lynch AM, Parry JM. 1993. The cytochalasin-B micronucleus/ kinetochore assay in vitro: studies with 10 suspected aneugens. Mutat Res 287:71–86.

Maes A, Collier M, Van Gorp U, Vandoninck S, Verschaeve L. 1997. Cytogenetic effects of 935.2-MHz (GSM) microwaves alone and in combination with mitomycin C. Mutat Res 393:151–156.

Maes A, Collier M, Slaets D, Verschaeve L. 1995. Cytogenetic effects of microwaves from mobile communication frequencies (954 MHz). Electro-Magnetobiology 14:91–98.

Maes A, Verschaeve L, Arroyo A, De Wagter C, Vercruyssen L. 1993: In vitro cytogenetic effects of 2450 MHz waves on human peripheral blood lymphocytes. Bioelectromagnetics 14:495–501.

Malyapa RS, Ahern EW, Straube WL, Moros EG, Pickard WF, Roti Roti JL. 1997a. Measurement of DNA damage after exposure to 2450 MHz electromagnetic radiation. Radiat Res 148:608–617.

Malyapa RS, Ahern EW, Straube WL, Moros EG, Pickard WF, Roti Roti JL. 1997b. Measurement of DNA damage after exposure to electromagnetic radiation in the cellular phone communication frequency band (835.62 and 847.74 MHz). Radiat Res 148:618–627.

Malyapa RS, Ahern EW, Bi C, Straube WL, LaRegina M, Pickard WF, Roti Roti JL. 1998. DNA damage in rat brain cells after in vivo exposure to 2450 MHz electromagnetic radiation and various methods of euthanasia. Radiat Res 149:634–645.

NCRP. 1986. Biological effects and exposure criteria for radiofrequency electromagnetic fields. Report No. 86, National Council on Radiation Protection and Measurements, Bethesda, MD.

Phillips JL, Ivaschuk O, Ishida-Jones T, Jones RA, Campbell-Beachler M, Haggren W. 1998. DNA damage in Molt-4 T-lymphoblastoid cells exposed to cellular telephone radiofrequency fields in vitro. Bioelectrochem Bioenerg 45:103–110.

Rojas E, Lopez MC, Valverde M. 1999 Single cell gel electrophoresis assay: methodology and applications. J Chrom B 722:225–254.

Singh NP, McCoy MT, Tice RR, Schneider EL. 1988. A simple technique for quantitation of low levels of DNA damage in individual cells. Exp Cell Res 175:184–191.

Strauss GHS. 1991. Nonrandom cell killing in cryopreservation: Implications for performance of the battery of leukocyte tests (BLT) I. Toxic and immunotoxic effects. Mutation Res 252:1–15.

Tice RR, Strauss GHS, Peters WP. 1992. Assessment of DNA damage in individual blood lymphocytes (PBLs) from breast cancer chemotherapy patients using the single cell gel electrophoresis (SCG) assay. Mutat Res. 271:101–113.

Tice RR, Furedi-Machacek M, Satterfield D, Udumudi A, Vasquez M, Dunnick JK. 1998. Measurement of micronucleated erythrocytes and DNA damage during chronic ingestion of phenolphthalein in transgenic female mice heterozygous for the *p53* gene. Environ Mol Mutagen 31:113–124.

Tice RR. 1995. The single cell gel/comet assay: a microgel electrophoretic technique for the detection of DNA damage and repair in individual cells. In: Phillips DH, Venitt S. (eds). Environmental Mutagenesis, Oxford: Bios Scientific Publishers, pp 315–339.

Tucker JD, Preston RJ. 1996. Chromosome aberrations, micronuclei, aneuploidy, sister chromatid exchanges, and cancer risk assessment. Mutat Res 365:147–159.

Vijayalaxmi, Mohan N, Meltz ML, Wittler MA. 1997. Proliferation and cytogenetic studies in human blood lymphocytes exposed in vitro to 2450 MHz radiofrequency radiation. Int J Radiat Biol 72:751–757.

Vijayalaxmi, Leal BZ, Szilagyi M, Prihoda TJ, Meltz ML. 2000. Primary DNA damage in human blood lymphocytes exposed in vitro to 2450 MHz radiofrequency radiation. Radiat Res 153:479–486.

Vijayalaxmi, Pickard WF, Bisht KS, Leal BZ, Meltz ML, Roti Roti J, Straube WL, Moros EG. 2001. Cytogenetic studies in human blood lymphocytes exposed in vitro to radiofrequency radiation at a cellular telephone frequency (835.62 MHz, FDMA). Radiat Res 155:113–121.

Int Arch Occup Environ Health (2009) 82:275–278
DOI 10.1007/s00420-008-0323-3

SHORT COMMUNICATION

Comments on "Radiofrequency electromagnetic fields (UMTS, 1,950 MHz) induce genotoxic effects in vitro in human fibroblasts but not in lymphocytes" by Schwarz et al. (Int Arch Occup Environ Health 2008: doi: 10.1007/s00420-008-0305-5)

Alexander Lerchl

Received: 26 February 2008 / Accepted: 3 April 2008 / Published online: 24 April 2008

Abstract
Background A recent publication by Schwarz et al. describes the effects of exposure of human fibroblast and lymphocytes to radiofrequency-electromagnetic fields at frequencies used for communication with mobile phones. Even at very low specific absorption rates of 0.05 W/kg, thus well below internationally accepted exposure limits, significant effects were seen in fibroblasts whose DNA molecules were damaged as assessed by their comet tail factor (CTF) in the comet assay.
Areas of concern The CTF mean values and the standard deviations of the replicates revealed very low coefficients of variation, ranging from 1.2 to 4.9% (average 2.9%), which are in contrast to much higher variations reported by others. Moreover, inter-individual differences of the CTF values strongly disagree with the previously published data from the same group of researchers.
Conclusion The critical analysis of the data given in the figures and the tables furthermore reveal peculiar miscalculations and statistical oddities which give rise to concern about the origin of the reported data.

Keywords Electromagnetic fields · UMTS · Non-thermal · DNA · Comet assay

Introduction

The question of whether or not radiofrequency-electromagnetic fields (RF-EMF) used for mobile communication pose a health risk is being intensely discussed between politicians, health officials, physicians, scientists, and the public. Whereas the majority of scientific publications do not indicate that these non-ionizing RF-EMFs cause biological damages at levels below the thermal threshold (Sommer et al. 2007; Tillmann et al. 2007; Vijayalaxmi and Obe 2004), some investigations demonstrated such effects. When replicated, however, even those studies were found to be non reproducible. One well-known example is the study by Repacholi et al. (1997)who have reported higher incidences of lymphoma in transgenic mice which were exposed to pulsed EMF at 900 MHz (Repacholi et al. 1997). Two independent replication studies did not confirm the earlier findings (Oberto et al. 2007; Utteridge et al. 2002).

Of particular importance is the possible damage of DNA molecules by EMF exposure. Despite the fact that no biophysical mechanism has been identified for such interactions, some results of studies apparently showed DNA damages which, if such studies were found to be reproducible, would give rise to concern about immediate and long-term safety issues of mobile phone use. In 2005, it was shown by a group of researchers from the Medical University Vienna that DNA molecules of human fibroblasts and rat granulosa cells, when exposed to EMFs at 900 MHz, were significantly damaged, as shown by the comet assay (Diem et al. 2005). A replication study, using the same exposure apparatus, however, did not confirm these initial findings (Speit et al. 2007). The same group from Vienna recently published their findings on human fibroblasts and lymphocytes, this time exposing the cells to RF-EMFs at frequencies of the new mobile phone communication standard UMTS at around 1,950 MHz (Schwarz et al. 2008). Like in their earlier investigation, exposed fibroblasts' DNA molecules were found to be severely damaged, even at specific absorption rates (SAR) of 0.05 W/kg, thus far

A. Lerchl (✉)
School of Engineering and Science, Jacobs University Bremen, Campus Ring 6, Res. II 28759, Bremen, Germany
e-mail: a.lerchl@jacobs-university.de

below the recommended exposure limits for whole-body exposure (0.08 W/kg) and partial-body exposure (2 W/kg), respectively, of the general public (ICNIRP 1998).

Areas of concern

Before the problems of the publication of Schwarz et al. are addressed, it is important to briefly summarize how the cells, after treatment (exposure, sham exposure, negative or positive control), were analyzed for their DNA damages: cells (10,000–30,000 per slide) were placed on slides in agarose and treated with lysis solution. After incubation (to allow unwinding of the DNA molecules), electrophoresis was performed so that the DNA molecules or fragments thereof moved along the slide to the anode. After electrophoresis, DNA molecules were stained with ethidium bromide, and the "comets" (tailing of the DNA spots) were inspected and examined microscopically at 400× magnification. The fraction of total DNA present in the tail of the comet reflects the frequency of DNA breaks. Per slide, 500 cells were examined. The comets were manually classified into five categories from A (no damage, no tail) to E (severe damage, longest tail). The resulting comet tail factor (CTF) was calculated per slide by multiplying the numbers of cells in each category with numbers representing the average of damage (in % tail DNA) of each category. These calibration factors, derived from previous work, are 2.5% for A cells (no tail), 12.5% for B cells, 30% for C cells, 67.5% for D cells, and 97.5% for E cells (longest tail). The cumulative sum of the products of numbers of cells × factors, divided by the number of cells (500) yielded the final result of CTF for each slide. For example, the following numbers of cells were counted: A, 445 cells; B, 39 cells; C, 13 cells; D, 2 cells; E, 1 cell. The resulting CTF value would be 4.45. These data were actually extracted from one of the data of sham-exposed cells given in Table 2 of the paper by Schwarz et al.

Low standard deviations

Per data point (i.e., for each of the five SAR values), three independent replicates with three cell culture dishes each were used for each treatment condition. It is evident that the numbers of severely damaged cells belonging to category E have a large impact on the CTF value for each slide. In the above mentioned example, one single E cell more or less would change the CTF value of the slide substantially to 4.64, or 4.26, respectively. Surprisingly, the coefficients of variation for the number of E cells of sham-exposed and negative control samples (both having the lowest numbers of E cells), as calculated by dividing the standard deviations by the respective means, is much higher (on average 57%) than the coefficients of variation for the respective CTF values (on average 4.0%). In other words, the very low coefficients of variation of the overall CTF values are difficult to explain, even provided that absolutely no biological or methodological variation would exist.

This argument is further underlined by looking at all coefficients of variation of all 20 CTF values given in Table 2 and Fig. 1 of the Schwarz et al. paper: on average, coefficients of variation are 2.9% and never exceed 5%, which is truly remarkable for this kind of biological experiment with a large number of possible confounders and methodological inaccuracies, among them differences in the cells' status and cycle, possible differences in cell culture conditions (from at least 15 independently performed experiments), differences in exposure to EMFs and UV, variations during electrophoresis and staining, and, most importantly, differences in microscopic examination and manual classification. What is even more surprising: the coefficients of variation are lower at higher CTF values: in sham-exposed cells or negative controls, the average coefficients of variation are 3.9 and 4.1%, respectively, whereas in RF-EMF exposed cells, the coefficients of variation are on average 2.6%, and in positive controls (irradiated with UV) only 1.2%. These extremely low variations are biologically and methodologically incomprehensible. For example, the SAR variations were already reported to be 26%, thus 10 times as large as the variations in the biological answer of the exposed cells. Furthermore, the low standard deviations are also in sharp contrast to results of a study (Speit et al. 2007) where the authors tried to replicate earlier results from the group of Vienna showing DNA breakage in cells exposed to 900 MHz RF-EMFs (Diem et al. 2005). Using the same cells as in the investigation by Schwarz et al., the authors found much higher coefficients of variation on the order of 30–40%. In this context a statement in the paper by Schwarz et al. is interesting: "Due to the scoring of 500 cells, being about ten times the cells usually processed by computer-aided image analysis, standard deviations become very low." Presumably, Schwarz et al. refer to the paper by Speit et al. where exactly 50 cells per slide were analyzed by means of a computer-assisted evaluation system for the DNA comets. It is, however, well known that the standard deviation does not depend on the number (n) of a sample, unlike the standard error. That in fact standard deviations were calculated in their publication is evident when looking at a publication by the same group (Rüdiger et al. 2006) where original (raw) data were presented in response to a critical letter (Vijayalaxmi et al. 2006) in reference to the two previous publications by the researchers from Vienna (Diem et al. 2005; Ivancsits et al. 2005). The standard deviations were in the same range as in the recent paper by Schwarz et al.

Unexpected low standard deviations are also seen in the time course study (Fig. 3) of the Schwarz et al. paper. Whereas after 4 h no effects by exposure are seen, the CTF values are significantly increased after 8 and 12 h of exposure with very low standard deviations. CTF values of sham-exposed and negative control cells are statistically indistinguishable and almost constant (range between 4.7 and 4.9). For these data ($n = 7$ for sham-exposed cells and $n = 7$ for negative controls), the coefficients of variation between the (independent) experiments were only 2.1 and 1.2%, respectively, thus even lower than the coefficients of variation between replicates which were reported to be 4.2% for "unexposed" samples. These low coefficients of variation are therefore statistically impossible.

The recent data by Schwarz et al. are also in sharp contrast to their own, previously published results (Diem et al. 2002), where inter-individual coefficients of variation for CTF values were reported to be on the order of 25–30% with age as a major factor. In the present paper (Schwarz et al. 2008) (Fig. 6a), inter-individual differences (coefficients of variation) for CTF values of cells from donors aged 6, 29, and 53 years, respectively, were only 6.1% (sham exposed), 3.8% (exposed), 7.1% (negative controls), and 4.0% (positive controls), respectively. Also, these low coefficients of variation are therefore difficult to comprehend.

Calculation errors and statistical analyses

The sums of the average values of all cell types (A–E) as given in Table 2 of the Schwarz et al. paper should be 500 since this was the number of cells which were analyzed. This is in fact the case for exposed and sham-exposed cells where the sums are 500 ± 0.2, the small deviations probably being due to rounding errors. In positive and negative controls, however, there are consistently different cell numbers with differences up to 14.6 cells.

The statistical analysis to check for significant effects of exposure was done by the non-parametric Mann–Whitney–Wilcoxon test, comparing $n = 3$ values of exposed cells with the combined ($n = 6$) values of sham-exposed and negative control cells. This way to analyze the data is odd, for several reasons. The data in Table 2 reveal that the variances of the CTF values of the three groups for each SAR value with $n = 3$ were statistically not different between exposed, sham-exposed and negative control cells, as tested by the F-test for equal variances. Thus, a parametric test would have been possible with much better significance levels by just comparing sham-exposed and exposed cells which should have been the difference of interest. This was actually the way in which the data from the previous study by the group were analyzed (Diem et al. 2005). In fact, based on the data given in Table 2 of the Schwarz et al. paper, all differences between sham-exposed and exposed CTF values turned out to be highly significantly different ($p < 0.001$) when using the parametric Student's t test. In none of these tests were the variances between the groups significantly different. Why the authors decided to perform a non-parametric test with a maximum level of significance of $p = 0.0238$ remains enigmatic. It is, however, interesting to note that a non-parametric test with $n = 3$ in both groups (exposed and sham-exposed) would not have been possible because irrespective of the differences, the lowest p value would be 0.1. In other words, it was essential to combine the CTF values of negative controls and sham-exposed cells to be able to perform a non-parametric test in the first place. This is only possible if the negative controls (cells which were placed in the incubator) and sham-exposed cells (which were placed in the exposure apparatus but were not exposed) showed about the same CTF values. Apparently and surprisingly, this was the case.

Summary and conclusion

The paper by Schwarz et al. (2008) apparently supports the earlier findings of the group (Diem et al. 2005), again showing significant deleterious effects of RF-EMF on DNA molecules of human fibroblasts (please note that the former name of the author Kratochvil was Diem). Despite the lack of any biophysical mechanism which would be able to explain such interactions, the results not only confirm the group's previous findings, but they apparently extend them to another frequency range (UMTS, around 1,950 MHz) and to lower SAR levels which are well below internationally accepted exposure limits for the general public (ICNIRP 1998).

The arguments given in this paper, focusing on the effects seen on DNA damage of fibroblasts, question the validity and the origin of the data published by Schwarz et al. (2008). Many of the arguments listed here, though, would be valid for the analysis of the micronuclei (MN), too (e.g., low standard deviations, low standard deviations at high MN numbers, low inter-individual differences, lack of random effects, etc.). For several reasons, the extremely low standard deviations are far too low for this kind of experiment in living cells with respect to the cells' status in many independently performed experiments, methodological variations (e.g., variations in the SAR levels), random effects of cells counted, and estimation errors due to microscopical inspection and manual classification. The statistical analysis was done inappropriately and several calculation errors are irritating. As long as no convincing evidence is provided rebutting all arguments as listed here, the paper of Schwarz et al. must be treated with extreme caution.

References

Diem E, Ivancsits S, Rüdiger HW (2002) Basal levels of DNA strand breaks in human leukocytes determined by comet assay. J Toxicol Environ Health A 65:641–648

Diem E, Schwarz C, Adlkofer F, Jahn O, Rüdiger H (2005) Non-thermal DNA breakage by mobile-phone radiation (1800 MHz) in human fibroblasts and in transformed GFSH-R17 rat granulosa cells in vitro. Mutat Res 583:178–183

ICNIRP (1998) Guidelines for limiting exposure to time-varying electric, magnetic, and electromagnetic fields (up to 300 GHz). Health Phys 74:494–522

Ivancsits S, Pilger A, Diem E, Jahn O, Rüdiger HW (2005) Cell type-specific genotoxic effects of intermittent extremely low-frequency electromagnetic fields. Mutat Res 583:184–188

Oberto G, Rolfo K, Yu P, Carbonatto M, Peano S, Kuster N, Ebert S, Tofani S (2007) Carcinogenicity study of 217 Hz pulsed 900 MHz electromagnetic fields in Pim1 transgenic mice. Radiat Res 168:316–326

Repacholi MH, Basten A, Gebski V, Noonan D, Finnie J, Harris AW (1997) Lymphomas in E mu-Pim1 transgenic mice exposed to pulsed 900 MHZ electromagnetic fields. Radiat Res 147:631–640

Rüdiger H, Kratochvil E, Pilger A (2006) Reply to the letter by Vijayalaxmi et al. Mutat Res 603:107–109

Schwarz C, Kratochvil E, Pilger A, Kuster N, Adlkofer F, Rüdiger HW (2008) Radiofrequency electromagnetic fields (UMTS, 1,950 MHz) induce genotoxic effects in vitro in human fibroblasts but not in lymphocytes. Int Arch Occup Environ Health

Sommer AM, Bitz AK, Streckert J, Hansen VW, Lerchl A (2007) Lymphoma development in mice chronically exposed to UMTS-modulated radiofrequency electromagnetic fields. Radiat Res 168:72–80

Speit G, Schutz P, Hoffmann H (2007) Genotoxic effects of exposure to radiofrequency electromagnetic fields (RF-EMF) in cultured mammalian cells are not independently reproducible. Mutat Res 626:42–47

Tillmann T, Ernst H, Ebert S, Kuster N, Behnke W, Rittinghausen S, Dasenbrock C (2007) Carcinogenicity study of GSM and DCS wireless communication signals in B6C3F1 mice. Bioelectromagnetics 28:173–187

Utteridge TD, Gebski V, Finnie JW, Vernon-Roberts B, Kuchel TR (2002) Long-term exposure of E-mu-Pim1 transgenic mice to 898.4 MHz microwaves does not increase lymphoma incidence. Radiat Res 158:357–364

Vijayalaxmi, McNamee JP, Scarfi MR (2006) Comments on: "DNA strand breaks" by Diem et al. [Mutat Res 583 (2005) 178–183] and Ivancsits et al. [Mutat Res 583 (2005) 184–188]. Mutat Res 603:104–106

Vijayalaxmi, Obe G (2004) Controversial cytogenetic observations in mammalian somatic cells exposed to radiofrequency radiation. Radiat Res 162:481–496

Int. J. Radiat. Biol., Vol. 85, No. 3, March 2009, pp. 196–213

informa
healthcare

Genetic damage in mammalian somatic cells exposed to extremely low frequency electro-magnetic fields: A meta-analysis of data from 87 publications (1990–2007)

VIJAYALAXMI[1] & THOMAS J. PRIHODA[2]

[1]*Department of Radiation Oncology, and* [2]*Department of Pathology, University of Texas Health Science Center, San Antonio, TX 78229, USA*

(Received 11 May 2008; revised 21 October 2008; accepted 4 December 2008)

Abstract

Purpose: A meta-analysis was conducted to obtain a 'quantitative' estimate of the extent of genetic damage in mammalian somatic cells exposed to non-ionizing radiation emitted from extremely low frequency electro-magnetic fields (ELF-EMF) and to compare with that in unexposed control cells.

Methods: The methods used for the meta-analysis were recommended in several standard text books. Three specific variables related to ELF-EMF exposure characteristics were examined in the meta-analysis: (i) frequency (Hz), (ii) flux density (mT), and (iii) in occupationally exposed individuals.

Result and conclusions: (1) The difference between ELF-EMF-exposed and control cells as well as the 'effect size' due to ELF-EMF exposure were biologically small (although statistically significant) with very few exceptions. (2) At certain ELF-EMF exposure conditions there was a statistically significant increase in genetic damage assessed from some end-points. (3) The mean indices for chromosomal aberrations and micronuclei end-points in ELF-EMF-exposed and control cells were within the spontaneous levels reported in historical database. (4) Considerable evidence for publication bias was found in the meta-analysis.

Keywords: *Meta-analysis, electromagnetic fields, DNA strand breaks, chromosomal aberrations, micronuclei, sister chromatid exchanges*

Introduction

The possible effects of exposure to non-ionizing radiation emitted from extremely low frequency electro-magnetic fields (ELF-EMF) on the genetic material (DNA) are very important. Damage in the DNA of somatic cells can lead to the development of cancer or cell death. Hence, during the last several decades, researchers have used recently developed experimental techniques as well as classical cytogenetic methods to determine the extent of genetic damage in mammalian somatic cells exposed in vitro and/or in vivo to ELF-EMF in the frequency range of 0–5000 Hz. The data were published in peer-reviewed scientific journals. Vijayalaxmi and Obe (2005) reviewed the literature published during 1990–2003 and made a 'qualitative assessment' of the data reported in 63 investigations. The extent of genetic damage in all these publications was determined using one or more end-points, namely, single- and/or double-strand breaks in the DNA evaluated using the comet assay in which the comet tail length was measured in microns (SBM) and the comet tail moment expressed as a ratio (SBR, derived from the amount of DNA in comet head and comet tail), and the incidence of chromosomal aberrations (CA), micronuclei (MN) and sister chromatid exchanges (SCE). The conclusions from 29 investigations (46%) did not indicate significantly increased genetic damage in ELF-EMF-exposed cells as compared with that in sham- and/or un-exposed cells while the results from 14 studies (22%) have suggested such an increase in the former as compared with the latter cells. The observations from 20 other studies (32%) were inconclusive. Similar conclusions were drawn in earlier reviews (McCann et al. 1993, 1998, Murphy et al. 1993, Moulder 1998). The details presented in these publications revealed several

Correspondence: Vijayalaxmi, PhD, Department of Radiation Oncology, University of Texas Health Science Center, 7703 Floyd Curl Drive, San Antonio, TX 78229, USA. Tel: +1 (210) 692 7874. Fax: +1 (210) 949 5085. E-mail: vijay@uthscsa.edu

ISSN 0955-3002 print/ISSN 1362-3095 online © 2009 Informa Healthcare USA, Inc.
DOI: 10.1080/09553000902748575

differences among the investigations including ELF-EMF exposure conditions, experimental protocols, etc. Any and/or all of these variables could have contributed to the controversial observations in the existing literature (Vijayalaxmi and Obe 2005).

Meta-analysis is widely used in biomedical research, especially when the outcomes of the observations in different investigations are controversial. If considered separately, any one study may be either too small or too limited in scope to arrive at a generalized and unequivocal conclusion. Analyses of the combined data from all such related studies represent an attractive alternative to strengthen the evidence from any individual study. The importance of precise methods used in analyzing the data to draw inferences from heterogeneous but logically related studies has been emphasized by Armitage (1984). A meta-analysis was conducted using all SBM, SBR, CA, MN and SCE data published in peer-reviewed scientific journals during the years 1990–2007 to obtain a 'quantitative' estimate of the extent of genetic and epigenetic damage (theoretically, it may well be that ELF-EMF exposure per se is not genotoxic, but that such exposure could enhance the damage induced by other biological, chemical and/or physical genotoxic agents, i.e., ELF-EMF+ known genotoxic agents) in mammalian somatic cells exposed in vitro and/or in vivo to ELF-EMF. Such analyses could also help in better understanding of the genotoxic/carcinogenic potential of ELF-EMF. The objectives were to: (i) Obtain a good 'quantitative' estimates of the damage reported in ELF-EMF-exposed cells compared with that in sham- and/or un-exposed control cells, (ii) study the correlation between certain specific ELF-EMF exposure characteristics (see below) and increased genotoxicity which is larger than the random variability, (iii) examine whether the damage indices in ELF-EMF-exposed cells were within the spontaneous levels reported in historical database, (iv) use multiple regression analysis to determine the combined effects of ELF-EMF characteristics (each adjusted for the others) on genotoxicity, and (v) test for heterogeneity of residual variability to indicate if other factors that were not considered in the meta-analysis could explain the effects reported in the publications. A similar meta-analysis was conducted using the genetic damage indices, reported from 1990–2005, in mammalian somatic cells exposed in vitro and in vivo to radiofrequency radiation (300 MHz to 300 GHz), and the conclusions were published recently (Vijayalaxmi and Prihoda 2008).

Materials and methods

The methods employed for the meta-analysis have been recommended in several standard textbooks: (i) *Statistical Methods for Meta-analysis* (Hedges and Olkin 1985), (ii) *Practical Meta-Analysis* (Lipsey and Wilson 2001), (iii) *Methods of Meta-Analysis*: *Correcting Error and Bias in Research Findings* (Hunter and Schmidt 2004), (iv) *How to Report Statistics in Medicine*: *Annotated Guidelines for Authors*, *Editors*, *and Reviewers* (Lang and Secic 2006) and (v) Cochrane Handbook for Systematic Reviews of Interventions 2006. A total of 87 papers were retrieved from peer-reviewed scientific publications. Each publication was examined in detail by both authors: the results reported as numbers in the Tables were documented as such while the Figures were 200% enlarged to enter the data (nearer to the actual numbers) in an Excel spreadsheet (Microsoft, WA). The quality of investigations, i.e., whether or not the researcher(s) have included sham-/unexposed-/positive-controls, 'blind' evaluations, provided detailed description of dosimetry, experimental protocols, data collection procedures, appropriate statistical analyses, and conclusions from results in the text, tables and figures being consistent were assessed and agreed upon by both authors. This information was not intended to 'rank' the publications either to exclude or include the data in meta-analysis. All data recorded from each publication in the Excel spread sheet was checked and re-checked (to ensure no errors were made during the recording process) before subjecting the data to meta-analysis.

For the same genotoxicity end-point, researchers have examined different numbers of cells in the same or different experiments. For example, investigators have reported the incidence of MN recorded in a total of 500, 1000 or 2000 cells. In such instances, Fleiss et al. (2003) have suggested a method using 'raw' data to calculate the mean, standard deviation (SD) and variance from varying number of cells examined in different experiments (when averaging over experiments and cells within experiments). However, it is almost impossible to obtain the raw data from individual investigators. Hence, for each end-point, a standardized 'unit' was obtained and used as a more homogeneous measure. The standardized unit for CA was in 100 cells, i.e., if an investigator has reported the incidence in 200 cells, it was divided by two to obtain the unit as CA/100 cells. Similarly, the standardized units were MN/1000 cells and SCE/cell. The results reported for DNA single- and double-strand breaks were pooled to obtain a standardized unit for the comet tail length in microns (SBM) and comet tail moment as radio (SBR) (the 'tail factor' used in some investigations was included in this category). The 'units' in ELF-EMF-exposed were integrated to obtain overall pooled mean and SD to designate to the 'ELF-EMF-exposed group' while similar data in controls were assigned to the 'control group'. These are the

'descriptive' data for standardized units from which the meta-analysis was conducted.

Meta-analysis

Several variables in the experimental protocols used by different investigators in different countries were identified and discussed in an earlier review by Vijayalaxmi and Obe (2005). It is beyond the scope and goals of this meta-analysis to determine the effect of all such variables. Only three specific variables related to ELF-EMF exposure characteristics were selected to determine their 'potential' influence on various genotoxicity end-points (based on 50 Hz used in Europe/Asia and 60 Hz used mainly in USA, and flux density exposure limits suggested by international organizations): (i) Frequency (Hz), (ii) flux density (mT) and (iii) occupational exposure (electric train drivers, power-line inspectors and maintenance personnel, and also individuals employed in high voltage electric supply substations). The frequency of ELF-EMF was sub-classified: (a) $\leq$50 Hz and (b) $\geq$60 Hz. The flux density was sub-classified: (a) 0.0–0.5 mT, (b) $>$ 0.5–1.0 mT, (c) $>$ 1.0 – 5.0 mT and (d) $>$ 5 mT. The issue related to epigenetic effects of ELF-EMF exposure was investigated in rodent and human cells which were treated in vitro with a known genotoxic agent prior/during/after ELF-EMF exposure: The data reported in a total of 33 publications were also subjected to meta-analysis. The Statistical Analysis System (SAS 2006) Version 9.1 for Windows was used for all analyses described below.

Magnitude of weighted difference between ELF-EMF-exposed and controls (E–C)

The existence of variability in the data obtained from one experiment to another experiment and from one laboratory to another laboratory is well known. One of the goals of the meta-analysis was to take this variability into consideration to summarize the descriptive data. Fixed-effects models described by Lipsey and Wilson (2001) were first used to calculate the magnitude of difference between ELF-EMF-exposed and control (E–C). These models assume a single 'fixed' effect that every study will approximate within each sub-group. This conservative approach provides very 'narrow' confidence intervals (CI) and is more likely to find significant differences between ELF-EMF-exposed and control groups (as compared with random effects models which yield 'wider' CI and would not find such differences). Furthermore, the variability in the results obtained from different experiments and from different laboratories was taken into consideration to provide a 'weight' which is based on the sample size and variance in ELF-EMF-exposed and controls in each publication (Lipsey and Wilson 2001). Separate statistical analyses were performed for each genotoxicity end-point because of the differences in their standardized units and for the interpretation of the units. The method used to obtain a quantitative estimate of E–C was described in detail in the supplementary information provided in an earlier publication (Vijayalaxmi and Prihoda 2008).

Effect size (ES) or standardized mean difference (d)

Another method regularly used in the meta-analysis is to determine 'unit-less' measures called 'effect size' (ES) between ELF-EMF-exposed and controls in each publication and for each endpoint. The ES was calculated using the random-effects models suggested by Hunter and Schmidt (2004). These models are recommended by the National Research Council (1992) and are more accurate than the traditional random effects models, and have several advantages: they allow for the possibility that p values vary from one study to another, make fewer assumptions, are more conservative, and use weighting by sample size (which is critical for meta-analysis). The method also corrected for 'bias' in the estimated ES and provided 'weights' for the data in each publication. The method used to obtain the ES was described in detail in the supplementary information provided in an earlier publication (Vijayalaxmi and Prihoda 2008).

Multiple regression analysis

The meta-analysis considered the influence of several sub-groups in ELF-EMF exposure characteristics on each end-point. The % contribution of each sub-group for the outcomes in E–C and ES were examined using the standard output of weighted multiple regression analysis with adjustments for meta-analysis as described in Hedges and Olkin (1985). Nine predictor variables in ELF-EMF exposure characteristics [ELF-EMF *frequency sub-groups* (*$\leq$50 Hz and $\geq$60 Hz*) *as 1 predictor variable*; flux *density sub-groups* (0.0–0.5 mT, $>$ 0.5–1.0 mT, $>$ 1.0–5.0 mT, $<$5 mT and occupationally exposed *individuals*) *as four predictor variables*; *interaction of Hz and flux density as four predictor variables*], adjusted for each other, provided 'weighted' regression coefficients and sums of squares for E–C (Lipsey and Wilson 2001) and for ES (Hunter and Schmidt 2004). The weighted regression coefficients and sums of squares for each predictor variable, for residual variability and for total variability in the regression were obtained from SAS software (SAS 2006). The standard error (SE) of these regression coefficients from SAS was adjusted (Hedges and Olkin 1985) for the weighted meta-analysis of

sub-group effects. The % variance due to the predictor variables was calculated from each of the weighted sums of squares as % of their total. The % contribution of each sub-group to the effect/outcome observed on E–C and ES on each genotoxicity end-point was estimated. The interaction effects are to test if the effect of Hz is the same or different at different flux densities. If there was no interaction, then the effect of Hz would be the same regardless of the flux density.

Heterogeneity

The meta-analysis considered several related studies. The degree of heterogeneity among the results from such studies can influence the overall conclusions. This was examined in the weighted multiple regression analysis (Hedges and Olkin 1985) using the random error for testing heterogeneity of effects to verify the validity of the models used for both E–C and ES. The residual weighted sums of squares were used in the Chi-square 'goodness of fit' hypothesis with appropriate degrees of freedom (Hedges and Olkin 1985). When the hypothesis was not rejected, the regression model was considered as adequate. Also, when the goodness of fit gave significant results, the data indicated heterogeneity in E–C and ES values obtained for each end-point, i.e., factors which were not considered in this meta-analysis had an influence on the differences between ELF-EMF-exposed and control conditions. Such data were further examined: (i) to explain which sub-group ELF-EMF exposure characteristic contributed to the heterogeneity, (ii) to compare minimum and maximum effects with those in controls, and (iii) interpret the magnitude of heterogeneity.

Publication 'bias'

Publication 'bias' refers to the fact that studies with statistically significant results, even with small sample size, are more likely to be published than those without statistically significant results (Dickersin 1990). When the data with 'no' publication bias were presented in a Figure, studies with small sample size would have the same mean ES (as in those with large sample size) but, indicate a greater variability with wider dispersion of low and high ES values around the mean ES. In contrast, if there is a publication bias, the smaller ES in studies with small sample size would be disproportionately absent since such studies will fail to accomplish statistical significance ($p < 0.05$). Sterne and Egger (2001) have suggested that the graphs/figures to represent publication bias should generally use standard error (SE) as the measure of study/sample size for the vertical axis. Hence, this method was used to assess the publication bias in ELF-EMF research investigations.

Historical database

To provide a proper perspective in the evaluation of potential 'adverse' effects of ELF-EMF exposure, the genotoxicity indices reported in ELF-EMF research investigations were compared with the 'spontaneous' indices in normal cells published in a large historical database. A simple descriptive meta-analysis was performed by pooling the spontaneous incidence of CA, MN or SCE reported in normal cells in several studies in which large sample size was used (Lloyd et al. 1980, Vijayalaxmi and Evans 1982, Fenech and Morley 1985, Obe 1986, Rudd et al. 1988, Bender et al. 1988, 1989, 1992, Bonassi et al. 1995, 2001, Bolognesi et al. 1997, Stephan and Pressl 1999, Fenech et al. 2003, Hagmar et al. 2004, Neri et al. 2005, Rossner et al. 2005) and weighted by the sample size and variance. The spontaneous indices obtained for each end-point was compared with those in ELF-EMF-exposed and controls in the meta-analysis database.

Results

There were a total of 87 peer-reviewed scientific publications during 1990–2007 (Tables I and II). The geographical distribution showed that a great majority of the publications were from Europe followed by the USA: consequently, large numbers of investigations were conducted using ELF-EMF exposure at 50 Hz. Only two studies have compared the effect of two different frequencies (32 Hz and 50 Hz, and 50 Hz and 60 Hz). With respect to flux density, 1 mT was predominantly used by the researchers. Other studies compared the effect of more than one flux density. Seven studies were conducted in human volunteers exposed to ELF-EMF. Investigations were conducted both in vitro and in vivo conditions in humans and experimental animals. The issue related to epigenetic effects of ELF-EMF exposure ($\pm$ physical and chemical mutagens) was addressed in vitro using human and rodent cells and the observations were reported in a total of 33 publications. A great majority of the researchers have used only one genotoxic end-point while 4 studies have compared the data obtained in all four different end-points. Twenty five different tissue/cell types have been used to examine the effect of ELF-EMF exposure.

DNA single- and double-strand breaks

The results of the meta-analysis of the weighted mean E–C for SBM and SBR, presented in Table III,

Table I. List of ELF-EMF publications in chronological order.

#	First author	Year	#	First author	Year	#	First author	Year
1	Frazier	1990	30	Lai	1997b	59	McNamee	2002
2	Garcia-Sagredo	1990	31	Scarfi	1997a	60	Nakahara	2002
3	Garcia-Sagredo	1991	32	Scarfi	1997b	61	Robison	2002
4	Khalil	1991	33	Scarfi	1997c	62	Zeni	2002
5	Livingston	1991	34	Singh	1997	63	Cho	2003
6	Scarfi	1991	35	Simko	1998a	64	Ding	2003
7	Fiorani	1992	36	Simko	1998b	65	Hone	2003
8	Ciccone	1993	37	Singh	1998	66	Ivancsits	2003a
9	Hintenlang	1993	38	Svedenstal	1998	67	Ivancsits	2003b
10	Khalil	1993	39	Ahuja	1999	68	Pasquini	2003
11	Scarfi	1993	40	Pacini	1999	69	Verheyen	2003
12	Skyberg	1993	41	Scarfi	1999	70	Lai	2004
13	Valjus	1993	42	Simko	1999	71	Lloyd	2004
14	Zwingelberg	1993	43	Svedenstal	1999a	72	Stronati	2004
15	Fairbairn	1994	44	Svedenstal	1999b	73	Testa	2004
16	Nordenson	1994	45	Yaguchi	1999	74	Zmyslony	2004
17	Scarfi	1994	46	Kindzelskii	2000	75	Ivancsits	2005
18	Antonopoulos	1995	47	Maes	2000	76	Luceri	2005
19	Cantoni	1995	48	Miyakoshi	2000	77	McNamee	2005
20	d'Ambrosio	1995	49	Yaguchi	2000	78	Moratti	2005
21	Galt	1995	50	Zmyslony	2000	79	Scarfi	2005
22	Paile	1995	51	Abramsson-Zetterberg	2001	80	Winker	2005
23	Tofani	1995	52	Heredia-Rojas	2001	81	Wolf	2005
24	Cantoni	1996	53	Jajte	2001	82	Yokus	2005
25	Okonogi	1996	54	Nordenson	2001	83	Udroiu	2006
26	Ahuja	1997	55	Othman	2001	84	Villarini	2006
27	Jacobson-Kram	1997	56	Simko	2001	85	Erdal	2007
28	Lagroye	1997	57	Skyberg	2001	86	Miyakoshi	2007
29	Lai	1997a	58	Ivancsits	2002	87	Wahab	2007

Table II. Publications characteristics.

Year:	1990 – 2; 1991 – 4; 1992 – 1; 1993 – 7; 1994 – 3; 1995 – 6; 1996 – 2; 1997 – 9; 1998 – 4; 1999 – 7; 2000 – 5; 2001 – 7; 2002 – 5; 2003 – 7; 2004 – 5; 2005 – 8; 2006 – 2; 2007 – 3	87
Countries:	Austria – 5; Belgium – 2; Canada – 2; Egypt – 1; Finland – 2; France – 1; Germany – 6; India – 3; Italy – 24; Japan – 7; Jordan – 2; Mexico – 1; New Zealand – 1; Norway – 2; Poland – 3; South Korea – 1; Spain – 2; Sweden – 7; Turkey – 2; UK – 2; USA – 11.	87
ELF-EMF frequencies:	16 Hz – 1; 50 Hz – 65; 60 Hz – 16; 100 Hz – 1; 4400 Hz – 2; 32 and 50 Hz – 1; 50 and 60 Hz – 1	87
Flux density: 0.0– > 5.0 mT	1 Flux density – 54; 2 different flux densities – 6; 3 different flux densities – 14; 4 different flux densities – 1; 5 different flux densities – 3; 6 different flux densities – 1; 8 different flux densities – 1; Occupational – 7;	87
Studies: In vitro-Human; In vitro-Rodent; In vivo-Human; In vivo-Rodent In vitro-Human ± Mutagen; In vitro-Rodent ± Mutagen In vivo-Rodent ± Mutagen	1 study – 78; 2 different studies – 8; 4 different studies – 1	87
Genotoxicity end-points: DNA strand breaks; Chromosomal aberrations Micronuclei; Sister chromatic exchanges	1 end-point – 72; 2 different end–points – 11; 3 different end–points – 2; 4 different end–points – 2	87
Cell types (*):	1 cell type only – 79; 2 different cell types – 5; 3 different cell types – 2; 6 different cell types – 1	87

(*): Freshly collected and cultured human cells: Human amniotic cells; Human blood lymphocytes; Human blood neutrophils; Human glioma cells; Human lymphoblastoid cells; Human melanocytes; Human monocytes; Human skeletal muscle cells; Human skin fibroblasts; Human tumor cells. (*): Freshly collected and cultured rodent cells: Chinese hamster lung cells; Chinese hamster ovary cells; Mouse blood lymphocytes; Mouse bone marrow cells; Mouse brain cells; Mouse liver cells; Mouse red blood cells; Mouse skin cells; Rat brain cells; Rat blood lymphocytes; Rat bone marrow cells; Rat granulosa cells; Rat lung cells; Rat skin fibroblasts; Syrian hamster embryo cells.

Table III. Meta-analysis of the pooled E-C[a] and ES[b] data for DNA strand breaks evaluated as comet tail length in microns (SBM) and comet tail moment expressed as ratio (SBR).

End Point	ELF-EMF Exposure	Group	Pooled data		E–C		ES
			N	Mean (SD)	Total N	Mean (SE)	Mean (SE)
SBM	Hz and Flux	Control	545	4.8 (5.8)			
		ELF-EMF-exposed	544	2.8 (10.9)	1089	1.07 (0.06)***	0.81 (0.08)***
SBM	≤50 Hz	Control	95	1.0 (3.8)			
		ELF-EMF-exposed	94	0.8 (4.3)	189	0.81 (0.06)***	1.34 (0.21)***
SBM	≥60 Hz	Control	450	30.9 (6.1)			
		ELF-EMF-exposed	450	42.9 (11.8)	900	3.34 (0.18)***	0.73 (0.08)***
SBM	0.0–0.5 mT	Control	269	6.0 (7.7)			
		ELF-EMF-exposed	268	2.1 (15.2)	537	0.35 (0.07)***	1.32 (0.12)***
SBM	>0.5–1.0 mT	Control	132	13.5 (2.9)			
		ELF-EMF-exposed	132	14.3 (3.2)	264	0.57 (0.25)***	0.26 (0.14)*
SBM	>1.0–5.0 mT	Control	108	2.6 (2.7)			
		ELF-EMF-exposed	108	5.6 (2.7)	216	1.39 (0.15)***	0.50 (0.16)***
SBM	>5.0 mT	Control	36	1.7 (1.1)			
		ELF-EMF-exposed	36	6.4 (1.1)	72	4.40 (0.15)***	1.84 (0.45)***
SBR	Hz and Flux	Control	1575	3.8 (0.8)			
		ELF-EMF-exposed	1575	5.4 (3.4)	3150	2.68 (0.00)***	0.57 (0.04)***
SBR	≤50 Hz	Control	1305	3.9 (0.9)			
		ELF-EMF-exposed	1305	5.7 (3.8)	2610	2.74 (0.00)***	0.75 (0.05)***
SBR	≥60 Hz	Control	270	0.8 (0.3)			
		ELF-EMF-exposed	270	0.7 (0.3)	540	−0.08 (0.01) ns	−0.21 (0.10)*
SBR	0.0–0.5 mT	Control	187	3.5 (0.4)			
		ELF-EMF-exposed	187	8.8 (0.9)	374	3.83 (0.01)***	−0.21 (0.14) ns
SBR	>0.5–1.0 mT	Control	1274	3.9 (0.9)			
		ELF-EMF-exposed	1274	5.0 (3.8)	2548	2.61 (0.00)***	0.71 (0.05)***
SBR	>1.0–5.0 mT	Control	104	0.4 (0.3)			
		ELF-EMF-exposed	104	0.4 (0.3)	208	0.00 (0.01) ns	−0.01 (0.16) ns
SBR	>5.0 mT	Control	10	1.8 (1.5)			
		ELF-EMF-exposed	10	2.1 (1.4)	20	0.30 (0.27) ns	0.17 (0.61) ns

[a]E–C: Magnitude of weighted difference between ELF-EMF-exposed and control groups based on sample size and variance; [b]ES: Effect size. N: Sample size (i.e., number of experimental units); SD: Standard Deviation; SE: Standard Error; *$p < 0.05$, **$p < 0.01$, ***$p < 0.001$; ns: Not significant.

indicated significant increases in mean ± SE values in ELF-EMF-exposed as compared with controls ($p < 0.001$). There were no significant differences between ELF-EMF-exposed and control groups for SBR at ≥60 Hz and at > 1.0 mT ($p > 0.05$). The weighted mean E–C for SBM and SBR ranged between 0.35 and 4.4 and −0.08 and 3.83, respectively. Also, see Table X for further results. A significantly increased ES was evident for SBM at all exposure conditions (Hz and flux densities, $p < 0.05$). Similarly, a significantly increased ES was evident for SBR at Hz and flux, ≤50 Hz and >0.5–1.0 mT ($p < 0.05$). On the other hand, a significantly decreased (negative) effect was observed for SBR at ≥60 Hz ($p < 0.05$) while the effect was not significant at 0.0–0.5 mT and >1.0 mT flux densities.

Chromosomal aberrations

The results of the meta-analysis of the weighted mean E–C for CA, presented in Table IV, indicated significant increases in mean ± SE values in ELF-EMF-exposed as compared with controls ($p < 0.01$); the only exception was at the flux density of >5.0 mT ($p > 0.05$). The weighted mean E–C for CA ranged between 0.12 and 0.89 (i.e., an increase of <1.0 CA in 100 ELF-EMF exposed cells). Also, see Table X for further results. The ES for CA was significant at all exposure conditions (Hz and flux densities, $p < 0.01$), the only exception being at flux density 0.0–0.5 mT.

Micronuclei

A majority of investigators in ELF-EMF research have used MN as a genotoxicity end-point to assess the damage. Consequently, the consolidated sample size is the largest among all of the end-points investigated, as given in Table V. The results of the meta-analysis of the weighted mean E–C for MN, indicated significant increase in mean ± SE values in ELF-EMF-exposed as compared with controls ($p < 0.05$) at all exposure conditions; the only exception was in cells from occupationally exposed individuals. The weighted mean E–C for MN ranged between 0.07 and 3.71 (i.e., <4.0 MN in 1000 ELF-EMF-exposed cells). Also, see Table X for further results. The ES for MN was significant at all

Table IV. Meta-analysis of the pooled, E–C[a] and ES[b] data for chromosomal aberrations/100 cells (CA).

End Point	ELF-EMF Exposure	Group	Pooled data		E–C		ES
			N	Mean (SD)	Total N	Mean (SE)	Mean (SE)
CA	Hz and Flux	Control	262	3.4 (0.9)			
		ELF-EMF-exposed	344	4.7 (1.7)	606	0.61 (0.03)***	0.67 (0.10)***
CA	≤50 Hz	Control	170	1.7 (0.8)			
		ELF-EMF-exposed	252	1.6 (1.9)	422	0.22 (0.07)***	0.59 (0.11)***
CA	≥60 Hz	Control	92	4.5 (0.9)			
		ELF-EMF-exposed	92	5.4 (0.9)	184	0.74 (0.04)***	0.91 (0.19)***
CA	0.0–0.5 mT	Control	48	0.5 (0.8)			
		ELF-EMF-exposed	48	0.8 (0.8)	96	0.12 (0.09)**	0.33 (0.24) ns
CA	>0.5–1.0 mT	Control	43	4.4 (1.0)			
		ELF-EMF-exposed	43	4.7 (1.1)	86	0.31 (0.07)***	0.96 (0.27)***
CA	>1.0–5.0 mT	Control	75	4.1 (0.4)			
		ELF-EMF-exposed	75	5.6 (1.6)	150	0.88 (0.04)***	1.49 (0.24)***
CA	>5.0 mT	Control	16	0.8 (0.4)			
		ELF-EMF-exposed	16	1.2 (4.1)	32	0.89 (0.50) ns	1.30 (0.45)**
CA	Occupational	Control	80	2.1 (1.1)			
		ELF-EMF-exposed	162	1.9 (1.7)	242	0.52 (0.19)***	0.37 (0.13)**

[a]E–C: Magnitude of weighted difference between ELF-EMF-exposed and control groups based on sample size and variance; [b]ES: Effect size; N: Sample size (i.e., number of experimental units); SD: Standard Deviation; SE: Standard Error; *$p < 0.05$, **$p < 0.01$, ***$p < 0.001$; ns: Not significant. The indices reported in the historical database: CA – mean 1.5/100 cells (SD = 3.7, $n = 15{,}594$).

Table V. Meta-analysis of the pooled, E–C[a] and ES[b] data for micronuclei/1000 cells (MN).

End Point	ELF-EMF Exposure	Group	Pooled data		E–C		ES
			N	Mean (SD)	Total N	Mean (SE)	Mean (SE)
MN	Hz and Flux	Control	828	9.5 (3.8)			
		ELF-EMF-exposed	832	10.1 (4.3)	1660	0.31 (0.02)***	0.66 (0.06)***
MN	≤50 Hz	Control	780	9.6 (3.9)			
		ELF-EMF-exposed	784	10.1 (4.4)	1564	0.31 (0.02)***	0.64 (0.06)***
MN	≥60 Hz	Control	48	8.2 (2.6)			
		ELF-EMF-exposed	48	9.2 (3.3)	96	1.45 (0.36)**	1.06 (0.27)***
MN	0.0–0.5 mT	Control	187	10.7 (4.9)			
		ELF-EMF-exposed	187	10.4 (4.9)	374	0.07 (0.02)*	0.47 (0.13)***
MN	>0.5–1.0 mT	Control	392	5.8 (3.5)			
		ELF-EMF-exposed	396	7.7 (3.9)	788	0.90 (0.06)***	0.63 (0.09)***
MN	>1.0–5.0 mT	Control	137	5.5 (2.5)			
		ELF-EMF-exposed	137	8.8 (4.6)	274	3.71 (0.14)***	0.86 (0.16)***
MN	>5.0 mT	Control	85	5.1 (0.9)			
		ELF-EMF-exposed	85	8.0 (1.3)	170	2.47 (0.15)**	1.61 (0.26)***
MN	Occupational	Control	27	11.0 (7.0)			
		ELF-EMF-exposed	27	11.5 (7.1)	54	0.50 (1.92) ns	0.07 (0.28) ns

[a]E–C: Magnitude of weighted difference between ELF-EMF-exposed and control groups based on sample size and variance; [b]ES: Effect size; N: Sample size (i.e., number of experimental units); SD: Standard Deviation; SE: Standard Error; *$p < 0.05$, **$p < 0.01$, ***$p < 0.001$; ns: Not significant. The indices reported in the historical database: MN – mean 9.0/1000 cells (SD = 8.0, $n = 8{,}667$).

exposure conditions (Hz and flux densities, $p < 0.001$), the only exception, again, was in cells from occupationally exposed individuals.

Sister chromatid exchanges

The results of the meta-analysis of the weighted mean E–C for SCE, presented in Table VI, indicated significant increase in mean ± SE values in ELF-EMF-exposed as compared with controls ($p < 0.05$); the exceptions were at >1.0–5.0 mT flux density and in cells from occupationally exposed individuals. The weighted mean E–C for SCE ranged between −0.06 and 1.42 (i.e., <2.0 SCE/cell in the ELF-EMF-exposed group). Also, see Table X for further results. The ES values for SCE were not significant at all exposure conditions ($p > 0.05$).

Epigenetic investigations

The pooled data for different exposure groups, E–C and ES, are presented in Table VII. The E–C data

Table VI. Meta-analysis of the pooled, E–C[a] and ES[b] data for sister chromatid exchanges/cell (SCE).

End Point	ELF-EMF Exposure	Group	Pooled data		E–C		ES
			N	Mean (SD)	Total N	Mean (SE)	Mean (SE)
SCE	Hz and Flux	Control	223	7.3 (1.6)			
		ELF-EMF-exposed	232	6.2 (1.5)	455	0.70 (0.03)***	0.10 (0.11) ns
SCE	≤50 Hz	Control	140	6.3 (1.7)			
		ELF-EMF-exposed	150	7.1 (1.6)	290	1.15 (0.04)***	0.03 (0.13) ns
SCE	≥60 Hz	Control	83	7.6 (1.4)			
		ELF-EMF-exposed	82	4.8 (1.2)	165	0.14 (0.05)**	0.24 (0.18) ns
SCE	0.0–0.5 mT	Control	70	10.0 (1.8)			
		ELF-EMF-exposed	69	7.7 (1.7)	139	0.14 (0.12)*	0.16 (0.20) ns
SCE	>0.5–1.0 mT	Control	34	4.4 (1.7)			
		ELF-EMF-exposed	34	4.6 (1.8)	68	0.16 (0.05)*	0.27 (0.31) ns
SCE	>1.0–5.0 mT	Control	58	4.7 (1.8)			
		ELF-EMF-exposed	60	5.0 (1.7)	118	−0.06 (0.13) ns	0.02 (0.22) ns
SCE	>5.0 mT	Control	13	6.1 (0.8)			
		ELF-EMF-exposed	14	7.2 (0.2)	27	1.42 (0.05)*	−0.13 (0.45) ns
SCE	Occupational	Control	48	6.9 (1.0)			
		ELF-EMF-exposed	55	6.4 (0.9)	103	0.04 (0.18) ns	0.07 (0.20) ns

[a]E–C: Magnitude of weighted difference between ELF-EMF-exposed and control groups based on sample size and variance; [b]ES: Effect size; N: Sample size (i.e., number of experimental units); SD: Standard Deviation; SE: Standard Error; *$p < 0.05$, **$p < 0.01$, ***$p < 0.001$; ns: Not significant. The indices reported in the historical database: SCE – mean 7.6/cell (SD = 1.6, $n = 4{,}576$).

Table VII. Meta-analysis of the pooled, E–C[a] and ES[b] for DNA strand breaks evaluated as comet tail length in microns (SBM) and comet tail moment expressed as ratio (SBR), chromosomal aberrations/100 cells (CA), micronuclei/1000 cells (MN) and sister chromatid exchanges/cell (SCE) in epigenetic investigations.

End Point	ELF-EMF Exposure	Group	Pooled data		E–C		ES
			N	Mean (SD)	Total N	Mean (SE)	Mean (SE)
SBM	Hz and Flux	Control	104	0.8 (11.6)			
SBM	Hz and Flux	ELF-EMF alone	106	0.2 (17.7)	210	−0.07 (0.07) ns (a)	1.72 (0.20)*** (a)
SBM	Hz and Flux	Mutagen alone	96	12.9 (14.1)			
SBM	Hz and Flux	ELF-EMF + Mutagen	111	28.0 (18.7)	195	4.63 (0.76)*** (b)	0.31 (0.16)* (b)
SBR	Hz and Flux	Control	90	0.3 (0.6)			
SBR	Hz and Flux	ELF-EMF alone	90	0.2 (0.6)	180	−0.01 (0.01) ns (a)	0.17 (0.20) ns (a)
SBR	Hz and Flux	Mutagen alone	90	2.8 (1.0)			
SBR	Hz and Flux	ELF-EMF + Mutagen	90	1.8 (0.9)	180	0.27 (0.03)*** (b)	0.48 (0.21)* (b)
CA	Hz and Flux	Control	55	1.3 (2.9)			
CA	Hz and Flux	ELF-EMF alone	55	0.9 (2.9)	110	−0.09 (0.07) ns (a)	0.33 (0.25) ns (a)
CA	Hz and Flux	Mutagen alone	55	5.5 (8.1)			
CA	Hz and Flux	ELF-EMF + Mutagen	55	4.2 (9.0)	110	0.16 (0.11) ns (b)	0.61 (0.27)* (b)
MN	Hz and Flux	Control	360	5.4 (5.6)			
MN	Hz and Flux	ELF-EMF alone	360	11.5 (4.9)	720	4.50 (0.10)*** (a)	0.57 (0.10)*** (a)
MN	Hz and Flux	Mutagen alone	365	14.6 (12.6)			
MN	Hz and Flux	ELF-EMF + Mutagen	346	12.5 (13.9)	711	−0.22 (0.13) ns (b)	−0.01 (0.10) ns (b)
SCE	Hz and Flux	Control	36	3.7 (0.5)			
SCE	Hz and Flux	ELF-EMF alone	36	3.8 (0.6)	72	0.16 (0.08) ns (a)	0.25 (0.31) ns (a)
SCE	Hz and Flux	Mutagen alone	36	7.3 (1.4)			
SCE	Hz and Flux	ELF-EMF + Mutagen	36	11.1 (1.3)	72	1.46 (0.13)** (b)	0.59 (0.35)* (b)

[a]E–C: Magnitude of weighted difference between ELF-EMF-exposed and control groups based on sample size and variance; [b]ES: Effect size; N: Sample size (i.e., number of experimental units); SD: Standard Deviation; SE: Standard Error; *$p < 0.05$, **$p < 0.01$, ***$p < 0.001$; ns: Not significant. (a): Difference between control and ELF-EMF exposure alone; (b): Difference between Mutagen treatment alone and ELF-EMF + Mutagen treatment.

for SBM, SBR, CA and SCE indicated no significance differences between ELF-EMF-exposure alone and control groups while the data for MN showed a significant increase in the former group as compared with the latter ($p < 0.001$). As expected, treatment with mutagen alone had significantly increased indices for all end-points ($p < 0.001$). A comparison between mutagen alone and ELF-EMF + mutagen treatment indicated significantly increased E–C for SBM, SBR, and SCE and non-significant effect for CA and MN; similar comparison of ES data indicated a significant effect for CA ($p < 0.01$).

Multiple regression analysis

The multiple regression analysis data for E–C and ES, and % contribution of Hz and flux density as well as their interaction on each end-point are presented in Table VIII. The details of the significant effects for the multiple regression analyses are given in Table IX.

The overall % contribution to the variability observed in E–C and ES for all end-points due to Hz groups and flux density groups were of smaller magnitude as compared with that obtained for goodness of fit data given in the last column of Table VIII. Nonetheless, some of them were significant ($p < 0.05$) and are explained in detail by the regression coefficients given in Table IX.

The variability in E–C for SBM, CA, MN and SCE due to Hz groups is not statistically significant ($p > 0.05$) while that for SBR is significant ($p < 0.001$). For all end-points, the variability in E–C due to flux density groups is statistically significant ($p < 0.01$). The interaction between Hz and flux density groups was also significant for all endpoints ($p < 0.01$) except for SCE which was not statistically significant. On the other hand, the variability in ES due to Hz and flux density groups are statistically significant for some endpoints, significant for Hz groups with SBR and CA ($p < 0.05$) and significant for flux density groups with SBM, CA, and MN ($p < 0.01$) . Similarly, the interaction between Hz and flux density groups was significant for only SBM and CA ($p < 0.05$). The detailed explanation for the coefficients which are significant in multiple regression analysis for the Hz and flux density groups and their interaction for E–C and ES values are presented in Table IX (the data in parenthesis describes the change due to Hz or flux density $\pm$ SE as well as their interaction).

Heterogeneity

The data for goodness of fit presented in the last column of Table VIII indicated that for each end-point (except SCE), random error accounted for a maximum variability (heterogeneity) observed in E–C values ($p < 0.01$). For ES values however, random error accounted for a significant amount of variability in SBM and CA ($p < 0.05$). When the goodness of fit showed a significant value ($p < 0.05$), the indication was that factors other than the ELF-EMF exposure characteristics are needed to explain more of the variability. The detailed explanation for these heterogeneity effects are described in Table X.

For SBM, the residuals for 18 out of 84 effects (21.4%) were outside the normal range, and this is due to the fact that 100% of these effects were from the studies that used longer electrophoresis duration. For SBR, the residuals for 95 out of 228 effects (41.7%) were outside the normal range, and 94.3% (90 of 95) of these effects were found to be from the studies that used the 'tail factor' method of assessment of DNA strand breaks. This leaves only five of 228 (2.2%) residuals outside of the normal range for SBR which is below the expected 5%. The effects for MN (1 out of 130, 0.8%) and SCE (0 out of 44, 0.0%) which are outside the normal range were found to be very few and the indices for these end-points were within the mean $\pm$ 2 SD observed in the historical database. Thus, the magnitude of heterogeneity for MN and SCE endpoints were small although they were not totally explained by Hz and/or flux density groups and their interaction alone.

The E–C multiple regression data obtained for CA indicated six of the 36 effects (16.7%) were larger than control mean + 2 SD (outside the expected normal range). These 16.7% effects were mainly due

Table VIII. Multiple regression analysis of the effects of ELF-EMF exposure characteristics on E–C[a] and ES[b] observed for each genotoxicity end-point. The data in the last column (goodness of fit) indicates unexplained variance. The multiple regression coefficients for significant effects ($p < 0.05$) are described in detail in Table IX.

End-point		Number of effects examined	Percentage contribution due to			
			Hz groups	Flux groups	Hz and Flux groups interaction	Regression 'goodness of fit'
SBM	E-C	84	0.11	21.26***	0.54***	78.09***
SBR	E-C	228	1.27***	0.00***	0.65***	98.09***
CA	E-C	36	0.27	8.28**	3.49***	87.96***
MN	E-C	130	0.19	6.66***	0.65**	92.51**
SCE	E-C	44	0.77	23.67***	1.55	74.01
SBM	ES	84	0.15	13.01***	2.25*	84.59*
SBR	ES	227	5.7***	0.23	0.72	93.35
CA	ES	36	3.34*	11.74**	8.91**	76.00**
MN	ES	130	0.29	4.52***	1.16	94.03
SCE	ES	42	13.50	17.99	14.43	54.08

[a]E–C: Magnitude of weighted difference between ELF-EMF-exposed and control groups based on sample size and variance; [b]ES: Effect size; *$p < 0.05$, **$p < 0.01$, ***$p < 0.001$; ns: Not significant.

Table IX. Detailed explanation for the E–C[a] and ES[b] coefficients which are significant in multiple regression analysis data in Table VIII. The data in parenthesis, [ ], describes the change due to Hz or flux (standard error).

Endpoint	Exposure effect on E–C or ES	E–C[a] or ES[b]	Explanation
Main effects			
MN	≤50 Hz	E–C	Effect of ≤50 Hz is larger than the effect of ≥60 Hz [0.91 (0.47), p 0.026].
SBM	≤50 Hz	E–C	Effect of ≤50 Hz is larger than the effect of ≥60 Hz [8.96 (5.48), p 0.050].
SBR	≤50 Hz	E–C	Effect of ≤50 Hz is larger than the effect of ≥60 Hz [2.70 (0.02), $p < 0.001$].
MN	0.0–0.5 mT	E–C	Effect of 0.0–0.05 mT is larger than >0.5–1.0 mT [2.37 (1.04), p 0.012].
SBM	0.0–0.5 mT	E–C	Effect of 0.0–0.05 mT is larger than >0.5–1.0 mT [2.37 (1.04), $p < 0.001$].
SBR	0.0–0.5 mT	E–C	Effect of 0.0–0.05 mT is smaller than >0.5–1.0 mT [2.37 (1.04), $p < 0.001$].
CA	>1.0–5.0 mT	E–C	Effect of >1.0–5.0 mT is larger than >0.5–1.0 mT [0.56 (0.09), $p < 0.001$].
MN	>1.0–5.0 mT	E–C	Effect of >1.0–5.0 mT is larger than >0.5–1.0 mT [4.34 (0.86), $p < 0.001$].
SCE	>1.0–5.0 mT	E–C	Effect of >1.0–5.0 mT is smaller than >0.5–1.0 mT [−0.30 (0.16), p 0.031].
MN	>5.0 mT	E–C	Effect of >5.0 mT larger than is larger than >0.5–1.0 mT [1.56 (0.16), $p < 0.001$].
SCE	>5.0 mT	E–C	Effect of >5.0 mT larger than is larger than >0.5–1.0 mT [1.54 (0.27), $p < 0.001$].
SBR	≤50 Hz	ES	Effect of ≤50 Hz is larger than the effect of ≥60 Hz [0.96 (0.15), $p < 0.001$].
CA	0.0–0.5 mT	ES	Effect of 0.0–0.5 mT is smaller than >0.5–1.0 mT [−0.72 (0.38), p 0.028].
SBM	0.0–0.5 mT	ES	Effect of 0.0–0.5 mT is larger than >0.5–1.0 mT [1.19 (0.19), $p < 0.001$].
CA	>1.0–5.0 mT	ES	Effect of >1.0–5.0 mT is larger than >0.5–1.0 mT [0.97 (0.45), p 0.015].
MN	>1.0–5.0 mT	ES	Effect of >1.0–5.0 mT is larger than >1.0–5.0 mT [1.52 (0.62), p 0.007].
MN	>5.0 mT	ES	Effect of >5.0 mT is larger than >1.0–5.0 mT[0.96 (0.27), $p < 0.001$].
CA	Occupationally exposed individuals	ES	Effect of occupational exposure is smaller than >1.0–5.0 mT [−0.64 (0.30), p 0.017].
MN	Occupationally exposed individuals	ES	Effect of occupational exposure is smaller than >0.5–1.0 mT [−0.58 (0.29), p 0.023].
Interaction of Hz and flux density.			
CA	50 Hz and >5.0 mT	E–C	Effect of >5.0 mT over >0.05–1.0 mT is larger in 50 Hz than in 60 Hz [6.40 (1.91), $p < 0.001$].
SBR	50 Hz and >5.0 mT	E–C	Effect of >5.0 mT over >0.5–1.0 mT is smaller in 50 Hz than in 60 Hz [−2.53 (0.92), p 0.003].
MN	50 Hz and 0.0–0.5 mT	E–C	Effect of 0.0–0.5 mT over >0.5–1.0 mT is smaller in 50 Hz than in 60 Hz [−3.21 (1.05), p 0.001].
SBM	50 Hz and 0.0–0.5 mT	E–C	Effect of 0.0–0.5 mT over >0.5–1.0 mT is smaller in 50 Hz than in 60 Hz [−19.01 (5.48), $p < 0.001$].
SBR	50 Hz and 0.0– 0.5 mT	E–C	Effect of 0.0–0.5 mT over >0.5–1.0 mT is larger in 50 Hz than in 60 Hz [1.60 (0.03), $p < 0.001$].
MN	50 Hz and >1.0–5.0 mT	E–C	Effect of >1.0–5.0 mT over >0.5–1.0 mT is smaller in 50 Hz than in 60 Hz [−1.57 (0.87), p 0.036].
SBR	50 Hz and >1.0–5.0 mT	E–C	Effect of >1.0–5.0 mT over >0.5–1.0 mT is smaller in 50 Hz than in 60 Hz [−1.57 (0.87), $p < 0.001$].
SBR	50 Hz and 0.0–0.5 mT	ES	Effect of 0.0–0.5 mT over >0.5–1.0 mT is smaller in 50 Hz than in 60 Hz [−1.96 ± 0.90, p 0.014].
CA	50 Hz and >1.0–5.0 mT	ES	Effect of >1.0–5.0 mT over >0.5–1.0 mT is smaller in 50 Hz than in 60 Hz [−1.57 ± 0.87, p 0.049].
MN	50 Hz and >1.0–5.0 mT	ES	Effect of >1.0–5.0 mT over >0.5–1.0 mT is smaller in 50 Hz than in 60 Hz [−1.57 ± 0.87, p 0.011].
SBM	50 Hz and >1.0–5.0 mT	ES	Effect of >1.0–5.0 mT over >0.5–1.0 mT is larger in 50 Hz than in 60 Hz [1.42 ± 0.87, p 0.052].

[a]E-C: Magnitude of weighted difference between ELF-EMF-exposed and control groups based on sample size and variance; [b]ES: Effect size; SBM: DNA strand breaks evaluated as comet tail length in microns; SBR: DNA strand breaks evaluated as comet tail moment expressed as ratio; CA: Chromosomal aberrations/100 cells; MN: Micronuclei/1000 cells; SCE: Sister chromatid exchanges/cell.

to two effects which were explained in Table IX: (i) When the cells were exposed to >1.0–5.0 mT flux density (0.56 ± 0.09 in main effects) and (ii) when there was an interaction effect of ≥50 Hz exposure at >5.0 mT (6.4 ± 1.91). Thus, exposure of the cells to >1.0–5.0 mT flux density (2 of 10 or 20% of the effects) and ≥50 Hz at >5.0 mT flux density (1 of 3 or 33% of the effects) resulted in an abnormally high incidence of CA. The remaining three large effects, when averaged in with 10 other effects in the same category resulted in a non-significant and small multiple regression effect for E-C. These three large effects could not be explained by Hz and flux density.

Publication bias

The publication bias was graphically presented in Figure 1. Although there were a total of 87 publications, some investigators have examined one

Table X. Heterogeneity in ELF-EMF exposure characteristics on the effects observed in the end-points investigated.

End-point		Number of E–C effects examined (N)	ELF-EMF publications		
			Sample size Controls	Controls (C)	ELF-exposed (E)
SBM	Mean		545	4.76	2.83
	SD			5.78	10.91
	Upper limit*			11.56	
	E–C Range**	84		−1.2 to 105.0 (18 of 84 = 21.4%)	
				100% (of 21.4%) studies used longer electrophoresis duration	
SBR	Mean		1575	3.80	5.39
	SD			0.82	3.43
	Upper limit*			1.64	
	E–C Range**	228		−5.3 to 12.5 (95 of 228 = 41.7%)	
				−5.3 to 12.5 (4 of 228 = 1.8% below the normal)	
				94.3% (of 41.7%) studies used tail factor method	
CA/100 cells	Mean		262	3.43	4.66
	SD			0.85	1.71
	Upper limit*			1.70	
	E–C Range**	36		−1.5 to 6.7 (6 of 36 = 16.7%)	
	Historical Controls:				
	Mean (SD)			1.5 (3.7)	
	Upper limit*			7.40	
	E–C Range**			−1.5 to 6.7 (0 of 36 = 0.0%)	
MN/1000 cells					
	Mean		828	9.55	10.07
	SD			3.82	4.31
	Upper limit*			7.64	
	E–C Range**	130		−6.0 to 7.9 (1 of 130 = 0.8%)	
	Historical Controls:				
	Mean (SD)			9.00 (8.00)	
	Upper limit*			16.00	
	E–C Range**			−6.0 to 7.9 (0 of 130 = 0.0%)	
SCE/cell					
	Mean		223	7.33	6.15
	SD			1.59	1.49
	Upper limit*			2.18	
	E–C Range**	44		−1.3 to 1.6 (0 of 44 = 0.0%)	
	Historical Controls:				
	Mean (SD)			7.60 (1.60)	
	Upper limit*			3.20	
	E–C Range**			−1.3 to 1.6 (0 of 44 = 0.0%)	

N: Number of E–C values examined in the multiple regression; *Upper limit is 2 × SD above control mean, i.e., 97.5 percentile; **E–C range is the minimum and maximum for all E–C residual values (i.e., deviations from predictions) used in the multiple regression; SBM: DNA strand breaks evaluated as comet tail length in microns; SBR: DNA strand breaks evaluated as comet tail moment expressed as ratio; CA: Chromosomal aberrations/100 cells; MN: Micronuclei/1000 cells. SCE: Sister chromatid exchanges/cell.

or more end-points in several different ELF-EMF exposure conditions. Consequently, the X-axis and Y-axis in Figure 1 has several data points each representing the ES value of one end-point indicating 'near zero' or 'no' effect in one ELF-EMF exposure condition, respectively. The overall data did not appear as 'pyramid' with the mean ES approximately at the center with 'negative' and 'positive' publications (absence and presence of significant differences between ELF-EMF-exposed and controls). In contrast, the data were largely 'skewed' indicating the existence of a significant publication bias ($p < 0.001$). The 'skew' was due to large SE in studies with large ES values despite a small mean E–C difference. Finally, since the meta-analysis strongly suggested the presence of publication bias, the conclusions should be regarded as 'tentative'. For example, there was only one instance in which the cells which were exposed to $\leq$50 Hz at $>$5 mT exhibited the largest increase in CA; these observations must be replicated. The practical reality is that the data from diverse investigations were used for meta-analysis and this needs to be accepted while drawing final conclusions.

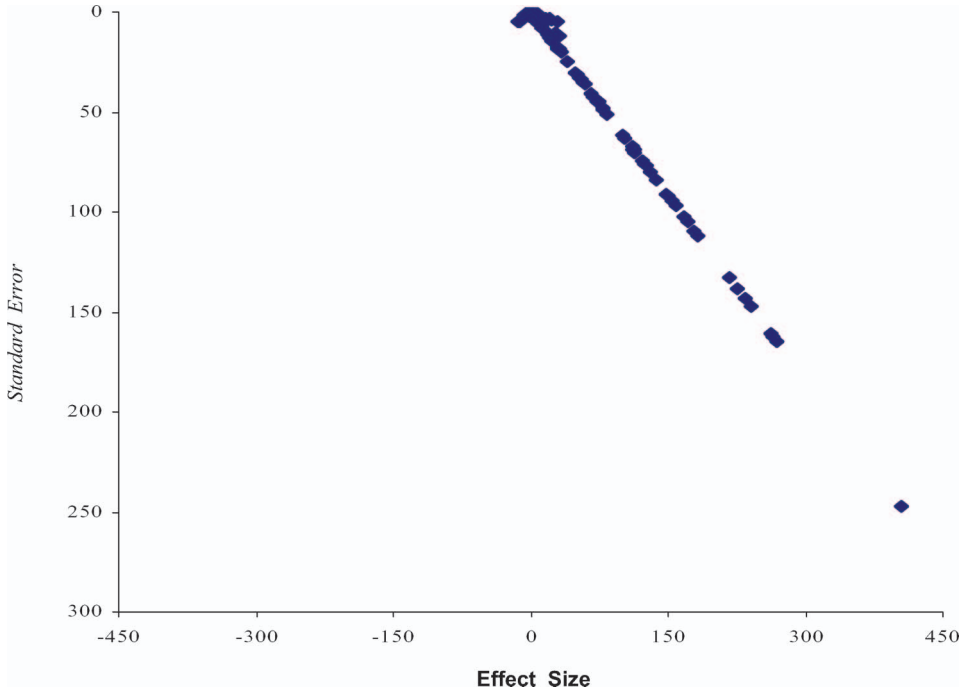

Figure 1. Each data-point in the figure represents one effect from a group of ELF-EMF-exposed and control conditions, in one publication, for one genotoxicity end-point. There were a total of 522 data-points (96 data-points <0 value, 49 data-points with 0 value and 377 data-points >0 value). The effect size and the standard error are represented on X-axis and Y-axis, respectively. The 'skewed' publication bias is due the investigations reporting 'positive' results (significant difference between ELF-EMF-exposed and control groups of cells) with large standard error. Detailed explanation is given in the text.

Comparison of meta-analysis data with those in historical database for CA, MN and SCE

Several hundred reports were the published literature (some were mentioned before) in which the incidence of CA, MN and SCE in normal normal/spontaneous cells were reported and the indices were used as biomarkers to predict the carcinogenic potential of exposure to genotoxic agents present in our environment. The mean incidence (and the range of values) for CA, MN and SCE reported for freshly collected peripheral blood lymphocytes from normal individuals in the historical database with large sample size are as follows: CA – 1.5/100 cells (SD 3.7; $n = 15594$); MN – 9.0/1000 cells (SD 8.0; $n = 8667$); SCE – 7.6/cell (SD 1.6; $n = 4576$). The maximum indices obtained in ELF-EMF-exposed and control groups in the meta-analysis were similar to the above indices in the historical database (with very few exceptions).

Cytogenetic end-points as biomarkers for cancer risk assessment

When the cells are exposed to genotoxic agents, the primary lesions that are induced in the DNA are base damage, single strand breaks, double strand breaks, etc. Cells also have inherent mechanism(s) to repair some or all of these lesions. The un-repaired and/or mis-repaired lesions lead to the formation of CA, MN and SCE (see below). The original technique for the evaluation of DNA strand breaks in single cells included embedding of cells in agarose, lysis and electrophoresis; cells which were exposed to gamma rays displayed a significant increase in the length of DNA migration as compared with those that were not irradiated (Ostling and Johanson 1984). Researchers in various laboratories have made several modifications to the laboratory protocol used for the comet assay (Singh et al. 1988, 1994, Olive et al. 1990, Vijayalaxmi et al. 1992) and reported the data in freshly collected and/or cultured rodent and human cells exposed in vitro and in vivo the ELF-EMF at various frequencies and flux densities. Ivancsits et al. (2002, 2003a, 2003b, 2005) exposed unsynchronized, continuously growing cultured rodent and human cells to 50 Hz ELF-EMF at 0.02–1.0 mT. The exposure period ranged from 1–24 h after which the cells were used in the comet assay. The comets were classified 'visually' into A, B, C, D and E categories which were then subjected to approximate transformation factors (weighted as A $\times$ 2.5, B $\times$ 12.5, C $\times$ 30.0, D $\times$ 67.5 and E $\times$ 97.5) to derive an 'objective' 'tail factor' (Diem et al. 2002). Vijayalaxmi et al. (2006) expressed concern over the presence and contribution of 'confounding' cells (in S-phase of the cell cycle and

apoptosis) to the tail factor. It is imperative for future researchers to include cell cycle analysis to determine the numbers of cells in S-phase as well as enumeration of apoptotic cells when the comet assay is applied to unsynchronized, continuously growing cells. So far, there has been no information on human health hazard risk evaluation using the data reported from DNA strand breaks (using the comet assay), although the assay has been increasingly used in recent years. It is worth mentioning the observations of the comet assay that was conducted in regular genetic toxicology investigations in which cells from eight different organs of mice treated with 208 chemicals (groups 1, 2A, 2B, 3 and 4) selected from the carcinogenicity database of the International Agency for Research on Cancer and from the U. S. National Toxicology Program were examined. The results were compared with those obtained from other genotoxicity end-points used for the assessment of genetic damage, namely, Ames test in bacterial tester strains, CA, MN and unscheduled DNA synthesis. The overall conclusion was that no single test was capable of detecting all relevant genotoxic/carcinogenic agents and the recommendation was to conduct a battery of in vitro and in vivo tests for genotoxicity (Sasaki et al. 2000).

The incidence of CA had been investigated for several decades to monitor whole-body and environmental exposures to genotoxic carcinogens. At the molecular level, the spontaneous and/or induced strand breaks in the DNA that remain un-repaired and/or that undergo aberrant repair lead to the formation of CA. The analysis CA is more refined in recent years so that the cells in their first mitotic metaphase only were examined since unstable aberrations such as dicentric and ring chromosomes are eliminated in successive cell divisions. At least 100 metaphases per sample were recommended for detailed CA evaluations. However, not all researchers in ELF-EMF field appeared to have followed the classification and recommendation. CA, as a biomarker to predict carcinogenic risk in humans, has been systematically examined by several researchers. The data from several studies have indicated that the aberration frequencies were increased even prior to the clinical manifestation of disease. Despite the fact that CA analysis is time-consuming, it is the most reliable biomarker to predict increased cancer risk in humans (Tucker et al. 1997, Hagmar et al. 2004, Bonassi et al. 2005, Norppa et al. 2006).

The existence of MN as a separate entity in a cell, apart from the main nucleus, was known for decades and the indices were widely used to monitor occupational and environmental exposure to genotoxic agents. MN may contain portions of broken chromosomes (clastogenic effect) or whole chromosomes which were not incorporated into daughter cells during cell division due to spindle disruption (aneugenic effect). Preliminary evidence has been presented that an increased incidence of MN predicts enhanced risk of cancer in humans (Bonassi et al. 2007). An important suggestion has been made to use fluorescence in situ hybridization techniques to recognize the presence or absence of centromere in order to explain the clastogenic or aneugenic effect of the test agent, respectively. However, the presence of broken chromosomal fragments with intact centromere which gives the appearance of whole chromosome in MN can not be ruled out.

SCE are cytological manifestation of consequences of errors in DNA replication resulting in interchanges between the two chromatids of the same chromosome at apparently homologous loci, possibly at the replication fork itself (Painter 1980). Although evaluation of SCE is generally considered a more sensitive indicator of exposure to genotoxic agents, their indices did not appear to have a predictive value for human health risk assessment. Nonetheless, SCE would remain a valuable end-point among the short-term assay systems because of the sensitivity and less effort is needed for their analysis, especially when the exposed cells/subjects and their matched controls were sampled simultaneously and scorer bias was eliminated.

The epigenetic investigations are important since in real life, people are exposed to a variety of environmental insults simultaneously and/or sequentially. Theoretically it may well be that ELF-EMF exposure *per se* is not genotoxic, but such exposure could enhance the cytogenetic damage induced by other chemical and/or physical genotoxic agents (i.e., the influence of ELF-EMF exposure could be epigenetic or non-genotoxic). Hence, this important issue was addressed in a total of 33 ELF-EMF investigations.

Considering the above discussion, it is note worthy that the genotoxicity indices for SBM, SBR, CA, MN and SCE obtained in the meta-analysis for ELF-EMF-exposed and control groups were similar to the 'spontaneous' indices reported in the historical database.

Perspectives from meta-analysis and conclusions

Cytogenetic investigations are important since most genotoxic agents are also carcinogens. Besides, the epigenetic effect of some non-genotoxic agents can contribute to the development of cancer by enhancing the damage induced by known genotoxic agents. It is clear from the above discussion that no single genotoxic end-point, by itself, is capable of providing a precise estimate of the genotoxic potential and the consequent cancer risk from

occupational and environmental agents (Sasaki et al. 2000). Perhaps, the evaluation of CA is the best among the end-points available for such purpose. In order to protect the general public and occupationally involved individuals, several national and international organizations have suggested guidelines for limiting exposure to ELF-EMF. For both 50 Hz and 60 Hz, the guidelines for the general public are 5 kV/m and 100 μT for continuous exposure and 10 kV/m and 1000 μT for short-term exposure; the guidelines for occupational exposures are 10 kV/m and 500 μT for continuous exposure and 30 kV/m and 5000 μT for short-term exposures (ICNIRP 1998). Also, the guidelines for residential and occupational exposures to 60 Hz are 10 kV/m and 1330 μT, and the standards for 50 Hz are 12 kV/m and 1600 μT (NRPB 2001). These standards are based on keeping the electric currents induced by power frequency fields to <10 mA/m^2. Above these levels, evidence was presented for a direct stimulation of neuronal and cardiac tissue. When the investigations were conducted under these recommended safety guidelines, the overall genotoxicity indices obtained in the meta-analysis were similar, in ELF-EMF-exposed and controls, to those reported in historical database. It must be pointed out that the meta-analysis focused on only three specific ELF-EMF exposure characteristics, and the multiple regression analysis and goodness of fit did indicate that factors other than the three ELF-EMF exposure characteristics are needed to explain more of the variability reported in the investigations. Since no single genotoxic end-point, by itself, is capable of determining the genotoxic potential and the consequent cancer risk from occupational and environmental agents (Sasaki et al. 2000, Bonassi et al. 2005), it is relevant to include more than one genotoxicity end-point for DNA damage assessment in future ELF-EMF research investigations.

Acknowledgements

The authors wish to thank the Forschungsstelle für Elektropathologie, Munich, Germany, for giving financial support for this meta-analysis. Dr Prihoda also thanks the Department of Pathology for support of this work. We thank Dr C-K Chou, Motorola, Florida, for providing the information on ELF-EMF exposure safety guidelines. We also thank Dr Guenter Obe, Teltow, Berlin, Germany and Dr Ferdinando Bersani, Professor, University of Bologna, Italy, for helpful suggestions and useful comments. We are grateful to Ms Lynda Howell MLS, University of Texas Health Science Center in San Antonio, for preparing the Tables and Figures.

Declaration of interest: The authors report no conflicts of interest. The authors alone are responsible for the content and writing of the paper.

References

Abramsson-Zetterberg L, Grawe J. 2001. Extended exposure of adult and fetal mice to 50 Hz magnetic field does not increase the incidence of micronuclei in erythrocytes. Bioelectromagnetics 22:351–357.

Ahuja, YR, Bhargava, A, Sircar, S, Rizwani, W, Lima, S, Devada, AH, Bhargava, SC. 1997. Comet assay to evaluate DNA damage caused by magnetic fields. In: Proceedings of International Conference on Electromagnetic Interference and Compatibility, Hyderabad, India. pp. 273–276.

Ahuja YR, Vijayashree B, Saran R, Jayashri EL, Manoranjani JK, Bhargava SC. 1999. *In vitro* effects of low-level, low-frequency electromagnetic fields on DNA damage in human leucocytes by comet assay. Indian Journal of Biochemistry and Biophysics 36:318–322.

Antonopoulos A, Yang B, Stamm A, Heller WD, Obe G. 1995. Cytological effects of 50 Hz electromagnetic fields on human lymphocytes *in vitro*. Mutation Research 346:151–157.

Armitage P. 1984. Controversies and achievements in clinical trails. Controlled Clinical Trials 5:67–72.

Bender MA, Preston RJ, Leonard RC, Pyatt BE, Gooch PC, Shelby MD. 1988. Chromosomal aberrations and sister chromatid exchange frequencies in peripheral blood lymphocytes of a large human population sample. Mutation Research 204:421–433.

Bender MA, Preston RJ, Leonard RC, Pyatt BE, Gooch PC. 1989. Chromosomal aberration and sister chromatid exchange frequencies in peripheral blood lymphocytes of a large human population sample. II. Extension of age range. Mutation Research 212:149–154.

Bender MA, Preston RJ, Leonard RC, Pyatt BE, Gooch PC. 1992. On the distribution of spontaneous SCE in human peripheral blood lymphocytes. Mutation Research 281:227–232.

Bolognesi C, Abbondandolo A, Barale R, Casalone R, Dalpra L, De Ferrari M, Degrassi F, Forni A, Lamberti L, Lando C, Migliore L, Padovani P, Pasquini R, Puntoni R, Sbrana I, Stella M, Bonassi S. 1997. Age-related increase of baseline frequencies of sister chromatid exchanges, chromosome aberrations, and micronuclei in human lymphocytes. Cancer Epidemiology Biomarkers and Prevention 6:249–256.

Bonassi S, Bolognesi C, Abbondandolo A, Barale R, Bigatti P, Camurri L, Dalpra L, De Ferrari M, Forni A, Lando C, Padovani P, Pasquini R, Stella M, Puntoni R. 1995. Influence of sex on cytogenetic end points: Evidence from a large human sample and review of the literature. Cancer Epidemiology Biomarkers and Prevention 4:671–679.

Bonassi S, Fenech M, Lando C, Lin Y, Ceppi M, Chang WP, Holland N, Kirsch-Volders M, Zeiger E, Ban S, Barale R, Bigatti MP, Bolognesi C, Jia C, Di Giorgio M, Ferguson LR, Fucic A, Lima OG, Hrelia P, Krishnaja AP, Lee T-K, Migliore L, Mikhalevich L, Mirkova E, Mosesso P, Muller W-U, Odagiri Y, Scarfi MR, Szabova E, Vorobtsova I, Vral A, Zijno A. 2001. Human micronucleus project: International database comparison for results with cytokinesis-block micronucleus assay in human lymphocytes. I. Effect of laboratory protocol, scoring criteria, and host factors on the frequency of micronuclei. Environmental and Molecular Mutagenesis 37:31–45.

Bonassi S, Ugolini D, Kirsch-Volders M, StrØmberg U, Vermeulen R, Tucker JD. 2005. Human population studies with Cytogenetic biomarkers: Review of the literature and future prospective. Environmental and Molecular Mutagenesis 45:258–271.

Bonassi S, Znaor A, Ceppi M, Lando C, Chang WP, Holland N, Kirsch-Volders M, Zeiger E, et al. 2007. An increased micronucleus frequency in peripheral blood lymphocytes predicts the risk of cancer in humans. Carcinogenesis 28:625–631.

Cantoni O, Sestili P, Fiorani M, Dacha M. 1995. The effect of 50 Hz sinusoidal electric and/or magnetic fields on the rate of repair of DNA single/double strand breaks in oxidatively injured cells. Biochemistry and Molecular Biology International 37:681–689.

Cantoni O, Sestili P, Fiorani M, Dacha M. 1996. Effect of 50 Hz sinusoidal electric and/or magnetic fields on the rate of repair of DNA single strand breaks in cultured mammalian cells exposed to three different carcinogens: methylmethane sulphonate, chromate and 254 nm U.V. radiation. Biochemistry and Molecular Biology International 38:527–533.

Cho YH, Chung HW. 2003. The effect of extremely low frequency electromagnetic fields (ELF-EMF) on the frequency of micronuclei and sister chromatid exchange in human lymphocytes induced by benzo(a)pyrene. Toxicology Letters 143:37–44.

Ciccone G, Mirabelli D, Leis A, Gavarotti P, Rege-Cambrin G, Davico L, Vineis P. 1993. Myeloid leukemias and myelodisplastic syndromes: Chemical exposure, histologic subtype and cytogenetics in a case-control study. Cancer Genetics and Cytogenetics 68:135–139.

Cochrane Handbook for Systematic Reviews of Interventions 4.2.6 – updated September 2006. Higgins JPT, Green S, editors. Section 8.7. The Cochrane Library. Issue 4. Chichester, UK: John Wiley & Sons, Ltd. pp 136–140.

d'Ambrosio G, Lioi MB, Massa R, Scarfi MR, Zeni O. 1995. Genotoxic effects of amplitude-modulated microwaves on human lymphocytes exposed in vitro under controlled conditions. Electro- and Magnetobiology 14:157–164.

Dickersin K. 1990. The existence of publication bias and risk factors for its occurrence. The Journal of the American Medical Association 263:1385–1989.

Diem E, Ivancsits S, Rüdiger HW. 2002. Basal levels of DNA strand breaks in human leukocytes determined by comet assay. Journal of Toxicology and Environmental Health, Part A 65:641–648.

Ding GR, Nakahara T, Miyakoshi J. 2003. Induction of kinetochore-positive and kinetochore-negative micronuclei in CHO cells by ELF magnetic fields and/or X-rays. Mutagenesis 18:439–443.

Erdal N, Gurgul S, Celik A. 2007. Cytogenetic effects of extremely low frequency magnetic field on Wistar rat bone marrow. Mutation Research 630:69–77.

Fairbairn DW, O'Neill KL. 1994. The effect of electromagnetic field exposure on the formation of DNA single strand breaks in human cells. Cellular and Molecular Biology 40:561–567.

Fenech M, Morley AA. 1985. The effect of donor age on spontaneous and induced micronuclei. Mutation Research 148:99–105.

Fenech M, Bonassi S, Turner J, Lando C, Ceppi M, Chang WP, Holland N, Kirsch-Volders M, Zeiger E, Bigatti MP, Bolognesi C, Cao J, de Luca G, Di Giorgio M, Ferguson LR, Fucic A, Lima OG, Hadjidekova VV, Hrelia P, Jaworska A, Joksic G, Krishnaja AP, Lee T-K, Martelli A, McKay MJ, Migliore L, Mirkova E, Muller W-U, Odagiri Y, Orsiere T, Scarfi MR, Silva MJ, Sofuni A, Suralles J, Trenta G, Vorobtsova I, Vral A, Zijno A. 2003. Intra- and inter-laboratory variation in the scoring of micronuclei and necleoplasmic bridges in binucleate human lymphocytes. Results of an international slide-scoring exercise by the HUMN project. Mutation Research 534:45–64.

Fiorani M, Cantoni O, Sestili P, Conti R, Nicolini P, Vetrano F, Dacha M. 1992. Electric and/or magnetic field effects on DNA structure and function in cultured human cells. Mutation Research 282:25–29.

Fleiss JL, Levin B, Paik MC. 2003. Statistical Methods for Rates and Proportions. 3rd ed, New York: Wiley and Sons Inc. pp 440–442.

Frazier ME, Reese JA, Morris JE, Jostes RF, Miller DL. 1990. Exposure of mammalian cells to 60-Hz magnetic or electric fields: Analysis of DNA repair of induced, single-strand breaks. Bioelectromagnetics 11:229–234.

Galt S, Wahlstrom J, Hamnerius D, Holmqvist D, Johannesson T. 1995. Study of effects of 50 Hz magnetic fields on chromosome aberrations and the growth-related enzyme ODC in human amniotic cells. Bioelectochemistry and Bioenergetics 36:1–8.

Garcia-Sagredo JM, Parada LA, Monteagudo JL. 1990. Effect on SCE in human chromosomes in vitro of low-level pulsed magnetic field. Environmental and Molecular Mutagenesis 16:185–188.

Garcia-Sagredo JM, Monteagudo JL. 1991. Effect of low-level pulsed electromagnetic fields on human chromosomes in vitro: Analysis of chromosomal aberrations. Hereditas 115:9–111.

Hagmar L, Stromberg U, Bonassi S, Hansteen I-L, Knudsen LE, Lindholm C, Norppa H. 2004. Impact of types of lymphocyte chromosomal aberrations on human cancer risk: Results from Nordic and Italian cohorts. Cancer Research 64:2258–2263.

Hedges, LV, Olkin, I. 1985. Statistical Methods for Meta-Analysis, New York: Academic Press. Chapter 8.

Heredia-Rojas JA, Rodriguex-De La Fuente AO, Velazco-Campos RM, Leal-Garza CH, Rodriguez-Flores LE, Fuente-Cortez B. 2001. Cytological effects of 60 Hz magnetic fields on human lymphocytes in vitro: Sister-chromatid exchanges, cell kinetics and mitotic rate. Bioelectromagnetics 22:145–149.

Hintenlang D. 1993. Synergistic effects of ionizing radiation and 60 Hz magnetic fields. Bioelectromagnetics 14:545–551.

Hone P, Edwards A, Halls J, Cox R, Lloyd D. 2003. Possible associations between ELF electromagnetic fields, DNA damage response processes and childhood leukemia. British Journal of Cancer 88:1939–1941.

Hunter JE, Schmidt FL. 2004. Methods of meta-analysis: Correcting error and bias in research findings. 2nd ed, London: SAGE Publications. pp 67 and 285–286.

ICNIRP (International Commission on Non-Ionizing Radiation Protection). 1998. Guidelines for limiting exposure to time-varying electric, magnetic, and electromagnetic fields (up to 300 GHz). Health Physics 74:494–522.

Ivancsits S, Diem E, Pilger A, Rudiger HW, Jahn O. 2002. Induction of DNA strand breaks by intermittent exposure to extremely-low-frequency electromagnetic fields in human diploid fibroblasts. Mutation Research 519:1–13.

Ivancsits S, Diem E, Jahn O, Rudiger HW. 2003a. Intermittent extremely low frequency electromagnetic fields cause DNA damage in a dose-dependent way. International Archives of Occupational and Environmental Health 76:431–436.

Ivancsits S, Diem E, Jahn O, Rudiger HW. 2003b. Age-related effects on induction of DNA strand breaks by intermittent exposure to electromagnetic fields. Mechanisms of Ageing and Development 124:847–850.

Ivancsits S, Pilger A, Diem E, Jahn O, Rudiger HW. 2005. Cell type-specific genotoxic effects of intermittent extremely low-frequency electromagnetic fields. Mutation Research 583:184–188.

Jacobson-Kram D, Tepper J, Kuo P, San RH, Curry PT, Wagner VO, Putman DL. 1997. Evaluation of potential genotoxicity of pulsed electric and electromagnetic fields used for bone growth stimulation. Mutation Research 388:45–57.

Jajte J, Zmylony M, Palus J, Dziubaltowska E, Rajkowska E. 2001. Protective effect of melatonin against in vitro iron ions and 7 mT 50 Hz magnetic field-induced DNA damage in rat lymphocytes. Mutation Research 483:57–64.

Khalil AM, Quasem W, Amoura F. 1991. Cytogenetic effects of pulsating electromagnetic field on human lymphocytes in vitro: Chromosome aberrations, sister-chromatid exchange and cell kinetics. Mutation Research 247:141–146.

Khalil AM, Quasem W, Amoura F. 1993. Cytogenetic changes in human lymphocytes from workers occupationally exposed to high-voltage electromagnetic fields. Electro- and Magnetobiology 12:17–26.

Kindzelskii AL, Petty HR. 2000. Extremely low frequency pulsed DC electric fields promote neutrophil extension, metabolic resonance and DNA damage when phase-matched with metabolic oscillators. Biochimica et Biophysica Acta 1495:90–111.

Lagroye I, Poncy JL. 1997. The effect of 50 Hz electromagnetic fields on the formation of micronuclei in rodent cell lines exposed to gamma radiation. International Journal of Radiation Biology 72:249–254.

Lai H, Singh NP. 1997a. Acute exposure to a 60 Hz magnetic field increases DNA strand breaks in rat brain cells. Bioelectromagnetics 18:156–165.

Lai H, Singh NP. 1997b. Melatonin and N-tert-butyl-a-phenylnitrone block 60-Hz magnetic field-induced DNA single and double strand breaks in rat brain cells. Journal of Pineal Research 22:152–162.

Lai H, Singh NP. 2004. Magnetic-field-induced DNA strand breaks in brain cells of the rat. Environmental Health Perspectives 112:687–694.

Lang TA, Secic M. 2006. Synthesizing the results of related studies: Reporting systematic reviews and meta-analyses. In: How to report statistics in medicine: Annotated guidelines for authors, editors, and reviewers. 2nd ed, Philadelphia: American College of Physicians. Chapter 17, pp 255–279.

Lipsey MW, Wilson DB. 2001. Practical meta-analysis, London: SAGE Publications. Chapter 7 and pp 72.

Livingston GK, Witt KL, Gandhi OP, Chatterjee I, Roti Roti JL. 1991. Reproductive integrity of mammalian cells exposed to power frequency electromagnetic fields. Environmental and Molecular Mutagenesis 17:49–58.

Lloyd DC, Purrott RJ, Reeder EJ. 1980. The incidence of unstable chromosome aberrations in peripheral blood lymphocytes from unirradiated and occupationally exposed people. Mutation Research 72:523–532.

Lloyd D, Hone P, Edwards A, Cox R, Halls J. 2004. The repair of gamma-ray-induced chromosomal damage in human lymphocytes after exposure to extremely low frequency electromagnetic fields. Cytogenetics and Genome Research 104:188–192.

Luceri C, De Filippo C, Giovannelli L, Blangiardo M, Cavalieri D, Aglietti F, Pampaloni M, Andreuccetti D, Pieri L, Bambi F, Biggeri A, Dolara P. 2005. Extremely low-frequency electromagnetic fields do not affect DNA damage and gene expression profiles of yeast and human lymphocytes. Radiation Research 164:277–285.

Maes A, Collier M, Vandoninck S, Scarpa P, Verschaeve L. 2000. Cytogenetic effects of 50 Hz magnetic fields of different magnetic flux densities. Bioelectromagnetics 21:589–596.

McCann J, Dietrich F, Rafferty C, Martin AO. 1993. A critical review of the genotoxic potential of electric and magnetic fields. Mutation Research 297:61–95.

McCann J, Dietrich F, Rafferty C. 1998. The genotoxic potential of electric and magnetic fields: An update. Mutation Research 411:45–86.

McNamee JP, Bellier PV, McLean JR, Marro L, Gajda GB, Thansandote A. 2002. DNA damage and apoptosis in the immature mouse cerebellum after acute exposure to a 1 mT, 60 Hz magnetic field. Mutation Research 513:121–133.

McNamee JP, Bellier PV, Chauhan V, Gajda GB, Lemay E, Thansandote A. 2005. Evaluating DNA damage in rodent brain after acute 60 Hz magnetic-field exposure. Radiation Research 164:791–797.

Miyakoshi J, Yoshida M, Shibuya K, Hiraoka M. 2000. Exposure to strong magnetic fields at power frequency potentiates X-ray-induced DNA strand breaks. Journal of Radiation Research 41:293–302.

Miyakoshi J, Horiuchi E, Nakahara T, Sakurai T. 2007. Magnetic fileds generated by an induction heating (IH) cook top do not cause genotoxicity in vitro. Bioelectromagnetics 28:529–537.

Moratti M, Villarini M, Simonucci S, Fatigoni C, Scassellati-Sforzolini G, Monarca S, Pasquini R, Angelucci M, Strappini M. 2005. Effects of co-exposure to extremely low frequency (ELF) magnetic fields and benzene or benzene metabolites determined in vitro by the alkaline comet assay. Toxicology Letters 157:119–128.

Moulder JE. 1998. Power frequency fields and cancer. Critical Reviews in Biomedical Engineering 26:1–116.

Murphy JC, Kaden DA, Warren J, Sivak A. 1993. Power frequency electric and magnetic fields: A review of genetic toxicology. Mutation Research 296:221–240.

Nakahara T, Yaguchi H, Yoshida M, Miyakoshi J. 2002. Effects of exposure of CHO-K1 cells to a 10-T static magnetic field. Radiology 224:817–822.

Neri M, Ceppi M, Knudsen LE, Merlo DF, Barale R, Puntoni R, Bonassi S. 2005. Baseline micronuclei frequency in children: Estimates from meta- and pooled analyses. Environmental Health Perspectives 113:1226–1229.

Nordenson I, Mild KH, Andersson G, Sandstrom M. 1994. Chromosomal aberrations in human amniotic cells after intermittent exposure to fifty hertz magnetic fields. Bioelectromagnetics 15:293–301.

Nordenson I, Mild KH, Jarventaus H, Hirvonen A, Sandstrom M, Wilen J, Blix N, Norppa H. 2001. Chromosomal aberrations in peripheral lymphocytes of train engine drivers. Bioelectromagnetics 22:306–315.

Norppa H, Bonassi S, Hansteen I-L, Hagmar L, StrØmberg U, RÖssner P, Boffetta P, Lindholm C, Gundy S, Lazutka J, Cebulsks-Wasilewsks A, Fabiánová E, Srám RJ, Knudsen LE, Barale R, Fucic A. 2006. Chromosomal aberrations and SCEs as biomarkers of cancer risk. Mutation Research 600:37–45.

NRC (National Research Council). 1992. Combining information: Statistical issues and opportunities for research, Washington, DC: National Academy of Science Press; 1992.

NRPB (National Radiological Protection Board). 2001. Electromagnetic Fields and the Risk of Cancer. Report of an advisory group on non-ionizing radiation, Vol. 12, No. 1. Chilton, UK: National Radiological Protection Board.

Obe G. 1986. Spontaneous levels of somatic chromosome aberrations in man. In: Sorsa M, Norppa H, editors. Monitoring of occupational genotoxicants, New York: Alan R. Liss; 1986.

Okonogi H, Nakagawa M, Tsuji Y. 1996. The effects of a 4.7 Tesla static magnetic field on the frequency of micronucleated cells induced by mitomycin C. Tohoku Journal of Experimental Medicine 180:209–215.

Olive PL, Banath JP, Durand RE. 1990. Heterogeneity in radiation-induced DNA damage and repair in tumor and normal cells measured using a ''comet'' assay. Radiation Research 122:86–94.

Ostling O, Johanson KJ. 1984. Microelectrophoretic study of radiation-induced DNA damage in individual mammalian cells. Biochemical and Biophysical Research Communications 123:291–298.

Othman O-El-M, Aly M-S, Nahas S-M-El. 2001. Aneuploidy in workers occupationally exposed to electromagnetic field detected by FISH. Cytologia 66:117–125.

Pacini S, Vannelli GB, Barni T, Ruggiero M, Sardi I, Pacini P, Gulisano M. 1999. Effect of 0.2 T static magnetic fields on human neurons: remodeling and inhibition of signal transduction without genome instability. Neuroscience Letters 267: 185–188.

Paile W, Jokela K, Koivistonen A, Saloma S. 1995. Effects of sinusoidal magnetic fields and spark charges on human lymphocytes in vitro. Bioelectochemistry and Bioenergetics 36:15–22.

Painter RB. 1980. A replication model for sister-chromatid exchange. Mutation Research 70:337–341.

Pasquini R, Villarini M, Scassellati-Sforzolini G, Fatigoni C, Moretti M. 2003. Micronucleus induction in cells co-exposed in vitro to 50 Hz magnetic field and benzene, 1,4-benzenediol (hydroquinone) or 1,2,4-bensenetriol. Toxicology In Vitro 17:581–586.

Robison JG, Pendleton AR, Monson KO, Murray BK, O'Neill KL. 2002. Decreased DNA repair rates and protection from heat induced apoptosis mediated by electromagnetic field exposure. Bioelectromagnetics 23:106–112.

Rossner P, Boffetta P, Ceppi M, Bonassi S, Smerhovsky Z, Landa K, Juzova D, Sram RJ. 2005. Chromosomal aberrations in lymphocytes of healthy subjects and risk of cancer. Environmental Health Perspectives 113:517–520.

Rudd NL, Hoar DI, Greentree CL, Dimnik LS, Henning UGG. 1988. Micronucleus assay in human fibroblasts: A measure of spontaneous chromosomal instability and mutagen hypersensitivity. Environmental and Molecular Mutagenesis 12:3–13.

SAS (Statistical Analysis System). 2006. Version 9.1 for Windows, SAS Institute, Cary, North Carolina.

Sasaki YF, Sekihashi K, Izumiyama F, Nishidate E, Saga A, Ishida K, Tsuda S. 2000. The comet assay with multiple mouse organs: Comparison of comet assay results and carcinogenicity with 208 chemicals selected from the IRRC monographs and US. NTP carcinogenicity data base. Critical Reviews in Toxicology 30:629–799.

Scarfi MR, Bersani F, Cossarizza A, Monti D, Castellani G, Cadossi R, Franceschetti G, Franceschi C. 1991. Spontaneous and mitomycin-C-induced micronuclei in human lymphocytes exposed to extremely low frequency pulsed magnetic fields. Biochemical and Biophysical Research Communications 176:194–200.

Scarfi MR, Bersani F, Cossarizza A, Monti D, Zeni O, Lioi MB, Franceschetti G, Capri M, Franceschi C. 1993. 50 Hz AC sinusoidal electric fields do not exert genotoxic effects (micronucleus formation) in human lymphocytes. Radiation Research 135:64–68.

Scarfi MR, Lioi MB, Zeni O, Franceschetti C, Franceschi F, Bersani F. 1994. Lack of chromosomal aberration and micronucleus induction in human lymphocytes exposed to pulsed magnetic fields. Mutation Research 306:129–133.

Scarfi MR, Lioi MB, Noci MD, Zeni O, Franceschi C, Monti D, Castellani G, Bersani F. 1997a. Exposure to 100 Hz pulsed magnetic fields increases micronucleus frequency and cell proliferation in human lymphocytes. Bioelectrochemistry and Bioenergetics 43:77–81.

Scarfi MR, Prisco F, Lioi MB, Noci MD, Zeni O, Franceschi C, Monti D, Castellani G, Bersani F. 1997b. Extremely low frequency pulsed magnetic field cytogenetic effects on lymphocytes from Turner's syndrome subjects. Bioelectrochemistry and Bioenergetics 43:221–226.

Scarfi MR, Prisco F, Lioi MB, Zeno O, Della Noce M, Di Pietro R, Franceschi C, Bersani F. 1997c. 50-Hz, 1-mT sinusoidal magnetic fields do not affect micronucleus frequency and cell proliferation from normal and Turner's syndrome subjects. Electro- and Magnetobiology 16:301–307.

Scarfi MR, Lioi MB, Zeni O, Della Noce M, Franceschi C, Bersani F. 1999. Micronucleus frequency and cell proliferation in human lymphocytes exposed to 50 Hz sinusoidal magnetic fields. Health Physics 76:244–250.

Scarfi MR, Sannino A, Perrotta A, Sarti M, Mesirca P, Bersani F. 2005. Evaluation of genotoxic effects in human fibroblasts after intermittent exposure to 50 Hz electromagnetic fields: A confirmatory study. Radiation Research 164:270–276.

Simko M, Kriehuber R, Weiss DG, Luben RA. 1998a. Effects of 50 Hz EMF exposure on micronucleus formation and apoptosis in transformed and nontransformed human cell lines. Bioelectromagnetics 19:85–91.

Simko M, Kriehuber R, Lange S. 1998b. Micronucleus formation in human amnion cells after exposure to 50 Hz MF applied horizontally and vertically. Mutation Research 418:101–111.

Simko M, Dopp E, Krichuber R. 1999. Absence of synergistic effects on micronucleus formation after exposure to electromagnetic fields and asbestos fibers *in vitro*. Toxicol Letters 108:47–45.

Simko M, Richard D, Kriehuber R, Weiss DG. 2001. Micronucleus induction in Syrian hamster embryo cells following exposure to 50 Hz magnetic fields, benzo(a)pyrene, and TPA *in vitro*. Mutation Research 495:43–50.

Singh NP, Lai H. 1998. 60 Hz magnetic field exposure induces DNA crosslinks in rat brain cells. Mutation Research 400:313–320.

Singh NP, McCoy MT, Tice RR, Schneider EL. 1988. A simple technique for quantitation of low levels of DNA damage in individual cells. Experimental Cell Research 175:184–191.

Singh NP, Stephens RE, and Schneider EL. 1994. Modifications of alkaline microgel electrophoresis for sensitive detection of DNA damage. International Journal of Radiation Biology 66:223–228.

Singh S, Khanduja KL, Mittal PK. 1997. Mutagenic potential of benzo(a)pyrene and N-nitrosodiethyamine is not affected by 50-Hz sinusoidal electromagnetic field. Electro- and Magnetobiology 16:169–175.

Skyberg K, Hansteen IL, Vistnes AI. 1993. Chromosome aberrations in lymphocytes of high-voltage laboratory cable splicers exposed to electromagnetic fields. Scandinavian Journal of Work, Environment and Health 19:29–34.

Skyberg K, Hansteen IL, Vistnes AI. 2001. Chromosomal aberrations in lymphocytes of employees in transformer and generator production exposed to electromagnetic fields and mineral oil. Bioelectromagnetics 22:150–160.

Stephan G, Pressl S. 1999. Chromosomal aberrations in peripheral lymphocytes from healthy subjects as detected in first cell division. Mutation Research 446:231–237.

Sterne JAC, Egger M. 2001. Funnel plot for detecting bias in meta-analysis: Guidelines on choice of axis. Journal of Clinical Epidemiology 54:1046–1055.

Stronati L, Testa A, Villani P, Marino C, Lovisolo GA, Conti D, Russo F, Fresegna AM, Cordelli E. 2004. Absence of genotoxicity in human blood cells exposed to 50 Hz magnetic fields as assessed by comet assay, chromosome aberration, micronucleus, and sister chromatid exchange analyses. Bioelectromagnetics 25:41–48.

Svedenstal BM, Johanson KJ. 1998. Leukocytes and micronucelated erythrocytes in peripheral blood from mice exposed to 50-Hz or 20-kHz magnetic fields. Electro- and Magnetobiology 17:127–143.

Svedenstal BM, Johanson KJ, Mattsson MO. Paulsson LE. 1999a. DNA damage, cell kinetics and ODC activities studied in CBA mice exposed to electromagnetic fields generated by transmission lines. In Vivo 13:507–513.

Svedenstal BM, Johanson KJ. Mild KH. 1999b. DNA damage induced in brain cells of CBA mice exposed to magnetic fields. In Vivo 13:551–552.

Testa A, Cordelli E, Stronati L, Marino C, Lovisolo GA, Fresegna AM, Conti D, Villani P. 2004. Evaluation of genotoxic effect of low level 50 Hz magnetic fields on human blood cells using different cytogenetic assays. Bioelectromagnetics 25: 613–619.

Tofani S, Ferrara A, Anglesio L, Gilli G. 1995. Evidence for genotoxic effects of resonant ELF magnetic fields. Bioelectochemistry and Bioenergetics 36:9–13.

Tucker JD, Eastmond D, Littlefield LG. 1997. Cytogenetic endpoints as biological dosimeters and predictors of risk in epidemiological studies, Lyon: International Agency for Research on Cancer (IARC). pp 185–200.

Udroiu I, Cristaldi M, Ieradi LA, Bedini A, Giuliani L, Tanzarella C. 2006. Clastogenicity and aneuploidy in newborn and adult mice exposed to 50 Hz magnetic fields. International Journal of Radiation Biology 82:561–567.

Valjus J, Norppa H, Jarventaus H, Sorsa M, Nykyri E, Salomaa S, Jarvinen P, Kajander J. 1993. Analysis of chromosomal aberrations, sister chromatid exchanges and micronuclei among power linesmen with long-term exposure to 50-Hz electromagnetic fields. Radiation Environment and Biophysics 32:325–336.

Verheyen GR, Pauwels G, Verschaeve L, Schoeters G. 2003. Effect of coexposure to 50 Hz magnetic fields and an aneugen on human lymphocytes, determined by the cytokinesis block micronucleus assay. Bioelectromagnetics 24:160–164.

Vijayalaxmi, Evans HJ. 1982. *In vivo* and in vitro effects of cigarette smoke on chromosomal damage and sister-chromatid exchange in human peripheral blood lymphocytes. Mutation Research 92:321–332.

Vijayalaxmi, Tice RR, Strauss GHS. 1992. Assessment of radiation-induced DNA damage in human blood lymphocytes using single-cell gel electrophoresis technique. Mutation Research 271:243–252.

Vijayalaxmi, Obe G. 2005. Controversial cytogenetic observations in mammalian somatic cells exposed to extremely low frequency electromagnetic radiation: A review and future research recommendations. Bioelectromagnetics 26:412–430.

Vijayalaxmi, McNamee JP, Scarfi MR. 2006. Comments on DNA strand breaks reported by Diem et al. in Mutation Research 2005;583:178–183, and Ivancsits et al. in Mutation Research 2005;583:184–188. Mutation Research 603:104–106.

Vijayalaxmi, Prihoda TJ. 2008. Genetic damage in mammalian somatic cells exposed to radiofrequency radiation: A meta-analysis of data from 63 publications (1990–2005). Radiation Research 169:561–574.

Villarini M, Moretti M, Scassellati-Sforzolini G, Boccioli B, Pasquini R. 2006. Effects of co-exposure to extremely low frequency (50 Hz) magnetic fields and xenobiotics determined in vitro by the alkaline comet assay. Science of the Total Environment 361:208–219.

Wahab MA, Podd JV, Rapley BI, Rowland RE. 2007. Elevated sister chromatid exchange frequencies in dividing human peripheral blood lymphocytes exposed to 50 Hz magnetic fields. Bioelectromagnetics 28:281–288.

Winker R, Ivancsits S, Pilger A, Adlkofer F, Rudiger HW. 2005. Chromosomal damage in human diploid fibroblasts by intermittent exposure to extremely low-frequency electromagnetic fields. Mutation Research 585:43–49.

Wolf FI, Torsello A, Tedesco B, Fasanella S, Boninsegna A, D'Ascenzo M, Grassi C. Azzena GB, Cittadini A. 2005. 50-Hz extremely low frequency electromagnetic fields enhance cell proliferation and DNA damage: Possible involvement of a redox mechanism. Biochimica et Biophysica Acta 1743:120–129.

Yaguchi H, Yoshida M, Ejima Y, Miyakoshi J. 1999. Effect of high-density extremely low frequency magnetic field on sister chromatid exchanges in mouse m5S cells. Mutation Research 440:189–194.

Yaguchi H, Yoshisa M, Ding GR, Shingu K, Miyakoshi J. 2000. Increased chromatid type aberrations in mouse m5S cells exposed to power-line frequency magnetic fields. International Journal of Radiation Biology 76:1677–1684.

Yokus B, Cakir DU, Akdag MZ, Sert C, Mete N. 2005. Oxidative DNA damage in rats exposed to extremely low frequency electro magnetic fields. Free Radical Research 39:317–323.

Zeni O, Bersani F, Scarfi MR. 2002. Radiological workers sensitivity to 50 Hz pulsed magnetic fields: preliminary results. Radiation and Environmental Biophysics 41:275–279.

Zmyslony M, Jajte J, Dziubaltowska E, Rajkowska E. 2000. DNA damage in rat lymphocytes treated in vitro with iron cations and exposed to 7 mT magnetic fields (static or 50 Hz). Mutation Research 453:89–96.

Zmyslony M, Palus J, Dziubaltowska E, Politanski P, Mamrot P, Rajkowska E, Kamedula M. 2004. Effects of in vitro exposure of power frequency magnetic fields on UV-induced DNA damage of rat lymphocytes. Bioelectromagnetics 25:560–562.

Zwingelberg R, Obe G, Rosenthal M, Mevissen M, Buntenkötter S, Löscher W. 1993. Exposure of rats to a 50-Hz, 30-mT magnetic field influences neither the frequencies of sister-chromatid exchanges nor proliferation characteristics of cultured peripheral lymphocytes. Mutation Research 302:39–44.

RADIATION RESEARCH **171**, 735–742 (2009)
0033-7587/09 $15.00

Induction of Adaptive Response in Human Blood Lymphocytes Exposed to Radiofrequency Radiation

Anna Sannino,[a] Maurizio Sarti,[a] Siddharth B. Reddy,[a] Thomas J. Prihoda,[b] Vijayalaxmi[c] and Maria Rosaria Scarfì[a,1]

[a] *CNR-Institute for Electromagnetic Sensing of Environment, Napoli, Italy;* [b] *Department of Pathology, University of Texas Health Science Center, San Antonio, Texas 78229; and* [c] *Department of Radiation Oncology, University of Texas Health Science Center, San Antonio, Texas 78229*

Sannino, A., Sarti, M., Reddy, S. B., Prihoda, T. J., Vijayalaxmi and Scarfì, M. R. Induction of Adaptive Response in Human Blood Lymphocytes Exposed to Radiofrequency Radiation. *Radiat. Res.* 171, 735–742 (2009).

The incidence of micronuclei was evaluated to assess the induction of an adaptive response to non-ionizing radiofrequency (RF) radiation in peripheral blood lymphocytes collected from five different human volunteers. After stimulation with phytohemagglutinin for 24 h, the cells were exposed to an adaptive dose of 900 MHz RF radiation used for mobile communications (at a peak specific absorption rate of 10 W/kg) for 20 h and then challenged with a single genotoxic dose of mitomycin C (100 ng/ml) at 48 h. Lymphocytes were collected at 72 h to examine the frequency of micronuclei in cytokinesis-blocked binucleated cells. Cells collected from four donors exhibited the induction of adaptive response (i.e., responders). Lymphocytes that were pre-exposed to 900 MHz RF radiation had a significantly decreased incidence of micronuclei induced by the challenge dose of mitomycin C compared to those that were not pre-exposed to 900 MHz RF radiation. These preliminary results suggested that the adaptive response can be induced in cells exposed to non-ionizing radiation. A similar phenomenon has been reported in cells as well as in animals exposed to ionizing radiation in several earlier studies. However, induction of adaptive response was not observed in the remaining donor (i.e., non-responder). The incidence of micronuclei induced by the challenge dose of mitomycin C was not significantly different between the cells that were pre-exposed and unexposed to 900 MHz RF radiation. Thus the overall data indicated the existence of heterogeneity in the induction of an adaptive response between individuals exposed to RF radiation and showed that the less time-consuming micronucleus assay can be used to determine whether an individual is a responder or non-responder. © 2009 by Radiation Research Society

INTRODUCTION

The phenomenon of adaptive response, analogous to that found in *Escherichia coli* (*1*), has been well documented *in vitro* and *in vivo* in human and rodent cells. Freshly collected and/or cultured human and animal cells that were exposed to an extremely small adaptation dose of a genotoxic agent were found to be less susceptible to the induction of genetic damage when given a higher challenge dose of the same or similar genotoxic agent. The induction of an adaptive response was shown to be influenced by several factors, including the dose used for adaptation, the dose rate (in the case of ionizing radiation), the time between the adaptation and challenge doses, and the stage of the cell cycle at which the adaptation dose is delivered. The induction of an adaptive response in these investigations was assessed using several genotoxicity assays: DSBs, chromosomal aberrations, micronuclei, sister chromatid exchange (SCE) and mutations (*2–18*). Several hypotheses have been proposed for the induction of an adaptive response, including efficient repair of damaged DNA and a possible role for the enzymes involved in the repair processes of damaged DNA and protein synthesis (*19–23*). Studies have also provided evidence that the peripheral blood lymphocytes of some individuals in the population exhibited an adaptive response (responders) while others did not (non-responders) (*24–32*). The latter observations suggested that the induction of adaptive response did not depend on transient physiological parameters but rather on some stable genetic constitutional traits.

Non-ionizing radiofrequency (RF) radiation in the frequency range of 300 MHz to 300 GHz has a significant and positive impact in modern society. A multitude of devices that emit RF radiation are used in medicine, in industry for heating, welding and sealing of plastics and metals, and for a variety of military purposes. A large increase in the number of people exposed to RF radiation occurred with the introduction of wireless communication services (handheld mobile phones as well as the newer personal communication devices that deliver voice, data and images). Consequently, public attention has been drawn to the potential for adverse human health effects from exposure to RF radiation. Since the damage to the DNA in somatic cells can lead to the development of cancer or to cell death while changes in the DNA of germ cells can lead to

[1] Address for correspondence: CNR-Institute for Electromagnetic Sensing of Environment, Via Diocleziano, 328 - 80124 Naples, Italy: e-mail: scarfi.mr@irea.cnr.it.

mutations that can be transmitted to subsequent generations, several researchers have investigated the extent of genetic damage (assessed from DSBs, chromosome aberrations, micronuclei, SCE, mutations) after *in vitro* and *in vivo* exposure of prokaryotic and eukaryotic cells to RF radiation. Vijayalaxmi and Prihoda (*33*) conducted a meta-analysis of genotoxicity data reported in 63 peer-reviewed scientific publications during 1990–2005. The overall data indicated the following: (1) The difference between RF-radiation-exposed and sham-/unexposed control cells was small; (2) in certain RF-radiation exposure conditions, there was a significant increase in some end points but not in all; (3) the mean indices for chromosome aberrations and micronuclei in RF-radiation-exposed and sham-/unexposed controls were within the spontaneous levels reported in the historical database.

The phenomenon of the adaptive response was investigated extensively using extremely small doses of ionizing radiation where the dose itself did not induce significantly increased genetic damage. The aim of this study was to investigate whether non-ionizing RF radiation exposure, given as an adaptation dose, renders the cells refractory to the genetic damage induced by a subsequent challenge dose with a known genotoxic agent, mitomycin C. So far, there has been no such information in the RF-radiation literature, and the preliminary data are reported here. The induction of an adaptive response in this preliminary investigation was assessed in peripheral blood lymphocytes collected from healthy human volunteers using the cytokinesis-block micronucleus (MN) technique (*34*) mainly because the assay is simple and less time-consuming and has been suggested as a genotoxic end point in investigations addressing the issues related to the induction of an adaptive response (*31*).

MATERIALS AND METHODS

Reagents

RPMI 1640 tissue culture medium, fetal bovine serum (FBS) and phytohemagglutinin (PHA-M form) were from BioWhittaker (Verviers, Belgium); penicillin, streptomycin and L-glutamine were from Gibco (Milan, Italy); cytochalasin B and mitomycin C (MMC) were from Sigma (St. Louis, MO); dimethyl sulfoxide (DMSO), EDTA, methanol, Giemsa, NH_4Cl and $KHCO_3$ were from Baker (Deventer, The Netherlands). Entellan was from Merck (Darmstadt, Germany). The same batches of culture reagents were used for all the experiments.

Radiofrequency-Radiation Exposure System

The exposure system used was described in detail earlier (*35, 36*). Briefly, it consisted of four wire patch cells (WPCs) placed in two separate commercial incubators (Forma Scientific, model 311) maintaining an average temperature of 36.9 ± 0.5°C and a humidified atmosphere of 5% carbon dioxide and 95% air. Two WPCs were assigned for RF-radiation exposure at an average specific absorption rate (SAR) of 1.25 W/kg, corresponding to 10 W/kg, peak value. The SAR used was considered as the worst-case scenario of maximum local exposure in the head region in a mobile phone user and is well above the safety guidelines recommended by international organizations (*37, 38*). The other two WPCs were used for sham exposure. Metal grid boxes provided the shielding to avoid both electromagnetic compatibility problems with the electronic system of the incubators and interferences between WPCs. A four-channel power supply was controlled entirely by a computer for the management of the power inside the WPCs. The software was developed using LabVIEW 6.1 (National Instruments, Austin, TX) to provide a user-friendly system interface. All data were recorded, coded and stored by this software in a database (Microsoft Access 97) in real time. The code was broken only after the completion of all microscope examinations. Numerical and experimental dosimetry was carried out using a commercial code that uses the FIT (Finite Integration Technique) method to measure the SAR distribution within the biological sample (CST Microwave Studio 5.0, Darmstadt, Germany). The efficiency of the measurement was about 0.35 ± 0.10 W/kg W^{-1}. The temperature in RF-radiation-exposed samples was maintained with two spiral coils positioned on the exterior faces of each WPC. The circulating water in each coil was maintained at 36.7°C to obtain an average temperature of 36.9 ± 0.5°C (*35*). The temperature was also monitored and recorded by means of a four-channel fiber-optic thermometer (Fiso UMI 4, Fiso Technologies, Quebec, Canada). The cells in separate culture dishes were exposed to RF radiation or sham radiation for a continuous period of 20 h (see below). Neither the pH nor volume of the culture medium was changed in all culture dishes. No condensation was observed in any of the culture dishes. These observations indicated that the relatively high peak SAR (10 W/kg) used did not induce any thermal-based or other stress response in RF-radiation-exposed cells.

Experimental Protocol

The experimental protocol was approved by the ethical committee of ASL-Napoli 1. Informed consent was obtained and peripheral blood samples were collected from nine healthy, non-smoking male donors aged between 21 and 38 years (mean 31.7 ± 5.9 years). Each donor's whole blood was then diluted (1:10) with RPMI 1640 culture medium containing 15% heat-inactivated FBS, 100 U/ml penicillin, 100 mg/ml streptomycin, 2 m*M* L-glutamine and 1% PHA. For each donor, several duplicate cultures were set up in petri dishes (internal diameter 3.5 cm), each having 3 ml of diluted blood. All cultures were kept in a laboratory incubator at 37 ± 1°C in a humidified atmosphere of 5% carbon dioxide and 95% air.

In the first set of experiments, diluted blood from four donors were examined. MMC was used for both the adaptation and challenge doses. The adaptation dose of MMC, 1, 5 or 10 ng/ml, was added to the cultures at 24 h. The challenge dose 100 ng/ml of MMC was added to all cultures at 48 h after PHA stimulation (Fig. 1a). In the second set of experiments, diluted blood from five donors was examined. The adaptation dose, 900 MHz RF radiation at a peak SAR of 10 W/kg (average SAR 1.25 W/kg) or sham exposure, was initiated in separate WPCs at 24 h after PHA stimulation and continued until 44 h, after which all cultures were returned to the laboratory incubator. One hour before the initiation of RF-radiation and sham exposures, the culture dishes were placed in WPCs to allow for temperature equilibration and settlement of cells at the bottom of the petri dish. At 48 h after culture initiation, the challenge dose of 100 ng/ml of MMC was added to RF-radiation- and sham-exposed cultures (Fig. 1b).

Cytochasin B was added to all cultures at 44 h, and the cells were collected for the MN assay at the end of 72 h (*39*). From each petri dish, 1 ml cell suspension was centrifuged and the cell pellets were resuspended in 3 ml lysis buffer (10 m*M* EDTA, 155 m*M* NH_4Cl and 10 m*M* $KHCO_3$) for 7 min at room temperature. The cells were then treated with hypotonic solution (one part RPMI 1640 medium supplemented with 2% FBS and four parts distilled water) for 15 min.

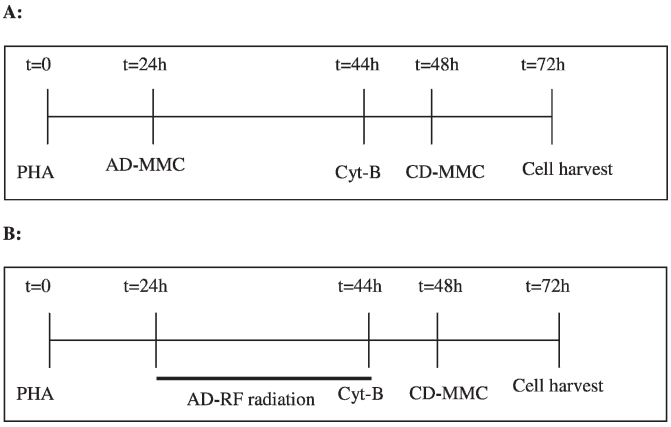

FIG. 1. Panel A: Experimental protocol used in the investigation using MMC as adaptation as well as challenge doses. Panel B: Experimental protocol used in the investigation using RF radiation as the adaptation dose and MMC as the challenge dose. AD-MMC: adaptation dose of MMC. CD-MMC: challenge dose of MMC (100 ng/ml). AD-RF radiation: adaptation dose of 900 MHz RF radiation at 10 W/kg peak SAR.

Cytospin centrifuge (Cytospin, Shandon; 7 min at 130*g*) was used to collect the cells on coded microscope slides. The cells on air-dried slides were fixed in 80% methanol for 10 min and stained with 10% Giemsa solution. All coded slides were examined at 1000× magnification. The criteria defined by Fenech *et al.* (*40*) were used for MN evaluation. For each donor and from each exposure condition, two separate slides prepared from duplicate cultures were examined. A total of 2000 consecutive cells (1000 cells from each slide) were examined to obtain the frequency of binucleate (BN) cells. The proliferation index (PI) was derived from [M1 + 2M2 + 3(M3 + M4)]/N, where M1 to M4 represent the numbers of cells with one to four nuclei, respectively, and N is the total number of cells scored. A total of 2000 binucleated cells (1000 binucleated cells from each slide) were analyzed to record the incidence of cells with one (BN1MN), two (BN2MN) or three (BN3MN) micronuclei. The total number of micronuclei was obtained from (1 × BN1MN) + (2 × BN2MN) + (3 × BN3MN).

Statistical Analysis

The expected frequencies of micronuclei in combined treatments (adaptation + challenge) were calculated as the sum of the micronuclei in two individual treatments minus the frequency in untreated controls. The statistical significance of reductions in observed frequencies relative to the expected incidences was evaluated for each blood sample using a two-tailed z test (Statistical Analysis System, Version 9.1 for Windows, SAS Institute, Cary, NC). A two-tailed paired Student's t test was also applied to compare all treatments with each other.

RESULTS

The percentage of binucleate cells, PI and the incidence of micronuclei in the lymphocytes of four donors where MMC was used for both the adaptation and challenge doses are presented in Table 1. There were no significant differences in percentage of binucleate cells and PI among the cells treated with adaptation and/or challenge doses of MMC. Lymphocytes treated with the adaptation dose of 1, 5 and 10 ng/ml MMC alone exhibited varying degrees of increases in the incidence of micronuclei, and there was no consistent dose response among the four donors. However, treatment with the 100-ng/ml MMC challenge dose alone resulted in a significantly increased frequency of micronuclei in all four donors. Lymphocytes from all four donors exhibited an adaptive response when treated with the adaptation + challenge dose of 1 + 100 ng/ml MMC, respectively, and the percentage decrease in the incidence of micronuclei ranged from 46% to 63%. All four donors were considered as responders. There was no consistent improvement in the adaptive response when the cells were treated with higher adaptation doses of MMC. The percentage decrease in the incidence of micronuclei observed in cells treated with 5 + 100 ng/ml and 10 + 100 ng/ml MMC was not significantly greater than that observed with 1 + 100 ng/ml MMC. In fact, in a majority of the combined treatments of the cells with 5 + 100 and 10 + 100 ng/ml MMC, the percentage decrease in micronuclei was lower than that observed with 1 + 100 ng/ml MMC. Hence, in the subsequent RF-radiation and sham exposure investigation in which blood samples from five donors were used, cultures treated with 1 ng/ml MMC, 100 ng/ml MMC and 1 + 100 ng/ml MMC were included to confirm whether the donor was a responder.

The data from the RF-radiation investigation are presented in Table 2. The PI in cells treated with 100 ng/ml MMC given alone or as challenge dose was significantly reduced compared with untreated control cells ($P < 0.01$), while the results for the percentage of binucleate cells were unaffected. Similar observations were also made when the cells were treated with 100 ng/ml MMC after RF-radiation and sham adaptation exposures. Lymphocytes from all five donors exposed to 1 ng/ml MMC, RF-radiation and sham exposure alone exhibited similar incidences of micronuclei, and the indices were not significantly different from those for untreated control cells. Also, there were no significant differences among the five donors. In contrast, there was a significant increase in the frequency of micronuclei when the cells were treated with the 100-ng/ml MMC challenge dose alone. Lymphocytes from four donors (nos. 2, 3, 4 and 5) that were treated with 1 + 100 ng/ml exhibited an adaptive response; the percentage decrease in the incidence of micronuclei ranged from 42% to 52%. Interestingly, cells from these four donors also exhibited an adaptive response when they were exposed to RF radiation prior to challenge with 100 ng/ml MMC. The percentage decrease in the frequency of micronuclei ranged from 35% to 56%, while no decrease was observed in cells adapted with the sham exposure and challenged with 100 ng/ml MMC. These donors were considered as responders. However, the extent of the adaptive response was not the same in all four donors, which suggested interindividual variability. In contrast,

TABLE 1
The Percentage of Binucleate Cells, Proliferation Index and the Incidence of Micronuclei in the Peripheral Blood Lymphocytes of Four Donors Exposed to the Adaptation Dose of 1, 5 or 10 ng/ml Mitomycin C and/or Challenge Dose of 100 ng/ml Mitomycin C

Treatment	Percentage binucleate cells	Proliferation index	Micronuclei		Difference (observed − expected)	Decrease (%)	*P* value
			Observed 2000 binucleate cells[b]	Expected[a] 2000 binucleate cells			
Donor 1							
Control	43.8	1.74	14				
100 ng/ml	46.2	1.50	82				
1 ng/ml	40.0	1.80	24				
1 + 100 ng/ml	50.0	1.54	40	92	52	56.5	0.002
5 ng/ml	43.2	1.75	16				
5 + 100 ng/ml	45.4	1.53	66	84	18	21.4	0.168
10 ng/ml	39.0	1.65	34				
10 + 100 ng/ml	48.0	1.52	44	102	58	56.9	<0.001
Donor 2							
Control	41.4	1.67	10				
100 ng/ml	48.2	1.54	94				
1 ng/ml	44.4	1.68	12				
1 + 100 ng/ml	48.4	1.54	36	96	60	62.5	<0.001
5 ng/ml	48.0	1.68	18				
5 + 100 ng/ml	54.0	1.62	30	102	72	70.6	<0.001
10 ng/ml	51.2	1.76	22				
10 + 100 ng/ml	53.2	1.57	58	106	48	45.3	0.006
Donor 3							
Control	41.2	1.76	12				
100 ng/ml	48.8	1.54	74				
1 ng/ml	42.4	1.74	34				
1 + 100 ng/ml	45.2	1.50	52	96	44	45.8	0.008
5 ng/ml	38.4	1.71	32				
5 + 100 ng/ml	52.4	1.79	76	94	18	19.1	0.178
10 ng/ml	39.4	1.78	48				
10 + 100 ng/ml	48.6	1.55	78	110	32	29.1	0.059
Donor 4							
Control	41.6	1.96	6				
100 ng/ml	46.2	1.66	98				
1 ng/ml	38.0	1.95	18				
1 + 100 ng/ml	52.0	1.68	54	110	56	50.9	0.001
5 ng/ml	36.4	1.82	36				
5 + 100 ng/ml	51.6	1.58	76	128	52	40.6	0.006
10 ng/ml	40.0	1.84	40				
10 + 100 ng/ml	46.8	1.66	78	132	54	40.9	0.005

[a] The expected values are the sums of two individual treatments minus the control.
[b] See the text for other details.

lymphocytes from donor no. 1 that were adapted to 1 ng/ml MMC, RF-radiation and sham exposures did not exhibit an adaptive response when challenged with 100 ng/ml MMC. There was no significant decrease in the incidence of micronuclei when the cells adapted to 1 ng/ml MMC, RF-radiation and sham exposures challenged with 100 ng/ml MMC. This donor was considered a non-responder.

DISCUSSION

In all of the earlier *in vitro* and *in vivo* studies related to the induction of an adaptive response, an extremely small dose of a known genotoxic agent (ionizing radiation in a great majority of the studies) was used to render the cells refractory to the induction of genetic damage induced by a higher challenge dose of the same or a similar genotoxic agent. Recent reviews of the published data suggested that non-ionizing RF radiation does not act like a genotoxic agent (*33, 41–44*). The results obtained in this study also confirmed that RF radiation itself was non-genotoxic, as seen by the absence of a significant increase in the incidence of micronuclei in the lymphocytes of all five donors. Thus the important observation made in this preliminary investigation is that a non-genotoxic agent, RF radiation, was capable of inducing an adaptive response: Lymphocytes collected from four (out of five) donors

TABLE 2
The Percentage Binucleate Cells, Proliferation Index and the Incidence of Micronuclei in the Peripheral Blood Lymphocytes of Five Donors Exposed to the Adaptation Dose of 1 ng/ml Mitomycin C, Radiofrequency Radiation or Sham and/or Challenge Dose of 100 ng/ml Mitomycin C

Treatment	Percentage binucleate cells	Proliferation index	Micronuclei		Difference (observed − expected)	Decrease (%)	*P* value
			Observed 2000 binucleate cells[b]	Expected[a] 2000 binucleate cells			
Donor 1							
Control	35.6	1.58	32				
100 ng/ml	38.3	1.42	83				
1 ng/ml	36.5	1.59	31				
1 + 100 ng/ml	37.7	1.41	83	82	−1	−1.22	0.527
Sham	36.8	1.58	30				
Sham + 100 ng/ml	37.8	1.40	72	81	9	11.11	0.267
RF radiation	33.3	1.46	26				
RF radiation + 100 ng/ml	36.7	1.36	58	77	19	24.68	0.089
Donor 2							
Control	43.0	1.67	20				
100 ng/ml	43.6	1.47	140				
1 ng/ml	43.2	1.69	31				
1 + 100 ng/ml	46.0	1.53	72	151	79	52.32	<0.001
Sham	43.6	1.72	36				
Sham + 100 ng/ml	45.6	1.49	104	156	52	33.33	0.001
RF radiation	41.5	1.70	35				
RF radiation + 100 ng/ml	45.0	1.48	68	155	87	56.13	<0.001
Donor 3							
Control	47.3	1.87	28				
100 ng/ml	43.1	1.49	101				
1 ng/ml	44.5	1.74	42				
1 + 100 ng/ml	44.3	1.51	67	115	48	41.74	<0.001
Sham	44.0	1.68	27				
Sham + 100 ng/ml	44.8	1.49	110	100	−10	−10.00	0.735
RF radiation	41.6	1.70	33				
RF radiation + 100 ng/ml	43.1	1.47	69	106	37	34.91	0.007
Donor 4							
Control	39.6	1.80	22				
100 ng/ml	47.1	1.52	88				
1 ng/ml	39.3	1.69	32				
1 + 100 ng/ml	49.7	1.54	53	98	45	45.92	0.001
Sham	44.5	1.71	30				
Sham + 100 ng/ml	43.4	1.46	85	96	11	11.46	0.228
RF radiation	42.3	1.72	28				
RF radiation + 100 ng/ml	43.1	1.44	58	94	36	38.30	0.004
Donor 5							
Control	44.6	1.92	18				
100 ng/ml	52.7	1.64	67				
1 ng/ml	42.7	1.92	23				
1 + 100 ng/ml	49.7	1.54	39	72	33	45.83	0.003
Sham	46.0	1.78	18				
Sham + 100 ng/ml	54.0	1.60	52	67	15	22.39	0.111
RF radiation	44.5	1.77	25				
RF radiation + 100 ng/ml	56.9	1.61	40	74	34	45.95	0.002

[a] The expected values are the sum of two individual treatments minus the control.
[b] See the text for other details.

exposed for 20 h to 900 MHz RF radiation at a peak SAR of 10 W/kg were found to be less susceptible to the induction of genetic damage (assessed from the incidence of micronuclei) by subsequent exposure to a genotoxic dose of MMC, a chemotherapeutic alkylating chemical mutagen that induces genetic damage (*45*). Perhaps RF-radiation exposure to the cells produces a "trigger" that is small and does not result in significantly increased genetic damage, but such a trigger is capable of inducing an adaptive response and thus provided protection from the subsequent challenge dose with a genotoxic agent. In this context, it is interesting to note that several reviewers (*46–48*) have suggested that exposure to non-ionizing electromagnetic radiation itself

is non-genotoxic (analogous to RF radiation), and L929 cells that were pre-exposed to non-ionizing extremely low-frequency 50 Hz magnetic fields at 100 mT flux density for 24 h exhibited significantly decreased proportions of G_1 cells and increased proportions of cells in the G_2/M phase, indicating a modification of the DNA damage response to subsequent exposure to a genotoxic chemical, menadione (*49*).

There are several reports in the literature in which researchers used a sequential exposure protocol that is similar to that used in the current investigation, i.e., exposure of human blood lymphocytes to RF radiation (*in vitro* for 2 h or occupational exposure for >2 years) followed by *in vitro* treatment of the cells with MMC. The results include a highly reproducible synergistic effect (*50*), very weak synergistic effect (*51*), inconsistent effect (*52, 53*) and no effect (*54, 55*). In these studies, unstimulated lymphocytes (G_0 stage of the cell cycle) were exposed to RF radiation followed by stimulation of the cells with PHA and treatment with MMC. It is possible that the RF-radiation exposure of the lymphocytes in the G_0 stage of the cell cycle (as an adaptation dose) failed to induce an adaptive response, as observed in the studies by Shadley *et al.* (*20*).

The data from the current investigation also indicated that the lymphocytes of one donor (no. 1) that were exposed to RF radiation (under similar exposure conditions) did not exhibit the induction of an adaptive response when subsequently challenged with MMC. The absence of an induction of an adaptive response in human blood lymphocytes has been reported previously (*26–27, 30*). This is more likely due to individual variability in eliciting an adaptive response and an indication that the induction of an adaptive response does not depend on transient physiological parameters, but rather on some stable genetic constitutional traits (*24, 25, 28, 31, 56–59*).

The ability of MMC to induce an adaptive response has been demonstrated in several earlier investigations (*9, 16, 18, 60–62*). The results obtained in the current study lend additional support to the data presented in the above reports. Lymphocytes from four donors exposed to an adaptation dose of 1 ng/ml MMC exhibited significantly decreased incidence of micronuclei when challenged with 100 ng/ml dose of MMC. Overall, such decrease in MN frequencies was greater than that observed in cells exposed to higher adaptation doses of 5 and 10 ng/ml MMC, suggesting that the dose used for adaptation is important to eliciting an adaptive response (*63, 64*).

Several mechanisms have been proposed for the induction of an adaptive response (*65–69*). The possible role of the enzymes involved in the repair of damaged DNA, particularly the activity of poly(ADP-ribosyl) polymerase, which responds to DNA strand breaks induced by free radicals generated by MMC, has been implicated in several earlier investigations (*19, 21, 22*). Other factors, such as (a) efficient repair of radiation-induced DNA damage in adapted cells (*23*), (b) the ability of the cells to perform protein synthesis (*70, 71*), (c) expression of different mRNA after exposure to an adaptation dose (*66*), (d) changes in chromatin conformation (*72*), (e) altered expression of several genes and gene products (*73, 74*), etc. appear to be important in the induction of an adaptive response. In addition, cell cycle regulation (*75*), altered G_1 checkpoint control (*76*) and mitotic delay (*12*) have been implicated in the induction of adaptive response. Similar studies are necessary to explain the mechanism of induction of an adaptive response in cells exposed to non-ionizing RF radiation.

In conclusion, the results obtained in the current preliminary investigation indicated that exposures to RF radiation at a frequency in use for wireless communications is capable of inducing an adaptive response in human blood lymphocytes. This finding deserves further research regarding whether an adaptive response can be elicited in other *in vitro and in vivo* experimental conditions including various frequencies, different SARs, timing of adaptation and challenge dose treatments, different cell types, etc.

Received: December 9, 2008; accepted: February 3, 2009

REFERENCES

1. L. Samson and J. A. Cairns, A new pathway for DNA repair in *Escherichia coli*. *Nature (London)* **267**, 281–283 (1977).
2. T. Ikushima, Chromosomal responses to ionizing radiation reminiscent of an adaptive response in cultured Chinese hamster cells. *Mutat. Res.* **180**, 215–221 (1987).
3. S. Wolff, V. Afzal, J. Wiencke, G. Olivieri and A. Micheli, Human lymphocytes exposed to low doses of ionizing radiation become refractory to high doses of radiation as well as chemical mutagens that induce double strand breaks in DNA. *Int. J. Radiat. Biol.* **53**, 39–48 (1988).
4. J. D. Shadley and G. Dai, Cytogenetic and survival adaptive response in G_1 phase human lymphocytes. *Mutat. Res.* **265**, 273–281 (1992).
5. S. Wolff, Is radiation all bad? The search for adaptation. *Radiat. Res.* **131**, 117–123 (1992).
6. S. Wolff, Low dose exposure and induction of adaptation. In *Low Dose Irradiation and Biological Defense Mechanisms* (T. Sugahara, L. A. Sagan and T. Aoyama, Eds.), pp. 21–28. Elsevier, Amsterdam, 1992.
7. I. Dominguez, N. Pannerselvan, P. Escalza and A. T. Natarajan, Adaptive response to radiation damage in human lymphocytes conditioned with hydrogen peroxide as measured by cytokinesis-block micronucleus technique. *Mutat. Res.* **301**, 135–141 (1993).
8. E. I. Azzam, G. P. Raaphorst and R. E. J. Mitchel, Radiation-induced adaptive response for protection against micronucleus formation and neoplastic transformation in C3H½ mouse embryo cells. *Radiat. Res.* **138** (Suppl.), S28–S31 (1994).
9. E. Madrigal-Bijaidar, M. Cassani, S. J. Matinez and T. Morales, Adaptive response induced by mitomycin C measured in the frequency of SCE in human lymphocyte cultures. *Mutat. Res.* **322**, 301–305 (1994).

10. J. Seong, C. O. Suh and G. E. Kim, Adaptive response to ionizing radiation induced by low doses of gamma rays in human cell lines. *Int. J. Radiat. Oncol. Biol. Phys.* **33**, 869–874 (1995).
11. T. Nikolova and E. Hüttner, Adaptive and synergistic effects of a low-dose ENU pre-treatment on the frequency of chromosomal aberrations induced by a challenge dose of ENU in human peripheral blood lymphocytes *in vitro*. *Mutat. Res.* **357**, 131–141 (1996).
12. B. Salone, V. Pretazzoli, A. Bosi and G. Olivieri, Interaction of low-dose radiation with subsequent mutagen treatment: role of mitotic delay. *Mutat. Res.* **358**, 155–160 (1996).
13. E. L. Anuszewska, B. M. Gruber and J. H. Koziorowska, Studies on adaptation to adriamycin in cells pretreated with hydrogen peroxide. *Biochem. Pharmacol.* **53**, 597–603 (1997).
14. N. I. Ryabchenko, M. M. Antoshchina, E. V. Fesenko, T. I. Ivanova, T. V. Kondrashova and V. A. Nasonova, Cytogenetic adaptive response in cultured human lymphocytes: dependence on the time of exposure to adapting and challenging doses of gamma-rays. *Mutat. Res.* **418**, 7–19 (1998).
15. G. Oliviera, M. Neves, A. S. Rodrigues, G. O. Monteiro, T. Chaveca and J. Rueff, Assessment of the adaptive response induced by quercetin using the MNCB peripheral blood human lymphocytes assay. *Mutagenesis* **15**, 77–83 (2000).
16. K. Schlade-Bartusiak, A. Stembalska-Kozlowska, M. Bernady, M. Kudyba and M. Sasiadek, Analysis of adaptive response to bleomycin and mitomycin C. *Mutat. Res.* **513**, 75–81 (2002).
17. L. M. Stoilov, L. H. F. Mullenders, F. Darroudi and A. T. Natarajan, Adaptive response to DNA and chromosomal damage induced by X-rays in human blood lymphocytes. *Mutagenesis* **22**, 117–122 (2007).
18. A. P. Krishnaja and N. K. Sharma, Variability in cytogenetic adaptive response of cultured human lymphocytes to mitomycin C, bleomycin, quinacrine dihydrochloride, ^{60}Co γ-rays and hyperthermia. *Mutagenesis* **23**, 77–86 (2008).
19. J. A. Wiencke, V. Afzal, G. Olivieri and S. Wolff, Evidence that the [^{3}H] thymidine-induced adaptive response of human lymphocytes to subsequent doses of X-rays involves the induction of a chromosomal repair mechanism. *Mutagenesis* **1**, 375–380 (1986).
20. J. D. Shadley, V. Afzal and S. Wolff, Characterization of the adaptive response to ionizing radiation induced by low doses of X rays to human lymphocytes. *Radiat. Res.* **111**, 511–517 (1987).
21. Vijayalaxmi and W. Burkart, Effect of 3-aminobenzamide on chromosome damage in human blood lymphocytes adapted to bleomycin. *Mutagenesis* **4**, 187–189 (1989).
22. H. E. Kleczkowska and F. R. Althaus, The role of poly(ADP-ribosyl)ation in the adaptive response. *Mutat. Res.* **358**, 215–221 (1996).
23. T. Ikushima, H. Aritomi and J. Morisita, Radioadaptive response: Efficient repair of radiation-induced DNA damage in adapted cells. *Mutat. Res.* **358**, 193–198 (1996).
24. K. Sankaranarayanan, A. von Duyn, M. J. Loos and A. T. Natarajan, Adaptive response of human lymphocytes to low-level radiation from radioisotopes or X-rays. *Mutat. Res.* **211**, 7–12 (1989).
25. A. G. Bosi and G. Olivieri, Variability of the adaptive response to ionizing radiations in humans. *Mutat. Res.* **211**, 13–17 (1989).
26. E. Schmid, M. Bauchinger and U. Nahrstedt, Adaptive response after X-irradiation of human lymphocytes? *Mutagenesis* **4**, 87–89 (1989).
27. M. Bauchinger, E. Schmid, H. Braselmann and U. Nahrstedt, Absence of adaptive response to low-level irradiation from tritiated thymidine and X-rays in lymphocytes of two individuals examined in serial experiments. *Mutat. Res.* **227**, 103–107 (1989).
28. G. Olivieri and A. Bosi, Possible causes of variability of the adaptive response of human lymphocytes. In *Chromosomal Aberrations. Basic and Applied Aspects* (G. Obe and A. T. Natarajan, Eds.), pp. 130–139. Springer-Verlag, Berlin, Heidelberg, 1990.
29. Z. Q. Wang, S. Saigusa and M. S. Sasaki, Adaptive response to chromosome damage in cultured human lymphocytes primed with low doses of X-rays. *Mutat. Res.* **246**, 179–186 (1991).
30. J. Hain, R. Jaussi and W. Burkat, Lack of adaptive response to low doses of ionizing radiation in human lymphocytes from five different donors. *Mutat. Res.* **283**, 137–144 (1992).
31. Vijayalaxmi, B. Z. Leal, T. S. Deahl and M. L. Meltz, Variability in adaptive response to low dose radiation in human blood lymphocytes: consistent results from chromosome aberrations and micronuclei. *Mutat. Res.* **348**, 45–50 (1995).
32. L. Zhang, Cytogenetic adaptive response induced by pre-exposure in human lymphocytes and marrow cells in mice. *Mutat. Res.* **334**, 33–37 (1995).
33. Vijayalaxmi and T. J. Prihoda, Genetic damage in mammalian somatic cells exposed to radiofrequency radiation: A meta-analysis of data from 63 publications (1990–2005). *Radiat. Res.* **169**, 561–574 (2008).
34. M. Fenech, The cytokinesis-block micronucleus technique: A detailed description of the method and its application to genotoxicity studies in human population. *Mutat. Res.* **285**, 35–44 (1993).
35. M. R. Scarfì, A. M. Fresegna, P. Villani, R. Pinto, C. Marino, M. Sarti, A. Sannino, P. Altavista and G. A. Lovisolo, Exposure to radiofrequency radiation (900 MHz, GSM signal) does not affect micronucleus frequency and cell proliferation in human peripheral blood lymphocytes. *Radiat. Res.* **165**, 655–663 (2006).
36. R. Palumbo, F. Brescia, D. Capasso, A. Sannino, M. Sarti, M. Capri, E. Grassilli and M. R. Scarfì, Exposure to 900 MHz radiofrequency radiation induces caspase-3 activation in proliferating human lymphocytes. *Radiat. Res.* **170**, 327–334 (2008).
37. International Commission on Non-Ionizing Radiation Protection, Guidelines for limiting exposure to time-varying electric, magnetic, and electromagnetic fields (up to 300 GHz). *Health Phys.* **74**, 494–522 (1998).
38. IEEE, *Standard for Safety Levels with Respect to Human Exposure to Radio Frequency Electromagnetic Fields, 3 kHz to 300 GHz*. Institute of Electrical and Electronics Engineers, Piscataway, NJ, 1999.
39. M. R. Scarfì, M. B. Lioi, M. Della Noce, O. Zeni, C. Franceschi, D. Monti, G. Castellani and F. Bersani, Exposure to 100 Hz pulsed magnetic fields increases micronucleus frequency and cell proliferation in human lymphocytes. *Bioelectrochem. Bioenerg.* **43**, 77–81 (1997).
40. M. Fenech, S. Bonassi, J. Turner, C. Lando, M. Ceppi, W. P. Chang, N. Holland, M. Kirsch-Volders, E. Zeiger and A. Zijno, Intra- and inter-laboratory variation in the scoring of micronuclei and nucleoplasmic bridges in binucleated human lymphocytes. Results of an international slide-scoring exercise by the HUMN project. *Mutat. Res.* **534**, 45–64 (2003).
41. L. N. Heynick, S. A. Johnston and P. A. Mason, Radiofrequency electromagnetic fields: Cancer, mutagenesis, and genotoxicity. *Bioelectromagnetics* **24** (Suppl. 6), S74–S100 (2003).
42. M. L. Meltz, Radiofrequency exposure and mammalian cell toxicity, genotoxicity, and transformation. *Bioelectromagnetics* **24** (Suppl. 6), S196–S213 (2003).
43. Vijayalaxmi and G. Obe, Controversial cytogenetic observations in mammalian somatic cells exposed to radiofrequency radiation. *Radiat. Res.* **162**, 481–496 (2004).
44. L. Verschaeve, Genetic effects of radiofrequency radiation. *Toxicol. Appl. Pharmacol.* **207**, S336–S341 (2005).
45. B. J. Sanderson and A. J. Shield, Mutagenic damage to mammalian cells by therapeutic alkylating agents. *Mutat. Res.* **355**, 41–57 (1996).
46. J. McCann, F. Dietrich and C. Rafferty, The genotoxic potential of electric and magnetic fields: An update. *Mutat. Res.* **411**, 45–86 (1998).
47. U. Bergqvist, J. Brix, F. de Gruijl, R. de Seze, M. Hietanen, J. G. R. Jeffereys, I. Lagroye, G. W. Lotz, R. D. Owen and

B. Veyret, Review of experimental investigations of EMF biological effects (0–100 kHz)—ICNIRP Standing Committee II. In *Exposure to Static and Low Frequency Electromagnetic Fields, Biological Effects and Health Consequences* (R. Matthes, A. McKinley, J. Bernhardt, P. Vecchia and B. Veyret, Eds.). ICNIRP, Oberschleissheim, 2003.

48. Vijayalaxmi and G. Obe, Controversial cytogenetic observations in mammalian cells exposed to extremely low frequency electromagnetic radiation. A review and future research. *Bioelectromagnetics* **26**, 412–430 (2005).
49. A. Markkanen, J. Juutilainen and J. Naarala, Pre-exposure to 50 Hz magnetic fields modifies menadione-induced DNA damage response in murine L929 cells. *Int. J. Radiat. Biol.* **84**, 742–751 (2008).
50. A. Maes, M. Collier, D. Slaets and L. Verschaeve, MHz microwaves enhance the mutagenic properties of mitomycin C. *Environ. Mol. Mutagen.* **28**, 26–30 (1996).
51. A. Maes, M. Collier, U. Van Gorp, S. Vandoninck and L. Verschaeve, Cytogenetic effects of 935.2-MHz (GSM) microwaves alone and in combination with mitomycin C. *Mutat. Res.* **393**, 151–156 (1997).
52. A. Maes, M. Collier and L. Verschaeve, Cytogenetic investigations on microwaves emitted by a 455.7 MHz car phone. *Fol. Biol.* **46**, 175–180 (2000).
53. P. K. Gadhia, T. Shah, A. Mistry, M. Pithawala and D. Tamakuwala, A preliminary study to assess possible chromosomal damage among users of digital mobile phones. *Electromag. Biol. Med.* **22**, 149–159 (2003).
54. A. Maes, M. Collier and L. Verschaeve, Cytogenetic effects of 900 MHz (GSM) microwaves on human lymphocytes. *Bioelectromagnetics* **22**, 91–96 (2001).
55. A. Maes, U. Van Gorp and L. Verschaeve, Cytogenetic investigation of subjects professionally exposed to radiofrequency radiation. *Mutagenesis* **21**, 139–142 (2006).
56. F. Cortes, I. Doinguez, M. J. Flores, J. Pinero and J. C. Mateos, Differences in adaptive response to radiation damage in G_0 lymphocytes conditioned with hydrogen peroxide to low-dose X-rays. *Mutat. Res.* **311**, 157–163 (1994).
57. I. Kaina and G. Nemethova, Variability of the adaptive response to low dose radiation in peripheral blood lymphocytes of twins and unrelated donors. *Fol. Biol.* **43**, 91–95 (1997).
58. S. H. Park, Y. Lee, K. Jeong, S. Y. Yoo, C. K. Cho and Y. S. Lee, Different induction of adaptive response to ionizing radiation and neoplastic cells. *Cell Biol. Toxicol.* **15**, 111–119 (1999).
59. S. M. J. Mortazavi, T. Ikushima and H. Mozdarani, Variability of chromosomal radioadaptive response in human lymphocytes. *Iran J. Radiat. Res.* **1**, 55–61 (2003).
60. J. E. Moquet, J. S. Prosser, A. A. Edwards and D. C. Lloyd, Sister-chromatid exchanges induced by mitomycin C after acute and chronic exposure of human lymphocytes to a low dose of X-rays. *Mutat. Res.* **227**, 207–213 (1989).
61. M. Osmak and D. Horvat, Chromosomal analysis of Chinese hamster V79 cells exposed to multiple γ-ray fractions: induction of adaptive response to mitomycin C. *Mutat. Res.* **282**, 259–263 (1992).
62. G. Oliviera, A. S. Rodrigues, T. Chaveca and J. Rueff, Induction of an adaptive response to quercetin, mitomycin C and hydrogen peroxide by low doses of quercetin in V79 Chinese hamster cells. *Mutagenesis* **12**, 457–462 (1997).
63. J. D. Shadley and S. Wolff, Very low doses of X-rays can cause human lymphocytes to become less susceptible to ionizing radiation. *Mutagenesis* **2**, 95–96 (1987).
64. Vijayalaxmi and W. Burkart, Resistance and cross-resistance to chromosome damage in human blood lymphocytes adapted to bleomycin. *Mutat. Res.* **211**, 1–5 (1989).
65. R. E. J. Mitchel, Mechanisms of adaptive response in irradiated mammalian cells. *Radiat. Res.* **141**, 117–118 (1995).
66. S. Wolff, Aspects of the adaptive response to very low doses of radiation and other agents. *Mutat. Res.* **358**, 135–142 (1996).
67. S. Wolff, The adaptive response in radiobiology: evolving insights and implications. *Environ. Health Perspect.* **106**, 277–283 (1998).
68. C. Stecca and G. B. Gerber, Adaptive response to DNA-damaging agents: a review of potential mechanisms. *Biochem. Pharmacol.* **55**, 941–951 (1998).
69. M. S. Sasaki, Y. Ejima, T. Tachibana, K. Ishizaki, T. Shimizu and T. Nomura, DNA damage response pathway in radioadaptive response. *Mutat. Res.* **504**, 101–118 (2002).
70. J. H. Youngblom, J. K. Wiencke and S. Wolff, Inhibition of the adaptive response of human lymphocytes to very low doses of ionizing radiation by the protein synthesis inhibitor cycloheximide. *Mutat. Res.* **227**, 257–261 (1989).
71. J. H. Kim, K. H. Hahm, C. K. Cho and S. Y. Yoo, Protein biosynthesis in low dose ionizing radiation-adapted human melanoma cells. *J. Radiat. Res.* **37**, 161–169 (1996).
72. I. Y. Belyaev, I. M. Spivak, A. Kolman and M. Harms-Ringdahl, Relationship between radiation induced adaptive response in human fibroblasts and changes in chromatin conformation. *Mutat. Res.* **358**, 223–230 (1996).
73. M. Martin, F. Crechet, B. Ramaounet and J. L. LeFaix, Activation of c-fos by low dose radiation: a mechanism of the adaptive response in skin cells. *Radiat. Res.* **141**, 118–119 (1995).
74. O. Rigaud and E. Moustacchi, Radio-adaptation for gene mutations and the possible molecular mechanisms of adaptive response. *Mutat. Res.* **358**, 127–134 (1996).
75. M. Meyers, J. McCaffrey, E. Odegaard and D. Boothman, X-ray-inducible transcripts and altered cell cycle regulation are involved in adaptive survival responses in human cells. *Radiat. Res.* **141**, 119–120 (1994).
76. D. A. Boothman, M. Meyers, E. Odegaard and M. Wang, Altered G_1 checkpoint control determines adaptive survival responses to ionizing radiation. *Mutat. Res.* **358**, 143–153 (1996).

Environmental and Molecular Mutagenesis 32:1–16 (1998)

Review Article

Genotoxicity of Radiofrequency Radiation

DNA/Genetox Expert Panel:
David Brusick, Chairman,* Richard Albertini, Donald McRee, Donald Peterson, Gary Williams, Phillip Hanawalt, and Julian Preston

During the past several years, concerns have been raised regarding the potential adverse effects of exposures to nonionizing radiation, particularly in the extremely low frequency (ELF) range (50 to 60 MHz) and radiofrequency radiation (RFR) with frequencies ranging from 30 KHz to 30,000 MHz. One focus of concern has been potential DNA interactions. Publications reviewing the genotoxicity of ELF radiation [McCann et al. (1993): Mutat Res 297(1):61–95; Murphy et al. (1993): Mutat Res 296:221–240; NAS (1997)], have been uniform in concluding that the weight of evidence does not indicate any genotoxic risk from exposure to this type of radiation.

Concern that RFR may be associated with adverse biological effects [WHO, 1993], including recent allegations that they may be involved in the production of brain tumors in humans [Elmer-Dewit (1993): *Time,* February 8:42], has resulted in the production of a large number of publications describing the effects of RFR on the integrity of nucleic acids. Data from studies conducted in a frequency range from 800 to 3,000 MHz were reviewed and subjected to a weight-of-evidence evaluation. The evaluation focused on direct toxicological effects of RFR as well as on studies addressing basic biological responses to RFR at the cellular and molecular level.

The data from over 100 studies suggest that RFR is not directly mutagenic and that adverse effects from exposure of organisms to high frequencies and high power intensities of RFR are predominantly the result of hyperthermia; however, there may be some subtle indirect effects on the replication and/or transcription of genes under relatively restricted exposure conditions. Environ. Mol. Mutagen. 32:1–16, 1998.

Key words: genotoxicity; microwave; radiowave; mutation; aberrations

INTRODUCTION

Use of wireless communication devices, such as cellular telephones, is increasing dramatically in the United States as well as internationally. Most current wireless devices operate by sending and receiving radio signals in the range of 800 to 900 MHz.* Frequencies on digital cellular telephones and other personal communication devices (PCDs) extend to 2,000 MHz. Most cellular telephones currently in use employ continuous analog transmission technology; however, the use of digital equipment, which employ pulse transmission of radio frequencies, will increase significantly in the next few years.

Expansion of this technology will result in substantial human exposure to radiofrequency radiation (RFR) on a chronic basis. During the past several years, concerns have been raised regarding the potential of RFR to initiate and/or promote tumor development, suppress components of the immune system, or induce genetic alterations [Elmer-Dewit, 1993; WHO, 1993]. Research focused on safety issues of chronic exposure to RFR, particularly in the frequency range associated with wireless communication devices, is limited. Interpretation of the data with respect to possible genetic risk has been inconsistent. To a large extent, the inability to develop a conclusive interpretation is the result of the absence of uniform exposure standards, accurate measurement techniques, and the small number of safety studies conducted in compliance with GLP regulations.

One of the most active areas of RFR testing is the assessment of direct and indirect effects on DNA. A database containing results from over 100 published studies was collected for this evaluation. The types of studies conducted range from investigations of RFR interactions with purified DNA in vitro to assessment of chromosome

Contract grant sponsor: Wireless Technology Research, L.L.C., Mississauga, Ontario.

*Correspondence to: Dr. David Brusick, Covance, 9200 Leesburg Pike, Vienna, VA 22182-1699.

Received 3 August 1997; Revised and accepted 1 March 1998

Abbreviations: hertz (Hz); kilohertz (KHz); megahertz (MHz); gigahertz (GHz); radiofrequency radiation (RFR); 12-O-tetra-decanoylphorbol-12-acetate (TPA); specific absorption rate (SAR); extremely low frequency (ELF).

damage in primary cells recovered from laboratory animals and humans exposed to RFR [WHO, 1993].

The purpose of this review is to examine the available database for RFR genotoxicity and evaluate the potential of RFR in the wireless communication range for genotoxic hazard and/or risk to exposed human populations.

The biological consequences of exposure to electromagnetic fields within a frequency range of 300 Hz to 300 GHz interact with biological systems [WHO, 1993]. Within this broad range, RFRs cover a range of frequencies from 30 KHz to 30,000 MHz. The most frequently studied RFR, however, is 2,450 MHz, associated with microwave ovens. Table I lists 105 studies from over 35 laboratories that have been directed toward defining the nature and biological significance of DNA interactions with RFR. This review will concentrate on an analysis of the genotoxicity of RFR studies listed in Table I with an independent assessment of those studies employing the frequency range associated with wireless communication devices (i.e., 800 MHz to 2,000 MHz). Unfortunately, the number of studies published in this frequency range is currently very small. A significant amount of new RFR research and testing is focused on this frequency range. These data will augment this evaluation over then next several years. Also present among the studies evaluated are three publications involving an assessment of DNA damage in humans with long-term exposure to RFR [Garaj-Vrhovac et al., 1990b; Garson et al., 1991; Maes et al., 1995]. The results of these studies are particularly relevant to the development of a hazard assessment.

The studies reviewed include those conducted on plants, insects, microorganisms, cultured mammalian cells (both primary cultures and continuous cell lines), and in vivo mammalian assays. Most of the studies are classified as being hazard identification evaluations and include assessments for mutation induction, a wide range of chromosome alterations, cell transformation, and evidence for the induction and/or integrity of DNA repair processes. A smaller subset of studies were designed to detect cellular and molecular changes occurring in DNA exposed to RFR in situ or in simulated extracellular matrices. These latter studies measured DNA responses not associated directly with genetic toxicity and were therefore not viewed as highly relevant to assessments of genetic hazard or risk, although they may provide extremely useful mechanistic information.

CHARACTERISTICS OF THE DATABASE

Although the majority of the articles were published within the past ten years and use state-of-the-art techniques for assessing genotoxicity, some of the studies included in the database were published almost two decades ago. Consequently, many of the studies were designed with controls and methods of data analysis that would be considered inadequate by current standards. There was an attempt to take these limitations into consideration in the overall data evaluation. The database can be characterized as:

1. Heterogeneous with respect to target organisms, exposure methods, and genetic endpoints employed.
2. Complex with respect to the variation of responses across similar types of endpoints and target organisms.
3. Redundant with respect to the frequency of replication of certain test methods (e.g., mutation induction in *Salmonella typhimurium*, chromosome aberration analyses in cultured human lymphocytes, mouse dominant lethal test).

Interpretation of results is also complicated by the high incidence of variables associated with RFR exposure. The most common variables are a) wave frequency, b) power, c) duration of exposure, d) modulation, and e) exposure temperature. Each of these parameters is critical for the interpretation of changes in biological activity and is potentially capable of affecting the outcome of an assay. For example, specific absorption rates (SAR) above 1 to 2 W/kg are capable of raising the body temperature of most laboratory animals 1°C or more, which can lead to a wide range of adverse effects [WHO, 1993]. Asanami and Shimono [1997] showed that elevations of core body temperatures in mice by 2°C produced increases in micronuclei in bone marrow. Therefore, it is theoretically possible to generate different responses in two trials of the same in vivo test method if the SAR varies enough to give a 1–2°C temperature differential.

STRATEGY FOR DATA EVALUATION

A weight-of-evidence strategy was used to evaluate the database because of its size, redundancy of tests, and heterogeneity of test methods. Small datasets that are not redundant are more amenable to a test-by-test assessment strategy because each assay exists only once in the dataset and an overall interpretation can be determined from the number and/or type of positive responses observed. In large datasets, assay redundancy accompanied by conflicting responses is commonly found, making interpretation difficult because plausible explanations for divergent responses generated by independent assay trials may not be possible. This characteristically results in selection of the positive (more conservative) responses for use in the final assessment.

A weight-of-evidence approach attempts to use test response patterns or trends to develop conclusions concerning the biological activity of an agent. There is a risk that a single test result may be disproportionately important and become lost in a weight-of-evidence approach.

Spontaneous mutation is a low-frequency event (i.e., 1

TABLE I. Database for Genotoxicity of Electromagnetic Radiation[1]

Endpoint	System	Exposure*	Result	Comments	Reference
Mutation—In vitro					
	Microbial	70,000–75,000 MHz, 10 mW/cm^2; 3 h	Negative	*Escherichia coli*	Bertraud et al., 1975
	Microbial	9,400, 17,000, 70,000–75,000 MHz, less than 60 mW/cm^2 & 28 mW/kg; 30 min	Negative	*Saccharomyces cerevisiae*	Dardalhon et al., 1981
	Microbial	9,400, 17,000, 70,000–75,000 MHz, less than 60 mW/cm^2 & 28 mW/kg; 30 min	Negative	*E coli*	Dardalhon et al., 1981
	Microbial	8,500–9,600 MHz, pulsed, 1, 5, 45 mW/cm^2; up to 2 h	Negative	*Salmonella typhimurium,* TA1535, TA100, TA98	Dutta and Nelson, 1978;[5] Dutta et al., 1979a
	Microbial	8,500–9,600 MHz, pulsed; up to 2 h	Negative	*S cerevisiae*	Dutta and Nelson, 1978;[5] Dutta et al., 1979a
	Microbial	7,000 or 7,500 MHz; 30 min	Negative	*E coli*	Averbeck et al., 1976
	Microbial	7,000 or 7,500 MHz; 30 min	Negative	*S cerevisiae*	Averbeck et al., 1976
	Microbial	3,100 MHz (PW) e&m,[3] 90 W/kg; 6 h	Negative	*S typhimurium,* TA100, TA98, TA1535, TA1537	Hamnerius et al., 1985
	Microbial	2,450 MHz, 10 and 50 mW/cm^2, 15 and 79 W/kg; 3–4 h	Negative	*E coli* strain WWU	Blackman et al., 1976
	Microbial	2,450 MHz, CW, 20 mW/cm^2, 40 W/kg; up to 2 h	Negative	*S typhimurium,* TA1535, TA100, TA98	Dutta and Nelson, 1978;[5] Dutta et al., 1979a
	Microbial	2,450 MHz, 3,070 MHz	Negative	*S typhimurium,* TA1535, TA1530, TA100	Anderstam et al., 1983
	Microbial	2,450 Mhz	Negative	*E coli* strain WP2	Anderstam et al., 1983
	Microbial	2,450 MHz, 5,100 mW/cm^2; up to 23 sec	Positive	*S typhimurium* TA98, TA100, TA1535, TA1537, TA1538	Blevins et al., 1980
	Microbial	2,450 MHz, CW, 20 mW/cm^2, 40 W/kg; up to 2 h	Negative	*S cerevisiae*	Dutta and Nelson, 1978;[5] Dutta et al., 1979a
	Microbial	2,450 MHz (CW), e&m 130 W/kg; 5.7 h	Negative	*S typhimurium,* TA100, TA98, TA1535, TA1537	Hamnerius et al., 1985
	Microbial	1,700 MHz, 3 W/kg; 3–4 h	Negative	*E coli* strain WWU	Blackman et al., 1976
	Microbial	27.12 MHz (CW), magnetic, 22 W/kg; 6 h	Negative	*S typhimurium,* TA100, TA98, TA1535, TA1537	Hamnerius et al., 1985
	Mammalian, in vitro	2,450 MHz, 48.8 mW/cm^2, 30 W/kg	Negative	Mouse lymphoma assay	Meltz et al., 1989, 1990a
Mutation—In vivo					
	D. melanogaster	3,100 MHz (PW) e&m, 60 W/kg; 6 h	Negative	Drosphilia somatic	Hamnerius et al., 1985
	D. melanogaster	2,450 MHz, 2.1, 2.75, 3.0 kW; 45 min	Negative	Drosophila SLRL	Pay et al., 1972
	D. melanogaster	2,450 MHz, CW, 110 W/kg; 6 h	Negative	Drosophila somatic	Hamnerius et al., 1979, 1985
	D. melanogaster	146 MHz, 12 h	Negative	Drosophila SLRL	Mittler, 1975, 1976
	D. melanogaster	146 MHz	Negative	Drosophila chromosome loss	Mittler, 1976
	D. melanogaster	98.5 MHz, 134 h/wk, 32 wk	Negative	Drosophila SLRL	Mittler, 1977
	D. melanogaster	29 MHz, 12 h	Negative	Drosophila chromosome loss	Mittler, 1975, 1976
	D. melanogaster	29 MHz	Negative	Drosophila SLRL	Mittler, 1976
	D. melanogaster	27.12 MHz (CW), e/m,[4] 0.3/0.05 W/kg; 6 h	Negative	Drosophila somatic	Hamnerius et al., 1985

TABLE I. *Continued*

Endpoint	System	Exposure*	Result	Comments	Reference
Mutation—In vivo					
	D. melanogaster	2,375 MHz, (15 W/cm^2 for 60 min; or 20 W/cm^2 for 10 min; or 25 W/cm^2 for 5 min) for 5 days	Negative	Drosophila SLRL	Marec et al., 1985
	Mammalian, in vivo	2,450 MHz, CW, 43 W/kg; 30 min	Negative	Male C3H mice: no dominant lethality (post-implantation survival), reduced pregnancy rate (weeks 3–6 post-expos) and pre-implantation survival: concluded to be a result of low sperm counts resulting from increased temp; temp not controlled	Saunders et al., 1983
	Mammalian, in vivo	2,450 MHz, CW, 100 W/m^2, 4 W/kg; 6 h/d = 120 h over 8 weeks	Negative	Male C3H mice: no increase in chromosome aberrations, no change in pregnancy rate or embryonic survival when mated to C3H/101 females, no increase in dominant lethalities or other chromosomal aberrations including reciprocal translocations	Saunders et al., 1988
	Mammalian, in vivo	2,450 MHz, a) 100 mW/cm^2 for 10 min; b) 50 mW/cm^2 for 10 min, 3 times over 1 day; c) 50 mW/cm^2 for 10 min, 4 times over 2 weeks	Mixed	Swiss mice (male): mated post-exposure for 6–7 weeks: no decrease in the number of implants or in the pregnancy rate; increase in mutagenicity index reported for A (overall, for weeks 1 and 6) and B, considered to be potentially a result of thermal increases, as no increase was observed in C (weeks 4 and 6)	Varma et al., 1976
	Mammalian, in vivo	2,450 MHz, CW, (5 mW/cm^2, 4 h/d, day 6 of gestation to 90 days of age) (10 mW/cm^2, 5 h/d, 5d beginning on day 90) (28 mW/cm^2, 4 h/d, 5 d/w, 4 wk, beginning on day 90)	Negative	Male rats: no sperm cell mutagenesis, temporary sterility at highest power density (effects on reproduction: no consistent pattern, increased fetal mortality not related to decrease live fetuses)	Berman et al., 1980
	Mammalian, in vivo	2,450 MHz, CW; 1.7 kW/m2 for 70 sec	Positive	Male Swiss albino mice: increased dominant lethality, reduced male fertility (pre- and post-implantation loss), abnormal sperm morphology; temperature not controlled (Beechey et al., 1986, implies lack of control is the cause of changes)	Goud et al., 1982
	Mammalian, in vivo	1,700 MHz; 50 W/kg; 30 min	Positive	Swiss mice: induction of dominant lethal mutations	Varma and Traboulay, 1976
Chromosome aberrations—In vitro					
	Mammalian, in vitro	7,700 MHz, 0.5 mW/cm^2; 15, 30, 60 min	Positive	V79 cells	Garaj-Vrhovac et al., 1990a, 1991
	Mammalian, in vitro	7,700 MHz, 0.5 (30 min), 10 (30 min), 30 mW/cm^2 (10, 30 or 60 min)	Positive	Human lymphocytes	Garaj-Vrhovac et al., 1992
	Mammalian, in vitro	2,450 MHz; 30 and 120 min	Positive	Human lymphocytes	Maes et al., 1993

TABLE I. ***Continued***

Endpoint	System	Exposure*	Result	Comments	Reference
Chromosome aberrations—In vitro					
	Mammalian, in vitro	2,450 MHz, CW; up to 200 W/kg; 20 min	Negative	Human lymphocytes	Lloyd et al., 1984, 1986
	Mammalian, in vitro	2,450 MHz, CW; 15 W/kg; up to 320 days (50 passages)	Positive	Rat kangaroo RH16 cells	Yao, 1976;[5] 1982
	Mammalian, in vitro	2,450 MHz, PW, 33.8 W/kg; 2 h	Negative	Chinese hamster ovary cells	Kerbacher et al., 1990
	Mammalian, in vitro	2,450 MHz, 30 min	Negative	Chinese hamster ovary cells	Alam et al., 1978
	Mammalian, in vitro	2,450 MHz, 20–500 mW/cm^2; 4–20 min	Positive	Chinese hamster cells	Chen et al., 1974
	Mammalian, in vitro	2,450 MHz, 0.2, 1.0, or 5.0 W/cm^2 for up to 30 min	Positive	Rat kangaroo bone marrow cells	Yao and Jiles, 1970
	Mammalian, in vitro	2,450 MHz, 49 mW/cm^2, 33.8 W/kg	Negative	Chinese hamster ovary cells	Meltz et al., 1990b
	Mammalian, in vitro	1,200 MHz, 24.33 W/kg	Negative	Chinese hamster ovary cells	Meltz et al., 1990b
	Mammalian, in vitro	850 MHz, 18 mW/cm^2, 14.4 W/kg	Negative	Chinese hamster ovary cells	Meltz et al., 1990b
	Mammalian, in vitro	954 MHz	Positive	Human lymphocytes	Maes et al., 1995
	Mammalian, in vitro	167 Mhz	Positive	Human lymphocytes	Khalil et al., 1993
	Mammalian, in vitro	100 MHz; 12.5 h	Negative	Chinese hamster ovary cells	Wolff et al., 1985
	Mammalian, in vitro	100 MHz; 12.5 h	Negative	Human lymphocytes	Wolff et al., 1985
	Mammalian, in vitro	15 MHz; 14 h	Negative	Chinese hamster ovary cells	Wolff et al., 1985
	Mammalian, in vitro	20 kHz; 72 h	Negative	Human amniotic cells	Nordesson et al., 1989[2]
Chromosome aberrations—In vivo					
	Mammalian, in vivo	30–300 GHz, 10–50 W/cm^2; occupational	Positive	Human subjects	Garaj-Vrhovac et al., 1990b
	Mammalian, in vivo	9,400 MHz (PW), 0.1–10 mW/cm^2; 1 h/d, 5 d/wk, 2 wk	Positive	BALB/c mice	Manikowska et al., 1979
	Mammalian, in vivo	2,450 MHz, CW; up to 21 W/kg; 15 min/d, 5 consec d	Negative	Chinese hamster blood lymphocytes	Huang et al., 1977
	Mammalian, in vivo	2,450 MHz; 12 min	Negative	Chinese hamster cells	Janes et al., 1969
	Mammalian, in vivo	2,450 MHz, CW, 100 W/m^2, 4 W/kg; 6 h/d = 120 h over 8 weeks	Negative	C3H mice	Saunders et al., 1988
	Mammalian, in vivo	2,450 MHz, CW; 0.05–20 W/kg; 30 min/d, 6 d/wk, 2 weeks	Positive	Sperm cells of male CBA/CEY mice increased chromosome translocations and other cytogenetic abnormalities (exposed as spermatocytes); rectal temperature did not change by 0.5°C	Manikowska-Czerska et al., 1985
	Mammalian, in vivo	2,450 MHz, CW; 1, 100, 400 W/m^2; 30 min/d, 6 d/wk, 2 weeks	Negative	Sperm cells of male mice: no increase in chromosomal aberrations (exposed as stem cells); temperature not controlled—significant increase in rectal temperature for 400 W/m^2 only; slight increases in chr aberrations thought to be due to change in temperature	Beechey et al., 1986

TABLE I. ***Continued***

Endpoint	System	Exposure*	Result	Comments	Reference
Chromosome aberrations—In vivo					
	Mammalian, in vivo	2,450 MHz	Negative	Mouse	Banerjee, et al., 1983
	Mammalian, in vivo	2,450 MHz, 100 mW/cm^2; 30 min	Positive	Chinese hamster corneal epithelium cells	Yao, 1978
	Mammalian, in vivo	2,375 (CW), 2750 (pulsed) MHz; 0.1, 0.5, 5.0 W/m^2; 7 h/d, 45 days	Positive	Mouse hepatocytes	Antipenko and Koveshnikova, 1987[2]
	Mammalian, in vivo	13 MHz (CW or PW)	Negative	Rat regenerating hepatic tissue	McLees et al., 1972
	Mammalian, in vivo	0.4 to 20,000 MHz; occupational	Negative	Human lymphocytes (radio-linemen)	Garson et al., 1991
	Mammalian, in vivo	Various frequencies, (incl. 450 × 950 MHz) ≥ 1 h/day for at least one year; occupational	Negative	Human lymphocytes (antenna maintenance workers	Maes, et al., 1995
Micronucleus formation—In vitro					
	Plant	10–21 MHz, 30 h	Positive	Tradescantia cuttings bearing young flower buds	Hadier et al., 1994
	Mammalian, in vitro	7,700 MHz, 0.5 mW/cm^2; 15, 30, 60 min	Positive	Chinese hamster V79 cells	Garaj-Vrhovac et al., 1991
	Mammalian, in vitro	2,450 MHz, 30 and 120 min	Positive	Human lymphocytes	Maes et al., 1993
	Mammalian, in vitro	7,700 MHz, 0.5 (30 min), 10 (30 min), 30 mW/cm^2 (10, 30 or 60 min)	Positive	Human lymphocytes	Garaj-Vrhovac et al., 1992
Micronucleus formation—In vivo					
	Mammalian, in vivo	Unknown (30–300 GHz); occupational	Positive	Human subjects	Garaj-Vrhovac et al., 1990b
Sister Chromatid Exchange (SCE)—In vitro					
	Mammalian, in vitro	2,450 MHz, CW; up to 200 W/kg; 20 min	Negative	Human lymphocytes	Lloyd et al., 1984, 1986
	Mammalian, in vitro	167 MHz	Positive	Human lymphocytes	Khalil et al., 1993
	Mammalian, in vitro	2,450 MHz; 30 and 120 min	Negative	Human lymphocytes	Maes et al., 1993
	Mammalian, in vitro	2,450 MHz, PW, 33.8 W/kg; 2 h	Negative	Chinese hamster ovary cells	Ciaravino et al., 1987
	Mammalian, in vitro	2,450 MHz, PW, 33.8 W/kg, 2 h	Negative	Chinese hamster ovary cells	Ciaravino et al., 1991
	Mammalian, in vitro	2,450 MHz, 49 mW/cm^2, 33.8 W/kg	Negative	Chinese hamster ovary cells	Meltz et al., 1990b
	Mammalian, in vitro	1,200 MHz, 24.33 W/kg	Negative	Chinese hamster ovary cells	Meltz et al., 1990b
	Mammalian, in vitro	850 MHz, 18 mW/cm^2, 14.4 W/kg	Negative	Chinese hamster ovary cells	Meltz et al., 1990b
	Mammalian, in vitro	100 MHz; 12.5 h	Negative	Chinese hamster ovary cells	Wolff et al., 1985
	Mammalian, in vitro	100 MHz; 12.5 h	Negative	Human lymphocytes	Wolff et al., 1985
	Mammalian, in vitro	15 MHz; 14 h	Negative	Chinese hamster ovary cells	Wolff et al., 1985
Sister chromatid exchange (SCE)—In vivo					
	Mammalian, in vivo	2,450 MHz, CW; 21 W/kg; 8 h/day, 28 days	Negative	Mouse bone marrow	McRee et al., 1981
	Mammalian, in vivo	2,450 MHz, CW, 100 W/m^2, 4 W/kg; 6 h/d = 120 h over 8 weeks	Negative	C3H mice	Saunders et al., 1988
	Mammalian, in vivo	2,450 MHz, CW; 0.05–20 W/kg; 6 h over 2 weeks	Positive	Sperm cells of male CBA/CEY mice	Manikowska-Czerska et al., 1985

TABLE I. ***Continued***

Endpoint	System	Exposure*	Result	Comments	Reference
Sister chromatid exchange (SCE)—In vivo					
	Mammalian, in vivo	800 MHz, 4 W/kg; 8 h	Negative	Mouse bone marrow	Brown and Marshall, 1982
	Mammalian, in vivo	2,450 MHz	Negative	Mouse bone marrow	Banerjee et al., 1983
	Mammalian, in vivo	400 MHz, 4 W/kg; 8 h	Negative	Mouse bone marrow	Brown and Marshall, 1982
DNA damage/repair—In vitro					
	Microbial	8,600, 8,800, 9,000 MHz, 1, 10, 20 mW/cm^2; 1, 5, 10, 15 h	Negative	*E coli* Pol A^+/A^- (normal/repair deficient)	Dutta et al., 1978
	Microbial	8,600 MHz, 12 W/kg; up to 7 h	Negative	*E coli* Pol A^+/A^- (normal/repair deficient)	Dutta et al., 1979b
	Microbial	2,600–4,000 MHz, 20 W/kg; 10–12 h	Negative	*E coli* B	Corelli et al., 1977
	Microbial	2,450 MHz (CW or PW), 10 mW/cm^2; 1 h	Negative	*Aspergillus nidulans*	Mezykowski et al., 1980
	Microbial	2,450 MHz, 10 mW/cm^2; 10–240 min	Negative	*A nidulans*	Baranski et al., 1976
	Mammalian, in vitro	1,200 MHz (CW or PW), 1 (or 5), 10 mW/cm^2, 2.7 ± 1.6 W/kg; 1–3 h	Negative	Human MRC-5 fibroblasts	Meltz et al., 1987, 1990b
	Mammalian, in vitro	850 MHz (CW or PW), 1 (or 5), 10 mW/cm^2, 4.5 ± 3.0 W/kg; 1–3 h	Negative	Human MRC-5 fibroblasts	Meltz et al., 1987, 1990b
	Mammalian, in vitro	350 MHz (CW or PW), 1 (or 5), 10 mW/cm^2, 0.39 ± 0.15 W/kg; 1–3 h	Negative	Human MRC-5 fibroblasts	Meltz et al., 1987, 1990b
DNA damage/repair—In Vivo					
	Mammalian, in vivo	2,450 MHz, 1 mW/cm^2; 2 h/d for 120, 150, 200 d	Positive	Swiss albino mice: DNA samples from testes and brain contained altered band patterns	Sarkar et al., 1994
	Mammalian, in vivo	1,700 MHz, CW; 50 W/kg; 30 min	Positive	Swiss male mice: chemical changes in testicular DNA (parameters assessed: hyperchromicity and melting temp, results indicate strand separation possible); temperature not controlled	Varma and Traboulay, 1977
	Mammalian, in vivo	1,700 MHz, 50 mW/cm^2 for 30 min; 10 mW/cm^2 for 80 min	Positive	Swiss mice: mutagenicity indicated by changes in properties of DNA (melting temperature, base composition, optical density) indicative of strand separation	Varma and Traboulay, 1976
	Mammalian, in vivo	985 MHz, 10 mW/cm^2; 80 min	Positive	Swiss mice: mutagenicity indicated by changes in properties of DNA (melting temperature, base composition, optical density) indicative of strand separation	Varma and Traboulay, 1976
	Mammalian, in vivo	2,450 MHz; 0.6 and 1.2 W/kg for 2 h	Positive	Comet assay measured single-strand breaks induced in rat brain DNA. Both continuous and pulsed exposures.	Lai and Singh, 1995
	Mammalian, in vivo	954 MHz; 1–5 weeks	Negative	Comet assay used for rat lymphocyte DNA. Breaks in controls and exposed animals were equivalent	Verschaeve et al., in press
Sperm abnormalities					
	Mammalian, in vivo	2,450 MHz, CW; 0.05–20 W/kg; 6 h over 2 weeks	Positive	Sperm cells of male CBA/CEY mice	Manikowska-Czerska et al., 1985

TABLE I. *Continued*

Endpoint	System	Exposure*	Result	Comments	Reference
Sperm abnormalities					
	Mammalian, in vivo	2,450 MHz, CW, 36 mW/cm^2; 16 h/30 d	Negative	Mice	Cairnie and Harding, 1981
Cell transformation					
	Mammalian, in vitro	2,450 MHz, with X-ray or benzo(a)pyrene; 4.4 W/kg; 24 h	Positive	Mouse embryo fibroblasts C3H/10T1/2	Balcer-Kubiczek and Harrison, 1985
	Mammalian, in vitro	2,450 MHz; 4.4 W/kg; 24 h	Negative	Mouse embryo fibroblasts C3H/10T1/2	Balcer-Kubiczek and Harrison, 1989, 1991
	Mammalian, in vitro	2,450 MHz, with TPA; 4.4 W/kg; 24 h	Positive	Mouse embryo fibroblasts C3H/10T1/2	Balcer-Kubiczek and Harrison, 1989, 1991

[1]Other than EFL—50–60 Hz.
[2]As cited in WHO, 1993.
[3]E&m indicates that the exposure conditions involved combined electric and magnetic fields.
[4]E/m indicates that the exposure conditions were assayed using electric and magnetic fields, separately.
[5]The result or reference indicated is an abstract only.
*Frequency, dose rates, deviation, and power only given where available.

$\times 10^{-6}$ per gene per generation). Bioassays used to detect DNA alterations have intrinsic rates of positive responses that occur sporadically. Therefore, the process of focusing only on the positive responses for decision-making may exclude valid data and may lead to erroneous conclusions about the genotoxicity of agents. Considering the impact of sporadic positive responses is probably useful only when reviewing large heterogeneous datasets where response patterns and trends are important interpretation factors.

Reviews of assay performance covering several in vitro assays [Kirkland and Dean, 1994] and the in vivo mouse micronucleus assay [Shelby et al., 1993] document the existence and occurrence of sporadic (nonreproducing) positive responses. Estimates of the incidences of sporadic positive responses provided in these reviews were approximately 8% for the Ames test, 20% for the Mouse Lymphoma assay, and for in vitro chromosome aberrations in CHO about 15%. The incidence of sporadic positive responses in the mouse micronucleus test was 10%. Estimates of these rates for other assays comes from personal experience when reviewing historical data. The basis of sporadic responses are complex, but can often be attributed to marginally positive, nonreproducible responses, associated with target organism toxicity, or responses associated with atypical concurrent control values in one of the trials. Some endpoints, such as mammalian cell transformation, mouse spermhead abnormalities, and plant cell clastogenicity, have high rates of sporadic positives presumably due to the susceptibility of these techniques to the production of change by nongenotoxic events (e.g., high osmolality, low pH, hyperthermia). Whole animal assays such as mutation in Drosophila, dominant lethal mutations in mice, and some DNA repair may be affected by indirect mechanisms associated with toxicity, but tend to be somewhat less susceptible than in vitro assays.

A thorough discussion of the rationale for using a weight-of-evidence approach when evaluating large, heterogenous, complex genotoxicity datasets has been published in a special issue of *Mutation Research* (Vol. 266, No. 1, 1992). An example of the application of this weight-of-evidence approach to an evaluation of a large genetic toxicity database, resistant to micro-assessment, was published by Brusick [1994].

EXPOSURE CONSIDERATIONS

The most frequently encountered confounding variable in the database was that associated with exposure conditions. RFR-emitting sources used to conduct the studies covered in this review ranged from relatively unsophisticated converted microwave ovens to highly reliable and calibrated exposure systems. This leads to nonuniform exposure conditions and may lead to high SARs producing localized thermal effects. Few exposure devices produced to date are able to generate uniform SARs in experimental units or monitor them accurately.

RFR doses are expressed as SARs to quantify the energy absorbed by the target organism in watts per kilogram (W/kg). SARs define both peak and average values for exposure. Because of the associated adverse physiological changes produced in the target organism by RFR exposures, reliable comparisons and interpretations were difficult for studies not reporting SARs.

RFR exposure parameters, in addition to frequency,

TABLE II. Expectations for Positive Responses in the Database Due to Sporadic Positives

Bioassay type	Intrinsic sporadic positives	Number of times used	Expected positives	Observed positives
Microbial	5%	24	1.2	1
In vitro cytogenetic	30%	32	9.6	12
Cell transformation	50%	3	1.5	1
Mouse lymphoma	20%	1	0	0
Drosophila	5%	12	1	0
UDS in vitro	5%	4	1	0
Plant cytogenetic	75%	1	1	1
Dominant lethal	5%	6	0	3*
In vivo cytogenetic	10%	18	1.8	8*
Spermhead abnormalities	50%	2	1	1

*Probable thermal effects: high temperature known to produce developmental effects and chromosome instability in vivo.

which may influence the outcome of a study, include modulation, polarization, and intermittent vs. continuous emission. Invariably, one or more of these parameters differed among independent studies with a given assay. Consequently, dose comparisons were not possible.

Kerbacher et al. [1990] reviewed the relationship between SAR and thermal effects for in vitro exposures at 2,450 MHz at an SAR of 33.8 W/kg. The conclusions of the authors were that many of the positive clastogenicity findings could be due to secondary thermal effects, and if thermal effects are eliminated RFR alone is not capable of inducing chromosome damage. Berman et al. [1980] attempted to provide similar information for germ cell damage in vivo following exposures to 2,450 MHz RFR. The authors concluded that male rats exposed to RFR (5 mW/cm^2) from day 6 of gestation to 90 days of age were not at risk for DNA damage to their sperm. Asanami and Shimono [1997] altered internal core body temperatures of ddY male mice and measured the frequencies of micronuclei in bone marrow cells. They showed that 1 hr at body temperatures of 39.5°C and higher significantly increased micronucleus frequency.

MACRO ASSESSMENT OF THE DATABASE

Table II summarizes the qualitative responses in the database, including the number of expected sporadic positive responses for specific assay types. With the exception of two test types, dominant lethality in mice and in vivo clastogenicity, the actual incidence of positive responses in the RFR database is close to the number expected from sporadic responses. This suggests that the basis of concern for RFR DNA damage is consistent with the response variability expected for a large sample of studies. This explanation is not intended to trivialize the interpretations of the authors of the investigations summarized in Table I, but it offers a plausible explanation for some of the increases that are inconsistent with observed response patterns or trends. The increased incidences seen in the in vivo assays may be attributable to hyperthermia-induced chromosome damage associated with microwave exposures [Leonard et al., 1983; Saunders et al., 1988].

DETAILED ASSESSMENT OF THE DATABASE

The database listed in Table I contains 105 studies. There are 65 in vitro studies, 28 mammalian in vivo studies, and 12 studies conducted in the fruit fly. Approximately 73% (77/105) of the studies showed no evidence of genotoxic activity. Studies designed to address basic research issues will be discussed separately from tests considered relevant to a hazard assessment (e.g., standard tests for mutation, chromosome alterations including sister chromatid exchange, induction of DNA repair processes, and tests for cell transformation). The following is a summary of results, by genetic endpoint, as assessed by the authors of the study reports.

HAZARD IDENTIFICATION/ASSESSMENT STUDIES

Gene Mutation

Thirty-four studies designed to measure the ability of RFR to induce recessive or dominant mutations were conducted in a range of microbial systems (i.e., bacteria, yeast, fungi), mammalian cell culture, and Drosophila. There was only a single study that reported a positive response [Blevins et al., 1980]. In this study, *S. typhimurium* strains TA1535, TA1537, TA1538, TA98, and TA100 were subjected to 2,450 MHz in a commercial microwave oven. Increases in reversion were observed, equally, in all five strains after ~8–10 sec at 5,100 mW/cm^2. In a control study, the same strains were incubated in a waterbath set at temperatures ranging from 45–100°C. Revertant frequencies increased starting at 65°C in all

strains but never reached the same magnitude as the frequencies observed following RFR. Blevins et al. [1980] concluded that RFR is mutagenic due to its producing single-strand breaks that lead to basepair substitutions and frame-shift alterations. It is clear that hyperthermia is able to induce mutations in all five tester strains and one might hypothesize that there are synergistic effects between RFR and heat. Because the investigators did not record temperatures in the 13 × 100 mm tubes used to hold the bacterial cultures, one cannot exclude hyperthermia as the primary factor in the observed increases. Failure to find reversion in *S. typhimurium* or other bacteria in studies controlling for hyperthermia support this interpretation.

A summary of the gene mutation studies within the database provides no convincing evidence supporting a conclusion that RFR is capable of inducing mutation.

Chromosome Alterations in Somatic Cells

The largest and most heterogenous subset of data summarized in Table I deals with chromosomal alternations. In vitro studies evaluated include those assessing structural aberrations, numerical alterations, micronuclei formation, and sister chromatid exchange (SCE) induction in cultured human cells as well as several primary and continuous animal cell cultures. If SCE studies are analyzed independent from aberration studies, there is a greater than expected number of positive aberration studies based on the sporadic positive response issue described above. The data strongly support the conclusion that induction of SCEs is not associated with RFR exposure. If in vitro genotoxicity studies (mutagenicity and clastogenicity) are combined, the incidence of positives was not higher than might be expected from sporadic positives.

The pattern of responses in vivo was similar to that seen in vitro and, again, there was a greater than expected number of positive responses in studies measuring chromosome aberrations, but not for SCE.

Among the studies listed in this group are three cytogenetic studies using cells collected from human populations exposed occupationally to RFR. Information concerning exposure metrics such as dose rates (SARs) is very limited in these studies.

The results of a study conducted by Garaj-Vrhovac et al. [1990b] measuring micronuclei and aberrations in ten workers from a radar station reported that incidences of micronuclei and aberrations in cultured lymphocytes from exposed subjects were significantly increased. The publication did not identify lifestyle factors which could influence the aberration levels in the control or treated groups, raising questions of potential bias. The increase in the average micronuclei reported for that study was based on increases in only five of the ten exposed individuals. The frequencies in the other five subjects were not significantly increased over control levels.

Two other studies examining the level of chromosome aberrations in human populations exposed to RFR from telecommunication transmission antennas did not find any evidence of increased chromosome alterations [Garson et al., 1991; Maes et al., 1995].

A number of studies suffered from technical problems (e.g., control of hyperthermia or appropriate study controls) which dampened confidence in the interpretation of the data. This was true for several reported positive responses. For example, the increases in aberrations reported by Alam et al. [1978] in CHO-K1 cells exposed to 2,450 MHz were found only at 42°C. When the exposures were controlled for hyperthermia and temperatures held at 29°C, the level of aberrations in the treated population was not increased.

The increased incidence of SCE reported by Khalil et al. [1993] in cultured human lymphocytes is also open to question because the cultures were mitogenically stimulated during exposure.

Two other in vitro studies were reported in which technical issues affect the overall interpretation. Yao [1982] reported increases in aberrations in cultured rat kangaroo cells but only after 20 passages of continuous exposure to 2,450 MHz. It is difficult to establish a mechanism to explain the late expression of accumulated damage. A study in which human lymphocyte cultures were exposed to 954 MHz reported a shielded control population of cells with aberration levels approximately equal to the exposed cells, indicating possible technical problems. The aberration frequencies in both the shielded control and the exposed cells were higher, however, than the culture controls [Maes et al., 1995].

Two of the in vivo studies reported as being positive were conducted with sample sizes too small to give reliable estimates of chromosome damage. Yao [1978] measured chromosome breakage in corneal epithelial cells of Chinese hamsters exposed to 2,450 MHz RFR at power densities of 100 mW/cm^2 and 25 mW/cm^2. Seventy-four cells were examined from control animals. Only two of the six treated groups had more than 100 cells evaluated for aberrations. The studies were considered positive on the basis of a single group achieving a significance level of $P = 0.05$.

A second study in which Chinese hamsters were exposed to 2,450 MHz RFR showed an increase in chromosome ''stickiness,'' an irregularity hypothesized to affect the mitotic process [Janes et al., 1969]. The level of ''stickiness'' was high in the controls, suggesting that it was a technical artifact. However, in the same study additional groups of animals were evaluated for aberrations using sample sizes of 50 metaphase per group. There was no significant increase in chromosome aberrations in the exposed animals.

Chromosome Damage in Mammalian Germ Cells

This group of studies includes studies of dominant lethality in mice and direct evaluation of aberrations in mouse meiotic chromosomes. Dominant lethal effects are generally considered to be the consequence of chromosome alterations in the germ cells of the exposed male mice.

The incidence of positive dominant lethal studies was higher than expected from sporadic positive responses, suggesting that the intensity of RFR used in these studies was associated with alterations in reproductive performance or chromosome damage in the original studies. The results of two studies reporting positive effects on germ cells by Varma and Traboulay [1976] and Varma et al. [1976] were not reproduced by Berman et al. [1980] nor by Cairnie and Harding [1981]. These latter investigators suggested that a combination of inappropriate evaluation methods and thermal effects were responsible for the reported positive effects. Goud et al. [1982] reported the induction of dominant lethality and spermhead abnormalities with 2,450 MHz RFR at a power density of 170 mW/cm^2 for 70 sec. This type of exposure would be reasonably certain to increase temperatures in gonadal tissues. Leonard et al. [1983] reviewed the RFR dominant lethal literature available at that time and concluded that the positive studies reported could be attributed to hyperthermia. Several recent studies by Saunders et al. [1988] and Beechey et al. [1986], in which hyperthermia was carefully controlled, did not find any evidence for dominant lethality or meiotic chromosome damage in mice exposed to 2,450 MHz RFR. While reports of positive dominant lethal studies were higher than expected due to sporadic positive responses, the fact that most of the positive studies were conducted without adequate control of temperature raises questions concerning direct effects of RFR on germ cell DNA. The contemporary studies measuring meiotic chromosome aberrations, spermhead abnormalities, and dominant lethal mutations were more careful in dosimetry measurements and were uniformly without genetic effects.

Conversely, the possibility of some nonthermal effects from RFR at frequencies in the range of 2,000 MHz to 10,000 MHz cannot be totally excluded.

Induction of DNA Repair Processes

Eight in vitro studies have been conducted to determine the ability of RFR to induce DNA damage that is subject to excision types of repair mechanisms (Table I). Among this group are five studies conducted in microorganisms and three in cultured mammalian cells. None produced positive results. There was no evidence in the existing database that RFR induced or altered DNA repair. Of six in vivo studies measuring DNA damage/repair conducted, five suggested evidence of DNA strand breakage or other molecular alterations. Some of these studies were not conducted under conditions appropriate for hazard assessment and will be reviewed in a following section.

In summary, in vivo studies suggest some biological effects from RFR, but additional studies with more stringent environmental controls will be needed to exclude hyperthermia as a cause.

Cell Transformation Assays

The database contains three assays measuring the induction of morphological cell transformation [Balcer-Kubiczek and Harrison, 1985, 1989, 1991]. The series of studies consisted of treating mouse C3H/10T1/2 cells with 2,450 MHz RFR a) alone, b) in combination with benzpyrene, and c) with the promoting agent TPA. RFR alone did not induce cell transformation, whereas the combined exposures with benzpyrene or TPA did increase morphological transformation. While the mechanisms involved in in vitro morphological transformation are not well understood, derivatives of the technology in which cells are exposed to co-carcinogenic exposures or are treated with promoting agents are even more difficult to interpret, especially in light of in vivo cancer studies in mice and rats which failed to find co-carcinogenic or promoting activities with RFR [Santini et al., 1988; Wu et al., 1989; Salford et al., 1993]. Preliminary results from more recent studies by Cain et al. [1997], in which C3H 10T1/2 cells were exposed to 836.55 MHz at SARs up to 7.8 W/g in the presence of TPA, showed no increase in transformed foci. Data evaluation of combination exposures is not well developed and the results of this study will be deferred to the discussion of carcinogenic effects.

BASIC MECHANISM STUDIES

RFR can cause chromosomes to uncoil. It is thought that RFR may disrupt histone bonds, resulting in chromosome uncoiling possibly leading to clastogenesis [Swicord and Czerski, 1984]. Other studies have suggested that RFR will inactivate repressor molecules activating gene expression and, therefore, affect cell differentiation. Swicord and Czerski [1984] studied the microwave absorption properties of DNA molecules in aqueous environments. Purified DNA extracted from *E. coli* was subjected to RFR at 2,450 MHz. The results indicated that DNA, specifically of certain lengths, absorbed microwaves more efficiently than water.

Further investigations reported by Sagripanti and Swicord [1986] showed that RFR in the range of 2,000 MHz to 9,000 MHz was absorbed by plasmid DNA. Using a 5,480 basepair plasmid designated pUC8.c2, RFR exposures of 2,000 MHz to 9,000 MHz produced both single- and double-stranded DNA breaks. The exposures inducing breaks were nonthermal, resulting in a temperature

increase of no more than 0.8°C. The method of exposure consisted of inserting the open end of a coaxial antenna into an aqueous sample containing the DNA molecules. The investigators found increases in strand breaks in both sham-exposed (contact with the copper antenna) and RFR-exposed DNA that exceeded the control DNA, which never contacted the antenna. This demonstrated that copper ions (cuprous only) were able to increase DNA strand breakage in the absence of RFR and complicated the interpretation of the studies.

Other in vitro studies indicated that RFR exposures of 2,450 MHz at SAR of 50 W/kg or less stimulate DNA and RNA synthesis and may, therefore, have effects on cell proliferation [Cleary et al., 1990].

Reports of in vivo effects range from shifts in testicular DNA hyperchromicity and thermal profiles in mice exposed to 2,450 MHz RFR [Varma and Traboulay, 1977] to alterations in the sequence of specific tandem repeats found in mouse testicular and brain DNA [Sarkar et al., 1994]. The mechanism(s) involved in these changes were not identified but tentatively attributed to nonspecific stress and not to hyperthermia.

A recent study conducted by Lai and Singh [1995] reports that acute, low-intensity RFR exposure to rats at 2,450 MHz induces single-strand breaks in brain DNA, as measured by gel electrophoresis (COMET assay). Interpretation of the results of this study was complicated by the fact that continuous exposure produced an increase in breaks immediately following exposure, whereas the increases following pulsed exposures were not seen until 4 hr postexposure. The extremely narrow range of COMET tail lengths in the exposed animals was also uncharacteristic of results from genotoxic agents evaluated in this test [McKelvey-Martin et al., 1993]. Malyapa et al. [1997] reported, in an abstract, preliminary data which failed to confirm the results of Lai and Shingh [1995]. A recent abstract published by Roti Roti et al. [1996] also failed to demonstrate DNA breakage in the Comet assay with C3H 10T1/2 cells using 835 and 847 MHz.

Weight-of-Evidence Summary for the Complete Database

The majority of studies conducted with RFR did not demonstrate genotoxic effects. This is true for the full range of RFR frequencies as well as the range more closely associated with wireless communication devices. Tests which measure gene mutation or recombinational effects such as SCE appear to be unaffected by RFR exposure. On the other hand, there appears to be a higher-than-expected number of positive responses from tests which measure DNA disruptions, such as cytogenetic analyses of somatic and/or germ cells. Closer inspection of these positive studies indicates that at least some of the effects are produced by hyperthermia. Other positive studies among this subgroup are attributable to study design deficiencies which may lead to sporadic positive results. Following a censoring of the database for studies with apparent technical or study design flaws, one finds no strong evidence supporting concerns that RFR in the range of 30 MHz to 30,000 MHz poses a genetic hazard to mammalian organisms. Responses at the molecular level also lack a consistent pattern, although limited evidence exists that RFR in the 2,000 MHz to 10,000 MHz range is absorbed by DNA leading to DNA breakage. Whether these effects can be extrapolated to cellular damage has not been determined.

While the overall evaluation of the data does not rule out the possibility that some reported genotoxic effects may be due to RFR exposure, the weight of evidence does not suggest a significant genetic risk associated with radiation frequencies in the range associated with existing communications devices.

ASSESSMENT OF RFR IN THE 800 MHZ TO 2,000 MHZ RANGE

Hazard Identification Studies

The number of studies using RFR exposures in the range of 800 MHz to 2,000 MHz constitutes only about 10% of the database listed in Table I. While the range of interest extends to 2,000 MHz, no studies have been published to date with frequencies at 2,000 MHz. A substantial amount of new research on RFR is being conducted in this frequency range and preliminary data are becoming available [Swicord, 1997]. While there is no reason to expect this frequency range would be any more or less biologically active, the data were reviewed independently.

The results of studies in the communication device range are summarized in Table III. They involved in vitro exposures to look for evidence of DNA breakage and repair, increases in SCE or chromosome aberrations, or cell transformation [Meltz et al., 1987, 1990b; Maes et al., 1995; Roti Roti et al., 1996; Cain et al., 1997].

Studies of possible effects of RFR on repair included studies of RFR on the induction of repair synthesis as well as the ability of RFR to interfere with the rate of repair in cells with previously existing damage [Meltz et al., 1987]. The in vivo study measured SCE induction in bone marrow cells [Brown and Marshall, 1982].

Among the ten studies listed in Table III, the only study reporting a positive effect was one conducted at 954 MHz in human lymphocyte populations [Maes et al., 1995]. The study consisted of splitting blood cultures from male and female donors into three samples. The treated samples were exposed by placing the tubes 5 cm from the emitting antenna for 2 hr. Temperature was maintained at 17 $\pm$ 1°C. The remaining samples were used for controls.

TABLE III. Summary of Effects From Exposure to RFR Frequencies Ranging From 800–2,000 MHz

Endpoint	System	Frequency	Result	SAR	Reference
Aberration	CHO	1,200 MHz	Negative	24.33 W/kg	Meltz et al., 1990b
	CHO	850 MHz	Negative	14.4 W/kg	Meltz et al., 1990b
	Human lymphocytes	954 MHz	Positive	1.5 W/kg	Maes et al., 1995
SCE	CHO	1,200 MHz	Negative	24.33 W/kg	Meltz et al., 1990b
	CHO	850 MHz	Negative	14.4 W/kg	Meltz et al., 1990b
	Mouse	800 MHz	Negative	4 W/kg	Brown and Marshall, 1982
DNA repair	MRC-5	1,200 MHz	Negative	4.5 W/kg	Meltz et al., 1987
	MRC-5	850 Mhz	Negative	4.5 W/kg	Meltz et al., 1987
	C3H10T1/2	835 MHz and 847 MHz	Negative	—	Roti Roti et al., 1996 (Abst.)
Cell transformation	C3H10T1/2	836.55 MHz plus TPA	Negative	7.8 W/kg	Cain et al., 1997 (Abst.)

Sham-exposed samples were placed in a metal container to shield them from RFR during the 2-hr period. Nonexposed controls were incubated in a room away from the antenna. Both the treated and sham-exposed cultures exhibited increased levels of chromosome aberrations compared with the nonexposed controls. The investigators were not able to explain the unexpected finding but suggested that the metal container did not adequately shield the cells from RFR. Apparently no measurements of RFR were taken from inside the metal container during the study.

STUDIES OF CELLULAR AND MOLECULAR INTERACTIONS FROM 800 MHz TO 2,000 MHz EXPOSURE

Verschaeve et al. (in press) conducted a COMET assay on lymphocytes of rats placed near a 954 MHz emitter. The rats showed increased COMET tails but the increases were attributed to stress during the transport and collection processes. This group also examined human blood lymphocytes for COMET tails and found increases when the blood samples were exposed within 5 cm of the antenna. At distances exceeding 5 cm, the effect disappeared. The investigators concluded that under restricted exposure conditions RFR is able to induce DNA strand breakage, but that the conditions required for induction of the DNA damage are not relevant as indications of human genetic risk. The study reported in an abstract by Cain et al. [1997] consisted of combined RFR and TPA exposures to C3H 10T1/2 cells. There was no evidence of cell transformation.

CARCINOGENIC EFFECTS

While this review is not intended to cover carcinogenic bioassays, it may be useful to determine whether the genotoxicity data and available carcinogenicity data are consistent. Although adequate human epidemiology studies associated with RFR exposures have not been conducted, animal cancer studies conducted at 2,450 MHz [Chou et al., 1992] did not show any increase in tumors. 915 MHz RFR did not enhance the growth of glioma tumor cells injected into the brains of Fisher 344 rats [Salford et al., 1993]. Most studies of co-carcinogenicity of RFR and other agents have been negative [Wu et al., 1989]. Other experimental work, such as that described in the Eu-*pim1* transgenic mouse model for tumor induction [Repacholi et al., 1997] and the tumor acceleration models reported by Szmigielski et al. [1982], in which RFR was implicated in tumor enhancement, complicate the picture.

SUMMARY

The data included in this review are derived from studies which evaluate the toxicological effects of RFR, as well as studies addressing basic biological responses to RFR at the cellular and molecular level. A small number of studies assessing the toxicological potential of RFR have reported alterations in chromosome replication and structure. Gene mutation and recombinational endpoints do not appear to be affected by RFR in the frequency ranges tested.

Adverse effects following exposure of organisms to high frequencies and high-power intensities of RFR appear to be predominantly the result of hyperthermia; however, there may be some subtle effects on the replication and or transcription of genes under relatively restricted exposure conditions [Stagg et al., 1997; Ivasvhuk et al., 1997]. In general, the data from a wide range of standard genetic test methods involving both mammalian and nonmammalian assays do not support the concern that RFR poses nonthermal genotoxic risk to somatic or germ cells of humans under normal exposure scenarios.

It is clear that additional confirmatory and new studies assessing the direct effects of RFR on DNA are needed. These studies must be conducted with more robust study designs and with exposure systems accurately defining dose and be capable of reducing and/or eliminating secondary thermal effects.

REFERENCES

Alam MT, Barthakur N, Lambert NC, Kasatiya SS (1978): Cytological effects of microwave radiation in Chinese hamster cells *in vitro*. Can J Genet Cytol 20:23–30.

Anderstam B, Hamnerius Y, Hussain S, Ehrenberg L (1983): Studies of possible genetic effects in bacteria of high frequency electromagnetic fields. Hereditas 98:11–32.

Asanami S, Shimono K (1997): High body temperature induces micronuclei in mouse bone marrow. Mutat Res 390:79–83.

Averbeck D, Dardalhon M, Berteaud AJ (1976): Microwaves action in procaryotic and eukaryotic cells and a possible interaction with X-rays. J Microw Power 11:143–144.

Balcer-Kubiczek EK, Harrison GH (1985): Evidence for microwave carcinogenesis *in vitro*. Carcinogenesis 6:859–864.

Balcer-Kubiczek EK, Harrison GH (1989): Induction of neoplastic transformation in C3H/10T 1/2 cells by 2.45-GHz microwaves and phorbol ester. Radiat Res 117:531–537.

Balcer-Kubiczek EK, Harrison GH (1991): Neoplastic transformation of C3H/10T 1/2 cells following exposure to 120-Hz modulated 2.45-GHz microwaves and phorbol ester tumor promoter. Radiat Res 126:65–72.

Banerjee R, Goldfeder A, Mitra J (1983): Sister chromatid exchanges and chromosome aberrations induced by radio sensitizing agents in bone marrow cells of treated tumor-bearing mice. JNCI 70:517–521.

Baranski S, Debiec H, Kwarecki K, Mezykowski T (1976): Influence of microwaves on genetical processes of *Aspergillus nidulans*. J Microw Power 11:146–147.

Beechey CV, Brooker D, Kowalczuk CI, Saunders RD, Searle AG (1986): Cytogenic effects of microwave irradiation on male germ cells of the mouse. Int J Radiat Biol 50:909–918.

Berman E, Carter HB, House D (1980): Tests for mutagenesis and reproduction in male rats exposed to 2,450-MHz (CW) microwaves. Bioelectromagnetics 1:65–76.

Berteaud AJ, Dardalhon M, Rebcyrotte N, Averbeck DM (1975): Action d'un rayonnement electromagnetique a longueur d'onde millimetrique sur la croissance bacterienne (Effect of an electromagnetic microwave radiation on the growth of bacteria).

Blackman CF, Surles MC, Benane SG (1976): The effect of microwave exposure on bacteria: Mutation induction. In Johnson CC, Shore M (eds): ''Biological Effects of Electromagnetic Waves.'' Washington, DC: US Food and Drug Administration (FDA), (USNC/URSI Annual Meeting — Selected Papers, Oct. 20–23, 1975, Boulder, CO) Vol. 1:406–413.

Blevins RD, Crenshaw RC, Houghland AE, Clark CE (1980): The effects of microwave radiation and heat on specific mutants of *Salmonella typhimurium* LT2. Radiat Res 82:511–517.

Brown RF, Marshall SV (1982): Sister chromatid exchange in marrow cells of mice exposed to RFR (400, 800, and 1200 MhzCW) (meeting abstract). In Bioelectromagnetics Society (BEMS): ''4th Bioelectromagnetics Society Annual Meeting — Abstracts.'' Los Angeles, June 28 – July 2, 1982, p 51, Abstr. No. G31.

Brusick DJ (1994): An assessment of the genetic toxicity of atrazine: Relevance to human health and environmental effects. Mutat Res 317–144.

Cain et al. (1997): Bioelectromagnetics 18:237–243.

Cairnie AB, Harding RK (1981): Cytological studies in mouse testis irradiated with 2.45-GHz continuous-wave microwaves. Radiat Res 87:100–108.

Chen KM, Samuel A, Hoopingarner R (1974): Chromosomal aberrations of living cells induced by microwave radiation. Environ Lett 6:37–46.

Ciaravino V, Meltz ML, Erwin DN (1987): Effects of radiofrequency radiation and simultaneous exposure with mitomycin C on the frequency of sister chromatid exchanges in Chinese hamster ovary cells. Environ Mutagen 9:393–399.

Ciaravino V, Meltz ML, Erwin DN (1991): Absence of a synergistic effect between moderate-power radio-frequency electromagnetic radiation and adriamycin on cell-cycle progression and sister-chromatid exchange. Bioelectromagnetics 12:289–298.

Cleary SF, Liu LM, Merchant RE (1990): Glioma proliferation modulated *in vitro* by isothermal radiofrequency radiation exposure. Radiat Res 121:38–45.

Comptes Rendus Hebdomadaires des Seances de l'Academie des Sciences (Ser D -Sciences Naturelles) 281(12):843–846.

Corelli JC, Gutmann RJ, Kohazi S, Levy J (1977): Effects of 2.6–4.0 Ghz microwave radiation on E-coli B. J Microw 12:141–144.

Dardalhon M, Averbeck D, Berteaud AJ (1981): Studies on possible genetic effects of microwaves in procaryotic and eukaryotic cells. Radiat Environ Biophys 20:37–51.

Dutta SK, Nelson WH (1978): Lack of genetic effects of short duration low power density 2.45 GHz CW and 8.5–9.6 GHz pulsed electromagnetic radiation on selected microbial tester strains. Environ Mutagen Soc — Ann Meet Program Abstr 9th:69–70.

Dutta SK, Nelson WH, Blackman CF, Brusick DJ (1978): Effects of chronic non-thermal exposures of pulsed microwaves on a repair-deficient mutant of *Escherichia coli*. Mutat Res 53:91–92.

Dutta SK, Nelson WH, Blackman CF, Brusick DJ (1979a): Lack of microbial genetic response to 2.45-GHz CW and 8.5- to 9.6-GHz pulsed microwaves. J Microw Power 14:275–280.

Dutta SK, Hossain MA, Ho HS, Blackman CF (1979b): Effects of 8.6-GHz pulsed electromagnetic radiation on an *Escherichia coli* repair-deficient mutant. In Stuchly SS (ed): ''Electromagnetic Fields in Biological Systems.'' Edmonton, AB: IMPI Ltd., (Symposium, June 28–39, 1978, Ottawa, ON) pp 76–95.

Elmer-Dewit P (1993): Dialing ''P'' for Panic. *Time*, February 8:42.

Garaj-Vrhovac V, Horvat D, Koren Z (1990a): The effect of microwave radiation on the cell genome. Mutat Res 243:87–93.

Garaj-Vrhovac V, Fucic A, Horvat D (1990b): Comparison of chromosome aberration and micronucleus induction in human lymphocytes after occupational exposure to vinyl chloride monomer and microwave radiation. Periodicum Biologorium 92:411–416.

Garaj-Vrhovac V, Horvat D, Koren Z (1991): The relationship between colony-forming ability, chromosome aberrations and incidence of micronuclei in V79 Chinese hamster cells exposed to microwave radiation. Mutat Res 263:143–149.

Garaj-Vrhovac V, Fucic A, Horvat D (1992): The correlation between the frequency of micronuclei and specific chromosome aberrations in human lymphocytes exposed to microwave radiation *in vitro*. Mutat Res 281:181–186.

Garson OM, McRobert TL, Campbell LJ, Hocking BA, Gordon I (1991): A chromosomal study of workers with long-term exposure to radiofrequency radiation. Med J Aust 155:289–292.

Goud SN, Usha Rani MV, Reddy PP, Reddi OS, Rao MS, Saxena VK (1982): Genetic effects of microwave radiation in mice. Mutat Res 103:39–42.

Haider T, Knasmueller S, Kundi M, Haider M (1994): Clastogenic effects of radiofrequency radiations on chromosomes of Tradescantia. Mutat Res 324:65–68.

Hamnerius Y, Olofsson H, Rasmuson A, Rasmuson B (1979): A negative test for mutagenic action of microwave radiation in *Drosophila melanogaster*. Mutat Res 68:217–224.

Hamnerius Y, Rasmuson A, Rasmuson B (1985): Biological effects of high-frequency electromagnetic fields on *Salmonella typhimurium* and *Drosophila melanogaster*. Bioelectromagnetics 6:405–414.

Huang AT, Engle ME, Elder JA, Kinn JB, Ward TR (1977): The effect of microwave radiation (2450 MHz) on the morphology and chromosomes of lymphocytes. Radio Sci 12:173–177.

Ivasvhuk et al. (1997): Bioelectromagnetics 18:223–229.

Janes ED, Leach WM, Mills WA, Moore RT, Shore ML (1969): Effects of 2450 MHz microwaves on protein synthesis and on chromosomes in Chinese hamsters. Non-Ionizing Radiat 1:125–130.

Kerbacher JJ, Meltz ML, Erwin DN (1990): Influence of radiofrequency radiation on chromosome aberrations in CHO cells and its interaction with DNA-damaging agents. Radiat Res 123:311–319.

Khalil AM, Qassem WF, Suleiman MM (1993): A preliminary study on the radiofrequency field-induced cytogenetic effects in cultured human lymphocytes. Dirasat 20:121–130.

Kirkland DJ, Dean SW (1994): On the need for confirmation of negative genotoxicity results *in vitro* and on the usefulness of mammalian cell mutation tests in a core battery: Experiences of a contract research laboratory. Mutagenesis 9:491–501.

Lai H, Singh NP (1995): Acute low-intensity microwave exposure increases DNA single-strand breaks in rat brain cells. Bioelectromagnetics (in press).

Leonard A, Berteaud AJ, Bruyere A (1983): An evaluation of the mutagenic, carcinogenic and teratogenic potential of microwaves. Mutat Res 123:31–46.

Lloyd DC, Saunders RD, Finnon P, Kowalczuk CI (1984): No clastogenic effect from *in vitro* microwave irradiation of Go human lymphocytes. Int J Radiat Biol 46:135–141.

Lloyd DC, Saunders DC, Moquet JE, Kowalczuk CI (1986): Absence of chromosomal damage in human lymphocytes exposed to microwave radiation with hyperthermia. Bioelectromagnetics 7:235–237.

Maes A, Verschaeve L, Arroyo A, de Wagter C, Vercruyssen L (1993): *In vitro* cytogenetic effects of 2450 MHz waves on human peripheral blood lymphocytes. Bioelectromagnetics 14:495–501.

Maes A, Collier M, Slaets D, Verschaeve L (1995): Cytogenetic effects of microwaves from mobile communication frequencies (954 MHz). Electro Magnetobiol 14:91–98.

Manikowska E, Luciani JM, Servantie B, Czerski P, Obrenovitch J, Stahl A (1979): Effects of 9.4 GHz microwave exposure on meiosis in mice. Experientia 35:388–390.

Manikowska-Czerska E, Czerski P, Leach WM (1985): Effects of 2.45 GHz microwaves on meiotic chromosomes of male CBA/CAY mice. J Hered 76:71–73.

Marec F, Ondracek J, Brunnhofer V (1985): The effect of repeated microwave irradiation on the frequency of sex-linked recessive lethal mutations in *Drosophila melanogaster*. Mutat Res 157:163–167.

McKelvey-Martin VJ, Green MHL, Schmezer P, Pool-Zobel BL, De Meo MP, Collins A (1993): The single cell gel electrophoresis assay (comet assay): A European review. Mutat Res 288:47–63.

McLees BD, Finch ED, Albright ML (1972): An examination of regenerating hepatic tissue subjected to radio-frequency irradiation. J Appl Physiol 32:78–85.

McRee DI, MacNichols G, Livingston GK (1981): Incidence of sister chromatid exchange in bone marrow cells of the mouse following microwave exposure. Radiat Res 85:340–348.

Meltz ML, Walker KA, Erwin DN (1987): Radiofrequency (microwave) radiation exposure of mammalian cells during UV-induced DNA repair synthesis. Radiat Res 110:255–266.

Meltz ML, Eagan P, Erwin DN (1989): Absence of mutagenic interaction between microwaves and mitomycin C in mammalian cells. Environ Mol Mutagen 13:294–303.

Meltz ML, Eagan P, Erwin DN (1990a): Proflavin and microwave radiation: Absence of a mutagenic interaction. Bioelectromagnetics 11:149–157.

Meltz ML, Holahan PK, Smith ST, Kerbacher JJ, Ciaravino V (1990b): Interaction of inoning radiation, genetically active chemicals, and radiofrequency radiation in human and rodent cells. Department of Radiology, University of Texas Health Science Center. USAF-SAM-TR-90-18.

Mezykowski T, Bal J, Debiec H, Kwarecki K (1980): Response of *Aspergillus nidulans* and *Physarium polycephalum* in microwave irradiation. J Microw Power 15:75–80.

Mittler S (1975): Non-thermal radio waves and genetic damage in *Drosophila melanogaster*. Mutat Res 31:316.

Mittler S (1976): Failure of 2- and 10-meter radio waves to induce genetic damage in *Drosophila melanogaster*. Environ Res 11:326–330.

Mittler S (1977): Failure of chronic exposure to nonthermal FM radio waves to mutate *Drosophila*. J Hered 68:257–258.

Pay TL, Beyer EC, Reichelderfer CF (1972): Microwave effects on reproductive capacity and genetic transmission in *Drosophila melanogaster*. J Microw Power 14:275–280.

Repacholi MH, Basten A, Gebski V, Noonan D, Finnie J, Harris AW, (1997): Lymphomas in Eu-*pim 1* transgenic mice exposed to pulsed 900 Mhz electromagnetic fields. Radiat Res 147:631–640.

Roti, Roti et al. (1996): Bioelectromagnetics Society, 18th Annual Meeting, Victoria British Columbia, June 9–14, Abstract.

Sagripanti J-L, Swicord ML (1986): DNA structural changes caused by microwave radiation. Int J Radiat Biol 50:47–50.

Salford LG, Brun A, Persson BR, Eberhardt J (1993): Experimental studies of brain tumor development during exposure to continuous and pulsed 915 MHz radiofrequency radiation. Bioelectrochem Bioenerg 30:313–318.

Sarkar S, Ali S, Behari J (1994): Effect of low power microwave on the mouse genome: A direct DNA analysis. Mutat Res 320:141–147.

Saunders RD, Darby SC, Kowalczuk CI (1983): Dominant lethal studies in male mice after exposure to 2.45 GHz microwave radiation. Mutat Res 117:345–356.

Saunders RD, Kowalczuk CI, Beechey CV, Dunford R (1988): Studies of the induction of dominant lethals and translocations in male mice after chronic exposure to microwave radiation. Int J Radiat Biol 53:983–992.

Shelby MD, Erexson GL, Hook GJ, Tice RR (1993): Evaluation of a three-exposure mouse bone marrow micronucleus protocol: Results with 49 chemicals. Environ Mol Mutagen 21:160–179.

Stagg et al (1997): Bioelectromagnetics 18:230–231.

Swicord ML, Czerski P (1984): Strong interactions of radiofrequency fields with nucleic acids. In Adey WR, Lawrence AF (eds): ''Nonlinear Electrodynamics in Biological Systems.'' New York: Plenum Press, pp 36–57.

Szmigielski S, Szudezenki A, Pietraszek A, Bielec B, Janiak M, Wrembel JK (1982): Accelerated development of spontaneous and benzopyrene-induced skin cancer in mice exposed to 2450 MHz microwave radiation. Bioelectromagnetics 3:179–191.

Varma MM, Traboulay EA Jr (1976): Evaluation of dominant lethal test and DNA studies in measuring mutagenicity caused by nonionizing radiation. In Johnson CC, Shore M (eds): ''Biological Effects of Electromagnetic Waves.'' Washington, DC: US Food and Drug Administration (FDA), (USNC/URSI Annual Meeting — Selected Papers, Oct. 20–23, 1975, Boulder, CO) Vol. 1:386–396.

Varma MM, Traboulay EA (1977): Comparison of native and microwave irradiated DNA. Experientia 33:1649–1650.

Varma MM, Dage EL, Joshi SR (1976): Mutagenicity induced by nonionizing radiation in swiss male mice. In Johnson CC, Shore M (eds): ''Biological Effects of Electromagnetic Waves.'' Washington, DC: US Food and Drug Administration (FDA), (USNC/URSI Annual Meeting — Selected Papers, Oct. 20–23, 1975, Boulder, CO) Vol. 1:397–405.

Verschaeve L, Slaets D, Van Gorp U, Maes A, Vankerkom L (1998): *In vitro* and *in vivo* genetic effects of microwaves form mobile telephone frequencies in human and rat peripheral blood lymphocytes. In press.

WHO (1993): ''Environmental Health Criteria 137: Electromagnetic

Fields (300 Hz to 300 GHz).'' Geneva: World Health Organization, pp 80–180.

Wolff S, James TL, Young GB, Margulis AR, Bodycote J, Afzal V (1985): Magnetic resonance imaging: Absence of *in vitro* cytogenic damage. JN Radiol 155:163–165.

Wu RY, Ghiang H, Shao BJ (1989): The effects of 2.54 GHz radiation on DMH-induced colon cancer in mice (meeting abstract). In Bioelectromagnetics Society (BEMS): ''11th Bioelectromagnetics Society Annual Meeting - Abstracts.'' Tucson, AZ: June 18–22, 1989, Abstr. No. P-2-34.

Yao KTS (1976): Cytogenetic consequences of microwave incubation of mammalian cells in culture. Genetics 83:S84.

Yao KT (1978): Microwave radiation-induced chromosomal aberrations in corneal epithelium of Chinese hamsters. J Hered 69:409–412.

Yao KTS (1982): Cytogenic consequences of microwave irradiation on mammalian cells incubated *in vitro*. J Hered 73:133–138.

Yao KTS, Jiles MM (1970): Effects of 2450 MHz microwave radiation on cultivated rat kangaroo cells. In Cleary SF (ed): ''Biological Effects and Health Implications of Microwave Radiation.'' Medical College of Virginia Symposium - Proceedings, 1969, pp 123–133. Department of Health, Education, and Welfare, US (DHEW), Public Health Service, Environmental Health Service, Bureau of Radiology.

Accepted by—
H. Evans

Bioelectromagnetics 30:129–141 (2009)

Microwaves From UMTS/GSM Mobile Phones Induce Long-Lasting Inhibition of 53BP1/γ-H2AX DNA Repair Foci in Human Lymphocytes

Igor Y. Belyaev,[1,2,3]* Eva Markovà,[1,2] Lena Hillert,[4,5] Lars O.G. Malmgren,[6] and Bertil R.R. Persson[7]

[1]*Department of Genetics, Microbiology and Toxicology, Stockholm University, Stockholm, Sweden*
[2]*Laboratory of Molecular Genetics, Cancer Research Institute, Bratislava, Slovak Republic*
[3]*Laboratory of Radiobiology, Institute of General Physics, Russian Academy of Science, Moscow, Russia*
[4]*Occupational and Environmental Health, Stockholm County Council, Stockholm, Sweden*
[5]*Department of Public Health Sciences, Division of Occupational Medicine, Karolinska Institutet, Stockholm, Sweden*
[6]*MAX-lab, Lund University, Lund, Sweden*
[7]*Department of Medical Radiation Physics, Lund University Hospital, Lund, Sweden*

We have recently described frequency-dependent effects of mobile phone microwaves (MWs) of global system for mobile communication (GSM) on human lymphocytes from persons reporting hypersensitivity to electromagnetic fields and healthy persons. Contrary to GSM, universal global telecommunications system (UMTS) mobile phones emit wide-band MW signals. Hypothetically, UMTS MWs may result in higher biological effects compared to GSM signal because of eventual ''effective'' frequencies within the wideband. Here, we report for the first time that UMTS MWs affect chromatin and inhibit formation of DNA double-strand breaks co-localizing 53BP1/γ-H2AX DNA repair foci in human lymphocytes from hypersensitive and healthy persons and confirm that effects of GSM MWs depend on carrier frequency. Remarkably, the effects of MWs on 53BP1/γ-H2AX foci persisted up to 72 h following exposure of cells, even longer than the stress response following heat shock. The data are in line with the hypothesis that the type of signal, UMTS MWs, may have higher biological efficiency and possibly larger health risk effects compared to GSM radiation emissions. No significant differences in effects between groups of healthy and hypersensitive subjects were observed, except for the effects of UMTS MWs and GSM-915 MHz MWs on the formation of the DNA repair foci, which were different for hypersensitive ($P < 0.02$[53BP1]//0.01[γ-H2AX]) but not for control subjects ($P > 0.05$). The non-parametric statistics used here did not indicate specificity of the differences revealed between the effects of GSM and UMTS MWs on cells from hypersensitive subjects and more data are needed to study the nature of these differences. Bioelectromagnetics 30:129–141, 2009.

Key words: DNA double-strand breaks; DNA repair foci co-localization; chromatin; nucleoid; apoptosis; stress response

---

Additional supporting information may be found in the online version of this article.

Grant sponsors: Swedish Council for Working Life and Social Research; Swedish Animal Welfare Agency; Swedish Radiation Protection Authority; National Scholarship Program of the Slovak Republic.

*Correspondence to: Igor Y. Belyaev, Department of Genetics, Microbiology and Toxicology, Stockholm University, S-106 91 Stockholm, Sweden. E-mail: igor.belyaev@gmt.su.se

Received for review 1 September 2006; Final revision received 7 March 2008

DOI 10.1002/bem.20445
Published online 6 October 2008 in Wiley InterScience (www.interscience.wiley.com).

INTRODUCTION

Microwave (MW) exposures vary in many parameters: power (specific absorption rate, incident power density), wavelength/frequency, near field–far field, polarization (linear, circular) continuous wave (CW) and pulsed fields (pulse repetition rate, pulse width or duty cycle, pulse shape, pulse to average power, etc.), modulation (amplitude, frequency, phase, complex), overall duration and intermittence of exposure (continuous, interrupted), acute and chronic exposures. With increased absorption of energy, thermal effects of microwaves are observed that deal with MW-induced heating. Specific absorption rate (SAR) or power flux density (PD) is a main determinant for the thermal MW effects. Many other physical parameters of exposure have been reported to be important for non-thermal biological effects, which are induced by MWs at intensities well below any heating. Reports of non-thermal effects started appearing in the 1970s and have previously been reviewed [Adey, 1981, 1999; Blackman, 1984, 1992; Gründler et al., 1988; Iskin, 1990; Devyatkov et al., 1994; Pakhomov et al., 1998; Belyaev et al., 2000; Betskii et al., 2000; Banik et al., 2003; Grigoriev et al., 2003; Grigoriev, 2004; Lai, 2005]. Some studies have reported stress response in exposed cultured cells [Kwee et al., 2001; Leszczynski et al., 2002; Blank and Goodman, 2004; Czyz et al., 2004]. In other studies, no effects of non-thermal microwaves were observed as it has recently been reviewed [Meltz, 2003]. Dependence of the MW effects on several physical parameters, including frequency, polarization, modulation and several biological variables could explain various outcomes of studies with non-thermal MWs [Adey, 1981, 1999; Blackman, 1984, 1992; Belyaev et al., 2000; Belyaev, 2005a]. Among other dependencies, the dependence of non-thermal effects of MWs on frequency has been reported [Pakhomov et al., 1998; Belyaev et al., 2000]. Frequency-dependent interactions of MWs with such targets as cellular membranes, chromosomal DNA, radicals, proteins and ions in protein cavities may be involved in effects of MWs [Ismailov, 1987; Belyaev et al., 1992b; Chiabrera et al., 2000; Binhi, 2002; de Pomerai et al., 2003; Ritz et al., 2004]. However, there is substantial lack of knowledge in biophysical modeling of MW-induced non-thermal biological effects.

It has been described that MWs under specific conditions of exposure either inhibited repair of radiation-induced DNA damage [Belyaev et al., 1992a,b,c,d, 1993] or induced single- and double-stranded DNA breaks (DSBs) [Lai and Singh, 1996; Lai and Singh, 1997]. The mechanisms of these effects are not understood but could be related to the induced changes in interaction of DNA with proteins [Belyaev et al., 1999].

Several proteins involved in DNA repair and DNA damage signaling such as phosphorylated H2AX (γ-H2AX) and the tumor suppressor TP53 binding protein 1 (53BP1) have been shown to produce discrete foci that co-localize to DSBs [Rogakou et al., 1999; Schultz et al., 2000; Rappold et al., 2001; Fernandez-Capetillo et al., 2002; Sedelnikova et al., 2002; Kao et al., 2003]. These foci are referred to as DNA repair foci and their identification is considered to be the most sensitive technique to study DSB. This technique allows measurement of a single DSB per cell.

The γ-H2AX and 53BP1 proteins are phosphorylated in response to DNA damage providing a scaffold structure for DSB repair [DiTullio et al., 2002]. According to the current model, this scaffold functions by recruiting proteins involved in the repair of DSB [Fernandez-Capetillo et al., 2002; Iwabuchi et al., 2003; Kao et al., 2003]. The scaffold is organized on a megabase-size chromatin domain containing a DSB regardless of the repair pathway that is involved in processing DSBs [Rogakou et al., 1999; Paull et al., 2000; Mochan et al., 2004]. Thus, identification of DNA repair foci provides ultimate sensitivity to detect DSBs regardless of the mechanism of their formation and repair.

We have recently described the effects of mobile phone MWs of global system for mobile communication (GSM) on chromatin conformation and 53BP1/γ-H2AX DNA repair foci in human lymphocytes from hypersensitive and healthy persons [Sarimov et al., 2004; Belyaev et al., 2005; Markova et al., 2005]. These data have shown that stress response, DNA repair inhibition and/or DNA damage is induced by GSM MWs under specific conditions of exposure and dependent on carrier frequency. Contrary to GSM, universal global telecommunications system (UMTS) mobile phones emit wide-band, 5 MHz, signals. MWs representing wide-band signal may hypothetically result in higher biological effects since they may include ''effective'' frequency windows, presumably around 1–10 MHz, in the frequency range of mobile communication, 200–2000 MHz [Sarimov et al., 2004]. In our previous studies, we analyzed effects of GSM MWs immediately after exposure. In the present study we investigated effects of UMTS MWs in comparison to the effects of GSM MWs within 72 h post-exposure. Another aim of our project was to compare the response of cells from hypersensitive and healthy persons. In a Dutch study, the group of persons recruited based on their experience of being sensitive to MWs and the healthy control group reported reduced well-being during exposure to UMTS MWs [Zwambron et al., 2003]. The reported hypersensitivity in humans to electromagnetic field (EMF) is a fairly new phenomenon and the etiology of the phenomenon is not

yet known. There are several symptoms that hypersensitive people report when they are in the proximity of different sources of EMF such as video display terminals of personal computers, electrical appliances or mobile phones. The symptoms are not specific to this illness and there is no known pathophysiological marker or diagnostic test [Hillert et al., 1999]. In studies aimed at identifying possible health effects of MWs it is of interest to include groups that may have an increased sensitivity to this exposure. Therefore, cells were included in this study from persons who, based on their own experience and ill health, report to have such hypersensitivity.

MATERIALS AND METHODS

Donors and Blood Samples

Blood samples were obtained from five healthy donors and five patients reporting hypersensitivity to EMF. Patients referred to the Department of Occupational and Environmental Health, Stockholm County Council, who reported hypersensitivity to EMF including microwaves from mobile phones were asked to participate in the study. The first patients to give consent to participate were included in the study.

The group reporting hypersensitivity to EMF consisted of four women and one man, 28–49 years old (Table 1, Supporting Information). Control healthy subjects were matched by age (±6 years) and gender. In the hypersensitive group one person was working, one was unemployed and three persons were on sick leave or received sickness compensation. Aforementioned hypersensitive persons were sick because of hypersensitivity to EMF, that is, no other causes of their ill health were identified in the medical work-up. There were no smokers among the participants and no subject was on any regular medication. All hypersensitive subjects reported symptoms triggered by electrical equipment including mobile phones that were not sources of light (in all five cases) and were characterized with regard to the symptom profile, triggering factors, time relation and avoidance behavior [Hillert et al., 1999]. In all pairs, the hypersensitive person scored higher than the matched control in the questionnaire on symptoms; mean score 86 compared to 12 (29 symptoms scored 0–4 for frequency and severity, maximum score 232) [Hillert et al., 1998]. In four of the persons reporting hypersensitivity to EMF the neurovegetative symptoms headache, fatigue and difficulties concentrating were more pronounced than skin symptoms. The mean score per question and person for neurovegetative symptoms was 2.3 in the hypersensitive group and 0.4 in the control group (maximum 4). The corresponding score for skin symptoms in the face and upper chest were 1.7 and 0.1, respectively. In all cases of reported hypersensitivity the symptoms were experienced within 24 h after exposure to a reported triggering factor, in most cases within 1 h. All patients reported that they tried to avoid triggering factors.

Fresh blood samples from persons reporting hypersensitivity and matched controls were coded and all data were analyzed in blind. Ethical permission was obtained from the Ethic Committee of the Karolinska Institutet, Stockholm, Sweden.

Chemicals and Reagents

Reagent grade chemicals were obtained from Sigma–Aldrich (St. Louis, MI) and Merck (Darmstadt, Germany). Double cytoslides coated with polylysine and cytoslide chambers were purchased from Shandon (Pittsburg, PA). Anti-53BP1 mouse antibody was kindly provided by Dr. T. Halazonetis, The Wistar Institute, University of Pennsylvania, Philadelphia, PA, USA. The antibody recognizes the C-terminal domain of the protein that corresponds to the BRCT domains. Anti-Phosphorylated histone H2AX (γ-H2AX) rabbit antibody was purchased from Trevigen-BioSite (Täby, Sweden).

Cells

Lymphocytes were isolated 30 min after drawing the peripheral blood by density gradient centrifugation in Ficoll-Paque (Pharmacia LKB, Uppsala, Sweden) according to the manufacturer's instructions. The cells were transferred to basal medium (BM): RPMI 1640 medium supplemented with 10% fetal bovine serum (FBS), 2 mM L-glutamine, 100 IU/ml penicillin, 100 μg/ml streptomycin (Gibco, BRL, Gaithersburg, MD) at 5% CO_2 and 37 °C in a humidified incubator. Adherent monocytes were removed by overnight incubation of the cell suspension in culture flasks (Falcon) at the cell density of 3×10^6 cells/ml in the volume of 10–40 ml. After this incubation, the cells in suspension were collected by centrifugation. The cell density was adjusted to approximately 2×10^6 cells/ml in fresh BM and the lymphocytes were pre-incubated for 2 h at 37 °C before exposure. The viability of cells was always above 98% as measured with trypan blue exclusion assay at the beginning of exposure and the fraction of blue cells did not exceed 10% at the end of cultivation. At different time points, samples were taken for assessment of apoptotic morphological changes. After staining with fluorescent dyes (acridine orange and propidium iodide), the cells with morphological changes characteristic for apoptosis, such as chromatin condensation, fragmentation of nuclei and

nuclei shrinkage, were scored by using fluorescence microscope as previously described [Belyaev et al., 2001].

Cell Exposure

Two samples with lymphocytes from matched hypersensitive and healthy persons, were simultaneously exposed to either GSM (905 MHz or 915 MHz) or UMTS (1947.4 MHz, middle channel), output power being the same, 0.25 W. Exposure of cells in 14 ml round-bottom tubes (Falcon), to GSM and UMTS MWs were performed using two specially designed installations, each based on a transverse electromagnetic line cell (TEM-cell) and a test mobile phone. The construction of the TEM-cells allowed relatively homogeneous exposure of samples in these specific frequency ranges [Martens et al., 1993; Malmgren, 1998]. Cells from each person were exposed at each exposure condition once in one tube.

All exposures were performed at 37 °C in a CO_2-incubator, in Falcon tubes, 2.5 ml of cell suspension per tube, 2×10^6 cells/ml. Duration of all exposures was 1 h. Lymphocytes were exposed to MWs using either a GSM900 test-mobile phone (model GF337, Ericsson, Lund, Sweden) or a UMTS/GSM test-mobile phone (model 6650, Nokia, Helsinki, Finland) as previously described [Sarimov et al., 2004; Belyaev et al., 2005]. The output of each phone was connected by the coaxial cable to the correspondent TEM-cell. For GSM900 exposure we used the channels 74 and 124 with the frequencies of 905 and 915 MHz, respectively. The GSM signal included standard modulation, Gaussian Minimum Shift Keying (GMSK). Discontinuous transmission mode was off during all exposures. For UMTS exposure we used 1947.4 MHz middle channel, 5 MHz-wide band. The UMTS signal included standard modulation, Quadrature Phase Shift Keying (QPSK). Voice modulation was applied neither in GSM nor in UMTS exposures. The power was kept constant during exposures to GSM and UMTS as monitored on-line using either a power meter (Bird 43, Bird Electronic, Cleveland, OH) or a power meter (Hewlett-Packard 435A, Palo Alto, CA), respectively.

The specific absorption rate (SAR) was determined by measurements and calculations. Transmitted and reflected power was measured using a power meter (Hewlett-Packard 435A) and a coaxial directional coupler (Narda 3001-20, Hauppage, NY). A signal generator (Agilent 7648C, Santa Rosa, CA) connected to a power amplifier (Mini-circuit ZHL-2-8-N, Brooklyn, NY) was used. The SAR was calculated from the absorbed power and the mass of the sample to be 37 mW/kg for the frequency of 915 MHz and 40 mW/kg for the frequency of 1947 MHz. Good correlation between these measurements and calculations using the finite different time domain (FDTD) method has been observed [Sarimov et al., 2004]. The SAR value varied from 15 to 145 mW/kg at different locations of the exposed samples as calculated with FDTD using 0.75 mm × 0.75 mm × 0.75 mm size cells. More than 50% of cells had SAR values between 20 and 40 mW/kg. The measurement uncertainty budget for our setups has been accessed according to Nikoloski et al. [2005]. The uncertainty budget of the exposures did not exceed 48% with a confidence level of 95%. Taking into account all possible uncertainties, the SAR values in all cells were always well below thermal effects. Changes of frequency by 10 MHz change neither the SAR value nor the SAR variation in the exposed samples. In our TEM-cells, the measured power loss did not exceed 1.2% and that could not cause any temperature rise. Our TEM-cells were well ventilated through the special holes in the wooden cages of the TEM-cells. Temperature was measured in the MW-exposed samples before, during and after exposure with a precision of 0.1 °C. No changes in temperature were induced during exposures.

Sham exposures were performed in the same TEM-cells as MW exposures with MW power off. The order of MW- and sham-exposures was randomized among sessions. In each experiment and for each donor, the sham exposures were performed in duplicate, in the TEM-cell for GSM exposure and in the TEM-cell for UMTS exposure. No differences were observed between sham-exposed samples (sham–sham exposures) and the data from two sham exposures were pooled for comparison with exposed samples. The 1-h heat treatment in a water bath, 41 °C, was used as a positive control for stress response. As a positive control for genotoxic effect, the cells were irradiated with ^{137}Cs γ-rays, 3 Gy, using a Gammacell 1000 (Atomic Energy of Canada, Ottawa, Canada) source. The dose rate was 10.6 Gy/min.

AVTD Measurements

The conformation of chromatin was studied by the method of anomalous viscosity time dependencies (AVTD). This technique was shown to be a sensitive assay to measure genotoxic effects and stress response [Belyaev et al., 2001; Sarimov et al., 2004; Torudd et al., 2005]. Cell lysis was performed immediately after exposure as has been previously described [Belyaev et al., 1999]. Briefly, lymphocytes were lysed in polyallomer centrifuge tubes (14 mm, Beckman, Fullerton, CA) by addition of 3.1 ml lysis solution (0.25 M Na_2EDTA, 2% (w/v) sarcosyl, 10 mM Tris-base, pH 7.4) to 0.1 ml of cell suspension. The lysates were prepared in triplicate and kept at 23 °C for 4 h in

darkness before AVTD measurements. The AVTDs in lysates were measured using an AVTD-analyzer (Archer-Aquarius, Moscow, Russia) as described previously [Belyaev et al., 1999]. The AVTDs were measured at the shear rate of 5.6 s^{-1} and shear stress of 0.007 N/m^2. For each experimental condition, AVTD was measured in three replicates. AVTD parameters were described in detail previously [Belyaev et al., 1998, 1999]. Briefly, the AVTD is characterized by three main parameters: (1) maximum value of viscosity; (2) area under AVTD, and (3) time for maximum viscosity. All these parameters depend on conformation, rigidity and molecular weight of nucleoids [Belyaev et al., 1999]. Normalized relative viscosity (NRV) measured as normalized ratio of maximum viscosities in exposed and sham-exposed samples is the most sensitive parameter and was used here to characterize condensation of chromatin.

Immunostaining and Foci Analysis

Immediately after exposure, the cells were placed on ice for 1 h to prevent repair of eventual DSBs. Cytoslide samples were prepared by using cytospin centrifugation according to the manufacturer's instructions (Shandon). The immunostaining was performed according to Schultz et al. [2000] with some modifications. Cells were fixed in cold 3% paraformaldehyde in PBS, pH 7.4, permeabilized with cold 0.2% Triton X-100 in PBS (for 15 and 10 min, respectively), stained with primary mouse antibody 53BP1 (1:20) and primary rabbit antibody γ-H2AX (1:100) prepared in 2% FBS in PBS for 1 h, followed by 3 washes in cold PBS and incubated for 1 h with secondary goat anti-mouse IgG (H + L) antibody conjugated with Alexa fluor 488 (Molecular Probes, Eugene, OR) together with goat anti-rabbit IgG (H + L) antibody conjugated with Alexa fluor 555 (Molecular Probes), both in 2% FBS and in 1:200 dilution, followed by 3 washes in cold PBS. After 20 min DNA staining in ToPro (3-iodide, 1 mM stock solution in DMSO, Molecular Probes) and 5 min washing in PBS, cytoslides were mounted with equilibration solution and antifade reagent (Slow fade Light Antifade Kit, Molecular Probes) and sealed with cover slides. The images were recorded from 5 to 10 fields of vision that were randomly selected from two slides on the confocal laser scanning microscope Zeiss Axiovert 100 M using the planapochromat 63×/1.4-numerical-aperture oil immersion objective and the LSM 510 software. Optical magnification was 630. Through-focus maximum projection images were acquired from optical sections 1.00 μm apart and with a section thickness of 2.00 μm in the *Z*-axis. Resolutions in the *X*- and *Y*-axis were 0.20 μm. Five optical sections were usually obtained for each field of vision and the final image was obtained by projection of all sections onto one plane. For each independent exposure experiment and for each exposure condition (subject, type of exposure, duration after exposure), 300–600 cells were analyzed.

Spatial co-localization of 53BP1 and γ-H2AX foci was analyzed in all cells and samples as previously described [Markova et al., 2007]. Briefly, at least partially overlapping foci were considered to co-localize while co-localization was not counted in the cases of a distinct gap between 53BP1 and γ-H2AX foci.

Statistical Analysis

We set the statistical power to 0.80 based on previously obtained data on effects of GSM MWs on human lymphocytes [Sarimov et al., 2004; Belyaev et al., 2005]. The data were analyzed with the Mann–Whitney *U*-test, Kruskal–Wallis test or by the Wilcoxon matched pairs signed rank test. A correlation analysis was performed using Spearman rank order correlation test. Results were considered as significantly different at $P < 0.05$.

RESULTS

Chromatin Conformation

Irradiation with 3 Gy resulted in a statistically significant 3-fold increase in AVTD dealing with radiation-induced relaxation of chromatin (data not shown). In Table 2 (Supporting Information), primary data for all subjects obtained immediately after exposure to MWs are provided to document the variability in responses between different exposures/subjects. These data indicate possible individual variability in the effects. However, this conclusion seems to be premature. Repeated experiments with cells from the same donors are needed to prove individual variability; this was not the aim of our study. In those cases where heat shock significantly affected cells (donors 314, 315, and 906) a decrease in NRV that corresponds to chromatin condensation was observed immediately following 1 h treatment. MWs at the frequency of 915 MHz induced significant chromatin condensation in cells of four subjects (314, 315, 809, and 906) ($P < 0.05$, Mann–Whitney *U*-test). Significant decrease in NRV was also observed after exposure to MWs at 905 MHz in cells from three donors (314, 315, and 413). UMTS MWs at 1947.4 MHz resulted in significant condensation only in cells from donor 314. These data suggested that effects of MWs might be

frequency-dependent and various responses might be observed in cells from different individuals.

Although statistically significant chromatin condensation was observed in cells from some donors at all treatment conditions immediately after exposure (Table 2, Supporting Information), no such consistent response was seen 24 h following exposure to MWs when chromatin could be either condensed or decondensed (not shown). We tested the hypothesis that effects of different treatments would differ between groups of hypersensitive and normal persons using Wilcoxon matched pairs signed rank test. Only four matched pairs were included in this analysis because no cells from donor 801 were available to study changes in chromatin conformation by the AVTD technique. No statistically significant differences in the effects on chromatin conformation were seen, $P > 0.05$, between cells from control and hypersensitive groups as measured after all treatment conditions either immediately or 24 h following exposure. Therefore, the data pooled from all subjects, normal and hypersensitive, were analyzed for each treatment condition (Fig. 1). Based on the pooled data, statistically significant chromatin condensation was found in lymphocytes immediately after MW exposure at 915 MHz and heat shock at 41 °C ($P < 0.05$, Mann–Whitney U-test). From all treatments, only heat shock resulted in significant effects ($P < 0.02$, Mann–Whitney U-test) in the pooled data obtained 24 h following treatments (Fig. 1).

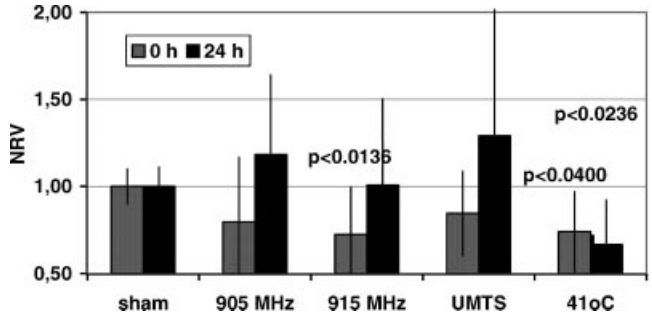

Fig. 1. The conformation of chromatin was studied by the method of anomalous viscosity time dependencies (AVTD) in five experiments with lymphocytes from nine subjects, four hypersensitive and five healthy subjects. Normalized relative viscosity (NRV) was used to characterize condensation of chromatin. For each subject and treatment condition the AVTD measurements of exposed and sham-exposed samples were performed in triplicate. Data are shown as mean and standard deviation (SD). In this figure and other histograms, *P*-values belong to bars that are situated below.

53BP1/γ-H2AX Foci

Irradiation of lymphocytes with 3 Gy resulted in a statistically significant increase in 53BP1/γ-H2AX foci dealing with radiation-induced DSBs, around 10 foci/Gy/cell as analyzed 1 h post-irradiation (data not shown). For three control donors, the data were obtained up to 72 h after irradiation of lymphocytes with doses of 0.5, 1, and 2 Gy providing clear dose response and time kinetics for radiation-induced 53BP1/γ-H2AX (data not shown). These data will be analyzed elsewhere. Typical images of lymphocytes with DNA repair foci under various treatment conditions are shown in Figure 2. The primary data obtained from cells of each subject immediately after 1 h exposure are shown in Tables 3A and 4A (Supporting Information). We observed a distinct MW-induced reduction in the level of 53BP1 and γ-H2AX foci both in cells from control and hypersensitive subjects in response to 915 MHz. UMTS MWs also consistently reduced 53BP1 foci in cells from all subjects and reduced γ-H2AX foci in most subjects. Very similar reductions in 53BP1/γ-H2AX foci were

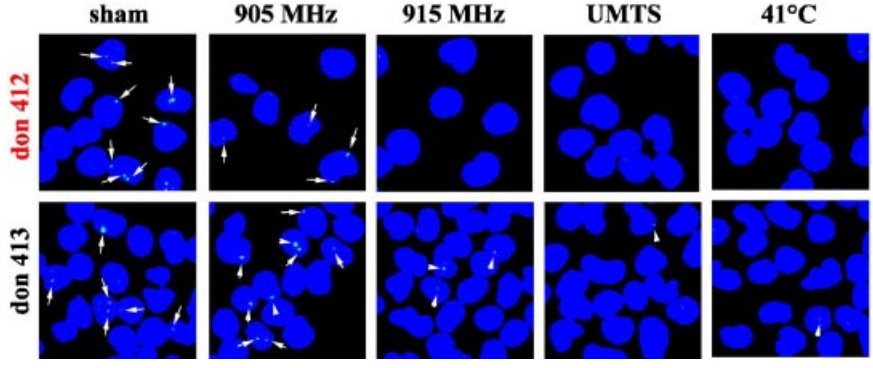

Fig. 2. Panels show typical images of fixed human lymphocytes (counterstained in blue with ToPro-3-iodide) from hypersensitive (subject 412) and matched healthy subject (subject 413) with 53BP1 foci (stained in green with Alexa fluor 488 and designated by arrows) as revealed by immunostaining and confocal laser microscopy. Foci were seen in sham-exposed cells. Significantly fewer foci were observed after 1-h exposure to GSM MWs at 915 MHz, UMTS MWs at 1947.4 MHz and heat shock, 41 °C (Table 3). [The color figure for this article is available online at www.interscience.wiley.com.]

observed in lymphocytes from control and hypersensitive subjects in response to heat shock at 41 °C (Tables 3A and 4A, Supporting Information).

The response to 905 MHz was not consistent among subjects and either increase or decrease in amount of 53BP1 and γ-H2AX foci or no effect was observed dependent on subject (Tables 3 and 4, Supporting Information). In particular, a statistically significant induction of γ-H2AX was seen in cells from donor 907, suggesting that 905 MHz may induce DSBs in cells from this donor (Table 4, Supporting Information).

There was no statistically significant difference in effects between groups of hypersensitive and healthy persons ($P > 0.05$, Wilcoxon matched pairs signed rank test) under all conditions of exposure. All data were pooled and highly significant inhibitory effects on formation of DNA repair foci were found as analyzed immediately after 1 h exposure to UMTS, 915 MHz and heat shock (Tables 3A and 4A, Supporting Information; Fig. 3).

The most striking observation was that these MW-induced inhibitory effects continued up to 3 days following 1 h exposure to MWs (Fig. 3). This long-lasting inhibition of the 53BP1/γ-H2AX foci was consistently observed in lymphocytes from both control and hypersensitive subjects in response to GSM MWs at 915 MHz and UMTS MWs (Tables 3B and C and 4B and C; Supporting Information). Responses to these MW exposures were stronger than response to heat shock at 41 °C that tended to disappear and was not statistically significant as analyzed 3 days following exposure (Tables 3C and 4C, Supporting Information; Fig. 3). The viability of cells was always above 98% as measured with trypan blue exclusion assay at the beginning of exposure and the fraction of blue cells did not exceed 10% at the end of cultivation. Apoptosis varied from 5% at the beginning to 20% at 72 h after beginning cultivation. These data are in line with previously published results [Torudd et al., 2005]. Despite increasing level of apoptosis, the inhibition of DNA repair foci was observed in a majority of cells at all time points showing that the observed effects did not correlate with onset of apoptosis. No activation of lymphocytes was observed by analysis of cell morphology and DNA content using obtained images of sham-exposed and MW-exposed lymphocytes. Therefore, inhibitory effects were unlikely to be caused by activation of lymphocytes or by alternation of cell cycle distribution from G0 to G1-S-phases.

Similar to the data obtained immediately after exposure, the response to 905 MHz was not consistent among subjects, and either an increase or decrease in the amount of foci was observed 24 and 72 h after exposure

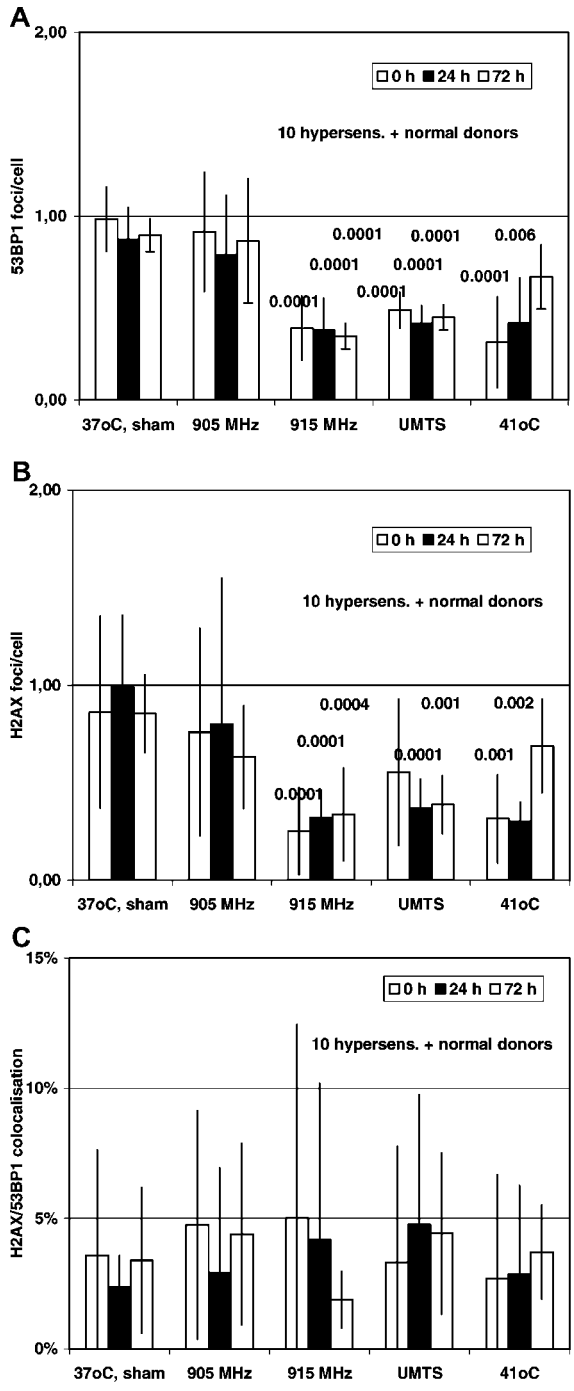

Fig. 3. 53BP1 foci (**A**), γ-H2AX foci (**B**), and co-localization of 53BP1/γ-H2AX foci as normalized to amount of γ-H2AX foci (**C**) in human lymphocytes immediately (0 h), 24 and 72 h following exposure to GSM MWs at 905 and 915 MHz, UMTS MWs at 1947.4 MHz, and heat shock at 41 °C, as measured by immunostaining and confocal laser microscopy. Mean values for cells from 10 subjects (five hypersensitive and five matched healthy subjects) and standard deviations are shown. Three hundred to 600 cells from 5 to 10 images were analyzed per treatment condition for each subject. *P*-values are shown for those treatments that were statistically significantly different from sham-exposure as analyzed by the Wilcoxon matched pairs signed rank test.

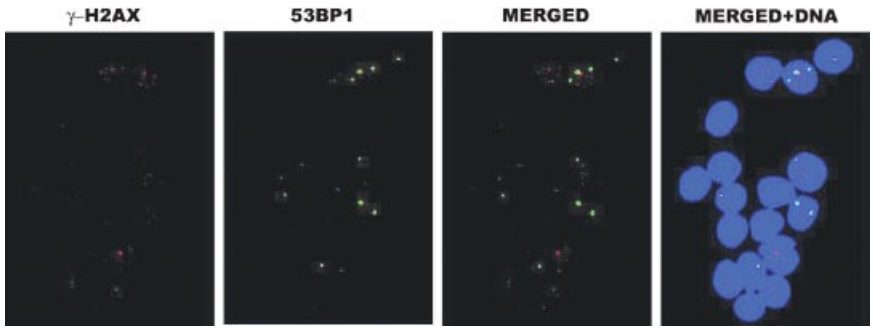

Fig. 4. Typical image showing the lack of co-localization between majorities of 53BP1 and γ-H2AX foci is shown in sham-exposed lymphocytes from one control donor. [The color figure for this article is available online at www.interscience.wiley.com.]

(Tables 3B and C and 4B and C, Supporting Information). Interestingly, γ-H2AX was statistically significantly induced by exposure to 905 MHz in cells from donor 907 as analyzed 24 h following exposure. This observation was in line with the induced level of foci as observed in cells of this donor immediately after exposure (Table 4, Supporting Information). Similar increases in 53BP1 foci, although statistically insignificant, were seen in cells from this donor (Table 3, Supporting Information).

For each group of subjects, we verified the hypothesis that MW exposure affects formation of 53BP1 and γ-H2AX foci. For this purpose, we compared effects of microwave exposures with sham (multiple comparisons of sham, 905, 915, and 1947.4 MHz) using the Kruskal–Wallis ANOVA by ranks. This multiple comparison showed that MWs affected both 53BP1 and γ-H2AX foci in cells from both hypersensitive and matched control persons at very high significance levels (Table 5, Supporting Information). Even stronger significance levels were obtained if the data from two groups were pooled and analyzed together with the Kruskal–Wallis ANOVA by ranks. These data show that the MW exposures as used in this study significantly affect the formation of DNA repair foci in human lymphocytes.

We next verified the hypothesis that the effects of GSM MWs are frequency-dependent. This was done by comparison of MW effects at 905 MHz and 915 MHz in cells from both hypersensitive and matched control persons by the Mann–Whitney *U*-test or Wilcoxon matched pairs signed rank test when applicable. This comparison showed that GSM MWs inhibit formation of the 53BP1/γ-H2AX foci dependent on frequency in cells from both normal and hypersensitive subjects (Table 6, Supporting Information).

We also tested whether effects of GSM MWs at the effective frequency of 915 MHz were the same as effects of UMTS MWs (Table 7, Supporting Information). Comparison of the MW effects on cells from hypersensitive subjects and matched control healthy persons was performed by the Wilcoxon matched pairs signed rank test. This comparison demonstrated that the effects of UMTS MWs and GSM MWs at 915 MHz on the formation of the 53BP1/γ-H2AX DNA repair foci were different for hypersensitive ($P < 0.02$ for 53BP1 and $P < 0.01$ for γ-H2AX, respectively) but not for control subjects ($P > 0.05$). The non-parametric statistics used here do not indicate the specificity of the differences between the effects of GSM and UMTS MWs on cells from hypersensitive subjects.

For all treatment conditions, a correlation between 53BP1 and γ-H2AX foci was observed ($R > 0.5$, $P < 0.000001$, Spearman rank order correlation test) both in cells from control and hypersensitive subjects. However, the majority of 53BP1 and γ-H2AX foci did not co-localize as the co-localization did not exceed 5% (Fig. 3C). These data are in line with results of our previous publications showing very low co-localization of γ-H2AX and 53BP1 foci in normal human lymphocytes and primary human fibroblasts [Markova et al., 2005, 2007]. Figure 4 shows that the majority of 53BP1 and γ-H2AX foci do not co-localize.

DISCUSSION

It is widely accepted that γ-H2AX and 53BP1 foci mark the locations of DSBs. Quantitative analysis of these foci show that these and other markers of DSB repair co-localize in the majority of DNA repair foci induced by radiations and genotoxic chemicals [Sengupta et al., 2004; Lee et al., 2005; Bocker and Iliakis, 2006; Markova et al., 2007]. However, this co-localization is usually only partial and, to our knowledge, 100% co-localization has never been established by quantitative analysis. We confirm here our previously reported finding that the majority

of 53BP1 and γ-H2AX foci do not co-localize in either untreated or MW/heat-shock treated lymphocytes [Markova et al., 2005]. Similarly, a low level of 53BP1 and γ-H2AX foci co-localization was observed in untreated primary human VH-10 fibroblasts [Markova et al., 2007]. However, radiation-induced foci showed significant co-localization that was dependent both on dose and post-irradiation time [Markova et al., 2007]. Perhaps different marker proteins have different kinetics of binding to and remaining at the locations of DSBs that may be dependent on treatment dose, post-treatment time, origin of DSB and cell type.

It has previously been shown that non-thermal MWs affected conformation of chromatin in *E. coli* cells, rat thymocytes and human lymphocytes under specific conditions of exposure [Belyaev et al., 2000, 2005; Markova et al., 2005]. Usually, in human lymphocytes, non-thermal MWs transiently condensed chromatin in contrast to decondensation, which has been observed immediately after genotoxic impacts such as ionizing radiation [Belyaev et al., 1999, 2001; Torudd et al., 2005]. The AVTD data obtained in this study are in line with the data published previously. GSM MWs at 915 MHz resulted in statistically significant and transient condensation of chromatin similar to condensation induced by heating (Table 2, Supporting Information). No heating was induced in samples exposed to MWs. The SAR values at different locations of the exposed samples were always well below thermal effects. Therefore, the MW effects could not be attributed to the heating, although a similar response was observed both after MW exposure and heat shock. This similarity indicates that MW exposure at 915 MHz is a stress factor for human peripheral blood lymphocytes. Stress response proteins and particularly hsp70 was activated by MWs of mobile phones in some previous studies as measured by Western blot [Kwee et al., 2001; Weisbrot et al., 2003] and even candidate gene sequences in molecular mechanism of this stress response were identified [Blank and Goodman, 2004]. Notably, both responses to heating and non-thermal MWs varied among donors, suggesting individual variability in chromatin condensation induced by these factors. In general, the effects of heating and MWs on chromatin condensation were less pronounced compared to the effects on DNA repair foci (Tables 2–4, Supporting Information).

We have recently described the effects of MWs from GSM mobile phones on 53BP1/γ-H2AX DNA repair foci in human lymphocytes [Belyaev et al., 2005; Markova et al., 2005]. GSM MWs at 915 MHz inhibited the formation of the DNA repair foci in lymphocytes from hypersensitive and control subjects [Belyaev et al., 2005; Markova et al., 2005]. Here, we extend the previously published data and report that exposure to GSM MWs at 915 MHz consistently inhibits formation of the 53BP1/γ-H2AX DNA repair foci in cells from 26 tested hypersensitive and normal persons. The prevalence of women among persons reporting hypersensitivity to electromagnetic fields, around 70%, is typical for Sweden. The ratio of women:men in this study, 8:2, represents the prevalence of women. Effects of UMTS MWs were observed in all eight samples obtained from women. Therefore, the UMTS findings seem to be general for women. There are reports that non-thermal effects of MWs may be gender-dependent [Belyaev, 2005a]. Thus, more data are needed to complement our finding on the UMTS effects on lymphocytes from men. Our findings regarding effects of GSM MWs at 915 MHz on chromatin conformation and DNA repair foci seem to be general with respect to gender because these effects were observed in cells from both men and women as has been shown in this paper and previously [Belyaev et al., 2005; Markova et al., 2005].

Our previous data have shown that MWs at specific frequencies inhibit repair of radiation-induced DNA damage in *E. coli* cells [Belyaev et al., 1992b, 1993]. Thus, our working hypothesis was that a decrease in 53BP1/γ-H2AX foci could be a manifestation of the inhibitory effects of MW on repair of spontaneous DSBs. Notably, both 53BP1 and γ-H2AX foci are similarly inhibited by heat shock and MWs from mobile phones. This inhibition may be caused by a decrease in accessibility of DSBs to proteins because of stress-induced chromatin condensation. The molecular mechanisms of the inhibitory effects observed here may also include downregulation of 53BP1 or delocalization of this protein from DNA repair foci. Analysis of these mechanisms was not within the scope of this study. While molecular mechanisms are unknown, the obtained data have clearly shown that MW from mobile phones, similar to moderate hyperthermia, can significantly inhibit DNA repair in human lymphocytes. Disruption of the balance between cellular repair systems and DNA damage may be of significant importance in the genotoxic effects of GSM/UMTS mobile communication including genomic instability and cancer [Galeev, 2000].

In contrast to 915 MHz exposures, MWs at 905 MHz did not affect cells in most cases. However, 905 MHz could either decrease or increase the amount of foci in cells from some subjects. Similar interindividual variability for the 905 MHz effects was observed in a previous study, where 905 MHz MWs induced DNA repair foci in cells of 4 donors out of 10 [Markova et al., 2005]. Does this mean that 905 MHz exposures

induced DSBs in those cases where foci increased? The data obtained here neither exclude nor directly support such a possibility. Replicated experiments with cells from the same donors may provide information regarding the nature of this variability in response to 905 MHz. Stronger variability of MW effects at 905 MHz compared to effects at 915 MHz provides additional evidence of the importance of carrier frequency in studies of MW effects.

It should be noted that the formation of DNA repair foci involves phosphorylation of 53BP1/γ-H2AX proteins [DiTullio et al., 2002; Fernandez-Capetillo et al., 2002]. It is thus possible that the observed effects of MWs and heat shock at the level of 53BP1/γ-H2AX foci formation were due to a change in phosphorylation.

Some recent publications show that heat shock can induce formation of γ-H2AX foci in cultured cells [Takahashi et al., 2004; Kaneko et al., 2005]. Mechanisms of this induction are not known. The strongest effects were observed in cancerous S-phase cells that usually have very high background levels of γ-H2AX foci, up to 20 foci/cell. It is therefore supposed that heat affects replication resulting in formation of DSBs at the replication forks [Takahashi et al., 2004]. However, this mechanism cannot account for our findings because we used primary human lymphocytes in G0 with relatively low background levels of foci, up to 2 foci/cell. Differences in cell type and stage of cell cycle may provide an alternative explanation for the discrepancies in our findings and the aforementioned literature data. This suggestion is supported by a recent publication where the authors did not observe induction of γ-H2AX foci by heat shock in cultured human amnion FL cells [Zhou et al., 2006]. It is interesting to note here, that effects of heat shock on chromatin as measured with AVTD technique in primary G0 human lymphocytes, had a nonlinear dependence on temperature within 40–45 °C [Sarimov et al., 2004]. Contrary to chromatin condensation that was induced in human lymphocytes at 40–42 °C and 0.5–2 h treatment, chromatin decondensation was observed at heat shock with higher temperature and longer duration of treatment. It may be another reason for discrepancies between data. Indeed, inhibitory effects of heat shock on γ-H2AX foci were observed at 41 °C and one-two h treatment in our studies. The temperature-dependent induction of H2AX phosphorylation was observed at temperatures of more than 41.5 °C and at longer durations of treatment [Takahashi et al., 2004].

Significant variations in the response of cells were observed in both hypersensitive and control groups of subjects. This investigation and previous studies [Belyaev et al., 2005; Markova et al., 2005] provide unequivocal evidence that MWs from mobile phones induce adverse effects in lymphocytes from hypersensitive and healthy subjects. However, the only difference between the groups was found here by comparing the effects of UMTS MWs and GSM MWS at 915 MHz on the formation of the 53BP1/γ-H2AX DNA repair foci (Table 7, Supporting Information). These effects were different for hypersensitive but not for control subjects. The non-parametric statistics that were used do not reveal the specificity of the differences between the effects of GSM and UMTS MWS on cells from hypersensitive subjects. More data are needed to study the nature of these differences.

In general, the comparison of pooled data obtained with all treatments did not show significant differences between the groups of controls and hypersensitive subjects. This result might be explained by the heterogeneity in groups of hypersensitive and control persons. Even if there is such a difference, it would be masked by the large individual variation between subjects, which was observed in both control and hypersensitive groups. An additional problem may be the lack of any objective criteria for selection of a study group consisting of persons that are either truly hypersensitive or insensitive to EMF (although this has yet to be proven). One cannot exclude that compensatory reactions are less efficient in the hypersensitive persons providing stronger connection of reactions to MWs at the cellular level with symptoms of hypersensitivity.

The data obtained in a previous study [Markova et al., 2005] and here clearly show that MWs from GSM mobile phones affect the formation of 53BP1/γ-H2AX DNA repair foci in human lymphocytes dependent on carrier frequency. This result, obtained in lymphocytes from 10 healthy and 10 hypersensitive persons, is of great importance. First, such frequency dependence suggests a mechanism for microwave effects that does not deal with heating. Investigation of this mechanism and the molecular targets of the frequency-dependent effects of MWs is a fundamental problem. Second, the data indicate that a possibility may exist to choose those carrier frequencies for GSM mobile communications that do not adversely affect human cells.

Inhibition of DNA repair foci in human lymphocytes was induced by specific GSM/UMTS signals from mobile phones at intensities well below the safety standards of the International Commission on Non-Ionizing Radiation Protection (ICNIRP) [ICNIRP, 1998]. The SAR values at different locations of the exposed samples were always well below thermal effects. In addition, the effects of GSM 915 MHz and UMTS MWs on DNA repair foci were observed in a majority of cells excluding any explanation based on micro-thermal points due to SAR variation. Therefore,

the MW effects were non-thermal. Changes of frequency by 10 MHz changed neither the SAR value nor the SAR variation between cells in the exposed samples. Dependence of the MW effect on frequency, 905 MHz versus 915 MHz, provided further evidence for the non-thermal nature of the MW effect described here. Thus, an important aspect of our findings is that criteria other than ''thermal'' criteria need to be established and utilized in the development of safety standards. In particular, our data indicate that different frequencies should be considered separately in setting the limits for safety standards.

In our pilot study on the effects of GSM MWs on the DNA repair foci we used 2 h exposure [Belyaev et al., 2005]. In the current study and in the previous one [Markova et al., 2005], the effects of 1 h exposure were investigated. Regardless of the time of exposure, formation of DNA repair foci was almost completely blocked by GSM MWs. These data suggest that the inhibitory effects of MWs reach saturation at least at 1 h exposure. Our yet unpublished results show that GSM-induced condensation of chromatin has approximately linear dependence on duration of exposure within 30 min and levels off at longer exposures. Similarly, inhibitory effects of MW exposure regarding DNA repair may be dependent on exposure time at short periods and leveling off for longer exposures.

Based on the established dependencies of non-thermal effects of MWs on frequency we hypothesized that MW representing wide-band signals such as UMTS (5 MHz) may result in higher biological effects compared to relatively narrower GSM signal (200 kHz) because of the higher probability of ''effective'' frequencies within the UMTS bands [Belyaev, 2005b]. The data obtained here are consistent with our hypothesis and show, for the first time, that UMTS MWs (1947.4 MHz, middle channel) inhibit formation of the 53BP1/γ-H2AX DNA repair foci in human lymphocytes both from hypersensitive and healthy subjects. In addition, UMTS signals significantly differ from GSM signals due to different modulation techniques. Modulation might be of great biological significance, thereby providing a possible alternative explanation for more pronounced effects in response to UMTS signals. Remarkably, inhibitory effects induced by MWs from UMTS mobile phones were rather stable and persisted for at least 72 h, even longer than the stress response following heat shock. Contrary to GSM communication, where all providers use the same fixed frequency channels, different UMTS frequency bands are usually assigned to different providers. Technically, it would be easy to adopt specific UMTS bands for mobile communication if it were proven in replicated studies that some of these frequency bands do not produce adverse effects compared to other bands. Identification of those signals and frequency channels/bands for mobile communication, which do not affect human primary cells, is a high priority task in the development of safe mobile communication.

CONCLUSIONS

Microwaves from UMTS/GSM mobile phones at non-thermal levels lower than the ICNIRP safety standards affect formation of 53BP1/γ-H2AX DNA repair foci and chromatin conformation in human lymphocytes from subjects reporting hypersensitivity to electromagnetic fields and healthy subjects. The MW effects on DNA repair foci were more pronounced. These effects depended on carrier frequency and type of signal and suggested misbalance between DNA damage and DNA repair. The results also show that inhibition of DNA repair foci is rather stable and observed up to 3 days following 1 h exposure to non-thermal microwaves from GSM/UMTS mobile phones. No significant differences in effects between groups of healthy and hypersensitive subjects were observed, except for the effects of UMTS MWs and GSM-915 MHz MWs on the formation of the DNA repair foci, which were different for hypersensitive but not for control subjects.

ACKNOWLEDGMENTS

We thank T. Halazonetis for donation of 53BP1 antibodies, L.E. Paulsson and G. Anger for verification of the experimental unit for exposure to microwaves, R. Sarimov for help with statistical analysis and E. Thunberg for obtaining and coding of blood samples. We are thankful to Dr. S. Lang and Mr. P. Sinisalo for valuable consultations and help with the UMTS exposure installation.

REFERENCES

Adey WR. 1981. Tissue interactions with nonionizing electromagnetic fields. Physiol Rev 61:435–514.

Adey WR. 1999. Cell and molecular biology associated with radiation fields of mobile telephones. In: Ueno S, editor. Review of radio science, 1996–1999. Oxford: Oxford University Press. pp. 845–872.

Banik S, Bandyopadhyay S, Ganguly S. 2003. Bioeffects of microwave—A brief review. Bioresour Technol 87:155–159.

Belyaev I. 2005a. Non-thermal biological effects of microwaves. Microwave Rev 11:13–29. Available from URL: http://www.mwr.medianis.net/pdf/Vol11No2-03-IBelyaev.pdf.

Belyaev I. 2005b. Nonthermal biological effects of microwaves: Current knowledge, further perspective, and urgent needs. Electromagn Biol Med 24:375–403.

Belyaev IY, Alipov YD, Shcheglov VS. 1992a. Chromosome DNA as a target of resonant interaction between Escherichia coli cells and low-intensity millimeter waves. Electro- Magnetobiol 11:97–108.

Belyaev IY, Alipov YD, Shcheglov VS, Lystsov VN. 1992b. Resonance effect of microwaves on the genome conformational state of E. coli cells. Z Naturforsch [C] 47:621–627.

Belyaev IY, Shcheglov VS, Alipov YD. 1992c. Existence of selection rules on helicity during discrete transitions of the genome conformational state of E.coli cells exposed to low-level millimeter radiation. Bioelectrochem Bioenerg 27: 405–411.

Belyaev IY, Shcheglov VS, Alipov YD. 1992d. Selection rules on helicity during discrete transitions of the genome conformational state in intact and X-rayed cells of E. coli in millimeter range of electromagnetic field. In: Allen MJ, Cleary SF, Sowers AE, Shillady DD, editors. Charge and field effects in biosystems. Basel, Switzerland: Birkhauser. pp. 115–126.

Belyaev IY, Shcheglov VS, Alipov YD, Radko SP. 1993. Regularities of separate and combined effects of circularly polarized millimeter waves on E. coli cells at different phases of culture growth. Bioelectrochem Bioenerg 31: 49–63.

Belyaev IY, Alipov YD, Matronchik AY. 1998. Cell density dependent response of E. coli cells to weak ELF magnetic fields. Bioelectromagnetics 19:300–309.

Belyaev IY, Eriksson S, Nygren J, Torudd J, Harms-Ringdahl M. 1999. Effects of ethidium bromide on DNA loop organisation in human lymphocytes measured by anomalous viscosity time dependence and single cell gel electrophoresis. Biochim Biophys Acta 1428:348–356.

Belyaev IY, Shcheglov VS, Alipov ED, Ushakov VL. 2000. Nonthermal effects of extremely high frequency microwaves on chromatin conformation in cells in vitro: Dependence on physical, physiological and genetic factors. IEEE Trans Microwave Theory Tech 48:2172–2179.

Belyaev IY, Czene S, Harms-Ringdahl M. 2001. Changes in chromatin conformation during radiation-induced apoptosis in human lymphocytes. Radiat Res 156:355–364.

Belyaev IY, Hillert L, Protopopova M, Tamm C, Malmgren LO, Persson BRR, Selivanova G, Harms-Ringdahl M. 2005. 915 MHz microwaves and 50 Hz magnetic field affect chromatin conformation and 53BP1 foci in human lymphocytes from hypersensitive and healthy persons. Bioelectromagnetics 26:173–184.

Betskii OV, Devyatkov ND, Kislov VV. 2000. Low intensity millimeter waves in medicine and biology. Crit Rev Biomed Eng 28:247–268.

Binhi VN. 2002. Magnetobiology: Underlying physical problems. San Diego: Academic Press.

Blackman CF. 1984. Sub-chapter 5.7.5, Biological effects of low frequency modulation of RF radiation. In: Cahill DF, editor. Biological effects of radiofrequency radiation: EPA-600/8-83-026F. Research Triangle Park, NC: U.S. Environmental Protection Agency. pp. 5-88–5-92.

Blackman CF. 1992. Calcium release from nervous tissue: experimental results and possible mechanisms. In: Ramel C, editor. Interaction mechanisms of low-level electromagnetic fields in living systems. Oxford: Oxford University Press. pp. 107–129.

Blank M, Goodman R. 2004. Comment: A biological guide for electromagnetic safety: The stress response. Bioelectromagnetics 25:642–646; discussion 647-648.

Bocker W, Iliakis G. 2006. Computational methods for analysis of foci: Validation for radiation-induced gamma-H2AX foci in human cells. Radiat Res 165:113–124.

Chiabrera A, Bianco B, Moggia E, Kaufman JJ. 2000. Zeeman-Stark modeling of the RF EMF interaction with ligand binding. Bioelectromagnetics 21:312–324.

Czyz J, Guan K, Zeng Q, Nikolova T, Meister A, Schonborn F, Schuderer J, Kuster N, Wobus AM. 2004. High frequency electromagnetic fields (GSM signals) affect gene expression levels in tumor suppressor p53-deficient embryonic stem cells. Bioelectromagnetics 25:296–307.

de Pomerai DI, Smith B, Dawe A, North K, Smith T, Archer DB, Duce IR, Jones D, Candido EP. 2003. Microwave radiation can alter protein conformation without bulk heating. FEBS Lett 543:93–97.

Devyatkov ND, Golant MB, Betskij OV. 1994. Peculiarities of usage of millimeter waves in biology and medicine (in Russian). Moscow: IRE RAN. 164 pp.

DiTullio RA Jr, Mochan TA, Venere M, Bartkova J, Sehested M, Bartek J, Halazonetis TD. 2002. 53BP1 functions in an ATM-dependent checkpoint pathway that is constitutively activated in human cancer. Nat Cell Biol 4:998–1002.

Fernandez-Capetillo O, Chen HT, Celeste A, Ward I, Romanienko PJ, Morales JC, Naka K, Xia Z, Camerini-Otero RD, Motoyama N, Carpenter PB, Bonner WM, Chen J, Nussenzweig A. 2002. DNA damage-induced G2-M checkpoint activation by histone H2AX and 53BP1. Nat Cell Biol 4:993–997.

Galeev AL. 2000. The effects of microwave radiation from mobile telephones on humans and animals. Neurosci Behav Physiol 30:187–194.

Grigoriev YG. 2004. Bioeffects of modulated electromagnetic fields in the acute experiments (results of Russian researches). *Annual of Russian National Committee on Non-Ionisng Radiation Protection.* Moscow: ALLANA. pp. 16–73.

Grigoriev YG, Stepanov VS, Nikitina VN, Rubtcova NB, Shafirkin AV, Vasin AL. 2003. ISTC Report. Biological effects of radiofrequency electromagnetic fields and the radiation guidelines. Results of experiments performed in Russia/ Soviet Union. Moscow: Institute of Biophysics, Ministry of Health, Russian Federation.

Gründler W, Jentzsch V, Keilmann F, Putterlik V. 1988. Resonant cellular effects of low intensity microwaves. Frölich H, Biological coherence and response to external stimuli. Berlin: Springer-Verlag. pp. 65–85.

Hillert L, Kolmodin Hedman B, Dolling BF, Arnetz BB. 1998. Cognitive behavioural therapy for patients with electric sensitivity - a multidisciplinary approach in a controlled study. Psychother Psychosom 67:302–310.

Hillert L, Kolmodin Hedman B, Söderman E, Arnetz BB. 1999. Hypersensitivity to electricity: Working definition and additional characterization of the syndrome. J Psychosom Res 47:420–438.

ICNIRP. 1998. ICNIRP Guidelines. Guidelines for limiting exposure to time-varying electric, magnetic, and electromagnetic fields (up to 300 GHz). Health Phys 74:494–522.

Iskin VD. 1990. Biological effects of millimeter waves and correlation method of their detection (in Russian). Kharkov: Osnova. p. 244.

Ismailov ES. 1987. Biophysical action of microwaves. Moscow: Energoatomizdat. p. 143.

Iwabuchi K, Basu BP, Kysela B, Kurihara T, Shibata M, Guan D, Cao Y, Hamada T, Imamura K, Jeggo PA, Date T, Doherty AJ. 2003. Potential role for 53BP1 in DNA end-joining repair through direct interaction with DNA. J Biol Chem 278:36487–36495.

Kaneko H, Igarashi K, Kataoka K, Miura M. 2005. Heat shock induces phosphorylation of histone H2AX in mammalian cells. Biochem Biophys Res Commun 328:1101-1106.

Kao GD, McKenna WG, Guenther MG, Muschel RJ, Lazar MA, Yen TJ. 2003. Histone deacetylase 4 interacts with 53BP1 to mediate the DNA damage response. J Cell Biol 160:1017–1027.

Kwee S, Raskmark P, Velizarov S. 2001. Changes in cellular proteins due to environmental non-ionizing radiation. I. Heat-shock proteins. Electromagn Biol Med 20:141–152.

Lai H. 2005. Biological effects of radiofrequency electromagnetic field. In: Bowlin GL, editor. Encyclopedia of biomaterials and biomedical engineering. New York, NY: Marcel Decker. pp. 1–8.

Lai H, Singh NP. 1996. Single- and double-strand DNA breaks in rat brain cells after acute exposure to radiofrequency electromagnetic radiation. Int J Radiat Biol 69:513–521.

Lai H, Singh NP. 1997. Melatonin and a spin-trap compound block radiofrequency electromagnetic radiation-induced DNA strand breaks in rat brain cells. Bioelectromagnetics 18: 446–454.

Lee AC, Fernandez-Capetillo O, Pisupati V, Jackson SP, Nussenzweig A. 2005. Specific association of mouse MDC1/NFBD1 with NBS1 at sites of DNA-damage. Cell Cycle 4:177–182.

Leszczynski D, Joenvaara S, Reivinen J, Kuokka R. 2002. Non-thermal activation of the hsp27/p38MAPK stress pathway by mobile phone radiation in human endothelial cells: Molecular mechanism for cancer- and blood-brain barrier-related effects. Differentiation 70:120–129.

Malmgren L. 1998. Radio frequency systems for NMR- imaging-coil development and studies of non-thermal biological effects [Doctoral Theses]. Lund, Sweden: Lund University, Lund, Sweden.

Markova E, Hillert L, Malmgren L, Persson BR, Belyaev IY. 2005. Microwaves from GSM mobile telephones affect 53BP1 and gamma-H2AX foci in human lymphocytes from hypersensitive and healthy persons. Environ Health Perspect 113:1172–1177.

Markova E, Schultz N, Belyaev IY. 2007. Kinetics and dose-response of residual 53BP1/gamma-H2AX foci: Co-localization, relationship with DSB repair and clonogenic survival. Int J Radiat Biol 83:319–329.

Martens L, Van Hese J, De Zutter D, De Wagter C, Malmgren L, Persson BRR, Salford LG. 1993. Electromagnetic field calculations used for exposure experiments on small animals in TEM-cells. Bioelectrochem Bioenergetics 30:73–81.

Meltz ML. 2003. Radiofrequency exposure and mammalian cell toxicity, genotoxicity, and transformation. Bioelectromagnetics Suppl. 6:S196–S213.

Mochan TA, Venere M, DiTullio RA, Jr, Halazonetis TD. 2004. 53BP1, an activator of ATM in response to DNA damage. DNA Repair (Amst) 3:945–952.

Nikoloski N, Frohlich J, Samaras T, Schuderer J, Kuster N. 2005. Reevaluation and improved design of the TEM cell in vitro exposure unit for replication studies. Bioelectromagnetics 26:215–224.

Pakhomov AG, Akyel Y, Pakhomova ON, Stuck BE, Murphy MR. 1998. Current state and implications of research on biological effects of millimeter waves: A review of the literature. Bioelectromagnetics 19:393–413.

Paull TT, Rogakou EP, Yamazaki V, Kirchgessner CU, Gellert M, Bonner WM. 2000. A critical role for histone H2AX in recruitment of repair factors to nuclear foci after DNA damage. Curr Biol 10:886–895.

Rappold I, Iwabuchi K, Date T, Chen J. 2001. Tumor suppressor p53 binding protein 1 (53BP1) is involved in DNA damage-signaling pathways. J Cell Biol 153:613–620.

Ritz T, Thalau P, Phillips JB, Wiltschko R, Wiltschko W. 2004. Resonance effects indicate a radical-pair mechanism for avian magnetic compass. Nature 429:177–180.

Rogakou EP, Boon C, Redon C, Bonner WM. 1999. Megabase chromatin domains involved in DNA double-strand breaks in vivo. J Cell Biol 146:905–916.

Sarimov R, Malmgren LOG, Markova E, Persson BRR, Belyaev IY. 2004. Non-thermal GSM microwaves affect chromatin conformation in human lymphocytes similar to heat shock. IEEE Trans Plasma Sci 32:1600–1608.

Schultz LB, Chehab NH, Malikzay A, Halazonetis TD. 2000. p53 binding protein 1 (53BP1) is an early participant in the cellular response to DNA double-strand breaks. J Cell Biol 151:1381–1390.

Sedelnikova OA, Rogakou EP, Panyutin IG, Bonner WM. 2002. Quantitative detection of (125)IdU-induced DNA double-strand breaks with gamma-H2AX antibody. Radiat Res 158:486–492.

Sengupta S, Robles AI, Linke SP, Sinogeeva NI, Zhang R, Pedeux R, Ward IM, Celeste A, Nussenzweig A, Chen J, Halazonetis TD, Harris CC. 2004. Functional interaction between BLM helicase and 53BP1 in a Chk1-mediated pathway during S-phase arrest. J Cell Biol 166:801–813.

Takahashi A, Matsumoto H, Nagayama K, Kitano M, Hirose S, Tanaka H, Mori E, Yamakawa N, Yasumoto J, Yuki K, Ohnishi K, Ohnishi T. 2004. Evidence for the involvement of double-strand breaks in heat-induced cell killing. Cancer Res 64:8839–8845.

Torudd J, Protopopova M, Sarimov R, Nygren J, Eriksson S, Markova E, Chovanec M, Selivanova G, Belyaev IY. 2005. Dose-response for radiation-induced apoptosis, residual 53BP1 foci and DNA-loop relaxation in human lymphocytes. Int J Radiat Biol 81:125–138.

Weisbrot D, Lin H, Ye L, Blank M, Goodman R. 2003. Effects of mobile phone radiation on reproduction and development in Drosophila melanogaster. J Cell Biochem 89:48–55.

Zhou C, Li Z, Diao H, Yu Y, Zhu W, Dai Y, Chen FF, Yang J. 2006. DNA damage evaluated by gammaH2AX foci formation by a selective group of chemical/physical stressors. Mutat Res 604:8–18.

Zwambron APM, Vossen SHJA, van Leersum BJAM, Ouwens MA, Mäkel WN. 2003. Effects of global communication system radio-frequency fields on well being and cognitive functions of human subjects with and without subjective complaints. The Hague, Netherlands: TNO Physics and Electronics Laboratory (TNO-report FEL-03-C148). Available from URL: www.ez.nl.

Bioelectromagnetics 4:281–292 (1983)

Suppression of T-Lymphocyte Cytotoxicity Following Exposure to Sinusoidally Amplitude-Modulated Fields

Daniel B. Lyle, Patricia Schechter, W. Ross Adey, and Robert L. Lundak

Division of Biomedical Sciences, University of California, Riverside (D.B.L.), Research Service, Jerry L. Pettis Memorial Veterans Hospital, Loma Linda, California (P.S., W.R.A.), and Techniclone International, Santa Ana, California (R.L.L.)

Significant inhibition of allogeneic cytotoxicity of the target cell MPC-11 by the murine cytotoxic T-lymphocyte line CTLL-1 was observed when the 4-h cytotoxicity assay was conducted in the presence of a 450-MHz field sinusoidally amplitude-modulated at 60 Hz. Exposure of the effector cells to the field prior to adding them to the target cells in the cytolytic assay resulted in a similar inhibition, suggesting a direct interaction of the field with the cytolytic T lymphocyte. The inhibition was preferentially expressed during the early allogeneic recognition phase. Field-exposed cytolytic cells recovered their full cytolytic capacity in 12.5 h. A differential susceptibility was observed with modulation frequencies from 0 to 100 Hz. Peak suppression occurred at 60 Hz modulation, with progressively smaller effects at 40, 16, and 3 Hz. The unmodulated carrier wave did not affect the cytotoxicity. Effects with 80- and 100-Hz modulation were smaller than at 60 Hz. These results demonstrate an inhibitory but recoverable effect by certain amplitude modulations of weak nonionizing radiation upon the cell-mediated cytolytic immune response.

Key words: microwaves, amplitude modulation, murine allogeneic cytotoxicity, T lymphocytes

INTRODUCTION

Exposure of laboratory animals to nonionizing radiation can produce both general and specific changes in immune competence. Cases reported involving perturbation of the general hematopoietic system include: decreased total cell volume of bone marrow and spleen in mice [Rotkovska and Vacek, 1975], decreased leukocyte counts in hamsters [Lappenbush et al, 1973], and decreased circulating lymphocytes with concomitant increasing circulating neutrophils in mice [Liburdy, 1977]. Specific changes in immune response observed after exposure of animals for various lengths of time to nonionizing radiation include increased lymphoblastoid transformation of cultured peripheral blood lymphocytes from rabbits [Czerski, 1975], decreased phytohemagglutinin (PHA)-induced mitosis of cultured lymphocytes from hamsters [Lysina, 1965], and enhanced PHA-

Received for review September 25, 1981; revision received November 17, 1982; final revision received January 10, 1983.

Address reprint requests to Dr. W. Ross Adey, Jerry L. Pettis Memorial Veterans Hospital, Loma Linda, CA 92357.

induced mitosis of cultured lymphocytes from rhesus monkeys [Prince et al, 1972]. Other specific immune changes reported include an increase in complement-receptor positive lymphocytes in the spleens of mice [Schlagel et al, 1980], decrease of the B-cell primary immune response to sheep red blood cells in immunized mice [Wiktor-Jedrzejczak et al, 1977], increase in response of cultured lymphocytes of rats to both T- and B-cell mitogens [Smialowicz, 1979], and increased antibody titer to *Streptococcus pneumoniae* in mice [Liddle et al, 1980]. Field strengths were clearly at levels, in some of these studies, that would produce raised temperatures in animal test subjects in the range of 0.5 °C or more, and in others marginal increases may have occurred. Direct exposure of leukocytes in vitro to nonionizing radiation where thermal effects were carefully excluded has also been demonstrated to be capable of altering immune competence, as in the decreased viability of rabbit granulocytes [Szmigielski, 1975], and a reduction in the numbers of granulocyte and macrophage colony-forming units from preparations of mouse bone marrow [Lin et al, 1979].

This report describes a reproducible inhibitory effect of 450-MHz fields, sinusoidally modulated at frequencies from 0 to 100 Hz, on the allogeneic cytotoxicity reaction conducted in vitro by CTLL-1 cytotoxic T lymphocytes. All radiation exposures were in an anechoic horn chamber at an incident field intensity of 1.50 mW/cm^2. The experiments reported here describe: (a) the magnitude of suppression of cytotoxic killing, (b) the cell population affected by the radiation (target cell or T-cytotoxic cell), (c) the phase of the cytotoxic event that is affected (recognition and induction or cytolysis), (d) reversibility of the suppressive effects, and (e) differential sensitivity to amplitude modulation of the carrier wave at frequencies between 0 and 100 Hz.

MATERIALS AND METHODS

Maintenance of the T Lymphocyte Line

The "CTLL-1" T-cytotoxic cell line was obtained from Dr. James Watson (University of Adelaide, Australia), and was characterized by Gillis and Smith [1977]. Log-growth phase CTLL-1 cells were cultured at an initial density of 1×10^4 cells/ml and subcultured when the density reached a maximum of 2×10^5 cells/ml. These cells that require T-cell growth factor [Schreier et al, 1980] were supplemented with new media every 48 h.

Preparation of T-Cell Growth Factor-Containing Medium

Sprague-Dawley rat spleens were disaggregated to a single cell suspension by teasing with sterile forceps, counted, and resuspended in 100-ml volumes in glass culture flasks at a final density of 1×10^8 cells/flask. The culture medium was RPMI 1640 with 10% fetal calf serum, 2 mM glutamine, antibiotics (100 μg/ml streptomycin, 100 U/ml penicillin, and 2.5 μg/ml fungizone), 5×10^{-5} M β-mercaptoethanol, and 5 μg/ml concanavalin A. Following 48 h of incubation at 37 °C the T-cell growth-factor (TCGF) containing supernatants were centrifuged, pooled, and sterile-filtered. Aliquots were frozen at −20 °C until needed. Before use, the TCGF medium was mixed with an equal volume of fresh medium and used to culture the CTLL-1 cell line. This medium was also used in the cytotoxicity assay.

Labeling of Allogeneic Target Cells

The tumor target cells used for the cytolytic assay were a H-2^d B lymphoma MPC-11 [Laskov and Scharff, 1970]. Log-phase target cells at a density of 1×10^7 cells/0.5

ml of RPMI-1640 were incubated with 100 μCi $Na^{51}Cr$ for 40 min at 37 °C. Labeled cells were washed three times in 50-ml volumes of Hank's balanced salt solution, then a fourth time immediately before being dispersed into the assay system. Labeling of target cells routinely produced 3,000–8,000 disintegrations per minute per 5×10^4 cells.

Cytotoxicity Assay

Chromium-labeled MPC-11 target cells were suspended in TCGF media and placed into microtiter wells (Linbro) at a cell density of 5×10^4 cells/well (0.1-ml volumes). CTLL-1 allogeneic cytolytic cells were then added to these wells in 0.1-ml volumes to give a final volume of 0.2 ml/well. Following 4 h of incubation at 37 °C, 0.1 ml was carefully removed from the top of each well and the radioactivity measured with a gamma-counter (Beckman Gamma 4000). Spontaneous release of radioactivity by labeled cells was determined by culturing the cells in media only. Maximal release was determined by analysis of supernatants from freeze-thawed labeled cells. Viabilities of all cultures were 99% or greater both at dispersal of cells into the plates and after a 4-h field exposure. Viabilities have also been determined for longer field exposure, both for 26-h and 40-h exposures, and have been measured at 99 ± 1.096 for control and test cultures (450 MHz modulated at 60 Hz). Specific allogeneic cytoxicity was determined using the following formula:

$$\% \text{ specific cytotoxicity} = \frac{(\text{test counts} - \text{spontaneous counts}) \times 100}{(\text{maximum releasable counts} - \text{spontaneous counts})}$$

Three-times freeze-thawed labeled MPC target cells routinely released 70% of the total counts in each culture. The maximum-releasable counts for each experiment was determined by taking 70% of the total counts in each culture, giving one maximum release value for each experiment. These values were statistically identical with or without field exposure. Microwave-exposed cultures were tested in parallel to identical plates in the absence of microwaves. Control cultures were prepared identically to the field-exposed cultures, and consisted of a separate culture plate with six spontaneous-release wells (target cells only), and six test wells (target cells plus effector cells). The control culture was prepared at the same time as the field-exposed culture, using the same cell population, and was gassed with 5% CO_2 and immediately covered with a pressure-sensitive adherent plastic film. The plate was placed into an incubator monitored at the same temperature as the anechoic exposure system. The field-exposed plate was placed on a plastic stand slanted at a 70° angle facing the field. The control plate was also placed on a stand at a 70° angle.

Anechoic 450-MHz Exposure System

The irradiation facility was constructed as a horn radiator, with a plywood frame lined with copper screening. The four walls and the plywood surface closing the wide end of the horn were lined with radiofrequency absorbing material (Echosorb). The absorber on the endwall had a surface geometry designed to maximize absorption at 450 MHz. The exposure area was located near the broad end of the horn 3 m from the point of excitation. The feed system used a terminated wave guide, and this wave guide could be rotated through 90° to allow either vertical or horizontal polarization of the E-vector. All materials inside the chamber were plywood, plastic, or paper. With an overall length of 4 m, the chamber was approximately 7 wavelengths long and was excited in the TE (transverse electric) mode. The chamber has a forced-air environmental control system

that recirculates heated air and ensures a uniform temperature throughout the chamber. This system was activated 2 h before exposure of cell cultures and maintained a temperature of 35 ± 1 °C at a constant relative humidity of 40% for all experiments.

A volume, in the exposure area near the broad end of the horn, in excess of 1.0 m^3 has an SWR of 1.2:1 or less, when unperturbed by biological preparations. The electrical characteristics of the chamber have been calibrated by H. Bassen (Bureau of Radiological Health, Rockville, MD). The field generating system was comprised of a low-frequency waveform generated with sine, square, and triangular wave outputs over the spectrum from 0.01 Hz to 100 kHz (Wavetek Model 159). The modulating signal was applied through a PIN diode modulator to the output of a 450-MHz phase-locked loop-controlled signal generator (Wavetek Model 3000). This generator drove a broadband linear power amplifier with a maximum power output of 80 W (Ailtech Model 35512). Depth of sinusoidal amplitude modulation was monitored with an oscilloscope and with an inline modulation meter/forward-reflected power meter (Bird Model 5483). Modulation depth was maintained at 75–85 percent. An input power to the chamber of 10 W produced a measured field intensity of 10 mW/cm^2 in the 1 m^3 at the exposure site described above, with less than 5% variation over the entire volume.

Incident field level at the exposure location was measured in two ways: with a commercial field intensity probe (Narda Model 8300); and with an experimental triple dipole probe provided for collaborative studies in tissue dosimetry (H. Bassen, Bureau of Radiological Health). A relationship between the sensitivity of this triple probe and an implantable tissue probe was established by exposing both to the same 450-MHz fields in a Crawford cell [Adey et al, 1981]. However, attempts to use the implantable tissue probe for direct dosimetry measurements in individual culture wells were unsuccessful, due to the small dielectric volume in the well (0.2 ml) with respect to the wave length of the incident field (67 cm). Each well plate has 96 wells uniformly spaced in a 12 × 8 matrix. Spacing between well centers was 9 mm. Each plate was 13 × 9 cm. During exposure, plates were tilted to an angle of 70° above the horizontal, with the wells facing the incident field. As many as three plates were exposed at one time. They were then placed vertically one above the other within the low SWR exposure site described above. Incident field levels were adjusted to 1.5 mW/cm^2 in all experiments. Harmonic and spurious content of the radiofrequency (RF) signal was periodically measured with a spectrum analyzer (Tektronix model 7L13) as a check against partial failure of the power amplifier output transistors, with possible contamination of the output spectrum by these components.

A further control on the cytotoxic sensitivities to modulated microwave fields reported here has been made in a Crawford cell exposure system at 37.0 ± 0.1 °C. With a 60-Hz modulated 450-MHz field (1.5 mW/cm^2 incident power), observed inhibition of cytotoxicity in four separate experiments was at the same 20% level noted in the horn chamber data reported here. Controls were placed adjacent to the Crawford cell in the same large incubator that housed it.

Pre- and postexposure temperature measurements were made in the horn exposure chamber, in wells on tissue plates in the exposure chamber, and in the control incubator. A digital thermistor thermometer was used with a resolution of 0.1 °C. The exposed thermistor tip diameter was 1.0 mm and its plastic sheath diameter was 3.5 mm. Well temperatures did not differ significantly from the air temperature of 35 °C in the exposure chamber at commencement and termination of field exposure, nor from incubator air temperatures at those same times for control preparations. Chamber temperature was

35 ± 1 °C. No significant increase in exposure chamber temperature occurred over the 4-h exposure epoch.

Statistical Analysis

The statistical significance of percent reductions in cytotoxicity were determined for each individual experiment, as indicated by the P values in Tables 1–5. The P values were determined using Student's t-test. Arcsin transformations of the six replicate decimal numbers from which the mean percent test cytotoxicity was determined were compared using Student's t-test to the arcsin transformations of the six replicate decimal numbers from which the mean percent control cytotoxicity was determined. Each decimal number was obtained by subtracting the appropriate spontaneous release mean from the individual counts per minute released in the assay and dividing that by the mean of the maximum releasable counts from which the spontaneous mean had been subtracted.

RESULTS

Exposure to the 450-MHz field sinusoidally modulated at 60 Hz during the 4-h allogeneic cytotoxicity assay resulted in a 20% inhibition of the observed cytotoxicity (Table 1). Similar suppression was observed in experiments in which the effector cells were exposed to microwave radiation for a 4-h period before the target cells were added for the 4-h cytotoxicity assay which was conducted in the absence of the field (Table 2). Since the target myeloma cells (MPC-11) were never field-exposed in the latter experiment, observed cytotoxicity changes are attributed to field actions on the effector T lymphocytes.

To evaluate the time-course of the cytotoxic suppression over the 4 h of field exposure, the cytotoxic cells were exposed to microwaves for the first 2 h only, for the last 2 h only, and for the entire 4 h of the cytotoxicity test (Table 3). Exposure to the field during only the first 2 h of the assay resulted in inhibition at levels similar to those noted from a full 4-h exposure to the field. In contrast, inhibition produced by exposure confined to the last 2 h of the assay produced only partial inhibition when compared with that elicited by the continuous 4-h exposure. This suggests a preferential effect upon the recognition phase of cytotoxicity.

TABLE 1. Inhibition of CTLL-1 H-2^d-Directed Cytotoxicity by Exposure During the 4-h Assay to a 450-MHz Field at 1.50 mW/cm^2, Sinusoidally Amplitude-Modulated at 60 Hz*

Experiment		Percent specific cytotoxicity	CPM during cytotoxicity	Spontaneous CPM	Maximum releasable counts	Percent inhibition of cytotoxicity	P value
1	Field	36	2,550 ± 115	1,309 ± 76	4,759 ± 101	20	<.05
	Control	45	2,903 ± 356	1,411 ± 222			
2	Field	58	4,959 ± 718	2,511 ± 796	6,759 ± 247	20	<.05
	Control	72	5,582 ± 278	2,580 ± 801			
3	Field	76	2,870 ± 368	861 ± 64	4,137 ± 216	24	<.05
	Control	81	3,500 ± 595	786 ± 16			
4	Field	25	1,839 ± 15	808 ± 31	5,009 ± 190	17	<.0001
	Control	30	2,125 ± 36	893 ± 58			
5	Field	30	885 ± 22	355 ± 24	2,121 ± 105	17	<.0005
	Control	36	1,015 ± 39	383 ± 18			

*These data represent five experiments, each with six replicates.

TABLE 2. Inhibition of CTLL-1 H-2^d-Directed Cytotoxicity by Exposure of the T Lymphocytes to a 450-MHz Field Modulated at 60 Hz at 1.50 mW/cm^2, for 4 h Prior to Cytotoxicity Assay*

Experiment		Percent specific cytotoxicity	CPM during cytotoxicity assay	Spontaneous CPM	Maximum releasable counts	Percent inhibition of cytotoxicity	P value
1	Field	19	2,410 ± 173	—[a]	7,587 ± 460	24	<.025
	Control	25	2,810 ± 307	1,223 ± 47			
2	Field	53	1,521 ± 145	—[a]	2,270 ± 51	15	<.025
	Control	62	1,663 ± 45	670 ± 36			
3	Field	47	3,524 ± 542	—[a]	6,141 ± 350	15	<.025
	Control	55	3,945 ± 350	1,232 ± 90			
4	Field	35	1,502 ± 84	—[a]	3,172 ± 306	17	<.025
	Control	42	1,676 ± 135	610 ± 56			
5	Field	12	1,334 ± 58	—[a]	5,226 ± 147	25	<.01
	Control	16	1,542 ± 104	857 ± 21			

*These data represent five experiments, each with six replicates.
[a]This table describes the effect on cytotoxicity when the T lymphocytes are irradiated before the cytotoxicity assay is begun. Target cells were added to wells containing CTLL-1 cells after the CTLL-1 had been exposed to the field.

TABLE 3. Inhibition of CTLL-1 H-2^d-Directed Cytotoxicity by Exposure to a 450-MHz Field, 1.50 mW/cm^2, Modulated at 60 Hz, During the Entire Assay, First 2 h, or Last 2 h of the 4-h Assay*

Field on during cytotoxicity test	Percent specific cytotoxicity	CPM during cytotoxicity	Spontaneous CPM	Percent inhibition of cytotoxicity	P value
Experiment 1					
All 4 h	58	4,959 ± 718	2,511 ± 796	19	<.05
First half	60	4,861 ± 263	1,992 ± 443	17	<.005
Last half	66	5,288 ± 207	2,449 ± 580	8	<.05
Control	72	5,582 ± 287	2,580 ± 80	—	—
Experiment 2					
All 4 h	30	885 ± 22	355 ± 24	17	<.0005
First half	32	977 ± 26	441 ± 61	11	<.01
Last half	36	990 ± 19	364 ± 16	0	>.25
Control	36	1,015 ± 39	383 ± 18	—	—

*These data are from two experiments, each with six replicates. (Maximum release counts: experiment 1, 759 ± 247; experiment 2, 121 ± 105.)

The effects of prior exposure of the cytotoxic T lymphocytes to the electromagnetic field at varying intervals prior to the cytotoxicity assay were also investigated. Field exposure was delivered 1, 4, 9, and 12.5 hours prior to the 4-h cytotoxicity assay. A 20% inhibition of cytotoxicity was observed in the assay 1 h post-field exposure (Fig. 1, Table 4). The inhibition of cytotoxicity had decreased to 13% and 12% at 4 h and 9 h post-field exposure, respectively. Cytotoxic inhibition was no longer observed after 12.5 h post-field exposure. As in the experiments in Table 2, target myeloma cells were not

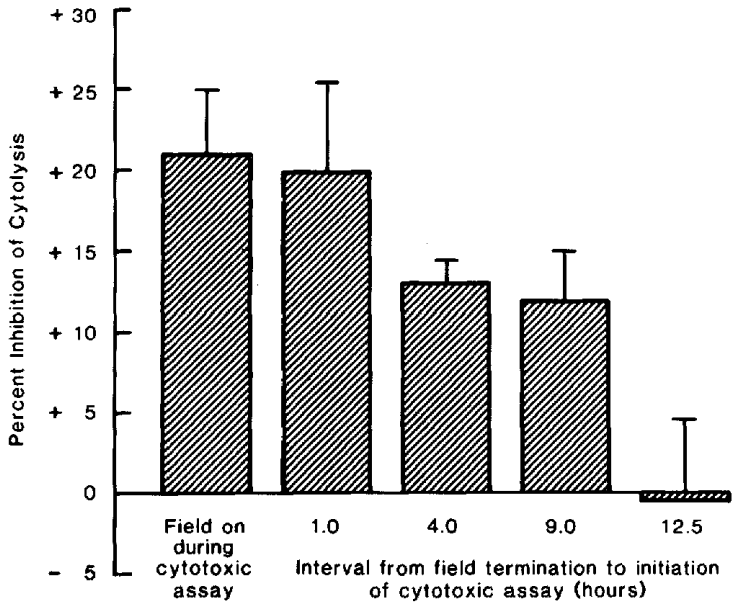

Fig. 1. Recovery of CTLL-1 H-2^d-directed cytotoxicity inhibited by a 4-h exposure of the T lymphocytes to a 450-MHz field, 1.50 mW/cm^2, 60-Hz modulation. Two experiments are averaged here. Final values for each experiment are the average of six replicate cultures exposed in parallel.

field-exposed, and altered cytotoxicity is attributed to modified effector action by field-exposed T lymphocytes. The cultures were supplemented with fresh medium every 2 h by replacement of 0.1 ml of liquid in each well. Cell viabilities at the end of the assay were the same for both control and test wells (99%).

The possibility of differential effects with amplitude modulation frequencies from 0 to 100 Hz was then examined (Fig. 2; Tables 5 and 6). The unmodulated carrier wave did not influence cytotoxicity, and 3-Hz modulation produced only an insignificant suppression. Differential suppression at higher frequencies was seen, with 16, 40, 80, and 100 Hz all producing suppression (9%, 11%, 10%, and 13% respectively), but at lower levels than that seen at 60 Hz (20% suppression).

DISCUSSION

A significant reproducible inhibition (20%) of allogeneic cytotoxicity of the TCGF-maintained murine lymphocyte CTLL-1 was observed when the 4-h cytotoxicity assay was conducted in the presence of a 450-MHz field sinusoidally amplitude-modulated at 60 Hz. This inhibition decreased sharply at higher and lower frequencies, with less suppression (9%, 11%, 10%, and 13% respectively) observed at 16, 40, 80, and 100 Hz. Reduction of allogeneic cytotoxicity was not seen at 3 Hz or in the presence of an unmodulated field. The suppression observed at 60 Hz was transient in nature. Complete recovery was observed 12.5 h following exposure to the microwave field.

The modulated field could inhibit T-cell mediated cytotoxicity by at least two potential mechanisms: (a) interaction with glycoprotein target cell receptor molecules in the membrane of the cytotoxic T lymphocytes; and (b) modulation of critical calcium ion flux. Field interactions with cell membrane surface glycoproteins may in itself involve

TABLE 4. Recovery of CTLL-1 H-2^d-Directed Cytotoxicity Inhibited by a 4-h Exposure of the T Lymphocytes to a 450-MHz Field, 1.50 mW/cm^2, 60-Hz Modulation

Interval from field termination to assay		Percent specific cytotoxicity	CPM during cytotoxicity	Spontaneous CPM	Maximum releasable counts	Percent inhibition of cytotoxicity	P value
Experiment 1							
During	Field-exposed	76	2,870 ± 368	861 ± 64	4,137 ± 216	24	<.05
assay	Control	81	3,500 ± 595	786 ± 16			
1 h	Field-exposed	35	1,502 ± 84	—[a]	3,172 ± 306	17	<.025
	Control	42	1,676 ± 135	610 ± 56			
4 h	Field-exposed	37	1,929 ± 150	—[a]	3,584 ± 69	14	<.025
	Control	43	2,143 ± 183	611 ± 48			
9 h	Field-exposed	36	1,816 ± 219	—[a]	3,980 ± 126	14	<.05
	Control	42	2,015 ± 111	597 ± 59			
12.5 h	Field-exposed	34	1,848 ± 124	—[a]	4,419 ± 102	−4	>.25
	Control	32	1,800 ± 337	513 ± 27			
Experiment 2							
During	Field-exposed	25	1,839 ± 15	808 ± 31	5,009 ± 190	17	<.0001
assay	Control	30	2,125 ± 36	893 ± 58			
1 h	Field-exposed	12	1,376 ± 58	—[a]	5,226 ± 147	25	<.01
	Control	16	1,542 ± 104	851 ± 21			
4 h	Field-exposed	15	1,286 ± 64	—[a]	4,199 ± 78	12	<.10
	Control	17	1,360 ± 94	787 ± 49			
9 h	Field-exposed	19	1,271 ± 43	—[a]	3,826 ± 132	10	<.10
	Control	21	1,340 ± 92	673 ± 9			
12.5 h	Field-exposed	32	1,282 ± 55	—[a]	2,699 ± 79	3	>.10
	Control	33	1,299 ± 32	608 ± 31			

[a]This table describes the recovery of cytotoxicity to control levels as measured by cytotoxicity assays initiated at different times after the CTLL-1 cells were exposed to the field.

modified calcium binding. It has been shown that weak electromagnetic fields can influence the aggregation of acetylcholine receptors on embryonic muscle fibers [Orida and Poo, 1978], and the aggregation of concanavalin A receptors on lymphocytes [Poo and Robinson, 1977]. Evidence has also been accumulated using a clonal line of osteoblast cells, as well as cultured bone preparations, that weak electromagnetic fields can alter the rate of formation of adenylcyclase in response to parathyroid hormone [Luben et al, 1980; Norton et al, 1980]. Adherence to the effector cytotoxic T lymphocyte via specific membrane receptor molecules to the target cell has been shown to be a necessary prerequisite to lysis of the target cell [Abler et al, 1970]. Furthermore, the target cell receptor has been implicated in directing or triggering the T cell cytotoxicity mechanism [Kuppers and Henney, 1976; Fishelson and Berke, 1978].

Although the mechanism of T-cell mediated lympholysis has not yet been agreed upon, considerable evidence supports the delivery of lytic molecules of lymphotoxin to the adhered target cell membrane as directed by specific target cell receptor molecules [Ware and Granger, 1981]. According to Ware and Granger's model of T-cell mediated lympholysis, lymphotoxin precursor subcomponents form part of a macromolecular complex upon the surface of the cell membrane. The complex is thought to have three essential

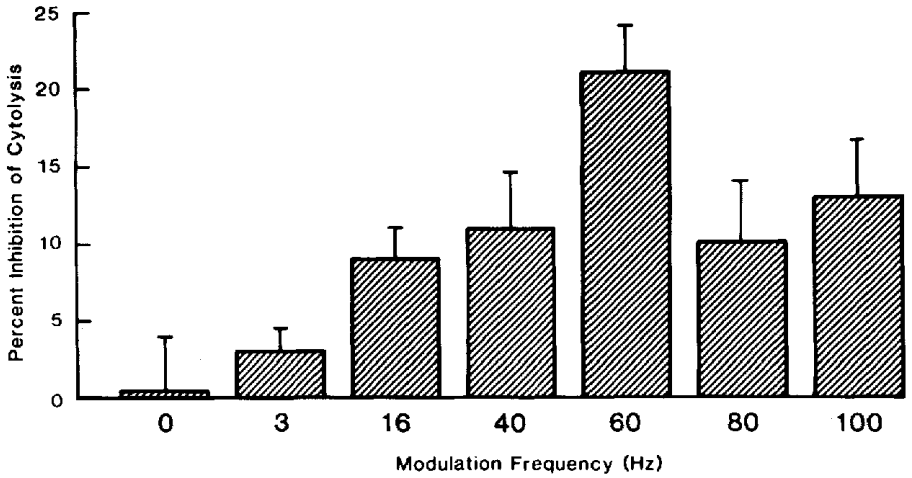

Fig. 2. Inhibition of CTLL-1 H-2^d-directed cytotoxicity by exposure to a 450-MHz field, 1.50 mW/cm^2, sinusoidally amplitude-modulated between 0 and 100 Hz. The inhibitions represented at 0, 3, 16, 40, and 80 Hz are the average of two experiments each. The inhibition at 100 Hz is the average of three experiments. The inhibition at 60 Hz is from the same five experiments of Table 1. Final values for each experiment are the average of six replicate cultures.

TABLE 5. Inhibition of H-2^d-Directed Cytotoxicity by Exposure to a 450-MHz Field, 1.50 mW/cm^2, Sinusoidally Amplitude-Modulated at 0, 3, and 16 Hz

Modulation frequency	Experiment		Percent specific cytotoxicity	CPM during cytotoxicity	Spontaneous CPM	Maximum releasable counts	Percent inhibition of cytotoxicity	P value
0	1	Field	50	3,355 ± 321	1,378 ± 124	5,299 ± 144	4	<.25
		Control	52	3,308 ± 138	1,160 ± 53			
	2	Field	34	2,038 ± 31	914 ± 80	4,270 ± 132	−3	>.25
		Control	33	1,998 ± 104	892 ± 84			
3 Hz	1	Field	73	2,269 ± 66	846 ± 18	2,787 ± 73	4	<.25
		Control	76	2,323 ± 102	884 ± 47			
	2	Field	49	1,521 ± 76	432 ± 44	2,644 ± 154	2	<.25
		Control	50	1,519 ± 163	380 ± 17			
16 Hz	1	Field	36	3,576 ± 194	1,079 ± 77	8,017 ± 450	10	<.01
		Control	40	3,875 ± 145	1,121 ± 77			
	2	Field	54	1,669 ± 58	432 ± 20	2,711 ± 86	8	<.10
		Control	59	1,784 ± 105	391 ± 24			

subunits: (a) the antigen-specific receptor, (b) a catalytic unit composed of inactive lymphotoxin subcomponents, and (c) an activation unit. Upon binding to antigen or lectin, two signals would occur: one to instruct the cytotoxic T lymphocyte to redistribute additional complexes to the area of effector-target cell membrane contact, and the other signal prompting the activation and delivery of the lymphotoxin unit to the target membrane surface. Following this "programming-for-lysis," the presence of the effector lym-

TABLE 6. Inhibition of CTLL-1 H-2^d-Directed Cytotoxicity by Exposure to a 450-MHz Field, 1.50 mW/cm^2, Sinusoidally Amplitude-Modulated at 40, 80, and 100 Hz

Modulation frequency	Experiment		Percent specific cytotoxicity	CPM during cytotoxicity	Spontaneous CPM	Maximum releasable counts	Percent inhibition of cytotoxicity	P value
40 Hz	1	Field	61	965 ± 50	231 ± 16	1,436 ± 41	9	<.025
		Control	67	1,045 ± 36	258 ± 14			
	2	Field	40	984 ± 73	306 ± 16	1,995 ± 40	13	<.05
		Control	46	1,069 ± 57	284 ± 22			
80 Hz	1	Field	22	1,656 ± 72	793 ± 17	4,768 ± 301	12	<.005
		Control	25	1,866 ± 51	907 ± 27			
	2	Field	47	1,344 ± 71	332 ± 19	2,471 ± 86	8	<.05
		Control	51	1,416 ± 49	328 ± 19			
100 Hz	1	Field	19	2,648 ± 74	1,201 ± 63	8,850 ± 259	9	<.10
		Control	21	2,953 ± 216	1,415 ± 62			
	2	Field	43	1,348 ± 52	378 ± 20	2,661 ± 116	14	<.0025
		Control	50	1,493 ± 80	338 ± 26			
	3	Field	61	1,062 ± 22	247 ± 32	1,590 ± 31	15	<.001
		Control	72	1,208 ± 66	245 ± 21			

phocyte is no longer necessary for subsequent lysis of the target cell, which may take up to several hours to occur [Martz and Benacerraf, 1973].

We observed that the murine allogeneic cytotoxicity reaction is preferentially inhibited by field exposure during the initial phase of the assay (first 2 h), in which programming-for-lysis occurs. The modulated field could be affecting any or all of the postulated functions of the target cell receptor which are crucial to the cytolytic mechanism. These sites for field-perturbation are: (a) interaction of the receptor with specific target cell antigen, (b) receptor-directed redistribution of additional macromolecular complexes to the area of lymphocyte-target cell membrane contact, or (c) receptor-mediated delivery of activated lymphotoxin units to the target cell membrane.

Another early requirement for lysis of the target cell is the presence of calcium [Goldstein, 1975]. The programming-for-lysis stage will not occur if Ca^{2+} is absent from the culture medium [Gately and Martz, 1979]. It has been established that calcium efflux from nervous tissue can be modulated by weak electromagnetic fields [Bawin et al, 1978]. Furthermore, calcium efflux from chick brain tissue was shown to be sensitive to amplitude modulation frequency, with a peak effect occurring at 16 Hz [Bawin et al, 1975; Blackman et al, 1979]. Exposure of chick cerebral hemispheres to 450-MHz fields amplitude-modulated at 16 Hz resulted in an increased calcium efflux of 10% or more at field intensity of 0.1–1.0 mW/cm^2. A similar effect, but with different field parameters, might be occurring during the calcium-dependent programming-for-lysis stage of T-cell mediated lympholysis.

Field-perturbation of critical calcium ion flux or membrane receptor function are thus possible explanations for the suppressive effect of weak nonionizing radiation on cell-mediated cytotoxicity described here. These observations add new evidence that the

functional capacity of the T lymphocyte in cell-mediated immune response is sensitive to weak microwave fields amplitude-modulated at low frequency, and that there is a differential sensitivity to the modulation frequency, with maximum effect at 60 Hz.

ACKNOWLEDGMENTS

We wish to thank Dr. James Watson, University of California, Irvine, Medical School (currently at University of Adelaide, Australia) for kindly supplying the CTLL-1 cell line. This research was supported in part by American Cancer Society Grant No. IM253, Department of Energy Contract DE-A101-79078, and Bureau of Radiological Health Contract R01-FD00063-03.

REFERENCES

Abler ME, Lee JC, Rosenau W (1970): Lymphocyte-target cell interation *in vitro*. Ultrastructural and cinematographic studies. Am J Pathol 60:421–427.

Adey WR, Bawin SM, Burge B, Bassen HI, Franke KE (1981): Electric fields in cat brain exposed to 450 MHz CW fields in semi-far fields. Bioelectromagnetics Society, Third Annual Meeting, Washington, D.C. Proceedings, p. 35 (Abstract)

Bawin SM, Kaczmarek LK, Adey WR (1975): Effects of modulated VHF fields on the central nervous system. Ann NY Acad Sci 247:74–81.

Bawin SM, Adey WR, Sabbot IM (1978): Ionic factors in release of $^{45}Ca^{2+}$ from chick cerebral tissue by electromagnetic fields. Proc Natl Acad Sci USA 75:6314–6318.

Blackman CS, Elder JA, Weil CM, Bennane SG, Eichinger DC, House DE (1979): Induction of calcium ion efflux from brain tissue by radio frequency radiation: Effects of modulation frequency and field strength. Radio Sci 14:93–98.

Czerski P (1975): Microwave effects on the blood forming system with particular reference to the lymphocyte. Ann NY Acad Sci 247:232–242.

Fishelson Z, Berke G (1978): T lymphocyte-mediated cytolysis: Dissociation of the binding and lytic mechanisms of the effector cell. J Exp Med 143:1121–1126.

Gately MK, Martz E (1979): Early steps in specific tumor cell lysis by sensitized mouse T lymphocytes. III. Resolution of two distinct roles for calcium in the cytolytic process. J Immunol 122:482–489.

Gillis S, Ferm MM, Ou W, Smith KA (1978): T cell growth factor: Parameters of production and a quantitative microassay for activity. J Immunol 120:2027–2032.

Gillis S, Smith KA (1977): Long term culture of tumor-specific cytotoxic T-cells. Nature 268:154–156.

Golstein P (1975): Post recognition Mg^{++} or Ca^{++} dependent events in cell-mediated cytotoxicity. In Seligmann M, et al (eds): "Membrane Receptors of Lymphocytes." New York: American Elsevier, pp 399–401.

Kimpel GR, Byus CV, Russel DH, Lucas DO (1979): Cyclic AMP-dependent protein kinase activtion and the induction of ornithine decarboxylase during lymphocyte mitogenesis. J Immunol 123:817–824.

Kuppers RC, Henney CS (1976): Evidence for a direct linkage between antigen recognition and lytic expression in effector T cells. J Exp Med 143:684–689.

Lappenbush WL, Gillespie LJ, Leach WM, Anderson GE (1973): Effect of 2450-MHz microwaves on the radiation response of X-irradiated Chinese hamsters. Radiat Res 54:294–303.

Laskov R, Scharff MD (1970): Synthesis, assembly, and secretion of gamma globulin by mouse myeloma cells. I. Adaption of the Merwin plasma cell tumor-II to culture, cloning, and characterization of gamma globulin subunits. J Exp Med 131:515–541.

Liburdy RP (1977): Effects of radiofrequency radiation on inflammation. Radio Sci 12(6S):179–183.

Liddle CG, Putnam JS, Ali JS, et al (1980): Alteration of circulating antibody response to mice exposed to 9-GHz pulsed microwaves. Bioelectromagnetics 1:397–404.

Lin JC, Ottenbreit MJ, Wang S-L, et al (1979): Microwave effects on granulocyte and macrophage precursor cells of mice *in vitro*. Radiat Res 80:292–302.

Luben RA, Chen M, Rosen D, et al (1980): Effects of therapeutic electromagnetically induced current on hormone responsiveness of bone cells *in vitro*. J Electrochem Soc 127:129c. (Abstract)

Lysina GG (1965) Effect of superhigh frequencies on the morphological composition of blood. Gigi Sanit 30:95–96.

Martz E, Benacerraf B (1973): An effector-cell independent step in target cell lysis by sensitized mouse lymphocytes. J Immunol 111:1538–1545.

Nabholz M, Conzelmann A, Acuto O, et al (1980): Established murine cytolytic T-cell lines as tolls for a somatic cell genetic analysis of T-cell functions. Immunol Rev 51:125–156.

Norton LA, Shteyer A, Rodan GA (1980): Electromagnetic field effects on DNA synthesis in bone cells. J Electrochem Soc 127:129. (Abstract)

Orida N, Poo MM (1978): Electrophoretic movement and localisation of acetylcholine receptors in the embryonic muscle cell membrane. Nature 275:31–35.

Poo MM, Robinson KR (1977): Electrophoresis of concanavalin A receptors along embryonic muscle membrane. Nature 265:602–605.

Prince JE, Mori LH, Frazer JW, Mitchell JC (1972): Cytologic aspect of radiofrequency radiation in the monkey. Aerospace Med 43:759–761.

Rasmussen H (1975): Ions as "second messengers." In Weissman G, Claiborne R (eds): "Cell Membranes." City: HP Publishing Co., pp 203–212.

Rotkovska D, Vacek A (1975): The effect of electromagnetic radiation on the hematopoietic stem cells of mice. Ann NY Acad Sci 247:243–250.

Schlagel CJ, Sulek K, Ho HS, et al (1980): Biologic effects of microwave exposure. II. Studies on the mechanisms controlling susceptibility to microwave-induced increases in complement receptor-positive spleen cells. Bioelectromagnetics 1:405–414.

Schreier MH, Iscove NN, Tees R, Aarden L, Von Boehmer H (1980): Clones of killer and helper T cells: Growth requirements, specificity and retention of function in long-term culture. Immunol Rev 51:315–335.

Smialowicz RT (1979): Hematologic and immunologic effects of nonionizing electromagnetic radiation. Bull NY Acad Med 55:1094–1118.

Szmigielski S (1975): Effect of 10-cm (3-GHz) electromagnetic radiation (microwaves) on granulocytes *in vitro*. Ann NY Acad Sci 247:275–280.

Ware CF, Granger GA (1981): Mechanisms of lymphocyte-mediated cytotoxicity. III. Characterization of the mechanism of inhibition of the human alloimmune lymphocyte-mediated cytotoxic reaction by poly-specific anti-lymphotoxin *in vitro*. J Immunol 126:1932–1940.

Wiktor-Jedrzejczak W, Ahmed A, Czerski P, et al (1977): Immune response of mice to 2450-MHz microwave radiation: Overview of immunology and empirical studies of lymphoid splenic cells. Radio Sci 12(6S):209–219.

Bioelectromagnetics 17:246–248 (1996)

Brief Communication

Effect on the Immune System of Mice Exposed Chronically to 50 Hz Amplitude-Modulated 2.45 GHz Microwaves

Erzsébet Elekes, György Thuróczy, and László D. Szabó

National "Frédéric Joliot-Curie" Research Institute for Radiobiology and Radiohygiene, Budapest, Hungary

The effect of continuous (CW; 2.45 GHz carrier frequency) or amplitude-modulated (AM; 50 Hz square wave) microwave radiation on the immune response was tested. CW exposures (6 days, 3 h/day) induced elevations of the number of antibody-producing cells in the spleen of male Balb/c mice (+37%). AM microwave exposure induced elevation of the spleen index (+15%) and antibody-producing cell number (+55%) in the spleen of male mice. No changes were observed in female mice. It is concluded that both types of exposure conditions induced moderate elevation of antibody production only in male mice.

Key words: immune response, AM or CW microwave radiation, chronic MW exposure, male and female mice

The level of electromagnetic radiation has increased in both occupational and residential environments due to the increasing number of long-term low-level and short-term medium- or high-power sources. In the study of biological effects, the role of various exposure parameters must be assessed (carrier frequency, power density, type of modulation, duration of exposure). Changes in these parameters can influence different phases of the immune response [Vinogradov et al., 1981; Nageswari et al., 1991; Veyret et al., 1991]. In our experiments, we used a carrier frequency of 2.45 GHz because of its use in industry and a modulation frequency of 50 Hz, which is similar to the frequency of some mobile phone systems (TDMA) and other ELF modulation systems. The incident power level of 0.1 mW/cm^2 corresponds to the value that is allowed in the work place for long-term exposure according to the Hungarian standard. The immune response against sheep red blood cells (SRBC) was tested.

Balb/c mice of both sexes were used. Experiments were repeated two or three times. Animals were kept in plastic cages, with food and water available ad libitum. Exposures were performed in an anechoic chamber (2.55 $\times$ 1.8 $\times$ 2.9 m) using a standard horn antenna (G = 14 dB). The microwave generator (TKI type TR-TK0603) was used in the external modulation mode. A function generator (OMSZOV type BE-104) was coupled to the microwave source. The carrier frequency was 2.45 GHz. The continuous-wave (CW) or amplitude-modulated (AM; 50 Hz square wave) microwave signal was amplified with a traveling-wave tube amplifier (Hughes model 1177). The time-averaged power density was 0.1 mW/cm^2 at the center of the cage. The specific absorption rate (SAR) was determined in polyacrylamide tissue equivalent phantoms of animals by the method of Andreucetti et al. [1988]. The averaged SAR for 0.1 mW/cm^2 was 0.14 $\pm$ 0.02 W/kg.

Animals were exposed in a circular cage (23 cm diameter, 5 cm high), which was divided into ten separated areas. To produce identical experimental circumstances for male and female and for control and exposed animals, male and female mice were placed side by side in the cages. Exposure occurred for 6 consecutive days, every day for 3 h. The control animals spent the duration of exposure in a cage identical to that used for the exposure, but out of the anechoic chamber in a separate room, where the humidity, temperature, and other

Received for review January 11, 1995; revision received June 21, 1995.

Address reprint requests to Erzsébet Elekes, National Research Institute for Radiobiology and Radiohygiene, POB 101, H-1775 Budapest, Hungary.

circumstances were the same as in the anechoic chamber. Following the daily exposure, the exposed and control animals were housed in the same room in an identical manner.

Mice were immunized on the second day of the exposure with 4×10^8 SRBC intraperitoneally and bled 5 days later. Spleen cell suspensions were prepared. The number of antibody-producing cells (PFC) was determined [Jerne et al., 1963]. In the serum samples, hemagglutinin titer [Takátsy, 1956] and IgG level [Mancini et al., 1965] were determined. Mean value ± SE and spleen index (spleen weight in mg/body weight in g) were calculated. The Mann-Whitney test (two-tailed) was used to determine the statistical significance of the differences between groups.

Body weight remained constant in all experiments. Moderate elevation of the spleen weight (+15%) and a nearly significant elevation (+15%) of the spleen index appeared only in the AM microwave-exposed male mice (Table 1). The number of spleen cells in control and exposed groups did not differ markedly from each other. The number of antibody-producing cells in the spleen of male mice was nearly significantly elevated in the CW and AM microwave-exposed males but did not differ from control in females (Table 1, Fig. 1). No difference in the titer of hemagglutinin or in the IgG level of serum could be observed.

AM microwaves induced an elevation of the spleen index without elevation in the number of spleen cells in male mice, indicating some alteration of the cell microenvironment. This might be due to changes in the water content or connective tissue in the spleen. The elevation of antibody production in male mice following exposure seems to be the consequence of excitation of the immune system.

Other groups have found that CW or pulsed microwaves at 10 and 15 mW/cm^2 induced elevated immune response against SRBC [Robert et al., 1981; Rama Roa et al., 1985]. The circulating antibody against *Streptococcus pneumoniae* was elevated at 10 mW/cm^2 but not at 1 mW/cm^2 [Liddle et al., 1986]. Veyret et al. [1991], using exposure to 30 μW/cm^2 pulsed modulated microwaves for 10 h/day for 5 days, demonstrated moderate elevation of PFC count with nonpulsed MW and a marked elevation in the case of AM MW at specific modulating frequencies in male mice. In other experiments, exposure to 450 MHz, 1.5 mW/cm^2 with 60 Hz sinusoidal modulation suppressed the mouse T-lymphocyte cytotoxicity [Lyle et al., 1983].

In our experiments, the AM exposure induced only moderately higher elevation of antibody production than that with CW exposure. We suppose that the low power density (0.1 mW/cm^2) and the short duration of the daily exposures are responsible for the small difference.

In the present experiments, MW exposures induced different effects in female and male mice. Similarly, different effects were found in male and female mice exposed to a 240 kV/m, 60 Hz field for 4500 hours [Fam, 1980]: Leukocyte count was significantly decreased only in female mice, whereas changes of blood proteins appeared only in male mice. This difference may be due to the different psychoneurohormonal regulation in the

TABLE 1. Spleen Index, Number of Spleen Cells, and PFCs in CW and AM Microwave-Exposed Mice (Mean ± SEM)

Sex	Group	n	Spleen index	Cells/spleen (×10^6)	PFC/spleen
Female	Control	8	6.93 ± 0.21	99.3 ± 6.6	18,239.8 ± 1997.7
	CW exposed	8	6.67 ± 0.18	84.3 ± 3.7	19,862.6 ± 2101.2
			-3.75%	-15.11%	+8.9%
Male	Control	8	5.46 ± 0.32	71.6 ± 7.2	15,343.3 ± 1700.5
	CW exposed	8	5.43 ± 0.11	63.5 ± 4.6	21,031.2 ± 2517.6**
			-0.55%	-11.32%	+37.07%
Female	Control	15	6.63 ± 0.24	110.0 ± 9.1	8852.1 ± 1262.5
	AM exposed	16	6.88 ± 0.19	112.8 ± 9.4	7936.6 ± 1021.4
			+3.77%	+2.36%	-10.34%
Male	Control	13	5.54 ± 0.21	99.2 ± 10.8	11,980.4 ± 1437.4
	AM exposed	13	6.37 ± 0.34*	89.6 ± 4.5	18,619.0 ± 3136.2***
			+14.98%	-9.68%	+55.41%

*P = 0.0687.
**P = 0.0929.
***P = 0.0918.

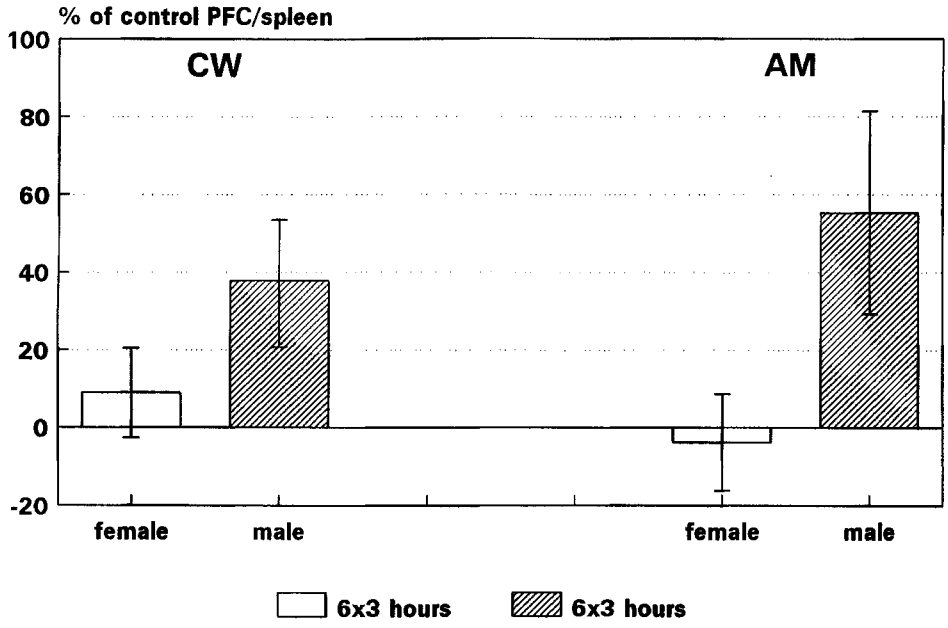

Fig. 1. Alteration of the antibody-producing cells of CW- or AM-exposed mice as percentage of corresponding control. Mice were exposed to 2.45 GHz CW or with 50 HZ AM MW, at 0.1 mW/cm^2 power density. Error bars represent SE.

two sexes. Furthermore, the exposure or other circumstances of the experiment might evoke different situational stress in male and female mice. The cause of sexual differences could be clarified by further baseline experiments. Our study can provide additional information on the effects of modulated and CW exposures in relation to mobile communications because of the ELF modulation frequency and field intensity.

ACKNOWLEDGMENTS

This research was supported by PHARE-ACCORD program 0492.

REFERENCES

Anderucetti D, Bini M, Ignesti A, Olmi R, Rubino N, Vanni R (1988): Use of polyacrylamide as a tissue-equivalent material in the microwave range. IEEE Biomed Eng 35:275–277.

Fam WZ (1980): Long-term biological effects of very intense 60 Hz electric field on mice. IEEE Biomed Eng 27:376.

Jerne NK, Nordin A, Henry C (1963): The agar plaque technique for recognizing antibody-producing cells. In Amos B, Koprowski H (eds): "Cell-Bound Antibodies." Philadelphia: Wistar Institute Press, pp 109–125.

Liddle CG, Putman JP, Lewter OH, West M, Morrow G (1986): Circulating antibody response of mice exposed to 9-GHz pulsed microwave radiation. Bioelectromagnetics 7:91–94.

Lyle DB, Schechter P, Adey WR, Lundak KR (1983): Suppression of T-lymphocyte cytotoxicity following exposure to sinusoidal amplitude-modulated field. Bioelectromagnetics 4:281–292.

Mancini G, Carbonari AO, Heremans JF (1965): Immunochemical quantitation of antigens by single radial immunodiffusion. Immunochemistry 2:235–254.

Nageswari KS, Sarma KR, Rajvanshi VS, Sharan R, Sharma M, Barathwal V, Singh V (1991): Effect of chronic microwave radiation on T cell mediated immunity in the rabbit. Int J Biotechnol 35:92–97.

Rama Roa GV, Cain CA, Tompkins WAF (1985): Effect of microwave exposure on the hamster immune system. IV. Spleen cell IgM hemolytic plaque formation. Bioelectromagnetics 6:41–52.

Robert D, Deschaux P, Pellisier JP, Santini R, Fontanges R (1981): Etude preliminaire d'effect cumulatif d'un rayonnement micro-onde a 2450 MHz sur la reponse immunitaire de la souris. CR Soc Biol 172:1148–1154.

Takátsy G (1956): The use of spiral loops in serological and virological micromethods. Acta Microbiol Acad Sci Hung 3:191–202.

Veyret B, Bouthet C, Deschaux P, de Seze R, Geffard M, Joussot-Dubien J, le Diraison M, Moreau J-M, Caristan A (1991): Antibody responses of mice exposed to low-power microwaves under combined pulse- and amplitude modulation, Bioelectromagnetics 12:47–56.

Vinogradov GI, Gonchar NM, Belonozhko NG, Zhelezniak AA, Vinarskaia EI (1981): Immunological and hematological effects of low-intensity extremely high frequency electromagnetic fields (Rus). Hygiene Residential Areas 20:29–33.

EHE'07 – 2nd International Conference on
Electromagnetic Fields, Health and Environment
Wroclaw, Poland, September 10-12, 2007

OXIDATIVE AND IMMUNE RESPONSE IN EXPERIMENTAL EXPOSURE TO ELECTROMAGNETIC FIELDS

Dana Dabala[1], Didi Surcel[2], Csabo Szanto[2], Simona Miclaus[3], Mariana Botoc[2], S.Toader[2], O. Rotaru[2]

1. Department of Occupational Medicine, Transport Regional Public Health Center, Cluj-Napoca, Romania
2. Department of Occupational Medicine, Institute of Public Health, Cluj-Napoca, Romania
3. Land Forces Academy, Sibiu, Romania

ABSTRACT

Although the physical techniques for measuring of the electromagnetic fields (EMF) are well developed, adequate characterization of the biological effects induced by EMF is subject of discussion yet. We don't know the effects that would be after a long term of exposure. Many scientific studies have been devoted to assessing what health risks are associated with EMF exposure. Data from the recent experiments suggest that EMF are associated with the iron-mediated free radical generation, that can cause damage in the biologic molecules such as lipids, proteins and can profundly affect cellular homeostasis.

The aim of this study was to show the effects of the chronic exposure to EMF on the immune and oxidative response.

In vivo experiment was carried out on 80 Wistar rats that were divided in 4 groups as following: 1. Control-group, without exposure, sacrificed at 1 month; 2. Control-group, without exposure sacrificed at 3 months; 3 .EMF–exposed group, sacrificed at 1 month; 4. EMF – exposed group, sacrificed at 3 months. The rats were exposed to RF EMF that covers a range of the frequencies between 140-160 MHz generated by a Motorola device.The components of EMF field were measured with an EMF 200 Monitor Water&Golterman (the measured Power density (S) was 8+/- 1 W/m2).

The following parameters were assessed : a) 3HTdR incorporation test; b) IL-1 assay; c) TNF-assay; d) Chemiluminiscence assay; e) Lipid peroxides.

The 3HTdR incorporation was decreased in the EMF- exposed groups, as compared with control groups, but with statistically significant difference (ssd) ($p>0.01$) only in third group. Increased values of the cytokines (IL-1 and TNF) were found in the 3 and 4 – groups, with ssd for both of the cytokines ($p> 0.05$ for IL-1 and $p> 0.01$ for TNF) Chemiluminescence assay and lipid peroxides were parameters with increased values for 3 and 4 groups, but ssd were found only in the forth -group. Our results point out an important increased of the oxidative response in the EMF- exposed groups, in special in the group sacrificed at 3 months. In the forth group, an important suppression of the immune response and increased activity of the cytokines was demonstrated.

Our results indicate an association between electromagnetic fields and immune and oxidative response, suggesting increased modifications in the group with EMF -prolonged exposure.

Introduction

The aim of this study was to show the effects of the chronic exposure to EMF on the immune and oxidative response.

Although the physical techniques for measuring EMF are well developed, adequate characterization of the biological effects induced by EMF is subject of discussion yet. We don't know the effects that would be after a long term of exposure. Many scientific studies have been devoted to assessing what health risks are associated with EMF exposure. Data from the

recent experiments suggest that EMF are associated with the iron-mediated free radical generation, that can cause damage in the biologic molecules such as lipids, proteins and can profoundly affect cellular homeostasis.

Materials and Methods

In vivo experiment was carried out on 80 Wistar rats that were divided in 4 groups as following:
1. Control-group, without exposure, sacrificed at 1 month;
2. Control-group, without exposure sacrificed at 3 months;
3.EMF–exposed group, sacrificed at 1 month;
4. EMF – exposed group, sacrificed at 3 months.

The rats were exposed to to RF EMF that covers a range of the frequencies between 140-160 MHz generated by a Motorola device.The components of EMF field were measured with an EMF 200 Monitor Water&Golterman (the measured Power density (S) was 8+/- 1 W/m2).
The following parameters were assessed :
a) 3HTdR incorporation test; b) IL-1 assay;
c) TNF-assay;
d) Chemiluminiscence assay;
e) Lipid peroxides.

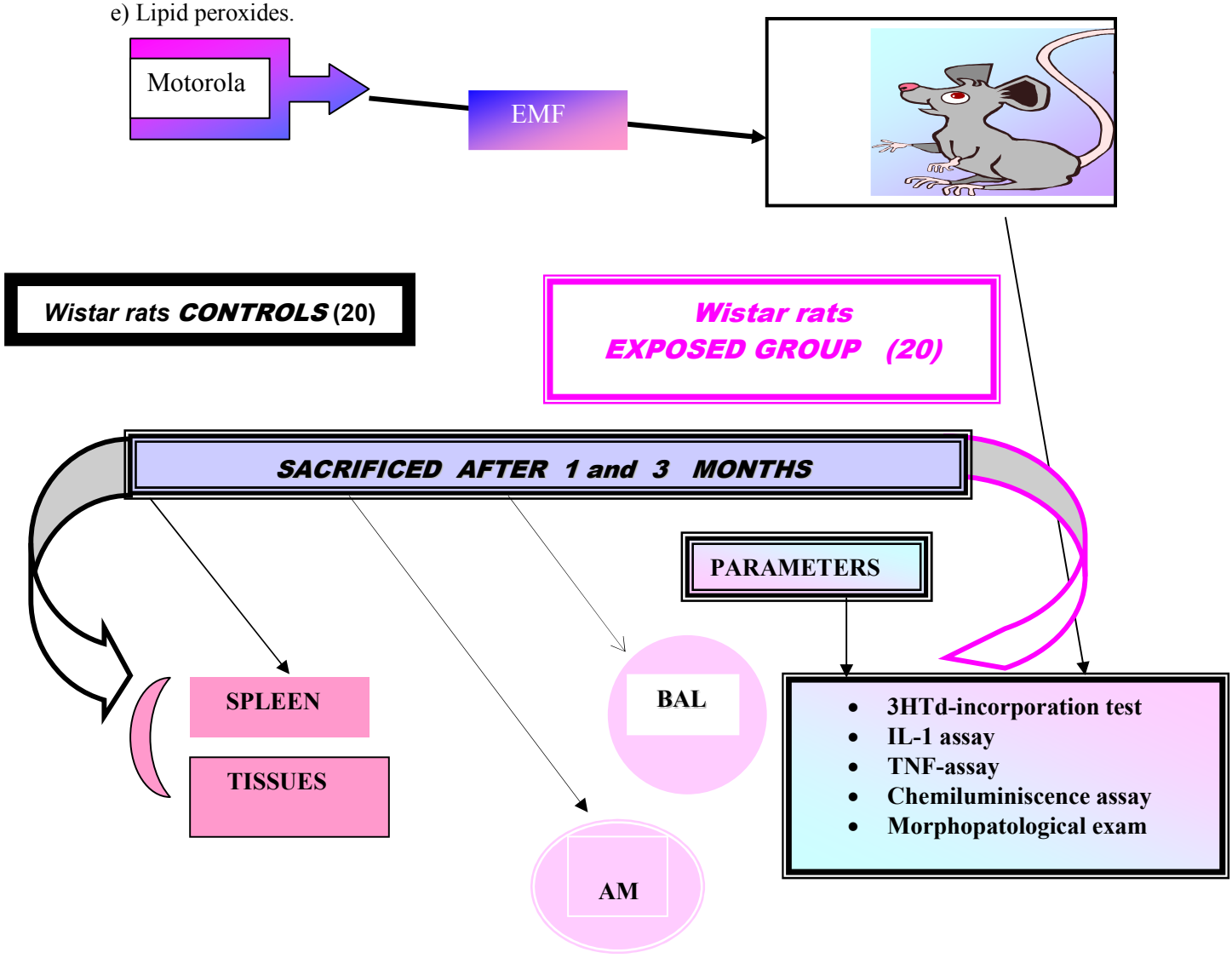

Results

The 3HTdR incorporation was decreased in the EMF- exposed groups, as compared with control groups, but with statistically significant difference (ssd) ($p>0.01$) only in third group. Increased values of the cytokines (IL-1 and TNF) were found in the 3 and 4 – groups, with ssd for both of the cytokines ($p> 0.05$ for IL-1 and $p> 0.01$ for TNF) Chemiluminescence assay and lipid peroxides were parameters with increased values for 3 and 4 groups, but ssd were found only in the forth -group. Our results point out an important increased of the oxidative response in the EMF- exposed groups, in special in the group sacrificed at 3 months. In the forth group, an important suppression of the immune response and increased activity of the cytokines was demonstrated.

Our results point out the following:

- an important increased of the oxidative response in the EMF- exposed groups, in special in the group sacrificed at 3 months.
- an important suppression of the immune response
- increased activity of the cytokines in all the groups exposed to EMF

Fig.1 ^{3}HTdR INCORPORATION TEST
Effect of the chronic exposure to EMF on the 3HTdR incorporation by PHA splenic Lys in the presence of the autologous AMs , at 30 and 90 days after EMF – exposure of the rats

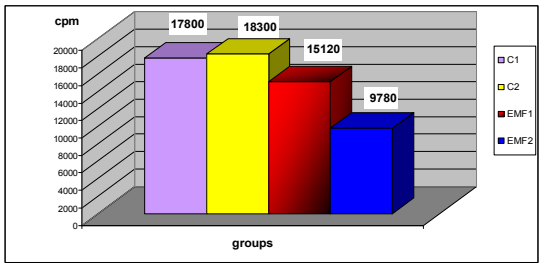

Fig. 2. IL-1 assay
Effect of on the chronic exposure to EMF on the IL-1 release by AMs obtained by BAL, 30 and 90 days after EMF – exposure of the rats.

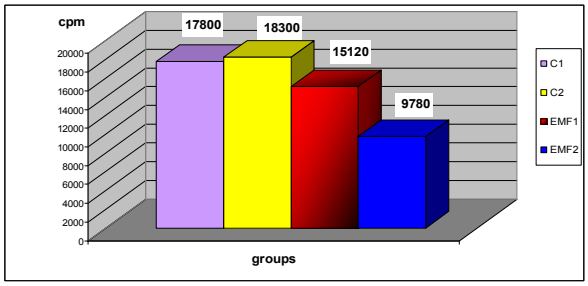

Fig. 3. TNF- assay

Effect of the chronic exposure to EMF on the TNF release by rats AMs,
obtained by BAL, 30 and 90 days after EMF – exposure of the rats.

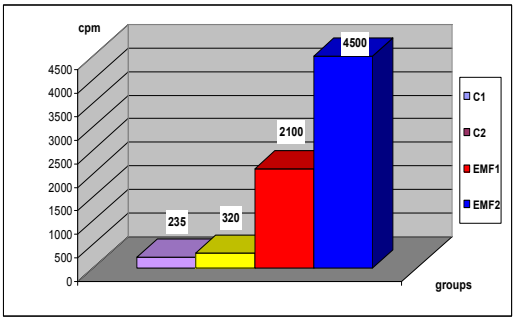

Fig. 4. LUMINOL -DEPENDENT CHEMILUMINISCENCE ASSAY.
Effect of the chronic exposure to EMF on ROS release from the rats AMs ,
obtained by BAL, 30 and 90 days after EMF – exposured rats.

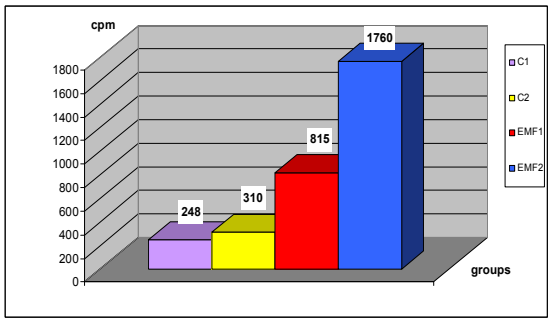

Fig. 5. LIPID PEROXIDES ASSAY
Effect of the chronic exposure to EMF on the release of the LP in the TBA- treated AMs, at 30 and 90 days after EMF – exposured rats.

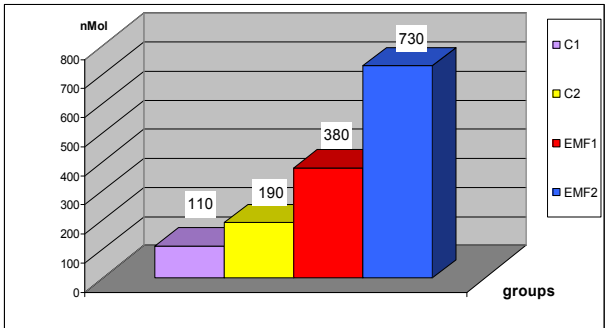

Conclusions

Although important issue are not yet resolved in this study, our results showed that EMFs caused changes in the immune system, possible mediated by the proliferative response of the T cells, by their distribution and by the cytokines 'activity. Our results clearly show that the exposure to EMF is connected to an increased release of free radicals. The increased levels of the ROS pointed out alterations in the oxidative stress parameters in the rat's macrophages that were exposed to EMF. Our results indicate an increased risk regarding development of the biological effects in EMF exposure correlated with intensity and period of the exposure.

References

1. Becker R.O., Marino A.A.- Electromagnetic pollution, The Sciences, January, 1978,pp 14, 15, 23
2. Bell G.B., Marino A.A., Chesson A.L- Human sensitivity to weak magnetic fields, Lancet 338: 1521- 1522, 1991
3. Bell G.B., Marino A.A., Chesson A.L.- Frequency –specific responses in the human brain caused by EMF , J. Neurol.Sci. 123:26-32, 1994
4. Bajinyan S, Hovhannisyan N., Arakelyan V. – The Effect of Millimeter-range Electromagnetic Waves of Low Intensity on Cellular Membranes, Effect of Electromagnetic Waves on Cellular Membranes 1999, 5(1):43- 49
5. Gianni M., Maggio F., Liberti M, Paffi A- Modeling Biological Noise in Firing and Bursting Neurons in the Presence of an EMF-Proceedings of the 2-the Iternational IEEE EMBSArington, Virginia, 2005
6. Kelsh M.A., Bracken T.D., Sahl J.D., Shum M., Ebi Kl.- occupat. Magnetic field exposure of garment workers- Bioelectromagnetics, 2003; 24(5): 316 -26
7. Kjell Hansson Mild, Mike Rapacholi, Emilie van Deventer, Paolo Ravazzani - EMF Hypersensitivity, Proceedings of the International Workshop on EMF Hypersensitivity, Prague, Oct.25-27, 2004
8. Leif G. Salford, Arne E. Brun, Jacob L. Eberhardt, Lars Malmgren , Bertil R. R. Persson-Nerve Cell Damage in Mammalian Brain after Exposure to Microwaves from GSM Mobile Phones- Environmental Health Perspectives,vol.111, number7, June 2003
9. Henry Lai, Narendra P. Singh-Magnetic-Field-Induced DNA Strand Breaks in Brain Cells of the Rat- Environmental Health Perspectives,vol 112, number 6, May 2004
10. Lantow M., Lupke E.M., Frahm E.J., Mattsson E.M.O. - ROS release and Hsp70 expresion afterexposure to1,800 MHzRMF in primary human monocytes and lympocytes- Radiat. Environ.Biophys, 2006
11. Marino A.A, Marcel Dekker, Environ. EMF and public health, New York, 965- 1044, 1988
12. Marino A.A, Morris D.M., Chronic electromagnetic stressors in the environment : A risk factor in human cancer, J. Environ. Sci.C3(2) 189- 219,1985
13. Mailhes J.B., Young D, Marino A.A – Mutagenesis, 12:347- 351,1997

14. Repacholi M.H. – Low –Level Exposure to Radiofrequency Electromagnetic Fields, Bioelectromagnetics 19: 1-19, 1988
15. Santini R., Santini P, Le Ruz P., Danze-Survey study of people living in the vicinity of cellular phone base stations. Electromagnetic biology and Medicine, 2003;22, 41-49
16. Zhang J. – the effect of low force chiropractic adjustments on body surface EMF- J. Can. Chiropr. Assoc.2004; 48(1)